CALIFORNIA REGIONAL WATER QUALITY CONTROL BOARD
CENTRAL VALLEY REGION

RESOLUTION NO. R5-2010-0043

AMENDMENTS TO THE WATER QUALITY CONTROL PLAN
FOR
THE SACRAMENTO RIVER AND SAN JOAQUIN RIVER BASINS
FOR
THE CONTROL OF METHYLMERCURY AND TOTAL MERCURY IN THE
SACRAMENTO-SAN JOAQUIN DELTA ESTUARY

WHEREAS, the California Regional Water Quality Control Board, Central Valley Region (Central Valley Water Board) finds that:

1. In 1975, the Central Valley Water Board adopted the Water Quality Control Plan for the Sacramento River and San Joaquin River Basins (Basin Plan), which has been amended occasionally.

2. The Basin Plan may be amended in accordance with the California Water Code (Water Code) section 13240, et seq.

3. Water Code section 13241 authorizes the Central Valley Water Board to establish water quality objectives and Water Code section 13242 sets forth the requirements for a program for implementation for achieving water quality objectives.

4. The federal Clean Water Act (CWA) section 303 requires the Central Valley Water Board to develop water quality objectives that are sufficient to protect beneficial uses designated for each water body found within its region.

5. The CWA section 303 requires the Central Valley Water Board to review the Basin Plan at least every three years and where appropriate modify water quality objectives or beneficial uses in the Basin Plan.

6. The Sacramento-San Joaquin Delta Estuary (Delta) has been identified under the federal Clean Water Act section 303(d) as impaired due to a fish consumption advisory for elevated concentrations of mercury in fish tissue, which poses a threat to humans. The mercury concentrations also pose a threat to wildlife and threatened and endangered species that consume Delta fish.

7. Pursuant to CWA section 303(d), a total maximum daily load (TMDL) is required to bring the impaired water bodies into compliance with water quality standards. These Basin Plan amendments satisfy the requirements of a TMDL. The draft staff report for the Basin Plan amendments contains TMDL elements including: the numeric targets used in the TMDL analyses; the source analyses for methylmercury and mercury; the linkage analysis between the targets and

methylmercury; seasonal variations and critical conditions analysis, load and waste load allocations; and a margin of safety.

8. The Consolidated Toxic Hot Spots Cleanup Plan (Water Code section 13394) adopted by the State Water Resources Control Board (State Water Board) identified the Delta as a toxic hot spot due to mercury. Water Code section 13392 requires that basin plans and water quality control policies be amended to prevent the creation of new toxic hot spots and the further pollution of existing hot spots.

9. The Water Quality Control Plan for the San Francisco Bay contains a TMDL for mercury in San Francisco Bay that assigned to the Central Valley a load allocation of 330 kilograms total mercury per year.

10. Section 131.38 of Title 40 of the Code of Federal Regulations (or the California Toxics Rule (CTR)) includes a criterion of 0.05 µg/L total recoverable mercury for freshwater sources of drinking water that is enforceable for all waters with a municipal and domestic water supply use designation, including the Delta.

11. The Central Valley Water Board recognizes that the Basin Plan does not include numeric fish tissue objectives for methylmercury, nor an implementation plan to control methylmercury and inorganic mercury discharges to the Delta; therefore, Basin Plan amendments are appropriate.

12. The proposed amendments modify Basin Plan Chapter II (Existing and Potential Beneficial Uses) to add the commercial and sport fishing (COMM) beneficial use as a designated beneficial use in the Delta and Yolo Bypass north of the Delta.

13. The proposed amendment modifies Basin Plan Chapter III (Water Quality Objectives) to add site-specific numeric fish tissue objectives for the Delta and Yolo Bypass north of the Delta.

14. The proposed amendments modify Basin Plan Chapter IV (Implementation) to include a methylmercury and inorganic mercury control program for the Delta and Yolo Bypass north of the Delta (Delta Mercury Control Program). The proposed amendments establish the loading capacity and allocations for methylmercury. The allocations are needed to provide a clear basis for implementation of actions to achieve compliance with applicable fish tissue objectives. The loading capacity and allocations also satisfy the federal requirements for a TMDL.

15. The proposed amendments modify Basin Plan Chapter IV (Implementation) to include interim total mercury limits for NPDES dischargers within the Delta and Yolo Bypass and total mercury reduction requirements for tributary watershed inputs to the Delta and Yolo Bypass. The draft final staff report for the Basin Plan amendments explains how the TMDL methylmercury allocations, interim total mercury limits for NPDES dischargers, and total mercury reduction requirements for tributary watershed inputs to the Delta and Yolo Bypass are set to attain all applicable water quality standards, including the CTR, the San Francisco Bay

mercury TMDL allocation, and site-specific numeric fish tissue objectives for the Delta and Yolo Bypass north of the Delta.

16. The proposed amendments divide implementation into two phases. In Phase 1, the proposed amendments require dischargers of methylmercury to conduct studies to identify potential methylmercury control methods and evaluate the effectiveness, cost, and potential environmental effects of identified methylmercury control methods. The proposed amendments also require specific point source dischargers to implement pollution minimization programs during the first phase of the control program, and non-point sources are required to reduce sediment in runoff.

    At the end of Phase 1, the Central Valley Water Board will evaluate the completed studies, and will consider: modification of methylmercury objectives, allocations, and implementation schedules for methylmercury controls; and a Mercury Offset Program to compensate for loads in excess of the methylmercury allocations. The proposed amendments require dischargers to implement methylmercury management practices during Phase 2 of the control program.

17. The proposed amendments modify Basin Plan Chapter V (Surveillance and Monitoring) to include monitoring requirements to allow the Central Valley Water Board to assess progress in reducing inorganic mercury and methylmercury discharges and to determine compliance with fish tissue objectives.

18. The Central Valley Water Board has considered the factors set forth in Water Code section 13241, including economic considerations, in developing this proposed amendment. The costs of implementing the proposed amendments are reasonable, considering the size of the geographic area and the number of methylmercury dischargers affected by the amendment.

19. The proposed amendments include an estimate of the cost of the implementation program to agriculture and identify potential sources of financing, as required by Water Code section 13141.

20. Central Valley Water Board staff developed a draft staff report and draft Basin Plan amendments for independent, external scientific peer review in June 2006 in accordance with Health and Safety Code section 57004. The draft final staff report and amendments have been changed to conform to the recommendations of the peer reviewers or staff has provided sound rationale for why individual recommendations were not adopted.

21. The Central Valley Water Board finds that the scientific portions of the proposed Basin Plan amendments are based on sound scientific knowledge, methods, and practices in accordance with Health and Safety Code section 57004.

22. The Central Valley Water Board finds that the proposed amendments are consistent with the State Water Board Resolution No. 68-16, in that the addition of

fish tissue objectives (i) considers maximum benefit to the people of the State, (ii) will not unreasonably affect present and anticipated beneficial use of waters, and (iii) will not result in water quality less than that prescribed in policies, and the proposed amendment is consistent with the federal Antidegradation Policy (40 C.F.R. § 131.12). The proposed amendments require actions to be taken to implement management practices to ensure compliance with the fish tissue objectives. Such actions are of maximum benefit to the people of the State. Control of discharges of inorganic mercury and methylmercury to the Delta is necessary to protect beneficial uses of the Delta. The proposed amendments will not unreasonably affect present and anticipated beneficial uses nor result in water quality less than described in applicable policies because the amendment is intended to result in compliance with the fish tissue objectives and contains an implementation plan that incorporates an adaptive management approach designed to avoid negative impacts to beneficial uses.

23. The regulatory action proposed meets the “Necessity” standard of the Administrative Procedures Act, Government Code section 11353, subdivision (b).

24. The Central Valley Water Board staff held a California Environmental Quality Act (CEQA)(Pub. Resources Code §21000, et seq.) scoping meeting on 29 September 2005, a Board workshop on 28 November 2005, public workshops on 18 and 19 September 2006, a Board workshop on 16 March 2007, Board hearings on 24-25 April 2008, and numerous meetings with stakeholders to receive comments on the draft amendments and to identify any significant issues that must be considered.

25. The basin planning process has been certified by the Resources Agency as an exempt regulatory program because its process adequately fulfills the purposes of CEQA. The Central Valley Water Board is therefore exempt from CEQA’s requirement to prepare an environmental impact report, negative declaration, or initial study for the proposed amendments. Central Valley Water Board staff has prepared the required documentation for adoption of a Basin Plan amendment, including an environmental checklist and written report (staff report) (23 Cal. Code Regs. § 3777).

26. Central Valley Water Board staff has prepared draft final Basin Plan amendments and a staff report dated April 2010. The staff report includes environmental documentation consisting of a description of the project and proposed amendments, environmental analysis and checklist, identification of potentially significant adverse environmental impacts, an analysis of reasonable alternatives to the proposed amendments, an analysis of the reasonably foreseeable alternative methods of compliance with the proposed amendments, and an analysis of the reasonably foreseeable environmental impacts of the methods of compliance and mitigation measures. The environmental documentation also includes stakeholder comments, staff responses to comments, and this Board resolution.

27. The proposed amendments have the potential to cause significant adverse impacts upon the environment, primarily because implementation of the amendments may cause the design and location of proposed wetlands restoration projects to be reconsidered and perhaps modified. However, there are mitigation measures that, if employed, would substantially lessen the potentially significant adverse impacts. These mitigation measures are within the responsibility and jurisdiction of the dischargers implementing control actions, and not the Central Valley Water Board. Water Code section 13360 precludes the Central Valley Water Board from dictating the manner in which responsible agencies comply with any of the Central Valley Water Board's regulations or orders. When the dischargers responsible for implementing this amendment determine how they will proceed, the dischargers responsible for those parts of the project can and should incorporate mitigation into any subsequent projects or project approvals. Until additional methylmercury studies have been completed, it is not known whether wetlands that may contribute methylmercury to the Delta and Yolo Bypass also provide critical habitat to species of concern, and whether it will be possible to mitigate the potential impacts to less than significant levels.

28. From a program-level perspective, incorporation of the mitigation measures outlined in the staff report will foreseeably reduce most potential impacts to less than significant levels. Other impacts could be significant and therefore staff prepared a Statement of Overriding Considerations.

29. The Statement of Overriding Considerations evaluates the ecological and health benefits of implementing the proposed Basin Plan amendments in relation to the potentially significant adverse impacts. A fishery with mercury-contaminated fish is an environmental justice issue and is a threat to wildlife. Implementation of the proposed amendments will result in an overall improvement in water quality in the Delta region and will have a significant positive impact upon the environment by enabling humans and wildlife to safely consume Delta fish. To the extent significant adverse environmental effects could occur, the Central Valley Water Board has balanced the economic, legal, social, and other benefits of the amendments against the potentially unavoidable environmental risks and finds that specific economic, legal, social, and other benefits of the amendments outweigh the potentially unavoidable adverse environmental effects, such that those effects are considered acceptable.

30. Central Valley Water Board staff has circulated a Notice of Public Hearing, Notice of Filing, a written staff report, response to public comments documents, environmental checklist, and draft amendments to interested individuals and public agencies, including persons having special expertise with regard to the environmental effects involved with the proposed amendments, for review and comment in accordance with state and federal environmental regulations (23 Cal. Code Regs. § 3775, 40 C.F.R. Part 25, and 40 C.F.R. § 131).

31. Stakeholders, including representatives from irrigated agriculture, managed wetlands, wastewater treatment plants, municipal stormwater, environmental advocates, environmental justice advocates, and State and federal agencies, participated in a collaborative stakeholder process with Central Valley Water Board staff that contributed to the development of the proposed Basin Plan amendments for the Delta Mercury Control Program.

32. A subset of the stakeholders, with support from Central Valley Water Board staff, is developing an adaptive management plan that can be used by dischargers and other stakeholders to develop and implement activities required under Phase 1 of the Delta Mercury Control Program in an effective and efficient manner. The adaptive management plan includes, among other information: guiding principles for the overall Delta Mercury Control Program and for future offset policy, an organizational structure with roles and responsibilities, guidance for the Phase 1 methylmercury control studies and exposure reduction program, and potential funding strategies.

33. Responses to all comments have been prepared and the proposed amendments, staff report and environmental checklist have been revised as appropriate in response to comments.

34. The Central Valley Water Board held a public hearing on 22 April 2010, to receive testimony and adopt the draft Basin Plan amendments. Notice of the public hearing was sent to all interested persons and published in accordance with Water Code section 13244.

35. Based on the record as a whole, including draft Basin Plan amendments, the environmental document, accompanying written documentation, and public comments received, the Central Valley Water Board concurs with staff's conclusion that some actions to comply with the Basin Plan amendments may result in significant impacts and the Central Valley Water Board concurs with the Statement of Overriding Considerations. The Central Valley Water Board finds that the record as a whole and the procedures followed by staff comply with applicable CEQA requirements (Pub. Resources Code § 21080.5, 14 Cal. Code Regs. §15250, et seq., 23 Cal. Code Regs. § 3775, et seq.).

36. Basin Plan amendments must be approved by the State Water Board, Office of Administrative Law (OAL), and the United States Environmental Protection Agency (USEPA). The proposed amendments become effective under State law after OAL approval and become effective under the federal Clean Water Act after USEPA approval.

37. The Central Valley Water Board finds that the amendments to the Basin Plan were developed in accordance with Water Code section 13240, et seq.

THEREFORE BE IT RESOLVED:

1. Pursuant to Water Code section 13240 et seq., the Central Valley Water Board, after considering the entire record, including all late revisions, staff responses to comments, and oral testimony at the hearing, hereby approves the staff report and adopts the amendments to the Basin Plan as set forth in Attachment 1.

2. The Central Valley Water Board supports stakeholder development and implementation of an adaptive management plan that will help implement activities required under Phase 1 of the Delta Mercury Control Program.

3. Central Valley Water Board staff is directed to continue working with stakeholders in the development and implementation of the Phase 1 activities.

4. The Executive Officer is directed to forward copies of the Basin Plan amendments to the State Water Board in accordance with the requirements of Water Code section 13245.

5. The Central Valley Water Board requests that the State Water Board approve the Basin Plan amendments in accordance with the requirements of sections 13245 and 13246 of the Water Code and forward it to OAL and the USEPA for approval. The Central Valley Water Board specifically requests USEPA approval of all Basin Plan amendment provisions that require USEPA approval.

6. If during its approval process the Central Valley Water Board staff, State Water Board or OAL determines that minor, non-substantive corrections to the language of the amendments are needed for clarity or consistency, the Executive Officer may make such changes, and shall inform the Central Valley Water Board of any such changes.

7. The Central Valley Water Board hereby approves and adopts the CEQA substitute environmental documentation, which was prepared in accordance with Public Resources Code section 21159 and California Code of Regulations, Title 14, section 15187, and directs the Executive Officer to sign the environmental checklist.

8. Following approval of the Basin Plan amendments by the OAL, the Executive Officer shall file a Notice of Decision with the Secretary for Resources in accordance with Public Resources Code section 21080.5, subsection (d)(2)(E), and California Code of Regulations, Title 23, section 3781.

I, PAMELA C. CREEDON, Executive Officer, do hereby certify the foregoing is a full, true, and correct copy of a Resolution adopted by the California Regional Water Quality Control Board, Central Valley Region, on 22 April 2010.

original signed by
PAMELA C. CREEDON, Executive Officer

Attachment 1: Amendments to the Water Quality Control Plan for the Sacramento River and San Joaquin River Basins for the Control of Methylmercury and Total Mercury in the Sacramento-San Joaquin River Delta Estuary

Attachment 1

Resolution No. R5-2010-0043
Amendments to the Water Quality Control Plan for the Sacramento River and San Joaquin River Basins for the Control of Methylmercury and Total Mercury in the Sacramento-San Joaquin River Delta Estuary

Revise Chapter II (Existing and Potential Beneficial Uses), Table II-1 for Sacramento San Joaquin Delta, to add as follows:

Yolo Bypass (8)

Sacramento San Joaquin Delta (8,9)

Addition to Table II-1 Footnote (8) under existing text:

COMM is a designated beneficial use for the Sacramento San Joaquin Delta and Yolo Bypass waterways listed in Appendix 43 and not any tributaries to the listed waterways or portions of the listed waterways outside of the legal Delta boundary unless specifically designated.

Addition to Table II-1 Footnote (9) under existing text:

COMM is a designated beneficial use for Marsh Creek and its tributaries listed in Appendix 43 within the legal Delta boundary.

Revise Chapter III (Water Quality Objectives), under "Methylmercury", to add as follows:

For the Sacramento-San Joaquin Delta and Yolo Bypass waterways listed in Appendix 43, the average methylmercury concentrations shall not exceed 0.08 and 0.24 mg methylmercury/kg, wet weight, in muscle tissue of trophic level 3 and 4 fish, respectively (150-500 mm total length). The average methylmercury concentrations shall not exceed 0.03 mg methylmercury/kg, wet weight, in whole fish less than 50 mm in length.

Revise Chapter IV (Implementation), under "Mercury Discharges in the Sacramento River and San Joaquin River Basins", to add as follows:

Delta Mercury Control Program

The Delta Mercury Control Program applies specifically to the Delta and Yolo Bypass waterways listed in Appendix 43.

This amendment was adopted by the Regional Water Quality Control Board on [date], and approved by the U.S. Environmental Protection Agency on [date]. The Effective Date of the Delta Mercury Control Program shall be [Effective Date], the date of U.S. EPA approval.

Program Overview
The Delta Mercury Control Program is designed to protect people eating one meal/week (32 g/day) of trophic levels 3 and 4 Delta fish, plus some non-Delta (commercial market) fish. The Regional Water Board recognizes that some consumers eat four to five meals per week (128-160 g/day) of a variety of Delta fish species. The fish tissue objectives will be re-evaluated during the Phase 1 Delta Mercury Control Program Review and later program reviews to determine whether objectives protective of a higher consumption rate can be attained as methylmercury reduction actions are developed and implemented.

Additional information about methylmercury source control methods must be developed to determine how and if Dischargers can attain load and waste load allocations set by the Board. Information is also needed about the methylmercury control methods' potential benefits and adverse impacts to humans, wildlife, and the environment. Therefore, the Delta Mercury Control Program will be implemented through a phased, adaptive management approach.

Phase 1 spans from [Effective Date] through the Phase I Delta Mercury Control Program Review, expected to be in [9 years after the Effective Date]. Phase 1 emphasizes studies and pilot projects to develop and evaluate management practices to control methylmercury. Phase 1 includes provisions for: implementing pollution minimization programs and interim mass limits for inorganic (total) mercury point sources in the Delta and Yolo Bypass; controlling sediment-bound mercury in the Delta and Yolo Bypass that may become methylated in agricultural lands, wetland, and open-water habitats; and reducing total mercury loading to San Francisco Bay, as required by the Water Quality Control Plan for the San Francisco Bay Basin.

Phase 1 also includes: the development of upstream mercury control programs for major tributaries; the development and implementation of a mercury exposure reduction program to protect humans; and the development of a mercury offset program.

At the end of Phase 1, the Regional Water Board shall conduct a Phase 1 Delta Mercury Control Program Review that considers: modification of methylmercury goals, objectives, allocations and/or the Final Compliance Date; implementation of management practices and schedules for methylmercury controls; and adoption of a mercury offset program for dischargers who cannot meet their load and waste load allocations after implementing all reasonable load reduction strategies. The review also shall consider other potential public and environmental benefits and negative impacts (e.g., habitat restoration, flood protection, water supply, fish consumption) of attaining the allocations. The fish tissue objectives, the linkage analysis between objectives and sources, and the attainability of the allocations will be re-evaluated based on the findings of Phase 1 control studies and other information. The linkage analysis, fish tissue objectives, allocations, and time schedules shall be adjusted at the end of Phase 1, or subsequent program reviews, if appropriate.

Phase 2 begins after the Phase 1 Delta Mercury Control Program Review or [11 years after the Effective Date], whichever occurs first, and ends in 2030. During Phase 2, dischargers shall implement methylmercury control programs and continue inorganic (total) mercury reduction

programs. Compliance monitoring and implementation of upstream control programs also shall occur in Phase 2.

Load and Waste Load Allocations
Final methylmercury waste load allocations for point sources and load allocations for non-point sources are listed in Tables A through D. For each subarea listed in Table A, the sum of allocations for agricultural drainage, atmospheric wet deposition, open water, urban (nonpoint source), and wetlands and the individual allocations for tributary inputs (Table D), NPDES facilities and NPDES facilities future growth (Table B), and NPDES MS4 (Table C) within that subarea equals that subarea's assimilative capacity. New or expanded methylmercury discharges that begin after [Effective Date] may necessitate adjustments to the allocations.

Load allocations are specific to Delta subareas, which are shown on Figure xx-x. The load allocations for each Delta subarea apply to the sum of annual methylmercury loads produced by different types of nonpoint sources: agricultural lands, wetlands, and open-water habitat in each subarea, as well as atmospheric wet deposition to each subarea (Table A), and runoff from urban areas outside of Municipal Separate Storm Sewer System (MS4) service areas. The subarea allocations apply to both existing and future discharges.

Waste load allocations apply to point sources, which include individual NPDES permitted facility discharges and runoff from urban areas within MS4 service areas within the Delta and Yolo Bypass (Tables B and C, respectively).

Methylmercury allocations are assigned to tributary inputs to the Delta and Yolo Bypass (Table D). Future upstream control programs are planned for tributaries to the Delta through which management practices will be implemented to meet load allocations for tributary inputs assigned by the Delta Mercury Control Program.

Load allocations for the tributary inputs, urban areas outside of MS4 service areas, open-water habitat, and atmospheric deposition, and waste load allocations for the MS4s, are based on water years 2000 through 2003, a relatively dry period. Annual loads are expected to fluctuate with rainfall volume and other factors. As a result, attainment of these allocations shall be assessed as a five-year average annual load. Allocations for these sources will be re-evaluated during review of the Phase 1 Delta Mercury Control Program as wet year data become available.

Margin of Safety
The Delta Mercury Control program includes an explicit margin of safety of 10%.

Final Compliance Date
Methylmercury load and waste load allocations for dischargers in the Delta and Yolo Bypass shall be met as soon as possible, but no later than 2030, unless the Regional Water Board modifies the implementation schedule and Final Compliance Date.

During Phase 1, all dischargers shall implement reasonable, feasible controls for inorganic (total) mercury.

All dischargers should implement methylmercury management practices identified during Phase 1 that are reasonable and feasible. However, implementation of methylmercury

management practices identified in Phase 1 is not required for the purposes of achieving methylmercury load allocations for nonpoint sources until the beginning of Phase 2.

The Regional Water Board will, as necessary, include schedules of compliance in NPDES permits for compliance with water quality-based effluent limits based on the waste load allocations. The compliance schedules must be consistent with the requirements of federal laws and regulations, including, USEPA regulations 40 CFR 122.47, State laws and regulations, including State Water Board Policy for Compliance Schedules in National Pollutant Discharge Elimination System Permits, and the Final Compliance Date. The Regional Board will review the feasibility of meeting wasteload allocations based on reliable data and information regarding variability in methylmercury concentrations and treatment efficiencies and time needed to comply with the wasteload allocations. The Phase 1 Control Studies are designed to provide this information. As needed, the Regional Board shall incorporate the Phase 1 Control Studies into compliance schedules. When Phase 1 studies are complete, the Regional Board will review the need for additional time during Phase 2 for NPDES permittees to comply with the final wasteload allocations.

Implementation Program

Point Sources

The regulatory mechanism to implement the Delta Mercury Control Program for point sources shall be through NPDES permits.

Requirements for NPDES Permitted Facilities

By [six months after Effective Date], all facilities listed in Table B shall submit individual pollutant minimization program workplans to the Regional Water Board. The dischargers shall implement their respective pollutant minimization programs within 30 days after receipt of written Executive Officer approval of the workplans. Until the NPDES permitted facility achieves compliance with its WLA, the discharger shall submit annual progress reports on pollution minimization activities implemented and evaluation of their effectiveness, including a summary of mercury and methylmercury monitoring results.

During Phase 1, all facilities listed in Table B shall limit their discharges of inorganic (total) mercury to facility performance-based levels. The interim inorganic (total) mercury effluent mass limit is to be derived using current, representative data and shall not exceed the 99.9^{th} percentile of 12-month running effluent inorganic (total) mercury loads (lbs/year). For intermittent dischargers, the interim inorganic (total) mercury effluent mass limit shall consider site-specific discharge conditions. The limit shall be assigned in permits and reported as an annual load based on a calendar year. At the end of Phase 1, the interim inorganic (total) mercury mass limit will be re-evaluated and modified as appropriate.

NPDES permitted facilities that begin discharging to the Delta or Yolo Bypass during Phase 1 shall comply with the above requirements.

Requirements for NPDES Permitted Urban Runoff Discharges

MS4 dischargers listed in Table C shall implement best management practices (BMPs) to control erosion and sediment discharges consistent with their existing permits and orders with the goal of reducing mercury discharges.

The Sacramento MS4 (CAS082597), Contra Costa County MS4 (CAS083313), and Stockton MS4 (CAS083470) permittees shall implement pollution prevention measures and BMPs to minimize total mercury discharges. This requirement shall be implemented through mercury reduction strategies required by their existing permits and orders. Annually, the dischargers shall report on the results of monitoring and a description of implemented pollution prevention measures and their effectiveness.

The Sacramento MS4 (CAS082597), Contra Costa County MS4 (CAS083313), and Stockton MS4 (CAS083470) shall continue to conduct mercury control studies to monitor and evaluate the effectiveness of existing BMPs per existing requirements in permits and orders, and to develop and evaluate additional BMPs as needed to reduce their mercury and methylmercury discharges into the Delta and Yolo Bypass.

Nonpoint Sources

Nonpoint sources shall be regulated through the authority contained in State and federal laws and regulations, including State Water Board's Nonpoint Source Implementation and Enforcement Policy.

Table A contains methylmercury load allocations for non-point sources in the Delta and Yolo Bypass waterways listed in Appendix 43.

During Phase 1, all nonpoint sources in the Delta and Yolo Bypass shall implement reasonable, feasible actions to reduce sediment in runoff with the goal of reducing inorganic mercury loading to the Yolo Bypass and Delta, in compliance with existing Basin Plan objectives and requirements, and Irrigated Lands Regulatory Program requirements.

Attainment of methylmercury load allocations at the end of 2030 will be determined by comparing monitoring data and documentation of methylmercury management practice implementation for each subarea with loads specified in Table A and Table D.

For subareas not in compliance with allocations by 2030, the Regional Water Board may develop load allocations for individual sources and require individual monitoring and waste discharge requirements.

In subareas needing reductions in methylmercury, proponents of new wetland and wetland restoration projects scheduled for construction after [Effective Date] shall (a) participate in Control Studies as described below, or shall implement site-specific study plans, that evaluate practices to minimize methylmercury discharges, and (b) implement methylmercury controls as feasible. New wetland projects may include pilot projects and associated monitoring to evaluate management practices that minimize methylmercury discharges.

Phase 1 Control Studies

Point and nonpoint source dischargers, working with other stakeholders, shall conduct methylmercury control studies (Control Studies) to evaluate existing control methods and, as needed, develop additional control methods that could be implemented to achieve their methylmercury load and waste load allocations. The Regional Water Board will use the Phase 1 Control Studies' results and other information to consider amendments to the Delta Mercury Control Program during the Phase 1 Delta Mercury Control Program Review.

A Technical Advisory Committee, described below, will review the Control Studies' designs and results.

Study Participants

Control Studies can be developed through a stakeholder group approach or other collaborative mechanism, or by individual dischargers. Individual dischargers are not required to do individual studies if the individual dischargers join a collaborative study group(s).

Control Studies are required for:

a. Irrigated agricultural lands that discharge to the Yolo Bypass and Delta subareas that require methylmercury source reductions.

b. Managed wetlands and wetland restoration projects that discharge to the Yolo Bypass and Delta subareas that require methylmercury source reductions.

c. Existing NPDES permitted facilities in the Delta and the Yolo Bypass (listed in Table B).

d. Sacramento Area MS4, Stockton MS4, and Contra Costa County MS4 service areas within and upstream of the legal Delta boundary.

e. State and Federal agencies whose activities affect the transport of mercury and the production and transport of methylmercury through the Yolo Bypass and Delta, or which manage open water areas in the Yolo Bypass and Delta, including but not limited to Department of Water Resources, State Lands Commission, Central Valley Flood Protection Board, U.S. Army Corps of Engineers, and U.S. Bureau of Reclamation. If appropriate during Phase 1, the Executive Officer will require other water management agencies whose activities affect methylmercury levels in the Delta and Yolo Bypass to participate in the Control Studies.

f. Other significant sources of methylmercury not listed above, as identified and deemed appropriate by the Executive Officer.

Dischargers in the Central Valley that are not subject to the Delta Mercury Control Program but may be subject to future mercury control programs in upstream tributary watersheds are encouraged to participate in the coordinated Delta Control Studies. Dischargers in and upstream of the Delta who participate in the Control Studies will be exempt from conducting equivalent Control Studies required by future upstream mercury control programs.

Study Objectives

The Control Studies shall evaluate existing control methods and, as needed, additional control methods that could be implemented to achieve methylmercury load and waste load allocations. The Control Studies shall evaluate the feasibility of reducing sources more than the minimum amount needed to achieve allocations.

Phase 1 studies also may include an evaluation of innovative actions, watershed approaches, offsets projects, and other short and long-term actions that result in reducing inorganic (total) mercury and methylmercury to address the accumulation of methylmercury in fish tissue and to reduce methylmercury exposure.

Dischargers may evaluate the effectiveness of using inorganic (total) mercury controls to control methylmercury discharges.

Dischargers may conduct characterization studies to inform and prioritize the Control Studies. Characterization studies may include, but not be limited to, evaluations of methylmercury and total mercury concentrations and loads in source waters, receiving waters, and discharges, to determine which discharges act as net sources of methylmercury, and which land uses result in the greatest net methylmercury production and loss.

Final reports for Control Studies shall include a description of methylmercury and/or inorganic (total) mercury management practices identified in Phase 1; an evaluation of the effectiveness, and costs, potential environmental effects, and overall feasibility of the control actions. Final reports shall also include proposed implementation plans and schedules to comply with methylmercury allocations as soon as possible.

If the Control Study results indicate that achieving a given methylmercury allocation is infeasible, then the discharger, or an entity representing a discharger, shall provide detailed information on why full compliance is not achievable, what methylmercury load reduction is achievable, and an implementation plan and schedule to achieve partial compliance.

Control Study Workplans

Control Studies shall be implemented through Control Study Workplan(s). The Control Study Workplan(s) shall provide detailed descriptions of how methylmercury control methods will be identified, developed, and monitored, and how effectiveness, costs, potential environmental effects, and overall feasibility will be evaluated for the control methods.

The Control Study Workplan(s) shall include details for organizing, planning, developing, prioritizing, and implementing the Control Studies.

The Control Studies will be governed using an Adaptive Management approach.

Technical Advisory Committee and Adaptive Management Approach

The Regional Water Board commits to supporting an Adaptive Management approach. The adaptive management approach includes the formation of a Stakeholder Group(s) and a Technical Advisory Committee (TAC). Regional Water Board staff, working with the TAC and Stakeholder Group(s), will provide a Control Study Guidance Document for stakeholders to reference.

The TAC shall be comprised of independent experts who would convene as needed to provide scientific and technical peer review of the Control Study Workplan(s) and results, advise the Board on scientific and technical issues, and provide recommendations for additional studies and implementation alternatives developed by the dischargers. The Board shall form and manage the TAC with recommendations from the dischargers and other stakeholders, including tribes and community organizations.

Board staff shall work with the TAC and Stakeholder Group(s) to review the Control Study Workplan(s) and results. As new information becomes available from the Control Studies or outside studies that result in redirection and/or prioritization of existing studies, dischargers may amend the Control Study Workplan(s) with Executive Officer approval.

Mercury Control Studies Schedule

1. By [six months after the Effective Date], entities required to conduct Control Studies shall submit for Executive Officer approval either: (1) a report(s) describing how dischargers and stakeholders plan to organize to develop a coordinated, comprehensive Control Study Workplan(s), or (2) a report describing how individual dischargers will develop individual Control Study Workplans. For dischargers conducting coordinated studies, the report shall include a list of participating dischargers, stakeholders, tribes, and community groups. Dischargers shall be considered in compliance with this reporting requirement upon written commitment to either be part of a group developing a Control Study Workplan or develop an individual Control Study Workplan.

2. Control Study Workplans shall be submitted to the Regional Water Board within [nine months of the Effective Date of this amendment]. With Executive Officer approval, an additional nine months may be allowed for Workplans being developed by a collaborative stakeholder approach. The Control Study Workplan(s) shall contain a detailed plan for the Control Studies and the work to be accomplished during Phase 1. Regional Water Board staff and the TAC will review the Workplans and provide recommendations for revising Workplans if necessary.

   Within four months of submittal, the Executive Officer must determine if the Workplans are acceptable. After four months, Workplans are deemed approved and ready to implement if no written approval is provided by the Executive Officer, unless the Executive Officer provides written notification to extend the approval process.

   Dischargers shall be considered in compliance with this reporting requirement upon timely submittal of workplans and revisions.

3. By [four years after the Effective Date], entities responsible for Control Studies shall submit report(s) to the Regional Water Board documenting progress towards complying with the Control Study Workplan(s). The report shall include amended workplans for any additional studies needed to address methylmercury reductions. The TAC will review the progress reports and may recommend what additional or revised studies should be undertaken to complete the objectives of the Control Studies. Staff will review the progress reports and recommendations of the TAC and provide a progress report to the Regional Water Board.

4. By [seven years after the Effective Date], entities responsible for Control Studies shall complete the studies and submit to the Regional Water Board Control Studies final reports that present the results and descriptions of methylmercury control options, their preferred methylmercury controls, and proposed methylmercury management plan(s) (including implementation schedules), for achieving methylmercury allocations. In addition, final report(s) shall propose points of compliance for non-point sources.

If the Executive Officer determines that dischargers are making significant progress towards developing, implementing and/or completing the Phase 1 Control Studies but that more time is needed to finish the studies, the Executive Officer may consider extending a study's deadlines.

The Executive Officer may, after public notice, extend time schedules up to two years if the dischargers demonstrate reasonable attempts to secure funding for the Phase 1 studies but experience severe budget shortfalls.

Annually, staff shall publicly report to the Regional Water Board progress of upstream mercury program development, discharger and stakeholder coordination, Control Study Workplan status, implementation of Control Studies, actions implemented or proposed to meet load and waste load allocations, and the status of the formation and activities of the TAC.

By [four years after the Effective Date], the Executive Officer shall provide a comprehensive report to the Regional Water Board on Phase 1 progress, including progress of upstream mercury control program development, Control Studies, actions implemented or proposed to meet Delta Mercury Control Program load and waste load allocations, and the status and progress of the TAC.

If dischargers do not comply with Control Study implementation schedules, the Executive Officer shall consider issuing individual waste discharge requirements or ordering the production of technical reports and/or management plans.

Phase 1 Delta Mercury Control Program Review

By [nine years after Effective Date] at a public hearing, and after a scientific peer review and public review process, the Regional Water Board shall review the Delta Mercury Control Program and may consider modification of objectives, allocations, implementation provisions and schedules, and the Final Compliance Date.

If the Executive Officer allows an extension for the Control Studies' schedule, then the Delta Mercury Control Program Review may be delayed up to two years. If the Delta Mercury Control Program Review is delayed more than one year, the Regional Water Board should consider extending the schedule for Phase 2 implementation of methylmercury controls, and the Final Compliance Date.

The Regional Water Board shall assess: (a) the effectiveness, costs, potential environmental effects, and technical and economic feasibility of potential methylmercury control methods; (b) whether implementation of some control methods would have negative impacts on other project or activity benefits; (c) methods that can be employed to minimize or avoid potentially significant negative impacts to project or activity benefits that may result from control methods; (d) implementation plans and schedules proposed by the dischargers; and (e) whether methylmercury allocations can be attained.

The Regional Water Board shall use any applicable new information and results of the Control Studies to adjust the relevant allocations and implementation requirements as appropriate. Interim limits established during Phase 1 and allocations will not be reduced as a result of early actions that result in reduced inorganic (total) mercury and/or methylmercury in discharges.

As part of the Phase 1 Delta Mercury Control Program Review and subsequent program reviews, the Regional Water Board may consider adjusting the allocations to allow methylmercury discharges from existing and new wetland restoration and other aquatic habitat enhancement projects if dischargers provide information that demonstrates that 1) all reasonable management practices to limit methylmercury discharges are being implemented and 2) implementing additional methylmercury management practices would negatively impact fish and wildlife habitat or other project benefits. The Regional Water Board will consider the merits of the project(s) and whether to require the discharger(s) to propose other activities in the

watershed that could offset the methylmercury. The Regional Water Board will periodically review the progress towards achieving the allocations and may consider additional conditions if the plan described above is ineffective.

The Regional Water Board shall conduct the Phase 1 Delta Mercury Program Review based on information received in Phase 1. If the Regional Water Board does not receive timely information to review and update the Delta Mercury Control Program, then allocations shall not be raised but may be lowered and the 2030 Final Compliance Date shall not be changed for those individual dischargers who did not complete the Phase 1 requirements.

The Regional Water Board shall require implementation of appropriate management practices. The methylmercury management plan(s) developed in Phase 1 shall be initiated as soon as possible, but no later than one (1) year after Phase 2 begins.

The Regional Water Board shall review this control program two years prior to the end of Phase 2, and at intervals no more than 10 years thereafter.

Compliance Monitoring

Within two years after the start of Phase 2, entities responsible for meeting load and waste load allocations shall monitor methylmercury loads and concentrations and submit annual reports to the Regional Water Board. The points of compliance for waste load allocations for NPDES facilities shall be the effluent monitoring points described in individual NPDES permits. The points of compliance for MS4s required to conduct methylmercury monitoring are those locations described in the individual MS4 NPDES permits or otherwise determined to be representative of the MS4 service areas and approved by the Executive Officer on an MS4-specific basis. The points of compliance and monitoring plans for non-point sources shall be determined during the Control Studies. Compliance with the load allocations for nonpoint sources and waste load allocations for MS4s may be documented by monitoring methylmercury loads at the compliance points or by quantifying the annual average methylmercury load reduced by implementing pollution prevention activities and source and treatment controls.

Entities will be allowed to comply with their mercury receiving water monitoring requirements by participating in a regional monitoring program, when such a program is implemented.

Chapter V, Surveillance and Monitoring, contains additional monitoring guidance.

Requirements for State and Federal Agencies

Open water allocations are assigned jointly to the State Lands Commission, the Department of Water Resources, and the Central Valley Flood Protection Board as applicable. Other agencies that are identified in Phase 1 that implement actions and activities that have the potential to contribute to methylmercury production and loss in open water will be required to take part in the studies. In the Phase 1 review, the Regional Water Board will modify, as appropriate, the list of entities that are responsible for meeting the open water allocations. Open water allocations apply to the methylmercury load that fluxes to the water column from sediments in open-water habitats within channels and floodplains in the Delta and Yolo Bypass.

The State Lands Commission, Central Valley Flood Protection Board, Department of Water Resources, and other identified agencies shall conduct Control Studies and evaluate options to reduce methylmercury in open waters under jurisdiction of the State Lands Commission and

floodplain areas inundated by flood flows. These agencies shall evaluate their activities to determine whether operational changes or other practices or strategies could be implemented to reduce ambient methylmercury concentrations in Delta open water areas and floodplain areas inundated by managed floodplain flows. Evaluations shall include inorganic mercury reduction projects. By [six months after Effective Date] these agencies shall demonstrate how the agencies have secured adequate resources to fund the Control Studies. Regional Water Board staff will work with the agencies to develop the Control Studies and evaluate potential mercury and methylmercury reduction actions.

Activities including water management and impoundment in the Delta and Yolo Bypass, maintenance of and changes to salinity objectives, dredging and dredge materials disposal and reuse, and management of flood conveyance flows are subject to the open water methylmercury allocations. Agencies responsible for these activities in the Delta and Yolo Bypass include, but are not limited to, Department of Water Resources, State Lands Commission, Central Valley Flood Protection Board, U.S. Bureau of Reclamation, U.S. Army Corps of Engineers (USACE), and the State Water Resources Control Board. Control Studies shall be completed for the activities that have the potential to increase ambient methylmercury levels. These agencies may conduct their own coordinated Control Studies or may work with the other stakeholders in comprehensive, coordinated Control Studies.

The agencies should coordinate with wetland and agricultural landowners during Phase 1 to characterize existing methylmercury discharges to open waters from lands immersed by managed flood flows and develop methylmercury control measures.

New wetland, floodplain, and other aquatic habitat restoration and enhancement projects, including but not limited to projects developed, planned, funded, or approved by individuals, private businesses, non-profit organizations, and local, State, and federal agencies such as USACE, U.S. Fish and Wildlife Service, National Oceanic and Atmospheric Administration Fisheries, U.S. Environmental Protection Agency, U.S. Bureau of Reclamation, State Water Resources Control Board, California Department of Water Resources, and California Department of Fish and Game, shall comply with all applicable requirements of this program, including conducting or participating in Control Studies and complying with allocations. To the extent allowable by their regulatory authority, Federal, State, and local agencies that fund, approve, or implement such new projects shall direct project applicants/grantees/loanees to apply to or consult with the Regional Water Board to ensure full compliance with the water quality requirements herein.

<u>Dredging and Dredge Material Reuse</u>
Dredging activities and activities that reuse dredge material in the Delta should minimize increases in methyl and total mercury discharges to Delta waterways (Appendix 43). The following requirements apply to dredging and excavating projects in the Delta and Yolo Bypass where a Clean Water Act 401 Water Quality Certification or other waste discharge requirements are required. The Clean Water Act 401 Water Quality Certifications shall include the following conditions:

1. Employ management practices during and after dredging activities to minimize sediment releases into the water column.

2. Ensure that under normal operational circumstances, including during wet weather, dredged and excavated material reused at upland sites, including the tops and dry-side of levees, is protected from erosion into open waters.

In addition to the above requirements, the following requirements apply to the California Department of Water Resources, U.S. Army Corps of Engineers, the Port of Sacramento, the Port of Stockton, and other State and federal agencies conducting dredging and excavating projects in the Delta and Yolo Bypass:

1. Characterize the total mercury mass and concentration of material removed from Delta waterways (Appendix 43) by dredging activities.

2. Conduct monitoring and studies to evaluate management practices to minimize methylmercury discharges from dredge return flows and dredge material reuse sites. Agencies shall:

   - By [two years from Effective Date] project proponents shall submit a study workplan(s) to evaluate methylmercury and mercury discharges from dredging and dredge material reuse, and to develop and evaluate management practices to minimize increases in methyl and total mercury discharges. The proponents may submit a comprehensive study workplan rather than conduct studies for individual projects. The comprehensive workplan may include exemptions for small projects. Upon Executive Officer approval, the plan shall be implemented.

   - By [seven years after the Effective Date], final reports that present the results and descriptions of mercury and methylmercury control management practices shall be submitted to the Regional Water Board.

   Studies should be designed to achieve the following aims for all dredging and dredge material reuse projects. When dredge material disposal sites are utilized to settle out solids and return waters are discharged into the adjacent surface water, methylmercury concentrations in return flows should be equal to or less than concentrations in the receiving water. When dredge material is reused at aquatic locations, such as wetland and riparian habitat restoration sites, the reuse should not add mercury-enriched sediment to the site or result in a net increase of methylmercury discharges from the reuse site.

The results of the management practices studies should be applied to future projects.

<u>Cache Creek Settling Basin Improvement Plan and Schedule</u>
Department of Water Resources, Central Valley Flood Protection Board, and USACE, in conjunction with any landowners and other interested stakeholders, shall implement a plan for management of mercury contaminated sediment that has entered and continues to enter the Cache Creek Settling Basin (Basin) from the upstream Cache Creek watershed. The agencies shall:

1. By [one year after Effective Date] the agencies shall take all necessary actions to initiate the process for Congressional authorization to modify the Basin, or other actions as appropriate, including coordinating with the USACE.

2. By [two years after the Effective Date], the agencies shall develop a strategy to reduce total mercury from the Basin for the next 20 years. The strategy shall include a description of, and schedule for, potential studies and control alternatives, and an evaluation of funding options. The agencies shall work with the landowners within the Basin and local communities affected by Basin improvements.

3. By [four years after the Effective Date], the agencies shall submit a report describing the long term environmental benefits and costs of sustaining the Basin's mercury trapping abilities indefinitely.

4. By [four years after the Effective Date], the agencies shall submit a report that evaluates the trapping efficiency of the Cache Creek Settling Basin and proposes, evaluates, and recommends potentially feasible alternative(s) for mercury reduction from the Basin. The report shall evaluate the feasibility of decreasing mercury loads from the basin, up to and including a 50% reduction from existing loads.

5. By [six years after Effective Date], the agencies shall submit a detailed plan for improvements to the Basin to decrease mercury loads from the Basin.

The agencies shall submit the strategy and planning documents described above to the Regional Water Board for approval by the Executive Officer. During Phase 1, the agencies should consider implementing actions to reduce mercury loads from the Basin. Beginning in Phase 2, the agencies shall implement a mercury reduction plan.

Tributary Watersheds

Table D identifies methylmercury allocations for tributary inputs to the Delta and Yolo Bypass.

The sum total of 20-year average total mercury loads from the tributary watersheds identified in Table D needs to be reduced by 110 kg/yr. Initial reduction efforts should focus on watersheds that contribute the most mercury-contaminated sediment to the Delta and Yolo Bypass, such as the Cache Creek, American River, Putah Creek, Cosumnes River, and Feather River watersheds.

Future mercury control programs will address the tributary watershed methylmercury allocations and total mercury load reductions assigned to tributary inputs to the Delta and Yolo Bypass. Additional methylmercury and total mercury load reductions may be required within those watersheds to address any mercury impairment within those watersheds.

Mercury control programs will be developed for tributary inputs to the Delta by the following dates:

2012: American River;
2016: Feather, Sacramento, San Joaquin, and Mokelumne Rivers, and Marsh and Putah Creeks; and
2017: Cosumnes River and Morrison Creek.

Mercury Offsets

The intent of an offset program is to optimize limited resources to maximize environmental benefits. The overall objectives for an offset program are to (1) provide more flexibility than the

current regulatory system provides to improve the environment while meeting regulatory requirements (i.e., load and wasteload allocations) at a lower overall cost and (2) promote watershed-based initiatives that encourage earlier and larger load reductions to the Delta than would otherwise occur.

On or before [nine years after Effective Date] the Regional Water Board will consider adoption of a mercury (inorganic and/or methyl) offsets program. During Phase 1, stakeholders may propose pilot offset projects for public review and Regional Water Board approval. The offsets program and any Phase 1 pilot offset projects shall be based on the following key principles:

- Offsets shall be consistent with existing USEPA and State Board policies and with the assumptions and requirements upon which this and other mercury control programs are established.
- Offsets should not include requirements that would leverage existing discharges as a means of forcing dischargers to bear more than their fair share of responsibility for causing or contributing to any violation of water quality standards. In this context "fair share" refers to the dischargers' proportional contribution of methylmercury load.
- Offset credits should only be available to fulfill a discharger's responsibility to meet its (waste) load allocation after reasonable load reduction and pollution prevention strategies have been implemented.
- Offsets should not be allowed in cases where local human or wildlife communities bear a disparate or disproportionate pollution burden as a result of the offset.
- Offset credits should be available upon generation and last long enough (i.e., not expire quickly) to encourage feasible projects.
- Creditable load reductions achieved should be real, quantifiable, verifiable, and enforceable by the Regional Water Board.

Alternatives to direct load credits may be developed.

Exposure Reduction Program

While methylmercury and mercury source reductions are occurring, the Regional Water Board recognizes that activities should be undertaken to protect those people who eat Delta fish by reducing their methylmercury exposure and its potential health risks. The Exposure Reduction Program (ERP) is not intended to replace timely reduction of mercury and methylmercury loads to Delta waters.

The Regional Water Board will investigate ways, consistent with its regulatory authority, to address public health impacts of mercury in Delta fish, including activities that reduce actual and potential exposure of and mitigate health impacts to those people and communities most likely to be affected by mercury in Delta caught fish, such as subsistence fishers and their families (*State Water Board Resolution No. 2005-0060*).

By [one year after Effective Date], Regional Water Board staff shall work with dischargers (either directly or through their representatives), State and local public health agencies (including California Department of Public Health, California Office of Health Hazard Assessment, and county public health and/or environmental health departments), and other stakeholders, including community-based organizations, tribes, and Delta fish consumers, to complete an Exposure Reduction Strategy. The purposes of the Strategy will be to recommend to the Executive Officer how dischargers will be responsible for participating in an ERP, to set

performance measures, and to propose a collaborative process for developing, funding and implementing the program. The Strategy shall take into account the proportional share of methylmercury contributed by individual dischargers. If dischargers (either directly or through their representatives) do not participate in the collaborative effort to develop the ERP, the Regional Water Board will evaluate and implement strategies, consistent with the Regional Water Board's regulatory authority, to assure participation from all dischargers or their representatives.

The objective of the Exposure Reduction Program is to reduce mercury exposure of Delta fish consumers most likely affected by mercury.

The Exposure Reduction Program must include elements directed toward:

- Developing and implementing community-driven activities to reduce mercury exposure;
- Raising awareness of fish contamination issues among people and communities most likely affected by mercury in Delta-caught fish such as subsistence fishers and their families;
- Integrating community-based organizations that serve Delta fish consumers, Delta fish consumers, tribes, and public health agencies in the design and implementation of an exposure reduction program;
- Identifying resources, as needed, for community-based organizations and tribes to participate in the Program;
- Utilizing and expanding upon existing programs and materials or activities in place to reduce mercury, and as needed, create new materials or activities; and
- Developing measures for program effectiveness.

The dischargers, either individually or collectively, or based on the Exposure Reduction Strategy, shall submit an exposure reduction workplan for Executive Officer approval by [two years after Effective Date]. The workplan shall address the Exposure Reduction Program objective, elements, and dischargers' coordination with other stakeholders. Dischargers shall integrate or, at a minimum, provide good-faith opportunities for integration of community-based organizations, tribes, and consumers of Delta fish into planning, decision making, and implementation of exposure reduction activities.

The dischargers shall implement the workplan by six months after Executive Officer approval of workplan. Every three years after workplan implementation begins, the dischargers, individually or collectively, shall provide a progress report to the Executive Officer. Dischargers shall participate in the Exposure Reduction Program until they comply with all requirements related to their individual or subarea methylmercury allocation.
The California Department of Public Health, the California Office of Environmental Health Hazard Assessment, and the local county public health and/or environmental health departments should collaborate with dischargers and community and tribal members to develop and implement exposure reduction programs and provide guidance to dischargers and others that are conducting such activities. The California Department of Public Health and/or other appropriate agency should seek funds to contribute to the Exposure Reduction Program and to continue it beyond 2030, if needed, until fish tissue objectives are attained.

The State Water Board should develop a statewide policy that defines the authority and provides guidance for exposure reduction programs, including guidance on addressing public health impacts of mercury, activities that reduce actual and potential exposure of, and mitigating health impacts to those people and communities most likely to be affected by mercury.

Exceptions for Low Threat Discharges

Discharges subject to a waiver of waste discharge requirements based on a finding that the discharges pose a low threat to water quality, except for discharges subject to water quality certifications, are exempt from the mercury requirements of this Delta Mercury Control Program.

Discharges subject to waste discharge requirements for dewatering and other low threat discharges to surface waters are exempt from the mercury requirements of this Delta Mercury Control Program.

Revise Chapter IV (Implementation), under "Recommended for Implementation by the State Water Board", to add:

Delta Mercury

1. The State Water Board should consider requiring methylmercury controls for new water management activities that have the potential to increase ambient methylmercury levels as a condition of approval of any water right action required to implement the project. The State Water Board Division of Water Rights should consider requiring the evaluation and implementation of feasible management practices to reduce or, at a minimum, prevent methylmercury ambient levels from increasing from those changes in water management activities and flood conveyance projects that have the potential to increase methylmercury levels. The State Water Board should consider funding or conducting studies to develop and evaluate management practices to reduce methylmercury production resulting from existing water management activities or flood conveyance projects.

2. During future reviews of the salinity objectives contained in the Bay-Delta Plan, the State Water Board Division of Water Rights should consider conducting studies to determine whether proposed changes to salinity objectives could affect methylmercury production and should consider the results of these studies in evaluating changes to the salinity objectives.

Revise Chapter IV (Implementation), under "Recommended for Implementation by Other Agencies", to add:

Delta Mercury

1. USEPA and the California Air Resources Board should work with the State Water Board and develop a memorandum of understanding to evaluate local and statewide mercury air emissions and deposition patterns and to develop a load reduction program(s).

2. The State of California should establish the means to fund a portion of the mercury control projects in the Delta and upstream watersheds.

3. Watershed stakeholders are encouraged to identify total mercury and methylmercury reduction projects and propose and conduct projects to reduce upstream non-point sources of methylmercury and total mercury. The Regional Water Board recommends that state and federal grant programs give priority to projects that reduce upstream non-point sources of methylmercury and total mercury.

4. Dischargers may evaluate imposed administrative civil liabilities projects for total mercury and methylmercury discharge and exposure reduction projects, consistent with Supplemental Environmental Project policies.

Revise Chapter IV (Implementation), under "Estimated Costs of Agricultural Water Quality Control Programs and Potential Sources of Financing", to add:

Delta Mercury Control Program

The total estimated costs (2007 dollars) for the agricultural methylmercury control studies to develop management practices to meet the Delta methylmercury allocations range from $290,000 to $1.4 million. The estimated annual costs for agricultural discharger compliance monitoring range from $14,000 to $25,000. The estimated annual costs for Phase 2 implementation of methylmercury management practices range from $590,000 to $1.3 million.

1. Potential funding sources include those identified in the San Joaquin River Subsurface Agricultural Drainage Control Program and the Pesticide Control Program.

Revise Chapter V (Surveillance and Monitoring), under "Mercury and Methylmercury", to add as follows:

Delta

Fish Methylmercury Compliance Monitoring

The Regional Water Board will use the following specifications to determine compliance with the methylmercury fish tissue objectives in the Sacramento-San Joaquin Delta. Beginning 2025, Regional Water Board staff will initiate fish tissue monitoring. Thereafter compliance monitoring will ensue every ten years, more frequently as needed where substantial changes in methyl or total mercury concentrations or loading occur, but not to exceed ten years elsewhere.

Initial fish tissue monitoring will take place at the following compliance reaches in each subarea:

- Central Delta subarea: Middle River between Bullfrog Landing and Mildred Island;
- Marsh Creek subarea: Marsh Creek from Highway 4 to Cypress Road;
- Mokelumne/Cosumnes River subarea: Mokelumne River from the Interstate 5 bridge to New Hope Landing;
- Sacramento River subarea: Sacramento River from River Mile 40 to River Mile 44;
- San Joaquin River subarea: San Joaquin River from Vernalis to the Highway 120 bridge;

- West Delta subarea: Sacramento/San Joaquin River confluence near Sherman Island;
- Yolo Bypass-North subarea: Tule Canal downstream of its confluence with Cache Creek; and
- Yolo Bypass-South subarea: Toe Drain between Lisbon and Little Holland Tract.

Compliance fish methylmercury monitoring will include representative fish species for comparison to each of the methylmercury fish tissue objectives:

- Trophic Level 4: bass (largemouth and striped), channel and white catfish, crappie, and Sacramento pikeminnow.
- Trophic Level 3: American shad, black bullhead, bluegill, carp, Chinook salmon, redear sunfish, Sacramento blackfish, Sacramento sucker, and white sturgeon.
- Small (<50 mm) fish: primary prey species consumed by wildlife in the Delta, which may include the species listed above, as well as inland silverside, juvenile bluegill, mosquitofish, red shiner, threadfin shad, or other fish less than 50 mm.

Trophic level 3 and 4 fish sample sets will include three species from each trophic level and will include both anadromous and non-anadromous fish. Trophic level 3 and 4 fish sample sets will include a range of fish sizes between 150 and 500 mm total length. Striped bass, largemouth bass, and sturgeon caught for mercury analysis will be within the CDFG legal catch size limits. Sample sets for fish less than 50 mm will include at least two fish species that are the primary prey species consumed by wildlife at sensitive life stages. In any subarea, if multiple species for a particular trophic level are not available, one species in the sample set is acceptable.

Water Methylmercury and Total Mercury Compliance Monitoring

Compliance points for irrigated agriculture and managed wetlands methylmercury allocations shall be developed during the Phase 1 Control Studies.

In conjunction with the Phase 1 Control Studies, nonpoint sources, irrigated agriculture, and managed wetlands shall develop and implement mercury and/or methylmercury monitoring, and submit monitoring reports.

NPDES facilities' compliance points for methylmercury and total mercury monitoring are the effluent monitoring points currently described in individual NPDES permits.

During Phase 1 and Phase 2, facilities listed in Table B shall conduct effluent total mercury and methylmercury monitoring starting by [one year after the Effective Date]. Monitoring frequencies shall be defined in the NPDES permits. Effluent monitoring requirements will be re-evaluated during the Delta Mercury Control Program Reviews.

Facilities that begin discharging to surface water during Phase 1 and facilities for which effluent methylmercury data were not available at the time Table B was compiled, shall conduct monitoring.

Compliance points and monitoring frequencies for MS4s required to conduct methylmercury and total mercury monitoring are those locations and wet and dry weather sampling periods currently described in the individual MS4 NPDES permits or otherwise determined to be

representative of the MS4 service areas and approved by the Executive Officer on an MS4-specific basis.

Annual methylmercury loads in urban runoff in MS4 service areas within the Delta and Yolo Bypass may be calculated by the following method or by an alternate method approved by the Executive Officer. The annual methylmercury load in urban runoff for a given MS4 service area during a given year may be calculated by the sum of wet weather and dry weather methylmercury loads. To estimate wet weather methylmercury loads discharged by MS4 urban areas, the average of wet weather methylmercury concentrations observed at the MS4's compliance locations may be multiplied by the wet weather runoff volume estimated for all urban areas within the MS4 service area within the Delta and Yolo Bypass. To estimate dry weather methylmercury loads, the average of dry weather methylmercury concentrations observed at the MS4's compliance locations may be multiplied by the estimated dry weather urban runoff volume in the MS4 service area within the Delta and Yolo Bypass.

ATTACHMENT 1
RESOLUTION NO. R5-2010-0043
DELTA MERCURY CONTROL PROGRAM

TABLE A
METHYLMERCURY LOAD AND WASTE LOAD ALLOCATIONS FOR EACH DELTA SUBAREA BY SOURCE CATEGORY

Source Type	DELTA SUBAREA													
	Central Delta		Marsh Creek		Mokelumne River		Sacramento River		San Joaquin River		West Delta		Yolo Bypass	
	Current Load (g/yr)	Allocation (g/yr)	Current Load (g/yr)	Allocation (g/yr)	Current Load (g/yr)	Allocation (g/yr)	Current Load (g/yr)	Allocation (g/yr)	Current Load (g/yr)	Allocation (g/yr)	Current Load (g/yr)	Allocation (g/yr)	Current Load (g/yr)	Allocation (g/yr)
Methylmercury Load Allocations														
Agricultural drainage [(d)]	37	37	2.2	0.40	1.6	0.57	36	20	23	8.3	4.1	4.1	19	4.1
Atmospheric wet deposition	7.3	7.3	0.23	0.23	0.29	0.29	5.6	5.6	2.7	2.7	2.4	2.4	4.2	4.2
Open water	370	370	0.18	0.032	4.0	1.4	140	78	48	17	190	190	100	22
Tributary Inputs [(a)]	37	37	1.9	0.34	110	39	2,034	1,129	367	133			462	100
Inputs from Upstream Subareas	(b)	(b)	- - -	- - -	- - -	- - -	- - -	- - -	- - -	- - -	(b)	(b)	- - -	- - -
Urban (nonpoint source)	0.14	0.14	---	---	0.018	0.018	0.62	0.62	0.0022	0.0022	0.066	0.066	---	---
Wetlands [(d)]	210	210	0.34	0.061	30	11	94	52	43	16	130	130	480	103
Methylmercury Waste Load Allocations														
NPDES facilities [(a)]	1.3	1.3	0.086	0.086	0	0	162	90	40	15	0.0019	0.0019	1.0	0.42
NPDES facilities future growth [(a)]	---	0.32 [(b)]	---	0.21	---	0	---	8.6	---	2.1	---	0.25 [(b)]	---	0.60
NPDES MS4 [(a)]	5.4	5.4	1.2	0.30	0.045	0.016	2.8	1.6	4.8	1.7	3.2	3.2	1.5	0.38
Total Loads [(c)] (g/yr)	**668**	**668**	**6.14**	**1.66**	**146**	**52.6**	**2,475**	**1,385**	**528**	**195**	**330**	**330**	**1,068**	**235**

Table A Footnotes:

(a) Values shown for Tributary Inputs, NPDES Facilities, NPDES Facilities Future Growth, and NPDES MS4 represent the sum of several individual discharges. See Tables B, C, and D for allocations for the individual discharges that should be used for compliance purposes.

(b) The Central Delta subarea receives flows from the Sacramento, Yolo Bypass, Mokelumne, and San Joaquin subareas. The West Delta subarea receives flows from the Central Delta and Marsh Creek subareas. These within-Delta flows have not yet been quantified because additional data are needed for loss rates across the subareas. Federal and state agencies whose activities affect methylmercury loss and production processes in the Delta and Yolo Bypass are assigned joint responsibility for the open water allocation. These subarea inflows are expected to decrease substantially (e.g., 40-80%) as upstream mercury management practices take place. As a result, reductions for sources within the Central and West subareas and tributaries that drain directly to these subareas are not required.

(c) For each Delta subarea, the allocations in Table A for agricultural drainage, atmospheric wet deposition, open water, urban (nonpoint source), and wetlands plus the individual allocations for tributary inputs (Table D), NPDES facilities and NPDES facilities future growth (Table B), and NPDES MS4 (Table C) within that subarea equal the Delta subarea's TMDL (assimilative capacity).

(d) The load allocations apply to the net methylmercury loads, where the net loads equal the methylmercury load in outflow minus the methylmercury loads in source water (e.g., irrigation water and precipitation).

TABLE B
MUNICIPAL AND INDUSTRIAL WASTEWATER METHYLMERCURY (MeHg) ALLOCATIONS

PERMITTEE [a]	NPDES Permit No.	MeHg Waste Load Allocation [b] (g/yr)
Central Delta		
Discovery Bay WWTP	CA0078590	0.37
Lincoln Center Groundwater Treatment Facility	CA008255	0.018
Lodi White Slough WWTP	CA0079243	0.94
Metropolitan Stevedore Company	CA0084174	[c]
Unassigned allocation for NPDES facility discharges	[d]	0.31
Marsh Creek		
Brentwood WWTP	CA0082660	0.14
Unassigned allocation for NPDES facility discharges	[d]	0.16
Sacramento River		
Rio Vista Northwest WWTP	CA0083771	0.069
Rio Vista WWTP	CA0079588	0.056
Sacramento Combined WWTP	CA0079111	0.53
SRCSD Sacramento River WWTP	CA0077682	89
Unassigned allocation for NPDES facility discharges	[d]	8.5
San Joaquin River		
Deuel Vocational Inst. WWTP	CA0078093	0.021
Manteca WWTP	CA0081558	0.38
Mountain House Community Services District WWTP	CA0084271	0.37
Oakwood Lake Subdivision Mining Reclamation [f]	CA0082783	0.38 [f]
Stockton WWTP	CA0079138	13
Tracy WWTP	CA0079154	0.77
Unassigned allocation for NPDES facility discharges	[d]	1.7
West Delta		
GWF Power Systems [e]	CA0082309	0.0052
Mirant Delta LLC Contra Costa Power Plant	CA0004863	[e]
Ironhouse Sanitation District	CA0085260	0.030
Unassigned allocation for NPDES facility discharges	[d]	0.22
Yolo Bypass		
Davis WWTP [g]	CA0079049	0.17 [g]
Woodland WWTP	CA0077950	0.43
Unassigned allocation for NPDES facility discharges	[d]	0.42

Table B Footnotes:

(a) If NPDES facilities that have allocations in Table B regionalize or consolidate, their waste load allocations can be summed.

(b) Methylmercury waste load allocations apply to annual (calendar year) discharge methylmercury loads.

(c) A methylmercury waste load allocation for non-storm water discharges from the Metropolitan Stevedore Company (CA0084174) shall be established in its NPDES permit once it completes three sampling events for methylmercury in its discharges. Its waste load allocation is a component of the "Unassigned Allocation" for the Central Delta subarea.

(d) Table B contains unassigned waste load allocations for new discharges to surface water that begin after [the effective date of this amendment]. New discharges that may be allotted a portion of the unassigned allocation may come from (1) existing facilities that previously discharged to land and then began to discharge to surface water or diverted discharges to another facility that discharges to surface water as part of ongoing regionalization efforts; (2) newly built facilities that have not previously discharged to land or water; and (3) expansions to existing facilities beyond their allocations listed in Table B where the additional allocation does not exceed the product of the net increase in flow volume and 0.06 ng/l methylmercury. The sum of all new and/or expanded methylmercury discharges from NPDES facilities within each Delta subarea shall not exceed the Delta subarea-specific waste load allocation listed in Table B.

(e) Methylmercury loads and concentrations in heating/cooling and power facility discharges vary with intake water conditions. To determine compliance with the allocations, dischargers that that use ambient surface water for cooling water shall conduct concurrent monitoring of the intake water and effluent. The methylmercury allocations for such heating/cooling and power facility discharges are 100%, such that the allocations shall become the detected methylmercury concentration found in the intake water. GWF Power Systems (CA0082309) acquires its intake water from sources other than ambient surface water and therefore has a methylmercury allocation based on its effluent methylmercury load.

(f) The waste load allocation for the Oakwood Lake Subdivision Mining Reclamation (CA0082783) shall be assessed as a five-year average annual methylmercury load.

(g) The City of Davis WWTP (CA0079049) has two discharge locations; wastewater is discharged from Discharge 001 to the Willow Slough Bypass upstream of the Yolo Bypass and from Discharge 002 to the Conaway Ranch Toe Drain in the Yolo Bypass. The methylmercury load allocation listed in Table B applies only to Discharge 002, which discharges seasonally from about February to June. Discharge 001 is encompassed by the Willow Slough watershed methylmercury allocation listed in Table G.

TABLE C
MS4 METHYLMERCURY (MeHg) WASTE LOAD ALLOCATIONS FOR URBAN RUNOFF WITHIN EACH DELTA SUBAREA

Permittee	NPDES Permit No.	MeHg Waste Load Allocation [a, b] (g/yr)
Central Delta		
Contra Costa (County of) [c]	CAS083313	0.75
Lodi (City of)	CAS000004	0.053
Port of Stockton MS4	CAS084077	0.39
San Joaquin (County of)	CAS000004	0.57
Stockton Area MS4	CAS083470	3.6
Marsh Creek		
Contra Costa (County of) [c]	CAS083313	0.30
Mokelumne River		
San Joaquin (County of)	CAS000004	0.016
Sacramento River		
Rio Vista (City of)	CAS000004	0.0078
Sacramento Area MS4	CAS082597	1.0
San Joaquin (County of)	CAS000004	0.11
Solano (County of)	CAS000004	0.041
West Sacramento (City of)	CAS000004	0.36
Yolo (County of)	CAS000004	0.041
San Joaquin River		
Lathrop (City of)	CAS000004	0.097
Port of Stockton MS4	CAS084077	0.0036
San Joaquin (County of)	CAS000004	0.79
Stockton Area MS4	CAS083470	0.18
Tracy (City of)	CAS000004	0.65
West Delta		
Contra Costa (County of) [c]	CAS083313	3.2
Yolo Bypass		
Solano (County of)	CAS000004	0.021
West Sacramento (City of)	CAS000004	0.28
Yolo (County of)	CAS000004	0.083

Table C Footnotes:

(a) Some MS4s service areas span multiple Delta subareas and are therefore listed more than once. The allocated methylmercury loads for all MS4s are based on the average methylmercury concentrations observed in runoff from urban areas in or near the Delta during water years 2000 through 2003, a relatively dry period. Annual loads are expected to fluctuate with water volume and other factors. As a result, attainment of these allocations shall be assessed as a five-year average annual load. Allocations may be revised during review of the Delta Mercury Control Program to include available wet year data.

(b) The methylmercury waste load allocations include all current and future permitted urban discharges not otherwise addressed by another allocation within the geographic boundaries of urban runoff management agencies within the Delta and Yolo Bypass, including but not limited to Caltrans facilities and rights-of-way (NPDES No. CAS000003), public facilities, properties proximate to banks of waterways, industrial facilities, and construction sites.

(c) The Contra Costa County MS4 discharges to both the Delta and San Francisco Bay. The above allocations apply only to the portions of the MS4 service area that discharge to the Delta within the Central Valley Water Quality Control Board's jurisdiction.

TABLE D
TRIBUTARY WATERSHED
METHYLMERCURY (MeHg) ALLOCATIONS

Tributary	MeHg Load Allocation [a] (g/yr)
Central Delta	
Bear Creek @ West Lane / Mosher Creek @ Morada Lane (sum of watershed loads)	11
Calaveras River @ railroad tracks u/s West Lane	26
Marsh Creek	
Marsh Creek @ Highway 4	0.34
Mokelumne River	
Mokelumne River @ Interstate 5	39.3 (39) [b]
Sacramento River	
Morrison Creek @ Franklin Boulevard	4.2
Sacramento River @ Freeport	1,125 (1,100) [b]
San Joaquin River	
French Camp Slough downstream of Airport Way	4.0
San Joaquin River @ Vernalis	129 (130)[b]
Yolo Bypass	
Cache Creek	30 [c]
Dixon Area	0.77
Fremont Weir	39
Knights Landing Ridge Cut	22
Putah Creek @ Mace Boulevard	2.4
Ulatis Creek near Main Prairie Road	2.1
Willow Slough	3.9

Table D Footnotes:

(a) Methylmercury allocations are assigned to tributary inputs to the Delta and Yolo Bypass. Mercury control programs designed to achieve the allocations for tributaries listed in Table D will be implemented by future Basin Plan amendments. Methylmercury load allocations are based on water years 2000 through 2003, a relative dry period. Annual loads are expected to fluctuate with water volume and other factors. As a result, attainment of these allocations shall be assessed as a five-year average annual load. Allocations will be revised during review of the Delta Mercury Control Program to include available wet year data.

(b) Tributary load allocations rounded to two significant figures for compliance evaluation.

(c) The allocation for water from Cache Creek entering the Yolo Bypass in this table is designed to achieve fish tissue objectives in the Yolo Bypass and Delta established by the Delta Mercury Control Program. The allocation in Table IV-6.1 assigned by the Cache Creek Mercury Control Program applies to the Cache Creek Settling Basin and requires a greater reduction so that fish within the Settling Basin can achieve water quality objectives for methylmercury in fish tissue that apply to Cache Creek, including the Settling Basin.

Add New Appendix 43 to the Basin Plan as follows:

APPENDIX 43

Delta and Yolo Bypass Waterways Applicable to the Delta Mercury Control Program

Table A43-1 lists the Sacramento-San Joaquin Delta waterways and the Yolo Bypass waterways within the Delta and north of the legal Delta boundary to which the COMM beneficial use, site-specific methylmercury fish tissue objectives, Delta mercury control implementation program, and monitoring provisions apply. The list contains distinct, readily identifiable water bodies within the boundaries of the "Legal" Delta (as defined in California Water Code section 12220) that are hydrologically connected by surface water flows (not including pumping) to the Sacramento and/or San Joaquin rivers. The list also includes Knights Landing Ridge Cut, Putah Creek, and Tule Canal in the Yolo Bypass north of the legal Delta boundary. Figures A43-1, A43-2, and A43-3 show the locations of these waterways.

The methylmercury allocations set forth in the Delta methylmercury control program are specific to Delta subareas, which are shown on Figure A43-4. Table A43-2 lists the waterways within each of the subareas.

TABLE A43-1: DELTA AND YOLO BYPASS WATERWAYS

Map Label #	Waterway Name	Map Label #	Waterway Name
1.	Alamo Creek	48.	Grizzly Slough
2.	Babel Slough	49.	Haas Slough
3.	Barker Slough	50.	Hastings Cut
4.	Bear Creek	51.	Hog Slough
5.	Bear Slough	52.	Holland Cut
6.	Beaver Slough	53.	Honker Cut
7.	Big Break	54.	Horseshoe Bend
8.	Bishop Cut	55.	Indian Slough
9.	Black Slough	56.	Italian Slough
10.	Broad Slough	57.	Jackson Slough
11.	Brushy Creek	58.	Kellogg Creek
12.	Burns Cutoff	59.	Latham Slough
13.	Cabin Slough	60.	Liberty Cut
14.	Cache Slough	61.	Lindsey Slough
15.	Calaveras River	62.	Little Connection Slough
16.	Calhoun Cut	63.	Little Franks Tract
17.	Clifton Court Forebay	64.	Little Mandeville Cut
18.	Columbia Cut	65.	Little Potato Slough
19.	Connection Slough	66.	Little Venice Island
20.	Cosumnes River	67.	Livermore Yacht Club
21.	Crocker Cut	68.	Lookout Slough
22.	Dead Dog Slough	69.	Lost Slough
23.	Dead Horse Cut	70.	Main Canal (Duck Slough tributary)
24.	Deer Creek (Tributary to Marsh Creek)	71.	Main Canal (Italian Slough tributary)
25.	Delta Cross Channel	72.	Marsh Creek
26.	Disappointment Slough	73.	Mayberry Cut
27.	Discovery Bay	74.	Mayberry Slough
28.	Donlon Island	75.	Middle River
29.	Doughty Cut	76.	Mildred Island
30.	Dry Creek (Marsh Creek tributary)	77.	Miner Slough
31.	Dry Creek (Mokelumne River tributary)	78.	Mokelumne River
32.	Duck Slough	79.	Mormon Slough
33.	Dutch Slough	80.	Morrison Creek
34.	Elk Slough	81.	Mosher Slough
35.	Elkhorn Slough	82.	Mountain House Creek
36.	Emerson Slough	83.	North Canal
37.	Empire Cut	84.	North Fork Mokelumne River
38.	Fabian and Bell Canal	85.	North Victoria Canal
39.	False River	86.	Old River
40.	Fisherman's Cut	87.	Paradise Cut
41.	Fivemile Creek	88.	Piper Slough
42.	Fivemile Slough	89.	Pixley Slough
43.	Fourteenmile Slough	90.	Potato Slough
44.	Franks Tract	91.	Prospect Slough
45.	French Camp Slough	92.	Red Bridge Slough
46.	Georgiana Slough	93.	Rhode Island
47.	Grant Line Canal	94.	Rock Slough

TABLE A43-1: DELTA AND YOLO BYPASS WATERWAYS, *Continued*

Map Label # / Waterway Name	Map Label # / Waterway Name
95. Sacramento Deep Water Channel	124. Toe Drain
96. Sacramento River	125. Tom Paine Slough
97. Salmon Slough	126. Tomato Slough
98. San Joaquin River	127. Trapper Slough
99. Sand Creek	128. Turner Cut
100. Sand Mound Slough	129. Ulatis Creek
101. Santa Fe Cut	130. Upland Canal (Sycamore Slough tributary)
102. Sevenmile Slough	
103. Shag Slough	131. Victoria Canal
104. Sheep Slough	132. Walker Slough
105. Sherman Lake	133. Walthall Slough
106. Short Slough	134. Washington Cut
107. Smith Canal	135. Werner Dredger Cut
108. Snodgrass Slough	136. West Canal
109. South Fork Mokelumne River	137. Whiskey Slough
110. Steamboat Slough	138. White Slough
111. Stockton Deep Water Channel	139. Winchester Lake
112. Stone Lakes	140. Woodward Canal
113. Sugar Cut	141. Wright Cut
114. Sutter Slough	142. Yosemite Lake
115. Sweany Creek	143. Yolo Bypass
116. Sycamore Slough	144. Deuel Drain
117. Taylor Slough (Elkhorn Slough tributary)	145. Dredger Cut
	146. Highline Canal
118. Taylor Slough (near Franks Tract)	147. Cache Creek Settling Basin Outflow
119. Telephone Cut	
120. The Big Ditch	148. Knights Landing Ridge Cut
121. The Meadows Slough	149. Putah Creek
122. Three River Reach	150. Tule Canal
123. Threemile Slough	

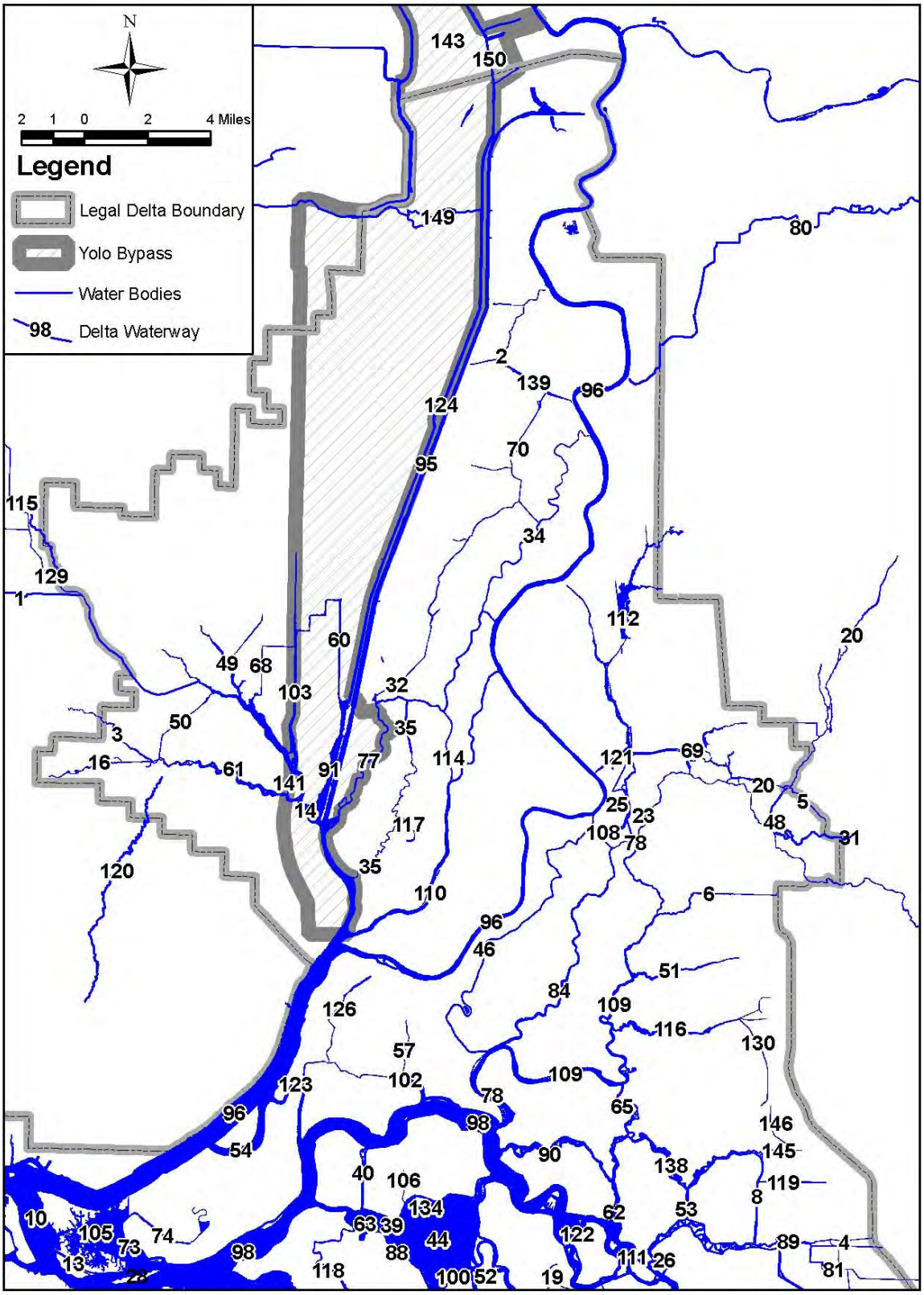

Figure A43-1: Delta Waterways (Northern Panel)

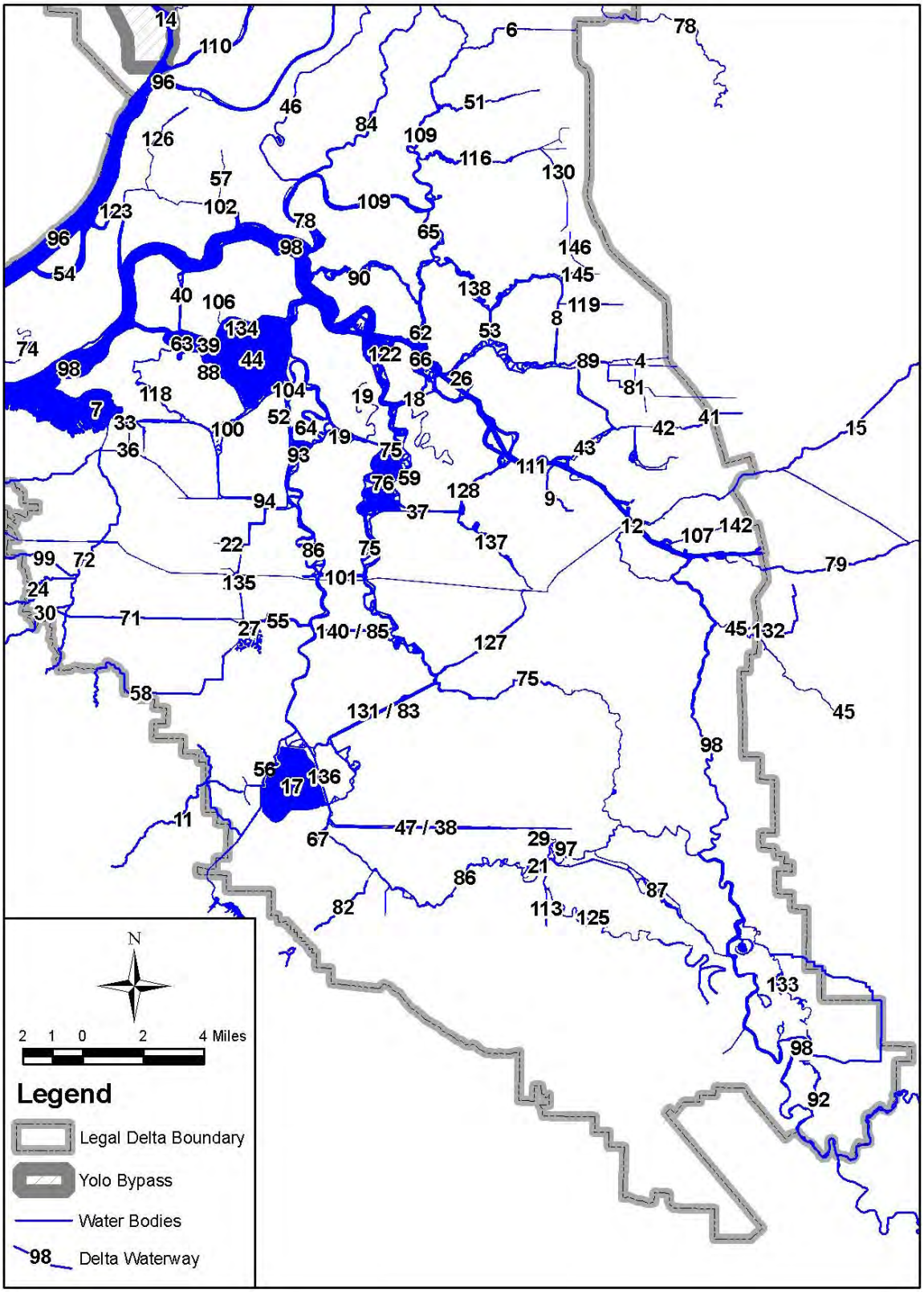

Figure A43-2: Delta Waterways (Southern Panel)

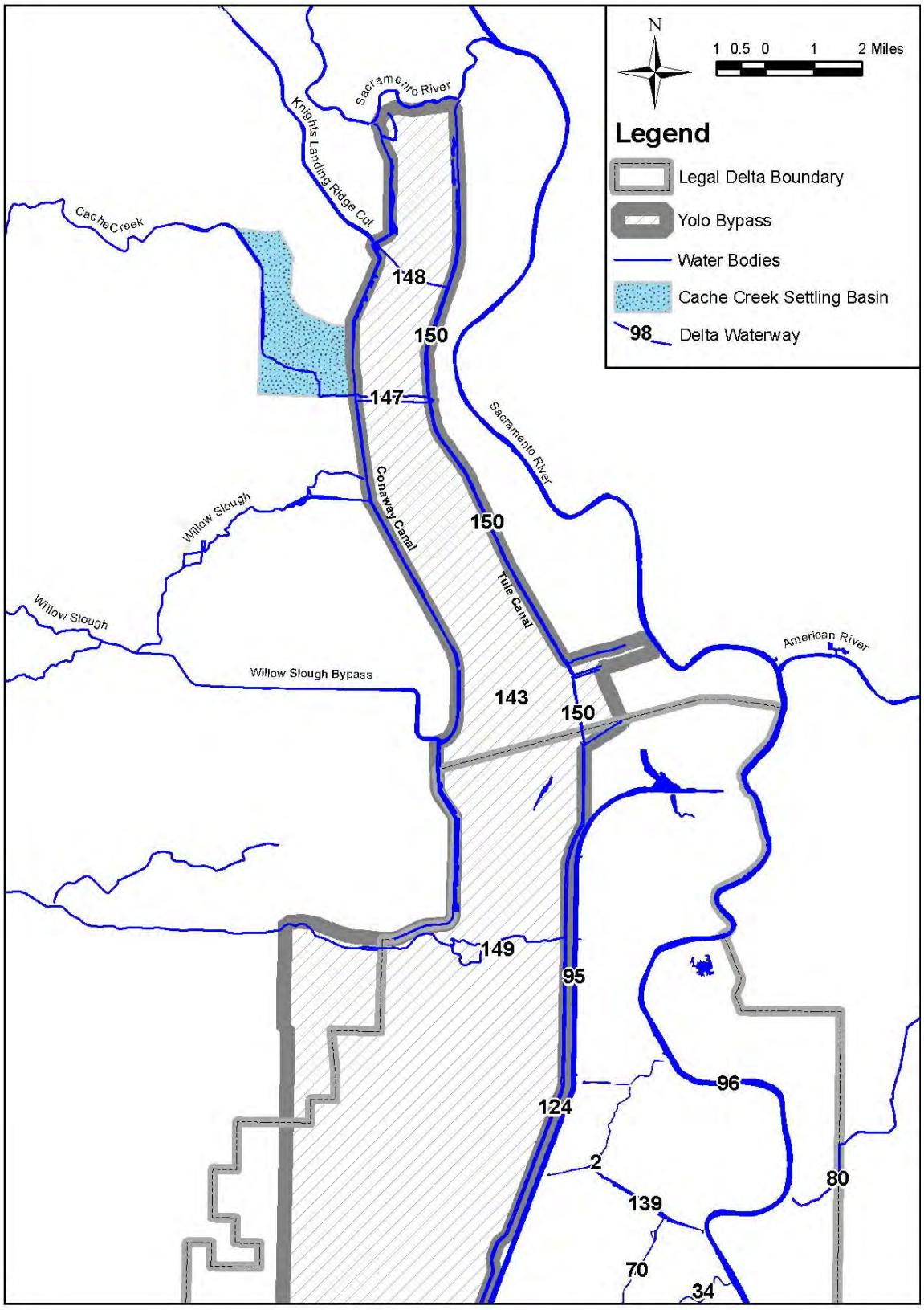

Figure A43-3: Northern Yolo Bypass

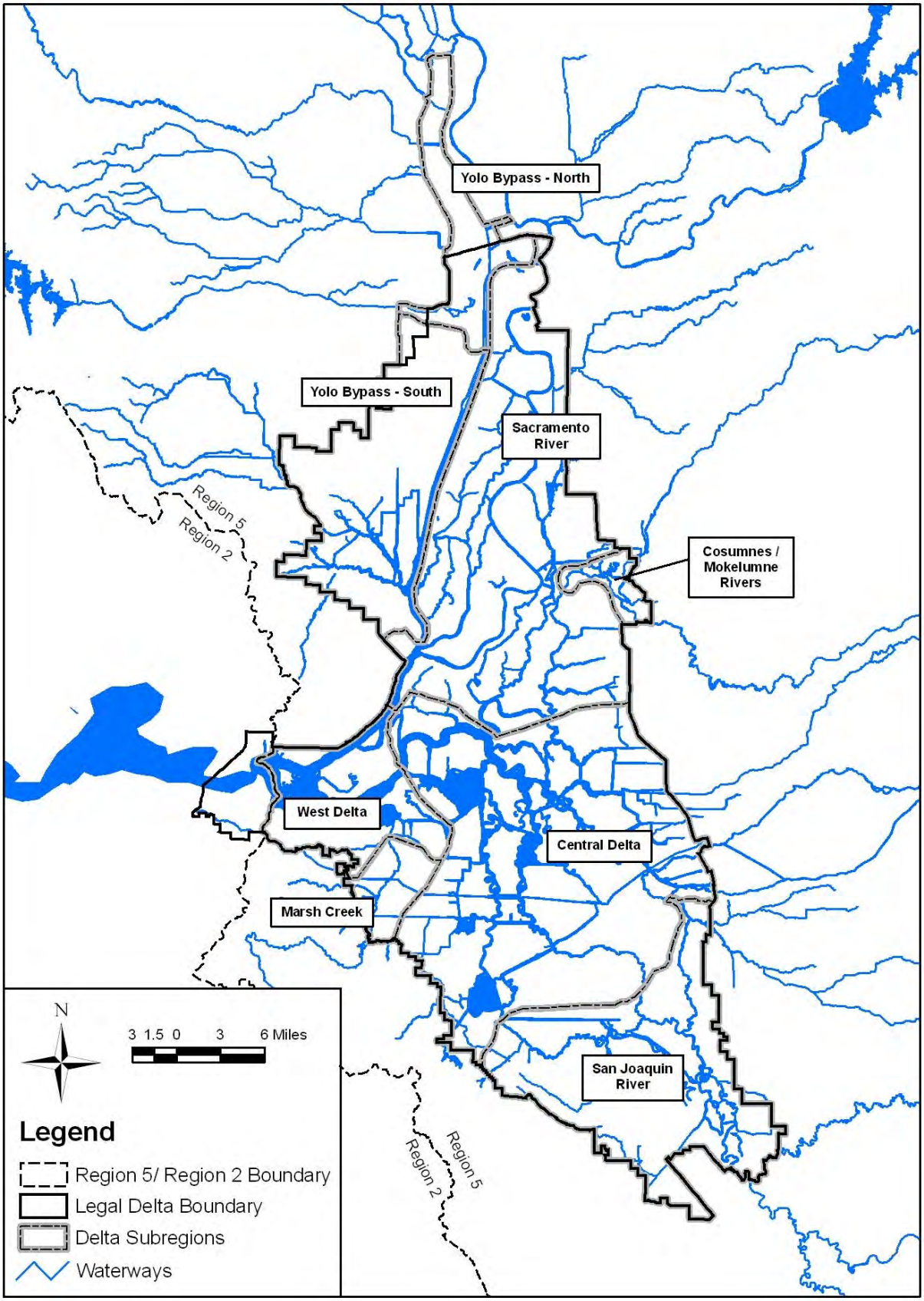

Figure A43-4: Subareas for the Delta Methylmercury Control Program

TABLE A43-2: DELTA AND YOLO BYPASS WATERWAYS BY METHYLMERCURY ALLOCATION SUBAREA

Waterway Name [Map Label #]	Waterway Name [Map Label #]	Waterway Name [Map Label #]
CENTRAL DELTA		
Bear Creek [4]	Indian Slough [55]	San Joaquin River [98]
Bishop Cut [8]	Italian Slough [56]	Sand Mound Slough [100]
Black Slough [9]	Jackson Slough [57]	Santa Fe Cut [101]
Brushy Creek [11]	Kellogg Creek [58]	Sevenmile Slough [102]
Burns Cutoff [12]	Latham Slough [59]	Sheep Slough [104]
Calaveras River [15]	Little Connection Slough [62]	Short Slough [106]
Clifton Court Forebay [17]	Little Franks Tract [63]	Smith Canal [107]
Columbia Cut [18]	Little Mandeville Cut [64]	Stockton Deep Water Channel [111]
Connection Slough [19]	Little Potato Slough [65]	Taylor Slough [nr Franks Tract] [118]
Dead Dog Slough [22]	Little Venice Island [66]	Telephone Cut [119]
Disappointment Slough [26]	Livermore Yacht Club [67]	Three River Reach [122]
Discovery Bay [27]	Main Canal [Indian Slough trib.] [71]	Threemile Slough [123]
Dredger Cut [145]	Middle River [75]	Tomato Slough [126]
Empire Cut [37]	Mildred Island [76]	Trapper Slough [127]
Fabian and Bell Canal [39]	Mokelumne River [78]	Turner Cut [128]
False River [39]	Mormon Slough [79]	Upland Canal [Sycamore Slough tributary] [130]
Fisherman's Cut [40]	Mosher Slough [81]	
Fivemile Creek [41]	North Canal [83]	Victoria Canal [131]
Fivemile Slough [42]	North Victoria Canal [85]	Washington Cut [134]
Fourteenmile Slough [43]	Old River [86]	Werner Dredger Cut [135]
Franks Tract [44]	Piper Slough [88]	West Canal [136]
Grant Line Canal [47]	Pixley Slough [89]	Whiskey Slough [137]
Highline Canal [146]	Potato Slough [90]	White Slough [138]
Holland Cut [52]	Rhode Island [93]	Woodward Canal [140]
Honker Cut [53]	Rock Slough [94]	Yosemite Lake [142]
MOKELUMNE/COSUMNES RIVERS		
Bear Slough [5]	Dry Creek [Mokelumne R. trib.] [31]	Lost Slough [69]
Cosumnes River [20]	Grizzly Slough [48]	Mokelumne River [78]
MARSH CREEK		
Deer Creek [24]	Main Canal [Indian Slough trib.] [71]	Rock Slough [94]
Dry Creek [Marsh Creek trib.] [30]	Marsh Creek [72]	Sand Creek [99]
Kellogg Creek [58]		
SACRAMENTO RIVER		
Babel Slough [2]	Little Potato Slough [65]	Stone Lakes [112]
Beaver Slough [6]	Lost Slough [69]	Sutter Slough [114]
Cache Slough [14]	Main Canal [Duck Slough trib.] [70]	Sycamore Slough [116]
Dead Horse Cut [23]	Miner Slough [77]	Taylor Slough [Elkhorn Slough tributary] [117]
Delta Cross Channel [25]	Mokelumne River [78]	
Duck Slough [32]	Morrison Creek [80]	The Meadows Slough [121]
Elk Slough [34]	North Mokelumne River [84]	Tomato Slough [126]
Elkhorn Slough [35]	Sacramento River [96]	Upland Canal [Sycamore Slough tributary] [130]
Georgiana Slough [46]	Snodgrass Slough [108]	
Hog Slough [51]	South Mokelumne River [109]	Winchester Lake [139]
Jackson Slough [57]	Steamboat Slough [110]	

TABLE A43-2: DELTA AND YOLO BYPASS WATERWAYS BY METHYLMERCURY ALLOCATION SUBAREA, *Continued*

Waterway Name [Map Label #]	Waterway Name [Map Label #]	Waterway Name [Map Label #]
SAN JOAQUIN RIVER		
Crocker Cut [21]	Middle River [75]	San Joaquin River [98]
Deuel Drain [144]	Mountain House Creek [82]	Sugar Cut [113]
Doughty Cut [29]	Old River [86]	Tom Paine Slough [125]
Fabian and Bell Canal [38]	Paradise Cut [87]	Walker Slough [132]
French Camp Slough [45]	Red Bridge Slough [92]	Walthall Slough [133]
Grant Line Canal [47]	Salmon Slough [97]	
WEST DELTA		
Big Break [7]	Horseshoe Bend [54]	San Joaquin River [98]
Broad Slough [10]	Marsh Creek [72]	Sand Mound Slough [100]
Cabin Slough [13]	Mayberry Cut [73]	Sherman Lake [105]
Donlon Island [28]	Mayberry Slough [74]	Taylor Slough [near Franks Tract] [118]
Dutch Slough [33]	Rock Slough [94]	Threemile Slough [123]
Emerson Slough [36]	Sacramento River [96]	
False River [39]		
YOLO BYPASS-NORTH [(a)]		
Cache Creek Settling Basin Outflow [147]	Toe Drain [124]/Tule Canal [150] Putah Creek [149)]	Sacramento Deep Water Ship Channel [95]
Knights Landing Ridge Cut [148]		
YOLO BYPASS-SOUTH [(a)]		
Alamo Creek [1]	Liberty Cut [60]	Sweany Creek [115]
Babel Slough [2]	Lindsey Slough [61]	Sycamore Slough [116]
Barker Slough [3]	Lookout Slough [68]	The Big Ditch [120]
Cache Slough [14]	Miner Slough [77]	Toe Drain [124]
Calhoun Cut [16]	Prospect Slough [91)]	Ulatis Creek [129]
Duck Slough [32]	Sacramento Deep Water Ship Channel [95]	Wright Cut [141]
Haas Slough [49]		
Hastings Cut [50]	Shag Slough [103]	

(a) Both the "Yolo Bypass-North" and "Yolo Bypass-South" subareas contain portions of the Yolo Bypass flood conveyance channel shown in Figure IV-4. When flooded, the entire Yolo Bypass is a Delta waterway. When the Yolo Bypass is not flooded, the Toe Drain [127] (referred to as Tule Canal [C] for its northern reach), Cache Creek Settling Basin Outflow [A], and Knights Landing Ridge Cut [B] are the only waterways within the Yolo Bypass hydrologically connected to the Sacramento River.

SAN FRANCISCO ESTUARY & WATERSHED SCIENCE
Sponsored by the Delta Science Program and the UC Davis John Muir Institute of the Environment

Peer Reviewed

Title:
Levee Decisions and Sustainability for the Sacramento-San Joaquin Delta

Journal Issue:
San Francisco Estuary and Watershed Science, 8(2)

Author:
Suddeth, Robyn J, University of California, Davis
Mount, Jeff, University of California, Davis
Lund, Jay R, University of California - Davis

Publication Date:
2010

Publication Info:
San Francisco Estuary and Watershed Science, John Muir Institute of the Environment, UC Davis

Permalink:
http://escholarship.org/uc/item/9wr5j84g

Keywords:
levee, decision analysis, reliability, policy, Delta

Abstract:
California's Sacramento-San Joaquin Delta has fragile levees subject to several trends that make them increasingly prone to failure. To assess the likely extent of Delta island flooding, this study presents an economic decision analysis approach for evaluating Delta levee upgrade and repair decisions for 34 major subsided agricultural islands that make up most of the Delta's Primary Zone and include all subsided, non-urban islands. The decision analysis provides a quantitative framework to address several relevant questions about reasonable levee upgrade and repair investments. This initial analysis indicates that it is economically optimal not to upgrade levees on any of the 34 subsided Delta islands examined, mostly because levee upgrades are expensive and do not improve reliability much. If upgrades can improve reliability more, it becomes optimal to upgrade some levees. Our analysis also suggests that, accounting for land and asset values, it is not cost effective to repair between 18 and 23 of these islands when they fail. When property values for all islands were doubled, only four islands originally not repaired become cost effective to repair. The decision analysis provides a quantitative framework for addressing several relevant questions regarding reasonable levee upgrade and repair investments. These initial results may act as a springboard for discussion, and the decision analysis model as a working framework for islands of high priority. An inescapable conclusion of this analysis is that maintaining the current Delta landscape is unlikely to be economical from business and land use perspectives.

AUGUST 2010

SAN FRANCISCO ESTUARY & WATERSHED SCIENCE
Sponsored by the Delta Science Program and the UC Davis John Muir Institute of the Environment

Levee Decisions and Sustainability for the Sacramento-San Joaquin Delta

Robyn Suddeth[1], Jeffrey Mount, and Jay Lund
Center for Watershed Sciences, University of California, Davis
One Shields Avenue, Davis, CA 95616

ABSTRACT

California's Sacramento-San Joaquin Delta has fragile levees subject to several trends that make them increasingly prone to failure. To assess the likely extent of Delta island flooding, this study presents an economic decision analysis approach for evaluating Delta levee upgrade and repair decisions for 34 major subsided agricultural islands that make up most of the Delta's Primary Zone and include all subsided, non-urban islands. The decision analysis provides a quantitative framework to address several relevant questions about reasonable levee upgrade and repair investments. This initial analysis indicates that it is economically optimal not to upgrade levees on any of the 34 subsided Delta islands examined, mostly because levee upgrades are expensive and do not improve reliability much. If upgrades can improve reliability more, it becomes optimal to upgrade some levees. Our analysis also suggests that, accounting for land and asset values, it is not cost effective to repair between 18 and 23 of these islands when they fail. When property values for all islands were doubled, only four islands originally not repaired become cost-effective to repair. The decision analysis provides a quantitative framework for addressing several relevant questions regarding reasonable levee upgrade and repair investments. These initial results may act as a springboard for discussion, and the decision analysis model as a working framework for islands of high priority. An inescapable conclusion of this analysis is that maintaining the current Delta landscape is unlikely to be economical from business and land use perspectives.

KEYWORDS

Levee, decision analysis, reliability, policy, Delta

INTRODUCTION: THE DELTA'S LEVEE SYSTEM

California's Sacramento-San Joaquin Delta is currently defined by its 1,770 km (1,100 miles) of levees. The Delta levee network was developed during the late 19th and early 20th centuries to reclaim more than 450,000 acres of freshwater and brackish marsh, mainly for agriculture. By the mid- and late-20th century, these levees became integral to local, state, and federal efforts to export water for urban and agricultural use. Four drivers are increasing probabilities of levee failure and island flooding: sea level rise, subsidence, changing inflows, and earthquakes (Mount and Twiss 2005; URS Corporation and J. R. Benjamin & Associates 2009; Cayan 2008a, 2008b; Church and White 2006; Deverel 2007; IPCC 2007; Stewart and others 2005). Physically and financially, the Delta cannot easily withstand these increasing pressures (Lund and others 2007, 2008, 2010).

1 Corresponding author: robynsuddeth@gmail.com

Deltas around the world are having similar problems (Syvitski and others 2009).

Physically, the Delta's levee network is rigid and brittle. Most levees were poorly constructed on weak, seismically unstable foundations. They are the descendents of originally small, private structures that have been expanded to cope with gradual land subsidence, sea level rise, and erosion. This expansion, accomplished by adding material to the top and sides, was, until recently, not subject to modern engineering standards.

Delta levees can fail in several ways (Linsley and others 1964; Wood 1977; Mount and Twiss 2005; Moss and Eller 2007). Most commonly, levees fail from slumping, rupturing, erosion or overtopping during storm events, or when high winds create large waves at high tides. Levees also may fail on a relatively calm day from internal degradation that has occurred over time with seepage, or from slumping and cracking that allows water to flow through and over the levee. Seepage is common in most levees and usually does not lead to failure, but when water pressure gradients are great, seepage can erode material within and under the levee, causing sand boils on the levee interior that eventually lead to collapse. Poor foundations, weak construction materials, and rodents all exacerbate these problems. Finally, a levee can fail during earthquakes. Shaking causes the foundation or embankments to lose cohesion, deform, and collapse. With continued levee degradation and increasing external forces, these failure pressures are all likely to become worse and more frequent (Mount and Twiss 2005). Without intervention, it seems likely that levee failures will increase in the future.

The levees are under growing financial pressure as well, often competing with other public interests in the Delta and elsewhere for funds, amidst great concern for the region's declining ecosystem and native species. The fragile levee system depends largely on the willingness of landowners and state and federal governments to invest in upgrading the levees or repairing them when they fail. With 166 levee failures over the past 100 years, that willingness to pay has kept all but three major islands intact. However, the roughly $90 million cost of the 2004 Jones Tract failure highlighted the high costs of levee failures and caused some state planners to question the economic viability of funding repairs and upgrades, especially when this money might be applied towards other public benefits or focused on prioritized islands (L. Harder, Senate Hearing, May 2006)

Acting together, these physical and financial drivers or constraints are likely to shift the Delta from its current configuration of narrow channels and subsided islands toward a system with several additional bodies of open water. In this analysis, we first present current estimates of failure probabilities for Delta levees, based principally on the recently released Delta Risk Management Strategy (DRMS) Phase 1 report (URS Corporation and J. R. Benjamin & Associates 2009), and identify resource allocation decisions the State currently faces. We evaluate the economic costs of maintaining the current levee configuration in the Delta and present a simplified, yet thoughtful, decision analysis to economically optimize levee repair and upgrades for individual islands. Our conclusions about upgrade and repair policies in the Delta extend those found in earlier studies (Logan 1989). Decision analysis is broadly used as a tool for public policy makers, both as a way to understand, organize, and quantify a problem, and as a way to compare the costs and benefits of various strategies. Decision analysis is valuable because it forces the decision maker to articulate how various parameters interact with each other, and identify a realistic and holistic set of alternatives (Hobbs and others 1997; Cheng and others 2008; Lund 2009).

Failure Probabilities: Certain Future, Uncertain Timing

Delta levees are a certain to fail. For more than 100 years, federal and state governments and Delta landowners have adapted to this reality. If the past were a reliable predictor of the future, the state could simply maintain the current Delta policy of supporting levee maintenance and repairs, fighting floods, and repairing islands when their levees fail. However, conditions are not static in the Delta, and risks and costs are increasing.

Using data from the DRMS Phase 1 report (URS

Corporation and J. R. Benjamin & Associates 2009), we calculated the annual probability of island levee failure from either hydrologic events or earthquakes for 34 Delta islands that have subsided below mean sea level (based on analysis in Mount and Twiss 2005). Figure 1 shows the range of failure probabilities for 36 islands (including the two urbanized islands, Bethel Tract and Hotchkiss Tract) over the next 100 years. Based on current flood and seismic failure probabilities, the median Delta island has a 95% probability of failure between now and 2050 and a 99% probability of failure by 2100. This probability of failure over extended periods is especially high for western Delta islands where, based on the DRMS data, each island has a roughly 99 percent

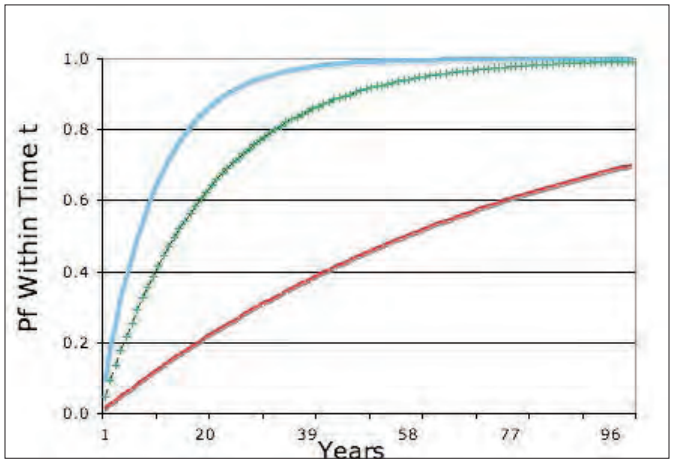

Figure 1 Maximum, median, and minimum probability of flooding from either earthquakes or floods for 36 Delta islands

probability of at least one failure by 2050.

These estimates are based solely on current likelihoods of failure; without major investments in levees, the probabilities of island failures will increase. Additionally, the effects of four processes—subsidence, flood inflows, sea level rise, and earthquakes—mutually re-enforce levee failure. Increasing Delta inflows and sea level rise together reduce the freeboard of the levees, increasing the frequency of levee overtopping. Subsidence, sea level rise, and increasing inflows act together to increase the relative difference in elevation between island interiors and surrounding water surfaces. All three factors increase hydraulic gradients within the levees, increasing through-seepage and under-seepage failures, and amplify the effects of poor levee construction and foundation conditions to increase the likelihood of levee failure during earthquakes. And all four processes increase the frequency and consequence of island failures, while increasing the costs of repair and upgrades.

Without substantial and sustained levee investments, levee failures will transform some Delta islands to extensive bodies of open water. State and federal policy and funding for improving, repairing, restoring or abandoning levees will play a key role in determining future Delta landscapes.

Current Levee Policy and Policy Challenges

Roughly a third of Sacramento-San Joaquin Delta levees are within federally authorized flood control projects, known as "project levees." The other two-thirds are owned and maintained by local reclamation districts on behalf of private land-owners ("non-project levees"). Most project levees are maintained by local reclamation districts with oversight and inspection from the state, following federal levee policies. This analysis focuses on non-project levees.

After significant floods in the Delta in 1986, the state set new standards for Delta levees to reduce the frequency of island flooding. The Sacramento District of the Army Corps of Engineers and the California Department of Water Resources (DWR) set standards for levee crown height and width and levee slopes for agricultural levees. The State Hazard Mitigation Plan (HMP) standard was viewed as an intermediate standard with the long-term goal of upgrading to a higher federal standard, termed "PL 84-99." These standards are summarized below in Figure 2. Levees meeting PL 84-99 standards qualify for federal aid if they are damaged by flooding. Discussions with several state and private Delta engineers indicate that most non-project Delta levees meet HMP standards, but few meet PL 84-99 standards.

Allocating Resources

Given the current fragility of the Delta levee system and the increasing risks of failure, the state will need

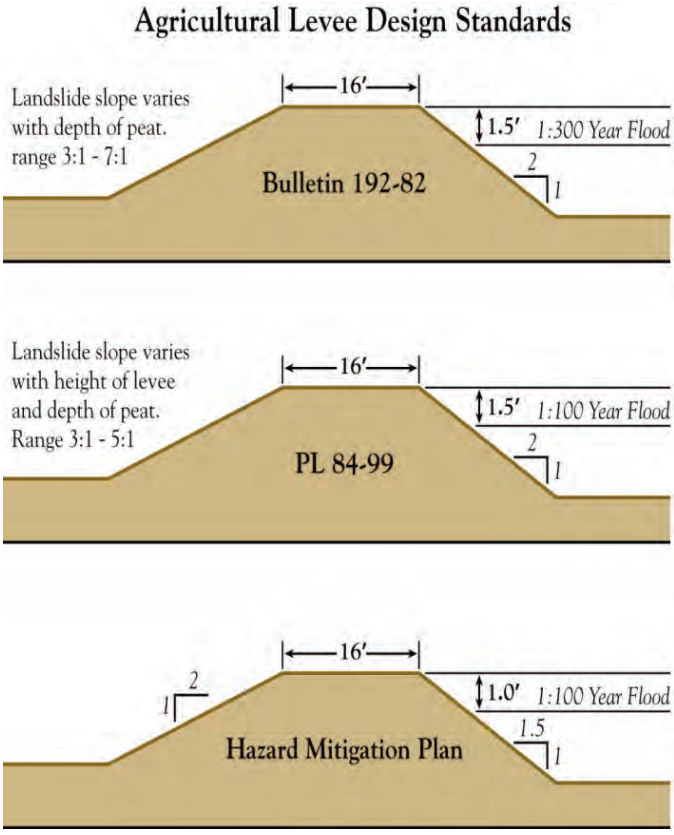

Figure 2 Comparison of state and federal levee standards

to address at least three critical policy issues.

1. Distribution of Available Resources. California voters, by passing Proposition 1E and Proposition 84 in 2006, allocated more than $3 billion in state bond funds to support levee improvements in the Central Valley (including the Delta). These funds and any future state and federal funds can be distributed in two ways:

- Equally everywhere to mitigate flood risk throughout the 1,770 kilometers of Delta levees and the 2,735 kilometers of project levees outside of the Delta, or
- Concentrated at specific locations to meet broader state objectives such as water supply, ecosystem restoration, transportation, and recreation, or to reduce the economic impacts of levee failures. In the Delta, the state's historical approach has been to apply a modest level of resources broadly without prioritization, principally through the Subventions Program (averaging roughly $6 million per year), which helps fund levee maintenance. However, as shown below, the costs of upgrading all Delta levees to even minimal current standards would require extraordinary increases in state contributions, with only small decreases in flood risk.

2. Repair and Restoration of Islands After Levee Failure. When island levees fail, state and local entities incur considerable island repair and recovery costs. As highlighted by the Jones Tract failure in June 2004, the economic impacts and costs to repair an island will often exceed the value of the land, often by several-fold. The cost of repairing a levee breach is typically $20 million to $40 million, depending on local conditions, with roughly equal additional costs from damages to island assets and losses to the local economy (URS Corporation and J. R. Benjamin & Associates 2009). The substantial investments needed to repair an island do little to reduce the likelihood of future failures since the size of a levee breach is usually small compared to the length of levee on an island. Given the high cost of these repairs, the low values of land they restore, and that repairs do not reduce future failure rates, the state might adopt a policy of not repairing all islands that fail and to prioritize repairs, particularly when multiple island failures occur in a single storm or earthquake. California's Department of Water Resources (DWR) announced such a policy after Jones Tract flooded, but it has yet to be tested.

3. Levee Upgrades and Climate Adaptation. California is recognized as a national leader in climate change mitigation policies. However, to date, the state does not have well-defined policies regarding climate change adaptation (Luers and Moser 2006; California Natural Resources Agency 2009). This problem is particularly acute in flood management in California in general (Galloway and others 2007) and in the Delta specifically. Climate change will require developing adaptation strategies that go beyond simply improving all Delta levees. This issue can be partly addressed with elements of the two policy challenges described above: selective investments in levee upgrades and repair of islands that flood.

METHODS: EVALUATION OF LEVEE POLICY DECISIONS

To address the three policy issues concerning future levee investments and repairs—how to distribute funds, whether investments to repair islands are worth the cost, and how to adapt levee policies to climate change—we developed the Levee Decision Analysis Model (LDAM). This model supports a comparison of strategic options for levee management from an economic perspective.

Six combinations of levee upgrade and post-failure repair are considered, with three upgrade levels each having two post-failure repair strategies (”repair” or ”no repair”). The three upgrade actions considered are

1. No upgrade to levees
2. Upgrade to PL 84-99 standards
3. Upgrade to PL 84-99 standards plus 0.3 m (1 ft) to mitigate for expected sea level rise by mid-century (denoted upgrade PL 84-99 + 0.3 m SLR)

For each island, each upgrade policy comes with an accompanying decision of whether or not to repair that island when its levees fail (Table 1).

Table 1 Levee Decision Analysis Model (LDAM) policy options

Option Number	Current Upgrade Policy	Future Repair Decision
1	No Upgrade	Repair
2	No Upgrade	No Repair
3	PL 84-99	Repair
4	PL 84-99	No Repair
5	PL 84-99 + 0.3 m SLR	Repair
6	PL 84-99 + 0.3 m SLR	No Repair

We begin with a summary of the decision analysis framework and method, and then describe how this analytical framework can be applied to the Delta’s levees. We exclude heavily urbanized islands from the decision analysis results. Levee upgrades for urbanized islands will be subject to Federal Emergency Management Agency (FEMA) National Flood Insurance Program standards that are not accommodated well in this initial decision analysis.

Decision Analysis: Framework and Methodology

Formal analysis of levee and other flood-control decisions requires a comparison of costs and benefits, weighed by probabilities, for several alternatives. Most levee or dike investments aim to reduce net flood damages (damages plus levee costs). This presents a dilemma for the decision-maker because the value of his or her investment is in part a function of an uncertain future. Decision analysis provides a logical framework for cost-benefit comparisons of decisions options with uncertainty about their outcomes (Hobbs and others 1997; Cheng and others 2008; Lund 2009). All decision analyses require a probability model and a “value” model (Maguire 2004). For flood structure analyses, the probable effectiveness of a levee or dike investment is factored into its economic evaluation by including probabilistic reliability analysis in the economic decision theory framework.

Reliability analysis developed independently from decision analysis. Assessing the probability of structural failure for a levee or dike is a complicated geotechnical endeavor, depending on several other stochastic variables such as storm events, underlying soils, river discharge, and location of an initial breach (Wood 1977; Moss and Eller 2007). Many studies focus almost exclusively on determining the appropriate probability distribution for flood events or a structural failure (Ang and Tang 1975; Van Manen and Brinkhuis 2005). Given the complexity of reliability analysis, it is common for decision analyses to adopt failure probabilities determined by a separate effort (Van Dantzig 1956; Eijgenraam 2006). In this analysis, we use the current failure probabilities for Delta levees provided in the DRMS Phase 1 report (URS Corporation and J. R. Benjamin & Associates 2009), and then, as sensitivity analysis, explore how results change for lower failure probabilities.

Some studies bridge the gap between reliability and cost-benefit analysis by assessing the “risk” or “expected value” for a given levee height, width, or other characteristic (Voortman and others 2002; USACE 1996, 1999a, 1999b). These risk-based performance values are typically attained by summing the net cost or benefit of future events multiplied by their probability of occurrence. Probabilistic

weighting for the value of a current decision was pioneered in the Netherlands in Van Dantzig's 1956 assessment of optimal dike heights, and generally in the United States in a body of economic decision theory work (Pratt and others 1964; Raiffa 1968). Reliability-based design uses these calculations to determine flood protection investments based upon a pre-accepted probability of failure (van Manen and Brinkhuis 2005; Bouma and others 2005; Woodall and Lund 2009).

Decision analysis brings risk or expected benefit calculations into a broader decision framework to allow comparison of several alternatives, as well as to incorporate a sequence of possible future decisions and/or events. Decision analysis is common in work on optimal flood-protection design (Davis and others 1972; USACE 1999a; Aven and Kørte 2002; Voortman and others 2002; Cheng and others 2008). An expected value is derived for each alternative, which provides the expected benefits (or costs) of a project, given an amount of uncertainty in its future performance. For cases where economic consequences are small relative to the overall wealth of the society or decision-maker, risk-aversion should be negligible, and expected-value calculations are appropriate (Arrow and Lind 1970). The structure of decision options and outcomes is often represented in a decision tree.

The framework for organizing the sequence of decisions necessary for levee investments appears in Figure 3. Decision points among options (in our case to upgrade levees, and to repair or abandon levees) are represented by boxes. Chance events and their outcome probabilities, such as levee failures, are represented by circles. The outcome values for each chain of decisions and events appear at the right side of the tree, and are used to assess the expected costs of the decision options. The tree branches out into

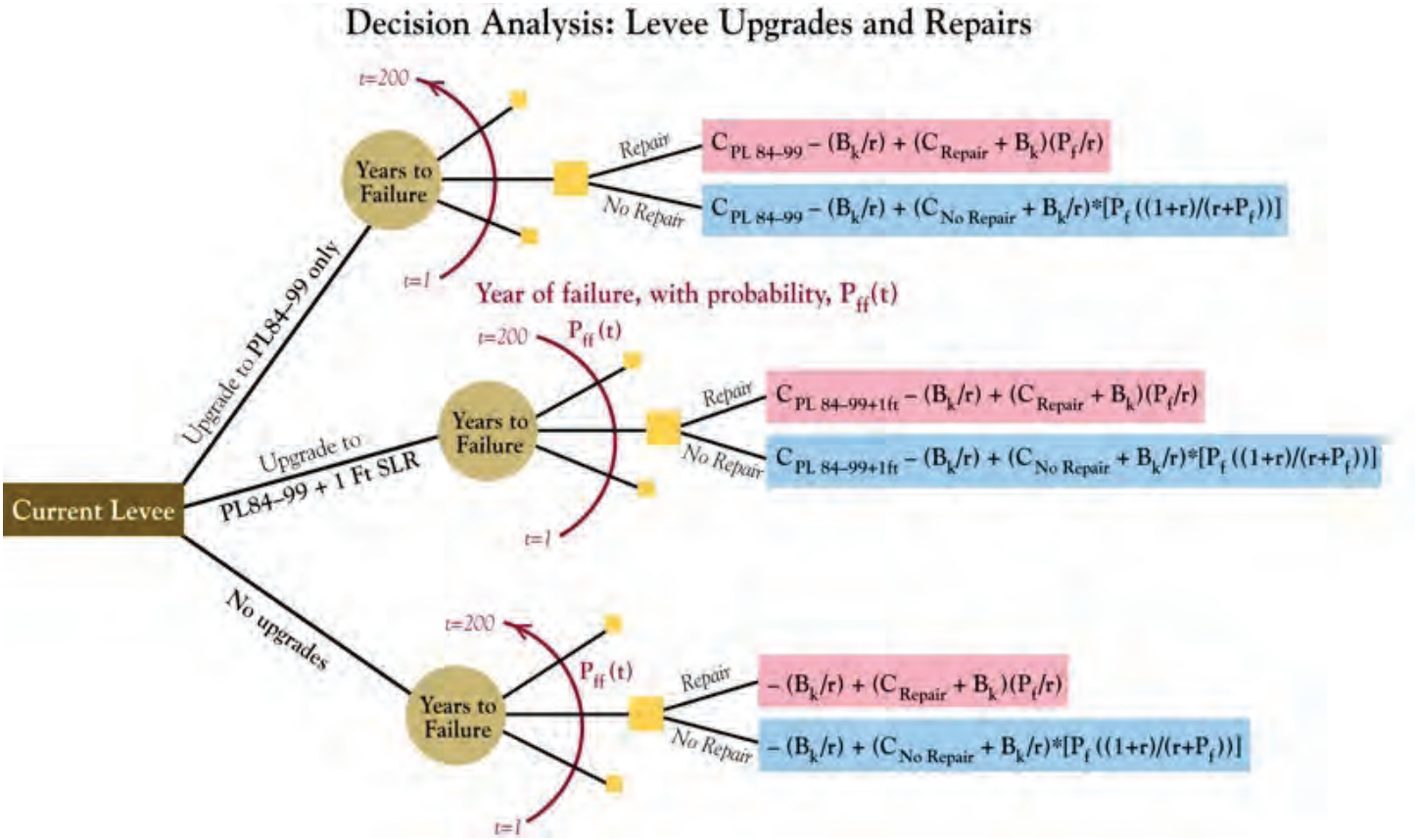

Figure 3 Island levee decision analysis tree for assessing whether to upgrade levees and to restore islands following flooding. $P_{ff}(t)$ = probability of first failure at time t, P_f = current probability of failure, r = discount rate, B_k = one year of island profits.

the future. In this way, a decision analysis facilitates the logical structuring and comparison of alternatives under uncertainty.

The LDAM presented here applies these ideas. As mentioned earlier, the state has three initial options for Delta levees: (1) no upgrade to levees, (2) upgrade to PL 84-99 standards, or (3) upgrade to PL 84-99 standards plus 0.3 m (1 ft) to mitigate for expected sea level rise by mid-century. Regardless of which direction is taken now, in some (uncertain) future year the state will need to decide whether to repair an island when its levee fails. This formulation is a variant of a classic decision tree: the node of uncertainty does not split off into different uncertain events with varying probabilities, but rather into different uncertain time-frames in which one event will occur. In other words, like life insurance, uncertainty revolves around *when* failure will occur, not *if* failure will occur.

Because the present value of a current upgrade decision depends on the possible future flood and repair events that follow, it must be calculated by working backwards. This procedure is called "folding back" in some analyses, and has been compared to backward dynamic programming (Hobbs and others 1997). Values are estimated for repair choices occurring furthest into the future for each upgrade strategy, and then the costs of those choices are weighted by an outcome probability and assigned to the present value of that strategy. In other words, the first step in the analysis is to look at the choices remaining *after* an initial policy has been employed (for which costs are sunk) and a future uncertain event has occurred. More complex, non-stationary decision analysis problems, such as long-term adaptation of levees to climate change, can be optimized using dynamic programming (Zhu and others 2007).

Decision to Repair after Failure

The first step is to look at a point in the future just after an island has failed, and determine if the economic value of the failed island justifies the costs of its repair. The costs of each choice for an individual island are discussed next.

Cost of Repairing an Island when it fails is a function of the materials and engineering costs of fixing and re-enforcing breached levees, pumping out the island, and the lost profits from one year of lost agricultural production on the island (assuming annual crops), plus those same costs occurring again and again further into the future each time the island fails. This second future cost term is represented by an infinite series of future costs for repairing the island each (probabilistic) time it fails again. The present value benefits of all future profits of the island (here, assumed equivalent to a property value corrected for failure rate) are subtracted from these costs. In mathematical terms:

$$\text{Cost} = C_{Repair} + B_k + (C_{Repair} + B_k)(P_f/r) - (B_k/r)$$

Where C_{Repair} is the average cost of repairing a failure, B_k is one year of island profits, r is the inflation-corrected interest (discount) rate, and P_f is the probability of island failure in any given year. The first term (C_{Repair}) is the cost of repairing the first failure. The second term, B_k, is the loss of one year's farm profit from island failure. The third term, $[(C_{Repair} + B_k)(P_f/r)]$ is the present value cost of all future failures (derived under "Present Cost of Repair" below), and the fourth term $[(B_k/r)]$ is the present value of island profits (a negative cost).

Cost of Not Repairing an Island when it fails is the sum of the cost of rebuilding or re-locating existing infrastructure (such as highways, towns and railroads) and the cost of fortifying nearby islands that would be newly vulnerable to wind and waves from newly open water. In mathematical terms:

$$\text{Cost of No Repair} = \text{Cost to Reinforce Downwind Islands} + \text{Cost of Lost Infrastructure}$$

Once the cost of no repair and the cost of repair for each island have been estimated, the least expensive (or most profitable) action (repair or no repair) can be identified. The cost of this action is brought back to the present time and assigned a present value. This is where probabilities and discount rates are important for the analysis. Because the costs of funding or not funding repair are summed over an infinite range of potential times to failure, formulas are derived to express these present values (Suddeth and others 2008).

Decision to Repair or Not Repair after Failure with Upgrades

This logic can now be extended to the costs of repair or no repair for levees that have been upgraded.

Present Cost of Repair is the present value of all present and future repair costs, plus the cost of upgrades, minus the present value of all future profits. Mathematically:

$$\text{Cost} = \text{Upgrade Cost} - (B_k/r) + (C_{Repair} + B_k)(P_f/r)$$

The first cost term will not exist in the "no upgrade" case. In the case of an enhanced upgrade to mitigate for 0.3 m (1 ft) of sea level rise, it will include the cost of that additional fortification. The only significant change in this formula from that of repair costs when an island fails (presented above) is that there is no current cost of repairing the island today (because it has not yet failed), so that $(C_{Repair} + B_k)$ only appears once and is multiplied by (P_f/r). The cost of current upgrades is incorporated to allow comparison of the three strategies.

The derivation of the infinite series of future repair costs (third term) is as follows:

Let C be the cost of each failure episode, and the repair and damage costs of a failure event. Friedenfelds (1981) provides a useful formula for understanding the present value of an infinite series of future costs (W), $W = C + W(1+r)^{-t}$, which can be re-arranged algebraically to:

$$W = \frac{C}{1-(1+r)^{-t}}.$$

As the time between failures (t) increases, the present value cost decreases both because failures are becoming less frequent and because of the increased effects of discounting. For Freidenfeld's derivation, the infinite series begins with a failure in the present. When the time of failure is uncertain and represented by a probability distribution, this becomes:

$$W = C + W\sum_{i=1}^{\infty} P_f\left(1-P_f\right)^{i}\left(1+r\right)$$

or

$$W = \frac{C}{1-\sum_{i=1}^{\infty} P_f\left(1-P_f\right)^{i-1}\left(1+r\right)^{-i}}$$

For our problem, there is no failure in the present, but the first failure occurs at some uncertain time in the future, so $W' = W - C$, or:

$$W' = \frac{C}{1-\sum_{i=1}^{\infty} P_f\left(1-P_f\right)^{i-1}\left(1+r\right)^{-i}} - C.$$

Note that

$$\sum_{i=1}^{\infty} P_f\left(1-P_f\right)^{i-1}\left(1+r\right)^{-i} = \frac{P_f}{1-P_f}\sum_{i=1}^{\infty}\left(\frac{1-P_f}{1+r}\right)^{i} = \frac{P_f}{r+P_f}$$

since this part is an infinite geometric series. This allows the entire expression to be simplified to $W' = C\,P_f/r$. Or, $DF_{isf} = P_f/r$ for the present value (DF = discount factor). The annualized value of these costs over an indefinite future period would be calculated by simply multiplying the cost C by the probability of failure P_f.

The Present Cost of No Repair is the cost of upgrades applied today to the island, plus the net present expected cost of upgrading surrounding islands and rebuilding infrastructure (roads, houses, railroads), minus the profit made from the island until the time of failure. In mathematical terms:

$$\text{Cost} = \text{Upgrade Cost} - (B_k/r) + (C_{No\ repair} + B_k/r)^*[P_f\ ^*\ [(1+r)/(r+P_f)]]$$

Where $(B_k/r) - (B_k/r)^*[P_f\ ^*\ [(1+r)/(r+P_f)]]$ is the present expected value of the profit made on the island until time of failure. The profits made before failure are subtracted from the total cost of abandoning the island.

$(C_{No\ repair})^*[P_f\ ^*\ [(1+r)/(r+P_f)]]$ is the present expected cost of upgrading surrounding islands and rebuilding infrastructure (roads, houses, railroads).

The expected value of the discount factor for a failure cost occurring at an uncertain future time (third

term) is derived as follows:

$$DF_{sf} = \sum_{t=0}^{\infty} P_f \left(1 - P_f\right)^t \left(1+r\right)^{-t} = P_f \sum_{t=0}^{\infty} \frac{1 - P_f}{1+r}^t$$

Here the probability of failure is the same in each year, yielding a geometric probability distribution for the time of first failure. This probability distribution of the time of failure is used to weight each year's discount factor.

Using geometric series expansions, this reduces to:

$$DF_{sf} = P_f \frac{1+r}{r+P_f},$$

which is used in the above equation to weight the profits made on the island before time of failure. Our use of a geometric probability distribution here is in accordance with other engineering studies interested in the time to first failure, or the recurrence interval for a given event (Ang and Tang 1975). Alternatively, some studies choose to use a continuous probability distribution, so that time need not be divided into intervals. The exponential distribution is similar to the geometric, and is likewise used for problems involving failure probabilities and recurrence intervals (Voortman and others 2002; Eijgenraam 2006).

Because upgrading an island to any standard will always cost more in cash today than not upgrading the island, the net expected present value of upgrades will only be cheaper than no upgrades if the upgrade significantly reduces the probability of failure for that island. In other words, if the upgrades significantly increase protection, upgrades should have a lower expected cost than no upgrades. Otherwise, the costs of upgrading are not justified.

The above analysis can be used to estimate the present value of the three upgrade strategy options for each island. The strategy for each levee is composed of two successive decisions. The first is the level of island upgrade: (1) no upgrade, (2) upgrade to PL 84-99 standards or (3) upgrade to PL 84-99 + 0.3 m (1ft) sea level rise. The second decision (which was actually analyzed first in this discussion) is what to do when that island fails: fund or not fund repairs. A complete strategy for an island might look something like this: "Upgrade to PL 84-99; Do not fund repair." The six logically available strategies for each island are summarized in Table 1.

In some cases, it might be worthwhile to add another option to the analysis. A "Prepare to Abandon" option for an island would include hardening or removing infrastructure to reduce flood damage or better survive permanent flooding. Although we did not include this option in our assessment, the results of this analysis suggest that such preparations might be prudent for some Delta islands.

Parameter Values

The results of this decision analysis depend on the values assigned to the costs and failure probabilities for each island. For instance, increasing the profitability or property value of an island makes repair more attractive. Likewise, a high cost of repair coupled with a low property value makes repair less likely.

This initial analysis employs values from various data sources. Refinements of cost valuations for Delta islands would enhance the resolution of the model. These initial results serve as a springboard for discussion, and this analysis as a working framework for developing an optimal strategy. We calculated costs using the following sources, assumptions and methods.

Property Value

The analysis summed annual crop productivity with island assets as a minimum measure of property value, presented in Table 2. The assets estimate, taken from the DRMS Phase 1 report (URS Corporation and J. R. Benjamin & Associates 2009), contained buildings, equipment, and infrastructure such as roads and rail lines. Land values were extracted from data and agricultural production modeling assembled in Lund and others (2007) in which crop acreage on each island was identified as either high or low value, and assigned the appropriate multiplier for annual profit yield per acre. The nominal property values here are not market values and assume island reliability. These property values were then increased in several steps to a maximum value triple that of the crop and asset

Table 2 Land and asset values

Island Name	Land Value (Lund and others 2007)	Asset Value (URS Corp. and J.R. Benjamin & Associates 2009, Table 12-7)	Land + Asset Values
Bacon Island	$16,248,424	$34,664,000	$50,912,424
Bouldin Island	$13,040,542	$21,511,000	$34,551,542
Brack Tract	$23,205,096	$13,647,000	$36,852,096
Bradford Island	$5,518,842	$19,003,000	$24,521,842
Brannan-Andrus Island	$73,173,177	$177,734,000	$250,907,177
Canal Ranch Tract	$27,692,544	$15,622,000	$43,314,544
Coney Island	$2,438,255	$14,614,000	$17,052,255
Dead Horse Island	$862,581	$910,000	$1,772,581
Empire Tract	$9,114,605	$9,511,000	$18,625,605
Grand Island	$64,673,235	$181,275,000	$245,948,235
Holland Tract	$8,823,343	$14,669,000	$23,492,343
Jersey Island	$7,272,961	$24,238,000	$31,510,961
Jones Tract	$42,496,164	$497,784,000	$540,280,164
King Island	$12,081,613	$30,840,000	$42,921,613
Mandeville Island	$11,731,203	$5,212,000	$16,943,203
McDonald Tract	$20,591,848	$30,780,000	$51,371,848
Medford Island	$2,221,145	$7,594,000	$9,815,145
Orwood Tract	$8,893,034	$239,425,000	$248,318,034
Palm Tract	$5,346,593	$21,107,000	$26,453,593
Quimby Island	$1,565,687	$584,000	$2,149,687
Rindge Tract	$19,906,394	$18,094,000	$38,000,394
Roberts Island	$164,103,230	$538,471,000	$702,574,230
Ryer Island	$38,670,068	$55,877,000	$94,547,068
Sherman Island	$27,023,167	$110,416,000	$137,439,167
Staten Island	$26,409,675	$20,191,000	$46,600,675
Terminous Tract	$50,975,498	$80,050,000	$131,025,498
Twitchell Island	$9,023,367	$12,105,000	$21,128,367
Tyler Island	$33,202,759	$91,184,000	$124,386,759
Union Island	$80,672,567	$140,909,000	$221,581,567
Venice Island	$6,839,964	$13,308,000	$20,147,964
Victoria Island	$22,618,787	$47,053,000	$69,671,787
Webb Tract	$11,554,466	$416,000	$11,970,466
Woodward Island	$4,437,580	$124,671,000	$129,308,580
Wright-Elmwood Tract	$26,166,120	$15,967,000	$42,133,120

estimate. This was done to account for uncertainty in input data, crop changes over time, and potential additional values (cultural, habitat, etc.) unaccounted for in crop and assets data.

Repair Costs

An average cost of $25 million dollars was assumed to repair a levee breach, plus an additional $0.34 per cubic meter to pump water from the island. These numbers are based on interviews with engineers familiar with the Delta who estimated that the typical levee breach repair costs $20 to 30 million, recorded costs of the Jones Tract Failure, and the DRMS Phase 1 report (URS and J. R. Benjamin & Associates 2009 2009).

PL 84-99 Upgrade Costs

Three estimates for upgrade costs were evaluated. Initial costs were calculated assuming $1.74 million dollars per kilometer of levee. This figure was based on evaluation of a range of PL 84-99 upgrade costs taken from multiple islands, including Twitchell, Sherman, Bouldin, and King, based on conversations with levee engineers and DWR engineers. This cost is close to that cited by DRMS for upgrades. We were also provided higher and lower estimates, of $2.48 million dollars per kilometer and $0.53 million dollars per kilometer, respectively. These other two costs also were evaluated in subsequent model runs. In all cases we noted which islands have already partially undergone PL 84-99 upgrades, and subtracted the appropriate amount from their estimated upgrade costs.

PL 84-99 Upgrade + 1 ft Sea Level Rise Costs

These were calculated by taking the lengths of each island's levees and applying a geometric formula for increased cut volumes needed to raise the island levee 0.3 meters (one foot), in keeping with PL 84-99 geometric standards. Levee lengths were obtained from GIS data derived from DWR, cited in Mount and Twiss (2005). Once we calculated the volume of material needed, we assigned the following costs: $13.08 per cubic meter ($10 per cubic yard) for fill and 1.4 cut cubic meters per cubic meter. These values were obtained from interviews with Delta levee engineers. We assigned no costs for engineers and contractors because in our analysis, we assume that such extra upgrades would occur at the same time as the PL 84-99 upgrade, for which engineering costs have already been included. This estimate biases the model toward this enhanced upgrade because it does not account for additional subsidence commonly following placement of fill on levees. Depending upon local conditions, subsidence can significantly increase the volume of fill needed to raise levee elevations.

Cost of No Repair

We assumed the two biggest costs of not repairing an island after failure to be the cost of rebuilding or diverting infrastructure and the cost of upgrading surrounding islands. Cost estimates for rebuilding roads, highways, or railroads are based on a simple, per mile cost obtained from the DRMS Preliminary Strategies Report Section 12, which reports an estimated cost of $45 million per mile (approximately $28 million per kilometer) of seismically resistant levee. Levees of this caliber would have to be built to support the roads or highways on top of them (these costs are conservative in that they do not include the actual cost of the road or rails themselves). The length of roads and railroads on each island used in the assessment of seismically resistant levee needs (above) were obtained from GIS Tele Atlas StreetMap Premium data, and included only the lengths on the interior of the island without counting road length along the levees themselves. The relevant roads used were the major highways routes (4, 12, 160); other highways were grouped (mostly Highway 5 and 84).

Costs of reinforcing surrounding islands were calculated with these assumptions:

1. The approximate length of levee upgrades needed for these surrounding islands should equal roughly half the circumference of the failed island (geometrically).
2. The surrounding levees need to be raised 0.3 m (1 ft) to account for this increased exposure.
3. Cost of these upgrades should thus equal half the cost of materials for raising the levee of the failed

island by 0.3 m (obtained from earlier calculations of PL 84-99 + 0.3 m SLR costs).

4. A multiplier of 1.3 is assigned to account for a 20% cost for engineers and construction management, along with 10% state costs for management and processing.

As with several other inputs, we allowed for the possibility of higher costs than those estimated with the above procedure. These initial numbers were taken as a minimum value, and were increased systematically by 10% increments to test results against a wider range of potential costs for not repairing an agricultural island.

Failure Probabilities

Equally as influential to the outcomes of this analysis are the probabilities of failure assigned to each island, and the change in failure probability that occurs with each potential upgrade. For our probabilities of failure without upgrades, we use the Levee Optimization Assessment from the DRMS Phase 1 report (URS Corporation and J. R. Benjamin & Associates 2009). The report evaluated risk to individual Delta levees from three events: sunny-day failures, flooding, and seismic activity. In this analysis, we ignore the smaller risk from sunny-day failures, and instead calculate the annual probability of levee breaches from floods or earthquakes. After assigning islands to one of several "vulnerability classes," DRMS calculations of annual failure probabilities for each class involved three steps:

1. Creating a "levee response function" to represent the levee's ability to withstand either hydrostatic (floods) or ground acceleration (seismic) forces

2. Creating a conditional probability of failure function to relate the conditional probability of a levee breach to a given exit gradient internal to the levee (for flooding) or the loss of freeboard (slumping from seismic ground accelerations)

3. The development of a "levee fragility function" to relate the probability of failure to channel water surface elevations or earthquake magnitudes. These functions were developed using a mixture of geotechnical models, expert elicitation, and Monte Carlo simulations.

The DRMS report went through several revisions in response to comments from CALFED's Independent Review Panel (IRP). In its final assessment of the report, the IRP generally found the analysis much improved and reliable for planning purposes, except for a few caveats.

The IRP stressed several points for the analysis of seismic and flood risk (CALFED IRP 2008). First, the IRP felt the DRMS report may have over-estimated failure from earthquake ground accelerations. The IRP points out that the frequencies predicted by the DRMS Phase 1 Report for earthquakes are significantly higher than the historical record suggests, and even for the seismically active period of 1850 through 1906, earthquakes of similar magnitude hitting the Delta region today would not necessarily cause the widespread failure suggested by the DRMS Phase 1 Report assessment. However, in a separate study, the U.S. Geological Survey (USGS) predicts a 30% chance of a 6.8 to 7.0 magnitude earthquake in the region within the next 30 years (Brocher and others 2008). This USGS study may help substantiate the higher frequencies predicted by the DRMS Phase 1 Report. Second, because the fragility curves relating levee failure to channel stage are steep, and some error occurs in predicting stage for specific sloughs and channels, it was thought that the risk from flood events may have been overstated for some islands, and understated for others. However, it was also noted that estimated seepage rates may have been low, which would tend to bias the models towards lower failure probabilities.

In this study we also attempted to assess how well PL 84-99 upgrades improved levee performance. That is, to assess the amount such an upgrade would reduce a levee's annual failure probability. We contacted many state, federal, and private engineers and asked their opinion of the reduced annual failure probability achieved through upgrading levees from the HMP to the PL 84-99 standard. All engineers noted that local differences in levee and foundation conditions lead to high variability in the value of improvements, but we were able to adopt a rough rule that this

upgrade reduces the levee failure rates by an average of approximately 10% for failures from levee overtopping, through-seepage and under-seepage. These upgrades, which occur mainly on the surface of the levee, do little to improve levee foundations and the risk of failure from earthquakes.

Because of concerns about the DRMS report and the necessarily coarse assessment of upgrade effectiveness, and also to test the economics against a wide range of uncertain futures, we took the DRMS probabilities of failure with a 10% decrease from upgrades as maximum values for this analysis. After we ran the model with these higher failure probabilities, we reduced them incrementally, first without upgrade and then via different upgrade options, to what we considered the lowest failure probability expected from agricultural levees in the Delta: 0.01 per year, or what is required under the Federal Emergency Management Act for urban levees. While this may be an optimistic and perhaps unrealistic lower bound, it serves to test the sensitivity of our results while also distinguishing those islands that may remain economically unsustainable even under very favorable conditions.

Discount Rate

Discount rate estimation is a routine concern in economic evaluation studies. A 5% annual real (inflation-corrected) discount rate is assumed for the base calculations. Discount rates between 3% and 7% were examined in sensitivity analysis.

Uncertainty

This analysis is used to organize and explore several uncertainties. These include: (1) pre-upgrade failure probabilities, (2) failure probability reduction with levee upgrades, (3) costs of not repairing islands, and (4) island economic production value. More generally, uncertainties can be grouped into three categories: (1) physical uncertainties, (2) parameter uncertainties, and (3) structural uncertainties with regards to the model itself (Tebbens and others 2008; Ramsey 2009). For this analysis, physical uncertainties for Delta levees and the effectiveness of various upgrade efforts are the most easily quantified, and are explicitly factored into the decision analysis. Parameter uncertainty refers to values used for inputs such as island assets and repair costs. These are accounted for by exploring different scenarios in which key inputs are varied. Structural uncertainty is difficult to quantify because it refers to the conceptual framing or formulation of the decision analysis itself, which relies on the logical formulation of the problem. Alternative logical formulations, such as expanding the problem to include dynamics and climate change (Zhu and others 2007), might be explored in later work at some cost of model comprehensibility for public policy purposes. For this analysis, structural (and other forms) uncertainty are addressed by using an "indeterminate" category for the repair decision in the base case, where the absolute net benefit (or cost) of repair is not large enough for this initial analysis to be persuasive.

RESULTS

Results are presented for a base case and sensitivity analyses regarding probabilities of failure, effectiveness of upgrades, property values, and costs of not repairing islands.

Base Case

The base case used DRMS failure probabilities with a 10% decrease from upgrades, property values reflecting only crop production and assets, and medium upgrade costs. The results suggested "no upgrade" as the economically optimal decision for every island, regardless of whether it would be optimal to repair the island in the future. Levee upgrades have a high cost for a small increase in reliability. This initial analysis also suggested that 11 islands fall in the "repair" category and 18 islands in the "no repair" category, with five classified as "indeterminate" (Figure 4). An island was assigned to the indeterminate category if the difference in cost between repairing and not repairing the island differed by less than a factor of two (Figure 4 and Table 3). Figure 4 also highlights islands that, in a separate analysis (Fleenor and others 2008), have been identified as critical for export water quality. Since Delta water exports were

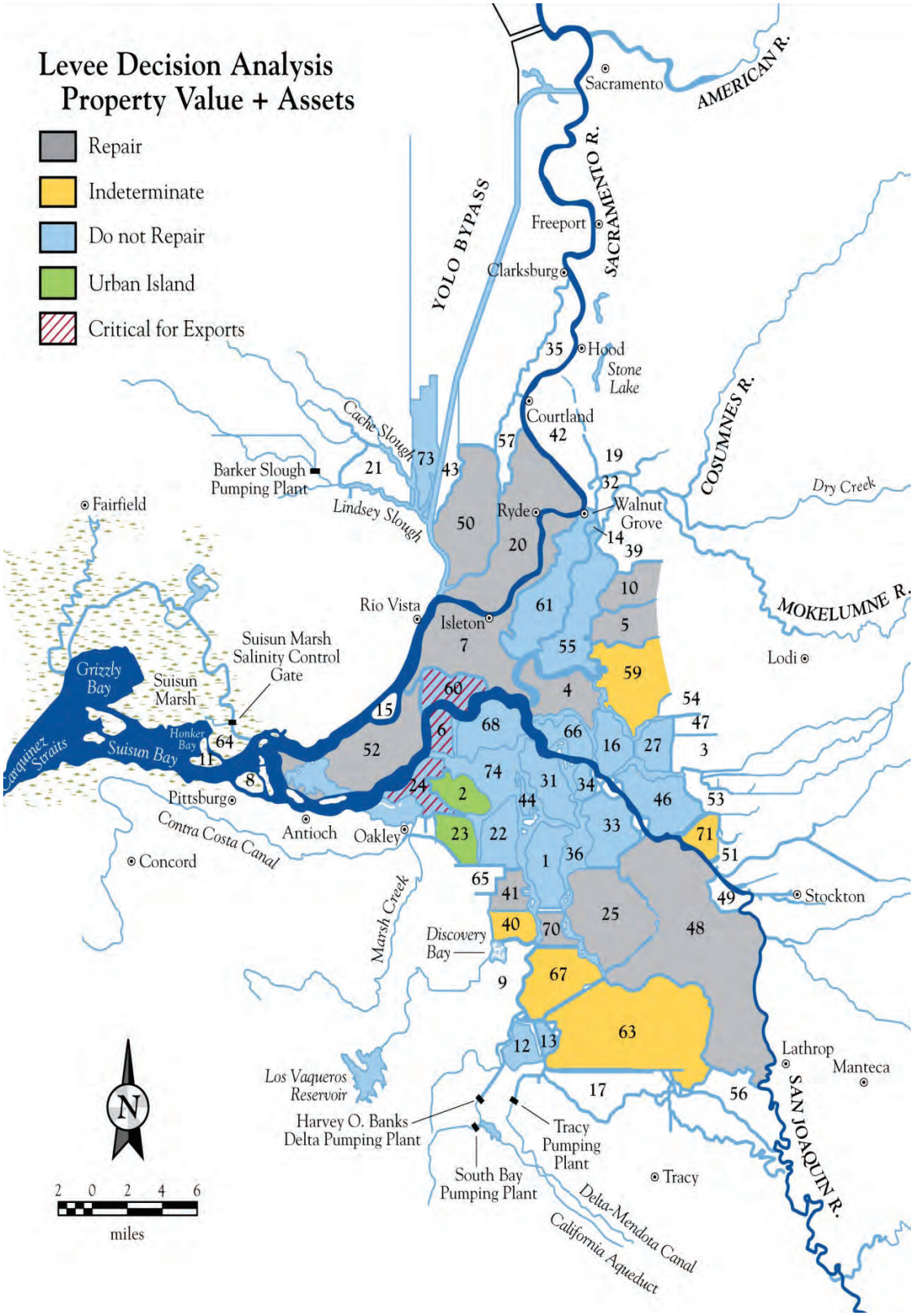

Figure 4 Base case repair decisions

Table 3 Summary of LDAM base case results for 34 subsided Delta islands

		Repair Costs, No Upgrade		Expected Present Cost of Upgrade Strategy			Decision Summary		
# on Map	Island Name	Cost of Repair	Cost of No Repair	No Upgrade	PL 84-99	PL 84-99 & 1 ft SLR	Upgrade Decision	Repair Spread / Min Cost	Repair Decision
1	Bacon Island	$74,170,946	$4,930,479	-$21,432,120	$17,803,803	$24,575,354	No Upgrade	14.04	Not Repair
4	Bouldin Island	$50,701,075	$213,036,975	$6,280,319	$54,666,794	$62,447,509	No Upgrade	3.02	Repair
5	Brack Tract	$30,779,601	$290,128,755	-$152,294	$29,286,637	$33,074,630	No Upgrade	8.43	Repair
6	Bradford Island	$47,396,917	$2,547,863	-$11,211,402	$9,336,404	$13,100,248	No Upgrade	17.60	Not Repair
7	Brannan-Andrus Island	$143,136,217	$534,606,881	-$40,079,378	$41,055,338	$57,601,934	No Upgrade	2.73	Repair
10	Canal Ranch Tract	$21,153,000	$100,338,229	-$17,274,655	$11,419,514	$16,505,363	No Upgrade	3.74	Repair
13	Coney Island	$53,101,021	$1,888,373	-$10,712,759	$4,464,574	$7,205,908	No Upgrade	27.12	Not Repair
14	Dead Horse Island	$29,734,105	$882,166	-$1,234,006	$5,915,590	$7,251,142	No Upgrade	32.71	Not Repair
16	Empire Tract	$44,204,857	$2,580,558	-$7,540,314	$21,567,527	$25,284,449	No Upgrade	16.06	Not Repair
20	Grand Island	$161,079,249	$632,108,744	-$76,175,303	-$74,971,324	-$62,331,264	No Upgrade	2.92	Repair
22	Holland Tract	$41,054,683	$3,762,228	-$10,349,819	$20,093,890	$25,746,214	No Upgrade	9.91	Not Repair
24	Jersey Island	$41,213,403	$5,298,546	-$9,183,422	$33,460,372	$41,194,943	No Upgrade	6.78	Not Repair
25	Jones Tract	-$242,826,036	$246,264,918	-$380,607,659	-$337,110,891	-$335,040,129	No Upgrade	-2.01	Repair
27	King Island	$60,034,074	$3,112,987	-$25,106,531	-$326,670	$3,966,906	No Upgrade	18.29	Not Repair
31	Mandeville Island	$47,779,653	$4,920,445	-$4,795,895	$34,929,662	$42,230,873	No Upgrade	8.71	Not Repair
33	McDonald Tract	$63,686,312	$$4,717,197	-$18,996,260	$18,683,638	$25,301,291	No Upgrade	12.50	Not Repair
34	Medford Island	$52,893,470	$2,021,808	-$3,420,891	$12,869,007	$15,837,938	No Upgrade	25.16	Not Repair
40	Orwood Tract	-$66,321,741	$2,905,255	-$159,659,980	-$141,971,477	-$142,843,340	No Upgrade	-1.04	Unsure
41	Palm Tract	$31,354,174	$124,503,940	-$2,859,112	$24,994,514	$30,100,025	No Upgrade	2.97	Repair
44	Quimby Island	$38,275,617	$2,413,574	-$390,020	$19,218,792	$22,916,823	No Upgrade	14.86	Not Repair
46	Rindge Tract	$31,242,597	$5,424,936	-$16,237,862	$27,536,440	$35,570,508	No Upgrade	4.76	Not Repair
48	Roberts Island	-$542,186,742	$604,431,954	-$618,820,393	-$496,727,006	-$472,037,573	No Upgrade	-2.11	Repair
50	Ryer Island*	$8,965,794	$138,815,097	-$53,438,418	-$55,028,153	-$45,743,380	Upgrade	14.48	Repair
52	Sherman Island	$31,404,098	$297,394,598	-$27,849,519	$19,976,484	$24,327,090	No Upgrade	8.47	Repair
55	Staten Island	$36,167,863	$12,011,078	-$11,437,213	$85,466,405	$103,220,536	No Upgrade	2.01	Not Repair
59	Terminous Tract	$55,819,068	$76,856,695	-$42,335,028	$14,501,533	$21,978,974	No Upgrade	.38	Unsure
60	Twitchell Island	$55,389,976	$4,087,597	-$7,229,820	$19,024,728	$25,067,144	No Upgrade	12.55	Not Repair
61	Tyler Island	$39,086,253	$8,665,380	-$37,544,331	-$2,899,668	$8,849,897	No Upgrade	3.51	Not Repair
63	Union Island	-$62,480,954	$11,580,883	-$154,202,742	-$64,900,064	-$48,689,736	No Upgrade	-1.19	Unsure
66	Venice Island	$56,168,608	$4,274,192	-$5,022,624	$29,358,610	$35,574,725	No Upgrade	12.14	Not Repair
67	Victoria Island	$77,047,296	$204,987,529	$8,325,075	$48,451,894	$54,583,650	No Upgrade	1.66	Unsure
68	Webb Tract	$44,674,014	$4,443,922	-$3,546,216	$32,458,763	$39,175,373	No Upgrade	9.05	Not Repair
70	Woodward Island	-$44,449,476	$70,569,861	-$87,822,876	-$64,016,738	-$60,334,101	No Upgrade	-2.59	Repair
71	Wright-Elmwood Tract	$4,611,486	$3,010,509	-$24,866,287'	-$620,551	$3,797,641	No Upgrade	0.53	Unsure
	Total for 34 Islands	$513,880,476	$3,629,524,149	-$1,875,929,756	-$602,031,629	-$360,532,435			

*Ryer Island has already been upgraded

not factored into this analysis, results for these five western islands may be unrealistic given the State Water Project and Federal Central Valley Projects' current reliance on lower-salinity water in the Delta for pumping. Under current state and federal project operations, it is likely that those islands would all be repaired.

Additional Analysis Exploring a Broader Range of Input Values

All analyses have uncertainties. Because this analysis includes the simplifying assumption that failure probabilities do not increase with time, results could be viewed as optimistic. On the other hand, our costs for not repairing an island are conservative in their estimation of infrastructure replacement costs. To explore a broader range of arguable reality, we can explore the sensitivity of decisions to changes in such parameter estimates. For this analysis, we varied failure probability, upgrade costs, the costs of not funding repair, property value estimates, and discount rate to assess potential changes in the foregoing conclusions. For these sensitivity analyses, the "indeterminate" category was eliminated.

Decreased Failure Probabilities and Varying Upgrade Costs

The failure probability of an island's levees acts together with upgrade costs to influence the estimation of the net present value of upgrades and repairs. Since these probability and cost estimates are imperfect and are likely to change as we understand more, we evaluated their effect on model results. First we focused on the repair decision, and found the number of islands repaired after lowering current failure probabilities (without levee upgrades). All islands were first set to the same annual probability of failure of 0.04 (higher than DRMS estimates for some islands, and lower for others), and decreased by increments of 0.005 to the urban FEMA standard of 0.01 (lower than the DRMS estimate for all of the 34 islands analyzed). When probabilities of failure were decreased from 0.04 to 0.01, and upgrade decisions were taken into account, only two additional islands were repaired. These results, summarized in Figure 5, reflect the relative importance of property values and repair costs in the repair decision. Second, we sought to find the number of islands optimally upgraded under increasingly effective upgrade scenarios, given low, medium, or high costs for those upgrades. This brackets our understanding into a "worst-case" through "best-case" continuum: The worst case being high upgrade costs for small increases in levee reliability, and the best case being low upgrade costs resulting in significantly more reliable levees. Because our initial results using medium-range values already suggest a policy of no upgrades, we can assume that a higher upgrade cost will not change this, and therefore call this our optimal policy under worst-case valuations as well. Under the best-case scenario, in which we assigned upgrade costs of $0.53 million per kilometer (versus the $1.74 million per kilometer used in the analysis above) and decreased every island's annual post-upgrade failure probability to 0.01 (the urban standard for levees), it is optimal to upgrade 23 of the 34 islands included in this analysis. Even if levee upgrades were relatively inexpensive and were thought to dramatically decrease failure probability (highly unlikely since these upgrades do not increase resistance to earthquakes), it still does not make economic sense to upgrade 11 islands of the 34 islands under review. These results support our initial conclusion that it

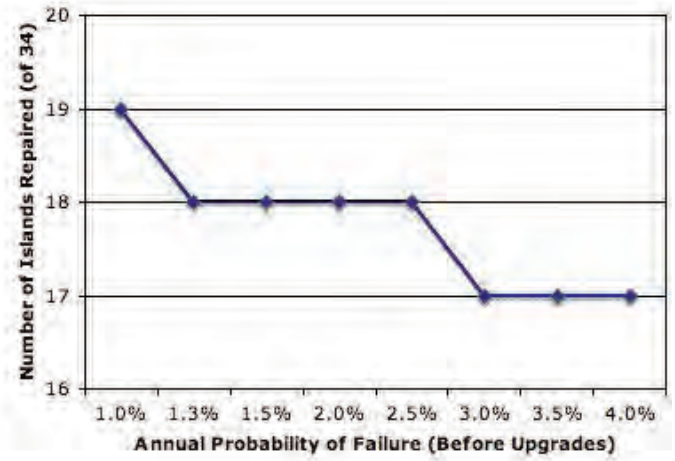

Figure 5 Effect of decreasing pre-upgrade failure probabilities on the economic repair decision

is not cost-effective to invest in upgrading all Delta islands to PL 84-99 standards or higher. The results of this analysis are summarized in Figure 6.

Increasing Property Values and "Do Not Repair" Costs

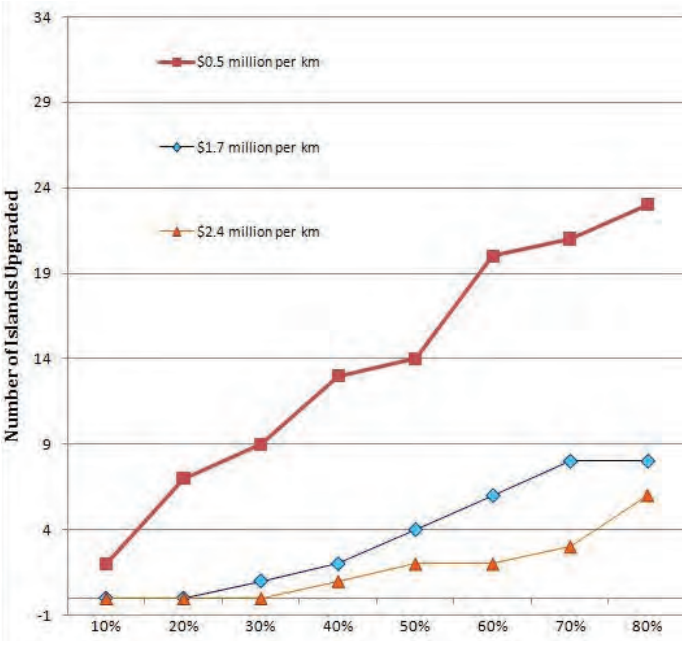

Figure 6 Effect of decreasing levee failure probabilities and upgrade costs on economic decision to upgrade islands

Because we only replace lost roads and rail lines in the case of no repairs, some other infrastructure replacement costs may not have been represented in the base case for a few islands. In addition, we did not consider potential additional costs of mitigating increased levee under-seepage that would occur on some islands adjacent to flooded islands. Finally, property values in the base case only account for crop production and on-island assets. Increases in all of these numbers could change a repair decision from "do not repair" to "repair." We first experimented with increasing "do not repair" costs by 10%. With 100% increases in the cost of not repairing an island, only five additional islands are repaired (summarized in Figure 7). This result demonstrates the relative importance of island property and asset values in evaluating whether to repair an island.

To evaluate the effect of property values in isolation from "do not repair" costs, we increased property values and assessed their effect on the "Abandon" versus "Repair" decision. Combined land and asset values were systematically increased by increments of 10 percent. Small increases in land and asset values had minimal effect. When values were increased by 100 percent, only four additional islands moved from the Abandon to Repair category (the indeterminate category was ignored for this sensitivity analysis.) This modest shift in the number of islands to repair reflects the high costs of levee repairs relative to island property values, even with substantial increases in those values. These results are summarized in Figure 8.

We finally looked at a more extreme case for both property values and "do not repair" costs, tripling both of them at the same time: 9 of 34 islands were

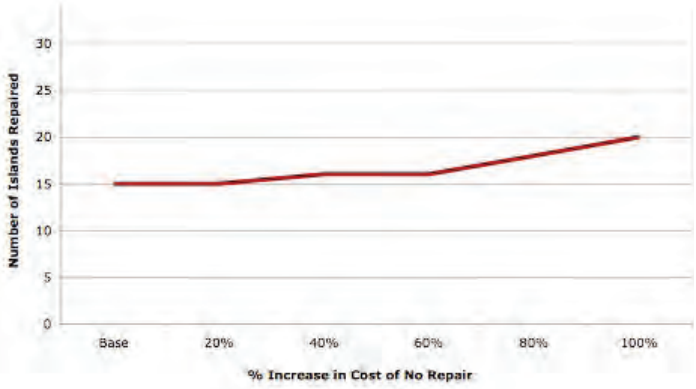

Figure 7 Islands repaired with increased costs of no repair

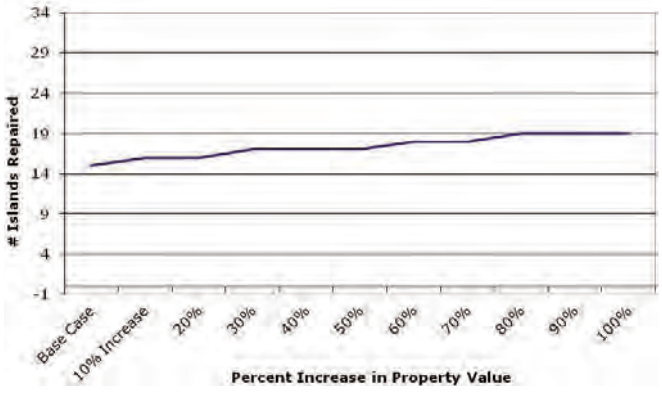

Figure 8 Effect of increasing property values on decision to repair islands after levee failure

not repaired by the model. These results are displayed in Figure 9.

Discount Rate

Discount rates were varied to see if results were sensitive to financial or social opportunity cost rates (a measure likely to depend on the decision-maker). For a high real annual discount rate of 7%, 16 islands were repaired. For the low discount rate of 3%, 14 islands were repaired. The upgrade decision responded to changes in discount rate in the opposite direction. One island (aside from Ryer, which is already at PL 84-99 standards) was upgraded with the low discount rate of 3%, with no islands upgraded for the base case of 5% and the higher discount rate. Less discounting of future costs and benefits encourages upgrades, but overall reduces the number of islands repaired.

Combining Optimistic Values

Unreasonably combining the most optimistic value for each parameter from the repair perspective (high discount rate, low initial probability of failure, low upgrade costs, tripled property value, and tripled "do not repair" cost), 30 islands of 34 are repaired and still no islands are upgraded. Unreasonably combining the most optimistic value of each parameter from the upgrade perspective (low discount rate, initial base case failure probabilities with reduction to 1% annual failure probability from upgrades, low upgrade costs, tripled "do not repair" costs and tripled property values), 28 islands are repaired and 24 islands are upgraded.

Results Summary

For all cases, we obtain a range of economic and risk-based upgrade and repair decisions. Results suggest that, of the 34 subsided islands analyzed, somewhere between 11 and 25 islands economically justify repair after a levee breach, and 0 to 23 islands justify current upgrades to PL 84-99 standards. For an unrealistic scenario in which *all* parameter values are altered to favor repair (within reasonable values) the number of islands repaired jumps to 30 of 34, and for a similarly unrealistic scenario for upgrades, the maximum number upgraded increases from 23 to 24. Even with unreasonably optimistic assumptions, it is uneconomical to upgrade all levees or to repair all islands.

The results of this analysis are similar to earlier work on upgrade and repair policy in the Delta. Logan (1990) studied the cost-effectiveness of a proposed DWR system-wide levee upgrade plan for the Delta. The cost for upgrading all islands was compared to the costs of a policy in which islands were not upgraded and were repaired post-failure. Logan's approach differs from ours in not using decision analysis or optimizing for individual islands. Instead, he pre-determined the number of islands to be repaired, and then applied Monte Carlo simulations to several stochastic variables to come up with a range of possible system-wide costs for each Delta levee policy. He calculated the expected costs of three reclamation policies: repairing all islands after they fail, repairing only 13 islands, or repairing no islands. His results suggested that *any* of the three policies analyzed would be more cost-effective than DWR's plan to upgrade the entire levee system. It did not make economic sense from a state-wide perspective to upgrade all Delta islands. These results are similar to ours, indicating much better economic value for a policy of limited and prioritized upgrades and repairs for Delta levees.

Caveats

This economic decision analysis for levee upgrades and repairs is based solely on the value of the land and assets of an island and the likelihood of failure under current conditions. There are four main limitations to this approach.

First, there are other reasons to assign higher values to specific islands. Most notably, allowing some islands to flood following failure might degrade Delta water quality for agricultural and urban uses (Lund and others 2008). Based on hydrodynamic modeling results, the western islands—Sherman, Twitchell, Brannan-Andrus, Jersey and Bradford—have the greatest effect on water quality and would be given higher value on this basis alone (Fleenor and oth-

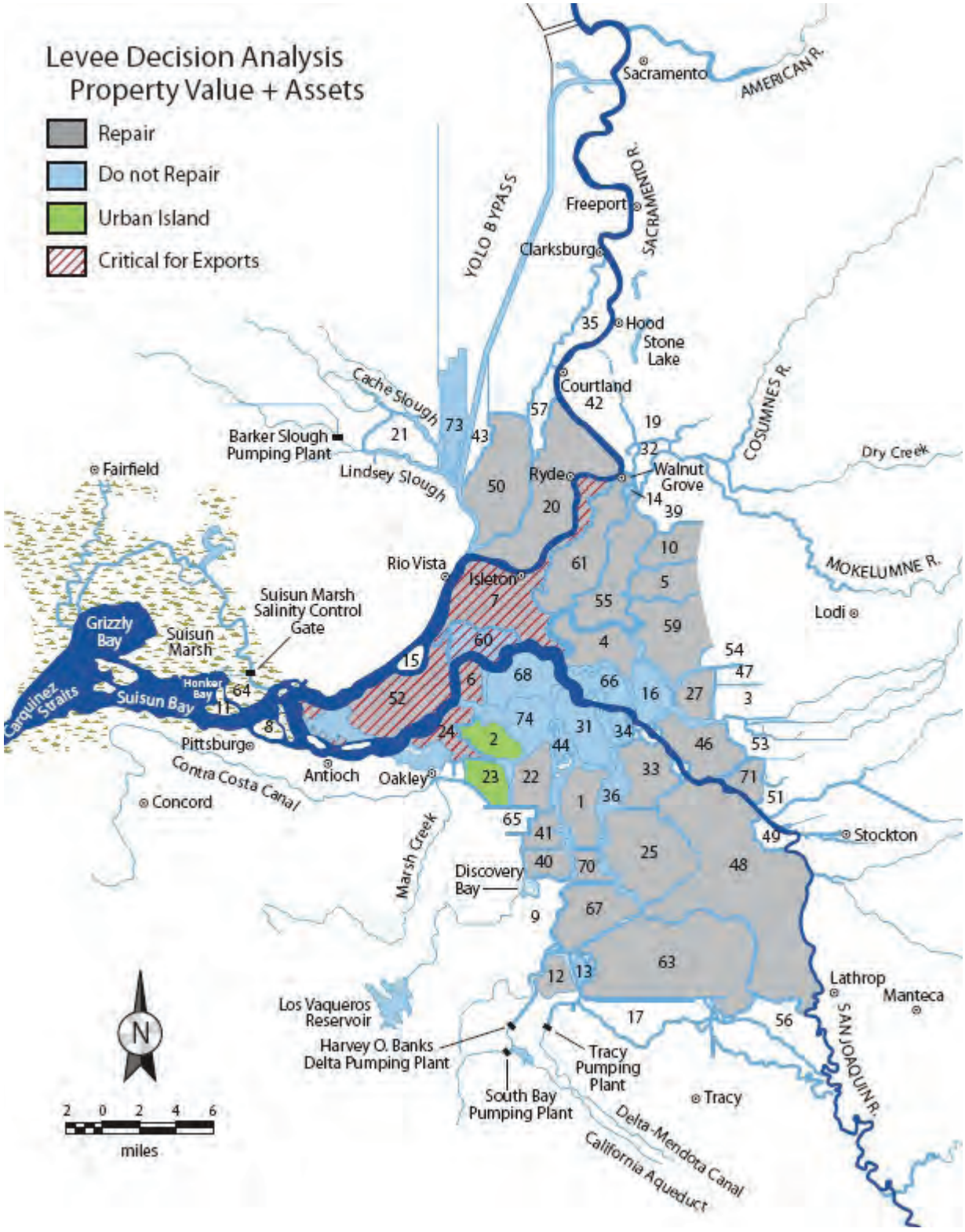

Figure 9 Repair decision using maximum property values and "do not repair" costs

ers 2008). It appears that other islands, in contrast, could be pre-flooded without harming water quality. A new state Delta levee policy would need to address how to mitigate effects for affected land-owners. Additionally, this model does not explicitly account for other cultural values such as legacy towns, or potential environmental costs and/or benefits, such as terrestrial sandhill crane habitat on Staten Island and potential positive habitat gains from flooded islands. However, the model can be used to experiment with the simple question of "how great must other values be" to alter a repair or upgrade decision, as our sensitivity analyses demonstrate.

The second main limitation is that the model does not yet incorporate future risk conditions. Since failure probabilities seem to be increasing due to subsidence, changing inflows, sea level rise and seismicity, the analysis presented here seems increasingly biased to favor upgrading and repairing islands with time. This limitation could be accommodated by a non-stationary dynamic programming formulation for each island (Zhu and others 2007), at some loss of simplicity and comprehensibility of the analysis.

Third, we computed the cost of not repairing an island, assuming that the flooding was unplanned, and that no private or public entity would be willing to fund repairs if the costs outweighed the economic value of the island. In other words, we did not calculate alternate lower "do not repair" costs where island flooding had been prepared for, either by previously moving or hardening infrastructure or by deciding to abandon particular groups of islands that might not greatly affect the vulnerability of other nearby levees. This also biases the model in favor of repairing islands, because "no repair" costs might be lower if the state or other infrastructure owners prepare in advance for flooding.

Finally, this analysis does not account for who pays for levee repairs and upgrades, nor the legal and political obstacles facing state-planned island flooding. The source and amount of funds available, whether federal, state or local, will have considerable influence on decision-making. Selective and well-planned island flooding in the Delta stands in stark opposition to California's current legal framework and policies for the Delta, which generally approach the Delta's levee network as a homogenous system (California Water Code Sections 12980–12985).

CONCLUSIONS

Linked human and natural systems that lack resiliency tend to undergo abrupt changes to new, irreversible regime states (Mount and Twiss 2005; Lund and others 2008, 2010). The Delta is a rigid, fragile system at high risk of undergoing just such an irreversible change. The current levee network that protects deeply subsided islands has high probabilities of failure, as a result of overtopping, seepage or collapse during earthquakes. These risks are likely to increase in the future, raising the likelihood of fundamental change. This common problem for deltas worldwide (Syvitski and others 2009) is exacerbated by California's susceptibility to earthquakes.

State and federal policy and the public's willingness to pay for upgrading and/or repairing Delta levees will modulate the nature of this change. Based solely on the net benefits and costs of such upgrades for 34 subsided islands in the Delta, it appears not to be cost-effective to upgrade all levees in the Delta to PL 84-99 standards or higher, based on the value of their land and built assets alone. In addition, it is not economically viable to repair between 4 and 23 islands (of 34 subsided non-urban islands examined) once they have flooded (Figure 4 and Table 3). We assume these islands will, with time, probably be abandoned by their owners, either before or after a levee failure. Conversely, some islands have sufficiently high value, either because of their land value and assets or the costs of replacing key infrastructure, to warrant repair investments after levee failure, at least for a time. Heavily urbanized islands require a more detailed analysis, and were not included in this assessment. The many islands that have not subsided below sea level, which we did not analyze, are likely to be sustainable for many decades.

The forces acting on the Delta and the costs of mitigating those forces lead us to conclude that much of the subsided Delta, composed of a network of levees that separate subsided land from the water, is about to undergo (or may already be undergoing) a transi-

tion. This new Delta will have little in common with the Delta of the early 1800s, since subsided island flooding will replace what was historically a freshwater tidal marsh—with open water more than 4.5 m deep in many places. The consequences of this transition are unknown, but will require those who manage the Delta to adapt to a new, evolving system with significant management challenges.

ACKNOWLEDGEMENTS

Sarah Swanbeck provided research support for this work. This analysis benefited greatly from discussions with levee experts familiar with the Delta, including Ross Boulanger, Gilbert Cosio, Joe Countryman, Gerald Galloway, Sergio Guillen, Roger Henderson, David Lawson, Michael Mirmazaheri, David Mraz, Michael Ramsbotham, Said Salah-Mars, Curt Schmutte, Raymond Seed, and several state and federal levee engineers who asked not to be identified. We also thank Ellen Hanak, Ignatius Anwanyu, Gerald Galloway, and Peter Rabbon for helpful reviews of an earlier draft. We are grateful for the funds provided by the David and Lucile Packard Foundation, Stephen D. Bechtel, Jr., and the Resources Law Foundation, which supported this work.

REFERENCES

Ang AH-S, Tang WH. 1975. Probability Concepts in Engineering Planning and Design, Vol. 1, Basic Principles. New York (NY): John Wiley & Sons.

Arrow K, Lind RC. 1970. Uncertainty and the Evaluation of Public Investment Decisions. American Economic Review 60(3):364-78.

Aven T, Kørte J. 2003. On the use of risk and decision analysis to support decision-making. Reliability Engineering and System Safety 79:289-299.

Bouma JJ, Francois D, Troch P. 2005. Risk assessment and water management. Environmental Modeling and Software 20:141-151.

Brocher TM, Boatwright J, Lienkaemper JJ, Prentice CS, Schwartz DP, Bundock H. 2008. The Hayward Fault — is it due for a repeat of the powerful 1868 earthquake? USGS Fact Sheet, U.S. Dept. of the Interior.

[CALFED IRP] CALFED Independent Review Panel. 2008. Review of the Delta Risk Management Strategy Phase 1 Report (Draft 4). Available from: http://calwater.ca.gov/science/drms/drms_irp.html.

Cayan DR, Bromirski PD, Hayhoe K, Tyree M, Dettinger MD, Flick RE. 2008a. Climate change projections of sea level extremes along the California coast. Climatic Change 87(1):S57–S73.

Cayan DR, Maurer EP, Dettinger MD, Tyree M, Hayoe K. 2008b. Climate change scenarios for the California region. Climatic Change 87(1):S21–S42.

Cheng C, Hsu N, Wei C. 2008. Decision-tree analysis on optimal release of reservoir storage under typhoon warnings. Natural Hazards 44:65-84.

Church JA, White NJ. 2006. Twentieth century acceleration in sea level rise. Geophysical Research Letters 33:(LO1602).

Davis DR, Kisiel CC, Duckstein L. 1972. Bayesian decision theory applied to design in hydrology. Water Resources Research 8(1):33-41.

Deverel S. 2007. Technical Memorandum Delta Risk Management Strategy (DRMS) Topical Area: Subsidence. Available from: http://www.drms.water.ca.gov/Updated2007/.

Eijgenraam CJJ. 2006. Optimal safety standards for dike-ring areas. Discussion paper. Netherlands: CPB Netherlands Bureau for Economic Policy Analysis.

Finch M. 1985. Earthquake damage in the Sacramento-San Joaquin Delta. California Geology (February):39-44.

Fleenor WE, Hanak E, Lund JR, Mount JR. 2008. Delta hydrodynamics and water salinity with future conditions. Appendix C. In: Lund J, Hanak E, Fleenor W, Bennett W, Howitt R, Mount J, Moyle P. Comparing futures for the Sacramento San Joaquin Delta. San Francisco (CA): Public Policy Institute of California. Available from: http://www.ppic.org/content/pubs/other/708EHR_appendixC.pdf.

Florsheim JL, Dettinger MD. 2007. Climate and floods still govern California levee breaks. Geophysical Research Letters 34:L22403.

Galloway GE, Boland JJ, Burby RJ, Groves CB, Longville SL, Link LE, Mount JF, Opperman J, Seed RB, Sills GL, Smyth JJ, Stork R, Thomas EA. 2007. A California challenge—flooding in the Central Valley. California Department of Water Resources. Independent Review Panel Report. Available from: http://www.water.ca.gov/news/newsreleases/2008/101507challenge.pdf.

Hobbs BF, Chao PT, Venkatesh BN. 1997. Using decision analysis to include climate change in water resources decision making. Climatic Change 37:177-202.

[IPCC] Intergovernmental Panel on Climate Change. 2007. Climate change 2007—impacts, adaptation and vulnerability. Contribution of Working Group II to the Fourth Assessment Report of the IPCC. Available from: http://www.ipcc.ch/ipccreports/ar4-wg2.htm.

Linsley RK, Franzini JB, Freyberg DL, Tchobanoglous G. 1992. Water resources engineering, 4th ed. U.S.: Irwin/McGraw-Hill. 768 p.

Logan SH. 1989. An economic analysis of flood control policy in the Sacramento-San Joaquin Delta. California Water Resources Center Report. University of California.

Logan SH. 1990. Simulating costs of flooding under alternative policies for the Sacramento-San Joaquin River Delta. Water Resources Research 26(5):799-809.

Luers AL, Moser SC. 2006. Preparing for the impacts of climate change in California: opportunities and constraints for adaptation. California Climate Change Center Report 500-2005-198-SF. Available from: http://www.energy.ca.gov/2005publications/CEC-500-2005-198/CEC-500-2005-198-SF.PDF

Lund J, Hanak E, Fleenor W, Bennett W, Howitt R, Mount J, Moyle P. 2007. Envisioning futures for the Sacramento-San Joaquin Delta. San Francisco (CA): Public Policy Institute of California. Available from: http://www.ppic.org/main/publication.asp?i=671

Lund J, Hanak E, Fleenor W, Bennett W, Howitt R, Mount J, Moyle P. 2008. Comparing futures for the Sacramento-San Joaquin Delta. San Francisco (CA): Public Policy Institute of California. Available from: http://www.ppic.org/content/pubs/report/R_708EHR.pdf.

Lund J, Hanak E, Fleenor W, Bennett W, Howitt R, Mount J, Moyle P. 2010. Comparing futures for the Sacramento-San Joaquin Delta. Berkeley (CA): University of California Press.

Maguire LA. 2004. What can decision analysis do for invasive species management? Risk Analysis 24(4):859-868.

Moss E, Eller M. 2007. Estimating the probability of failure and associated risk of the California Bay Delta Levee System. ASCE Geotechnical Special Publication, GSP 170 (Special Issue on Probabilistic Applications in Geotechnical Engineering).

Mount JF, Twiss R. 2005. Subsidence, sea level rise, seismicity in the Sacramento-San Joaquin Delta. San Francisco Estuary and Watershed Science [Internet]. Available from: http://www.escholarship.org/uc/item/4k44725p.

Pratt JW, Raiffa H, Schlaifer R. 1964. The foundations of decision under uncertainty: An elementary exposition. American Statistical Association Journal June 1964:353-375.

Ramsey MH. 2009. Uncertainty in the assessment of hazard, exposure, and risk. Environmental and Geochemical Health 31:205-217.

Stewart I, Cayan DR, Dettinger MD. 2005. Changes in snowmelt runoff timing in western North America under a 'business as usual' climate change scenario. Climate Change 62:217-232.

Suddeth R, Mount J, Lund J. 2008. Levee decisions and sustainability for the Sacramento-San Joaquin Delta. Appendix B. In: Lund J, Hanak E, Fleenor W, Bennett W, Howitt R, Mount J, Moyle P. Comparing futures for the Sacramento-San Joaquin Delta. San Francisco (CA): Public Policy Institute of California. Available from: http://www.ppic.org/content/pubs/other/708EHR_appendixB.pdf.

Syvitski JPM, Kettner AJ, Overeem I, Hutton EWH, Hannon MT, Brakenridge GR, Day J, Vörösmarty C, Saito Y, Giosan L, Nicholls RJ. 2009. Sinking deltas due to human activities. Nature Geoscience (2):681-686. Available from: http://www.nature.com/ngeo/journal/v2/n10/full/ngeo629.html.

Tebbens RJD, Pallansch MA, Kew OM, Sutter RW, Aylward RB, Watkins M, Gary H, Alexander J, Jafari H, Cochi SL, Thompson KM. 2008. Uncertainty and sensitivity analyses of a decision analytic model for posteradication polio risk management. Risk Analysis 28(4):855-876.

Torres RA, Abrahamson NA, Brovold FN, Harder LF, Marachi ND, Neudeck CH, O'Leary LM, Ramsbotham M, Seed RB. 2000. Seismic vulnerability of the Sacramento-San Joaquin Delta levees. Report of the Levees and Channels Technical Team, Seismic Vulnerability Sub-Team. Sacramento (CA): CALFED Bay-Delta Program.

URS Corporation, J. R. Benjamin & Associates. 2009. Delta Risk Management Strategy (DRMS) Phase 1 Risk Analysis Report. Prepared for the California Department of Water Resources.

[USACE] U.S. Army Corps of Engineers. 1996. Engineering and design – risk-based analysis for flood damage reduction studies. Department of the Army. Manual No. 1110-2-1619.

[USACE] U.S. Army Corps of Engineers. 1999a. Tools for risk-based economic analysis. Department of the Army, Institute for Water Resources. IWR Report 98-R-2.

[USACE] U.S. Army Corps of Engineers. 1999b. An overview of probabilistic analysis for geotechnical engineering problems. Department of the Army. Engineering Technical Letter 1110-2-556.

Van Dantzig D. 1956. Economic decision problems for flood prevention. Econometrica 24:276-287.

Van Manen SE, Brinkhuis M. 2005. Quantitative flood risk assessment for polders. Reliability Engineering and System Safety 90:229-237.

Voortman HG, van Gelder PHAJM, Vrijling JK. 2002. Risk-based design of large-scale flood defense systems. Cardiff 28th International Conference on Coastal Engineering July 2002:2373-2385.

Woodall DL, Lund JR. 2009. Dutch flood policy innovations for California. Journal of Contemporary Water Research and Education (141):1-16. Available from: http://cee.engr.ucdavis.edu/faculty/lund/papers/Woodall2009.pdf.

Wood E. 1977. An analysis of flood levee reliability. Water Resources Research 13(3):665-67.

WETLANDS SCIENCE PROGRAM

Mercury and Methylmercury Processes in North San Francisco Bay Tidal Wetland Ecosystems

Oakland, California

CONTRIBUTION NO. 621
MAY 2008

CalFed ERP02D-P62 Final Report

Submitted to
California Bay-Delta Authority Ecosystem Restoration Program

Donald Yee, Joshua Collins, Letitia Grenier, San Francisco Estuary Institute
John Takekawa, Danika Tsao-Melcer, Isa Woo, Steven Schwarzbach, USGS BRD
Mark Marvin-DiPasquale, Lisamarie Windham, USGS Menlo Park
David Krabbenhoft, Shane Olund, John DeWild, USGS Middleton, WI

SAN FRANCISCO ESTUARY INSTITUTE
7770 Pardee Lane, 2nd FLoor, Oakland, CA 94621 | www.sfei.org

USGS science for a changing world

This report should be cited as:
Yee, D., J. Collins, L. Grenier, J. Takekawa, D. Tsao-Melcer, I. Woo, S. Schwarzbach, M. Marvin-DiPasquale, L. Windham, D. Krabbenhoft, S. Olund and J. DeWild. 2008. Mercury and Methylmercury Processes in North San Francisco Bay Tidal Wetland Ecosystems. CalFed ERP02D-P62 Final Report. Submitted to California Bay-Delta Authority Ecosystem Restoration Program. SFEI Contribution #621. San Francisco Estuary Institute, Oakland, CA.

Mercury and Methylmercury Processes in North San Francisco Bay Tidal Wetland Ecosystems

CalFed ERP02D-P62 Final Report

Donald Yee, Joshua Collins, Letitia Grenier, San Francisco Estuary Institute*
John Takekawa, Danika Tsao-Melcer, Isa Woo, Steven Schwarzbach, USGS BRD
Mark Marvin-DiPasquale, Lisamarie Windham, USGS Menlo Park
David Krabbenhoft, Shane Olund, John DeWild, USGS Middleton, WI
*7770 Pardee Lane, Oakland, CA 94621 *tel*: (510)746-7334 *fax*: (510)746-7300 http://www.sfei.org *email*:donald@sfei.org

B. Introduction

1. Rationale

Efforts to restore wetland ecosystems are being proposed or underway in various areas of the San Francisco Bay estuary. Although wetland restoration provides ecological benefit, in some cases restoration of mercury-contaminated areas may negatively impact wildlife or human health. Among the concerns are impacts of accumulated mercury (Hg) on vertebrates such as state-listed threatened species like the California Black Rail that are linked closely with wetland habitats. The goals of this study are to improve understanding of environmental processes including: 1) mercury (Hg) and methylmercury (MeHg) distributions in tidal wetlands; 2) factors influencing the net methylation of Hg in these areas; 3) identifying key plant-Hg interactions; 4) MeHg exposure potential risk in California Black Rails and other wetland species; and 5) potential contribution of MeHg in tidal wetlands to the rest of the San Francisco estuary. Improved understanding of these ecosystem processes will allow better management of wetland restoration through informed decision-making to minimize negative impacts.

Previous studies (primarily freshwater) have found correlations between MeHg watershed loads and resident biota concentrations with percentage of wetland coverage in watersheds (Hurley et al. 1995; Rudd 1995; St. Louis et al. 1996), but identifying specific causal factors (chemical, physical, hydrological) with wetland abundance has remained elusive. Hg in soils and vegetation is released to aquatic environments after flooding and transformed into MeHg, with resulting increases in fish tissue concentrations (Bodaly et al. 1984; Hecky et al. 1987; Kelly et al. 1997). MeHg is particularly high in newly flooded wetlands, with large quantities of labile organic carbon and electron acceptors available for bacteria to generate anaerobic conditions (Kelly et al. 1997). Newly flooded restored wetlands in the Bay-Delta could also result in a similar spike in environmental MeHg concentrations, but a major concern for long-term ecosystem health is repeated production and distribution of MeHg.

Environmental parameters such as total mercury (THg) (Watras et al. 1995; Benoit et al. 1998), salinity (Mason et al. 1996; Barkay et al. 1997), sulfate (Oremland et al. 1995; Chen et al. 1997; Benoit et al. 1998; Gilmour et al. 1998), sulfide (Benoit et al. 1999), selenium (Pelletier 1985, Jin et al. 1999, Southworth et al. 2000), temperature (Choi et al. 1994), pH (Xun et al. 1987; Westcott and Kalff 1996; Rose et al. 1999), dissolved or total organic carbon (Krabbenhoft et al. 1995; Westcott and Kalff 1996; Barkay et al. 1997), and wetting and drying cycles (Krabbenhoft et al. 2005) have been shown to influence MeHg production, degradation, or bioaccumulation. Although these factors have been primarily studied in freshwater systems, some of these also may interact antagonistically or synergistically and vary in estuarine wetlands spatially and temporally. This project aims to improve understanding of these factors on Hg processes in salt marshes.

2. Current Conceptual Model

Combinations of interconnected factors can result in negative impacts from anthropogenic mercury contamination in wetlands. This can occur when: 1) Hg is elevated above natural concentrations; 2) Hydrologic and geomorphologic factors cause conditions suitable for mercury methylation; 3) Plants or other sources supply organic material and Hg to bacteria; 4) *In situ* bacterial production generates MeHg; 5) MeHg transfers from the zone of production to enter the base of the food web within the marsh or exported to other ecosystems; 6) MeHg bioaccumulates in the food web to harmful levels.

Tidal marsh morphology results from the interactions of abiotic and biotic forces shaping the landscape: rain, fluvial, and tidal flows transport water and sediments; vegetation builds the marsh plain, trapping sediments and adding organic detritus and lower molecular weight substrate. Problems may occur in tidal wetlands due to their tendency to entrap fine Hg laden sediments and hydro-geomorphic and soil characteristics conducive to net MeHg production in habitats supporting wildlife of concern. We expect these conditions will occur in predictable spatial and temporal patterns due to the physiographic template of mature marshes. These wetlands may be stratified into "habitat elements" which share geomorphic characteristics (e.g. large or small channels, marsh plains along channel edges or interiors away from channels). This template serves as our sample frame for assessing patterns of MeHg production that might be translated into habitat design and management recommendations.

3. Project Approach

Field sampling

Three wetlands along the tidal reach of the Petaluma River were studied: Black John Slough (BJ), nearest the mouth of the river; Mid-Petaluma Marsh (MP), a well-established ancient marsh approximately halfway between the city of Petaluma and San Pablo Bay; and Gambinini Marsh (GM), the site with most freshwater influence, adjoining a ranch just downstream of the City of Petaluma. A map of the study area is shown in Figure B.3.1. These wetlands were selected as our study areas for a number of reasons: 1) These wetlands are located within the California Bay-Delta Authority (CBDA) geographic area of interest. 2) The studied wetlands span a range of salinities (<2 to 30 ‰) found in various tidal wetlands in the region. 3) These are mature marshes with many of the desired endpoint habitat characteristics (e.g. elevation, channel networks, vegetation) for local wetland restoration efforts. 4) The location of these study areas within a single watershed would be expected to reduce potential variation from spatial factors such as differing water and sediment Hg sources which would otherwise require much more intensive sampling efforts to understand. 5) A state-listed threatened species of interest, the California black rail, resides in these wetlands and may be potentially affected by Hg exposure; avian experts in the group (USGS BRD and Avocet Associates) confirmed the suitability of habitat and presence of California black rail in the studied wetlands in pre-sampling surveys.

In 2005, this study focused on two components or "habitat elements" of the tidal marsh physiographic template: medium/large sloughs and marsh plains. One pair of replicate sites for each habitat element was sampled from each of the three wetlands (BJ, MP, GM), for a total of 12 sites (3 wetlands × 2 habitat elements × 2 replicates) sampled in each event (April and August) for sediments. Water samples were collected as grab samples pumped from near the surface (~10cm depth) of medium/large (3rd order, typically 1-2 m wide) slough channels

near high slack tide. Sediment samples from each site were collected as composites along defined transects, along the bottom of medium/large (3rd order) slough channels and perpendicular to these sloughs on the marsh plain (Figure B.3.2). Slough sediment samples transects were collected heading upstream of the channel flow in the slough at the time of sampling (generally during an ebbing tide) to minimize disturbance of samples collected later in the transect sequence.

For 2006, these habitat elements were more finely stratified between small (1st order, generally 20-50 cm wide) and medium/large (3rd order) sloughs, and edge (adjacent to medium/large sloughs) and interior (away from sloughs) marsh plain zones. These four habitat elements were each sampled in replicate (one pair of sites for each habitat element) within each of the three wetlands, for a total of 24 locations (3 wetlands × 4 habitat elements × 2 replicates). Water samples were collected as grab samples from the slough sites near high slack tide, pumped from ~10 cm depth in larger sloughs and from near the surface (~2-5 cm) in first order sloughs (which on some events had <20 cm water depth even at high slack tide) in order to minimize risk of stirring up bed sediments while sampling. Sediment samples in 2006 were composited from 7 m^2 areas, calculated for the geometry of the specific habitat element sampled, i.e. rectangular areas for slough and marsh plain edge sites, and circular areas for marsh plain interior sites (Figure B.3.3). Long rectangular zones were sampled for sloughs and marsh plain edge (of slough) sites to mirror slough geometry. Marsh plain interior sites, typically located >10 m from surrounding sloughs, were sampled in tighter (circular, although square would have been equally suitable) areas to better avoid approaching smaller channels and mosquito ditches than in the long transects sampled in 2005. Small (1 m^2) plots were devegetated in marsh plain edge and interior sites to examine plant interactions on the marsh plain. Although the smaller areas from which devegetated samples were collected could not capture or integrate spatial variation on >1 m scales, smaller plots were chosen to leave a smaller footprint of impact on the sampled sites than would occur if directly comparable areas of 7 m^2 were devegetated.

Water samples collected in the field were immediately chilled in dark coolers on wet ice. Upon return to local accommodations, water samples to be used for chemical analyses were filtered (0.7 μm nominal pore size quartz fiber filters) to separate particulate and filtered fractions, which were preserved by freezing, or by refrigeration after acidification, respectively. Water samples collected for net demethylation/reduction incubations were stored refrigerated without acidification. Most sediment samples collected from the field were analyzed as subsamples of the composites used in laboratory incubations to determine methylation and demethylation rates. The portions of sediment composites used for incubations were kept chilled from the time of field collection until use in laboratory incubations to maintain microbial viability. Subsamples of sediment composites taken for chemical analysis were immediately frozen in the field on dry ice to minimize degradation. Core samples taken in 2005 were not used in any incubation experiments and were frozen in the field and analyzed as individual sections to determine lateral and vertical spatial variations in MeHg and Hg concentrations within each of the sites. Similarly, several surface sediment samples from 2006 were frozen immediately in the field and analyzed as separate uncomposited grabs to examine within site variability.

Black rails were captured and marked under California Department of Fish and Game Memorandum of Understanding with USGS Scientific Collection permit SC-801158-03, U.S. Fish and Wildlife Service permit 22911, and with guidance and approval from the USGS

Western Ecological Research Center Animal Care and Use Committee. We captured a total of 130 black rails in the spring (10 March - 25 April 2005 and 6 March - 13 April 2006) and summer (12 -28 July 2005 and 10 - 25 July 2006). Each captured black rail was banded, and then mass (g), wing chord, culmen, and tarsus length (mm) were measured. Sex and age was determined from plumage characteristics (P. Pyle and S. Howell, Point Reyes Bird Observatory, personal communication). When plumage was not definitive, a small blood sample was collected for DNA-based sex determination (Zoogen Inc., Davis, CA). We collected a small number of feathers (10-15) from each bird's back (n=127), and collected blood samples (<1% body mass) when possible (n=66) for Hg, MeHg, Selenium (Se), and stable isotope analysis.

In spring 2005 and 2006, we fitted 48 black rails with 0.9 g radio transmitters with anterior and posterior suture channels. Transmitters were attached using cyanoacrylic glue and absorbable sutures anchored at the anterior and posterior ends of the transmitter according to methods previously described (Martin & Bider 1978; Wheeler 1991; Robert & Laporte 1999). Radio-marked individuals were monitored briefly to ensure ease of movement after transmitter attachment and released at the site of capture.

Target marsh invertebrates (surface scraper snails, detrivore amphipods, and predacious ground spiders) were identified prior to the study based on relative abundance at all sites, and by their representation of foraging guilds. Target invertebrates were collected in the summer of 2005 and 2006 at all sites and were kept alive for one day to purge gut contents. Snails were de-shelled and all other invertebrates were analyzed whole. Samples were triple-washed in DI water and sent to Batelle Marine Sciences Laboratory for MeHg analyses and Northern Arizona University for stable isotope analyses. Additional invertebrates found in the marsh were opportunistically collected, purged, cleaned, and analyzed for stable isotopes in 2005.

Target slough biota (filter feeding mussel, omnivorous crabs, and fish) were identified prior to the study based on their guild representation and presence at all sites. Target slough biota were collected in the summer of 2005 and 2006 and were kept alive for one day to purge their gut contents. Crabs, mussels, and clams were de-shelled, and all other invertebrates and small fish were analyzed whole. Samples were triple-washed in DI water and sent to Batelle laboratories for MeHg analyses and Northern Arizona University for stable isotope analyses. Additional invertebrates found in the marsh were opportunistically collected, purged, cleaned, and analyzed for stable isotopes.

Laboratory incubations

Stable isotopes of inorganic Hg (^{201}Hg) and MeHg ($Me^{199}Hg$) were used in controlled incubation experiments to determine the rates of Hg reduction and MeHg demethylation in sunlight. Photo-reduction is the light-mediated transformation of ionic Hg (Hg^{2+}) to elemental gaseous Hg (Hg^0) and subsequent evasion from the water. Photo-demethylation, on the other hand, is the cleaving of the methyl group from the Hg atom as a result of absorbing light. The reader is referred to Krabbenhoft (2002) for more details. For this study, we collected 5 liters of both filtered and unfiltered water from one of the large slough sites in each of the wetlands to test the effects of varying concentrations of turbidity and DOC on photo-chemical reactions. In each vessel, $^{201}Hg^{2+}$ and $Me^{199}Hg^{+}$ were added at environmentally relevant levels as tracers of these processes. The vessels were exposed to sunlight for 7 days, constantly sparged with air, and gold traps on the exhaust line for each

vessel captured any evaded Hg (both amended Hg isotopes and ambient Hg in the samples). The unfiltered water samples were constantly stirred with Teflon-coated, magnetic stir bars. The Hg reduction rate was calculated by the appearance of gaseous ^{201}Hg, whereas MeHg demethylation was estimated by the formation of un-methylated ^{199}Hg.

Mercury methylation and demethylation rates in sediment were also determined using laboratory incubations. Chilled sediment composite samples in jars with minimal/no headspace were taken to the laboratory for incubation within (48) hours of collection and opened in an anaerobic environment. Potential rates of MeHg production were calculated as the product of the radiotracer derived $^{203}Hg(II)$-methylation rate constant (k_{meth}) and the independently measured *in situ* $Hg(II)_R$ concentration. This approach factors in both a measure of the activity of the native Hg(II)-methylating microbial community and a measure of Hg(II) pool size that is available to that community. Sub-samples (3.0 g) of homogenized sediment from each site were incubated in duplicate for four hours after the addition of $^{203}HgCl$ (0.1 ml; specific activity adjusted to 1 μCi/μg; total Hg per sample = 500 ng/g wet sediment). Incubations were arrested by flash freezing samples on dry ice in ethanol. A single killed control (frozen at time = 0) was included with each site specific set. Radio labeled methylmercury ($Me^{203}Hg$) formed during the incubation was subsequently extracted with toluene and quantified via gamma radiation counting. Values for k_{meth} were subsequently calculated as previously described (Marvin-DiPasquale et al. 2003).

Reactive mercury ($Hg(II)_R$) is an operationally defined proxy measure of the pool of inorganic Hg(II) most readily available for Hg(II)-methylation, and is based upon the readily tin-reducible fraction of THg in a whole sediment sample. Previously sub-sampled and frozen sediment was thawed under anoxic conditions and slurried with anoxic 0.5 M HCl. The slurry was transferred to a gas purging bubbler and reacted with $SnCl_2$ for 15 minutes. The evolved Hg^0 gas was captured on a gold trap, thermally desorbed, and measured via cold vapor atomic fluorescence. Further details regarding this method are published elsewhere (Marvin-DiPasquale & Cox, 2007), and unpublished data indicates that this fraction is highly correlated with the amount of MeHg produced in controlled sediment incubation experiments (Bloom et al. 2006, Marvin-DiPasquale et al. 2006).

Microbial sulfate reduction (SR) rates were assayed via the $^{35}SO_4^{2-}$ amendment technique (Jørgensen 1978). Sub-samples for SR consisted of 1.5 g of sediment per vial and were collected under anoxic conditions and incubated in parallel with those for k_{meth}. Replication consisted of duplicate live (incubated) and one killed control sample per site. Samples for SR were amended with approximately 1.0 μCi of carrier-free $^{35}SO_4^{2-}$ (0.05 ml of a 20 μCi/ml working stock of $Na_2{}^{35}SO_4$). Incubations were arrested by the addition of 1 ml of 10% (w/v) zinc-acetate and subsequent freezing in an ethanol/dry ice bath. Upon thawing, total reduced sulfur (TRS) was extracted via distillation with an acidic chromium solution, and measured for beta radioactivity (Fossing & Jørgensen 1989). Rate constants for SR were calculated as the fraction of ^{35}S-TRS produced, relative the amount of $^{35}SO_4^{2-}$ added, normalized by the incubation time. Rates of SR were then calculated from the site-specific rate constants and the *in situ* whole sediment SO_4^{2-} concentration (Marvin-DiPasquale and Capone 1998).

Laboratory analyses

Brief descriptions of the methods for THg and MeHg analyses are provided here; the reader is referred to the cited reports in this section for more details. Water, sediment, and plant

biomass samples were analyzed at the USGS Mercury Research Laboratory located in Middleton, WI. Water samples were analyzed for THg using EPA method 1631 (USEPA 2002), which is a multi-step analysis with sample pre-oxidation, purge and trap, and cold vapor atomic fluorescence spectrometry (Olson & DeWild 1999). For sediment and tissue (plant) samples the USGS Mercury Lab employed additional acid digestion and oxidation steps to improve analytical performance. Water samples were analyzed for methylmercury by distillation, aqueous ethylation, purge and trap, and CVAFS (Olson & DeWild 1999; DeWild et al. 2002), and like the THg procedure, sediment and plant samples were first processed with an additional acid digestion step. Standard QC samples were run with all analytical batches. Digestion blanks using all reagents employed through all the analytical steps were measured, and subtracted from the final result. Field blanks were taken during each field sampling event, and the sample results used to provide quality assurance (QA) levels of the overall results. Standard Reference Materials (SRMs) were used for all THg and MeHg analyses on sediments and plants. For this study, the USGS Mercury Lab used IAEA 405 as an SRM to ensure the accuracy of the analytical results, with SRM acceptance limits within ± 10% of the certified value. Because there are no certified reference waters for Hg at concentrations relevant to environmental samples, the USGS lab used a commercially available Hg standard, which was verified against a certified NIST standard for THg. At least 10 percent of all THg analyses were run in replicate and agreed within ± 20% (acceptance criteria for the batches run).

Whole sediment acid volatile sulfur (AVS) was quantified by USGS WRD-CA using a modified acid distillation approach (Zhabina & Volkov 1978). Upon sub-sampling, 1.0-1.5 g of homogenized whole sediment was accurately weighed (± 0.01 g) and transferred into a 10 ml serum vial, under anoxic conditions. Sub-samples were preserved with the addition of 5.0 ml of anoxic 10% (w/v) zinc-acetate solution and stored frozen (-20 ^{o}C) until further analysis. Upon partial thawing, the sample was distilled under anoxic conditions in an acidic solution of titanium chloride. The liberated H_2S gas was trapped as ZnS precipitate in a 10 ml solution of 10% (w/v) zinc acetate. The ZnS precipitate solution was subsequently sub-sampled in duplicate and quantified by colorimetric analysis (Cline 1969).

Total mercury analyses of animal tissue samples (bird feathers, invertebrates) were performed by the U. S. Geological Survey, Davis Field Station Mercury Lab. Total mercury was analyzed following EPA Method 7473 on a Milestone DMA - 80 Direct Mercury Analyzer using an integrated sequence of drying (160 °C for 140 s), thermal decomposition (850 °C for 240 s), catalytic conversion, and then amalgamation, followed by atomic absorption spectroscopy. Prior to each analytical run, the analyzer was calibrated with dilutions of a certified mercury standard solution. Quality assurance measures included analysis of two certified reference materials (either dogfish muscle tissue (NRCC DORM-2), dogfish liver (NRCC DOLT-3), or lobster hepatopancreas (NRCC TORT-2), two system and method blanks, two duplicates, one matrix spike, and one matrix spike duplicate per sample batch. Total mercury was detected in blanks (range 0.01 ng/g to 0.45 ng/g dry weight, dw) and results were corrected then rounded to two significant figures μg/g. Recoveries on certified reference materials analyzed by the lab averaged (mean ± standard deviation, sd) 100 ± 4% of the target values, and duplicates were always within ± 10% RPD (average 2%).

Methylmercury in bird blood samples and invertebrate tissues was analyzed by Battelle using a modification of EPA Method 1630. Solid samples were freeze-dried and ball-milled to

homogenize. Samples were digested in a solution of 25% KOH in methanol at 45 °C for 4 hours, then diluted with methanol and DI water, ethylated, purged and trapped, and analyzed by CVAFS. MeHg was below detection limits in all blanks, and MeHg results were not blank corrected. Laboratory QC sample results were generally good, with measurements on sample replicate analyses all within ± 20% RPD (average 6% RPD), and recoveries on reference material (NRCC DORM-2, DOLT-2) always within ± 20% of the target value (mean ± sd of 106 ± 11% recovery).

Plant biomass metrics were assessed using standard methods, as described by Callway et al. (2001). Live root identification was confirmed with vital staining (tetrazolium red). Mercury analysis of additional plant material was performed according to Olson and DeWild (1999), and plant tissue samples were cleaned thoroughly, and rinsed with 1% EDTA prior to analysis to remove surface contamination. Porewater acetate was analyzed by HPLC (Hines et al. 1994). Dissolved mercury release onto leaf surfaces was assessed in field with short-term incubations, including control filters to account for atmospheric deposition (Windham et al. 2001).

Stable isotope samples for biota were analyzed by Northern Arizona University Colorado Plateau Stable Isotope Laboratory, where tissues were ground, dried, weighed, and packed into tin capsules for analysis. Isotopic composition and C and N concentrations of each sample were measured on continuous-flow mode using a ThermoFinnigan Delta ^{plus} Advantage gas isotope ratio mass spectrometer (Waltham, MA) interfaced with a Costech ECS 4010 elemental analyzer (Valencia, CA). Peach leaf (NIST 1547) was the main working standard to examine isotopic/elemental drift within and throughout the run. External precision on these standards were ± 0.10‰ or better for $\delta^{13}C$ and ± 0.20‰ or better for $\delta^{15}N$. As an added check of instrument performance and sample homogeneity and reproducibility, duplicates were interspersed throughout each run. Isotope values are expressed as $\delta^{13}C$ or $\delta^{15}N$ determined by the following equation:

$$\delta^{13}C \text{ or } \delta^{15}N = [(R_{sample}/R_{standard})-1] \times 1000,$$

where $R= {}^{13}C/{}^{12}C$ or $ {}^{15}N/{}^{14}N$. International standards used here include: carbonate rock from the Vienna Pee Dee Belemnite formation for carbon and atmospheric nitrogen (air).

4. Management goals and objectives addressed by the project

The CBDA Mercury Strategy (Wiener et al. 2003) included the following core components (in italics) that were most directly addressed by this project in the ways listed below:

1) *Quantification and evaluation of Hg and MeHg sources*- the study of MeHg processes in existing tidal wetlands helps in quantifying contribution to current Hg exposure to humans and wildlife;

3) *Quantification of effects of ecosystem restoration on MeHg exposure*- restoration effects can be projected by increases in wetland acreage with similar function as existing mature marshes; and

5) *Assessment of ecological risk*- California Black Rail, a species potentially at risk, and other food web components of tidal wetlands were directly studied for Hg exposure and accumulation in this project.

C. Project Timetable and Milestones

The project started in November 2004 with completion scheduled in April 2008. The first two field sampling events occurred in April and August 2005. After amendment to the sampling plan, two additional field collections were conducted in April and August 2006. Water and sediment field samples were primarily collected in those four sampling events, with the biota sampling occurring over several weeks following each of those events. Tidal monitoring to improve tidal parameter estimates (inundation frequency, mean tide, high water, and low water) was conducted March 2006- September 2007, and follow-up work mapping marsh plain elevations was done in spring and summer 2007. The research team has been engaged in final data synthesis since the latter part of 2007 to the project end, and plan to prepare manuscripts on various project components for publication in the peer-reviewed literature. Results from this project have been presented in numerous public forums (see Section F).

D. Project Highlights and Results

1. Hydro-Geomorphic Interactions (SFEI)

Hydrologic flows are critical to the morphology and function of wetlands. Daily tides transport water and sediments within wetland sloughs, while overbanking spring tides periodically transport water and sediments to the marsh plain. Episodic rains and river flows further add to the transport of water and sediment during the wet season, with potentially large interannual variation. Observations of wetland hydraulic processes provide a context for understanding much of the biogeochemical variation seen within and among wetlands.

1) Marsh plain and slough habitat components of wetlands responded on different time scales to hydraulic forcing, largely in relation to their connectivity.

A conceptual model of wetland form and hydrology is shown in Figure D.1.1. Although there are large hydrologic and geomorphic differences between wetland slough and marsh plain habitats, there are more subtle differences within these broader habitat elements which potentially influence the geochemical processes and distributions of THg, MeHg and other contaminants in wetlands. Differences were found in the hydrologic characteristics of these finer resolved habitats. A tide gage was deployed at one 3rd order slough channel site in each wetland to determine mean tide levels at each wetland, and additional continuous monitoring probes (channel water electrical conductivity, sediment redox potential, and temperature) were deployed at one site (only at GM due to vehicle accessibility within ~100 m of the gage site to allow data download and equipment servicing, yet restricted access to the general public to reduce tampering/disturbance, behind a locked gate on private property). Figure D.1.2 shows a typical rapid response of channel water and marsh plain edge groundwater levels in contrast to the muted response of marsh plain groundwater levels to tidal forces. Channel water levels often varied ~1 m within a day, while aside from overbanking events (when water inundated the marsh plain surface), levels at the marsh interior groundwater monitoring well location typically varied <0.1 m/day. Marsh plain edges, with groundwater rising nearly to the level of the channel in non-overbanking flood tides, and dropping rapidly during ebb tides, were better-drained than marsh plain interiors. During sampling events scheduled on days immediately following overbanking events, standing surface water was

seldom found at any marsh plain edge sites, except at higher high tide, when a narrow (<1 m wide) vegetated zone along channel banks would sometimes be covered with water.

2) Hydraulic and biotic forces interacted on daily and shorter time scales within the marsh, but MeHg in sediments did not respond on such short time scales.

We monitored one slough sampled (in 2005) at GM and a location on the adjacent marsh plain (~20 m from the slough) continuously for several 2-3 week periods during March to October 2006 to examine changes on small time scales. Figure D.1.3 shows influences of hydrology, solar radiation, plants, and microbiology on marsh plain redox potential (Eh measured at 2 cm depth) and groundwater level, monitored over daily and longer-term cycles. The groundwater level on the marsh plain responded to tidal, solar, and plant influences. Like in other monitored periods (e.g. Figure D.1.2) groundwater drew down in a sequence of neap tides. On the first overbanking tide (June 19), the water level at the marsh interior monitoring well tracked the flood and ebb of the overbanking tide, then drew down gradually over several hours as water infiltrated (laterally) from the well to equilibrate with the surrounding groundwater level, while water on the marsh surface infiltrated (vertically) to recharge the groundwater. In subsequent overbanking tides, the process repeated, until the groundwater level rose to equilibrate near the marsh plain surface, with minimal drawdown after the tide ebbed (e.g. June 27). On ensuing neap tides, the groundwater level resumed drawing down, primarily during daytime with higher temperatures and evapotranspiration rates (seen in higher slopes for mid-day versus overnight changes in groundwater level).

A midday maximum in sediment redox potential (a swing of 100-150 mV each day) also occurred, peaking with maximum solar radiation and photosynthetic activity, and dropping rapidly at night, when plant root and soil bacteria respiration dominated. Solar radiation was measured at a different site (in Santa Rosa, CA) ~30 km N-NW of GM, but the close response of surface redox to midday dips in radiation (e.g. 6/27 and 6/28) suggests similar weather conditions at both locations. Despite these rapid changes in sediment redox, MeHg concentrations in samples did not depend on the time of day a sample was collected. A small test in which follow-up grab samples were taken every two hours on the marsh plain interior at GM in August 2006 showed no significant change (Tukey HSD $p>0.05$) in sediment MeHg over the day, whereas redox potential increased (~150 mV) significantly ($p<0.05$) from morning to afternoon (Table D.1.1), similar to daily redox swings seen in continuous monitoring. A significant change in MeHg concentration over the course of a single day would be expected only if a large proportion of the sediment MeHg inventory were turned over (produced, transported, and/or degraded) each day, so this lack of significant change in measured MeHg concentrations despite large redox swings was not surprising.

Similar daily and spring/neap changes in near surface redox potential and groundwater levels in the marsh plain interior were typically observed in other periods monitored. Although redox was not monitored continuously at the marsh plain edge, redox measurements in near surface sediments at edge and interior collection sites taken during sediment grab sampling (Table D.1.2) showed greater aeration of channel edge surface soils, as would be expected given their rapid draining of groundwater to well below the surface during ebb tides.

3) Water source and quality varied greatly, particularly in spring.

In addition to variation in water quantity, changes in water source and quality could affect biogeochemical processes in marshes. Seasonal differences in rainfall and flow from the Petaluma River caused some of the largest differences in water quality. April 2006 sampling

occurred soon after a major storm event, with water grab samples collected from slough channels at all sites showing lower salinities than seen in all other sampling events (Table D.1.3). Waters sampled in April 2005 were also fresher than in summer but more saline than in April 2006, whereas summer salinities were much higher and similar for both years at each site. Conductivity at BJ, nearest the bay, was significantly higher (Tukey HSD $p<0.05$) than other sites for all sampling periods, while GM typically was lowest. Despite small scale temporal and spatial changes within marshes driven by hydrological (tides and rainfall) and plant forces (evapotranspiration, photosynthesis and respiration), we would expect these differences to only be reflected in biota and other matrices for processes which did not integrate across these scales.

2. Mercury and methylmercury distribution (USGS WI)

The abundance and distribution of THg in water and sediment were similar among sites, but MeHg largely reflected differences among wetlands and their habitat elements. Despite adjustments to the sampling scheme between years, similar patterns were seen in 2005 and 2006, with the largest differences in MeHg between slough and marsh plain interior habitats.

1) Petaluma wetland sediment THg was elevated above natural background (prior to Gold Rush), and similar to concentrations observed in nearby San Pablo Bay, but wetland sediment MeHg concentrations were ~10x higher.

Surface (0-2 cm) sediments in Petaluma wetlands ranged in THg content from 200 to 380 ng/g (dry weight (dw); Figure D.2.1). These results were similar to concentrations in San Pablo Bay sediments (~300 ng/g) previously measured in annual monitoring by the Regional Monitoring Program (RMP) for Water Quality in the San Francisco Estuary (Conaway et al. 2007, SFEI 2007) and in a National Oceanic and Atmospheric Administration/U.S. Environmental Protection Agency Environmental Monitoring and Assessment Program (NOAA/EMAP) survey of San Francisco Bay in 2000 and 2001 (unpublished data), but higher than background (pre-mining) THg concentrations observed in historical sediment cores in deep San Francisco Bay muds (~80 ng/g, Conaway et al. 2004). Similar THg concentrations observed in sediments from the Petaluma marshes and San Pablo Bay were expected given that the primary THg sources for these sites, and the northern San Francisco Bay-Delta ecosystem more generally, are suspended sediment loads from the Sacramento and San Joaquin Rivers and local watersheds, which are well-mixed by wind-wave and tidal action in the shallow bay and tidal portions of rivers (Schoellhamer et al. 2007). Significantly higher (Tukey, $p<0.05$) THg concentrations were observed for 2006 in sloughs and marsh plain edges compared to 2005, which may reflect loads of THg carried down during larger rain events seen in 2006. Whereas THg concentrations were similar to those found in San Pablo Bay, marsh plain interior site average MeHg concentrations were often 5 ng/g or higher, in contrast to San Pablo Bay subtidal sediments, which averaged ~0.3 ng/g in RMP monitoring between 2002-2006 (SFEI 2007).

2) Differences among habitat elements in sediment THg were ~30% or less, but average MeHg concentrations differed up to ~10-fold within each wetland.

At each study wetland site, THg concentrations were observed to be the greatest (and generally similar) at slough sites, with decreasing concentrations from high marsh plain edge to interior sites. Sediment THg was significantly ($p<0.001$, linear regression) inversely related

to percent loss on ignition (LOI), suggesting that organic material (plant roots and detritus) in the bulk sediments had lower concentrations of THg than inorganic material (Figure D.2.2). However, even adjusting for LOI (assuming THg was entirely in the inorganic portion of sediment, $THg_{inorganic} = THg_{bulk}/(100\%-\%LOI)$), this normalized measurement of $THg_{inorganic}$ (which would tend to overestimate THg in the inorganic portion of high LOI sediments) was still significantly (Tukey, $p<0.05$) higher in large sloughs (with low LOI) than in other habitat elements in the majority of cases (grouped by year and wetland).

In contrast, within each wetland, MeHg concentrations at high marsh interior sites were significantly greater ($p<0.05$, t-test for unequal variances) than at large slough sites, with the exception of MP. Lower MeHg levels in sediments nearer sloughs were likely due to a number of factors. Slough channel sediments typically experienced saturated conditions compared to interior marsh sites, where lower frequency wetting and drying cycles occurred. Drying and rewetting cycles have been shown to stimulate MeHg production in wetlands (Krabbenhoft et al., 2005). Those areas incurring the least drying (3rd order slough and marsh edge habitats) had correspondingly lower MeHg in surface sediments. In addition to more frequent wetting, slough channels and marsh plain edge habitat surface sediments had less organic matter (LOI). The impact of the latter on MeHg distributions in the marsh will be discussed below and in later sections on microbial and plant processes.

Sediment MeHg concentrations in individual sediment grab samples were highly variable at each site (within a single wetland habitat element), especially on the marsh plain, varying up to ~10 × between individual grab samples. However, average concentrations for individual grabs (3 grabs each at 24 sites in 2005, and 5 grabs each at 6 sites in 2006) were generally well-correlated to results for corresponding composite samples collected from the same site (Pearson coefficient = 0.75). Composite results were generally biased slightly lower than the means of grab samples (slopes for all data of 0.84, or 0.88 and 0.77 for 2005 and 2006 respectively, for linear regressions forced through the origin), but within a range similar to the acceptance range for precision on MeHg analyses of ± 20%).

3) Sediment profiles show MeHg maxima near the surface (0-2 cm); THg in contrast shows a subsurface peak.

Marsh plain interior (mid-transect in 2005) sediment cores showed maximum MeHg concentrations (8-20 ng/g) at the surface (0-2 cm), which sharply declined (to < 1 ng/g) with depth at all marsh sampling sites (Figure D.2.3). Declining MeHg concentrations with depth in sediment profiles is commonly observed in wetlands (Gilmour et al. 1998). This trend likely resulted from several factors: 1) the position of the oxic/anoxic transition zone near the sediment-water interface; 2) a higher density of plant roots supplying organic matter near the sediment surface; and 3) the overlying surface water serving as the source of sulfate to sustain co-location of maximum activity of sulfate reducing bacteria near the surface (Krabbenhoft et al. 1998).

Although transport of MeHg from adjacent waters (here Petaluma River/San Pablo Bay) to the marsh surface with subsequent (particulate) deposition and (dissolved phase) sorption to marsh surface sediments has been posited as a potential source of MeHg, it is unlikely to be a major source. The sum of filtered and particulate concentrations measured in slough waters in this study averaged <1 ng/L. If higher high tides overbanked the marsh plain during spring tide periods to an average depth of ~10 cm (e.g. Figures D.1.2 and D.1.3) on 4-7 days of each ~14 day spring/neap cycle, 1 ng/L MeHg concentrations in flooding water

would transport 4-7 ng MeHg to each 100 cm^2 of marsh surface. Assuming all the waterborne MeHg in each overbanking tide settled out or adsorbed to the marsh surface, a total of 0.04-0.07 ng/cm^2 of MeHg would be deposited on the marsh surface every two weeks. Using an average (dry) bulk density of marsh plain sediments of ~0.7 g/cm^3 (from a similar wetland in the region, Conaway et al. 2007), the top 2 cm of sediment would contain 1.4 g of sediment. Based on our measured MeHg concentrations of 3-7 ng/g for the high marsh interior (mean concentrations in composites measured in this study), an inventory of 4-10 ng of MeHg per cm^2 of marsh plain surface results. With two spring/neap cycles per month, MeHg transported and deposited via hydrologic flows could only account for ~2% of the inventory of MeHg in the top 2 cm of the marsh plain, even using a worst case assumption that all the MeHg transported in the water column during overbanking tides remained on the marsh plain.

In sloughs where concentrations and inventories of MeHg were lower and frequencies and depths of inundation higher, hydrologic transport of MeHg could be a more important component. Assuming ~1 m overlying water in a 3rd order slough channel, with inundation twice per day every day, net import of MeHg to sloughs could be up to 40 times higher than on the marsh plain, ~1.6-2.8 ng/cm^2 per spring/neap cycle. With concentrations in slough sediments of ~1-4 ng/g, such import could account for a larger portion of the pool of MeHg there. However, these concentrations were still higher than those in San Pablo Bay (~0.3 ng/g), so slough MeHg can not be accounted for by redistribution of San Pablo Bay sediments and require a suspended sediment source with higher MeHg concentrations (e.g. from the adjacent marsh plain), *in situ* production, or adsorption from the water column into the sediment. If the latter occurred substantially, filtered MeHg concentrations leaving the wetland on an ebb tide would be expected to be lower than in the preceding flood tide, counter to what was seen in sampling a 24 hour period described later in this section.

Mercury methylation in aquatic ecosystems largely results from microbial utilization of organic carbon (OC). Thus, good correspondence between sediment MeHg concentration and sediment THg and OC concentrations (note, in this study LOI is used as a proxy for OC) are commonly observed. However, data from these wetlands (Figure D.2.4) revealed a poor MeHg-THg relationship, and only a modest (but significant, $p<0.05$ for BJ and MP) relationship to LOI. Previous Hg research in the Delta has revealed similar poor MeHg-THg relationships (Slotton et al. 2000). One consideration is that sediments in these areas were beyond a Hg threshold or saturation point, so added THg would not notably contribute to additional MeHg. Previous research has suggested a threshold (ca. 5,000 ng/g dry wt.) for Hg(II) control on MeHg production may occur (Krabbenhoft et al. 1999; Rudd et al. 1983). However, these previous works were based on freshwater conditions and may not be transferable to estuarine environments. A second factor possibly explaining the lack of a MeHg-THg correlation was that only a small (and not linearly related) portion of the THg in these sediments was available to methylating microbial communities; thus THg exerted little influence on MeHg production. Bioavailability of Hg to methylating microbial communities is presently an active area of research, and most research points to the roles of sulfur and carbon (Barkay et al., 1997; Benoit et al., 1999). Variations in these two constituents can often explain observed differences in MeHg concentrations. These factors are discussed later in this report in the section addressing microbial transformations.

For the present study, LOI and MeHg showed a coefficient of determination (r^2) of 0.44. The MeHg/THg ratio is commonly used as an indicator of net methylation activity in

sediment because it normalizes for differences in Hg content, allowing the importance of other factors to be inferred. For sediments from Petaluma wetlands LOI and MeHg/THg results showed a better correspondence, with r^2=0.55 (p=0.015). If only sediment samples from surface 0-2 cm sections (where methylation activity is expected to be greatest) were included in the analysis, then the correspondence improved even more (r^2= 0.75, p=0.0003). These results suggest that net methylation activity in the Petaluma wetland was strongly influenced by the availability of organic carbon.

4) THg in surface water is primarily in the particulate phase, while MeHg is often found about equally in filtered and particulate phases.

Due to drier conditions in 2005 compared to 2006, water samples were only collected in sloughs for 2005. In 2006, water samples were also collected from pools of water on the surface at marsh interior locations (Figures D.2.5, D.2.6). Most (average 70%) THg in surface water was associated with suspended particulates (filtered using quartz fiber filters, 0.7 μm pore size), greater than is generally seen in many aquatic ecosystems (Krabbenhoft et al., 1999; 2005; Wiener et al., 2003). In contrast, less of the MeHg in surface water samples was observed in the particulate phase (about 50%). This result was likely due to two reasons. First, the suspended particulate load to the northern Bay-Delta is known to be enriched in inorganic Hg (Slotton 2000), and much of this solid phase Hg is not readily soluble and thus not likely available for methylation (see discussion above). Second, MeHg has a greater solubility than inorganic Hg, and thus should exhibit a greater relative fraction in the dissolved phase. In spring of 2006 the San Francisco region experienced an extended period of rainfall (25 days in March) shortly before we sampled, and contemporaneous changes in water column THg and MeHg concentrations were apparent. Increased THg concentrations in surface water were likely due to contributions from both Hg in rain and influx of resuspended bed sediment from the watersheds of the Delta. Three lines of evidence suggest that the flux of Hg from watershed derived bed sediment was the principal driver of the observed response. First, the net increase in surface water THg (particulate + filtered) of ~60 ng/L was considerably larger than typically observed levels of Hg in rainfall (5-10 ng/L, San Jose Mercury Deposition Network station, NADP 2006). Second, a significant majority of the increase in THg was observed in the particulate phase, consistent with observations from the watershed sources (Domagalski et al. 2004). Last, the BJ site, closer to the mouth of the Petaluma River, showed a larger net THg increase, with a greater proportion from particulate-associated Hg. If rainfall were the principal Hg source causing the April 2006 rise, a more even rise across our study sites would be expected. The relatively subtle rise in dissolved THg during April 2006 could also result from influx of particulate Hg if subsequent dissolution occurred on site. However, lab studies have revealed that leaching of Hg from sediments is generally quite limited (Puckett & Bloom 2001).

MeHg levels in April and August of 2006 were also elevated above those observed in 2005, but unlike THg, this probably was not predominantly due to watershed Hg delivery. Rather, because Hg in rainfall is dominantly in the dissolved state, and thus is likely readily available to methylating microbes, a greater fraction of Hg in rainfall (compared to particulate Hg) is likely available for methylation. In addition, the heavy rainfall in 2006 likely caused inundation of areas that were previously dry, which is known to give rise to intense periods of MeHg production (Krabbenhoft et al., 2005). It is interesting that the THg rise was relatively short lived compared to the extended period of elevated MeHg concentrations, further evidence that the cause for elevated MeHg was not well linked to the THg source.

5) Filtered MeHg and THg correlated to DOC concentration, which may also facilitate aqueous transport and bioavailability.

Researchers often observe strong correlations between DOC concentration and filter-passing THg and MeHg (Wiener et al. 2003), and the same observation was made in this study (Figure D.2.7). This observation is in part due to the fact that DOC is the primary ligand for inorganic Hg and MeHg in surface water, and in part related to the source of the DOC in most aquatic ecosystems: mineralization of organic carbon in sediments. Thus, as a result of sediment organic carbon breakdown, DOC is released, and a portion of the Hg originally associated with the sediment is carried to the surface water with the DOC. Similar to THg, particulate-bound MeHg is also released to surface water as a result of organic carbon mineralization. Furthermore, sulfate reduction, which leads to MeHg production, is also a carbon utilizing process. Thus for our sampled sites, as more organic carbon turnover occurred, these processes together increased net MeHg production and release, and the observed correlation of MeHg with DOC resulted.

6) MeHg demethylation and Hg(II) reduction under sunlight decreased ambient MeHg and THg concentrations, respectively; but, these processes were slower in turbid slough waters.

Due to the photo-sensitivity of Hg and MeHg, sunlight exposure to surface water can have a profound impact on the net speciation and concentration of Hg in aquatic ecosystems (Krabbenhoft et al., 1998; Krabbenhoft et al., 2002). For this study, controlled experiments using large slough water samples (filtered and unfiltered) from the three study wetlands and isotope tracers were used to evaluate aqueous reduction and demethylation. The Hg(II) reduction rate was estimated via stable isotope incubation experiments described previously (in the project approach section) by appearance of gaseous ^{201}Hg, whereas demethylation was estimated by the formation of un-methylated ^{199}Hg. For each reaction vessel, about 10 ng of each Hg isotope was added to achieve a starting concentration of ~2 ng/L. Results from these experiments are shown in Table D.2.1. Overall much shorter half-lives of ^{201}Hg clearly show that inorganic Hg was more photo reactive than MeHg. Ratios of ^{201}Hg/^{199}Hg mass evasion rates averaged 2.5 and 2.0 for photo-incubation experiments conducted in 2005 and 2006, respectively. Thus half-lives for Hg reduction were at most half those for MeHg demethylation. The demethylation half-lives of MeHg exposed to light in water from our studied wetlands ranged from 11-20 days in unfiltered water, and 5-20 days in filtered water. Although the ranges appeared similar for filtered and unfiltered water, in most cases filtered waters exhibited shorter half-lives when compared to unfiltered waters from the same locations. Like demethylation rates, reduction rates of ^{201}Hg were more rapid in filtered water in most of the tests. Calculated half-lives for Hg(II) reduction in filtered waters were estimated to be 2-5 days, versus 3-7 days in unfiltered waters. These results suggest that suspended particulates serve to decrease reduction and demethylation rates by scattering sunlight and reducing photo-mediated processes, or by sorption to particles, which would reduce availability to both photic and other aqueous phase reactions.

Comparing results only among experiments in filtered water, DOC also affected reactivity. Over the range of DOC concentrations exhibited by the site waters (6-12 mg C/L) there was an observed inverse relationship between DOC concentration and the measured reduction and demethylation rates. Although there was variability in the experimental results, the photo-demethylation rates determined for the low DOC site (BJ, 6 mg C/L) were 1.3-2.5 x faster than the rates determined for the high DOC waters (GM, with ~12 mg C/L). Demethylation rates measured for MP were in between these two sites, as were the

measured DOC concentrations (~9 mg C/L). Similarly, reduction rates at BJ were 1.4-1.5x greater than those measured for GM. From an environmental perspective, site waters with low suspended sediments, low DOC, and potentially long irradiation periods would be expected to show higher MeHg and Hg loss rates. In addition, these relatively fast half-lives illustrate the importance these processes play in regulating Hg and MeHg levels in shallow wetland waters and imply that these environments must be receiving ongoing inputs to maintain ambient concentrations.

7) Filtered MeHg concentrations in sloughs during ebb tides were elevated relative to concentrations coming from the Petaluma River during flood tides, indicating transport from wetland to river and bay waters.

MeHg concentrations of ~0.1-0.3 ng/L have been previously reported for northern San Francisco Bay (Choe and Gill 2003, RMP). Filtered MeHg collected in 2005 was generally in this range, but up to ~0.9ng/L was found in April 2006 and 0.6ng/L in August. Although we did not sample frequently enough to support accurate mass balances, in a 24-hour monitoring effort at BJ, greater MeHg in sloughs at low ebb compared to waters during flood tide from the Petaluma (Figure D.2.8) qualitatively suggests net export of filtered MeHg from the marsh. This event was the first overbanking tide following a neap period, so standing water on the marsh plain during the ebb likely increased the head, helping drive groundwater out through channel banks. Transport of particulate MeHg with subsequent dissolution and release from the wetland cannot be ruled out. An accurate particulate flux determination would require continuous integrated water column particle monitoring combined with frequent MeHg analysis through tidal cycles across seasons and various storm events, an approach that is a focus of another CBDA-funded project but beyond this project's scope. However, as described previously in this section, given concentrations of MeHg in slough water samples measured in this study, it appears unlikely that suspended particulate tidal transport could account for a substantial portion of the (0-2 cm sediment) inventory of MeHg on the marsh plain. With ~2% of the surface sediment MeHg inventory transported each month in overbanking tides, it would require ~4 years of accumulation from overbank transport to account for the MeHg in the top 2cm of marsh plain sediment, even assuming no degradation and complete retention of all (both filtered and particulate) transported MeHg.

3. Microbial mercury transformations (USGS CA)

Temporal and spatial variation in MeHg production, both within and among tidal marshes, was mediated by marsh hydrology and geophysical setting, which impacted site specific geochemistry and microbiology. Specifically, MeHg production was a function of 1) the activity of Hg(II)-methylating bacteria (k_{meth}), which was related to rates of microbial sulfate reduction, and 2) the pool size of reactive inorganic mercury ($Hg(II)_R$), which was mediated by sediment reduced sulfur concentrations. Key findings include the following:

1) Methylating activity of bacteria (k_{meth}) was greater on the vegetated marsh plain, compared to the sloughs, and greater in the marsh plain interior compared to marsh edge sites.

Differences in methylation rate constants *(k_{meth})* derived from tracer incubation studies were compared between wetland habitat elements and among wetlands. Analysis of variance (ANOVA) was conducted on 2005 k_{meth} data grouped by habitat element (marsh (plain) and slough) indicated that k_{meth} values associated with marsh sites were significantly ($p<0.05$)

greater than those from slough sites (Figure D.3.1A). For 2006 data, collected with more finely resolved habitat elements, pair-wise comparisons by the Tukey method verified that the marsh interior habitat element had significantly greater ($p<0.05$) k_{meth} than the three other habitat elements (marsh edge, 1st and 3rd order slough), and that none of the other habitat elements were significantly different from each other (Figure D.3.1B). Likely causes for these differences will be discussed in a following section addressing plant interactions.

In contrast, differences in k_{meth} values among the three wetlands (GM, MP, BJ) for any given habitat element were less evident than the above differences among geophysical habitat elements. The one exception was for the interior marsh habitat (2006 data only), where GM had a significantly higher k_{meth} (mean ± sd of 0.18 ± 0.05 d^{-1}) compared to BJ (0.022 ± 0.017 d^{-1}), while MP (0.086 ± 0.033 d^{-1}) was not significantly different from either of the other two sites, as assessed by the Tukey pair-wise comparison test. No other among-site differences were evident for the other habitat categories in either year. Temporally, there were no statistically significant differences in k_{meth} between months (April vs. August) for data grouped by habitat type.

2) The pool of $Hg(II)_R$ was higher on the vegetated marsh plain, and particularly at the marsh edge, whereas $Hg(II)_R$ in marsh interiors was similar to sloughs.

Reactive mercury ($Hg(II)_R$) is an operationally defined proxy measure using a method described earlier in this report (in section B.3 on project approach). ANOVA confirmed that for 2005 samples, marsh plain sites had significantly ($p<0.05$) higher $Hg(II)_R$ concentrations than did slough sites (Figure D.3.2A). Tukey pair-wise comparison verified that for 2006 data, marsh edge sites had significantly ($p<0.05$) higher $Hg(II)_R$ concentrations, compared to the three other habitat types (Figure D.3.2B). Among sites sampled during 2005, $Hg(II)_R$ (mean ± sd in ng g^{-1} dry wt.) in the marsh plain habitat was significantly higher at GM (5.66 ± 1.05) compared to MP (2.39 ± 0.62), while both were statistically similar to BJ (2.51 ± 0.72). In contrast, there were no significant differences among wetlands for the slough habitats sampled in 2005, nor were there any significant differences among wetlands for any of the four habitat elements sampled during 2006. ANOVA also revealed no statistically significant temporal differences in $Hg(II)_R$ between April and August samplings, nor between years, for any habitat type.

3) The calculated rates of microbial MeHg production were higher on vegetated marsh plains, compared to sloughs, and specifically highest for marsh interior sites.

Potential rates of MeHg production were calculated as the products of the $^{203}Hg(II)$-methylation rate constants (k_{meth}) and the *in situ* $Hg(II)_R$ concentrations described previously. For the 2005 sampling, calculated rates of MeHg production were consistently and significantly ($p<0.05$; ANOVA) higher in vegetated high marsh sites, compared to sloughs (Figure D.3.3A). This was driven both by the higher values of both k_{meth} (Figure D.3.1A) and $Hg(II)_R$ concentrations (Figure D.3.2A), compared to the slough sites. The expanded sampling design followed in 2006 gave further insight into the spatial variation of MeHg production, and the primary factors that controlled it. Tukey pair-wise comparison of habitat elements indicated that the marsh interior sites had significantly ($p<0.05$) higher MeHg production rates, compared to the other three habitat categories (marsh edge, 1st and 3rd order slough, Figure D.3.3B). Temporally, there was no statistically significant difference between months (April and August) within a given habitat type, for either 2005 or 2006 data.

Statistically significant differences in MeHg production rates (in pg g^{-1} d^{-1} dry wt.) among wetlands (GM, MP and BJ; assessed by Tukey pair-wise comparison) were noted for the marsh interior habitat element only (2006 data only, April and August data combined). Potential methylation rates (mean ± sd) for GM (91.1 ± 29.6) were significantly higher than those at either MP (23.5 ± 8.0) or BJ (17.7 ± 10.0). This spatial trend was similar to the among-site differences observed for k_{meth} described above.

4) The activity of Hg(II)-methylating bacterial (k_{meth}) was with a positive function of microbial sulfate reduction (SR) rate across all sites and sub-habitats.

Both k_{meth} and microbial SR rates varied over three orders of magnitude for the complete data set. Since specific species of sulfate reducing bacteria are also known to be able to carry out Hg(II)-methylation, a positive relationship between these two parameters was anticipated and was observed for logarithmically transformed data (Figure D.3.4). Both parameters were highest for marsh plain data (from 2005) and marsh interior sites (from 2006). In contrast, marsh edge habitat (adjacent to slough channels) was low for both parameters, while slough sites were intermediate.

5) Sediment reactive mercury decreased as solid phase reduced sulfur compounds increased.

One paradox of MeHg production is that while Hg(II)-methylation is partially a function of the activity of sulfate reducing bacteria, reduced-S end-products of sulfate reduction (e.g. sulfide or solid phase Fe-S minerals formed from sulfide) may strongly bind inorganic Hg(II) and decrease $Hg(II)_R$. In the current study, this was best demonstrated by the negative relationship between sediment acid volatile sulfur (AVS; largely solid phase FeS) and $Hg(II)_R$ concentration (Figure D.3.5). Across all sites and sub-habitats, marsh edge sites generally had the least AVS and the highest $Hg(II)_R$, while 1st order sloughs exhibited the opposite trend. This decrease in $Hg(II)_R$ with AVS, or similar metrics (e.g. sediment redox or total reduced sulfur), has been observed across a wide range of ecosystems in recent work conducted by USGS, including other portions of SF Bay, in southern Louisiana wetlands and estuaries, and across a wide range of river settings as part of the USGS NAWQA program (Marvin-DiPasquale, unpublished; Marvin-DiPasquale and others, in prep).

4. Plant-landscape-biogeochemical interactions (USGS CA)

Plant-microbial interactions influenced net MeHg production within the marsh plain. Experimental and comparative data show that potential and net MeHg production increased with higher live root density (% volume). Live root density in surface sediments was up to 3 orders of magnitude greater in marsh interiors than in marsh edges. This was one of the primary reasons that marsh interior sites, dominated by short pickleweed (*Salicornia virginica, or Sarcocornia pacifica*), had significantly greater MeHg pools and rates of MeHg production than marsh edge sites, dominated by gumplant shrubs(*Grindelia stricta*). Key findings include:

1) Methylmercury production rates and surface sediment pools were significantly correlated with live root density.

Root density (%volume=root volume/(root+sediment volume)) was positively related to k_{meth} ($r^2 = 0.62$, $p<0.0001$, Figure D.4.1a), and separated by season, live root density showed some of the highest environmental relationships with mercury methylation that were measured in this study ($r^2 = 0.78$-0.92, $p<0.0001$). However, root density had a negative relationship with $Hg(II)_R$ (Figure D.4.1b, $r^2 = 0.38$, $p<0.0042$), as well as with other oxidative

status factors such as redox potential (relationships not shown). Because live root density had contrasting effects on the two factors used to calculate MeHg production rates, the relationship between root density and methylmercury production (k_{meth} * $Hg(II)_R$) was significant but weaker (r^2 = 0.55, $p<0.0026$), Figure D.4.1c) than with k_{meth} alone. Sediment MeHg also increased linearly with increasing live root density (r^2 = 0.57, $p<0.0018$, Figure D4.1d).

2) Experimental devegetation of the marsh plain reduced rates of MeHg production by 80%.

In April 2006 we devegetated 1 m^2 plots (n=12), removing live aboveground biomass, trenching to 30 cm depth to sever roots, and covering with water permeable landscape shade cloth. We returned to collect samples from paired de-/vegetated plots in August 2006. The 80+% decrease in live root biomass led to a significant decrease in microbial activity (both SR and k_{meth}). Marsh interior sites, where live root density was 20-40% in control plots, were more strongly affected than marsh edge sites, where the biogeochemical differences were negligible. In devegetated marsh interior plots, SR dropped to rates consistent with slough subhabitats. Structural soil properties (e.g. % LOI, % moisture, temperature) and relatively large pools of ferric iron were not altered by devegetation. Whereas redox potential actually increased in devegetated plots, pools of $Hg(II)_R$ were not influenced by devegetation. This experiment demonstrated that the primary effect of plants on soil biogeochemistry was to promote sulfate and iron reduction (Figure D.4.2), and not to increase the pool size of surface sediment $Hg(II)_R$.

3) Reducing conditions associated with high root density are likely a function of increasing labile organic matter released into the rhizosphere zone by vegetation, with subsequent increase in anaerobic microbial activity.

Porewater DOC correlated positively with root density in August and April 2006 (r^2 = 0.39), decreasing by 54% when devegetated (Figure D.4.2). Porewater acetate concentrations were similarly decreased in devegetated plots (84% reduction, $p<0.0001$), and had a positive logarithmic relationship with root densities (r^2 = 0.521, $p<0.0094$). Removing aboveground vegetation decreased pools of reduced sulfur and iron species ~50%, and increased redox potential 64 ± 6 mV relative to paired vegetated plots. Transfer of O_2 into the rhizosphere zone by plants was originally hypothesized to increase redox potential in densely vegetated portions of the marsh plain. However, wetland soils were generally more reducing with increasing live root density, suggesting a conceptual model with the rhizosphere acting as a zone of high anaerobic bacterial activity, where $Hg(II)_R$ pools are bound by reduced sulfur species.

4) Hg released by plant salt exudation could represent a significant input of Hg(II) to salt marsh surface sediments.

Spikegrass (*Distichlis spicata*), the primary subdominant plant and a salt excreting C4 species, released ~21-fold more THg onto leaf surfaces than the succulent and dominant pickleweed (a C3 species) or atmospheric deposition onto glass fiber filters (both neutral and KCl-encrusted to mimic denuders for atmospheric reactive Hg, Figure D.4.3). Greater concentrations of sodium (Na) were found on spikegrass leaf surfaces than on pickleweed leaf surfaces, and sodium concentrations were linearly correlated with Hg concentrations for spikegrass (r=0.64), but not for pickleweed or control filters (Figure D.4.4). Spikegrass THg release likely occurred through use of salt glands (hydathodes) which provide a pathway for sodium Na release in salt tolerant species. In contrast, pickleweed appeared to concentrate

THg in the distal tips of senescing tissue, as THg in these tips was on average 5-7 fold higher than in fresh green leaf tissue (up to 78 ng/g). Per unit area (m^2), THg released onto leaf surfaces from daily salt excretion in spikegrass dominated plots represented ~3-5% of the $Hg(II)_R$ pool in 0-2 cm surface sediments. Rates of THg excretion at BJ were greater than at GM, likely due to a higher marine input of sodium (Figure D.4.4).

5) Hg fluxes through plant uptake and decomposition were not significantly different among habitats and were not significant pools and fluxes of Hg and MeHg relative to other more active processes.

Biomass accumulation from April to August 2006 was greater along the marsh edge than in the marsh interior ($p=0.0190$), but high leaf turnover in the marsh interior suggests that primary productivity in short pickleweed plots is underestimated by using only two seasonal measures of aboveground biomass. Live roots were significantly deeper in marsh edges versus marsh interiors (32 vs. 8 cm max, respectively), with more live root mass per plot, but with much lower root densities in the 0-2cm surface sediment compared to marsh interiors (Figures D.4.1a-d). THg in leaf biomass was low (<10 ng/g dry weight), and the only spatial pattern was slightly higher THg in senescent pickleweed and *Grindelia* at BJ. In lab-based decay experiments, mass loss and Hg release were slow for both pickleweed and spikegrass; decomposition rate constants (k_{dec}) were 0.021 and 0.007 d^{-1}, respectively, proportional to their tissue C:N ratios (12 and 33, respectively). The importance of tissue decay in redistributing $Hg(II)_R$ to surface sediment is likely low given the slow decomposition rates, at least for these species.

5. Mercury bioaccumulation (USGS Western Ecological Research Center)

Patterns in food web Hg contamination, including resident California Black Rails, generally reflected patterns seen in MeHg distributions in sediment or water, although differences in biota Hg concentrations were not as distinct among habitat elements. Details are given below:

1) California Black Rails occupied small home ranges, preferring pickleweed dominated marsh plain with taller vegetation.

We obtained enough locations (n>10) from 41 radio-marked rails in 2005 and 2006 to calculate fixed kernel home ranges. Black rails had small home ranges (average 95% fixed kernel home range 0.65 ha) and exhibited strong site fidelity in the breeding season. Thus, MeHg concentrations in individual rails may reflect patterns of MeHg levels within small wetland areas. Black Rails preferred areas in the marsh plain dominated by short pickleweed (*Sarcocornia pacifica,* formerly *Salicornia virginica;* Figure D.5.1) near taller natural structures such as upland levee vegetation or marsh gumplant (*Grindelia stricta*) within the marsh. These taller structures may provide refuge during high tides, so they are likely critical habitat elements for breeding Black Rails.

2). Black rail feather THg concentrations differed by year, site, sex, and age, whereas blood MeHg concentrations differed only by sex.

Geometric mean Hg for all rails averaged 6.94 μg/g fresh weight (fw) for feathers and 0.38 μg/g wet weight (ww) for blood. MeHg and THg in blood were strongly correlated ($r^2=0.903$). Average feather THg was higher in 2006 than 2005 (8.53 vs 5.45 μg/g fw; $p<0.001$) but did not differ by season. Blood MeHg concentrations did not differ by year or season ($p=0.13$ and 0.68, respectively). Feathers collected from black rails at MP had higher

THg concentrations than at BJ and GM (9.04, 6.46, and 6.61 μg/g fw, respectively; p=0.04; Figure D.5.2). MeHg in blood at MP and GM (0.44, 0.48 μg/g ww) was slightly higher, but not significantly different than at BJ (0.29 μg/g ww; p=0.09). Males had higher MeHg concentrations in blood (8.22 and 6.63 μg/g, respectively; p<0.001) and higher THg in feathers than females (0.62 and 0.23 μg/g, respectively; p=0.04), and adults had higher THg in feathers than hatch year birds (7.36 and 4.61 μg/g, respectively; p=0.001), but blood MeHg concentrations did not differ significantly (0.49 and 0.38 μg/g, respectively; p=0.817).

3) A majority of adult Black Rail MeHg concentrations were above levels associated with reproductive impairment in birds (9 μg/g in feathers, Heinz 1979), and fell within the low- to moderate- risk range of reproductive effects levels established for Common Loons (Evers et al. 2004).

Avian species exhibit differing sensitivity to MeHg contamination (Scheuhammer 1987), and toxicity thresholds have not been established for black rails. Although it is unknown if toxicity thresholds established for other species are appropriate for black rails, it was useful to compare our results with those of other avian species where reproductive and physiological effects have been measured in order to understand potential impacts of observed MeHg concentrations. Seventy-eight percent of black rail feathers were above the LOAEL established for mallards (5 μg/g, Heinz 1979). Evers et al. (2004) established risk categories for common loons. The low risk category upper limit is the no observed adverse effect level (NOAEL: 1 μg/g ww blood, 9 μg/g fw feathers); the lower limit of the high risk category is the lowest observed adverse effect level (LOAEL: 20 μg/g ww feathers, 3 μg/g fw blood). In this study, 67% of feathers and 91% of blood samples were in the low risk range, 32% of feathers and 9% of blood in the moderate risk range, and <1% of feathers and no blood samples were in the high risk range. Two birds captured at MP were in the high risk range. Average THg in 8 non-viable eggs was 0.01 μg/g fw, with no embryo deformities observed.

A substantial portion of the threatened black rail population in SFB may be at risk of adverse effects from MeHg if they are more sensitive to chronic levels of MeHg contamination than their relatively low concentrations imply. Even if the most conservative estimates of risk are used, with relatively small proportions of the population considered to be adversely affected by elevated MeHg contamination, any reduction in reproductive success or juvenile survival could have detrimental effects on at-risk subspecies such as the black rail that are already in decline. Individuals at MP and other similar marshes may be at even greater risk, as MeHg concentrations in both invertebrates and birds were higher than at other sites, with two birds in the high risk range established for common loons. This could indicate that there are potential localized "hot spots" for MeHg contamination within SFB.

4) Selenium concentrations in Black Rail blood samples were below published effects thresholds.

We measured total Selenium (Se) concentrations in 34 adult black rail blood samples in 2005 and 2006 in order to better understand the potential toxic effects of MeHg. Selenium can bind to MeHg and form stable, non toxic complexes, therefore reducing the toxicity of MeHg (Scheuhammer 1987). Dietary Se concentrations of 4-8 μg/g ww were associated with impaired reproduction in mallards (Heinz et al. 1989). Blood Se concentrations in this study (mean ± sd = 0.45 ± 0.11 μg/g ww) were far below the lower limit of this threshold, thus black rails probably did not experience reproductive impairment due to Se contamination. Black rails from BJ had higher (p=0.002) Se concentrations in blood [0.51 ± 0.09 μg/g (n=13)] than those at MP [0.42 ± 0.09 μg/g (n=15)] and GM [0.35 ± 0.04 μg/g (n=7)].

The mean (± sd) molar ratio of MeHg:Se in black rail blood samples was 0.37 ± 0.23. There was no correlation between MeHg and Se concentrations. The effect of interactions between MeHg and Se on birds is still unclear. Adult mallards exposed to 10 μg/g dietary MeHg and Se exhibited reduced toxicity compared to birds exposed to MeHg or Se alone (Heinz et al. 1998), similar to effects also found with increasing Se in other birds (El-Begearmi et al. 1977) and mammals (Ralston et al. 2007), even at MeHg:Se molar ratios higher than 1:1. Both elements can sometimes act synergistically to impair reproduction, as adult mallards exposed to both MeHg and Se had reduced breeding success and greater mortality and teratogenic effects to embryos than birds dosed with MeHg or Se alone (Heinz et al. 1998), but these were seen at dietary MeHg and Se (10 μg/g) much higher than any potential diet items measured in our study. Further (ideally species specific) study of MeHg and Se interactions would be required to evaluate potential effects at lower concentrations typically seen.

5) Black Rails opportunistically feed on a variety of marsh plain biota.

U.C. Davis Bohart Museum of Entomology identified 16 different invertebrate taxa in 42 regurgitated diet samples collected in the summers of 2005 and 2006. We calculated percent frequency (the times each taxon appeared in a diet sample) because highly digested stomach contents did not allow quantitation of total numbers or masses. Invertebrates targeted for MeHg analyses [beetles (*Bembidion* sp.), wolf spiders (*Pardosa* sp.), beach hopper amphipods (*Traskorchestia traskiana*, marsh snails (*Myosotella myosotis)]* were found in most samples. Among invertebrates, beetles and spiders occurred most frequently (97% and 72%, respectively), with amphipods and snails found less often (44% and 28%, respectively). Other taxa found include flies (*Diptera*), leaf hoppers, shore bugs (*Saldidae*), and macroveliid shore bugs (*Macroveliidae*) (53%, 31%, 23%, and 23%, respectively). Seeds occurred in 10% of samples. Nematodes, *Hemiptera, Heteroptera, Hymenoptera, Orthoptera*, and shaft lice were found in <5% of samples. Composition of black rail diet samples did not differ by site.

6. Prey items with the highest occurrence in diet samples (beetles and spiders) also had the highest MeHg concentrations.

MeHg concentrations in invertebrates were log-transformed for normality and analyzed with ANOVA. Overall, spiders consistently had the highest dry weight MeHg concentrations (0.412±0.021 μg/g; N=47), followed by snails (0.124±0.006 μg/g), and amphipods (0.102±0.005 μg/g; N=67). Since beetles were frequently detected in black rail diet samples, we collected beetles in 2006. We detected an interaction between taxa, site, and year (ANOVA, $F_{4,151} = 6.363$, $p < 0.0001$; Figure D.5.3) for MeHg concentration within marsh invertebrates. Beetles had a greater dry weight concentrations (0.443±0.126 μg/g at GM, N=2; 0.630±0.034 μg/g at MP, N=2; and 0.510 μg/g at BJ, N=1) than our target marsh invertebrates. In 2005, spiders at BJ had the greatest MeHg concentration, followed by MP and GM (Figure D.5.3). In 2006, MeHg concentrations in spiders were greatest at MP, followed by GM and BJ. Amphipod MeHg concentrations were consistently lower than snails at MP and BJ for 2005 and 2006, except for GM, where amphipod MeHg concentration was greater than snails in 2006. MeHg concentrations in target amphipods, snails, or spiders invertebrates were similar for marsh edge and marsh interior (Figure D.5.4).

We analyzed marsh and slough biota for carbon and nitrogen stable isotopes in 2005. We compared isotopes for pickleweed, a C3 plant, and saltgrass (*Distichlis spicata*, a C4 plant; L. Windham, unpublished data) collected in summer 2006. Though we did not analyze stable isotopes from algae, benthic diatoms, or phytoplankton, we listed values previously reported

for San Francisco Bay Estuary (Cloern et al. 2002). Saltgrass averaged -13.5 δ ^{13}C and -13.7 δ ^{13}C from GM and BJ, respectively) and pickleweed at GM and BJ averaged -27.9 δ ^{13}C and -26.8 δ ^{13}C. These data fell within the typical range found within San Francisco Bay tidal marshes; C4 plants (i.e., *Spartina* or saltgrass) ranged from -17.7 to -12.8 δ ^{13}C) and C3 plants (i.e., pickleweed or gumplant) ranged from -31.3 to -22.1 δ ^{13}C; as in Cloern et al. 2002). Benthic diatoms (δ 13C range -24.0 to -19.6), and phytoplankton (δ ^{13}C range -26.7 to -17.4; Cloern et al. 2002) are other possible carbon sources for marsh and slough biota. Since consumers are typically enriched within 1 ‰ for carbon (Michener & Kaufman 2007), stable isotopes are often used to identify carbon sources of consumer diets. Due to the variability in δ 13C values for primary producers and the considerable overlap in the range of δ ^{13}C values, we were not able to determine the relative contribution of C3 plants, phytoplankton, or diatoms to the food web; however, the dual carbon-nitrogen isotope diagram reflected a relatively little importance of C4 plants (Figure D.5.5).

We plotted carbon and nitrogen stable isotopes for major taxa in 2005, including black rail feathers that were collected in 2006 but grown in 2005. Marsh predators were more enriched in nitrogen: black rail feathers had the highest δ ^{15}N, followed by black rail blood, beetles, *Pardosa* spiders, non-target invertebrates (*Saldidae* shorebugs, *Coccinellidae* ladybugs, *Cicadellidae* leafhoppers, and *Mantidae* mantis), snails, and amphipods. Consumers typically display a trophic enrichment factor of 3.4‰ $\pm$ 1.1 for ^{15}N and within 1‰ for ^{13}C relative to their diet (Michener & Kaufman 2007). From their isotopic position, black rails are likely marsh generalists, feeding on predators such as beetles and spiders, but also detrivorous amphipods and snails. Stable isotopes indicated black rails were not ingesting slough biota including slough macroinvertebrates (i.e., aquatic amphipods and shrimp). These results are consistent with diet analyses.

MeHg concentrations increased with trophic position, as determined by delta^{15}N, for marsh biota (Figure D.5.6). Black rails were grouped within a range of δ ^{15}N (14.0 to 17.8) and had a range of MeHg values (3.7 to 19.5 μg/g). Marsh invertebrates had a wide range of δ ^{15}N (9.0 to 16.3) with some overlap with black rails, but a low range in MeHg concentrations (0.05 to 0.60).

7. Black Rail MeHg correlated with MeHg in beetles but not spiders.

Beetles had the highest frequency of detection in black rail diet samples and may reflect the trophic transfer of MeHg to black rails. Beetles were not previously included as target invertebrates for collection, but were collected in 2006 after their high detection rates in diet samples. Similar to MeHg in black rail blood, and THg in feathers, beetles had the highest MeHg concentration at MP (0.63 $\pm$ 0.03 MeHg μg/g dw, N=2), while BJ (0.51 MeHg μg/g dw, N=1) and GM (0.44 $\pm$ 0.13 MeHg μg/g dw, N=2) had lower MeHg values. Spiders were also frequently detected in black rail diet samples; however, site differences in spider MeHg concentrations did not correlate with MeHg patterns in Black Rail blood or THg in feathers. Feather THg concentrations were highest at MP; however, spiders had the greatest MeHg μg/g dw concentrations at BJ.

8. MeHg concentrations in slough biota did not increase with trophic level.

MeHg in slough biota were highest in fish, mussels, and clams (Figure D.5.7). Unlike marsh plain biota, we detected no relationship between MeHg concentrations in slough organisms with trophic position (Figure D.5.8). Filter feeding mussels grouped at a lower δ ^{15}N than

fish; however they also had high levels of MeHg, probably because MeHg is bound to fine particulates that the mussels filtered out of the water column.

E. Potential Management Implications of Findings

Management implications of findings related to our current conceptual model are as follows:

1) THg is elevated above natural concentrations in wetland sediments, but poor correlation between sediment THg and biota MeHg suggests that factors controlling MeHg production and/or transport are more influenced by wetland processes, seen in other inherent variables such as organic carbon content of sediment, rather than by ambient THg concentrations. Given that MeHg in water and sediment was generally less than 2% of THg concentrations, only a small proportion of THg needs to be methylated to account for the MeHg inventory found in the environment. Given the excess of THg generally present at these sites, efforts to reduce MeHg risks should especially be focused on identifying which forms of Hg are more bioavailable, and targeting decreasing loads of these Hg sources where possible.

2) Geomorphologic factors cause variations in MeHg production and uptake; sloughs, and marsh plain edges and interiors are markedly different in hydrology and vegetation. As a result, MeHg shows much variability on small spatial and temporal scales, which can be better understood using these habitat elements as sampling strata or for post-stratifying collected results during data analysis to help reduce some of the apparent variability within tidal marshes. However, even within these habitat elements, there is substantial small-scale heterogeneity, particularly in marsh plain sediments. Although this can be overcome by collecting and analyzing a large number of individual samples from each environment, collecting many samples to analyze as a smaller number of composites or employing other integrative techniques are less cost and labor intensive approaches to representatively characterizing these environments.

3) Plants supply organic material to anaerobic bacteria; this is the major critical role of macrophytes in the wetland biogeochemical Hg cycle. Although roots supply both O_2 and organic carbon to the rhizosphere, the net result of root activity is a reducing environment in shallow marsh plain interior sediments caused by bacterial iron and sulfate reduction of supplied labile organic matter. Although devegetation of marsh plain plots reduced MeHg concentrations, devegetation is obviously not a viable design or control action option given the importance of plants for biological function in high marsh habitat. However, if immature newly restored wetlands have lower elevation and consequently lower vegetation density and organic carbon content, there may be less potential MeHg impacts than would be expected for the mature marshes we studied.

4) *In situ* bacterial production generates much of the MeHg found in wetlands; methylation rates calculated in tracer incubations combined with $Hg(II)_R$ measurements can account for up to ~5% of the standing inventory of MeHg per day. In contrast, even using worst case assumptions (e.g. complete deposition and retention of all MeHg transported via water in overbanking tides), hydrologic transport of MeHg to the marsh plain over the course of a month can at best account for ~2% of the MeHg inventory.

5) Demethylation will decrease the MeHg pool in both water and sediment. Half lives in water ranged from ~5 days in clear (filtered) surface waters to ~3 weeks for unfiltered waters. Hg(II) is also lost via reduction, requiring ongoing inputs via various pathways such

as hydrologic transport and atmospheric deposition to maintain ambient THg concentrations found in the environment. A longer period of monitoring is needed to determine long term trends, but if ambient sediment concentrations do not change greatly (sediment concentrations were similar in the two years studied), sediment demethylation rates and other loss pathways are likely to be a similar order of magnitude as *in situ* production and transport inputs; if ~5% of the sediment MeHg inventory were demethylated each day (to offset transport and *in situ* production), steady state concentrations would be maintained roughly at current levels.

6) The mechanism for transfer of MeHg from the zone of production into the base of the food web is unclear, but MeHg in sediment epiphytes or detritus and water particulate microbes or phytoplankton are likely to be entry points to the food web. MeHg differences between high marsh edge and interior sediments are not reflected in invertebrates (except amphipods) collected at those locations, suggesting multiple possible factors: 1) mobility between habitat elements causing loss of differentiation ; 2) sediment MeHg remaining within production zones, or transported and mixed, with primarily a more uniformly distributed source supplying MeHg to the marsh food web; 3) sediment MeHg entering the food web through organisms not measured in this study; and/or 4) spatial differences in biodilution or other processes affecting MeHg uptake and accumulation by biota masking or overriding concentration differences in the various habitat elements. Invertebrate organisms studied largely do not travel among marshes, and transport mechanisms did not mix sufficiently on larger scales to distribute MeHg uniformly among marshes, so some inter-marsh differences in food web MeHg concentrations were still apparent.

Movements between marsh interior and marsh edge habitat elements were not likely to affect MeHg concentrations within marsh snails and amphipods because of their limited mobility; however, spiders may conceivably travel further and integrate prey from across the marsh. Although mercury may not enter the marsh food web through organisms measured in this study, we conducted a preliminary survey of marsh invertebrates and selected those that were present at all sites and that represented foraging guilds (surface scraper snails, detrivorous amphipods, predatory spiders) and also likely black rail prey items.

7) MeHg increased with trophic level in the marsh food web. There is moderate evidence that MeHg can bioaccumulate to levels that might impact Black Rails; 78% of black rail feathers were above the LOAEL established for mallards and 32% of California Black Rail feathers and 9% of blood samples were within a moderate risk category that was established for loons. THg in non-viable eggs were at concentrations at low risk levels (no embryo deformities found) for other species, but effects levels specific for Black Rails are unknown for all these tissue matrices. Further study is also needed to better understand possible interactions of MeHg and Se.

8) There is evidence that MeHg may be sometimes exported to other ecosystems. Although water MeHg concentrations are often similar to those of nearby San Pablo Bay, sampling of BJ over 24 hours during an overbank event indicated greater filtered MeHg concentrations in ebbing slough waters than flooding tides from the Petaluma River. Thus for at least some periods there is potential for net MeHg discharge from wetlands. Flow volumes and more detailed concentrations over longer periods and extrapolation to larger areas would be required to estimate loads discharged. Attempts to characterize loads from these and other wetlands should also examine special hydraulic circumstances that may discharge MeHg, even if net discharge during typical tidal or fluvial flows may appear small.

F. Products to date (list reports, publications, and presentations)

Reports

Yee, D., J. Collins, L. Grenier, J. Takekawa, S. Schwarzbach, M. Marvin-DiPasquale, D. Krabbenhoft, J. Evens (2005). Mercury and Methylmercury Processes in North San Francisco Bay Tidal Wetland Ecosystems. Annual Project Report to California Bay-Delta Authority. Sacramento, CA. November 7, 2005.

Yee D., J. Collins, L.Grenier, J. Takekawa, D. Tsao-Melcer, I. Woo, S. Schwarzbach, M. Marvin-DiPasquale, L. Windham, D. Krabbenhoft, S. Olund, J. Evens (2007). Mercury and Methylmercury Processes in North San Francisco Bay Tidal Wetland Ecosystems. Annual Project Report to California Bay-Delta Authority. Sacramento, CA. April 2007.

Publications

Tsao-Melcer, D. C. (2007). Space use and mercury concentrations of California black rails (*Laterallus jamaicensis coturniculus*), north San Francisco Bay, California. Master's Thesis. Graduate Group in Ecology, University of California, Davis.

Tsao-Melcer, D. C., A. K. Miles, J. Y. Takekawa, and I. Woo (*In review*). Mercury, methylmercury and Selenium concentrations in threatened California Black Rails at San Francisco Bay. Archives of Environmental Toxicology and Contamination.

Oral Presentations

Marvin-DiPasquale, M. (USGS, Menlo Park, CA). Toxic Mercury in Aquatic Ecosystems: Why Quality Trumps Quantity. Presented at USGS Menlo Park (CA) as part of the USGS Western Region Public Lecture Series. U. S. Geological Survey, Menlo Park, CA. September 29, 2005. Video-archived on-line at: http://online.wr.usgs.gov/calendar/2005.html

Marvin-DiPasquale, M., B. D. Hall, J. R. Flanders, N. Ladizinski1, J. L. Agee, L. H. Kieu, L. Windham. 2006a. Ecosystem Investigations of Benthic Methylmercury Production: A Tin-Reduction Approach for Assessing the Inorganic Mercury Pool Available for Methylation. Oral presentation abstract for the *8th International Conference on Mercury as a Global Pollutant*. Madison WI. August 6-11, 2006.

Marvin-DiPasquale, M., J. L. Agee, N. Ladizinsky, L. Windham-Myer, S. Wren, D. Yee, J. Collins, S. Olund, D. Krabbenhoft, R. Mason, A. Heyes (2006b). Controls on Mercury-Methylation in Sediments From Freshwater, Delta, and Salt-Marsh Regions of the San Francisco Bay Watershed. Abstract for CBDA Science Conference, Sacramento, CA. October 23-26, 2006.

Olund, S. D., D. P. Krabbenhoft, T. Sabin, M. Marvin-DiPasquale, L. Windham, J. Takekawa, D. Yee (2006). Dynamics of Mercury and Methylmercury in San Francisco Bay Estuarial Marshes Oral presentation and abstract for the *8th International Conference on Mercury as a Global Pollutant*. Madison WI. August 6-11, 2006.

Tsao-Melcer, D. C., J. Y. Takekawa, I. Woo, A. K. Miles (2007). Habitat use and mercury exposure in California Black Rails, Petaluma River, CA. Oral presentation at the 2007 Society of Wetland Scientists International Conference. Sacramento, CA. June 2007.

Tsao-Melcer, D. C., A. K. Miles, J. Y. Takekawa, I. Woo (2006). Mercury concentrations in Black Rails along the Petaluma River, CA. Talk presented at the 2006 Wildlife Society National Conference, Anchorage, AK. September 2006.

Windham-Myers, L., A. Jew, M. Marvin-DiPasquale (2006a). The uptake, release, and remobilization of mercury by wetland plants – implications for the "reactive" pool of mercury available for methylation, Poster presentation and abstract for the *8th International Conference on Mercury as a Global Pollutant*. Madison WI. August 6-11, 2006.

Windham-Myers, L., A. Jew, S. L. Wren, M. Marvin-DiPasquale (2006b). Plant-mercury interactions: The role of submerged and emergent macrophytes in mercury cycling of San Francisco Bay and Delta wetlands. Abstract for CBDA Science Conference, Sacramento, CA. October 23-26, 2006.

Woo, I., J. Y. Takekawa, D. Tsao-Melcer. 2006. Methylmercury concentrations in marsh invertebrates in relation to the food web structure of Black Rails. Oral Presentation. 4th Biennial CALFED Science Conference 2006 Making Sense of Complexity: Science for a changing environment. 23-25 Oct, 2006. Sacramento, CA

Woo, I., J. Y. Takekawa, D. Tsao-Melcer. 2007. Methylmercury concentrations of invertebrates in tidal marshes and food web relations to the California Black Rail. Oral presentation. Society of Wetland Scientists, June 2007. Sacramento, CA

Poster Presentations

Marvin-DiPasquale, M, J. L. Agee, L. H. Kieu, N. Ladizinski, L. Windham, D. Yee, J. Collins, S. Olund, D. Krabbenhoft, R. Mason, A. Heyes, C. Miller (2005b). Mercury-Methylation Dynamics In Sediments From Freshwater, Delta and Saltmarsh Regions of the San Francisco Bay Watershed. Poster Presentation at the California Bay-Delta Authority sponsored Mercury Project Review, Sacramento,CA. Nov. 29 – Dec. 1, 2005.

Tsao-Melcer, D. C., J. Y. Takekawa, A. K. Miles, I. Woo (2007). Space use and mercury concentrations in Black Rails along the Petaluma River, CA. Poster presented at the 2006 CalFed Science Conference. Sacramento, CA. October 2006.

Tsao-Melcer, D. C., J. Y. Takekawa, A. K. Miles, I. Woo (2006). Home range, habitat use, and Mercury concentrations in Black Rails along the Petaluma River, CA. Poster presented at the 2006 Wildlife Society Western Section Conference, Sacramento, CA. February 2006.

Windham, L., M. Marvin-DiPasquale (2005). The Role of Submerged and Emergent Macrophytes in the Mercury Cycle of San Francisco Bay Wetlands. Poster Presentation at the California Bay-Delta Authority sponsored Mercury Project Review, Sacramento,CA. Nov. 29 – Dec. 1, 2006.

Woo, I., J. Y. Takekawa, D. Tsao-Melcer (2006). Methylmercury concentrations in marsh invertebrates and food web structure of California Black Rails (Laterallus jamaicensis cotuniculus). Oral Presentation. 4th Biennial CALFED Science Conference 2006 Making Sense of Complexity: Science for a changing environment. Sacramento, CA. October 23-25, 2006.

Woo, I., J. Y. Takekawa, D. Tsao-Melcer (2006). Assessing mercury concentrations in the California Black Rail (*Laterallus jamaicensis cotuniculus*) food web. Poster Presentation. 4th

Biennial CALFED Science Conference 2006 Making Sense of Complexity: Science for a changing environment. 23-25 October, 2006. Sacramento, CA.

G. Literature Cited

Barkay, T., M. Gillman, R. R. Turner (1997). Effects of dissolved organic carbon and salinity on bioavailability of mercury. Applied and Environmental Microbiology. 63(11): 4267-4271.

Benoit, J. M., C. C. Gilmour, R. P. Mason, A. Heyes (1999). Sulfide controls on mercury speciation and bioavailability to methylating bacteria in sediment pore waters. Environmental Science & Technology 33(6): 951-957.

Benoit, J. M., C. C. Gilmour, R. P. Mason, G. S. Riedel, G. F. Riedel (1998). Behavior of mercury in the Patuxent River estuary. Biogeochemistry (Dordrecht) 40(2-3): 249-265.

Bloom, N., A. Bollen, M. Briscoe, G. Hall, M. Horvat, C. Kim, B. Lasorsa, M. Marvin-DiPasquale, J. Parker (2006). International Solid Phase Mercury Speciation Exercise (ISPMSE): Introduction and Preliminary Results, in Mercury 2006 Abstracts Book: Eighth International Conference on Mercury as a Global Pollutant, Madison, Wisconsin August 6-11, 2006.

Bodaly, R. A., R. E. Hecky, R. J. P. Fudge (1984). Increases in fish mercury levels in lakes flooded by the Churchill River diversion, northern Manitoba. Can. J. Fish. Aquat. Sci. 41: 682-691.

Callaway, J., G. Sullivan, J. Desmond, G. Williams, J. Zedler (2001). Assessment and monitoring. in Zedler (editor) Handbook for Restoring Tidal Wetlands. CRC Press. Boca Raton, FL

Chen, Y., J. -C. J. Bonzongo, W. B. Lyons, G. C. Miller (1997). Inhibition of mercury methylation in anoxic freshwater sediment by group VI anions. Environmental Toxicology and Chemistry 16(8): 1568-1574.

Choe, K. Y., G. A. Gill (2003). Distribution of particulate, colloidal, and dissolved mercury in San Francisco Bay estuary. 2. Monomethyl mercury. Limnol. Oceanogr. 48(4):1547–1556

Choi, S. -C., T. Chase, R. Bartha (1994). Enzymatic catalysis of mercury methylation by Desulfovibrio desulfuricans. Applied and Environmental Microbiology 60(4): 1342-1346.

Cloern, J. E., E. A. Canuel, D. Harris. (2002). Stable carbon and nitrogen isotope composition of aquatic and terrestrial plants of the San Francisco Bay estuarine system. Limnol. Oceanogr. 47(3): 713-729.

Cline, J. D. (1969). Spectrophotometric determination of hydrogen sulfide in natural waters. Limnology and Oceanography (14): 454-458.

Conaway, C. H., E. B. Watson, J. R. Flanders, A. R. Flegal (2004). Mercury deposition in a tidal marsh of south San Francisco Bay downstream of the historic New Almaden mining district, California. Marine Chemistry 90: 175– 184.

Conaway, C. H., J. R. M. Ross, R. Looker, R. P. Mason, A. R. Flegal (2007) Decadal mercury trends in San Francisco Estuary sediments. Environmental Research 105(1): 53-66.

DeWild, J. F., M. L. Olson, S. D. Olund (2002). Determination of Methyl Mercury by Aqueous Phase Ethylation, Followed by Gas Chromatographic Separation with Cold Vapor Atomic Fluorescence Detection. U. S. Geological Survey OFR 01-445

Domagalski, J. L., D. G. Slotton, C. N. Alpers, T. H. Suchanek, R. Churchill, N. Bloom, S. M. Ayers, and J. Clinkenbeard (2004). Summary and Synthesis of Mercury Studies in the Cache Creek Watershed, California, 2000–01: U. S. Geological Survey Water-Resources Investigations Report 03-4335, 30 p.

El-Begearmi M. M., M. L. Sunde, H. E. Ganther (1977). A mutual protective effect of mercury and selenium in Japanese quail. Poult Sci. 56(1):313-22.

Evers D. C., Lane O. P., Savoy L., Goodale W. M. (2005). Assessing the impacts of methylmercury on piscivorous wildlife using a wildlife criterion value based on the Common Loon, 1998-2003. Unpublished Report BRI 2004-5 submitted to the Maine Department of Environmental Protection. BioDiversity Research Institute, Gorham, Maine, USA.

Fossing, H., B. Jørgensen (1989). Measurement of bacterial sulfate reduction in sediments: Evaluation of a single step chromium reduction method: Biogeochemistry (8): 205-222.

Gill, G. A. (2001). Assessment of Ecological and Human Health Impacts of Mercury in the Bay-Delta Watershed: CALFED Bay-Delta Mercury Project Final Report (2001). 38 pp.

Gilmour, C. C., G. S. Riedel, M. C. Ederington, J. T. Bell, J. M. Benoit, G. A. Gill, M. C. Stordal (1998). Methylmercury concentrations and production rates across a trophic gradient in the northern Everglades. Biogeochemistry (Dordrecht) 40(2-3): 327-345.

Haitzer, M., G. R. Aiken, J. N. Ryan (2003). Binding of mercury(II) to aquatic humic substances: Influence of pH and source of humic substances. Environmental Science & Technology 37(11): 2436-2441.

Hecky, R. E., R. A. Bodaly, D. J. Ramsay, P. S. Ramlal, N. E. Strange (1987). Evolution of limnological conditions, microbial methylation of mercury and mercury concentrations in fish in reservoirs of Northern Manitoba. B/ Report for the Canada-Manitoba agreement on the study and monitoring of mercury in the Churchill River Division, Governments of Canada and Manitoba.

Heinz G. H., D. J. Hoffman (1998) Methylmercury Chloride and Selenomethionine Interactions on Health and Reproduction in Mallards. Environmental Toxicology and Chemistry. 17(2): 139–145.

Hines, M. E., G. T. Banta, A. E. Giblin, J. E. Hobbie (1994). Acetate concentrations and oxidation in salt-marsh sediments. Limnol. Oceanogr. 39: 140–148.

Hurley, J. P., J. M. Benoit, C. L. Barbiarz, M. M. Shafer, A. W. Andren, J. R. Sullivan, R. Hammond, D. Webb (1995). Influences of watershed characteristics on mercury levels in Wisconsin rivers. Environmental Science and Technology. 19: 1867-1875.

Jin, L., P. Guo, X. Xu (1999). Effect of Selenium on Mercury Methylation in Facultative Lake. Sediments. Toxicolog. Environ. Chem. 69 (1–2): 255–261.

Jørgensen, B. B. (1978). A comparison of methods for the quantification of bacterial sulfate reduction in coastal marine sediments. 1. Measurement with radiotracer techniques. Geomicrobiology Journal, (1): 11-27.

Kelly, C. A., J. W. M. Rudd, R. A. Bodaly, N. P. Roulet, V. L. St Louis, A. Heyes, T. R. Moore, S. Schiff, R. Aravena, K. J. Scott, B. Dyck, R. Harris, B. Warner, G. Edwards (1997). Increases in fluxes of greenhouse gases and methyl mercury following flooding of an experimental reservoir. Environmental Science & Technology 31(5): 1334-1344.

Krabbenhoft, D. P., J. P. Hurley, M. L. Olson, L. B. Cleckner (1998). Diurnal variability of mercury phase and species distributions in the Florida Everglades, Biogeochemistry, 40, p. 311-325.

Krabbenhoft, D. P., J. M. Benoit, D. L. Babiarz, J. P. Hurley, A. W. Andren (1995). Mercury cycling in the Allequash Creek watershed, northern Wisconsin. Water Air and Soil Pollution 80(1-4): 425-433.

Krabbenhoft, D. P., J. G. Wiener, W. G. Brumbaugh, M. L. Olson, J. F. DeWild, T. J. Sabin (1999). A National Pilot Study of Mercury Contamination of Aquatic Ecosystems along Multiple Gradients- Contamination of Hydrologic Systems and Related Ecosystems, Charleston, South Carolina, March 8-12, 1999, U. S. Geological Survey WRI Report.

Krabbenhoft, D. P., J. M. Benoit, C. L. Babiarz, J. P. Hurley, A. W. Andren (1995). Mercury cycling in the Allequash Creek watershed, northern Wisconsin. Water Air and Soil Pollution,. 80(. 1-4,): 425-433.

Krabbenhoft, D. P., B. A. Branfiruen, A. Heyes, (2005). Biogeochemical Cycles Affecting the Speciation, Fate, and Transport of Mercury in the Environment, in Mercury: Sources, Measurements, Cycles and Effects (Parsons, M., and Percival, J. eds), Mineralogical Society of Canada, 2005.

Krabbenhoft, D. P., C. C. Gilmour, J. M. Beniot, C. L. Babiarz, A. W. Andren, J. P. Hurley, (1998). Methylmercury dynamics in littoral sediments of a temperate seepage lake, Canadian Journal of Fisheries and Aquatic Sciences 55: 835-844.

Krabbenhoft, D. P., M. L. Olson, J. F. Dewild, D. W. Clow, R. S. Striegl, M. M. Dornblaser, P. VanMetre (2002). Mercury Loading And Methylmercury Production And Cycling In High-Altitude Lakes From The Western United States, Water, Air and Soil Pollution 2(2): 233-249.

Legare, M. L., W. R. Eddleman (2001). Home range size, nest-site selection and nesting success of Black Rails in Florida. Journal of Field Ornithology 72:170-177.

Mason, R. P., J. R. Reinfelder, F. M. M. Morel (1996). Uptake, toxicity, and trophic transfer of mercury in a coastal diatom. Environmental Science & Technology 30(6): 1835-1845.

Martin, M. L., and J. R. Bider. (1978). Transmitter attachment for blackbirds. Journal of Wildlife Management 42:613-685.

Marvin-DiPasquale, M. C., and D. G. Capone (1998). Benthic sulfate reduction along the Chesapeake Bay central channel. I. Spatial trends and controls. Marine Ecology Progress Series, v. 168, p. 213-228.

Marvin-DiPasquale, M., J. Agee, R. Bouse, B. Jaffe (2003). Microbial cycling of mercury in contaminated pelagic and wetland sediments of San Pablo Bay, California. Environmental Geology, v. 43, no. 3, p. 260-267.

Marvin-DiPasquale, M., B. D. Hall, J. R. Flanders, N. Ladizinski, J. L. Agee, L. H. Kieu, L. Windham-Myer (2006). Ecosystem Investigations of Benthic Methylmercury Production: A Tin-Reduction Approach for Assessing the Inorganic Mercury Pool Available for Methylation, in Mercury 2006 Abstracts Book: Eighth International Conference on Mercury as a Global Pollutant, Madison, Wisconsin August 6-11, 2006.

Marvin-DiPasquale, M., and M. H. Cox (2007). Legacy Mercury in Alviso Slough, South San Francisco Bay, California: Concentration, Speciation and Mobility U. S. Geological Survey, Open-File Report number 2007-1240, 98 p. On-line: http://pubs.usgs.gov/of/2007/1240/

Marvin-DiPasquale, M., M. A. Lutz, M. E. Brigham, D. P. Krabbenhoft, G. R. Aiken, W. H. Orem, B. D. Hall (2008 in prep). Mercury Cycling in Diverse Stream Ecosystems: 2. Benthic Methylmercury Production and Bed Sediment/Pore Water Partitioning: Environ. Sci. Tech.

Michener, R. H., L. Kaufman. 2007. Stable isotope ratios as tracers in marine food webs: an update. in R. Michener and K. Lajtha (Eds). Stable Isotopes in Ecology and Environmental Science: ecological methods and concepts 2nd edition. Blackwell Publishing. Malden MA.

NADP (2006). Mercury Deposition Network: a NADP Network. Monitoring Location CA72, San Jose, CA. Sample data query. http://nadp.sws.uiuc.edu/sites/siteinfo.asp?id=CA72&net=MDN

Olson, M. L., J. F. DeWild (1999). Low-level techniques for the collection and species-specific analysis of low levels of mercury in water, sediment, and biota, in Morganwalp, D. W., and Buxton, H. T., eds., Contamination of Hydrologic Systems and Related Ecosystems: U. S. Geological Survey Water-Resources Investigations Report 99-4018B: 191-200.

Oremland, R. S., L. G. Miller, P. Dowdle, T. Connell, T. Barkay (1995). Methylmercury oxidative degradation potentials in contaminated and pristine sediments of the Carson River, Nevada. Applied and Environmental Microbiology 61(7): 2745-2753.

Pelletier, E. (1985). Mercury-Selenium Interactions in Aquatic Organisms: A Review. Marine Environmental Research 18: 111-132.

Puckett, M., N. S. Bloom (2001). Fish mercury distribution in Massachusetts, USA lakes. Environmental Toxicology and Chemistry 18(7): 1370-1379.

Ralston, N. V. C., J. L. Blackwell III, L. J. Raymond (2007). Importance of Molar Ratios in Selenium-Dependent Protection Against Methylmercury. Biol Trace Elem Res (2007) 119:255–268

Robert, M., P. Laporte. (1999). Numbers and movements of Yellow Rails along the St. Lawrence River, Quebec. Condor 101:667-671.

Rose, J., et al. (1999). Fish mercury distribution in Massachusetts, USA lakes. Environmental Toxicology and Chemistry 18(7): 1370-1379.

Rose, J., M. S. Hutcheson, C. R. West, O. Pancorbo, K. Hulme, A. Cooperman, G. DeCesare, R. Isaac, A. Screpetis (1999). Fish mercury distribution in Massachusetts, USA lakes. Environmental Toxicology and Chemistry 18(7): 1370-1379.

Rudd, J. W. M. (1995). Sources of methyl mercury to freshwater ecosystems: A review. Water Air and Soil Pollution 80(1-4): 697-713.

Rudd, J. W. M., M. A. Turner, A. Furutani, A. Swick, B. E. Townsend (1983). A synthesis of recent research with a view towards mercury amelioration. Canadian Journal Fisheries Aquatic Sciences 40: 2206-2217.

Scheuhammer, AM. (1987). The chronic toxicity of Aluminum, Cadmium, Mercury, and Lead in birds: a review. Environ. Pollut. 46:263-295.

Schoellhamer, D. H., T. E. Mumley, J. E. Leatherbarrow (2007). Suspended sediment and sediment-associated contaminants in San Francisco Bay. Environmental Research, 105(1): 119-131.

SFEI (2007). The 2006 RMP Annual Monitoring Results. Regional Monitoring Program for Water Quality in the San Francisco Estuary. SFEI Contribution No. 542. San Francisco Estuary Institute, Oakland, CA. http://www.sfei.org/rmp/annualmonitoringresults/RMP_AMR2006_Final4web.pdf

Slotton, D. G., T. H. Suchanek, S. M. Ayers (2000). CalFed UC Davis Mercury Study: Year 2 Findings. CalFed Science Conference October 3-5, 2000, Sacramento, CA.

Southworth, G. R., M. J. Peterson, M. G. Ryon (2000). Long-Term Increased Bioaccumulation of Mercury in Largemouth Bass Follows Reduction of Waterborne Selenium. Chemosphere 41 (7): 1101–5.

St. Louis, V. L., J. W. M. Rudd, C. A. Kelly, K. G. Beaty, R. J. Flett, N. T. Roulet (1996). Production and loss of methylmercury and loss of total mercury from boreal forest catchments containing different types of wetlands. Environmental Science & Technology. 30(. 9,): 2719-2729.

USEPA 2002, Method 1631, Revision E: Mercury in water by oxidation, purge and trap, and cold vapor atomic fluorescence spectrometry. U. S. Environmental Protection Agency, Office of Water, Washington D. C. : EPA-821-R-02-019, 36 pp.

Watras, C. J., K. A. Morrison, N. S. Bloom (1995a). Chemical correlates of Hg and methyl-Hg in northern Wisconsin lake waters under ice-cover. Water Air and Soil Pollution 84(3-4): 253-267.

Watras, C. J., K. A. Morrison, J. S. Host, N. S. Bloom (1995b). Concentration of mercury species in relationship to other site-specific factors in the surface waters of northern Wisconsin lakes. Limnology and Oceanography 40(3): 556-565.

Westcott, K., J. Kalff (1996). Environmental factors affecting methyl mercury accumulation in zooplankton. Canadian Journal of Fisheries and Aquatic Sciences 53(10): 2221-2228.

Wheeler, W. E. (1991). Suture and glue attachment of radio transmitters on ducks. Journal of Field Ornithology 62:271-278.

Wiener, J. G., D. P. Krabbenhoft, G. H. Heinz, A. M. Scheuhammer (2003). Ecotoxicology of Mercury, Chapter 16 in D. J. Hoffman, B. A. Rattner, G. A. Burton, Jr., and J. Cairns, Jr. (editors), Handbook of Ecotoxicology, 2nd edition. CRC Press, Boca Raton, Florida, USA, pp. 407-461.

Wiener, J. G., B. C. Knights, M. B. Sandheinrich, J. D. Jeremiason, M. E. Brigham, D. R. Engstrom, L. G. Woodruff, W. F. Cannon, J. Balogh (2006). Mercury in Soils, Lakes, and Fish in Voyageurs National Park (Minnesota): Importance of Atmospheric Deposition and Ecosystem Factors, Environmental Science & Technology 40: 6261-6268

Wiener, J. G., C. C. Gilmour, D. P. Krabbenhoft (2003). Mercury Strategy for the Bay-Delta Ecosystem: A Unifying Framework for Science, Adaptive Management, and Ecological Restoration. Final Report to the California Bay Delta Authority: Association of Bay Area Governments. December 31, 2003.

Windham, L., J. Weis, P. Weis (2001). Patterns and processes of mercury (Hg) release from leaves of two dominant salt marsh plants: Spartina alterniflora (salt cordgrass) and Phragmites australis (common reed). Estuaries 24(5): 787-799.

Wolfe, M. F., S. Schwarzbach, R. A. Sulaiman (1998). Effects Of Mercury On Wildlife: A Comprehensive Review. Environmental Toxicology and Chemistry. 17: 146–160.

Xun, L., N. E. R. Campbell, J. W. M. Rudd (1987). Measurements of Specific Rates of Net Methyl Mercury Production in the Water Column and Surface Sediments of Acidified and Circumneutral Lakes. Canadian Journ. Fish. Aquat. Sci. 44: 750-757.

Zhabina, N., I. Volkov (1978). A method of determination of various sulfur compounds in sea sediment and rocks, in Krumbein, ed., Environmental Biogeochemistry and Geomicrobiology (Vol. 3): Ann Arbor, Ann Arbor Sci. Publ., : 735-746.

H. Acknowledgements

We would like to acknowledge and thank the CalFed Bay-Delta Authority under the Ecosystem Restoration Program, for funding the research described in this report under project ERP-02D-P62, and thank the peer reviewers for suggestions to make this document more complete and clear. The authors would also like to thank the following group of people whose professionalism and energy significantly contributed to this scientific program: J. Hunt, S. Bezalel, C. Striplen, A. Gilbreath, M. Williams, S. Pearce, B. Greenfield, M. Odaya, A. Robinson, S. Shonkoff for field assistance and data management at SFEI, J.L. Agee, L.H. Kieu, J.R. Flanders, S. Becking, N. Ladizinsky, A. Jew, S. Wren at USGS (Menlo Park, CA) for field and laboratory analytical support; D. Barfuss at GA State Univ. (Atlanta, GA) and NIEHS (Project # RO-1 ES05980 granted to D. Barfuss) for supplying radiotracer ^{203}Hg(II) for Hg-cycling studies; this project was additionally supported by R. Morat (FWS) and the USGS-SFBE Wetland Restoration Program. We gratefully thank R. Phelan and S. Brand for site access at Gambinini, CA Department of Fish and Game for access and permission at Mid Petaluma and Black John Slough, and J. Gustafson and D. Steele (CDFG) for state permits to work on the California Black Rail. Special thanks to J. Yee (USGS) for statistical advice, C. Eagles-Smith for stable istope expertise, Wes Maffei (Napa Solano Mosquito Abatement) and the UC Bohart Museum for insect and invertebrate identification, M. Nagendran D.V.M. and P. Gibbons as our veterinarian consultants, and field volunteers: A. Rowan, R. Gardiner, K. Turner, H. Bohlmann, A. Westhoff, and R. Melcer. We also wish to thank Leann Androvich of GCAP services for assistance with contract management and Mary Menconi of DFG for technical guidance on the project.

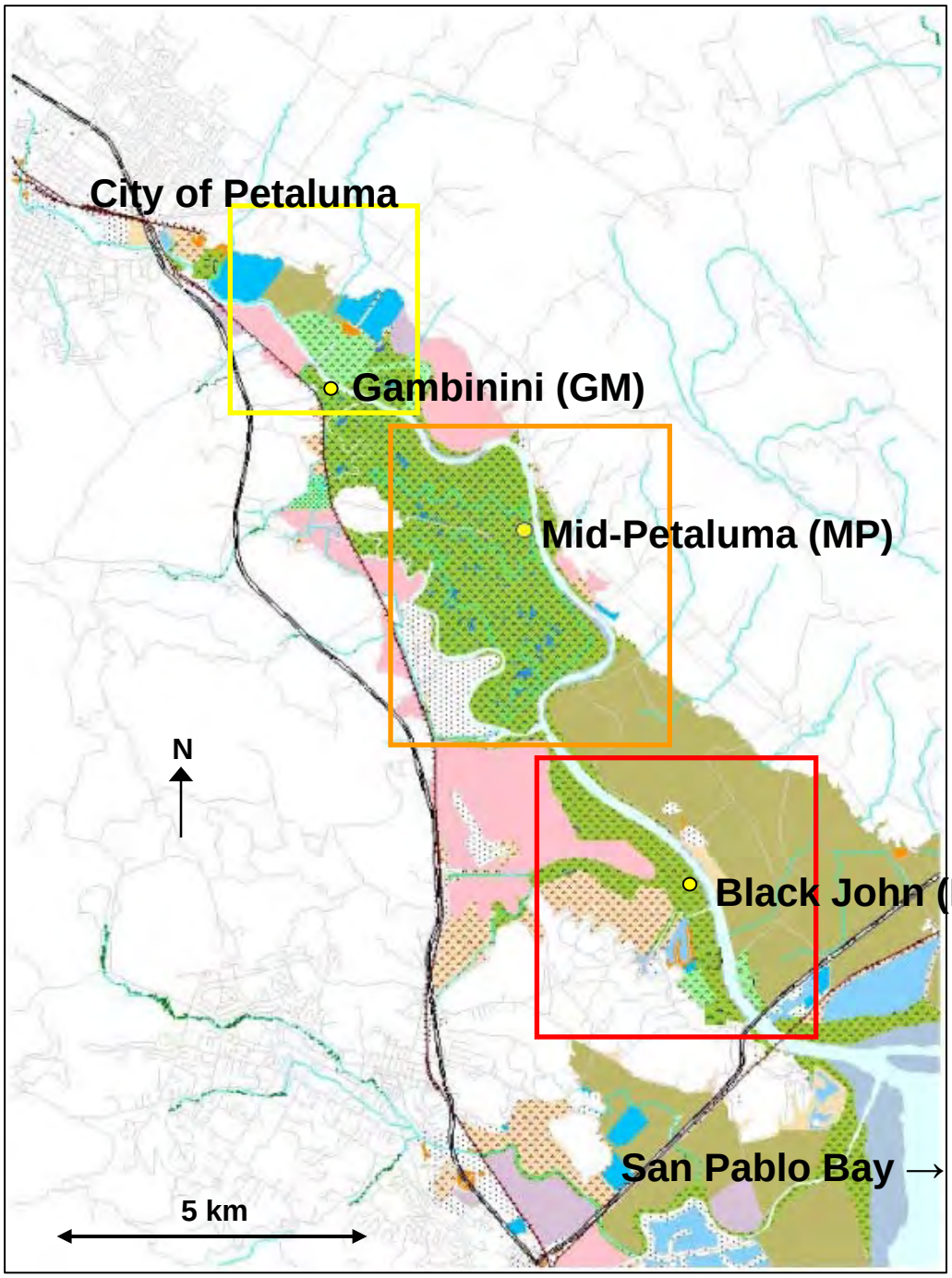

Figure B.3.1. Map of studied wetlands along the Petaluma River from least (yellow square) to most (red square) saline areas.

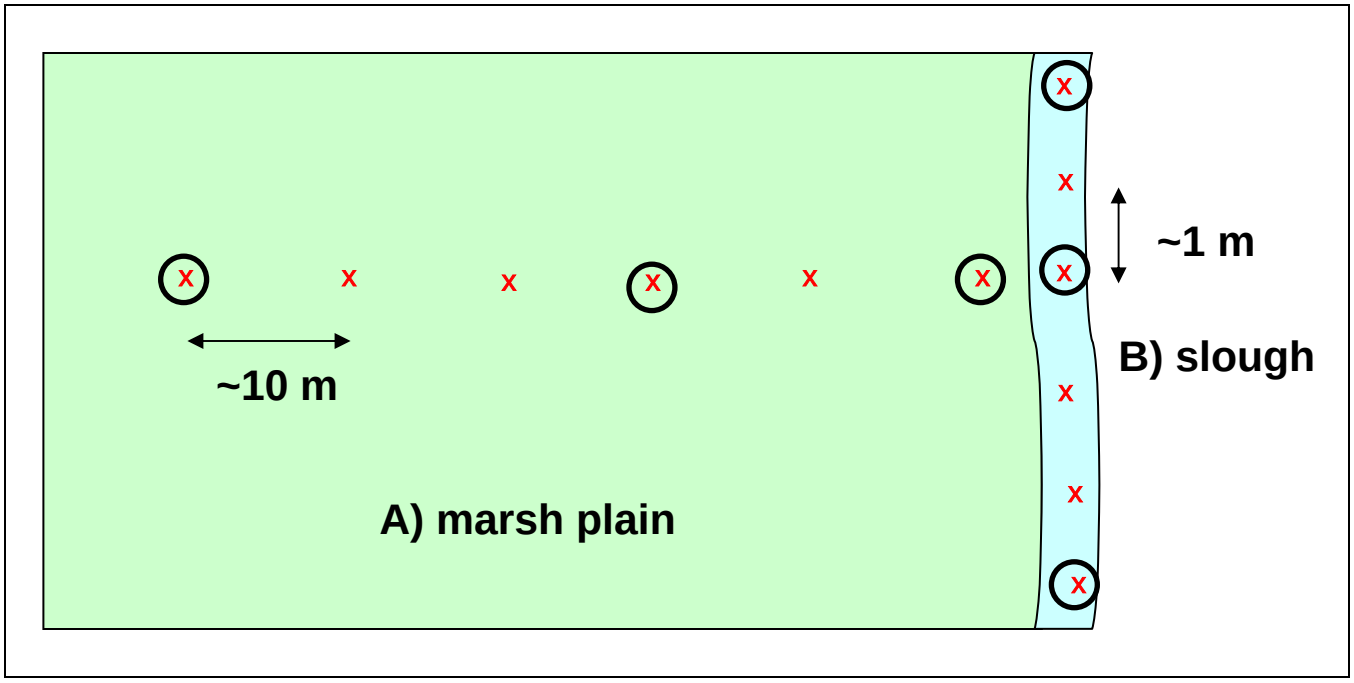

Figure B.3.2. Sediment locations sampled in April & August 2005. Samples were collected from the following habitat elements for each wetland: A) marsh plain and B) 3rd order (typically ~1-2 m wide) sloughs. Replicates of each habitat element were sampled in each wetland. Surface sediments (0- 2 cm depth) were taken from points (marked with "x") and composited for each replicate site; core samples (up to 25 cm depth) were taken from a subset of (circled) points and analyzed as individual grabs. The marsh core sample adjacent to the slough, when analyzed separately, was treated as equivalent to a marsh edge sample for comparison to 2006 data. The figure is not drawn to scale: marsh plain subsamples for composites were taken at ~10 m intervals starting from ~1m from the slough edge and moving along a transect away from 3rd order slough channels; slough samples were taken from bottoms of channels, with surface subsamples taken at ~1 m intervals composited for each slough site replicate.

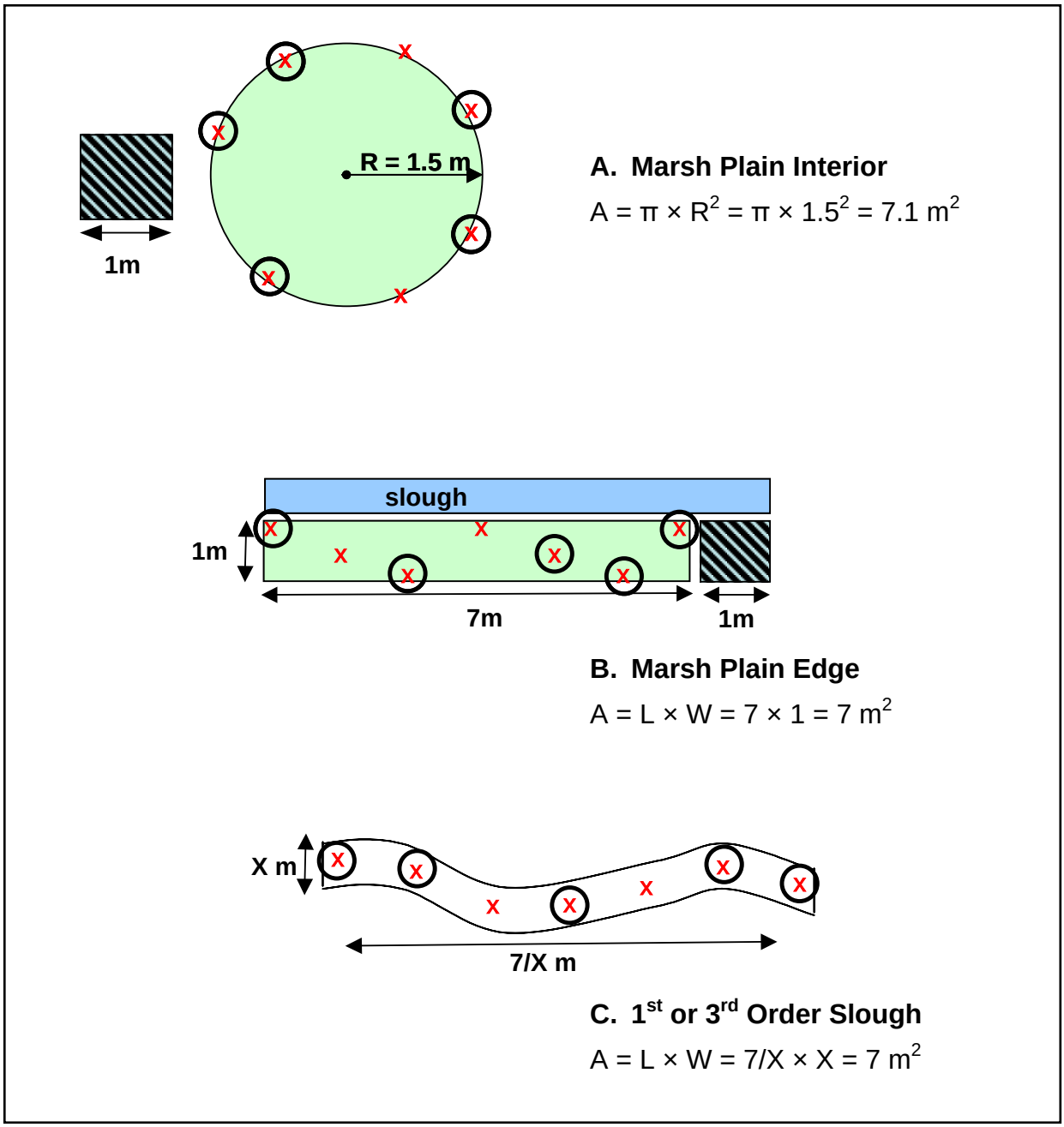

Figure B.3.3 Sediment sampling approach and geometry for April & August 2006 sampling events. Sampled areas included the following habitat elements: A) marsh plain interior, B) marsh plain edge and C) 1st or 3rd order sloughs. All sites were sampled as 7 subsamples (red X's) of the 0-2 cm surface interval that were composited for microbial assays, THg and MeHg analysis, and ancillary sediment geochemistry. Samples were collected from a 7 m^2 area in each habitat element, in a geometry adjusted to that of the habitat feature being sampled. Five individually analyzed sub-samples (circles) were also collected for a study of THg and MeHg variability. In marsh sites, an adjacent 1 m^2 plot was devegetated for plant veg/deveg experiments (hashed area).

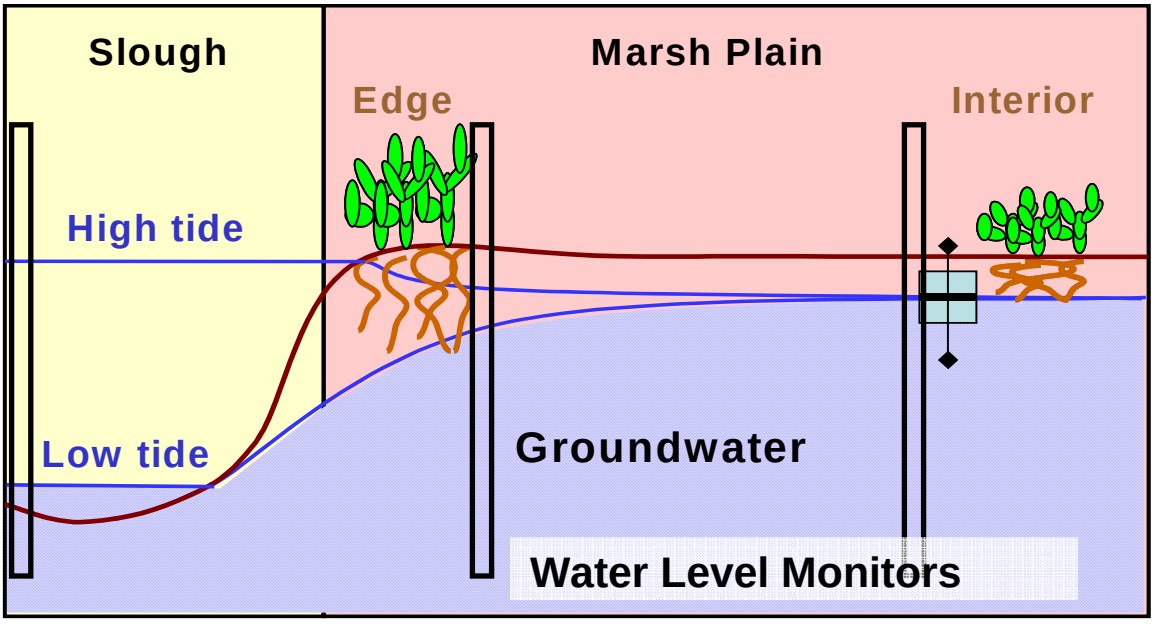

Figure D.1.1. Conceptual model of hydrology in tidal wetland habitat elements. High and low tide lines illustrate the water level in the slough and saturated zone of the marsh plain within a single (non –overbanking) tidal cycle. A groundwater monitoring well located at the marsh plain edge responds to tidal oscillations, whereas a monitoring well in the marsh plain interior shows little to no response to tides. The box plot and whiskers on the marsh plain interior illustrates hypothetical interquartile (25-75 percentile) and full ranges of the water level, respectively, over the course of a full spring and neap tidal cycle series at the marsh plain interior location.

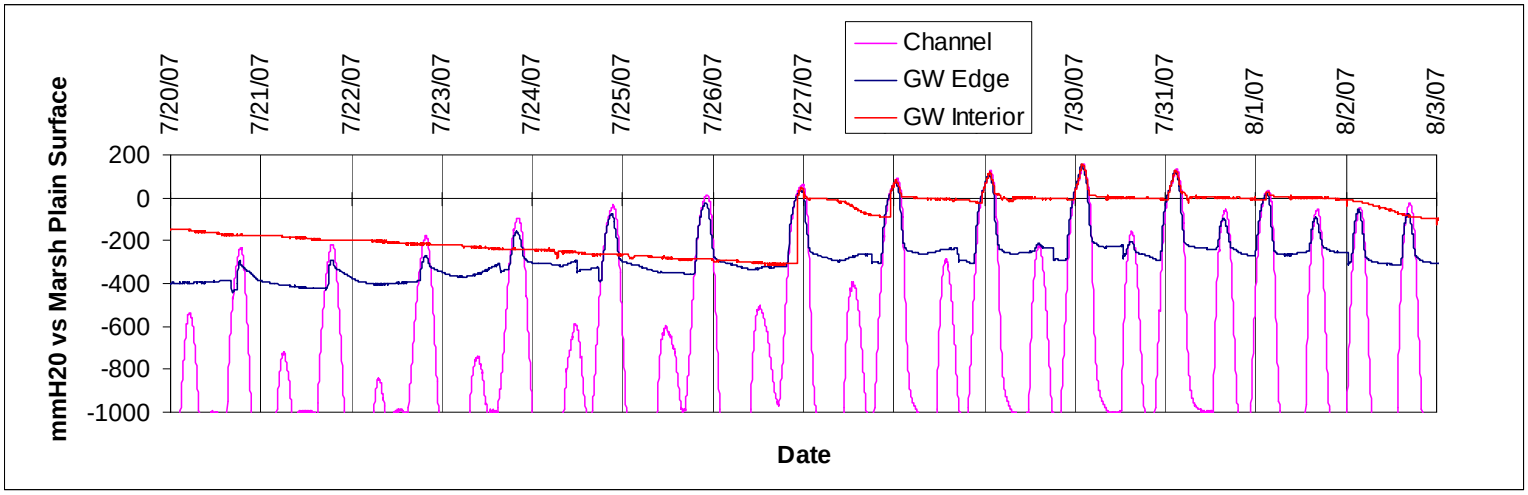

Figure D.1.2. Gambinini slough channel and marsh plain (edge and interior) groundwater levels during a spring/neap tide cycle. The marsh plain edge groundwater level responds to water infiltrating from the channel in non-overbanking high tides during a period of neap tides (July 20-26), while the marsh plain interior continually draws down.

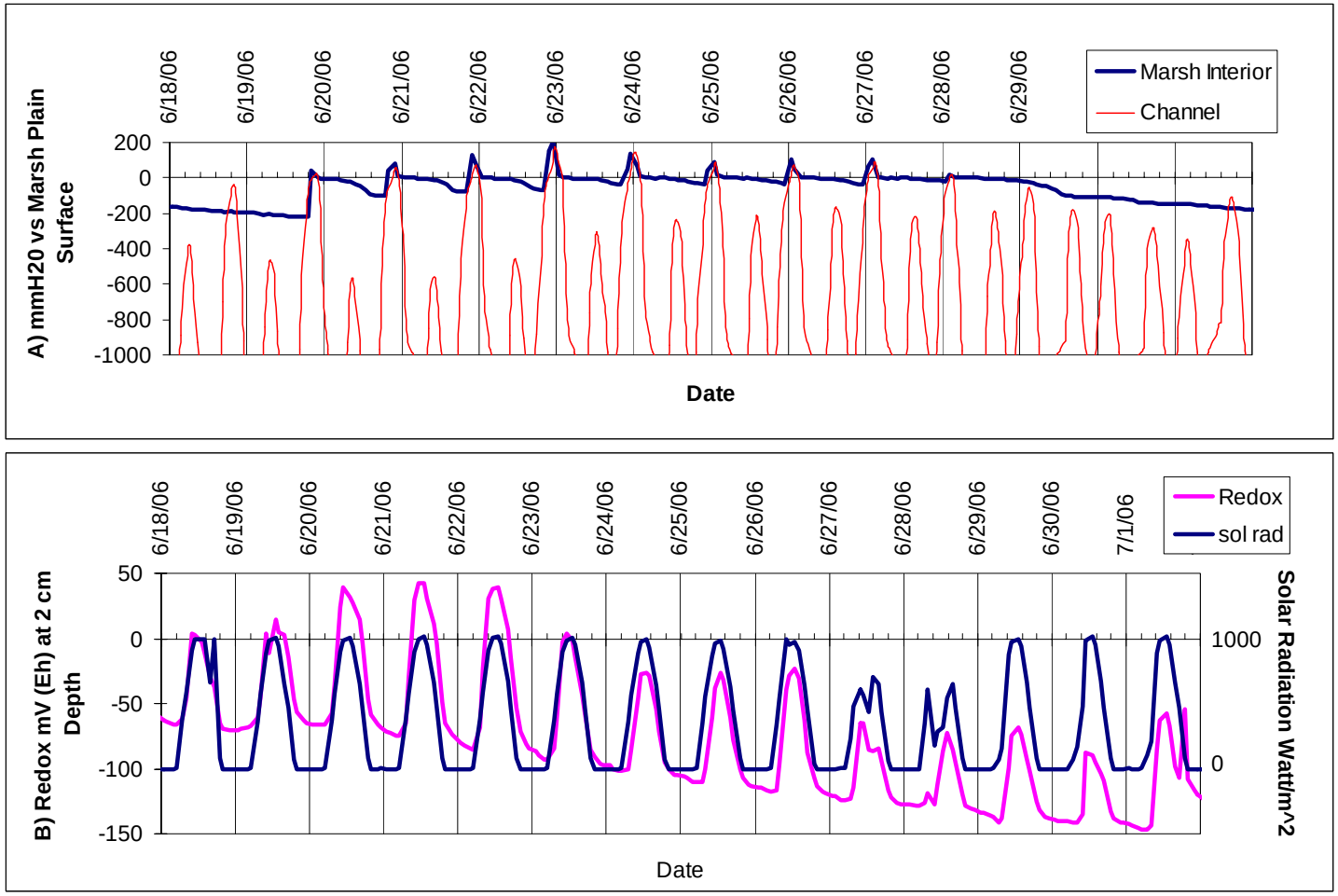

Figure D.1.3. Gambinini A) marsh plain and channel water levels and B) redox (at 2cm depth) and nearby solar radiation during a spring tide cycle. Marsh plain interior water levels show cycles similar to other periods (e.g. Figure D.1.2). Soil redox responds to solar radiation (data from CA Dept. of Forestry Santa Rosa (STA) meteorology station, ~30 km N-NW of Gambinini (lat/lon 38.479/-122.712) http://cdec.water.ca.gov/cgi-progs/queryF?s=sta).

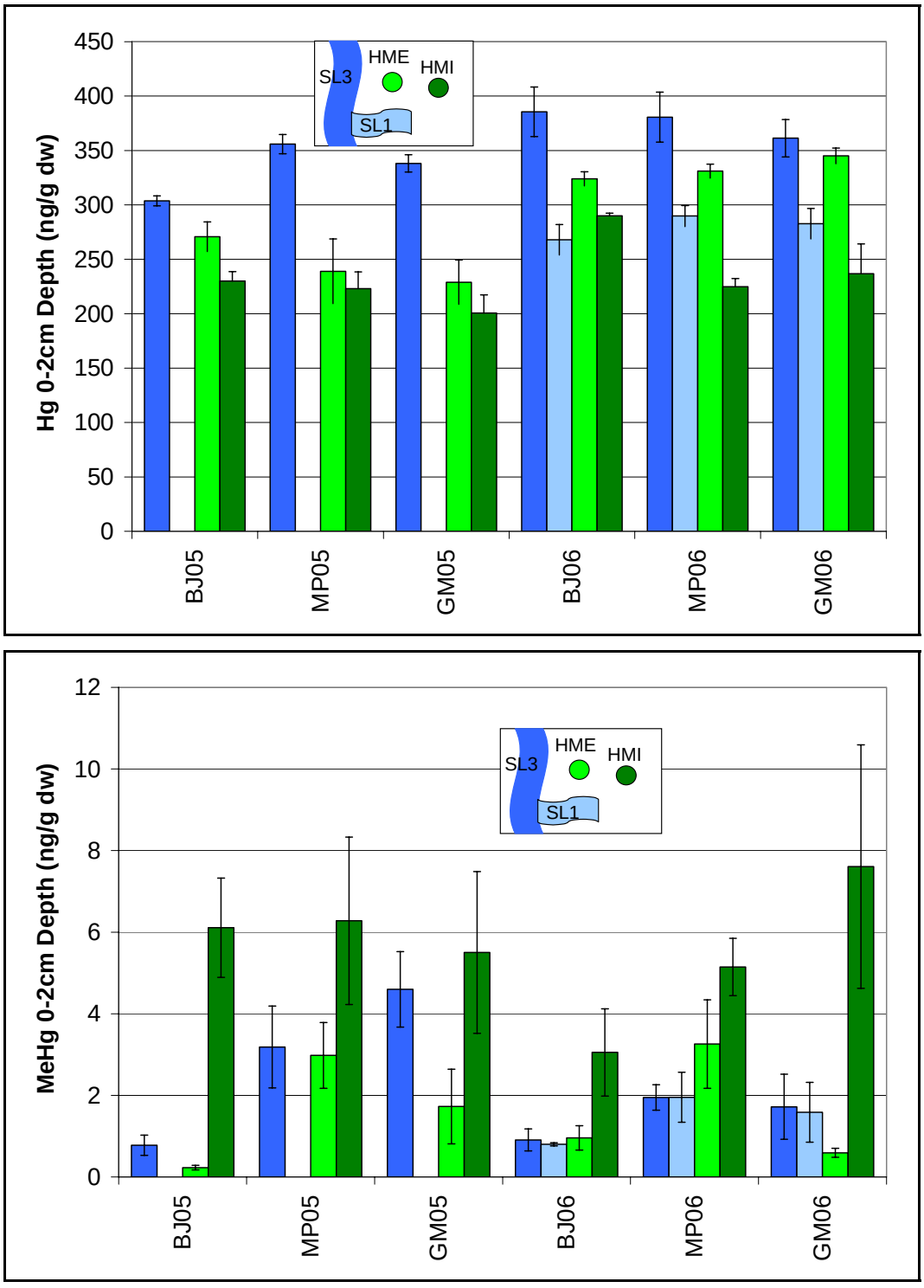

Figure D.2.1. Sediment THg and MeHg concentrations (mean±se (standard error bars)) for triplicate grabs taken in studied wetlands (BJ, MP, GM) in 2005 and 2006. Grabs taken in April and August combined within each year. Color-coded inset maps correspond to colors of bars, and show relative spatial position of sampling locations at each site. Sampling sites are 1st (SL1) or 3rd (SL3) order sloughs, or high marsh edge (HME) or interior (HMI) locations. 1st order sloughs (SL1) were not sampled in 2005.

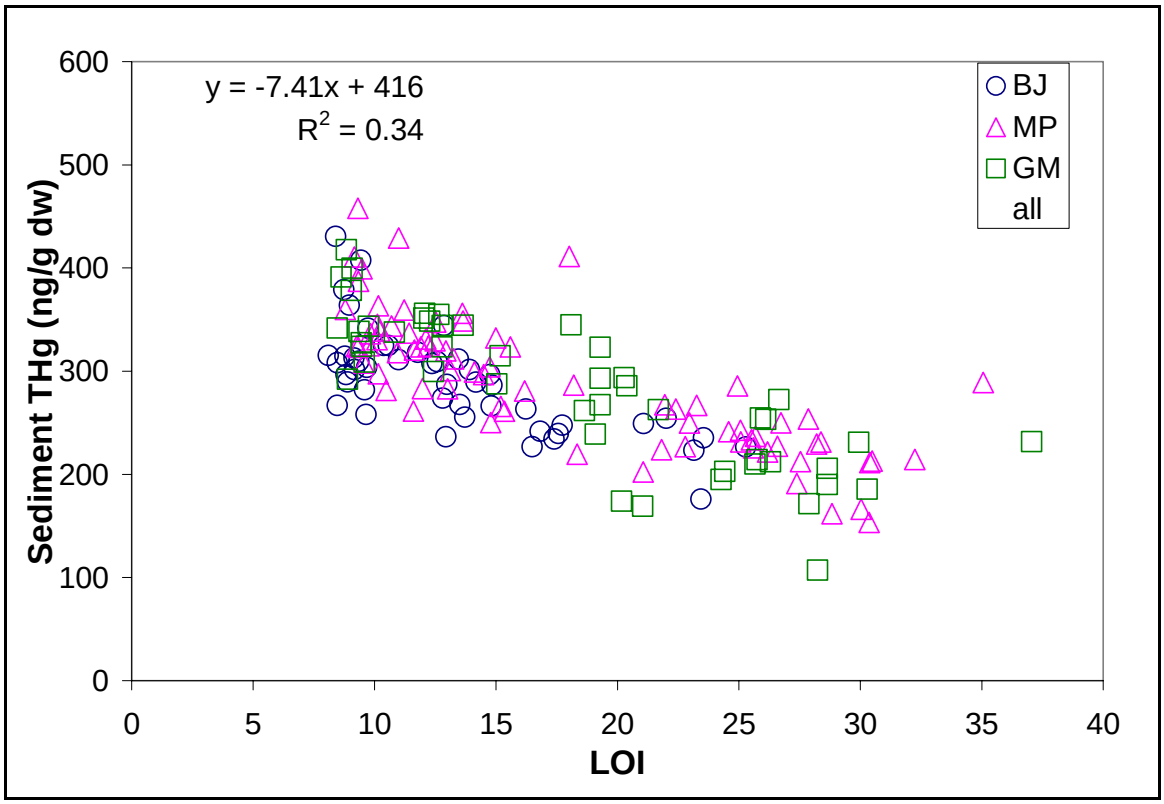

Figure D.2.2. Linear regression of Shallow (0-2cm) Sediment THg to Loss on Ignition. Regression conducted on data for all wetlands and habitat elements combined.

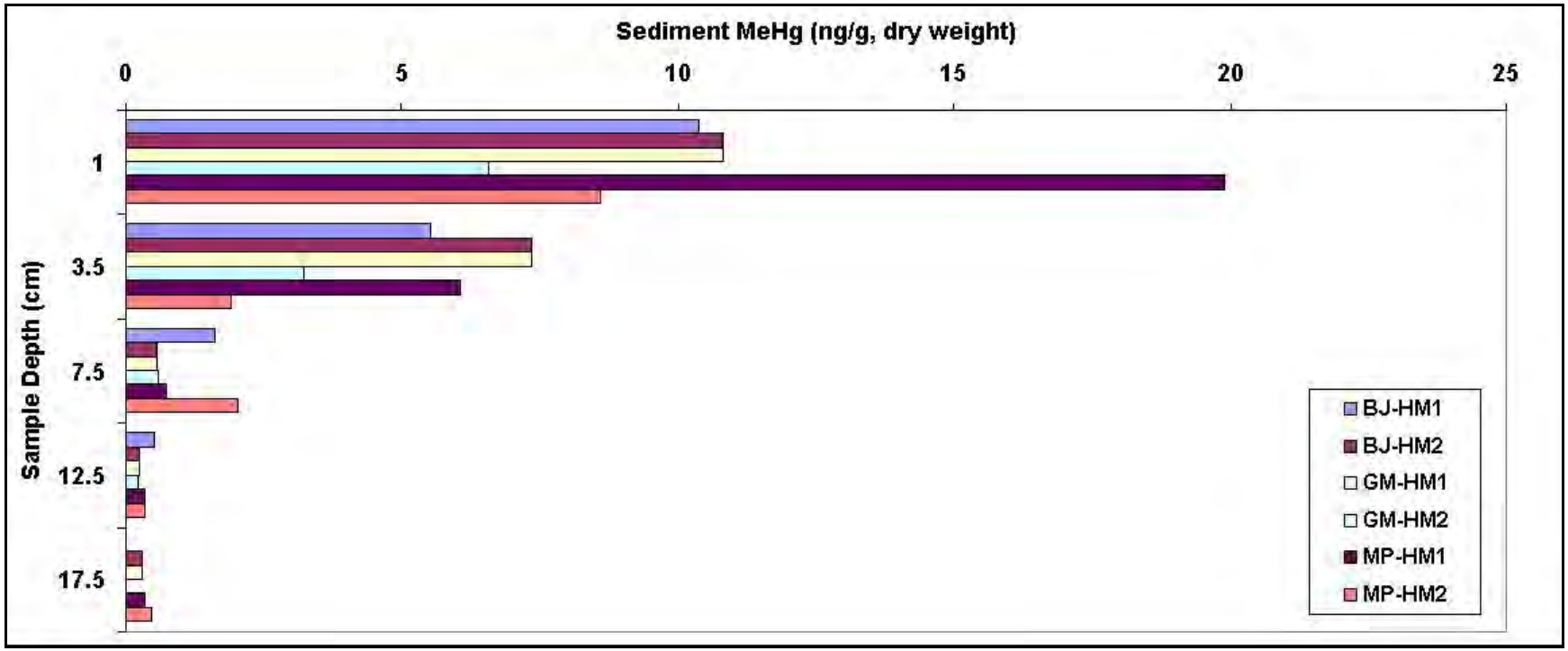

Figure D.2.3. Sediment MeHg concentrations for sediment cores collected from three principal study wetlands (BJ, GM, and MP) from two high marsh (HM) sites.

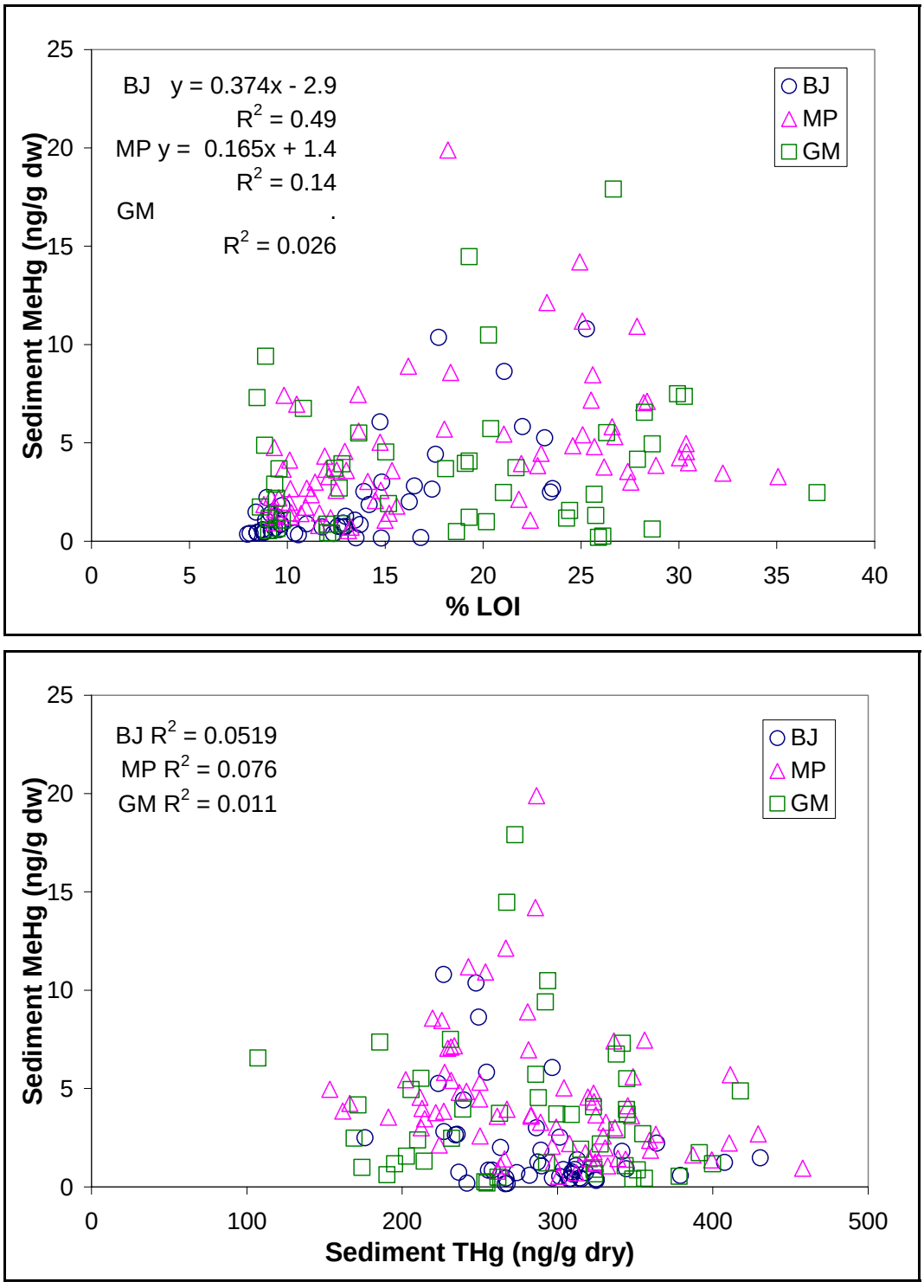

Figure D.2.4. Regressions of Shallow (0-2cm) Sediment MeHg to Loss on Ignition and THg. MeHg showed a moderate to weak relationship to LOI at two of the study wetlands, but no significant relationship to THg at any wetland. Linear regressions conducted on data for each wetland individually. Equations shown only for significant ($p<0.05$) relationships.

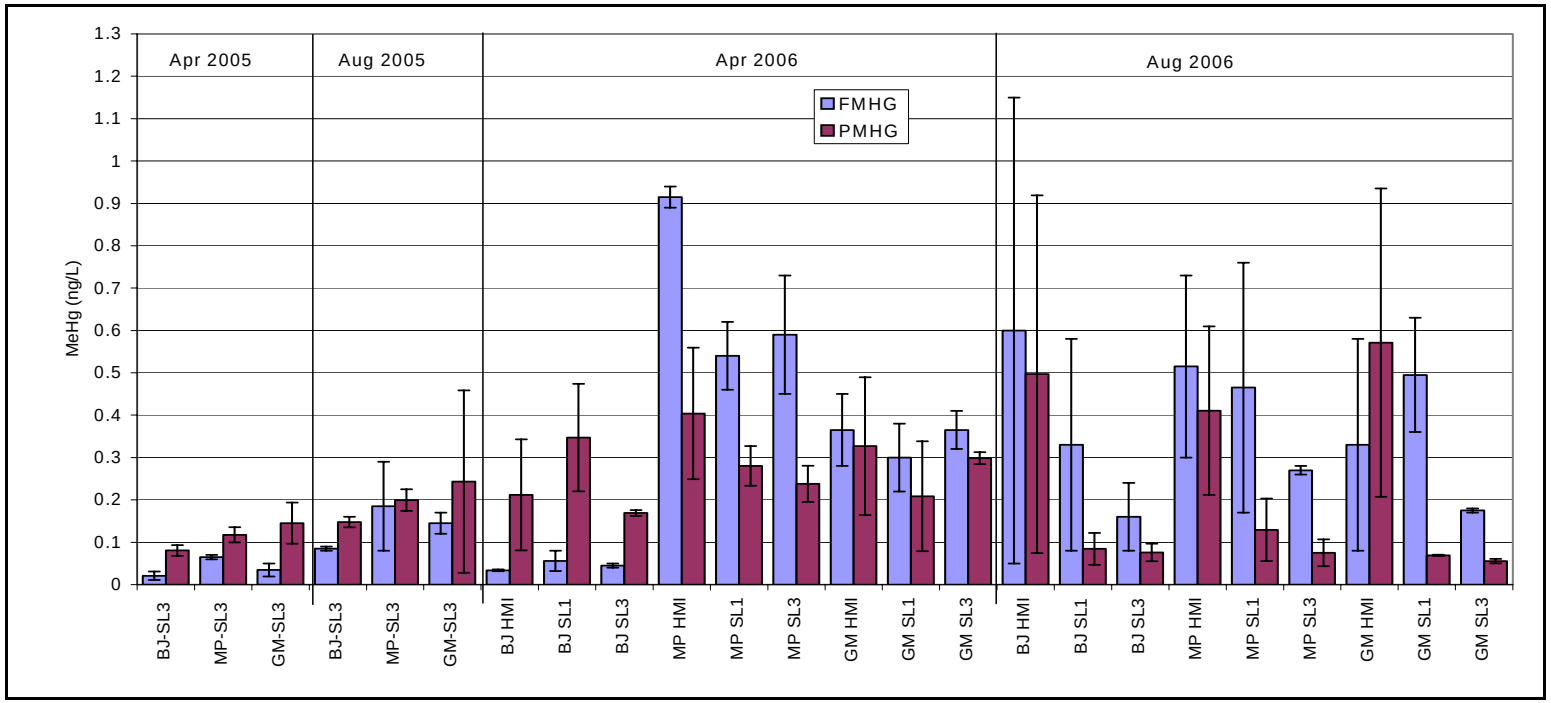

Figure D.2.5. Filtered (FMHg) and Particulate (PMHg) MeHg Concentrations in Wetland Waters (ng/L). Samples filtered using quartz fiber filters, 0.7 μm nominal pore size. Bars represent mean (±std err, n=2 to 4) for replicate water samples collected from 3rd (SL3) and first (SL1) order sloughs, pooled water on high marsh interior (HMI) surfaces.

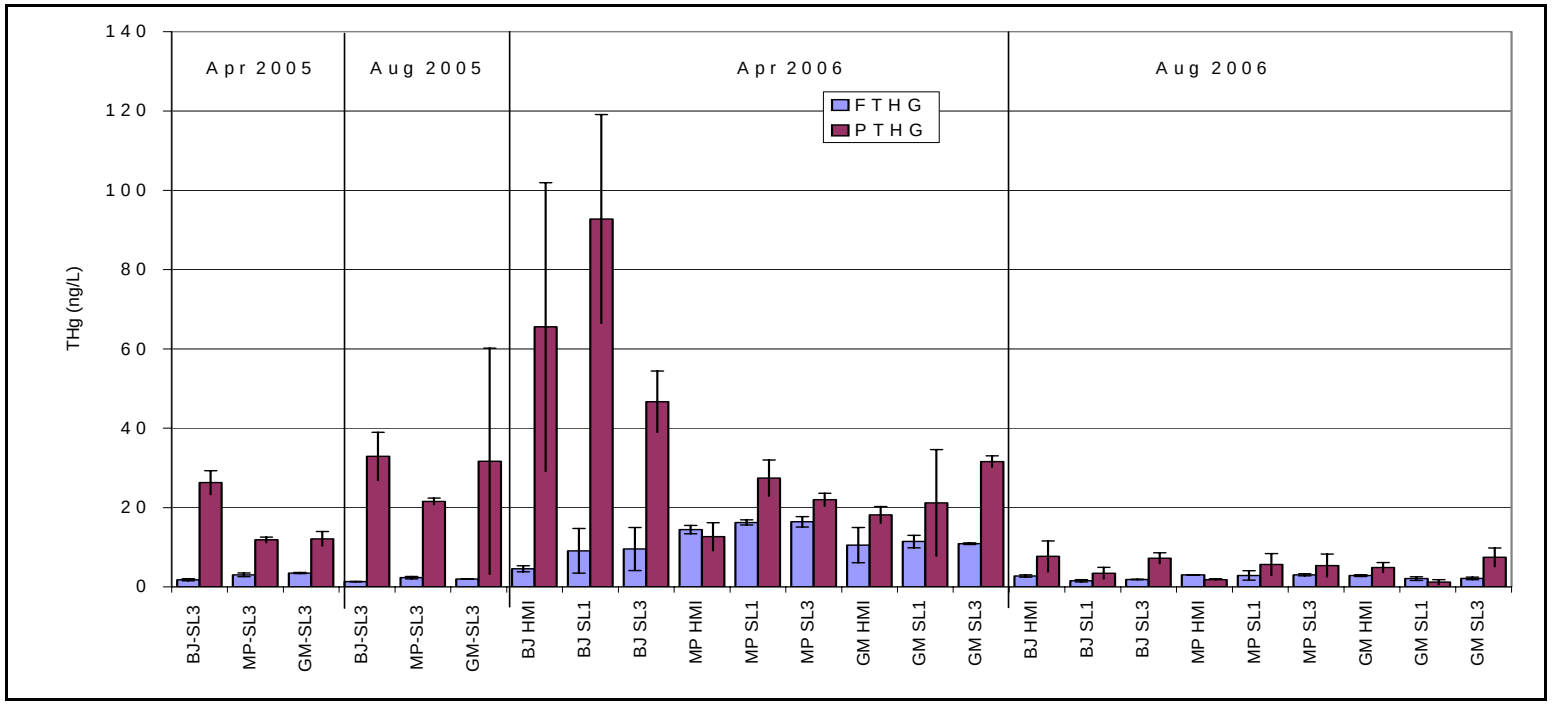

Figure D.2.6. Filtered (FTHg, ng/L) and Particulate (PTHg, ng/L) THg Concentrations in Wetland Waters. Samples filtered using quartz fiber filters, 0.7 μm nominal pore size. Bars represent mean (±std err, n=2 to 4) for replicate water samples collected from 3rd (SL3) and first (SL1) order sloughs, pooled water on high marsh interior (HMI) surfaces.

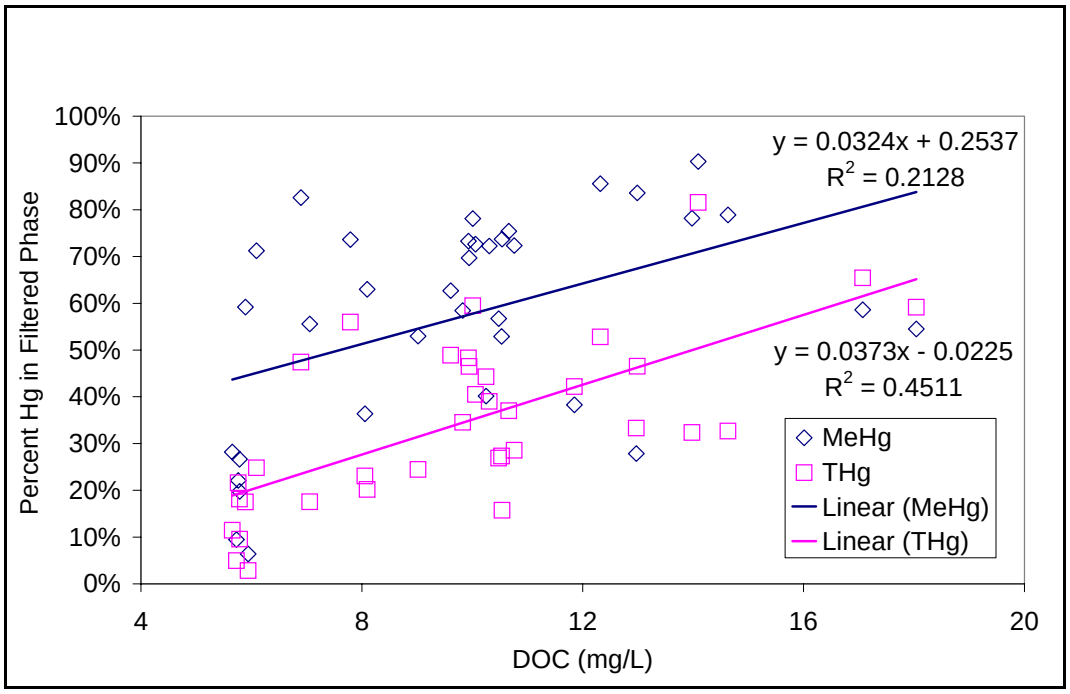

Figure D.2.7. Filtered MeHg and THg (as % of total water column concentration) vs DOC concentrations (mg/L) in water samples (quartz fiber filters, 0.7 um pore size)

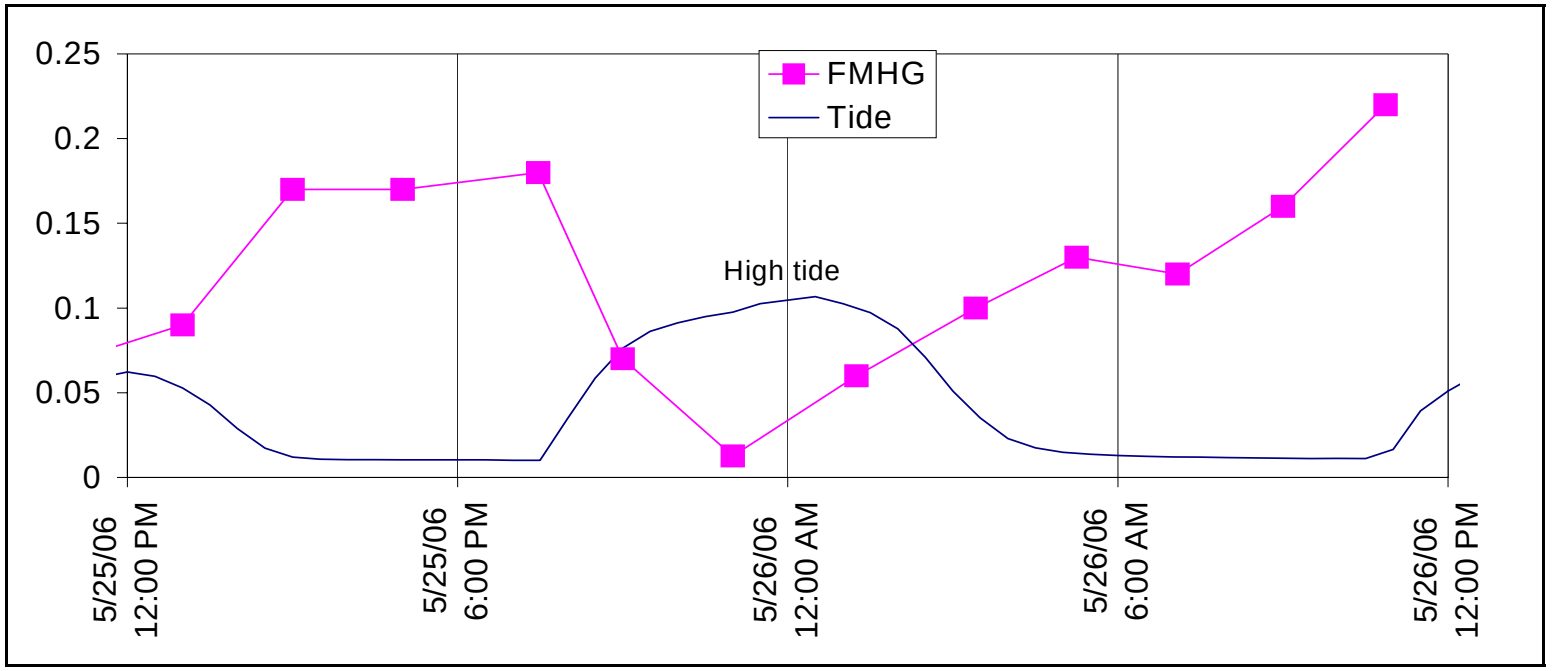

Figure D.2.8. Filtered MeHg (FMHg) During Overbank Tide Event at BJ. Grab samples were collected from a 3rd order channel every two hours for 24 hours, filtered (quartz fiber filters, 0.7 um pore size) within ~4 hours of collection in the field or on return to laboratory. Vertical axis is filtered MeHg concentration in ng/L, tidal height is arbitrarily scaled to fit graph, shown only to illustrate timing of tidal level changes.

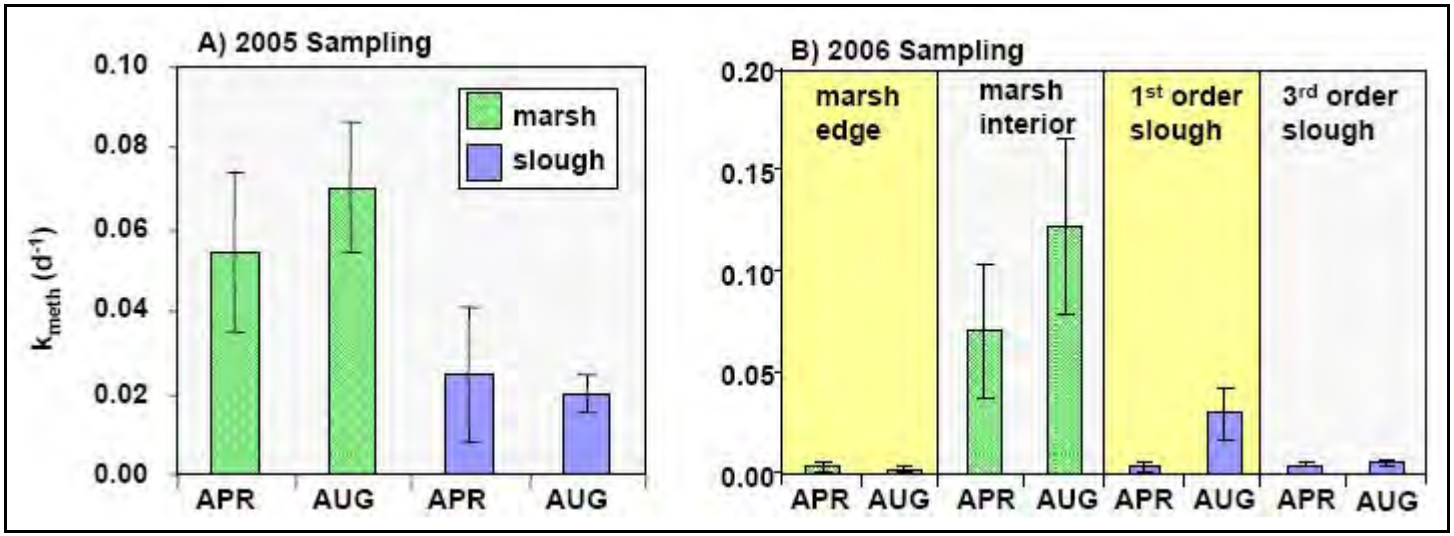

Figure D.3.1. Average microbial Hg(II)-methylation rate constants (k_{meth}) in 0-2 cm surface sediment for specific sub-habitat types, during A) 2005 and B) 2006. Values of k_{meth} were assessed by the ^{203}Hg(II)-methylation assay (Marvin-DiPasquale and Agee 2003). Each bar represents N = 6 sites. Error bars reflect standard deviations.

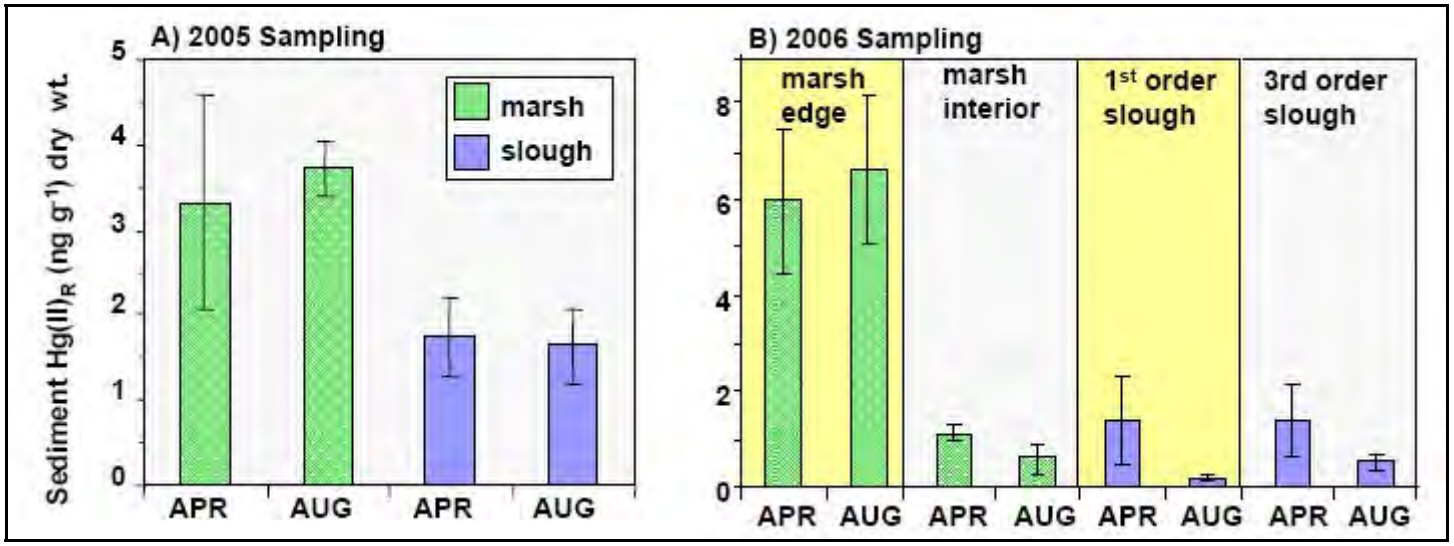

Figure D.3.2. Average reactive inorganic mercury ($Hg(II)_R$) in 0-2 cm surface sediment for specific sub-habitat types by month, for A) 2005 and B) 2006. Each bar represents N = 6 sites (n = 2 x 3 marshes). Error bars reflect standard deviations.

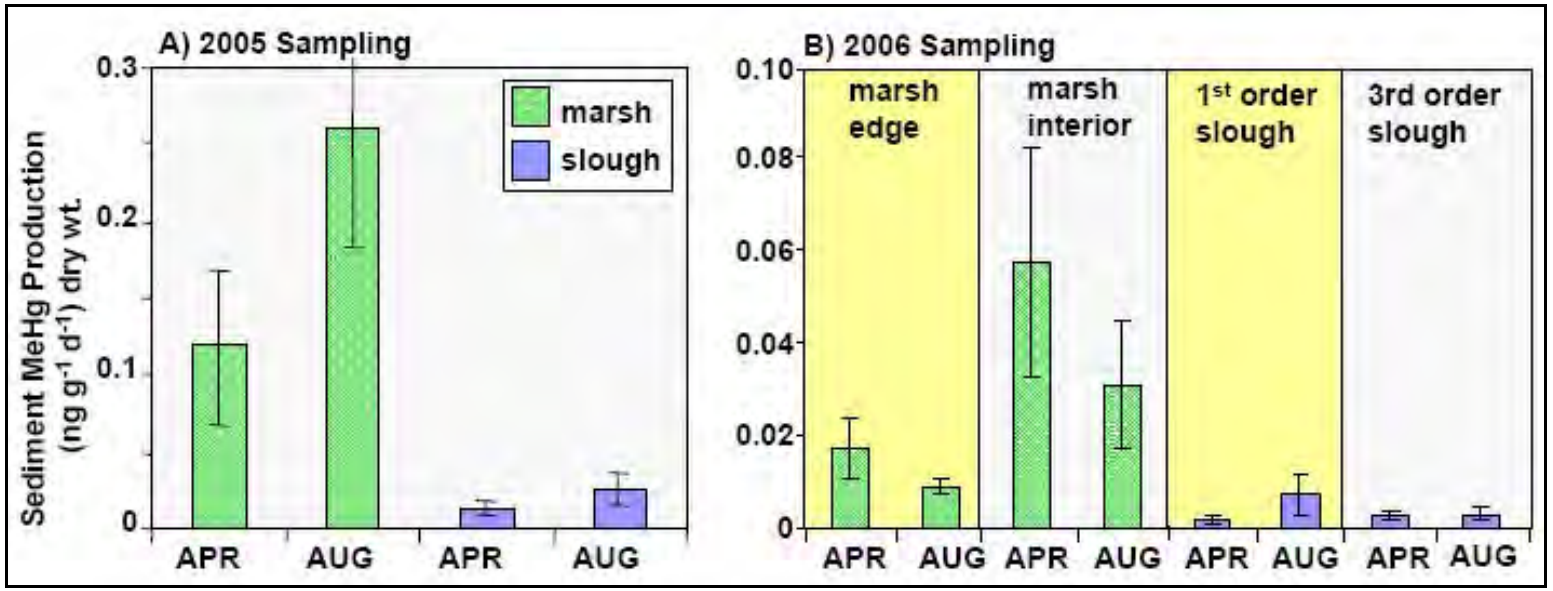

Figure D.3.3. Average MeHg production [potential] rates in 0-2 cm surface sediment by habitat type and month, for A) 2005 and B) 2006. Each bar represents N = 6 sites. Error bars reflect standard deviations

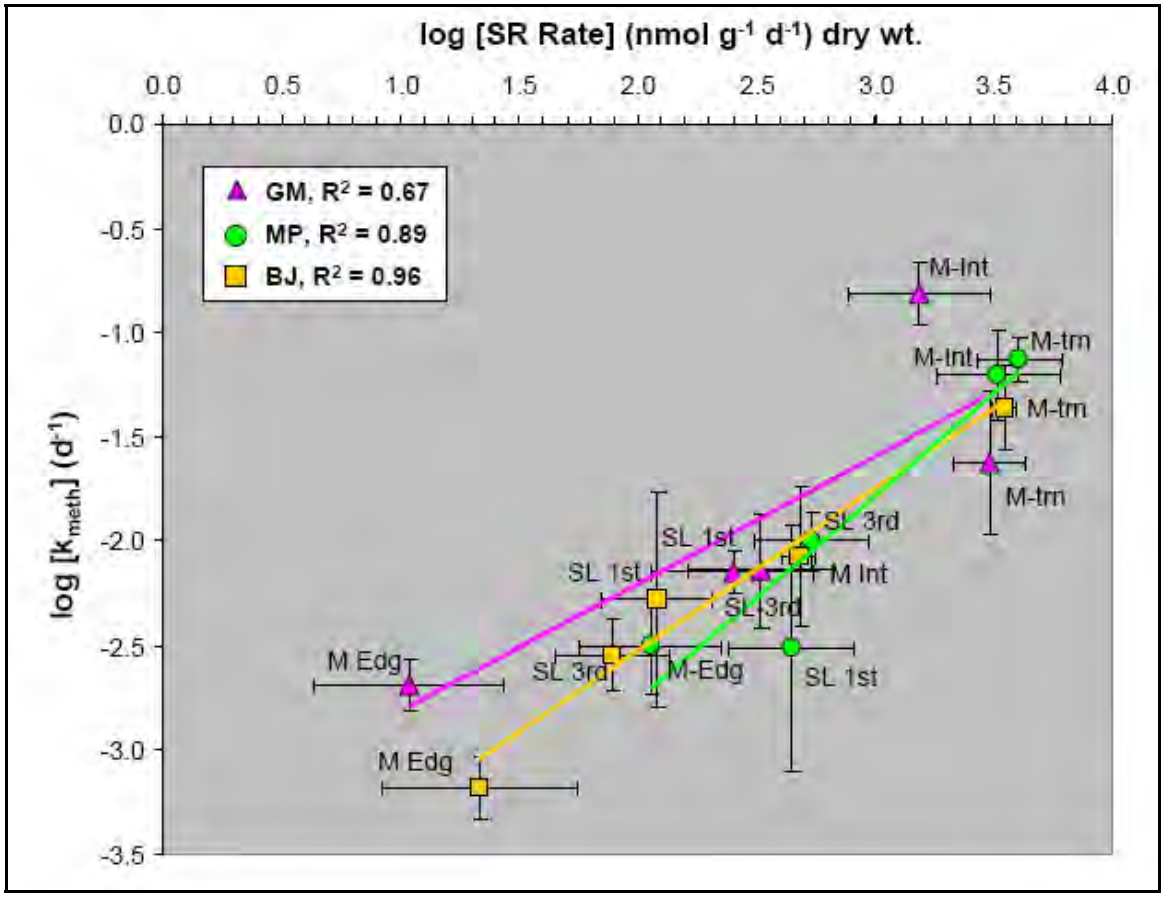

Figure D.3.4. Linear regression between logarithmic (log) transformed SR and k_{meth} data by site (GM, MP and BJ) and sub-habitat type, with three marsh (M) types (interior = int, edge = Edg, (both collected in 2006) and transect = trn (collected in 2005)) and two slough (SL) types (1st and 3rd order). Data points represent the average values for each site/sub-habitat combination. Errors bars represent standard errors. Regression lines are shown for each site.

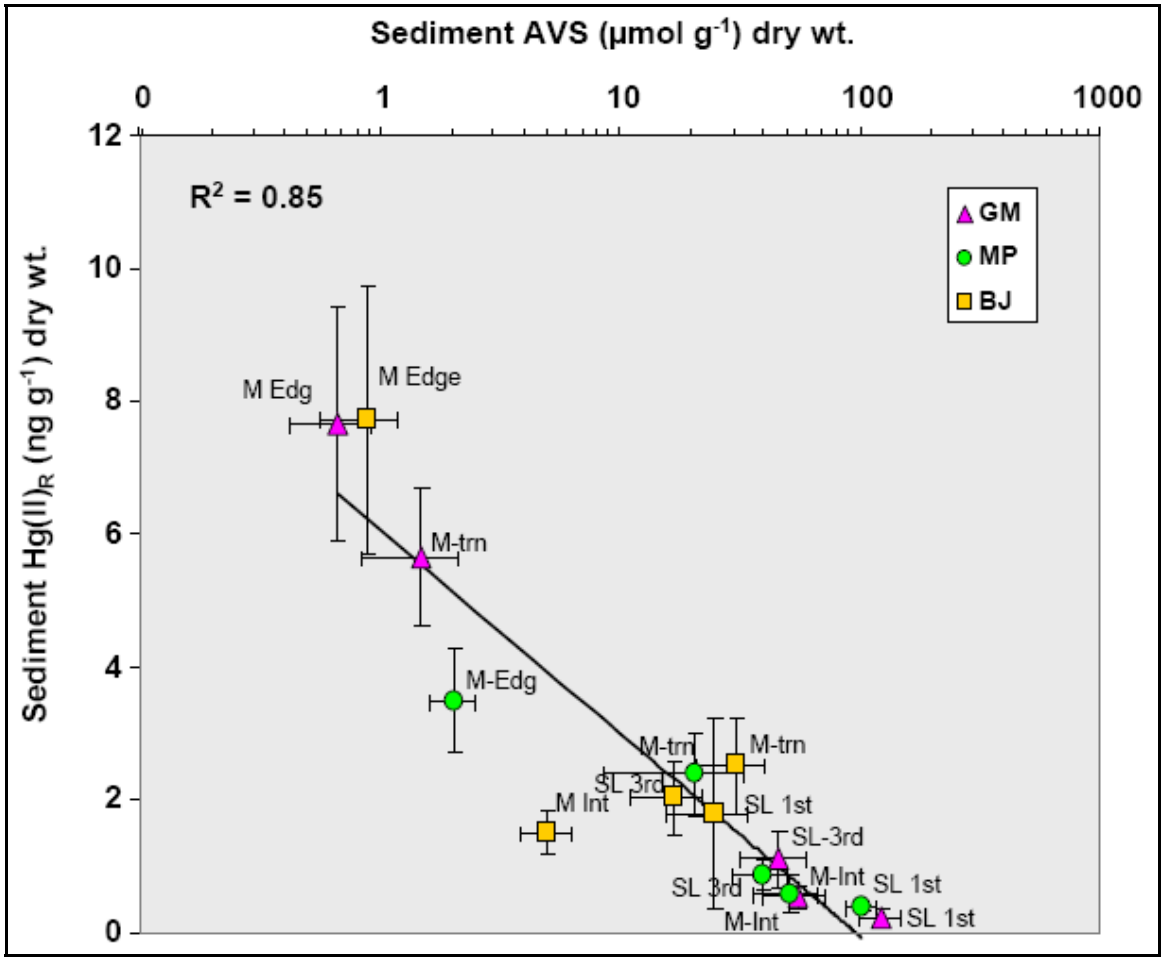

Figure D.3.5. The log-linear regression between acid volatile sulfur (AVS) and reactive mercury ($Hg(II)_R$) in 0-2 cm surface sediment, by site (GM, MP and BJ) and sub-habitat type (as per Figure D.3.4). Data points represent the average values (n = 4 to 8) and errors bars represent standard errors.

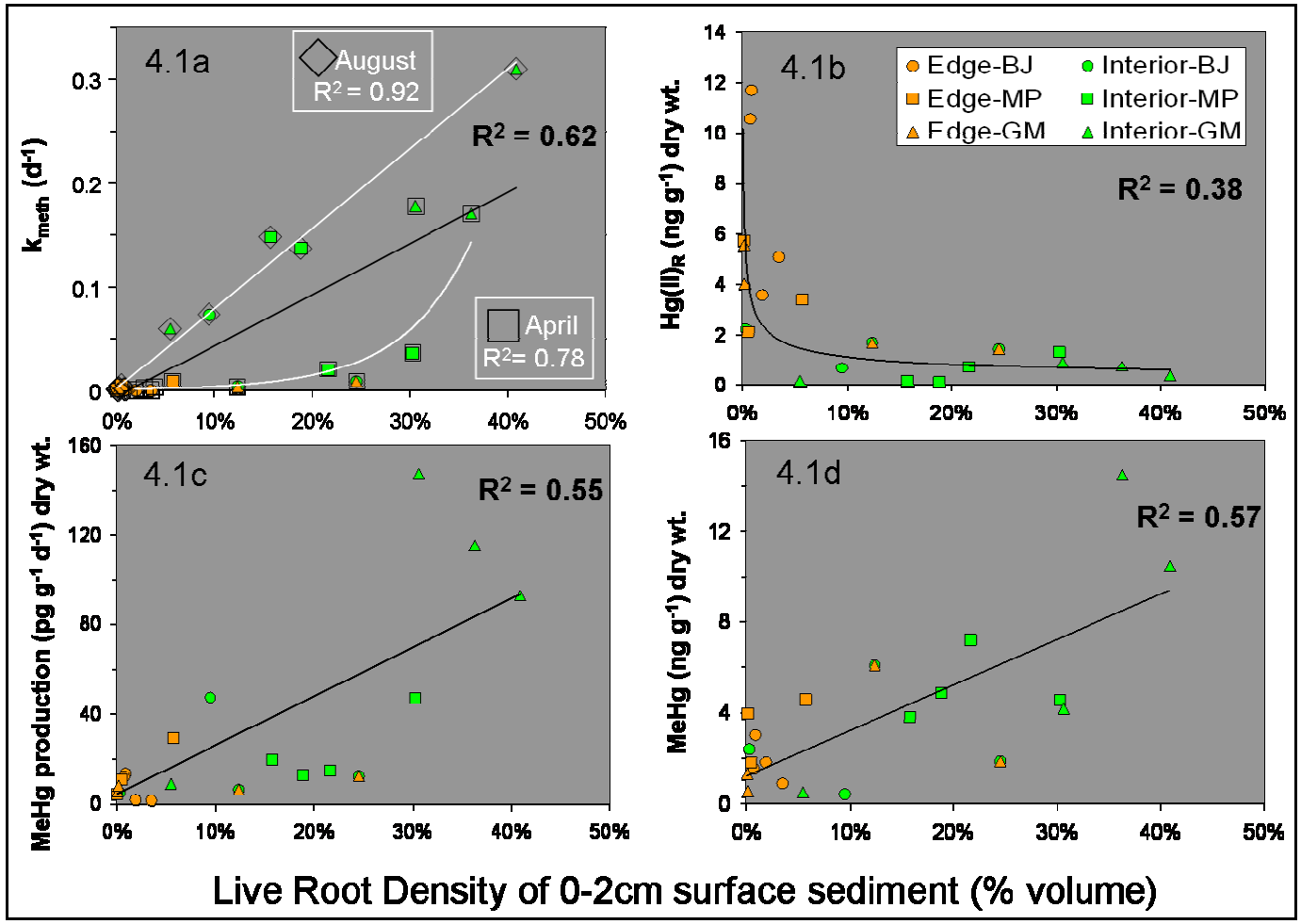

Figure D.4.1a-d. Surface sediment (0-2 cm) live root density vs mercury metrics: a) MeHg Production Rate constant (k_{meth}), b) reactive inorganic mercury ($Hg(II)_R$), c) MeHg production rate (k_{meth} x $Hg(II)_R$), and d) MeHg concentrations, for sampling year 2006. Seasonal differences are denoted for figure 4.1a (k_{meth}) by encircling data with squares for April and diamonds for August.

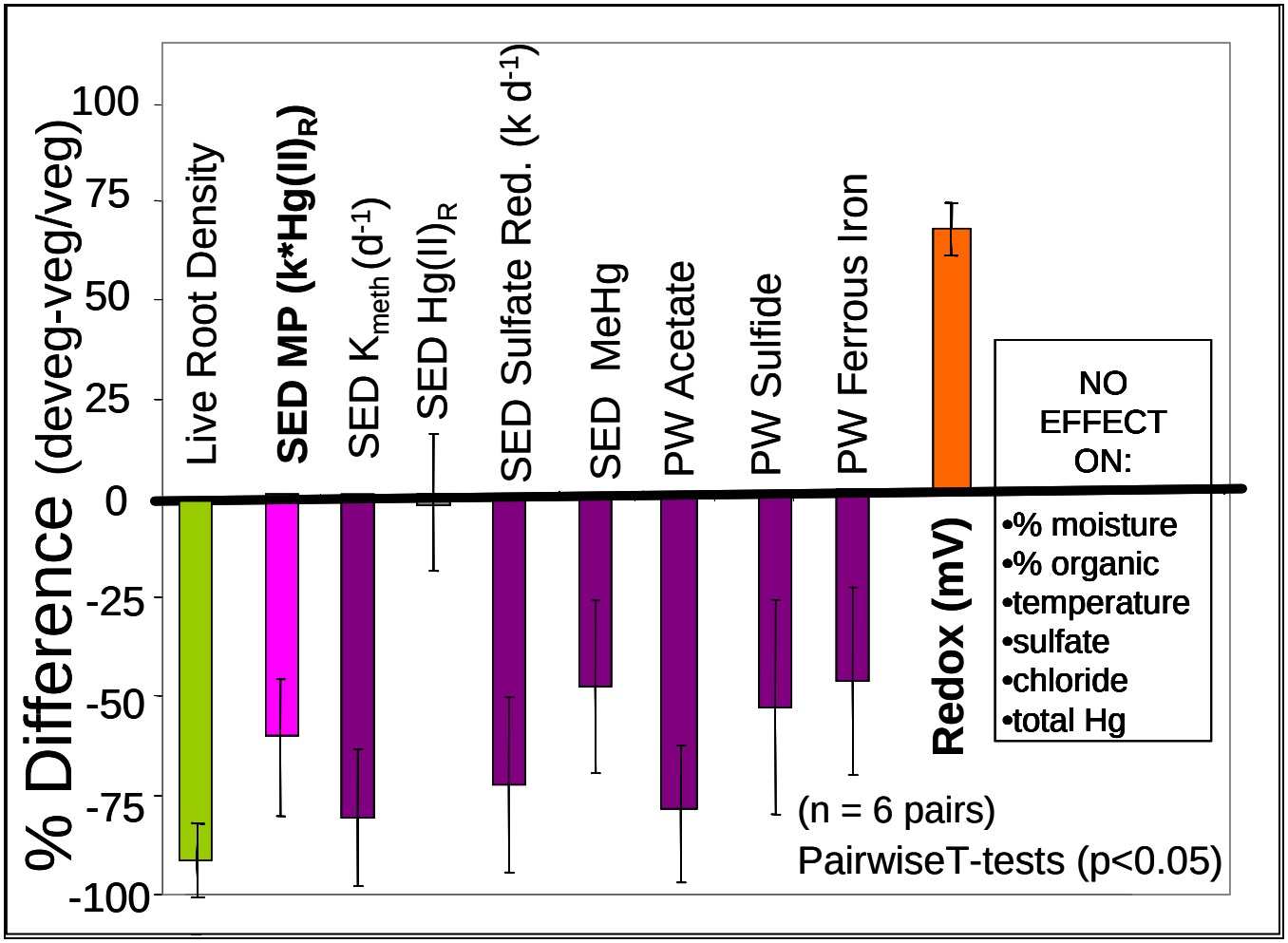

Figure D.4.2. Devegetation effect on microbial and biogeochemical factors August 2006. Values <0 indicate a decrease (as labeled). Only redox potential increased upon devegetation. Data for all plots but effects in marsh interior plots > in marsh edges (not shown). Error Bars = 1 std dev. Devegetation led to >80% reduction in live roots in all interior marsh plots. All bars shown represent significant differences between devegetated and control plots.

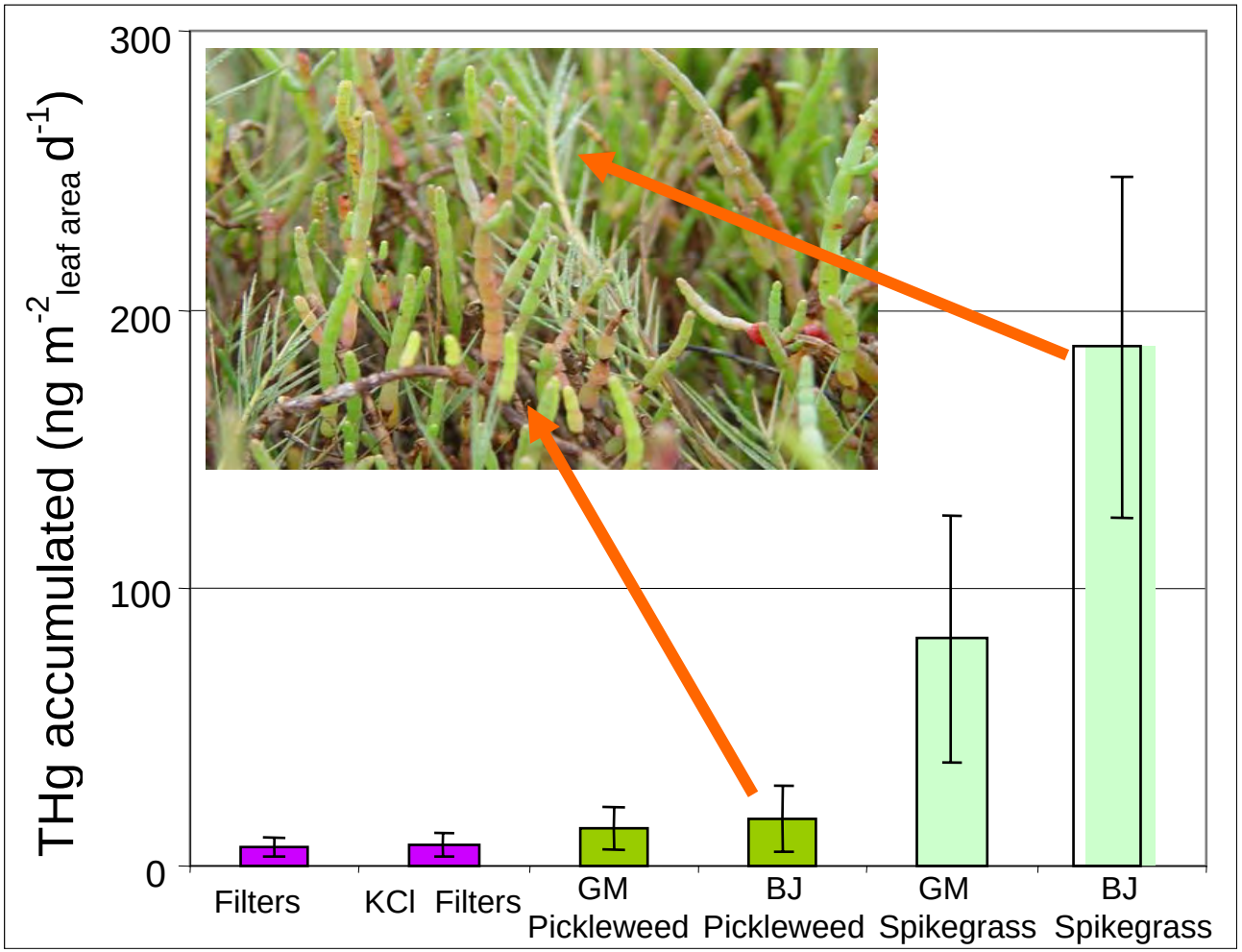

Figure D.4.3. Accumulated THg (ng m^2 leaf area) on surfaces of control filters, pickleweed, and spikegrass during 3-6 day incubations in June and August 2006 at GM and BJ. Bars represent averages of data pooled across months for individual filters (KCl encrusted), plants and months (n=12-16) and error bars represent 1 std dev.

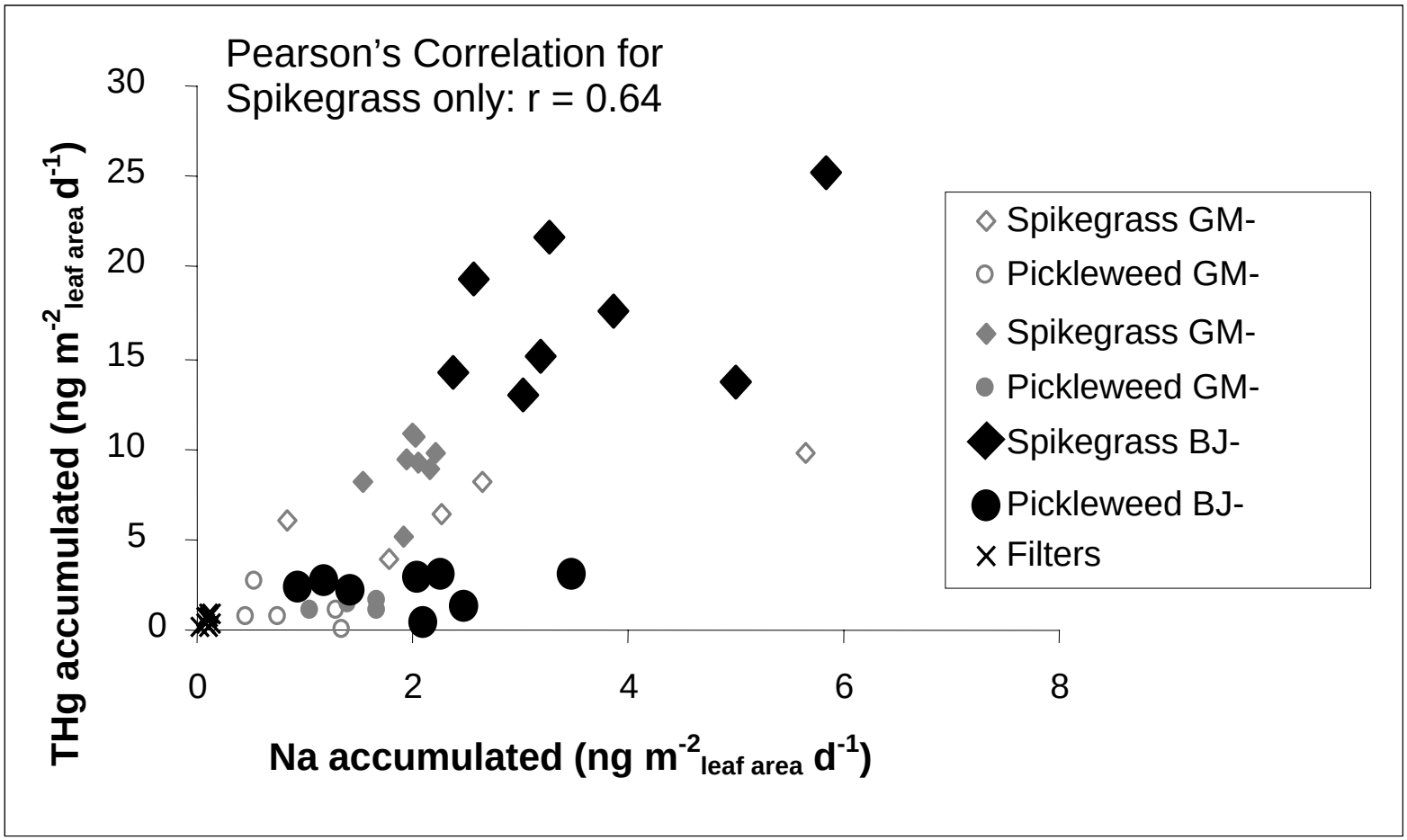

Figure D.4.4. Correlation of Na and THg on surfaces of control filters, pickleweed, and spikegrass during 3-6 day incubations in June and August 2006 at GM (open and gray symbols) and BJ (black symbols). Pickleweed = circles, Spikegrass = diamonds, Filters (atmospheric deposition) = crosses. N=8 for each plant category, N = 24 for filters, 16 neutral filters, and 8 KCl-encrusted filters.

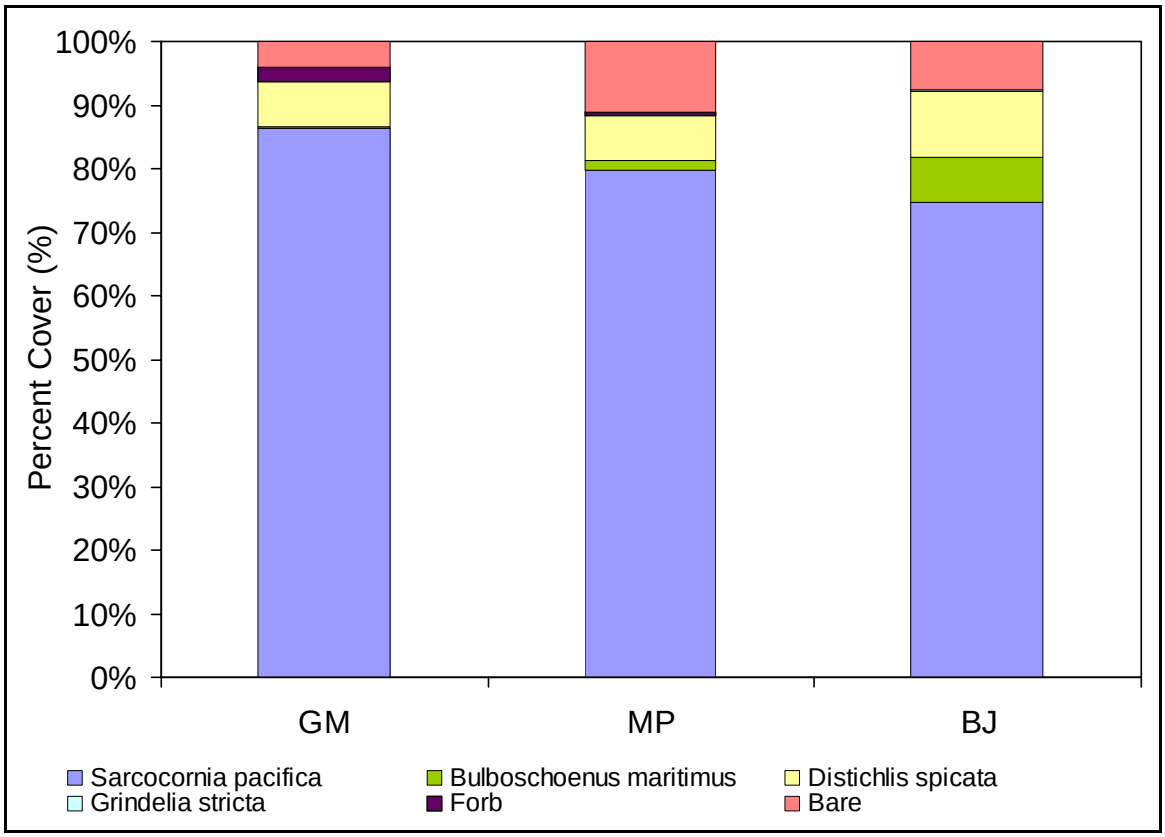

Figure D.5.1. Percent vegetation cover at locations within Petaluma marshes where Black Rails located via radio-telemetry. Radio-telemetry results indicate that Black Rails used high marsh habitats characterized by high percent cover of pickleweed (*Sarcocornia*).

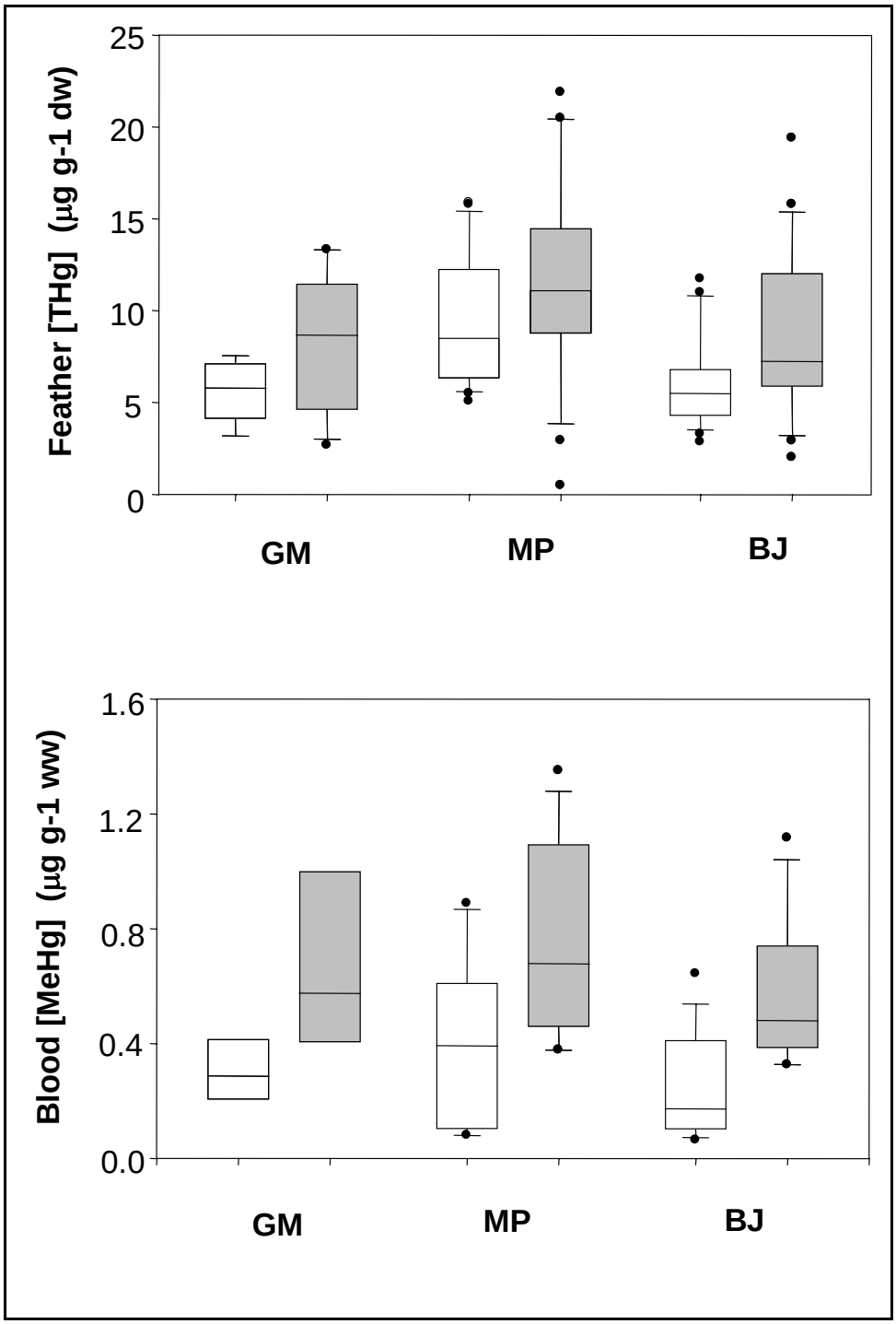

Figure D.5.2. Box plots showing geometric mean mercury concentrations (µg g^{-1}) by site and sex in total mercury (THg) in feathers and (b) methylmercury (MeHg) in blood of Black Rails sampled at three tidal marsh sites along the Petaluma River, California in 2005 and 2006. White bars represent females, and gray bars represent males.

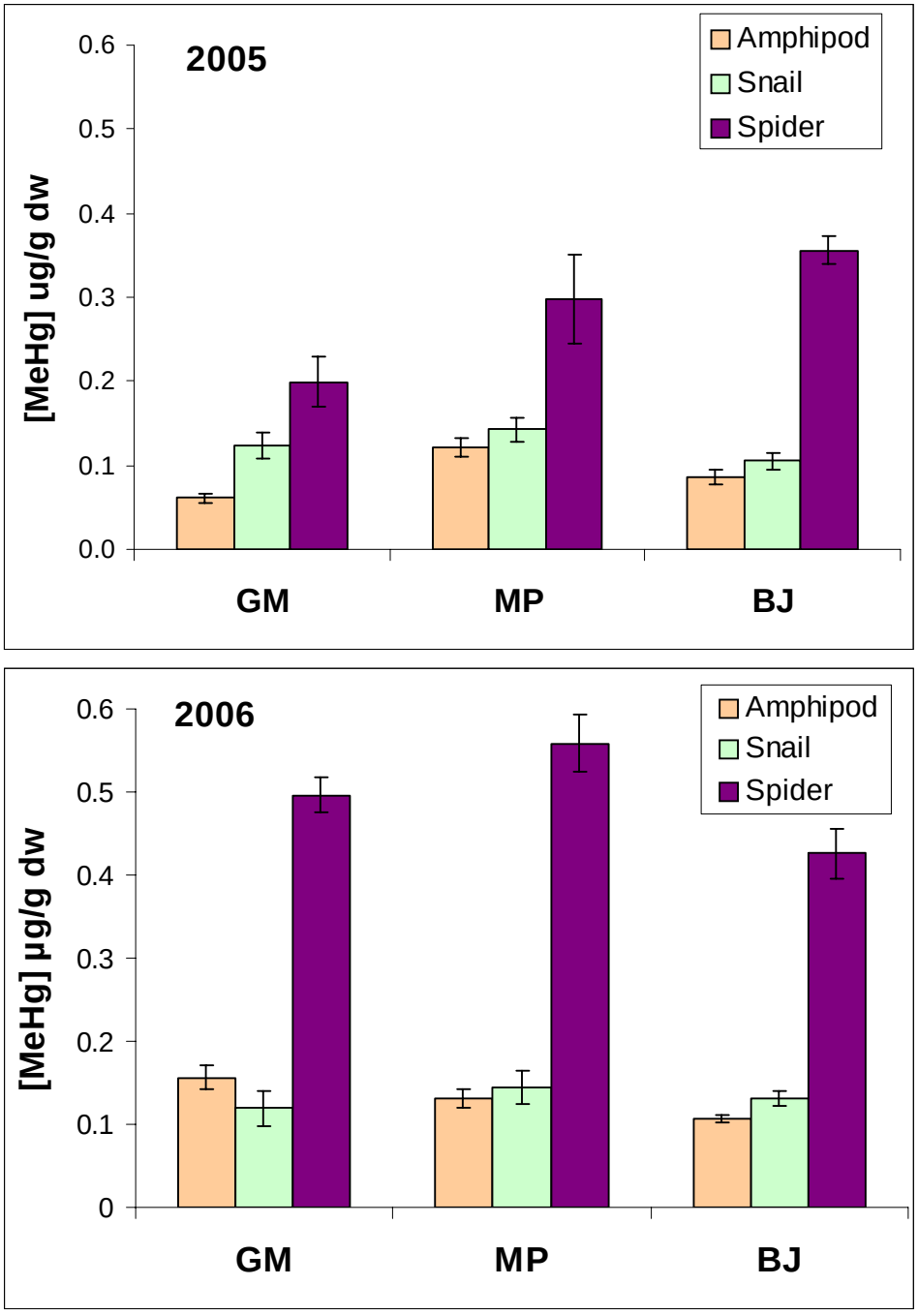

Figure D.5.3. Methylmercury (MeHg) concentrations (mean ± se) of target invertebrates at Gambinini Marsh, Petaluma Marsh, and Black John (GM, PM, BJ, respectively) in (a) 2005 and (b) 2006.

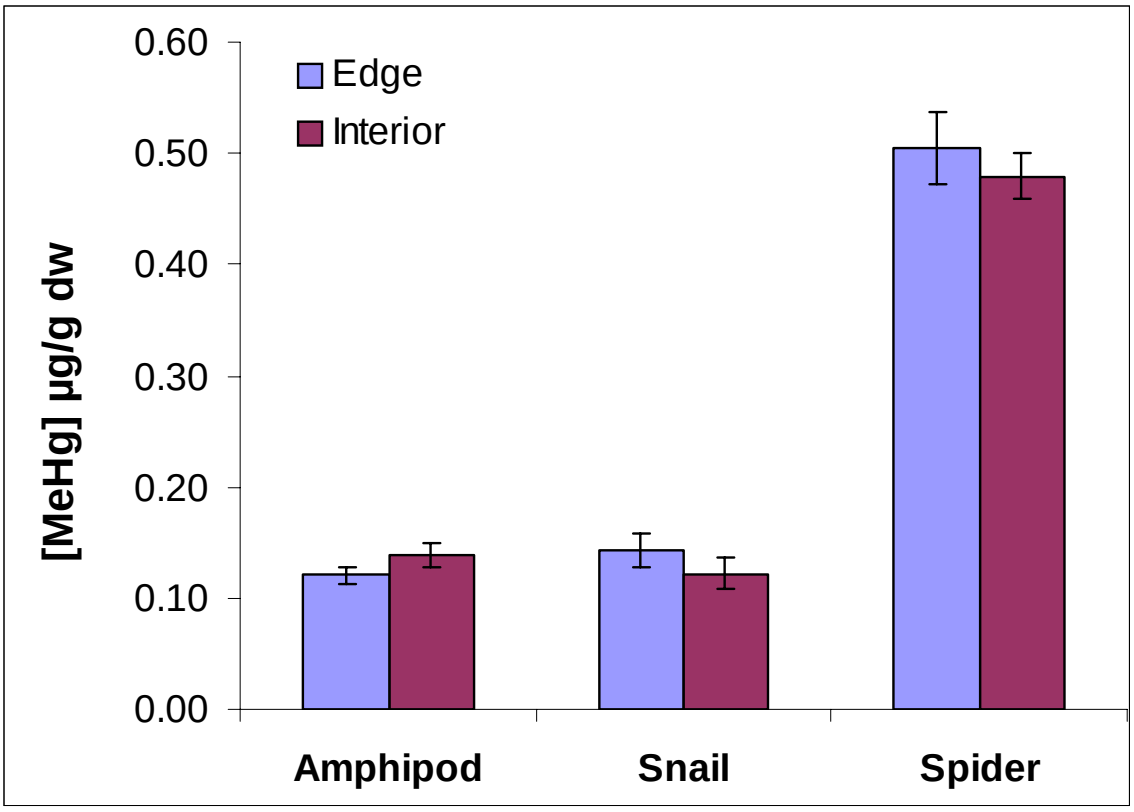

Figure D.5.4. Methylmercury (MeHg) concentrations (mean ± se) of amphipods, snails, and spiders by marsh edge and interiors.

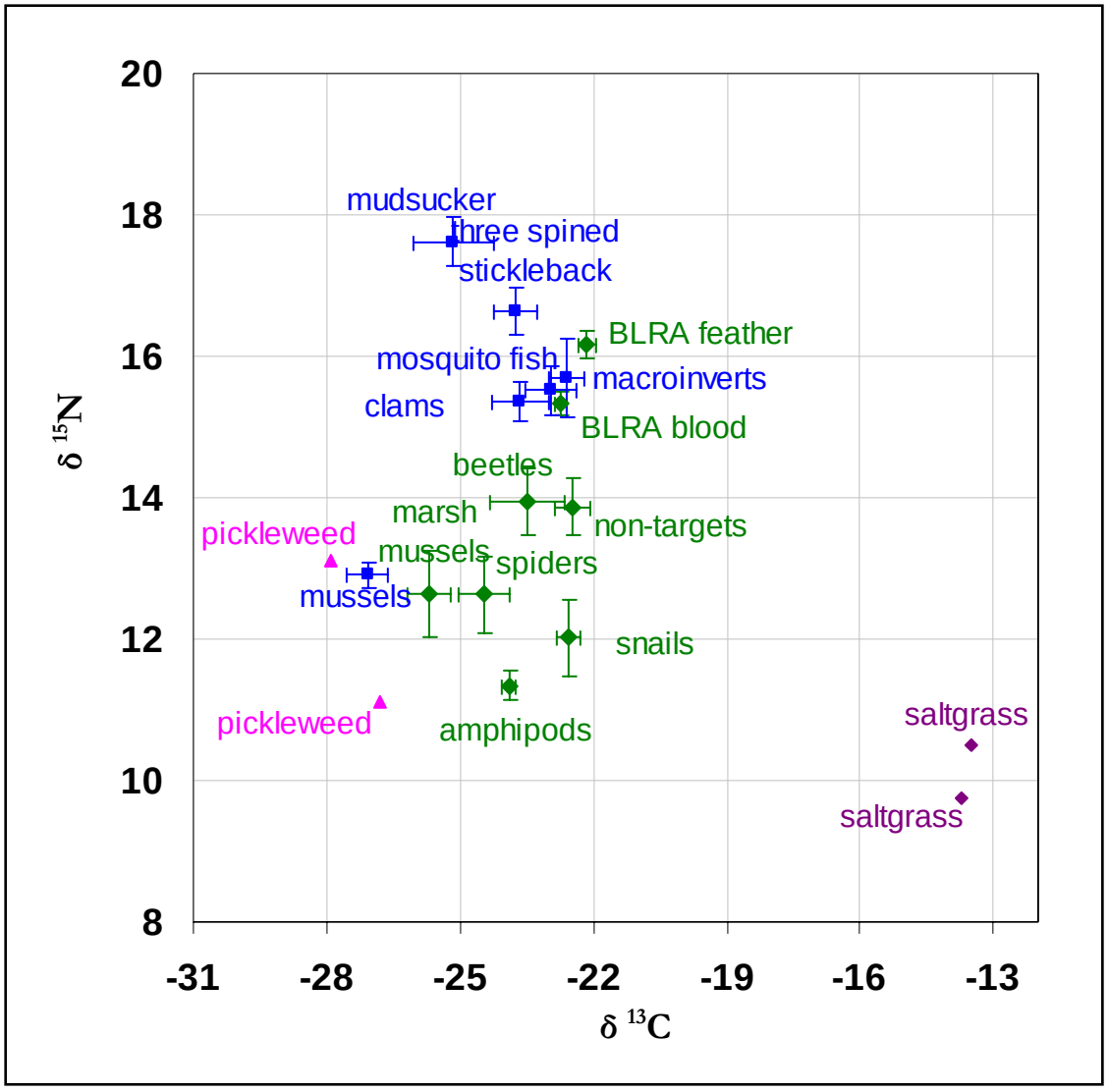

Figure D.5.5. Carbon and nitrogen stable isotope for marsh (green text) and slough (blue text) biota. Marsh non-target invertebrates included: praying mantis, ladybugs, leafhoppers, and shorebugs and slough macroinvertebrates include shrimp and aquatic amphipods.

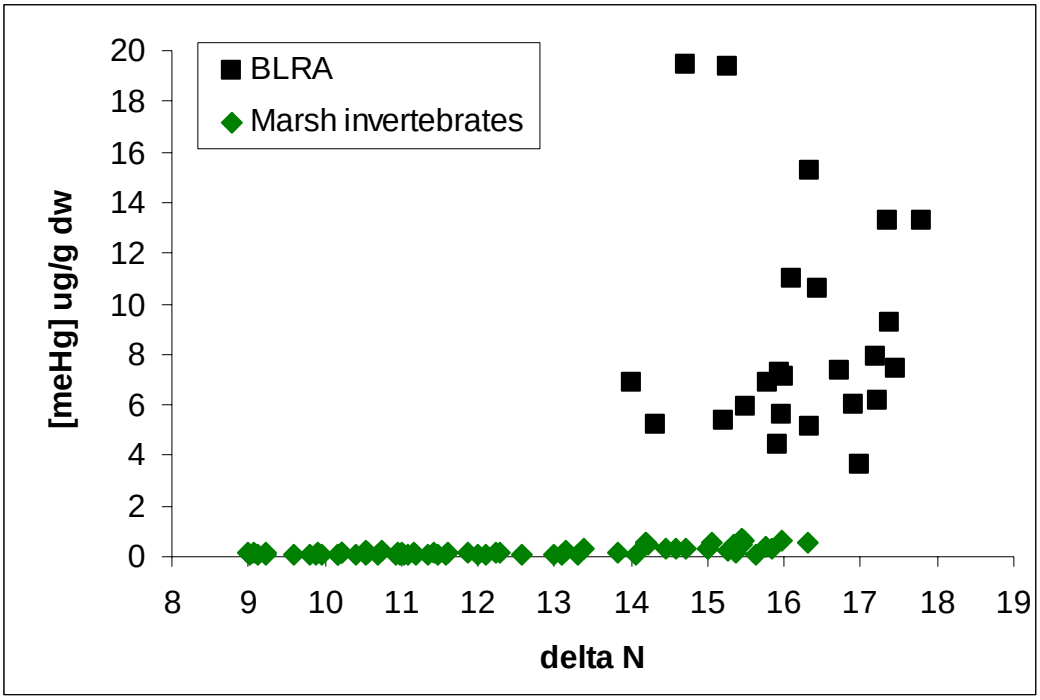

Figure D.5.6. MeHg concentrations in marsh biota increased by tropic level. Male black rails (BLRA) had the greatest MeHg concentrations, followed by female rails, juvenile rails, and target marsh invertebrates. Within target marsh invertebrates, predators (spiders and beetles) occupied a higher trophic level and had greater MeHg concentrations than detritivores (amphipods) and surface scrapers (snails).

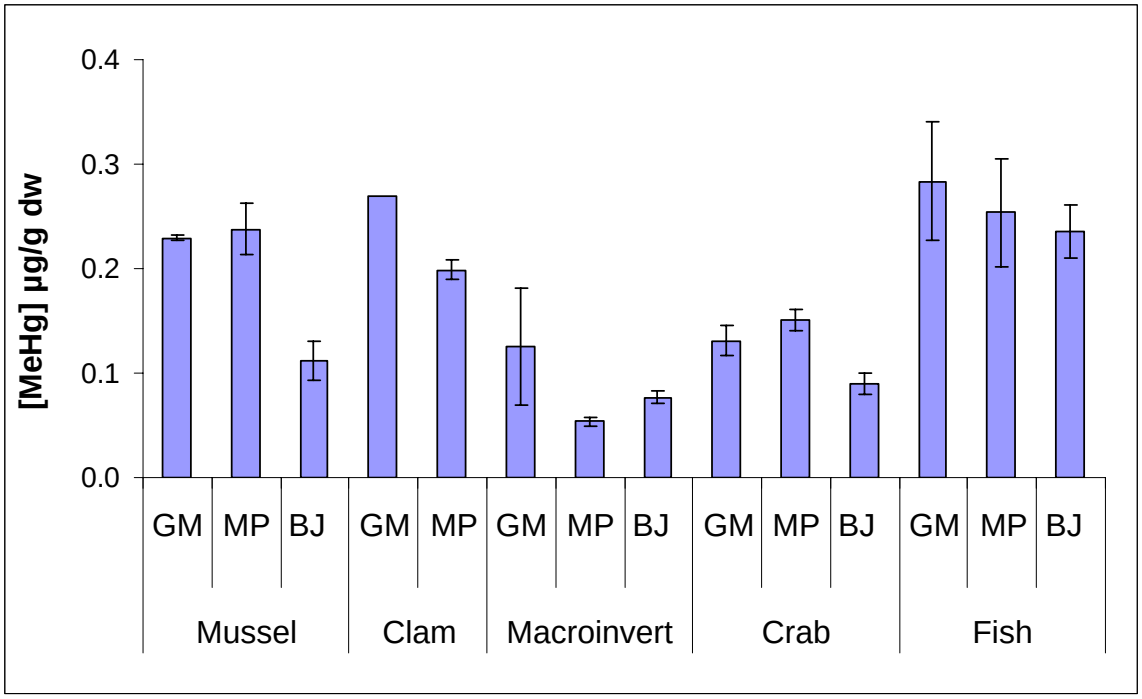

Figure D.5.7. MeHg concentrations in slough biota by site (mean ± se). "Macroinverts" included aquatic amphipods and shrimp and "fish" included longjaw mudsucker, mosquito fish, and three spine stickleback. Filter feeding mussels had similar MeHg concentrations as fish.

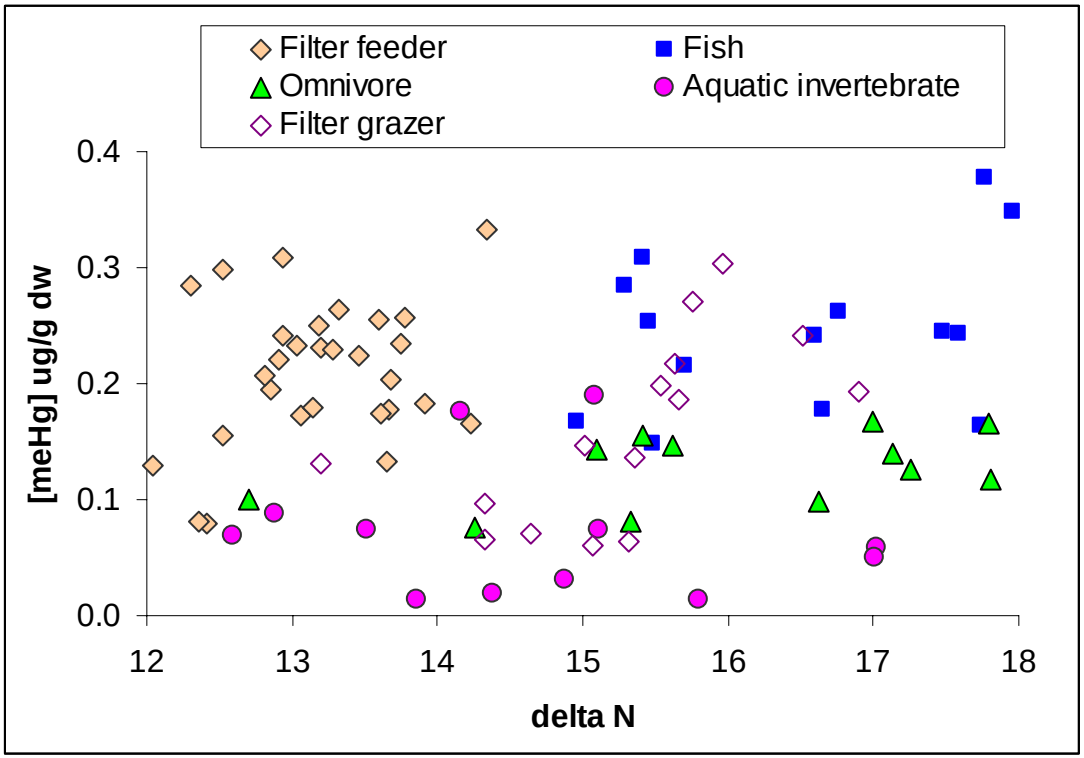

Figure D.5.8. MeHg concentrations in slough biota did not vary by trophic level. Filter feeders (mussels) had similar MeHg concentrations as fish (longjaw mudsucker, threespine stickleback, and mosquitofish). Aquatic invertebrates (aquatic amphipod and shrimp), filter grazer (Macoma clams), omnivore (Hemigrapsus crab) also had wide variations in delta N that did not correlate with MeHg concentrations.

Table D.1.1. Changes in Surface Sediment MeHg, Redox Potential, and Temperature Grabs were taken over the course of a day at five points (spaced ~1m apart) in Gambinini marsh plain interior. Mean ± se for measurements of the five grab locations shown.

Time	MeHg (ng/g dw)	Eh (mV)	Temp (C)
8:30	5.9 ± 1.7	32 ± 7	15.5 ± 0.1
10:30	8.4 ± 2.1	44 ± 51	16.8 ± 0.1
12:30	5 ± 1.3	140 ± 36	21.4 ± 0.3
14:30	7.3 ± 0.6	185 ± 28	22 ± 0.3

Table D.1.2. Differences in Habitat Element Redox Potential (Measured at 2 cm depth at grab sampling sediment locations).

Gambinini	Eh (mV) mean ± se
Edge	256 ± 10
Interior	117 ± 17
1st Slough	117 ± 55
3rd Slough	161 ± 43

Table D.1.3. Conductivity (mS/cm) of Slough Channel Surface Water (Measured in collected grab water samples)

	Marsh	(mean ± se)
April 2005	BJ	16.9 ± 1.1
	MP	9.5 ± 0.5
	GM	6 ± 0.6
August 2005	BJ	36.3 ± 1.0
	MP	31.6 ± 0.5
	GM	30.3 ± 1.2
April 2006	BJ	0.044 ± 0.006
	MP	0.021 ± 0.002
	GM	0.018 ± 0.002
August 2006	BJ	35.4 ± 0.7
	MP	29.9 ± 0.6
	GM	29.5 ± 0.5

Table D.2.1. Degradation Half-Lives (days), MeHg and Hg. Half lives based on rates of ^{201}Hg removal from solution and appearance of ^{199}Hg.

		$Me^{199}Hg$ Half-life		**^{201}Hg Half-life**	
Site	**Date**	Filtered	Unfiltered	Filtered	Unfiltered
BJ	Jun-05	6	20	2	3
MP	Jun-05	8	12	4	4.5
GM	Jun-05	14	18	2	6
BJ	Jun-06	5	10	2	7
MP	Jun-06	7	11	5	4
GM	Jun-06	20	15	5	4

Methylmercury cycling, bioaccumulation, and export from agricultural and non-agricultural wetlands in the Yolo Bypass

Cooperator Report Prepared by:
U.S. Geological Survey
California Department of Fish and Game
Moss Landing Marine Laboratory
Battelle Marine Sciences
Bachand and Associates
Yolo Basin Foundation

Responsible Organization: San Jose State University Research Foundation

FINAL REPORT
September 30, 2010

Title:	Name:	Signature:	Date:
Project Manager	Mark Stephenson	_____	_____
SWRCB Contract Manager	Janis Cooke	_____	_____

Dates: December 2006-December 2008
Watershed: Yolo Bypass, Yolo County, CA
Funds: Central Valley Regional Water Quality Control Board
Cost of Project: $999,760

This project is supported by Proposition 40 as part of the Agricultural Water Quality Grant Program and local and federal matching funds.

"Funding for this project has been provided in full or in part through an agreement with the State Water Resources Control Board. The contents of this document do not necessarily reflect the views and policies of the State Water Resources Control Board, nor does mention of trade names or commercial products constitute endorsement or recommendation for use." (Gov. Code 7550, 40 CFR 31.20)

GRANT SUMMARY FORM

2005 - 2006 CONSOLIDATED GRANTS - PROPOSITION 40/50 AGRICULTURE WATER QUALITY GRANT PROGRAM
GRANT AGREEMENT
BETWEEN THE
STATE WATER RESOURCES CONTROL BOARD, hereinafter called "State" or "State Water Board"
AND

SAN JOSE STATE UNIVERSITY FOUNDATION, hereinafter called "Grantee"

Methylmercury cycling and export from agricultural and natural wetlands in the Yolo Bypass, hereinafter called "Project"

AGREEMENT NO. 06-232-555-0

State and Grantee hereby agree as follows:

PROVISION(S). The following provision(s) authorize the State Water Board to enter into this type of Grant Agreement:
PRC §§ 5096.650, 30940(a) (Pr 40 Agricultural Water Quality)
WC § 79540.1(b), PRC § 30940(a) (Pr 50 Agricultural Water Quality)

PURPOSE. State shall provide a grant to and for the benefit of Grantee for the purpose of developing effective Total Maximum Daily Load (TMDL) by quantifying seasonal and spatial processes through laboratory and statistical analyses.

GRANT AMOUNT. The maximum amount payable under this Agreement shall not exceed $999,881.00. Global Positioning System (GPS) locations for any monitoring must be identified for this Project prior to any disbursements.

TERM OF AGREEMENT. The term of the Agreement shall begin on DECEMBER 1, 2006 and continue through Project completion plus three (3) years unless otherwise terminated or amended as provided in the Agreement. HOWEVER, ALL WORK SHALL BE COMPLETED BY MARCH 1, 2009. ABSOLUTELY NO FUNDS MAY BE REQUESTED AFTER APRIL 1, 2009.

PROJECT REPRESENTATIVES. The Project Representatives during the term of this Agreement will be:

State Water Board		Grantee: San Jose University Foundation	
Name:	Stephanie Fong, Grant Manager	Name:	Mark Stephenson, Project Director
Address:	11020 Sun Center Drive, Suite #200	Address:	544 Sandholt Road
City, Zip:	Rancho Cordova, CA 95670	City, Zip:	Moss Landing, CA 95039
Phone:	(916) 464-4822	Phone:	(831) 771-4177
Fax:	(916) 464-4780	Fax:	(831) 633-0805
e-mail:	swfong@waterboards.ca.gov	e-mail:	mstephenson@mlml.calstate.edu

Direct all inquiries to:

State Water Board		Grantee: San Jose University Foundation	
Section:	Division of Financial Assistance	Section:	
Attention:	Carmen Rios, Program Analyst	Name:	Chris Thompson, Grant Contact
Address:	1001 "I" Street, 16th Floor	Address:	210 N. 4th Street, 4th Floor
City, Zip:	Sacramento, CA 95814	City, Zip:	San Jose, CA 95112-5569
Phone:	(916) 341-5659	Phone:	(408) 924-1440
Fax:	(916) 341-5296	Fax:	(408) 924-1496
e-mail:	crios@waterboards.ca.gov	e-mail:	cthompso@foundation.sjsu.edu

Either party may change its Project Representative upon written notice to the other party.

Methylmercury cycling, bioaccumulation, and export from agricultural and non-agricultural wetlands in the Yolo Bypass

Lisamarie Windham-Myers[1], Mark Marvin-DiPasquale[1], Jacob Fleck[1], Charles N. Alpers[1], Josh Ackerman[1], Collin Eagles-Smith[1], Craig Stricker[1], Mark Stephenson[2,3], David Feliz[2], Gary Gill[4], Philip Bachand[5], Ann Brice[6], and Robin Kulakow[6]

[1]U.S. Geological Survey
[2]California Department of Fish and Game
[3]Moss Landing Marine Laboratory
[4]Battelle Marine Sciences
[5]Bachand and Associates
[6]Yolo Basin Foundation

Executive Summary

This 18-month field study addresses the seasonal and spatial patterns and processes controlling methylmercury (MeHg) production, bioaccumulation, and export from natural and agricultural wetlands of the Yolo Bypass Wildlife Area (YBWA). The data were collected in conjunction with a Proposition 40 grant from the State Water Resources Control Board in support of the development of Best Management Practices (BMP's) for reducing MeHg loading from agricultural lands in the wetland-dominated Yolo Bypass to the Sacramento-San Joaquin River Delta. The four management-based questions addressed in this study were:

1. **Is there a difference among agricultural and managed wetland types in terms of MeHg dynamics (production, degradation, bioaccumulation, or export)?**
2. **Does water residence time influence MeHg dynamics?**
3. **Does the application of sulfate-based fertilizer impact MeHg production rates?**
4. **Does the presence (or absence) of vegetation influence MeHg production rates?**

Measurements of MeHg concentrations in sediment, water, and biota (plants, invertebrates, and fish) were made to assess management-level patterns in five wetland types, which included three types of shallowly-flooded agricultural wetlands (white rice, wild rice, and fallow) and two types of managed wetlands (permanently and seasonally flooded). To strengthen our understanding of the processes underlying the seasonal and spatial patterns of MeHg cycling, additional explanatory factors were measured including ancillary sediment and water quality parameters, stable isotope fractionation (oxygen, sulfur, carbon, and nitrogen), photodemethylation rates, and daily-integrated hydrologic budgets. Samples and field data were collected from May 2007 to July 2008, and nearly all sample analyses were completed by September 2008 as per the Quality Assurance Program Plan (QAPP) requirements.

Although wetland type was a major factor that drove the study design, within-field hydrology also proved to be an important factor controlling aqueous MeHg and total mercury (THg) concentrations and export. Overall, agricultural wetlands exhibited higher MeHg concentrations in overlying water, sediment, and biota than did managed seasonal and permanent wetlands. This appears to be partly due to higher rates of sediment microbial production of MeHg in agricultural wetlands during the fall through spring period. Both sulfate- and iron-reducing bacteria have been implicated in the MeHg production process, and both were demonstrably active in all wetlands studied; however, sulfate-reducing bacteria were not stimulated by the addition of sulfate-based fertilizer to agricultural wetlands, suggesting that easily-degraded (labile) organic matter, rather than sulfate, was limiting their activity in these field types. The data suggest that agriculturally-managed soils promoted MeHg production through 1) enhanced microbial activity via higher temperatures and larger pools of labile carbon, and 2) enhanced pools of microbially available inorganic divalent mercury (Hg(II)) resulting from a decrease in reduced-sulfur, solid-phase minerals under oxic or only mildly reducing conditions.

MeHg mass balances were assessed by comparing field-specific MeHg loads for inlets vs. outlet flows. The overall mass balance for MeHg in surface water during the summer irrigation period (June – September 2007) indicated little to no net MeHg export from the six agricultural wetlands taken as a whole. Of the six agricultural wetlands, there was net overall MeHg export from two fields (one fallow and one white rice) during August, and from four of the six fields (one fallow, one white rice, and two wild rice) during September. Over the entire summer irrigation period, two of the fields (one fallow and one wild rice) showed net MeHg export, and the other four fields showed either net import or no significant change. Rates of measured photodemethylation and exchange between sediment and water pools suggest that both processes may be responsible for the lack of MeHg export. Despite significant differences during winter months between fields in surface water concentrations of MeHg, MeHg loads were not calculated in mid-winter because flood waters had overtopped field boundaries and field fidelity could not be established.

During the summer 2007 irrigation season, surface water out-flows from agricultural wetlands were 9%-36% of inlet flows, and evaporation rates explained most of this water loss, with infiltration likely accounting for the remainder. Unfiltered aqueous MeHg concentrations increased from <1 ng L^{-1} in source waters to up to10 ng L^{-1} in agricultural wetland drains during the summer irrigation period. Increases in solute concentration caused by evapoconcentration were estimated by determining concentration factors (outflow / inflow) for chloride (a conservative dissolved constituent) and by measuring oxygen isotope ratios ($^{18}O/^{16}O$, expressed as $\delta^{18}O$) in water. Increases in MeHg concentration from inflows-to-outflows exceeded those caused by evapoconcentration on several fields during the summer irrigation season. This was especially true when initial surface water MeHg concentrations were low, as seen in the southern block of fields receiving irrigation water directly from the Toe Drain. The northern block of fields received irrigation water from Greens Lake, which included Toe Drain water plus recirculated drain water from other agricultural fields within the Yolo Bypass and west of the Yolo Bypass; as such, the northern fields showed a smaller percentage increase in MeHg concentration because initial MeHg concentrations in surface water inflows were greater than in inputs to the southern fields.

Mercury concentrations in fish were greater in agricultural wetlands (white rice and wild rice) than in the two permanently flooded wetlands. Additionally, Hg concentrations in biota

showed a general increase from inlets to outlets within agricultural wetlands, but not within permanent wetlands. This was particularly evident in white rice fields where caged western mosquitofish at the outlets had Hg concentrations that were more than 4 times higher than in caged fish held at the inlets. Similar spatial patterns in Hg bioaccumulation in agricultural and permanent wetlands were seen for wild populations of western mosquitofish and Mississippi silversides. In contrast to fish, invertebrates, such as water-boatmen (Corixidae) and back swimmers (Notonectidae), had greater Hg concentrations in permanent wetlands than in temporarily flooded agricultural wetlands. Fish THg concentrations were weakly correlated with water MeHg, and not correlated with sediment MeHg. In contrast, invertebrate MeHg concentrations were more strongly correlated with sediment MeHg than with water MeHg concentrations. These results illustrate the complexity of MeHg bioaccumulation through food webs and indicate the importance of simultaneously using multiple biosentinels when monitoring MeHg production and bioaccumulation.

Despite high sediment MeHg production rates and water concentrations in agricultural wetlands, MeHg export was physically limited by hydrologic export for all wetlands studied. We suggest that load reduction is maximized by limiting water throughput, but that on-site biota exposure is maximized by this longer water residence time. While field-specific hydrologic loads could not be fully quantified during flood conditions in February 2008, we suggest that the primary period of MeHg export from Yolo Bypass Wildlife Area is during those winter flooding periods when overall microbial activity and MeHg production in agricultural soils is fueled by the decomposition of rice straw, and when hydrologic flowthrough is maximal.

Local stakeholders participated in two workshops related to this study, demonstrating an interest in understanding factors controlling MeHg production, export, and bioaccumulation. The results of this field study show that permanently flooded, naturally vegetated wetlands are unlikely to be a large source of MeHg production within the YBWA, in contrast with agriculturally-managed wetlands. MeHg loading to Toe Drain waters of the Yolo Bypass may be reduced by lowering rates of hydrologic export from agricultural wetlands during the growing season and especially during rice harvest. However, under these water-holding conditions, biota living within agricultural wetlands may thus be exposed to higher MeHg concentrations in surface water. As observed in this study, rapid bioaccumulation over a 2-month period led to MeHg concentrations in invertebrates and fish more than 6 and 11 times higher, respectively, than proposed TMDL target values to protect wildlife (0.03 ppm ww).

The results of this field study, together with the information from YBWA stakeholders, provide a more definitive understanding of how MeHg cycling and bioaccumulation respond to habitat differences and specific management practices. These results directly address 4 core components of CBDA's Mercury Strategy for the Bay-Delta Ecosystem (**Wiener et al., 2003a**):

a) Quantification and evaluation of THg and MeHg sources,

b) Quantification of effects of ecosystem restoration on MeHg exposure,

c) Assessment of ecological risk, and

d) Identification and testing of potential management approaches for reducing MeHg contamination.

In addition, the quantitative results reported here assess the effect of current land use practices in the Yolo Bypass on MeHg production, bioaccumulation and export, and provide process-based advice towards achieving current goals of the RWQCB-CVR's *Sacramento – San Joaquin Delta Estuary TMDL for Methyl & Total Mercury* (**Wood et al., 2010b**). Further work is necessary to evaluate biotic exposure in the Yolo Bypass Wildlife Area at higher trophic levels (e.g. birds), to quantify winter hydrologic flux of MeHg to the larger Delta ecosystem, and to evaluate rice straw management options to limit labile carbon supplies to surface sediment during winter months.

In summary, agricultural management of rice fields — specifically the periodic flooding and production of easily degraded organic matter — promotes the production of MeHg beyond rates seen in naturally vegetated wetlands, whether seasonally or permanently flooded. The exported load of MeHg from these agricultural wetlands may be controlled by limiting hydrologic export from fields to enhance on-site MeHg removal processes, but the tradeoff is that this impoundment increases MeHg exposure to resident organisms.

Table of Contents

NOTE: **The** *Quality Assurance Performance Plan* **(QAPP) and** *Project Assessment and Evaluation Plan* **(PAEP) referenced herein are publically available from the *Regional Water Quality Control Board – Central Valley Region***

List of Tables

List of Figures

Methylmercury cycling, bioaccumulation, and export from agricultural and non-agricultural wetlands in the Yolo Bypass

1 Project Structure

This project involved scientists and land managers from the following institutions:

U.S. Geological Survey (USGS)
- California Water Science Center (CWSC)
- Western Ecological Research Center (WERC)
- National Research Program (NRP)

California Department of Fish and Game (CDFG)
Moss Landing Marine Laboratory (MLML)
Yolo Basin Foundation (YBF)
Battelle Marine Sciences Laboratories (BMSL)
Bachand and Associates

San Jose State University Foundation was the submitting organization and the project manager. There were 11 Principal Investigators for the project, and **Table 1.1** describes the expertise and organizational affiliation of each. Principal Investigators were responsible for the quality assurance of work done by their own institution. The project QA officer was Ms. Autumn Bonnema, Moss Landing Marine Laboratories. She was not involved with any data collection or analyses for this project. Janis Cooke, with the Regional Water Quality Control Board – Central Valley Region (RWQCB-CVR), maintains the official Quality Assurance Program Plan (QAPP) and the Project Assessment and Evaluation Plan (PAEP) for this project, which were approved by the State Water Resources Control Board (SWRCB) on August 29, 2007 and January 29, 2008, respectively.

The project involved 8 Tasks, which included project management, research, monitoring, assessment, and outreach / education. These were as follows:

i. ***Task 1*** - Project Management
ii. Research/Monitoring/Assessment
   - ***Task 2*** - Manage fields and water levels in Yolo Bypass
   - ***Task 3*** - Collect and measure MeHg concentrations and loads
   - ***Task 4*** - Collect and measure water-quality parameters
   - ***Task 5*** - Measure MeHg production rates and associated factors
   - ***Task 6*** - Measure MeHg concentrations in bio-indicators
   - ***Task 7*** - Measure MeHg photodegradation rates in water column
iii. Education/Outreach/Capacity-building
   - ***Task 8*** - Administer workshops and produce outreach publications

2 Introduction

2.1 Mercury contamination in the Sacramento-San Joaquin Delta and the Yolo Bypass

The Sacramento–San Joaquin River Delta (hereinafter referred to as "the Delta") within California's Central Valley is highly contaminated with mercury (Hg) from historic Hg mining and gold extraction (**Davis et al., 2003; Wiener et al., 2003b; Alpers et al., 2005**). Elevated Hg concentrations in fish in the Delta have led to fish-consumption advisories to protect human health (**Gassel et al., 2007, 2008**) as well as concerns regarding exposure of wildlife to methylmercury (MeHg), the toxic organic form of mercury that is readily bioaccumulated (**Wiener et al., 2003a,b**). Available information indicates that about 60% of MeHg loads to the Delta come from tributary inputs and about 40% is estimated to be produced *in situ* within Delta wetlands and open-water habitats **(Foe et al., 2008)**.

Of the 8 sub-watersheds in the Delta, the wetland-dominated Yolo Bypass has the highest average annual surface water MeHg concentration (**Wood et al., 2010a**). These high MeHg concentrations in the Yolo Bypass may be due in large part to the predominance of wetlands within this sub-watershed (**Wood et al. 2010a**). Wetlands within the Delta and Yolo Bypass are estimated to account for 19% of all MeHg loadings into the Sacramento-San Joaquin River Delta (**Wood et al. 2010a**). However, the relative contribution of MeHg production from different wetland habitats is unknown.

2.2 Mercury cycling in wetlands

Wetlands are known to be significant MeHg production sites in the San Francisco Bay-Delta (SFB-D) (**Davis et al., 2003; Marvin-DiPasquale et al., 2003a**) and elsewhere (**Zillioux et al. 1993; Rudd 1995; St. Louis et al., 1994, 1996; Hurley et al. 1995; Rumbold and Fink 2006**). The production of MeHg is facilitated by sulfate-reducing and iron-reducing bacteria (SRB and FeRB, respectively) in sediments **(Compeau and Bartha, 1984; Fleming et al., 2006)**, and is largely controlled by the activity of those bacteria (limited by sulfate, ferric iron and/or organic matter), and by the availability of divalent inorganic Hg(II) to these bacteria **(Marvin-DiPasquale and Agee, 2003)**. The degradation of MeHg is controlled both by a wide range of microbes and by abiotic processes, particularly photodegradation **(Hammerschmidt and Fitzgerald, 2006; Byington, 2007; Gill, 2008a)**.

The role of wetland plants (both type and density) is a critical factor mediating MeHg production by bacteria in sediments, as plant root zones have recently been shown to be locations of enhanced microbial activity and Hg cycling **(Windham-Myers et al. 2009)**. Because Hg forms strong bonds with dissolved organic matter (DOM), the production and flux of DOM from wetlands is a key process controlling both THg and MeHg transport **(Ravichandran, 2004)**. The uptake of MeHg into the base of the food web, and its bioaccumulation up food webs is of particular concern for both wildlife and human health.

The wet-dry cycle experienced by seasonal wetlands, both non-agricultural wetland maintained for wildlife habitat and agricultural wetlands used for rice production, may promote Hg(II)-methylation more than that observed in permanent wetlands (**Alpers et al., 2008 and references therein; Marvin-DiPasquale et al., 2009a**). This effect is likely caused by the continued cycling of redox-sensitive elements such as sulfur and iron, which are critical to the metabolism of SRB and FeRB. Despite the importance of agricultural wetlands in California and

globally, there are no well-documented studies that examine the detailed cycling of Hg, Fe, and S in adjacent agricultural and non-agricultural wetlands.

2.3 Landuse and socioeconomic context for the Delta Methylmercury TMDL

The Central Valley historically contained 1.6-2.0 million hectares (ha) of natural wetland habitat (**U. S. Fish and Wildlife Service, 1978**), much of which was comprised of ephemeral wetlands that were primarily inundated in winter and spring. Over 90% of these wetlands have been lost to agriculture and development over the past century, with only 121,000 ha remaining (**U. S. Fish and Wildlife Service, 1978; Gilmer et al., 1982; Frayer et al., 1989; Dahl, 1990**). In contrast, 216,100 ha of white rice (**U. S. Department of Agriculture, National Agricultural Statistics Service, 2007**) and 8,575 ha of wild rice (**International Wild Rice Association, 2007**) were planted in the Central Valley in 2007. In contrast to the historic, ephemeral wetlands, rice fields are shallowly flooded (<50 cm) during spring and summer for rice production. Moreover, rice fields are often allowed to dry immediately post-harvest, then shallowly flooded again during the winter to speed rice straw decomposition (**Elphick and Oring, 1998; Bird et al., 2000**). These wetting and drying cycles may strongly impact rice field MeHg production and subsequent bioaccumulation.

Currently, the California RWQCB-CVR is developing a MeHg Total Maximum Daily Load (TMDL) for the Sacramento-San Joaquin River Delta, with a goal of meeting water-quality criteria as soon as possible, but no later than 2035 (**Wood et al., 2010b**). The current version of the Delta TMDL plan recommends an unfiltered aqueous MeHg level goal of 0.06 ng L^{-1} or below for the entire legal Delta and Yolo Bypass. To meet water-quality goals in the TMDL, substantial reductions of current loads were calculated for each Delta tributary region, with a stated recommendation of a more than 70% reduction in current MeHg loads from the Yolo Bypass specifically (**Wood et al., 2010a, 2010b**).

The long-term goal of reducing MeHg levels in sport fish has benefits to fish consumers in the area, including several environmental justice communities in Yolo and Sacramento Counties. Native Americans, African Americans, Russian, Ukrainian, Hmong/Mien, and several other southeast Asian and Pacific Islander groups have been identified by the California Dept. of Health Services as groups with below-average socioeconomic profile that consume above-average amounts of sport fish with elevated Hg levels. This situation puts members of these groups, especially children, at risk for Hg-related medical consequences that may affect neurological development and their ability to learn.

2.4 Land use and previous mercury studies in the Yolo Bypass

Within the Yolo Bypass is the 16,000-acre Yolo Bypass Wildlife Area (YBWA), managed by the California Department of Fish and Game (CDFG), which is tasked with restoring wetland habitat (**Elphick, 2000**) and encouraging agriculture, all while maintaining the primary function of the Yolo Bypass for flood control. Accordingly, there are four predominant wetland management strategies during the rice-growing season: white rice, wild rice, permanent wetlands, and shallowly-flooded fallow fields. Both white rice (*Oryza sativa*) and, to a lesser extent, wild rice (*Zizania palustris*) are grown extensively throughout the YBWA and represent

the largest wetland area during the late spring and summer. Additionally, former rice fields that are rotated out of production and left fallow are shallowly flooded during the late summer (typically during July through September) to provide foraging habitat for migrating shorebirds. Finally, there are several wetlands that are permanently flooded throughout the year. These different wetland types and the various approaches for managing them were expected to result in different rates of MeHg production, bioaccumulation and export. A more definitive understanding of these habitat differences, and the impact of specific management practices, is critical to achieving the stated TMDL MeHg reduction goals.

A pilot study during 2005–06 investigated concentrations of Hg and MeHg in shallow sediment and surface water at two sites within the YBWA (a non-agricultural, seasonal wetland and a permanent wetland) as well as two similar sites in the adjacent Cache Creek Settling Basin (CCSB) (**Marvin-DiPasquale et al., 2009a**). Results of that study indicated:

(a) a large degree of spatial and temporal variability with regard to Hg concentration and speciation;
(b) a rapid increase in benthic MeHg production and (or) release of previously formed MeHg to the water column within days of flooding seasonal wetlands;
(c) the speciation and methylation of Hg in seasonal and permanent wetlands in response to the chemistry of sulfur (S) and iron (Fe), and associated microbial reduction pathways;
(d) the period of inundation (hydroperiod) as an important factor mediating MeHg production among various wetland types; and
(e) the YBWA as more active with regard to MeHg production than the CCSB

Despite the predominance of agricultural wetlands in California's Central Valley, MeHg production, export, and bioaccumulation in rice fields has not previously been quantified relative to adjacent seasonal and permanent wetlands. This study represents an initial effort to fill that important information gap.

2.5 Project Purpose and Scope

This 18-month field study addresses the seasonal and spatial patterns and processes controlling methylmercury (MeHg) production, bioaccumulation, and export from natural and agricultural wetlands of the Yolo Bypass Wildlife Area (YBWA). The data were collected in conjunction with a Proposition 40 grant from the State Water Resources Control Board (SWRCB) in support of the development of Best Management Practices (BMP's) for reducing MeHg loading from agricultural lands in the wetland-dominated Yolo Bypass to the Sacramento−San Joaquin River Delta, and in support of the RWQCB-CVR's current *Sacramento – San Joaquin Delta Estuary TMDL for Methyl & Total Mercury*, which is currently in draft form (**Wood et al., 2010a, 2010b**) and can be accessed in its entirety on-line: http://www.waterboards.ca.gov/centralvalley/water_issues/tmdl/central_valley_projects/delta_hg

Through an assessment of current land use practices in the Yolo Bypass and their effect on MeHg production and export, this study was specifically designed to provide the necessary scientific background in support of achieving the goal of >70% reduction of MeHg export from the Yolo ByPass, as set out in the current Delta TMDL. In addition, the study addresses several core components of the *CALFED Mercury Strategy for the Bay-Delta Ecosystem* (**Wiener et al., 2003a**): 1) Quantification and evaluation of mercury and methylmercury sources, 3)

Quantification of effects of ecosystem restoration on methylmercury exposure, 4) Monitoring of mercury in fish…, and 6) Identification and testing of potential management approaches for reducing methylmercury contamination. This plan was completed in December 2003 and can be accessed in its entirety on-line at:
http://www.calwater.ca.gov/science/pdf/MercuryStrategyFinalReport.pdf

2.5.1 Management questions as project drivers

As the TMDL process moves forward, agencies and managers responsible for lands that may be source zones for MeHg to the Delta, have many questions regarding how their current practices may affect MeHg export to the Delta. In anticipation of some of these uncertainties, this study focuses on four questions that are both fundamental (yet currently unresolved) and useful to managers in terms of land use practices in the watershed. These questions were:

1. *Is there a difference among agricultural and managed wetland types in terms of MeHg dynamics (production, degradation, bioaccumulation, or export)?*
2. *Does water residence time influence MeHg dynamics?*
3. *Does the application of sulfate-based fertilizer impact MeHg production rates?*
4. *Does the presence (or absence) of vegetation influence MeHg production rates?*

2.5.2 Project Goals

Given the above management questions, the primary project **goals** were to determine:

1. *the extent to which seasonal and annual MeHg production and export loads differed for dominant wetlands in the Yolo Bypass: managed permanent and seasonal wetlands, white rice fields, wild rice fields, and rotational fields under fallow management;*
2. *the effect of specific management practices on observed differences in Hg cycling and export;*
3. *if MeHg bioaccumulation was measurable and different between wetland habitat types;*
4. *the underlying processes that led to any observed differences in Hg cycling among wetland types or management practices.*

2.5.3 Project Objectives

We considered two overarching project **objectives** to address these goals.

Objective 1: to examine the linkage between Hg/MeHg cycling, bioaccumulation and export with respect to the following environmental variables:

a) dissolved organic matter quality and quantity
b) vegetation type and density
c) flooding duration, timing, and water residence time
d) post-harvest flooding of rice straw

e) sulfur-based fertilizer application
f) sediment microbial processes and geochemistry

Objective 2: to use the information gained to help the SWRCB develop best management practices (BMP's) for rice farming and wetland management that minimize MeHg production and export.

2.5.4 Project Approach - Overview

Measurements of MeHg concentrations in sediment, water, and biota (plants, invertebrates, and fish) were made to assess land management activities in five wetland types, which included: three types of shallowly-flooded agricultural wetlands (white rice, wild rice, and fallow fields) and two types of managed non-agricultural wetlands (permanently and seasonally flooded). To strengthen our understanding of the processes underlying the seasonal and spatial patterns of MeHg cycling, additional explanatory factors were measured including ancillary sediment and water quality parameters, stable isotope fractionation (oxygen, sulfur, carbon, and nitrogen), photodemethylation rates, and daily-integrated hydrologic budgets. Samples and field data were collected from May 2007 to July 2008, and analyses were completed according to methods and procedures described in the project's Quality Assurance Program Plan (QAPP) (**U.S. Geological Survey et al., 2008**). Pre- and post-study workshops associated with this project were held to promote bi-directional information sharing among local stakeholder groups about Hg issues, including the risks from fish consumption from the Yolo Bypass and areas of the Delta and Sacramento River affected by MeHg export from the Yolo Bypass.

The structure of this report is described below. The next section (**Section 3**) includes a summary of the study design, results, and management implications. Following sections provide detailed results for specific aspects of the study: Hydrology (**Section 4**); MeHg loads and water quality (**Section 5**); Sediment MeHg production (**Section 6**); Plant-Hg interactions (**Section 7**); MeHg bioaccumulation (**Section 8**); MeHg photodemethylation (**Section 9**); Public outreach and stakeholder involvement (**Section 10**). Appendices include results of quality assurance / quality control (QA/QC) for sediment and plant samples (**Appendix 1**), QA/QC results for water-quality samples (**Appendix 2**), Tables of water-quality data (**Appendix 3**), and a summary of MeHg photodecomposition data (**Appendix 4**).

3 Summary of Study Design, Results, and Management Implications

3.1 Study Design

3.1.1 Research Questions

The 4 management questions posed above (**Section 2.5.1**) were expanded and structured to address the 6 research questions below, which systematically focus on comparing processes among wetland types undergoing different management regimes.

Question 1: Did MeHg dynamics vary by type of managed wetland **(habitat effect)**?

Quesiton 2: Did MeHg dynamics vary by field locations or source water such as Toe Drain vs. Toe Drain/Davis Drain/ Greens Lake **(block effect)**?

Question 3: Did MeHg dynamics vary seasonally within the different field types **(season effect)**?

Question 4: Did MeHg dynamics vary with hydrologic factors such as water depth and flowrate **(hydrology effect)**?

Question 5: Did application of sulfate-bearing fertilizers influence MeHg production **(fertilizer effect)**?

Question 6: Did the presence of non-disced rice straw influence MeHg production **(rice straw effect)**?

3.1.2 Location

The 40-mile-long Yolo Bypass located within the Sacramento River watershed and Yolo County, Calif., is part of the Sacramento River Flood Control Project, and serves to divert excess water from the Sacramento River during flood periods, relieving pressure on the main levee system along the river channel. Water primarily enters the basin through the Fremont Weir in the north, which allows inflows from the Sutter Bypass, the Feather River and the Sacramento rivers (**Figure 3.1**). Excess water safely returns to the Sacramento River at the southern end of the Bypass.

Within the Yolo Bypass is the 16,700 acre YBWA, (**Figures 3.1 and 3.2**) of which the CDFG manages 3,700 acres, the Yolo Wildlife Management Area (YWMA), for mixed-use as both wildlife habitat and agrigultural wetlands. The study area for this project was within the YWMA (**Figure 3.2**). The satellite image in **Figure 3.3** depicts the various wetland types (hereafter identified as **fields** (i.e. agricultural fields = white rice, wild rice, and fallow; non-agricultural fields = seasonally and permanently flooded wetlands)) sampled during the study, as well as the flow paths for irrigation waters. Sampling locations for water, sediment, plants and biota are illustrated in **Figure 3.4**. The GPS coordinates for all sampling locations are given in **Table 3.1**. Photodemethylation and solar radiation measurement study site locations are illustrated in **Figure 3.5**. The seasonally flooded wetland sampling site (SW) was also sampled during a recent previous study of Hg cycling within the YBWA and Cache Creek (**Marvin-DiPasquale et al., 2009a**).

3.1.3 Schedule

The sampling schedule reflected the needs and activities of the rice farmer (Jack DeWit) and CDFG wetland managers, with the first sampling occurring in late May 2007, immediately following the first flood-up event for that year, and the last sampling occurring during April 2008 when all fields were again drained in preparation for the 2008 rice planting season. A timeline of the field management activities and project field sampling events is diagrammed in **Figure 3.6**.

3.2 Results Summary: Methylmercury Export

3.2.1 Habitat Effect

Habitat effects were observed regarding several aspects of MeHg loading during the study period.

Wild Rice Harvest: The most prominent habitat effect was the large export of aqueous unfiltered MeHg (hereafter, u-MeHg) that occurred in the wild rice fields. This effect was largely attributed to wet harvest activity activity and elevated particulate MeHg in the surface waters of wild rice fields during September 2007 while outlets were still flowing. Despite relatively low water flow at the outlets during harvest, extremely high concentrations of u-MeHg resulted in increased export from the wild rice agricultural fields during the harvest period.

White Rice Detritus in Late Winter: Another habitat-specific effect occurred during the late winter (February 2008) following the Cache Creek flood event (Jan.24 – Feb.10, 2008). White rice fields had elevated u-MeHg concentrations relative to the other fields and thus exported a larger amount of MeHg compared to the other fields. This effect appears to be related to the amount and quality of decomposing rice straw (detritus) on the field when the flooding occurred. White rice fields had the greatest amount of detritus left on the fields at the time of the flood whereas the other fields had little detritus left by February. The amount of detritus on the field correlated with u-MeHg concentrations. In addition, the two white rice fields were higher than the other agricultural fields in MeHg export during the December period.

Permanent Wetland Water Retention: A significant habitat difference related to differences in water management is that the permanent wetland (PW5) did not have significant MeHg export because there was not much water exported. This, combined with relatively low MeHg concentrations, resulted in the permanent wetland having the lowest export rates of all the fields. Exports of MeHg from the seasonal wetland were not consistently higher or lower than those from the rice fields.

3.2.2 Block Effect

Block (north vs. south) was not a dominant driver of MeHg export over the course of the study. The only observed block effect occurred during the summer irrigation season, when the northern fields were receiving supply waters with elevated MeHg concentrations relative to the southern fields. As a result there was net export of MeHg from two southern fields (fallow and white rice) during August and September whereas the corresponding northern fields showed net import of MeHg during August and had imports approximately equal to exports during September. In terms of concentration factors relative to chloride (a conservative constituent indicative of evapoconcentration), the southern fields showed increases in MeHg from inflow to

outflow that were much greater than the corresponding increases in chloride, whereas the northern fields showed increases in MeHg comparable to those for chloride. In addition to the effect of higher MeHg in the input water, it is possible that longer residence time for water in the northern fields relative to the southern fields contributed to increased photodemethylation.

3.2.3 Season Effect

Season was the major driver of MeHg net export in the study. Winter exports were greater than summer exports for all agricultural fields. Most fields were a sink, or at most a very small source, of MeHg during the summer growing season. This was likely the effect of photo-demethylation and sedimentation processes. In contrast, all fields were a source of MeHg net export during winter/early spring.

3.2.4 Hydrology Effect

Hydrology was a dominant driver of MeHg exports throughout the summer but was less important between seasons. The greatest sink of MeHg in the summer occurred in the fields with restricted outflows and thus longer hydraulic residence times, greater evapo-transpiration (ET), potentially higher rates of photodemethylation, and lower outflow. Despite increases in MeHg concentration across the fields, the water management on the two fallow fields where inflow was ten times that of outflow led to lower MeHg loads leaving the field relative to the inputs. The greatest MeHg exports occurred when the fields were drained in winter/early spring **(Section 5.3.3.3)**, and also when the harvest operations dominated export in the wild rice fields **(Section 5.3.3.2)**. The importance of hydrology was also seen between blocks, as the block effect observed in August **(Section 5.3.3.2)** was associated with increased flows in southern fields as more water became available.

3.3 Results Summary: Methylmercury Production in Surface Sediment

3.3.1 Habitat Effect

There were a number of statistically significant differences, based upon habitat (agricultural vs non-agricultural fields), associated with both Hg biogeochemistry and factors that directly impact MeHg production. For data grouped by either agricultural or non-agricultural (experimental devegetated sites excluded) and averaged across all sampling events: sediment THg and reactive or bioavailable inorganic mercury ($Hg(II)_R$) concentrations were higher in agricultural fields, while values of k_{meth} (a measure of Hg(II)-methylating bacterial activity) were higher in non-agricultural fields. Calculated rates of MeHg production are a product of both $Hg(II)_R$ and k_{meth}, and were not significantly different between the two habitat groupings. However, average sediment MeHg concentrations were significantly higher (1.5-fold) in agricultural fields.

These trends in mercury metrics were driven by strong habitat differences in a number of key biogeochemical and microbial processes. Across all sites $Hg(II)_R$ concentrations decreased as sediment solid phase reduced sulfur concentrations increased, as a result of the strong bonds formed between inorganic Hg(II) and reduced sulfur species. Since average total reduced sulfur (TRS) was significantly lower (8-fold) in agricultural sites, compared to non-agricultural sites, concentrations of $Hg(II)_R$ were comparatively elevated in agricultural fields. Conversely, the activity of the resident microbial community, as assessed by radiotracer $^{203}Hg(II)$ amendment

experiments (k_{meth}), increased as sediment conditions transition from those more conducive to microbial iron-reduction to those more conducive to microbial sulfate-reduction. While both processes occur in all fields, iron speciation data indicate that sediments associated with the agricultural fields were generally more poised for iron reduction and non-agricultural fields were more poised for sulfate reduction. As a result, values of k_{meth} were significantly higher in non-agricultural fields. Thus, due to higher $Hg(II)_R$ concentrations and lower k_{meth} values in agricultural fields, and lower $Hg(II)_R$ concentrations and higher k_{meth} values in non-agricultural fields, average calculated MeHg production rates were similar for both groupings.

Across all sites for both agricultural and non-agricultural habitats, sediment MeHg concentrations were poorly correlated with calculated MeHg production (MP) rates, suggesting that temporal and spatial processes of MeHg degradation and/or loss within sediments are variable, significant and poorly understood. The exception to this was in white rice fields, where calculated MP rates explained 48% of the variability in MeHg concentration. MP, again, was calculated as the product of microbial rate measurements (k_{meth}) and the poolsize of reactive mercury in sediment ($Hg(II)_R$). Sediment MeHg concentrations were also significantly correlated with sediment organic content across all non-agricultural sites, but not across agricultural sites. In fact, no single factor adequately explained MeHg concentration across all agricultural fields.

A strong linear relationship between THg concentration and longitude was found, with THg concentrations increasing 4-fold moving from east to west. Much weaker, yet significant relationships were also found between longitude and other mercury metrics (k_{meth}, $Hg(II)_R$ and MeHg concentration), but not for calculated MP rates. Since all of the agricultural sites were located to the west of all of the non-agricultural study sites, we can not exclude the possibility that some of the significant differences found between agricultural and non-agricultural sites were at least partially caused by this spatial gradient in THg concentration.

3.3.2 Block Effect

The effect of northern block fields (F20, W23 and R31) versus southern block fields (F66, W65 and R64) was statistically tested across all agricultural fields. There were no significant differences in any of the measured sediment parameters, with the exception of pH, where northern block fields had slightly (yet significantly) higher average (± standard error) pH (7.01 ± 0.05) than southern block fields (6.88 ± 0.03). No mercury metrics were significantly different among the northern and southern blocks.

3.3.3 Season Effect

Seasonal effects were statistically tested by comparing growing season data (June, July and August 2007) to post-harvest data (December 2007 and February 2008) for agricultural sites (only). While there were no significant seasonal differences in most mercury metrics, average sediment MeHg concentrations were almost 2-fold higher during the post-harvest period (3.70 ± 0.38 ng g^{-1} dw) compared to the growing season (1.91 ± 0.17 ng g^{-1} dw). In addition, post-harvest agricultural fields had significantly lower pore water chloride and DOC, presumably due to winter flooding.

3.3.4 Hydrology Effect

Hydrology had a pronounced effect on sediment geochemical conditions on agricultural fields, as a function of field flooding and draining/drying cycles. Across all agricultural fields, sediment redox explained 51% of $Hg(II)_R$ concentration. Once flooded, agricultural fields became more chemically reduced as a result of the stimulation of sediment bacteria and the build-up of reduced sulfur and iron end-products. As sediment condition became more reduced (e.g throughout the June thru September growing season), concentrations of $Hg(II)_R$ decreased. In contrast, once fields were drained (e.g. during the September thru October harvest), fields became more oxidized and $Hg(II)_R$ increased. Post-harvest, fields were reflooded and sediments again became more reduced (during fall/winter) and sediment $Hg(II)_R$ concentrations tended to decrease as a result. Thus, since $Hg(II)_R$ concentrations partially control MeHg production rates, these changes in hydrology and sediment redox had a significant effect on where and when MeHg production rates were elevated or reduced.

3.3.5 Fertilizer Effect

A primary hypothesis of this study was that the addition of sulfate containing fertilizers to rice fields would stimulate microbial sulfate reduction (SR) and subsequently MeHg production. Although sulfate application rates were significant, at approximately 50-70 kg $acre^{-1}$ on rice fields during the growing season, neither SR nor MeHg production were measurably or systematically stimulated. Prior to fertilizer amendment, sediment pore water sulfate concentrations were elevated (> 1 mmol L^{-1}) at levels where SR is generally not limited by sulfate concentrations, but instead by organic substrates. Thus, the additional sulfate input as fertilizer did nothing to increase microbial SR, nor MeHg produced by resident sulfate reducing bacteria.

3.3.6 Rice Straw Effect

The seasonal increase in MeHg production observed for the white and wild rice fields during the post-harvest season appears to be at least partially driven by decaying rice straw (**Section 6.4.5**). The first line of evidence supporting this is that benthic microbial SR was not limited by sulfate (electron acceptor) concentration (**Section 6.4.4**), and thus was limited by available organic matter (electron donor) and/or temperature. Secondly, MeHg production rates and concentrations were not highest during the summer growing season when temperature was highest (23 ± 4°C), as might be predicted if temperature was the primary driver of microbially produced MeHg. Instead, MeHg production rates and concentrations were highest during the post-harvest period when sediment temperatures were significantly colder (12 ± 4°C). Thirdly, pore water acetate concentrations increased from 148 ± 73 µmol L^{-1} during the growing season to 385 ± 265 µmol L^{-1} post-harvest in white and wild rice fields (combined), which had decaying rice straw. In contrast, pore water acetate in the fallow fields decreased from 156 ± 87 µmol L^{-1} during the growing season to 16 ± 15 µmol L^{-1} post-harvest. Finally, white and wild rice fields (combined) had higher sediment MeHg concentrations by February than did the fields that were fallow during the previous growing season. Taken together, this evidence strongly suggests that the decaying rice straw supplied labile organic matter (in the form of low molecular weight compounds, such as acetate) that readily fueled the microbial community involved in Hg(II)-methylation.

Because none of the agricultural fields were disced in the post-harvest season, we were not able to compare the observed field reflooding effects of decomposing rice straw with discing (physical incorporation of straw into the surface soil horizon), which is another common practice to remove post-harvest rice straw..

3.3.7 Plant Effect

Experimental evidence suggests that the presence of actively growing vegetation increases rates of MeHg production. MeHg production and concentration were significantly greater during the growing season in vegetated (control) plots compared to devegetated (manipulated) plots. This vegetation effect appeared to be due primarily to rhizosphere stimulation of 1) the supply of labile carbon pools such as acetate (fermentation product) that serve as fuel for Hg(II)-methylating bacteria, and to a lesser extent 2) enhanced iron cycling, including the reoxidation of reduced iron pools – Fe(II) to amorphous Fe(III) – an effective electron acceptor for iron-reducing bacteria. Along with comparative data between fields and seasons, these experimental data suggest the potential importance of iron-reducing bacteria in Hg(II)-methylation in these agricultural wetlands.

3.4 Results Summary: Methylmercury Bioaccumulation

3.4.1 Habitat Effect

Mercury in Invertebrates: Wetland habitat type had an important influence on THg concentrations in invertebrates, but this effect depended on the sampling time period and taxa. In particular, Notonectidae, but not Corixidae, THg concentrations were higher in permanent wetlands (average concentrations exceeding 2.0 $\mu g\ g^{-1}$ dw) than in white rice, wild rice, or shallowly-flooded fallow fields, which all had similar average concentrations ranging between 1.1 and 1.3 $\mu g\ g^{-1}$ dw. The effect of wetland habitat type was especially prevalent at the end of the rice growing season, when Notonectidae THg concentrations increased by approximately 1.5-2 times over their flood-up levels, and were at their highest in permanent wetlands. Additionally, invertebrate THg concentrations were higher at field outlets ($1.14\pm0.06\ \mu g\ g^{-1}$ dw) than inlets ($0.93\pm0.06\ \mu g\ g^{-1}$ dw).

Mercury in Caged Fish: THg concentrations and total Hg burdens in caged fish differed among wetland types at all cage sites, with white rice and wild rice fields having higher Hg concentrations than permanent wetlands. THg concentrations were higher at outlets than inlets in white rice, higher at inlets than outlets in wild rice, and did not differ in permanent wetlands. Total Hg burdens were higher at outlets than inlets in white rice, higher at inlets than outlets in permanent wetlands, and did not differ in wild rice. Our results indicate that THg concentrations in caged mosquitofish increased by 12, 6, and 3 times over reference levels in white rice, wild rice, and permanent wetlands outlets in just 60 days, respectively.

Across all wetland habitat types and sites, THg concentrations in mosquitofish removed from cages after 60 days of exposure were $1.07\pm0.03\ \mu g\ g^{-1}$ dw, $1.13\pm0.02\ \mu g\ g^{-1}$ dw, and $0.40\pm0.01\ \mu g\ g^{-1}$ dw in white rice, wild rice, and permanent wetlands, respectively, and $0.71\pm0.02\ \mu g\ g^{-1}$ dw, $0.81\pm0.02\ \mu g\ g^{-1}$ dw, and $0.84\pm0.02\ \mu g\ g^{-1}$ dw at the inlets, centers, and outlets, respectively.

Mercury in Wild Fish: Similar to caged fish, THg concentrations in wild fish differed among habitats, with white rice and wild rice having THg concentrations higher than in permanent wetlands. THg concentrations in wild mosquitofish were higher at outlets than inlets in white rice and wild rice, and inlets were higher than outlets in permanent wetlands. THg concentrations in wild silversides also were higher at white rice outlets than inlets, but not in wild rice or permanent wetlands.

Across all wetland habitat types and sites, THg concentrations in wild mosquitofish (*N*=140) were 0.63±0.04 μg g^{-1} dw, 0.69±0.05 μg g^{-1} dw, and 0.45±0.02 μg g^{-1} dw in white rice, wild rice, and permanent wetlands, respectively, and 0.43±0.03 μg g^{-1} dw and 0.77±0.03 μg g^{-1} dw at the inlets and outlets, respectively. THg concentrations in wild silversides (*N*=136) were 0.82±0.05 μg g^{-1} dw, 0.66±0.05 μg g^{-1} dw, and 0.30±0.02 μg g^{-1} dw in white rice, wild rice, and permanent wetlands, respectively, and 0.48±0.03 μg g^{-1} dw and 0.62±0.04 μg g^{-1} dw at the inlets and outlets, respectively.

Wild Versus Caged Fish for Wetland Hg Monitoring: Our results from wild fish are similar to caged fish, except that THg concentrations in caged fish were higher than in wild fish that were presumably exposed to Yolo Bypass Hg concentrations their entire lives. This illustrates the importance of using caged fish as site specific bioindicators of Hg contamination since wild fish are free to move in and out of the wetlands studied and into canals where MeHg concentrations are known to be lower.

3.4.2 Block Effect

We did not test for a block effect on biota Hg concentrations due to inherent intercorrelations between block and habitat type.

3.4.3 Season Effect

We tested for a seasonal effect on biota Hg concentrations using invertebrates that were sampled upon rice flood-up and again just before rice harvest. THg concentrations in Corixidae did not differ between flood-up and pre-harvest time periods (difference: 0.11±0.09 μg g^{-1} dw), whereas THg concentrations in Notonectidae were higher during the pre-harvest than the flood-up time period (difference: 0.40±0.10 μg g^{-1} dw).

3.4.4 Hydrology Effect

As stated above, invertebrate Hg concentrations tended to be higher at the end of the rice growing season than upon flood-up. Additionally, mosquitofish that were experimentally caged at wetland centers had nearly as high Hg concentrations than mosquitofish caged at wetland outlets. These results indicate that Hg bioaccumulation occurred rapidly within wetlands' hydrological gradient from inlets to outlets.

3.4.5 Biota Hg Correlations with Hg in Water and Sediment

Our results indicate that temporarily flooded shallow wetlands, such as white rice and wild rice fields, have elevated THg concentrations in both caged and wild fish compared to permanent wetlands at the Yolo Bypass. In contrast, THg and MeHg concentrations in invertebrates were higher in permanent wetlands than in white rice or wild rice fields.

These conflicting results are partially explained by the fact that fish THg concentrations were correlated with water MeHg, but not with sediment MeHg, whereas invertebrate MeHg concentrations were more correlated with sediment MeHg than with water MeHg. These results illustrate the complexity of MeHg bioaccumulation in food webs and indicate the importance of using several bioindicators simultaneously when monitoring MeHg production and bioaccumulation.

3.4.6 Fish and Invertebrate Hg Concentrations Exceed Harmful Levels to Wildlife in Yolo Bypass Wetlands

Hg concentrations in Yolo Bypass wetlands exceeded levels potentially harmful to wildlife. Hg concentrations in invertebrates and fish were more than 6 and 11 times higher, respectively, in Yolo Bypass wetlands than stated TMDL target values to protect wildlife (0.03 ppm ww). In fact, 99% of wild fish sampled in Yolo Bypass wetlands exceeded stated TMDL target values to protect wildlife (0.03 ppm ww) and 75% of invertebrates sampled in Yolo Bypass wetlands exceeded reported MeHg dietary effect levels of 0.50 µg g^{-1} dw on avian reproduction. Therefore, Yolo Bypass wetlands should be considered a hot-spot for MeHg bioaccumulation and higher trophic level predators, such as waterbirds, should be monitored to make sure Hg is not having detrimental effects on avian reproduction.

3.5 Summary / Discussion of Results

Despite high benthic MeHg production rates (**Section 6**) and water concentrations in agricultural fields (**Section 5**), MeHg exports were physically limited by hydrologic export (**Section 4**) for all wetlands studied. While photodemethylation may have been partially responsible for limiting MeHg export (see **Section 9**), high aqueous MeHg concentrations led to rapid bioaccumulation of MeHg within caged and wild fish (**Section 8**). We suggest that load reduction is maximized by limiting water throughput, but that on-site biota exposure is maximized by this longer water residence time. Seasonally, we observed that the primary period of MeHg export from the Yolo Bypass Wildlife Area is during winter flooding periods when overall microbial activity and MeHg production in agricultural soils is fueled by the decomposition of rice straw (**Section 7**), and when hydrologic flowthrough in maximal. Because both photodemethylation and particle settling processes of MeHg removal are relatively inactive in winter months, we suggest that efforts to reduce MeHg production during this period would limit export from the fields.

The most dramatic difference in MeHg loads exported from the fields was found in the comparison of permanent ponds with the other fields. There was limited water export from the permanent ponds, and therefore, the MeHg export loads were minimal in comparison to the other fields. The concentrations of MeHg in the permanent ponds were also the lowest of all the fields, which also contributed to the relatively low MeHg exports.

The within-field comparisons are limited because of the variability in MeHg exports both seasonally and spatially and the limited sample size. It is unlikely the loads of MeHg coming from the fields in the Yolo Bypass are raising the concentrations of MeHg in the Delta during the active crop growing season, due to three factors:

1. Water discharge from YBWA agricultural fields are minimized by current management practices.

2. When water is exported, it is generally "recycled" and used again within the YBWA for irrigation.
3. Water use and evapotranspiration losses in rice fields is substantial during the summer irrigation season, such that the net flow of water is from the Delta to the YBWA.

3.6 Management Implications and Next Steps

1. The practice of wet harvesting of wild rice (active harvesting while outflows were open and flowing) led to the highest exports of u-MeHg the study. Restricting outflow during the wet harvest would minimize summer exports and potentially allow MeHg in the field's water column to be reduced by particle settling and photodemethylation. The efficacy of this control mechanism could be tested during peak MeHg load periods of wild rice post harvest or ag fields in winter months.

2. Lower outflow generally results in lower u-MeHg exports. Minimizing surface water exports, wherever practicable, may limit the export of MeHg loads, as the more water is exported, the higher the loads. For rice management, however,a long residence time with minimal water export might be detrimental.Minimum water depths are needed during critical periods of the rice life cycle (so that flower buds are protected from low evening air temperatures which can cause sterilization). Further, input water is relatively saline, and additional evaporation can cause salt (osmotic) stress on the rice plants. Only the minimal amount of water that is needed should be flowed through the rice fields to minimize MeHg export. More attention to water management to optimize water use might require more resources.

3. MeHg removal from the water column via photodemethylation or particle settling may explain the reduction aqueous MeHg concentrations from inlet to outlet in the permanent wetland. If waters are held continuously in a permanently flooded deep wetland, particle settling and photodemethylation may provide an important MeHg removal function that could be utilized for tail-water cleaning. In future studies, it may be valuable to evaluate the whether the restoration or creation of permanent wetlands at the landscape scale will significantly influence hydrologic export and biotic exposure, especially outside of the wetland boundaries.

4. The surficial layer of rice straw that is generated late in the season is likely responsible for the high MeHg concentrations in surface water and sediments (biota were not monitored in winter). Alternative management that limits the availability of this labile carbon source prior to continuous winter flooding (e.g. discing or rice straw removal) may limit the carbon supply to mercury methylating microbes, and thus limit MeHg production and subsequent export.

5. Source water concentrations of u-MeHg are difficult to mitigate at the field scale, and may be a dominant control on net exports. Next steps may include a tracer experiment and/or measurements of processes related to advection and diffusion, as well as percolation.

6. Yolo Bypass wetlands should be considered a hot-spot for MeHg bioaccumulation and higher trophic level predators, such as waterbirds, should be monitored to make sure Hg within the YBWA is not having detrimental effects on avian reproduction.

4 Detailed Results for Hydrology

4.1 Introduction

Understanding hydrology in aquatic systems is important because many of the factors that control water quality in these systems are dependent on hydrologic conditions. Constituent concentrations provide only a snapshot of water quality at a particular window of time without any insight into the processes that led to the snapshot. Water supply, controls, pathways, and losses are all required to understand the processes leading to the water quality of an aquatic system at any particular moment in time.

The role of hydrology is of particular importance in the YBWA because the various wetland systems managed within the YBWA are largely defined by their hydrologic conditions, such as time and duration of flooding. Other systems within the YBWA have similar hydrologic conditions but differ in other ways such as crop type, fertilization, pesticide use, and a host of other operational variables that may impact water quality. To be able to understand the impact of these variables on water quality in the YBWA, hydrology must first be excluded as a driving factor. The only way to address the role of hydrology, and its impact on these systems, is to measure the hydrology for each field and identify its role prior to assessing the impact of other variables on water quality. Furthermore, hydrology in the YBWA is widely manipulated for water supply and therefore provides a variable that can be relatively easily manipulated by managers in the interest of controlling water quality in the YBWA.

In this study, hydrology was characterized for five wetland types managed within the YBWA to provide a basis for understanding the fate and transport of nutrient, organic carbon and pollutants for different wetland habitats: rice, wild rice and fallow fields as well as seasonal and permanent wetlands. Hydrologic analyses and seasonal water budgets were developed for fields currently being managed by farmers and wildlife managers in Yolo County, CA through routine hydraulic and meteorological data. The objective of the research was to quantify the differences in the water budget and hydrologic management of the different cropping systems in order to better understand the potential drivers for water quality, in particular MeHg.

4.2 Approach

4.2.1 Site Description

Eight fields were studied in this investigation ranging in size from 16 to 78 hectares **(Table 4.1, also see Figures 3.3 and 3.4)**. Two fields were fallow under shallow flooding (F20, F66), two fields were in white rice (R31, R64), two fields were in wild rice (W32, W65), and two fields were managed wetlands (SW – seasonal wetland, PW –permanent wetland). The YBWA fields have silty-clay soils and shallow groundwater maintained at 1 to 2 meters below land surface during the irrigation season. Ditch water levels are maintained for routing water from three reservoirs: the Toe Drain, Green's Lake and return water from the Davis Drain. Losses in the recycled water in Greens Lake and Davis Drain are replenished by pumping water up the Toe Drain from the Sacramento - San Joaquin Delta and into the South Supply Ditch. The fields were managed in the spring, summer and fall according to their use: rice, wild rice, fallow or wetlands. The cropped fields were managed by the farmer to maximize crop yields. Wetlands were

managed by the California Department of Fish and Game for wildlife use. Field activities such as planting and harvesting were tracked through discussions with land managers and field observations.

Land managers controlled the hydrology of the study area's fields through the use of various hydraulic control structures. Water enters these fields through either valved pipes or flashboard risers depending upon the hydraulic design of each field. The fields are divided into checks, with a check defined as a subfield with a set bed elevation (plus or minus a few centimeters) with a minimal slope to carry the water from the upstream check to the downstream check. Check berms are set up along field contours, thus enabling the farmer to manage the water depths throughout each check. The number of checks within a field is determined by the total elevation drop across the field from inlet to outlet. Water enters and exits each check through risers with water level and flow controlled through the placement of boards in these weir structures. Each check typically has two weirs at the inlet and two at the outlet although field management may only utilize one weir box for an inlet or outlet from each check based on water demand and field mixing.

4.2.2 Hydrologic measurements

To characterize the hydrology of these systems, a hydrologic unit (HU) was defined for each field **(Table 4.1)**. The HU approach was used so that all flow measurements could be made using weirs and thus would be subject to the same constraints and errors. Each HU was defined so that both the inflows and outflows would have weirs. Since all fields do not have weirs at the inflows, the first check berms with weirs for inflows were defined as the upstream end of HUs. The downstream end of the fields, all fitted with weirs, were defined as outflow of the HUs. Thus, all flows were estimated using standard equation describing flow over weirs **(Heald, 2002)**:

$$Q = C(L - 0.2H)H^{1.5} \qquad \textbf{Equation 4.1}$$

Where
Q = flow in cubic feet per second,
L = length of weir opening in feet,
H = head on weir in feet

Data from a previous study with similar weirs were used to determine the C-value for this equation (C = 3.207, R^2=0.9394). **(Bachand and Associates et al., 2006)**. This equation is valid under critical flow conditions, where water drops over the end of the weir with no backing up of flow or other restrictions to gravity flow. Flow estimates could not be made in the managed wetlands (permanent and seasonal) because beaver dams interfered with the operation of the weirs.

A staff gauge was installed at each inflow and outflow location. Each height over weir measurement was accompanied by a staff gauge reading. These readings were used to provide a quick assessment of changes in water levels and were calibrated against the manual measurements of water height over the weir as a QAQC check. Staff gauge measurements at HU outflow locations were used to estimate changes in water levels across the fields. Along with

quantitative measurements, metadata was collected and photographs were taken to document the hydrologic conditions (e.g. critical flow, signs of disturbance, malfunctioning equipment, staff gauge levels).

For a subset of inflow and outflow locations, pressure transducers were installed and data recorded at 15 minute intervals. In wetland fields, pressure transducers were installed at outflow and center locations. Each pressure transducer was attached to a staff gauge and housed in an open-ended, vented PVC pipe. Pressure transducers measured water levels and were calibrated against staff gauge readings and measurements of heights over the weir. The calibrated data were converted to flow estimates using **Equation 4.1**, providing high frequency calculations of flow rates. Thus, the pressure transducers were used to track rapid changes in water level and flow not captured by discrete measurements.

Measurements began in June 2007 and continued through early April 2008 for the rice, wild rice and fallow fields. Transducer measurements began in July 2007, delayed by contractual issues. Monitoring of the wetland fields began in October 2007. Measurements were most intensive during the irrigation season; sites were visited several times a week during that time. Fewer measurements were made during the fall or spring because little or no water was flowing. Hydrologic measurements were made when possible in the late fall and winter, flooding limited access. After early December, few estimates of flow could be made because critical flow conditions were rarely met.

We were not able to calculate flow rates during the initial flooding of the fields because irrigators removed all boards in the weirs and water flowed freely. This phase occurred during the first week of irrigation; once standing water was present, irrigators began to add boards and measurements could be made. The flood-up period for fallow fields was approximately 50 days and we measured the flow rates during much of that time. We estimated that flow rates during the unmeasured flood-up period as equal to the average of the flows measured in July, the first month of flood-up for the fallow fields.

For rice and wild rice fields, we estimated inflow volume during initial flooding as the amount of water needed to saturate the unsaturated soil above the plow sole plus the height of water in the field at the end of the initial flooding phase. Several studies have shown through empirical data or modeling results that water does not quickly infiltrate the plow sole in rice fields **(Liu et al., 2001; Wopereis et al., 1994, Bouman et al., 1994)**. The soils at the YBWA, Sacramento Series (ref) are classified as having very poor drainage and a plow layer approximately 18 cm deep. We estimated that the soil initially had a water content of 25% based upon its field capacity of 30 – 35% and its hygroscopic coefficient (wilting point) of 10 – 18% **(Brady and Weil, 2002)**. Based on a porosity of about 50% for cultivated soils **(Brady and Weil, 2002)**, we estimated that 6 cm of water was needed to saturate the soil in the plow layer. We then doubled that amount based upon an expectation that some water would flow past the plow layer during the flooding period. Thus, to calculate the total volume of inflow during the initial flooding phase, 12 cm of water was added to the amount necessary to raise surface water levels. Flow rates were calculated for the initial flooding, depending on the elapsed time during this period.

All hydrologic data was entered into an MS-ACCESS database and processed to develop flow rates. Extensive QAQC of the hydrologic data was conducted to ensure that predicted flows were only made for conditions of critical or zero flow, and that instrumentation was working effectively. Data that failed to meet these objectives were excluded from the analyses. Hydrologic trends and statistical significance using ANOVA was conducted using Statistica **(Statsoft Inc)**.

4.2.3 Meteorological data

Precipitation measurements and reference evapotranspiration data was obtained from California Irrigation Management Information System (CIMIS) UCD station, located approximately 15 km to the northwest of YBWA. Actual evapotranspiration (ET) was calculated from ET_o using crop coefficients (Kc) according to:

$$ET = Kc\ ET_o \qquad \textbf{Equation 4.2}$$

where ET is in mm day^{-1}, the Kc value is dimensionless, and ET_o is the reference crop evapotranspiration measured by CIMIS in mm day^{-1}. During the growing season, Kc was based on crop development stage, as defined by the Food and Agriculture Organization Irrigation and Drainage Paper 56 (FAO 56) **(Allen et al., 1998)**. Kc values for fields and periods where no crop was present and no Kc value published were estimated according to their state of inundation, vegetative condition and soil water content.

4.2.4 Water sample collection and analyses

Water samples were collected for calibration of the hydrologic model using conservative tracers (SC, Cl^-, Br^-) measured at inflow, middle and outflow of HUs in late August 2007 to help assess the degree of mixing in the HUs. Specific conductance was measured in the field at the hydrologic monitoring locations using a YSI multiprobe **(YSI 6-series)**. Chloride and bromide samples were collected as part of the water quality sampling effort (see **Section 5**) at field inlets, outlets and center locations. Laboratory analyses are described in **Section 5**.

4.2.5 Mass balance calculations

Two models were used to develop mass budgets: the Plug Flow Reactor (PFR) model and Continuous Flow Stirred Tank Reactor (CFSTR). The CFSTR model assumes that the field is well mixed throughout whereas the PFR model assumes that each check is well mixed but independent from each other **(Figure 4.1)**. The equations derived above were used in the PFR and CFSTR model development to estimate the contributions of surface and groundwater to meeting evapotranspiration needs, and to estimate subsurface flow rates into or out of the field system. These equations were applied for selected conditions during the summer irrigation season including 1) Inflow was greater then zero; 2) Outflow was greater then zero; 3) Inflow was greater then outflow; and 4) All flow, electroconductivity and water level data was available for each date. These conditions allow for the best resolution of flow paths that could then be used to guide calculations for the entire hydrologic period.

Water and mass budgets were derived to describe the aquatic crop fields, including the underlying soil near the rootzone as illustrated in **Figure 4.2**. The total water budget can be described with the following expression:

$$Q_i + Q_{ssf} + Q_{pr} = Q_o + Q_{ET} + Q_{\Delta WL} \qquad \textbf{Equation 4.3}$$

where
Q_i = surface flow into the system,
Q_o = surface flow out from the system
Q_{Pr} = flow into the system from precipitation
$Q_{\Delta WL}$ = Change in water storage due to changes in surface water levels
Q_{ET} = flow from the system as evapotranspiration
Qssf = subsurface flow into the system.

Using the soil water interface as a boundary between the above and below ground water balance, a surface water budget can be described by

$$Q_i + Q_{pr} = Q_o + Q_P + Q_E + Q_{\Delta WL} \qquad \textbf{Equation 4.4}$$

For flooded fields, subsurface soil can be assumed to remain saturated and so no change in water storage occurs. The subsurface water can be described by

$$Q_P = Q_T - Q_{ssf} \qquad \textbf{Equation 4.5}$$

Where
Q_P = flow to root zone through percolation
Q_E = flow out as evaporation (surface) and
Q_T= flow out as transpiration (subsurface).
Q_{ssf} = flow to rootzone from groundwater

Importantly, this water budget separates transpiration and evaporation when describing evapotranspiration.

4.3 Results

4.3.1 General trends

Field based manual measurements tracked *in situ* measurements well and produced similar water fluxes **(Figure 4.3)**. Because of the good relationship between manual and automated measurements and because not all fields were equipped with transducers, manual measurements were used to calculate all field water budgets to maintain maximum consistency across all fields in the study.

Using the steady state analysis of a conservative tracer (Cl^-) with the models during the summer irrigation period, white rice fields were found to follow the PFR model where each check is individually well-mixed and concentrations increase along the flow paths, whereas wild rice fields behaved more like the CFSTR model with concentrations being similar across the entire field independent of checks.

4.3.2 Seasonal analyses

Measurements were separated into "seasons" based on agricultural practices, water level, and flow **(Table 4.2)**: Two of the "seasons" were periods of inundation for most fields including the summer agricultural production season, in which seven of the fields were flooded for at least 60 days, and the winter flooded period in which all eight of the fields were flooded. The winter flooded period was further broken down into three separate periods: the winter irrigation, winter flood, and winter drainage periods. The spring and autumn seasons are periods of no irrigation when fields are extensively dry so that land preparation and harvest activities can be performed, because no surface water transport occurred during these seasons, no analysis of those seasons is included in this report.

4.3.2.1 *Summer irrigated period*

For all fields, irrigation water dominated the inputs during the summer. **Table 4.3** presents a summer water budget with values reported as cm of water, standardized to the area of the field. Irrigation water applied to the fallow fields was less than that applied to the domestic white and wild rice fields largely because the fallow fields were flooded for a shorter period of time and were not managed as flow-through systems, instead allowing the water to stand in the field and slowly move from check to check. Surface drainage was much less than surface irrigation (12% to 31%) due to significant loss mechanisms during the time water passed over the fields. During stable flow conditions, the CFSTR model predicted that 38% of ET losses were from E and 63% from transpiration whereas the PFR model predicted 27% ET losses were from E and 73% from transpiration. Irrigation management in the summer growing season differed between white and wild rice. Flow across the fields was greater in wild rice than white rice early in the period whereas wild rice flows across the field decreased late in the season and flow across the white rice fields increased. Because the wild rice fields were not drained post-harvest, there is a relatively large amount of water stored on the field whereas the other fields were drained entirely during the irrigation period. Budget imbalance for the season ranged from -7 to +15 cm of water. When including the water deficit of the soils from the spring dry-down the budget imbalances range from -38 to +1 cm. The models suggest groundwater utilization by plants through upward flow in the soil strata during transpiration as the balance for the water deficits; however, these figures are within the error of measurement and are as likely to be the result of the initial flood-up estimates and ET demands during the dry period.

4.3.2.2 *Winter irrigated period*

This period is defined as the period when the fields are reflooded for waterfowl habitat and decomposition of summer vegetation. Precipitation and river flows commonly preclude the need for irrigation except in the fallow fields and seasonal wetlands which require irrigation because they typically get flooded earlier in the year before the rainy season begins. The end of the period was defined by overbanking of the fields by high Cache Creek flows, as this impacted the ability to accurately measure water and constituent fluxes. The value of 25 cm water depth was chosen as the point at which water quality measurements were reasonable for the measured water volumes. Losses due to transpiration were negligible because the plants were either harvested or senesced. Losses to evaporation were small because of cooler temperatures and less solar radiation. As seen in **Table 4.4**, the large calculated imbalance in the fallow fields and W65 likely reflects difficulties encountered in measuring the surface inflows to the fields during the

winter irrigation period. Many of the measurements collected early in this period failed to meet the critical flow requirement for measurement because of the manner in which the managers maintained the weirs. This resulted in a likely underestimation of surface irrigation for the early part of the record.

4.3.2.3 *Winter flood period*

Flow measurements onto and off of the fields could not be made during this period because high storm flows from Cache Creek over-topped the berms used to isolate the fields, resulting in a large, undefined expanse of water encompassing the fields. Unconfined flow dominated this period. Also, access was restricted during the flooded period for safety concerns. Because no measurements were possible during this period, there are no measurements that can be used to estimate this period, we can only estimate water fluxes during this period using theoretical approach. As a means to estimate water on and off the fields during this period, the pressure transducer measurements were used to estimate field depths. Elevation changes more from east to west so fields without pressure transducers that lie on the same longitude as field with transducers were estimated as having similar changes in water depth over the flooded period. Using the most conservative scenario, that there was no flow component to the flood inflow and outflow volumes and water merely rose and dropped on each field, the 17-day flood period accounted for roughly 50% of the annual water budgets for each field **(Table 4.5)**. Using the average change in water depth from the beginning of the flood and the end (from 1/25/08 – 2/10/08) and the lower end of published floodplain velocity estimates (0.1 m s^{-1}; **Sommer et al., 2001**)**,** we estimated a less conservative range of 200 to 500 cm of water flowed onto and off of each field during the 17-day period of inundation. There is little doubt that the flow regime across the greater Yolo Bypass was complex and likely included greater velocities than the 0.1 m s^{-1} used for this estimate, equating to much greater water volumes passing through the fields. We did not further evaluate the less conservative estimates of flow or areal differences between fields during this period because this very rough estimate of water flux was an order of magnitude greater than the irrigation values for the rest of the year, accounting for the vast majority of the annual water budget for each field despite the short duration of the regional flooding.

4.3.2.4 *Winter drainage period*

The winter drainage period is defined as the point at which the fields re-established their boundaries as floodwaters receded below the berms and back to the baseline 25cm depth established as the end to the winter irrigation period. Because the flood breached some berms and open irrigation supply pipes acted as drains following the flood, no direct measurements of flow could be made during this period. Therefore, the drainage period water budget was estimated as the export of water that was present on the field, based on the 25cm baseline assumption pre-flood. Because the start of this period was the re-establishment of individually flooded fields and the end was defined as fully drained conditions, a net export of 25 to 30 cm of water was calculated for all fields **(Table 4.6**). When added to the total winter budget (**Table 4.7**), this outflow of flood water was the greatest term for hydrologic export within all fields.

4.3.2.5 *Spring and autumn dry-down periods*

Precipitation and ET dominated in these periods as they have, by definition, no irrigation inputs or surface drainage from the fields. When drying fields, managers rely on ET to outpace precipitation to dry-out the soils for machinery access for harvest and field preparation activities. These periods make up a minor portion of the annual hydrologic budget except that they set the water deficit for the fields and drive the irrigation requirements at the initial flooding.

4.3.3 Annual water budget

It is apparent that a bulk of the surface irrigation of the agricultural fields occurs in summer (approx. 80%), as would be expected, however, the bulk of the surface water exports occur during winter (approx. 80%) because of lower ET and higher precipitation. As shown in **Table 4.8**, irrigation demand of the managed wetlands was similar to that of the agricultural fields in spite of having lower ET during the flooded period, largely due to longer periods of flooding which resulted in higher ET demand. Also, although we excluded the contribution of the regional flooding from the calculated annual budget because of the large uncertainties in the estimates, estimates of the contribution of the flood to the annual water budget is large even under the highly conservative methods used indicating the relative importance of this event to actual annual loads and the importance for capturing these events in future efforts. The high irrigation demand for field R64 was a result of the herbicide management requirement for that field. To apply the type of herbicide used, the field had to be completely drained and reflooded during the growing season. Irrigation demand for the fallow fields was lowest likely due to the short period of flooding; however, the budget imbalance was greatest for these fields, suggesting a large water deficit which may be a result of difficulties in measuring the initial flooding of these fields.

4.4 Discussion

Much of the irrigation water applied to the agricultural fields was never exported through surface outlets during the summer irrigation period **(Tables 4.3)**. Surface outflows constituted only 15 to 30% of the irrigation water in summer. Transpiration was the largest vector of water loss from the surface water column during this period, carrying constituents into the soil stratum, leaving the question of what the ultimate fate of the constituents might be: concentrated in soil root zone, leached out with some seepage into surrounding drains or taken up by plants through the roots, exported during flood periods in the winter due to diffusion from substratum into surface waters. Further impacts include the fact that advective flow of water downward into the soil from the overlying water to meet transpiration demand (during actively transpiring periods) would greatly reduce the diffusion of constituents produced in sediments upward into the surface water column.

In contrast, winter precipitation accounted for at least as much water inputs to the fields as surface irrigation, even without including the 17-day Cache Creek flood period. Also, evaporation was minor and transpiration is negligible during winter. This results in a bulk of the surface export of water to occur in the winter period. The differences in hydrology between seasons are likely to have a profound impact on water quality and constituent exports. Also, it is important to note that in the YBWA, even under the most conservative estimate of the winter flood to the annual budget, the flood waters accounted for at least 50% and more likely in excess

of 99% of the annual water budget despite being only 17 days long. It is imperative that a greater effort be attributed to the examining this winter period in future studies.

Also of note is the difficulty of measuring the water budget in these wetland systems, particularly in the fallow fields. The effort required for assessing hydrology should never be underestimated when designing a study or in prescribing management practices to growers. It was good that manual measurements mirrored *in situ* measurements in this study, but this relationship and datset should not be expected in all cases or locations, as it required a great amount of time and effort to make the measurements. It is imperitive that efforts be made for coordination between irrigation managers in the field and *in situ* data collection to reduce assumptions and error in measurements. Future efforts should be made to instrument flow structures in such a way as to capture flood-up and drainage of large events as they can dominate water flux on and off field as well as uncertainties that are carried on in the calculation of constituent fluxes.

In conclusion, hydrology may be the most important variable in understanding water quality in the YBWA. The flow of supply water, evaporative and plant transpiration demand and impacts of flow path all influenced water quality. Of particular interest in this study was the recognition of the different roles of evaporation (E) and transpiration (T) in the water budget as opposed to evapotranspiration (ET) considered as a single component of the water budget as there is a significant difference in their effect on surface water quality. Distinguishing evaporative losses from transpiration losses was necessary to reconcile the hydrologic and tracer mass budgets. Evaporation acts on the surface water of the system, removing water but not constituents, thus increasing concentrations in surface water (evaporative concentration). In contrast, transpiration occurs in the root zone of the plants which acts similarly to a surface outlet except that the constituents can be trapped in the soil or taken up into the plants. The implications of not capturing these realities in hydrology are profound in that the improper allocation of hydrologic flowpaths can result in the fundamental misunderstanding of ecosystem function and resulting water quality.

5 Detailed Results for Methylmercury loads and Water Quality

5.1 Introduction

There are several reasons to study MeHg cycling and export from wetland habitats hydraulically connected to the Delta: 1) there are fish consumption advisories issued for limiting the amount of fish consumed by anglers in the Delta; 2) there is concern that any changes to restore the Delta, including creating more wetlands, will exacerbate the Hg problem: 3) there are goals by the California Bay Delta Authority to create and restore thousands of acres of wetlands and to drastically alter the structure and functioning of the Delta; and 4) the Central Valley RWQCB has proposed a Basin Plan Amendment (**Wood et al., 2010b**) that would require wetland managers to conduct research to develop BMPs for reducing MeHg releases from wetlands.

There have been few publications reporting loads of MeHg from different wetland habitats, particularly in California's Delta where wetlands are a prominent land type. Internationally, wetlands have been identified as important sources of MeHg. For example, in the experimental lakes area of Ontario, Canada it was shown that watersheds with wetlands contributed far more MeHg than watersheds with lakes (stratified and non-stratified) and riparian habitats (**St. Louis et al., 1994**). In other areas in the U.S.A. and Canada these results were confirmed (**Krabbenhoft et al., 1995**; **Branfireun et al., 1996**; **Driscoll et al. 1998**). Of particular interest is that periodically flooded wetlands were found to be habitats with particularly high MeHg production (**Hecky et al., 1991; Rudd, 1995)**

Wetlands and rice fields from the YBWA were selected for study because of their wide wetland variety in close proximity, from typical seasonal wetlands and permanent wetlands to white rice, wild rice, and fallow fields. The YBWA wetlands represent important habitat for birds along the Pacific Flyway, a migratory corridor of manythousands of acres of wetlands throughout California.

The primary objectives of this task element of the study are to quantify and compare mercury and MeHg concentrations and exports from different wetland types within the YBWA and to determine the dominant processes that lead to methylation, export and Hg bioaccumulation under different land management schemes commonly used in the YBWA. Both *in situ* (within the YBWA) concentrations and exports are important because *in situ* concentrations will govern the exposure of local biota to Hg and MeHg, whereas exports may impact sensitive downstream environments.

5.2 Approach

5.2.1 Field sampling

The field sampling plan consisted of four levels of intensity: Schedules A, B, C and D. Schedules A and B were multidisciplinary and designed to coordinate with sediment, plant, and biota sampling teams involved in the greater study objective of providing a wholistic view of Hg cycling in different wetland habitats. These schedules consisted of the most extensive list of analytes collected at five time points considered indicative of the dominant management

activities in the wetlands under study, including initial flooding, mid-irrigation-season (top dressing fertilizer application), pre-harvest, winter flood-up (prior to Bypass flood) and winter pre-drainage (post Bypass flood) (see ***Table 11.1*** and ***11.2*** in ***QAPP*** (**U.S. Geological Survey et al., 2008**) for sampling schedules and analytes). Schedule C sampling included a subset of analytes from Schedules A and B with the focus of enhancing the time series of particular analytes of interest (i.e., MeHg, DOC, and SO_4) to provide greater certainty in the export loads calculation. Schedule D sampling included a subset of analyses performed for the purpose of calibrating *in situ* measurements used to discern the high frequency temporal variation in water chemistry in the fields that may be important to the methylation or demethylation processes. Procedures for the collection of samples in Schedules A, B, C, and D are described in the project's Quality Assurance Project Plan (***QAPP Table 4.2***) and Management Plan; a summary of procedures is provided below. Abbreviations for water-quality analytes are given in **Table 5.1**.

5.2.1.1 *Interdisciplinary study (Schedules A and B)*

Schedules A and B were collected as part of the multidisciplinary sampling plan. Sampling was conducted by the USGS Sacramento sampling team. Samples were collected from the inlets, outlets and a central location of each field using 2- or 3-liter acid-cleaned Teflon® bottles attached to an acid-rinsed PVC pole (**US Geological Survey, 2006**). Additional samples were collected from the supply ditches upstream of the inlets to determine if differences existed between concentrations of constituents going onto the fields and the source water in the supply ditches.

Water collected in the Teflon® bottles was poured into two acid cleaned 13-L Teflon®-lined containers until approximately nine liters had been collected in each container. The 13-L containers were placed on ice in a dark cooler with wet ice for immediate transport to the USGS laboratory in Sacramento for processing. In the cases where fields had multiple inlets or outlets, the water samples were composited in the field in proportion to the flow at each location.

Upon arrival at the USGS laboratory, samples were poured into a 20-L acid cleaned, Teflon®-lined, stainless-steel churn splitter to perform sub-sampling for the full suite of analyses for the appropriate sample schedule using clean-hands, dirty-hands techniques (**Olson and Dewild, 1999**). Aliquots were collected for various analyses, in various containers as per ***QAPP Figure 12.1*** and ***QAPP Table 12.1.*** Aliquots for all unfiltered analyses were collected from the churn prior to the collection of any filtered aliquots to ensure there was no biasing of the sample during processing with regard to suspended sediment concentration.

5.2.1.2 *Loads assessment extras (Schedule C)*

Schedule C samples were collected temporally between the Schedule A and B sample collections and during drainage events. The samples were collected primarily by the California Department of Fish and Game sampling team, although the USGS team from Sacramento assisted with several sampling events. Samples were collected at each sampling location using individual sample bottles. The bottles for MeHg and TSS analyses were preserved and shipped directly to the Moss Landing Marine Laboratory (MLML) in Moss Landing, CA. A single 2-L or 3-L sample was collected for the remaining analytes and was delivered to the USGS Sacramento

laboratory for processing similar to that performed in the Schedule A and B samplings. Aliquots for Schedule C analyses were collected as per ***QAPP Figure 12.1*** and ***QAPP Table 12.1***.

5.2.1.3 *Diel study (Schedule D)*

Schedule D samples were collected over three deployment periods. Diel measurements were conducted in Field W65 in July 2007; Field R64 in August 2007 and in Fields R20, W31 and PW5 in July 2008. The instrumentation was deployed for at least 48 hours to capture a sense of the diel variability in each field. Hourly to bihourly samples were collected for instrument calibration and to determine relationships between mercury species and the optical measurements. Isolated bottle and bag measurements were collected for comparison to *in situ* measurements of DOM and optical properties to help isolate possible mechanisms for diel trends.

The *in situ* instrumentation package consisted of a similar organic matter characterization system as described by **Downing et al. (2008)**. In summary, the system included a multi-channel spectrophotometer (AC-9, Wetlabs Inc.), a CDOM fluorometer (Wetlabs Inc.), a ChlA fluorometer (Wetlabs Inc.), a YSI multiprobe (YSI 6-series), and an UV-vis spectrophotometer (ISUS, Satlantic Inc.) The system included both filtered and unfiltered flow paths to capture measurements of the dissolved and particulate components of the water at short-term intervals, generally averaged over 15 minutes. The filtered flow path was pumped through a 0.2µm pore diameter filter with a 40-mesh screen and 10 µm pore diameter pre-filter. The unfiltered path was pumped in parallel to the filtered channel. Difficulties organic buildup within the filtered channel led to censoring of large portion of these data; data presented in this report focus primarily on the unfiltered channel.

Discrete grab samples were collected using modified clean-hands methods, as described in the ***QAPP***. Samples were collected in acid-cleaned glass bottles. *In situ* flowpaths were cleaned and well rinsed to reduce contamination. For Field W65, filtered samples were collected directly from the instrument flowpath whereas unfiltered samples were collected from the weir next to the instrument set-up. For the other fields, both samples were collected from their respective instrument flowpaths with care to pull from the center of the water column. Additional measurements of DOM character and optical properties were collected from Tedlar bags (http://www.keikaventures.com/s_tedlar.php#FAQ) during the 24-hr grab sampling effort on field R64 to isolate photolytic reactions from biological impacts. Six tedlar bags (3 filtered and 3 unfiltered) were filled with surface water from field R64 following sunset (9PM) and six bags were similarly filled at dawn (5AM). Each bag was left in the field near the *in situ* sampling apparatus to mimic photo-environment at the *in situ* measurement location. The tedlar bags were not tested for mercury cleanliness and thus were used only for DOM evaluations. Results from the tedlar bags were compared to *in situ* measurements and laboratory DOM measurements collected in coordination with the photodemethylation bottle experiments (**Section 9**).

5.2.2 Laboratory analyses

Laboratory analyses were completed for surface water samples using methods described in the ***QAPP*** **(U.S. Geological Survey et al., 2008)**. Results of quality assurance and quality control analyses are given in **Appendix 2**.

5.2.3 Meteorological data

Meteorological data were obtained from the California Irrigation Management System (http://wwwcimis.water.ca.gov) site #6, Davis (N38˚32'09", W121˚46'32") which is located approximately seven miles west of the YBWA.

5.2.4 Statistical analyses

Normality of data was checked using SigmaPlot, version 11 (Systat Software, Inc., San Jose, Calif.). Correlation coefficients for relationships among variables were determined using two different methods, a parametric method for normally distributed data and a non-parametric method for data that are not normally or log-normally distributed. The parametric method used was the Pearson Product Moment Correlation, for which the correlation coefficient is denoted as r_P. The non-parametric method used was the Spearman Rank Order, for which the correlation coefficient is denoted as r_S. Linear least-squares regression, for which the correlation coefficient is denoted as r and the coefficient of determination is R^2, was done using SigmaPlot, version 11.

A Mann-Whitney test (a non-parametric test for assessing whether two sets of observations come from the same distribution) was applied to various subgroups of the water quality data to assess whether or not statistically significant differences were found. The Mann-Whitney testing was done using MINITAB, version 14 (Minitab, Inc., State College, PA).

5.2.5 Load calculations

Loads were calculated for each field by interpolating measured concentrations for each flow sampling location to create a daily record and then multiplying by the daily flow at that location.The hydrology and flow determination are described in detail in **Section 4**. Water quality interpolations using data collected at the field inflow and outflow locations were combined with flow interpolation data collected at the inflow and outflow locations. These calculations were totaled over the season to estimate total surface load onto and off of the system. Because a concentration gradient exists within each field, and on most fields, the hydrologic measurements were collected at a different location than water-quality inflow measurements, we corrected the load estimates onto the fields using a linear interpolation of water-quality spatial gradients using the average seasonal concentrations. This correction did not need to be applied to outflow locations as the hydrology and water quality measurements were collected concurrently. Surface storage for each constituent was estimated using the total change in water level for the season multiplied by the average concentration on each field during a season.

Mass fluxes through the soil water interface were estimated using chloride as a tracer. Chloride is neither produced nor consumed by chemical reactions involving water and soil, and can be used as a conservative, natural tracer in aquatic systems (e.g. **Schemel et al., 2006**).

Chloride flux to the root zone (percolation) was taken as the difference between chloride inflow and outflow from each field. The percent of the inflow load passing through the soil-water interface was estimated by the differences between the surface-water load of chloride onto the field minus the sum of surface-water export of chloride and surface-water storage. A ratio was calculated for each field relating calculated chloride flux passing through the soil-water interface and surface-water chloride inflow. That ratio was applied to the other constituents to estimate the amount of each constituent fluxing through the soil-water interface because of hydrologic effects.

5.3 Results and Discussion

5.3.1 Mercury and Methylmercury Concentrations

5.3.1.1 *Seasonal trends*

5.3.1.1.1 Total Mercury

Concentrations of THg were highly variable over time. A large increase in THg concentration occurred shortly after early summer flood-up, followed by a quick decline. A second concentration pulse occurred in winter in the rice fields (**Figures 5.1 and 5.2**). A large proportion (about 50%) of the THg released in the initial pulse was in the dissolved (<0.45μm) fraction (f-THg), whereas the winter pulses tended to be the result of higher particulate concentrations (**Figures 5.1 and 5.2**). The proportion of THg that passed through 0.45μm filters varied from about 5% to about 95% (**Figure 5.3**). This proportion was relatively low in the permanent wetland (5 to 50%), relatively high in the seasonal wetland (30 to 95%), and highly variable (5 to 95%) in the agricultural fields.Over the period of study, u-THg concentrations exceeded the EPA water-quality criterion of 50 ng L^{-1} (California Toxics Rule; U.S. Environmental Protection Agency, 2000b) on 14 occasions, mostly following the initial flooding of the agricultural fields. Although the water-quality criterion in the California Toxics Rule is not typically enforced in agricultural systems, it is often used as an indicator of potential important sources of THg to downstream environments. Concentrations of u-THg and f-THg were consistently higher on agricultural fields (means of 26 and 7.1 ng L^{-1}, respectively) vs. non-agricultural fields (means of 7.8 and 1.9 ng L^{-1}, respectively) (**Table 5.2**). The differences in aqueous THg between agricultural and non-agricultural fields coincide with a general east-west gradient (lower in east, higher in west) noted in THg concentrations in sediment (**Section 6).** The east-west gradient in THg is believed to reflect the source of deposited sediments with high THg sediments from Cache Creek being deposited in the western part of the Bypass and lower THg sediments of the Sacramento River dominating deposition in the eastern portion of the Bypass, according to the east-west gradient of water flows identified by **Sommer et al. (2008**). No statistically significant differences were noted when comparing aqueous THg data from the northern block of fields to the southern block (**Table 5.3**) or between seasons (**Table 5.4**). The similarity between blocks is consistent with the lack of a north-south spatial gradient for THg in sediment at the scale of the study area (**Section 6**). High variability in THg concentrations explains the lack of statistically significant difference between seasons.

5.3.1.1.2 Methylmercury

Whole-water (u-MeHg) and filter-passing (f-MeHg) concentrations generally increased from inlet to center and inlet to outlet, however there was no significant difference between center and outlet for all fields considered together (**Figures 5.4 and 5.5**; **Table 5.5**). All measured u-MeHg concentrations far exceeded 0.06 ng L^{-1}, the TMDL goal (**Wood et al. 2010a,b**). Supply water

for the wetlands exceeded the TMDL goal by at least 4-fold throughout the year; the most elevated concentrations entered the northern water supply from the Davis Drain. Center and outlet locations on white rice and fallow fields had the highest u-MeHg concentrations shortly after flooding and maintained similar concentrations through the water year, whereas concentrations on wild rice fields started relatively low following irrigation flooding and increased throughout the growing season, peaking during wet harvest activities and decreasing during the winter to levels similar to those in mid-summer (**Figure 5.4**). The permanent wetland maintained low u-MeHg and f-MeHg concentrations throughout the year, except when inundated by floodwaters that covered much of the bypass in early February 2008. The dissolved fraction (<0.45 μm) of MeHg (f-MeHg) exhibited a temporal trend opposite to that of f-THg, starting low in early summer and increasing with time flooded. The temporal trend in f-MeHg mirrored the trend in sediment MeHg (**Figures 5.5** and **6.5**). For MeHg, the percent filter-passing varied from about 10 to 90%; most values were in the range of 30 to 60 % (**Figure 5.6**).Concentrations of f-MeHg on white rice fields increased throughout the year and were markedly higher than the other wetlands in winter. During August, surface-water concentrations of f-MeHg were similar among all of the agricultural fields .

The ratio of MeHg to THg (MeHg/THg) is often used as a measure of the methylation efficiency of a wetland (e.g. **Krabbenhoft et al., 1999**). The MeHg/THg ratio in unfiltered water generally ranged from about 1 to 100% (**Figure 5.7**) whereas the ratio in filtered water was mostly between about 10 and 100% (**Figure 5.8**). In both unfiltered water (**Figure 5.9)** and filtered water (**Figure 5.10**), the MeHg/THg ratio increased markedly throughout the summer growing season in all agricultural fields. In contrast, MeHg/THg ratio in the permanent wetland increased with time only in the filtered fraction (**Figure 5.9**). Although the relatively high MeHg/THg ratio in the northern supply water might confound the use of this metric, the consistency of temporal trends in both the northern and southern field blocks suggest that this effectis minor.

5.3.1.1.3 Evapoconcentration effects

Evapoconcentration was quantified using two independent approaches: (1) concentrations of chloride and (2) stable isotopes of oxygen and hydrogen. Because chloride is a conservative ion, it tends to be residually concentrated in surface water in direct proportion to the amount of evaporation. Stable isotopes of hydrogen and oxygen in water show a systematic trend with evaporation that commonly shown on plots of $\delta^{18}O$ vs. δH as a characteristic slope between 3 and 5, in constrast to unevaporated waters which tend to follow the Global Meteroric Water Line with a slope of 8 (**Clark and Fritz, 1997**). A plot of $\delta^{18}O$ vs. δH for water samples collected in this study (**Figure 5.11**) shows a slope of 4.42, which is consistent with evaporation being the dominant mechanism affecting the oxygen and hydrogen isotope ratios. The empirical fraction factor, alpha, is equal to 1.009 for $\delta^{18}O$ during evaporation (**Clark and Fritz, 1997**). On a log-linear plot of chloride concentration versus $\delta^{18}O$, the expected slope for water affected by evapoconcentration, based on Raleigh fractionation (**Clark and Fritz, 1997**) is 20.7 (9 times 2.303). The data from this study plot in a distribution very close to the expected slope (**Figure 5.12**), and a linear least-squares regression indicates a slope of 20.1, which corresponds to an empirical alpha value of 1.0087 (20.1 divided by 2.303).

The degree of evapoconcentration for given “snapshots” in time can be quantified by taking the ratio of chloride concentration of outflow to that of the inflow (Out/In) for each field. A similar ratio can be computed for other constituents to assess whether observed changes in concentration from inflow to outflow might be due entirely or in part to evaporative

concentration. By normalizing the Out/In ratio of MeHg to the Out/In ratio for chloride, the resulting values, if greater than 1.0, indicate the enhancement of MeHg caused by processes other than evaporative concentration. In **Table 5.6**, the Out/In ratio of u-MeHg and u-THg relative to chloride is shown for each season for each field. In general, the non-evaporative enhancement for u-MeHg was much higher for agricultural fields in the southern block than those in the northern block in the summer period. This effect is caused primarily by lower concentrations of u-MeHg in the inflow water for this zone compared with the inflow water to the northern block, which tended to include a higher degree of recirculated agricultural drainage water that was higher in MeHg. In contrast, the greatest non-evaporative enhancement in the winter period occurred in the white rice fields, one of the wild rice field (W32) and the seasonal wetland (SW). The enhancement for THg was largely caused by evaporative concentration, as indicated by values near 1.0. Only field F20 showed non-evaporative enhancement of THg.

5.3.1.2 *Diel Trends*

Diel trends were found to be widely variable between fields and years. During a series of intensive, high-frequency 24-hour sampling events in 2007, a strong diel trend in u-MeHg concentration was observed in a wild rice field (W65) varying from less than 1.0 ng L^{-1} to 2.1 ng L^{-1}. In contrast, no trend was observed in a white rice field (R64) with concentrations remaining around 0.73 ($^{+}$/- 0.08) ng L^{-1} (**Figure 5.13**) throughout a 24-hr period. In 2008, there was a trend in the white rice field R20 varying from 0.53 to 0.95 ng L^{-1}, although the trend was not clearly diel like the trend observed in W65 in 2007. No trend was observed in a wild rice field (W31) monitored in 2008, with concentrations holding constant at 0.51 ($^{+}$/- 0.02). The higher MeHg concentrations observed in field W65 during 2007 were likely caused by the higher THg concentrations in the wild rice field relative to the other fields (11.6 vs 3.2, 3.9 and 4.3 ng L^{-1}) because the percentage of THg as MeHg (MeHg/THg) was similar between fields. No significant diel trends were observed in THg concentrations at either site. The MeHg/THg ratios in unfiltered surface water (**Figure 5.14**) followed similar diel trends as u-MeHg concentrations in all fields, except with a greater skew towards dawn for W65. The primary difference between observed diel trends in MeHg concentration and those in MeHg/THgare the relative magnitudes between the sites.

The diel trends differed markedly between fields. The trend for u-MeHg in field W65 during the 2007 experiment was nearly sinusoidal; rising at night, peaking in the early morning hours (3 AM) and slowly decreasing throughout the daylight hours. In contrast, in field R20 during the 2008 diel experiment, MeHg concentrations remained relatively constant through much of the diel cycle but spiked in the early evening through midnight. During the 2007 experiment, the white rice field (R64) had a consistently high MeHg/THg (20%), whereas the wild rice field (W65) had a similar MeHg/THg at dawn (18%) and lower ratios during daylight hours (8%), suggests that the diel trend was more likely a result of a removal mechanism affecting MeHg during daylight than an increase in MeHg production during nighttime hours. In contrast, during the 2008 experiment, the fields had relatively constant MeHg/THg ratios around 15% with R20 decreasing slightly to 13% near sunset and increasing to 22% near midnight, before returning to 15% in the early AM which suggests a source of MeHg increasing concentrations in field R20.

The differences in the diel trends suggest different mechanisms affecting MeHg in R20 and W65; however, the influence of hydrology cannot be ruled out. The location of each deployment

differed because of differences in field management and condition of the crop. The field with the most pronounced diel trend, W65, was the field with the lowest flow rates during the deployments; in comparison the fields monitored in 2008 were observed to have greater flow rates and denser stands than the fields monitored in 2007. These differences in hydrology and crop density may explain some differences in trends between years do not explain differences observed within years.

5.3.2 Biogeochemical relationships

The complexities of Hg cycling can be explained in part by relationships of various forms of mercury with various forms of sulfur, iron, manganese, and DOM, all of which are redox-active constituents. With regard to DOM, both quantity (concentration) and quality (composition) may be important to THg and MeHg cycling (e.g. **Barkay et al., 1997; Haitzer et al., 2003; Ravichandran, 2004**).

5.3.2.1 Sulfur

Sulfate-reducing bacteria (SRB) are thought to play a major role in methylation of mercury in many environments (**Compeau and Bartha, 1984**; **Benoit et al., 2003**). Because sulfate (SO_4) was added to the white rice and wild rice fields as part of fertilizer applications, possible effects on Hg cycling were investigated. Because evapoconcentration affected all solutes, chloride (Cl) concentrations were used as a natural tracer to understand the degree of this effect. The ratio SO_4/Cl was higher on the white rice and wild rice fields relative to the fallow fields which did not receive fertilizer (**Figure 5.15**). The temporal trend on all irrigated fields during the summer months was toward lower values of SO_4/Cl. One explanation for the observed decrease in SO_4/Cl during the period June through September 2007 is the reduction of SO_4 by SRB. During late February, 2008, a series of water samples taken from white rice fields showed marked decrease in SO_4/Cl (**Figure 5.15**).

In some situations, stable isotopes of sulfur can provide a tracer both for sulfate-reduction processes as well as for sources of sulfur in hydrogeochemical systems (e.g. **Seal et al., 2000**). During periods of active sulfate reduction, the ratio $^{34}S/^{32}S$ (expressed as $\delta^{34}S$ relative to the reference standard Vienna Cañon Diablo Troilite or VCDT) becomes enriched in residual sulfate because SRB preferentially reduce ^{32}S relative to ^{34}S. The end-member fertilizer products used on the white rice and wild rice fields had $\delta^{34}S$ values ranging from 1.2 to 8.3 permil VCDT (**Appendix 3, Table A3-8**). The fertilizers were applied in mixtures such that the material applied to each field had $\delta^{34}S$ values ranging from 2.5 to 4.0 permil VCDT (**Figure 5.16**). Values of $\delta^{34}S$ in sulfate of input water ranged from about -2 to +2 permil. Aqueous sulfate from numerous water samples from field centers and outlets had $\delta^{34}S$ values greater than 4.0 permil (**Figure 5.16**), indicating that sulfate reduction was active. A significant correlation ($p < 0.001$) was found between log(SO_4/Cl) and $\delta_{34}S$ for all water samples (**Figure 5.16**), with a Spearman rank order correlation coefficient (r_S) of -0.74. This correlation was considerably stronger on two individual fields, W32 and F66, where r_S values were -0.87 and -0.96, respectively (**Figure 5.17**). These data provide additional evidence that SRB were actively removing sulfate from the water column. Furthermore, it is unlikely that interactions between sulfate and plants are responsible for the variations in aqueous $\delta^{34}S$, because isotope fractionation during plant uptake of sulfate is minimal (**Trust and Fry, 1992**).

Because SRB have been frequently mentioned in the literature as the main cause of Hg methylation, the relations between SO_4/Cl, $\delta^{34}S$ and u-MeHg concentration are of interest. Plots of log(SO_4/Cl) vs. log(u-MeHg) (**Figure 5.18**) and $\delta_{34}S$ vs. log(u-MeHg) (**Figure 5.19**) show poor correlations (R^2 = 0.13 and 0.20, respectively). Working with data for individual fields for plots similar to those in **Figure 5.18** and **5.19**, R^2 values were universally less than 0.5. These analyses suggest that SRB activity explains less than half of the variability in u-MeHg. It is important to consider that the fields are not closed systems, in that mass transfer between geochemical reservoirs (i.e. sediments, pore water, surface water, biofilms, etc.) is likely occurring to some extent. This is true both for sulfur species and MeHg, for which production and consumption are co-occurring and are not distinctly tied to one particular reservoir. Therefore one would not expect a perfect correlation in plots such as **Figures 5.18** and **5.19** even if SRB were the dominant process in u-MeHg production.These results are consistent with the conclusions from the sediment and pore water analyses (**Section 6**), which suggest that microbial reduction of iron (and perhaps also manganese) may be important in the study area.

5.3.2.2 Iron (Fe) and Manganese (Mn)

Because iron-reducing bacteria (and possibly manganese-reducing bacteria) also have been identified as contributors to mercury methylation **(Fleming et al., 2006; Kerin et al., 2006**), the relations between filtered iron (f-Fe), filtered manganese (f-Mn), and f-MeHg are also of interest. In the circum-neutral pH range for the surface waters in this study, f-Fe is likely to occur primarily as Fe(II) and f-Mn as Mn(II) because the more oxidized forms of Fe and Mn are relatively insoluble. Fe(II) and Mn(II) represent the end products of iron-reduction and manganese-reduction reactions, respectively. Measuring their concentration in surface water represents an indication of the extent to which Fe reduction and Mn reduction are taking place. Time series plots of f-Fe and f-Mn concentration **(Figure 5.20)** indicate that both of these metals were higher in concentration during the *early winter* and *late winter* sampling periods compared with the *summer irrigation season*. This suggests a flux of reduced species from the soils during winter flooding. The plots of f-Fe vs. u-MeHg **(Figure 5.21A)** shows a relatively weak positive correlation (R^2 = 0.20, Spearman rank order correlation = 0.492), whereas the plot of f-Mn vs. u-MeHg **(Figure 5.21B)** shows a relatively stronger correlation (R^2 = 0.52, Spearman rank order correlation = 0.718). Analysis of correlation between f-Mn vs. u-MeHg for specific field types indicates a stronger correlation for wild rice (**Figure 5.22A**, R^2= 0.58) and fallow fields (**Figure 5.22B**, R^2 = 0.68). Because log(f-Mn) and log (f-MeHg) are normally distributed for these individual field types, but log(f-Mn) is not normally distributed for the full data set, the non-parametric Spearman rank order correlation is more appropriate. These results indicates that f-Mn potentially explains more than half of the variation in f-MeHg in selected wetland types, and suggests the hypothesis that Mn-reducing bacteria may play a role in Hg methylation, perhaps to a greater extent than Fe-reducing bacteria. **Gill (2008b)** showed significant correlations between MeHg and dissolved Fe and Mn in pore water from two tidal marshes in the Delta, Little Break and Mandeville Cut. Additional work on distribution of Mn species in pore water and sediment, as well as microbial assays to demonstrate the presence of Mn-reducing bacteria, would be needed to demonstrate this hypothesis.

5.3.2.3 Organic Matter (OM)

Relationships between organic matter and mercury were highly variable in both space and time. For the ease of comparison, the analysis of the relationship is separated into two temporal scales: seasonal and diel.

5.3.2.3.1 Seasonal scale

Aqueous THg concentrations were closely related to DOC concentrations but the relationships varied across three distinct periods of field conditions (**Figure 5.23**). The relationship between f-THg and DOC during the first 30 days following the initial irrigation of the rice fields was poor. This poor relationship was likely a result of THg partitioning to suspended particles or algal uptake as u-THg was strongly related with DOC during this period (**Figure 5.24**). The linear least-squares regression between f-THg vs. DOC was strong throughout the growing season and into the winter during normal flow-through conditions prior to the regional flooding of the YBWA by Cache Creek (**Figure 5.23**; $R^2 = 0.66$). Finally, a strong relationship between f-THg and DOC was also observed following the flood of the Bypass, but THg was elevated relative to DOC during this period resulting in a different regression slope (**Figure 5.23**).

The relationship between DOC and f-MeHg was poor because both MeHg and DOC concentrations were highly variable within and between fields in the YBWA (**Figure 5.25**). However, a strong relationship was observed between DOC and f-MeHg in the seasonal and permanent wetlands although the relationship was markedly different after the regional flooding of Cache Creek (**Figure 5.26**). The relationship between DOC and f-MeHg in the permanent wetland was strikingly similar to that observed in a Delta tidal wetland, with both wetlands having nearly identical linear least-squares regression slopes (**Figure 5.27**). This may indicate a similar fundamental driving process in the permanent wetland as the tidal wetland with the difference in intercept being the result of differences in background conditions in each system.

DOM character appeared to be less important than concentration in relation to Hg cycling over the seasonal time-scale of this study. No strong relationships were observed between measurements of DOM character and either THg or MeHg across sites or seasons. One explanation for this result is that DOM and Hg are both subjected to extreme cycling in these low-flow, shallow water systems that disconnects them from the dominant processes that control them in other habitats where the biogeochemical controls on the production of MeHg and DOM are more tightly linked. The character of the DOM in this study appeared to be a result of extensive production and processing within the water column (via algal processing and photochemical reactions) more than the result of different sources (sediment vs. algal). It is likely to be similar for Hg and MeHg speciation.

In contrast to DOM character, particulate organic matter (POM) character appeared to have an impact on Hg cycling. MeHg in suspended particulates was very high with all concentrations exceeding 7 ng g^{-1}, which is an order of magnitude greater than typical environmental levels (e.g. **Rudd 1995**). Relationships between aqueous concentrations of MeHg in the particulate fraction (measured by difference between unfiltered and filtered subsamples) and particle concentration and character were mixed. TSS and POM concentration did not appear to be related to particulate MeHg (data not shown); however, MeHg was related to algae-derived particles (**Figure 5.28**).

The relationship was dependent on field type with white rice and fallow fields having the highest MeHg-to-algae ratio followed by wild rice and the permanent wetland with the lowest (**Figure 5.28**). This trend in MeHg-to-algae ratio corresponds well with biota Hg concentration trends across fields reported in **Section 8** of this report, potentially linking water column processes with Hg contamination in consumer organisms.

The importance of solid-phase OM to Hg cycling was further expressed in the winter period. Within the winter period, the amount of plant residue, or detritus, remaining on the fields in December and February was closely related to the ratio of MeHg (outlet/inlet) across field types and blocks (**Figure 5.20**; also see **Section 7:** plant interactions). The greater degree of scatter in February is likely due to uncertainty in the inlet water concentrations following the regional flooding of Cache Creek and any impacts the flooding had on resetting the relationship between the soils, detritus and water columns. This suggests that MeHg production in the winter season is largely driven by the amount of readily available organic matter for stimulating the microbial activity that produces MeHg (see **Sections 6 and 7**).

5.3.2.3.2 Diel scale

The relationships between DOM and MeHg differed markedly between seasonal and diel time-scales. Diel trends in MeHg were observed to differ greatly between fields but were much more tightly coupled to DOM character than over the seasonal timescale. MeHg concentrations were most closely related to ChlA fluorescence (**Figure 5.30**) and the fluorescence index of the DOM (FI) across all sites (**Figure 5.31**). The relationship between MeHg and ChlA is dominated by W65 which had the greatest magnitude and range in ChlA fluorescence (**Figure 5.30**). In contrast, the FI varied over the diel cycle in three of the four sites. In 2007, MeHg concentrations were positively correlated with FI, indicating higher MeHg concentrations corresponded with more algal or microbial DOM, whereas in R20 in 2008, MeHg concentrations were negatively correlated with FI, which suggests MeHg increases were more related to terrestrial DOM (**McKnight et al., 2001**). These results indicate the potential for different MeHg sources for diel trends with algal cycling likely driving MeHg diel trends in W65 and soil exchange with the water column likely driving the trend in R20.

Alternatively, photodemethylation may play a pivotal role in the MeHg diel trends in the fields (see **Section 9**: photodemethylation). Coincident decreases in MeHg and FDOM were observed in both the bottle experiments and *in situ* measurements. FDOM, an indicator of DOM photobleaching (**Frimmel 1998 a,b**; **Del Vecchio and Blough, 2002**), decreased with increasing radiation for all fields in the bottle experiments, and all fields except field W31 and part of the deployment in field R64 (when grab samples were collected) for the *in situ* measurements (**Figure 5.32**). Although there was not a direct relationship between MeHg concentration and FDOM, the MeHg/THg ratio was related to the carbon normalized fluorescence (FDOM/DOC) across the three fields where FDOM changed with photoexposure (**Figure 5.33**).

The absence of measurable MeHg diel trends in fields R64 and W31 is difficult to explain given the available data. All fields had similarly extreme weather conditions and relatively constant inorganic water chemistry. Optical measurements collected *in situ* revealed that field R64 optical measurements changed over the diel cycle, just not during the period of MeHg sampling (**Figure 5.32**). Furthermore, the Tedlar bags deployed at R64 showed changes in DOM

over the period of photo-exposure (especially *Sr*, HI). Perhaps shading was not equal across all sites as spot measurements of leaf area indices (LAI) suggested (see **Section 7**). Qualitative field observations suggest that W65 probably had the highest photoexposure due to poor canopy development in large areas of the field not included in the LAI assessment. Qualitative observations would support W31 having the greatest shading; however, measurements of PAR penetration through the canopies and water columns conducted in 2008 showed little difference between fields R20 and W31 (22% ± 9% vs 29% ± 21%, respectively). Perhaps differences in hydrology impacted the potential diel trends as higher flow rates in a field could limit the impact of photobleaching by reducing residence time and the cumulative photoexposure of DOM. The field with the strongest diel cycle, W65, had the lowest flow rate during the deployments. Also, some optical measurements of DOM character suggested W65 had more overall photoexposure ($Sr_{\text{uv-vis}}$, HI); however, these optical measurements are not merely measures of photoexposure but also of DOM source which complicates interpretation without supporting ancillary measurements.

Results from the bottle experiment suggest that DOM from fields R20 and W65 monitored in 2008 (which had similar properties as W64, monitored ing 2007) were more susceptible to photoexposure than field W31 (2008), suggesting that DOM character may play a role in overall diel cycling as well. Further research is necessary to address these potential mechanisms driving diel trends. Another explanation for the differences in the trends observed in 2007 and 2008 was that the measurements in 2007 were made in the southern fields which received relatively clean irrigation water from the Toe Drain whereas the fields measured in 2008 were in the north unit which received a higher proportion of recycled agricultural drain water that had higher MeHg concentrations in the irrigation water and may have suppressed the diffusional exchange between soil and water column, thus minimizing MeHg exchange mechanisms responsible for diel trends.

The strength of observed relationships suggests that algal activity was the greatest driving force for diel trends in MeHg in field W65; however, there are some perplexing aspects to this hypothesis. First, the maximum chlorophyll measurements would not normally be expected during the night. Potential explanations include: 1) the algae migrated from the benthos to the water column during the night and back to the sediments during the day to escape extreme environmental conditions such as low dissolved oxygen in the sediments at night or high temperatures and extreme solar radiation in the water column or 2) bioturbation caused by migrating invertebrates and feeding by zooplankton may have elevated chlorophyll in the water column at night. Perhaps the most important difference between fields that may have impacted algal activity was the application of herbicides. W65 was the most pristine of the fields studied, having not received herbicide in several years whereas the white rice fields receive several applications during the growing season and W31 had received herbicide applications the previous year when the field was used for white rice production. The application of herbicides would negatively impact the benthic algal community which may impact both the DOM and the algal activity. Reduced benthic ChlA was observed in the white rice fields when compared to W65 in 2007 (see **Section 7**).

The importance of understanding diel variations in these systems cannot be overstated. The disconnect between diel-scale and seasonal-scale relationships may indicate a decoupling of the mechanisms over time because of different rates of production and degradation, which merely

exposes the limitation that seasonal-scale sampling is insufficient for understanding Hg cycling. Furthermore, diel variations in MeHg concentration provide a potential large source of error in loads assessments depending on the time of sampling for each field. In fields where diel variations occur, early morning sampling would bias MeHg loads high whereas late afternoon sampling would bias loads low - assuming diel variations are caused by processes occurring within the fields such as photodemethylation and biological (algal) forcings which may not be equal for all fields. A need to better understand the processes that control diel cycling of MeHg in different systems and managements is essential to identifying optimal representative sampling strategies and may also provide insights to mitigations strategies for MeHg by identifying source and loss mechanisms that may be manipulated for MeHg control. The evidence for possible biological impacts on the diel trends of MeHg also provides potentially vital information for the entry of MeHg into the food web. If there is active movement of algae into the sediment, which is the primary source of MeHg, that would likely increase MeHg movement into the pelagic food web as rates of MeHg movement would likely increase compared to diffusive movement from the soil to water column. Also the diel pattern of possible algal movement and MeHg concentrations could affect biota differently through different temporal or event-based feeding patterns (e.g. **Krumme et al., 2008**).

5.3.3 Loads

5.3.3.1 *General trends*

Loading rates of MeHg in the YBWA fields differed greatly over both space and time. There was a wide range in area-normalized average daily export rates ranging from -195 μg m^{-2} d^{-1} in field F20 during the summer irrigation period to +310 μg m^{-2} d^{-1} in field R64 in winter (**Figure 5.34**). The most prominent difference was between the summer and winter seasons. Differences were observed between field blocks, type and management within seasons. For this reason, data analyses were performed within each season to explore the dominant controlling processes leading to the differences in MeHg loadings in the differently managed fields of the YBWA.

5.3.3.2 *Summer irrigation*

Within the summer irrigation season, there was a significant difference ($p<0.01$) in MeHg loadings between field units (north versus south) as the northern fields acted as MeHg sinks whereas the southern fields acted as sources of MeHg (**Figure 5.34**). The driver for this pattern is likely the irrigation source water because the northern fields' irrigation source water was higher in MeHg concentration than the southern irrigation source water leading to a greater enhancement of MeHg in the southern fields (**Table 5.6**). The two fields with net MeHg surface water losses, F20 and R31, received a large portion of their irrigation water from the Davis Drain, which had high MeHg concentrations during the mid- to late-summer irrigation period. The other fields received irrigation water dominated by Toe Drain water which had consistently lower MeHg concentrations throughout the summer period compared to the Davis Drain (see **Section 4**: hydrology). The load losses from transpiration were calculated according to the fields' mean concentrations and the percolation rates of water into the soil from plant water demand according to the water balance of the conservative tracers (see **Section 4**: hydrology). The ultimate fate of the MeHg percolated into the soil via transpiration demand is unknown but may build up in the soil strata, be taken up into plant components or possibly converted to Hg(0) and released to the atmosphere. Evidence exists for soil build-up (see **Section 6**: sediment) and plant uptake (see **Section 7**: plant interactions) supporting the total imbalance for the period which

points towards net MeHg production of about 1 to 1.5 μg m^{-2} d^{-1} produced in the fields, except F20 and PW which remained net sinks for the period (**Table 5.7**). Actual benthic flux from sediment to the water column, however, was not measured, so this estimate represents a potential flux.

We propose three mechanisms responsible for the trends observed during summer. First, the source of MeHg to the water column is assumed to be at least partially dependent on diffusion from the soils and into the water column. In the northern fields, the relatively high concentration of MeHg present in the irrigation supply water reduced the diffusional gradient of MeHg from the soils into the water column compared to the low MeHg concentration irrigation supply in the southern fields. Therefore, the MeHg flux from soil to water column would be greater in the southern fields than in the northern fields. In fact, the concentrations in the Davis Canal water were high enough in mid-summer to potentially promote diffusion from the water column into the soil. This mechanism also explains the relatively low MeHg concentrations in the permanent wetland (PW). Because the PW remains flooded throughout the year, diffusion gradients are minimized by the absence of the wet-dry cycle of flooding and draining and by the presence of a larger ratio of water volume to sediment area than the agricultural fields. The second mechanism we propose is a MeHg loss term: photodemethylation. In the fields with higher irrigation MeHg concentrations, more photodemethylation would be acting on the irrigation waters as the same MeHg coming into the field would be exposed to solar radiation throughout its residence time in the field whereas the fields where MeHg is diffused from soil to water column, there would be a lower solar radiation exposure rate.

The loss of MeHg by photodemethylation is further supported by the differences in loss rates within the blocks. The greatest loss rates in the northern block occur on the fields with the greatest residence times and thus greatest exposure to solar radiation (F20>R31>W32). The third mechanism that would contribute to summer losses of MeHg across the fields is particle settling. The higher concentrations of inlet waters would lead to greater particle loss across the fields.

Differences between fields were multifaceted. The management on F20 turned out to be optimal for MeHg removal with high inlet concentrations and minimal outlet flow following a long residence time on the field. The wild rice field monitored in 2008 (W32) had the lowest loss rate because the majority of the MeHg export from W32 occurred during the harvest operations. Wild rice requires a wet harvest to optimize harvest yield but this disturbs the soils such that u-MeHg concentrations increased markedly. During the 2007 harvest, outlets were allowed to flow during the operations thus greatly increasing outlet loads during and following this activity. Within the southern unit, the agricultural fields were all net sources of MeHg (F66>R64>W65). The MeHg loss observed in F20 was not reflected in F66, which showed the highest MeHg export rate in the southern unit. However, F66 acted as a MeHg sink for most of the summer period except for a large export due to the final drainage at the end of the summer period (**Figure 5.35**). The high export from F66 may be attributed to high bird use in the field, particularly a large pelican colony. If the management of W65 and R64 are taken into account, F66 loads were even higher relative to the other agricultural fields. W65 was wet harvested in 2007, thus increasing the outlet loads markedly during those operations compared to pre-harvest when there was a net MeHg loss in the field. The white rice field, R64, was drained in mid July 2007 for herbicide application, thus also increasing the outlet loads relative to F66.

5.3.3.3 *Winter*

The trends in the winter season were very different from those in the summer irrigation period (**Figure 5.34**), due in part to different hydrologic patterns, as summarized in **Section 4.3.2**. The absence of percolation due to transpiration demands and photodemethylation lead to a strong connection between MeHg concentration ratios and loads. The white rice fields were clearly the greatest exporters of MeHg in the winter, mirroring the MeHg production fueled by plant residues during this period (**Figure 5.34**; also **Section 7**). With the assumption of no MeHg loss from the water column due to transpiration-driven percolation, the total imbalance suggests higher MeHg production in the white rice fields and relatively low MeHg production in the wild rice fields (**Table 5.8**). The seasonal wetland (SW) shows a similar net MeHg production (1 μg m^{-2}) as in the white rice fields and all the agricultural fields in the summer period. The relatively low export from field W32 was due to the backing up of Green's Lake, which limited exports from this field and increased imports onto the field and was not a result of typical management conditions.

Unfortunately, the study design was focused on the irrigation period and water sampling was sparse during the winter period making interpretation difficult and limiting our ability to evaluate the dominant processes occurring during that period. Nonetheless, it appeared that the white rice fields produced the greatest amount of MeHg due to drying of fields for harvest operations, ample plant residue at flood-up and low photodemethylation and transpiration post-flooding for winter irrigation – all of which promote enhanced methylation (see **Sections 6, 7, and 9**). The seasonal wetland (SW) also showed high MeHg production in winter with ample plant residue, extended drying period, and relatively low transpiration, but water management was limited to maintaining the water level of the wetland and, similar to F20, the flooding began early in the season while the rice fields were still in the summer irrigation period such that the removal mechanisms dominating the summer loads in the rice fields discussed earlier might have an impact on the export from the seasonal wetland that would not have been observed in the white rice fields in the winter period. We note that our initial study design was to have "replicate" field types, but given water source differences and hydrologic management variation between fields, the pairs of agricultural fields with similar land use did not serve as replicates.

5.3.3.4 *Comparison between seasons*

The stark differences in MeHg loadings between seasons in the agricultural fields were likely the result of the different mechanisms responsible for both production and loss within each season. Summer exports from the water column were split between surface outlets, percolation into the soil from transpiration demands, and photodemethylation. In contrast, both photodemethylation and transpiration losses from the water column were small in the winter. Transpiration was nearly zero in winter because most vegetation was either senesced or had been cut during the rice harvest, with little growth of new vegetation following harvest. Photodemethylation was much lower in winter because the solar intensity and duration was reduced to a fraction of that occurring in the summer. The lack of these two loss mechanisms in winter would permit greater diffusion of MeHg from the soils into the water column, thus increasing surface water MeHg concentration available for surface transport off the fields. The MeHg production rates also increased in winter despite lower temperatures because of the large reservoir of organic matter left on the fields in the form of plant residue (see **Sections 6 and 7**: sediment and plant interactions).

The annual average exports measured in this study fall into a similar range as other wetland and agricultural systems (**Table 5.9**). MeHg losses in rice systems have been observed elsewhere in recent Delta studies (**Fleck, unpublished data; Heim, unpublished data**).

Comparing the loads measured in this study to the ***Delta Methylmercury Mass Balance*** (**Foe et al. 2008**), the contribution from the entire 6,500 hectares of the YBWA would range from -1.3 g d^{-1} to +0.2 g d^{-1} in the summer depending on the distribution of management types and operations. In winter, the range would be from -0.06 g d^{-1} for permanent wetlands to +2 g d^{-1} for the white rice fields. The contribution from the entire 24,000 hectares of the greater Yolo Bypass would be -5 g d^{-1} to +0.8 g d^{-1} in summer and -0.2 g d^{-1} to 7 g d^{-1} in winter. It is not feasible to manage the entire YBWA or the entire Yolo Bypass as permanent wetlands so the loss of MeHg in winter is an unrealistic scenario. Furthermore, the winter numbers do not include any regionally flooded conditions when the greatest loadings are likely to occur in the Bypass. The higher end of the estimated loadings calculated in this study concur with previous speculation that the Yolo Bypass contributes a large proportion of the tributary MeHg loads to the Delta in winter (16.6 g d^{-1} total tributary load estimated by Foe et al. 2008). The range of winter loads is comparable to other sources in the Delta including total benthic flux and wastewater exports (0.6 g d^{-1}, each) whereas summer loads are more comparable to the smaller sources to the Delta such as urban runoff and precipitation inputs (< 0.1 g d^{-1}). The annual average loads for the entire YBWA (-0.1 to 0.5 g d^{-1}) are similar in magnitude to the estimated agricultural return loads in the Delta Mass Balance (0.3 g d^{-1}).

Opportunities for improved management of MeHg loads from the Yolo Bypass are difficult to pinpoint because of the large variability in loads over both space and time observed in this study. Perhaps most important to note is that the annual loads from the Yolo Bypass are dominated by winter loads when agricultural operations are largely suspended. However, the impact of agriculture on the winter loads cannot be entirely ruled out. The highest winter loads were measured in the fields that had been used to grow white rice and where plant residues were left on the field and may have stimulated MeHg production. In contrast, wild rice fields had relatively low loading rates in winter, possibly due to the decomposition of plant residues during the period of no outflow. The holding of water on the field post-harvest reduced the export of MeHg from the fields but did not reduce *in situ* MeHg concentrations which may still lead to an ecological impact on birds and other animals that feed off the biota within the wild rice fields. Management of the fallow fields suggest a possible mitigation strategy for MeHg exports but the feasibility of this management option for widespread use in the Bypass is questionable. Another option for export management is the use of holding ponds or permanent ponds at the outlets of agricultural and seasonal wetlands. The ponds would remove suspended sediments through settling and promote photodemethylation in the drainage water prior to its release to downstream environments.

5.4 Summary and Conclusions

5.4.1 Summary

THg concentrations were high, exceeding 50 ng L^{-1} on 14 separate occasions, mostly following initial irrigation of rice fields and following the Cache Creek flood in February. On average 30% (stdev=20%) of the THg was in the filter-passing phase. This is of interest

because THg in the dissolved and colloidal phases have a greater potential for further cycling and transport than Hg bound to suspended sediments (e.g. Benoit et al. 2003). Concentrations of THg were positively correlated to DOC, iron, and manganese concentrations.

The multiple abiotic and biotic interactions affecting water MeHg concentrations and export are diagrammed in **Figure 5.36**. As shown in the synthesis table (**Table 5.10**), despite a marked increase in MeHg concentrations from inlets to outlets within individual fields in the YBWA wetlands, net exports of aqueous MeHg were minimal because outlet flows were small relative to inlets (approx 10%) because of evaporative losses and percolation into the soil to meet plant transpiration demands (see **Section 4**). MeHg was produced in the fields but concentrations in water were likely reduced *in situ* through a combination of loss mechanisms including photo-demethylation (see **Section 9**), percolation of surface waters into the soil (see **Section 4**), algal uptake, sedimentation, and uptake into plants (see **Section 7**) and bioaccumulation in the foodweb (see **Section 8**). The concentration of MeHg in irrigation source water appeared to control summer loads via two possible mechanisms:

1) source water MeHg concentrations affected the diffusion gradients from the soils to the water column, with high concentration source water depressing the diffusion of constituents upward, and

2) MeHg losses to photodemethylation, where the rate of photodemethylation is concentration-dependent with high concentrations having higher loss rates, especially in the case of source water where the exposure to solar radiation is maximized as the water crosses the field (see **Section 9**). Observed seasonal and diel trends illustrate the complex and highly variable nature of both Hg cycling and Hg-organic matter (Hg-OM) interactions in natural systems. Dissolved organic matter (DOM) and particulate organic matter (POM) appear to play significant roles in Hg cycling in ways that may impact both estimates of exports and uptake of MeHg into the foodweb.

5.4.2 Conclusions

MeHg cycling in the water column of the YBWA wetlands is variable and complex. Comparison with MeHg flux data from other wetland systems (**Table 5.9**), a wide range of imports and exports is shown within the YBWA complex. In this study the most important variable controlling net MeHg export from all the wetland types during the agricultural production period (summer) was the MeHg concentration of the irrigation source water. It appears that irrigation water already high in MeHg reduces the primary source of MeHg to the water column: diffusion of MeHg from the soil and promotes the losses: settling, advection into the soil via transpiration demand and photodemethylation. Summer net exports of MeHg could be minimized by utilizing irrigation water already high in MeHg if the option is available. However, the ultimate fate of MeHg in these fields is still in question. The impact of this approach only addresses net export concerns and does not consider impacts of MeHg in the rice grain (see **Section 7**) or resident biota on birds using the wetlands for foraging (see **Section 8**). Also, winter MeHg loads exceeded those of summer even though the period of regional flooding, when greatest loads would be expected, was left out of the calculations because it could not be reasonably estimated. The fields in winter were more consistent exporters across all field types and blocks. The magnitude of MeHg export appeared to be most dependent on the amount of plant residue present upon flooding, though a more extensive study of this mechanism is necessary to confirm this finding. Natural

seasonal flooding is difficult to manage but efforts to reduce outlet flow, increase particulate deposition and maximize exposure of the aqueous MeHg to sunlight, and finally to remove plant materials that may enhance MeHg formation priot to winter flooding could be utilized to minimize MeHg loads during winter.

6 Detailed Results for Sediment Methylmercury Production

The data reported in this section relates to summary **Section 3.3: Methylmercury Production in Surface Sediment.**

6.1 Introduction

Microbial processes are at the root of the Hg 'problem'. If certain microbes did not readily convert inorganic mercury (Hg(II)) to toxic and readily bioaccumulated MeHg, the Hg problem in the San Francisco Bay – Delta region and elsewhere would be largely a non-issue. The fact is that select bacteria that are common in freshwater and saline environments do indeed readily carry out the Hg(II)-methylation process. Thus, understanding the key environmental factors that stimulate their activity, as well as make Hg(II) readily available to them, is at the heart of managing the Hg problem in aquatic systems everywhere.

Some general things are well established in terms of what controls the activity of Hg(II)-methylating bacteria and what controls the availability of Hg(II) to those bacteria, with reviews on the subject of microbial Hg(II)-methylation previously published (**Ullrich et al., 2001; Barkay and Wagner-Döbler, 2005; Merritt and Amirbahman, 2009**). First, only a comparatively small subset of all microbes can convert Hg(II) to MeHg, and most of these are sub-sets from two general classes bacteria, sulfate reducers and iron reducers, both of which are anaerobic (i.e. do not persist in the presence of oxygen) and heterotrophic (i.e. require small organic substrates for energy and growth). The role of sulfate reducing bacteria in the Hg(II)-methylation process has been recognized since the mid-1980's (**Compeau and Bartha, 1985**), while the role of iron reducing bacteria in this process has only recently been established (**Fleming et al., 2006; Kerin et al., 2006**). A defining feature of all sulfate reducing bacteria is that they transfer electrons from the breakdown of organic substrates (the electron donor) to sulfate (the electron acceptor) and generate sulfide as an end-product (**Skyring, 1987**). Likewise, a defining feature of all iron reducing bacteria is that they transfer electrons from the breakdown of organic substrates to ferric iron (Fe(III), the oxidized form of Fe) and generate ferrous iron (Fe(II), the reduced form of Fe) (**Thamdrup, 2000**). Thus, in addition to universal effect of temperature on microbial rates, the availability of organic substrates and the above noted electron acceptors are key factors that mediate the activity of these bacteria, and thus MeHg formation in the environment.

A second important factor in understanding and managing the Hg problem is that only a comparatively small percentage of total Hg(II) in the environment is readily available for bacteria to methylate. However, measuring this fraction of bioavailable Hg(II), or even defining its exact chemical composition, remains both a challenge and an area of active research on the part of many mercury scientists. Since Hg(II) and reduced forms of sulfur (S) form very strong bonds, it is not surprising that Hg(II) availability for methylation has been shown to be affected by the relative availability of reduced sulfur compounds (**Benoit et al., 1999**) (REFS). In addition factors such as DOC concentration (**Benoit et al., 2001; Drexel et al., 2002; Waples et al., 2005**) (ref) and particle grain size (**Marvin-DiPasquale et al., 2009b**) have all been shown to play a role in mediating the relative 'availability' of Hg(II).

In recent years a number of mercury studies have been conducted that focus on reconciling the relative contributions of the activity of the resident Hg(II)-methylating microbial community

and the availability of Hg(II) to those microbes, both within the San Francisco Bay ecosystem (**Grenier et al., 2010; Marvin-DiPasquale and Agee, 2003; Marvin-DiPasquale et al., 2003a, 2007, 2009a; Yee et al., 2008**) and elsewhere (**Marvin-DiPasquale et al., 2009b**). Habatat type clearly plays a major role in determining if a particular location is a 'hot spot' for MeHg production or not, and wetland environments appear to be particularly efficient areas for Hg(II)-methylation **(Lacerda and Fitzgerald, 2001; Marvin-DiPasquale, et al., 2003a; Zillioux et al., 1993)**. A national study of 20 U.S. watersheds concluded that wetland density was the leading determinant of MeHg productions within a study basin **(Krabbenhoft et al., 1999**), and that MeHg concentrations in water were correlated with Hg accumulation in fish (**Brumbaugh et al., 2001**). There are many reasons why wetlands may be effective zones for MeHg production, including that a) they are typically organic rich, thus suppling plenty of organic 'fuel' for microbial processes, b) the generally have anoxic sediment, which is important for both iron and sulfate reducing bacteria, c) there are generally emergent plants, the root zones of which have been shown to be important zones of MeHg production (**Windham et al., 2009**), and d) they often go through wetting and drying cycles that is thought to 'reset' the pool of available Hg(II) (**Gilmour et al. 2004; Marvin-DiPasquale et al., 2009a**).

A primary focus of the current project is to better understand what controls MeHg production in the various agricultural and non-agricultural wetland habitats that dominate the Yolo Bypass, and specifically in terms of what environmental factors regulate both the activity of the resident Hg(II)-methylating microbial community and the availability of Hg(II) to that community. This work is a follow-up to a recent study conducted within the YBWA and Cache Creek (including the settling basin), which focused exclusively on non-agricultural wetlands (**Marvin-DiPasquale et al., 2009a**).

6.2 Approach

6.2.1 Field and Laboratory Analyses

Three agricultural settings (white rice, wild rice and fallow fields) and two hydrologically distinct non-agricultural settings (seasonally flooded and permanently flooded wetlands) were studied as part of the sediment biogeochemistry portion of the larger YBWA Mercury Project. Prior to the initial sampling, fixed sites were selected for sediment collection and mapped with GPS. All were located near the field centers, as opposed to near hydrologic inputs and outputs, (**Figures 3.3 and 3.4**). During the first sampling event (June '07) two separate sites, approximately 100 meters apart, were sampled to examine within-field variability. Afterwards only one site was sampled per field, with the exception of permanent wetland PW5, which contained three sub-habitats (non-vegetated open-water (PW5-ow), cattail dominate (PW5-cat) and tule dominated (PW5-tule)), all of which were within 20 meters of each other. To increase the number of non-agricultural sites, and for comparison to PW5-ow, an extra open water permanent wetland site (PW2) was added later in the study (December '07).

There were six sediment sampling events (**Figure 3.6**), which included: June '07 (soon after initial fertilization and rice seed planting; white and wild rice fields and PW5), July '07 (all agricultural fields and PW5), August '07 (all agricultural fields and PW5), October '07 (seasonal wetland SW only; two weeks following initial flooding), December '07 (all sites including PW2), February '08 (all sites). This sampling schedule reflected the fact that only flooded fields were sampled for sediment Hg cycling studies (**Figure 3.6**).

In all cases, the surface 0-2 cm depth interval was sampled, with sediment transferred to glass mason jars, which were filled to the brim such that no trapped air remained. To slow all microbial processes and abiotic reactions, the jars of sediment were stored on ice until further sub-sampling at the USGS laboratory in Menlo Park. Sample holding times prior to sub-sampling under laboratory conditions ranged from 1 to 2 days.

To understand what factors control temporal and spatial mercury dynamics across the range of YBWA habitats studied, a large suite of both mercury-related and non-mercury parameters were measured (**Table 6.1**). Field parameters measured include sediment temperature, pH, and redox (oxidation-reduction) potential. Samples that were incubated to measure microbial rates of MPP and SR were incubated at the average field temperature (± 1 ^{o}C) for that sampling event. Further details describing field sampling techniques, subsequent sediment and pore water sub-sampling under anaerobic laboratory conditions, and individual analyses associated with all of the parameters listed in **Table 6.1** are published elsewhere (**Marvin-DiPasquale et al., 2008** and references within) and are described in the Quality Assurance Performance Plan (QAPP) developed for the current study (**U.S. Geological Survey et al., 2008**).

The one method not detailed in the QAPP is the one used for assaying ^{34}S isotope fractionation in pore water sulfate ($\delta\ ^{34}SO_4^{2-}$), which is described brie here. Pore water was initially sub-sampled into crimp sealed vials under anaerobic conditions by the USGS Menlo Park group (**Marvin-DiPasquale et al., 2008; U.S. Geological Survey et al., 2008**), preserved frozen, and subsequently shipped frozen to the Denver, CO, USGS facility. Sample preparation was conducted according to previously published methods (**Carmody et al., 1998**). Upon thawing, samples were acidified with HCl to a pH of 3-4, then stripped of dissolved sulfide with nitrogen gas. Samples were the diluted with deionized water and dissolved SO_4^{2-} was precipitated as $BaSO_4$. The precipitate was filtered onto 0.45 µm cellulose acetate membrane filters, dried at 50º C, and transferred into borosilicate glass vials until further processing. Precipitate subsamples (ca. 1.5 mg) were transferred into 5 x 9 mm tin capsules, amended with of V2O5, and crimp sealed. Samples were then combusted and analyzed for δ^{34}S according to methods of **Giesemann et al. (1994)** using a Costech Analytical Inc. elemental analyzer (model ECS4010) coupled to a Thermo-Finnigan Delta Plus XP mass spectrometer operated in continuous flow mode. Stable isotope compositions are expressed in delta (δ) notation:

$$\delta = (R_{sample} / R_{standard}) - 1 \qquad \textbf{Equation 6.1}$$

where R refers to $^{34}S/^{32}S$. Values of δ^{34}S are expressed relative to Vienna-Cañon Diablo Troilite (V-CDT) with a precision of +/-0.2‰. Samples are normalized to the V-CDT scale using internationally accepted standards (IAEA-SO-6 = -34.1‰, NBS127 = 21.1‰).

6.2.2 Data analysis

The MeHg production potential (MPP) rate was calculated as a pseudo-first order reaction:

$$MPP = Hg(II)_R - Hg(II)_R * EXP(-k_{meth} * t) \qquad \textbf{Equation 6.2}$$

Where: $Hg(II)_R$ is 'inorganic reactive mercury' and a measure of the pool of inorganic Hg(II) that is available to microbes for Hg(II)-methylation; k_{meth} is the radiotracer derived ^{203}Hg(II)-methylation rate constant' and a measure of the activity of the sediment Hg(II)-methylating

community; t equals time (set to 1 day); and EXP indicates exponent (base e). At moderate to low values of k_{meth}, **Equation 6.2** approximates:

$$\mathbf{MPP = Hg(II)_R \times k_{meth}} \qquad \textbf{Equation 6.3}$$

Data was analyzeb for both temporal and spatial trends using S-Plus® 7.0 (Insightful Corp.) statistical software. Type II error probability was set at $p < 0.05$ for all statistical tests. Analysis of variance (ANOVA) was used to compare three primary paired relationships: a) agricultural vs non-agricultural fields, b) northern vs southern block fields (agricultural fields only), and c) growing season [June, July and August data] vs the post-harvest period [December and February data] (agricultural fields only).

6.3 Results

6.3.1 Mercury Parameters

Key mercury parameters (THg, $Hg(II)_R$, k_{meth}, MPP, and MeHg,) are plotted by 'habitat type' and in 'time series' to best illustrate both spatial and temporal data trends (**Figures 6.1** thru **6.5**). Summary statistics (mean, standard error and median) for individual fields are given in **Table 6.2** for all mercury and non-mercury parameters. ANOVA results for tests of spatial and temporal differences between paired groupings (agricultural vs non-agricultural fields; northern vs southern agricultural blocks; growing vs post-harvest season) are given in **Tables 6.3** thru **6.5**. While sediment THg concentration varied little over time at any given site, there were differences among habitat types (**Figure 6.1**), with agricultural fields having significantly more THg in surface sediments than did non-agricultural fields (**Table 6.3**). This difference in THg concentration among habitat types was unexpected, and was at least partially due to an east-west gradient in THg, with concentrations increasing approximately 4-fold overall from east to west (**Figure 6.6**). However, there was no significant east-west gradient in the data when grouped solely by agricultural or by non-agricultural habitat type (not shown). Instead there appeared to be a marked increase in overall THg concentration west of -121.603 degrees longitude, with a more than 2-fold higher average THg concentration in the agricultural field (west) grouping than for the non-agricultural field (east) grouping (**Table 6.3**). Further, the overall range of THg concentrations in the agricultural (western) fields was significantly larger than the range of concentrations observed for the non-agricultural fields (**Figure 6.6**). There were no significant differences in THg concentration among agricultural fields grouped by block (northern vs southern; **Table 6.4**) or by season (growing vs post-harvest, **Table 6.5**). For individual fields, median THg concentrations ranged 3-fold, from 124 ng g^{-1} (PW2) to 382 ng g^{-1} (white rice field R31), across all sampling dates (**Table 6.2**).

Average values of k_{meth} were significantly higher in non-agricultural wetlands compared to agricultural fields, across all sampling dates (**Table 6.3**, **Figure 6.2A**). After initially rising through the June through August growing season, k_{meth} values in most fields decreased during the period surrounding the rice harvest (**Figure 6.2B**), when agricultural fields were drained between early September thru mid-November (duration varied for individual fields; see **Figure 3.6**. Values of k_{meth} then increased again between early December and February, particularly for the white rice fields. There were no significant differences in k_{meth} values among agricultural fields grouped by block (northern vs southern; **Table 6.4**) or by season (growing vs post-harvest, **Table 6.5**). For individual fields, median k_{meth} values ranged 200-fold, from 0.003 d^{-1} (white rice field R31) to 0.52 d^{-1} (PW5-cat), across all sampling dates (**Table 6.2**).

Both spatial and temporal trends in sediment $Hg(II)_R$ concentration were largely the mirror opposite of what was seen for k_{meth}. Agricultural fields had significantly higher $Hg(II)_R$ concentrations than did non-agricultural wetlands (**Table 6.3, Figure 6.3A**). During the June through August growing season, $Hg(II)_R$ concentrations decreased in agricultural fields, followed by an increase during the September thru November periods the fields were drained, and finally a decrease again (post-reflooding) between early December and February (**Figure 6.3B**). There were no significant differences in $Hg(II)_R$ concentrations among agricultural fields grouped by block (northern vs southern; **Table 6.4**) or by season (growing vs post-harvest, **Table 6.5**). For individual fields, median $Hg(II)_R$ concentrations ranged 46-fold, from 0.14 ng g^{-1} (SW) to 6.4 ng g^{-1} (fallow field F66) across all sampling dates (**Table 6.2**).

Since MPP is a function of both k_{meth} and $Hg(II)_R$, the opposing spatial and temporal trends of these two parameters (**Figures 6.2 and 6.3**) resulted in overall similar trends in calculated MPP rates (**Figure 6.4**), with no significant difference between agricultural and non-agricultural sites (**Table 6.3**), by block (**Table 6.4**) or by season (**Table 6.5**). For individual fields, median MPP rates ranged 22-fold, from 5.4 pg g^{-1} d^{-1} (PW2) to 120 pg g^{-1} d^{-1} (PW5-CAT), across all sampling dates (**Table 6.2**).

In contrast to MPP, MeHg concentrations (and %MeHg) did show significant differences by both habitat type (agricultural fields > non-agricultural wetlands; **Table 6.3** and **Figure 6.5A**) and by season (post-harvest > growing season; **Table 6.5** and **Figure 6.5B**), but not by block (**Table 6.4**). Rice growing fields had the widest range of MeHg concentrations over the study period, although pooled by habitat type, fallow fields had the highest median MeHg concentration (**Figure 6.5A**). For individual fields, median MeHg concentrations ranged over 4-fold, from 0.65 ng g^{-1} (PW2) to 3.0 ng g^{-1} (wild rice field W65) across all sampling dates (**Table 6.2**).

6.3.2 Non-mercury parameters

Of the many sediment and pore water parameters measured during this study (**Table 6.1** and **6.2**), the ones that are discussed in detail below are the most relevant with respect to the ensuing discussion regarding what controls Hg(II)-methyation among the multiple habitat types studied.

6.3.2.1 *Sediment Redox*

Sediment 'redox' or oxidation-reduction potential (ORP) is a semi-quantitative and qualitative measure of the net impact of all competing chemical oxidation and reduction reactions occurring in the sediment aqueous (pore water) phase. When ORP probe measurements (in millivolts; mV) are corrected for the 'reference' half-reaction associated with hydrogen, redox is expressed in terms of E_h (in mV). Conditions of $E_h > 0$ are said to be 'oxidized, while those < 0 are said to be 'reduced'. Sediment redox was measured both in the field at the time of sample collection, and once again in the laboratory at the time the mason jars of sediment were again sub-sampled under anaerobic conditions. This repeated measure gives some indication as to if sediment chemistry changed significantly during the intervening holding period. There was an average decrease in E_h of -75 ± 9 mV (n = 55) between the time of field collection and laboratory sub-sampling (**Figure 6.7**), which is modest given the > 430 mV range in values (-80

to +353 mV) for the complete dataset of field measurements. Apart from this modest decrease in E_h during the 1-4 day holding period, the qualitative integrity of the sediment samples was verified to be preserved, as the plots for both field and laboratory E_h track each other very closely over the study period and by individual field (**Figure 6.7**).

Similarly, temporal changes in sediment redox at a given location indicate whether sediment chemistry is changing significantly throughout the year. Sediment redox changed dramatically throughout the study period in the agricultural fields, where in a pattern strikingly similar to that for $Hg(II)_R$ (**Figure 6.3B**), E_h decreased during the June through August growing season, then increased during the September thru November when the fields were drained, and finally decreased again (post-reflooding) between early December and February (**Figure 6.7**). There were significant habitat differences in E_h with agricultural fields more chemically oxidized and non-agricultural fields more chemically reduced (**Table 6.3**). While there was no significant north-south block effect for agricultural fields, there was a significant seasonal difference with the growing season being more reduced than the post-harvest period (reflooded) (**Table 6.5**), although this effect was only seen in the laboratory measurements, and not with the field collected E_h data.

6.3.2.2 *Sediment Sulfur Chemistry*

Microbial sulfate reduction (SR) rate varied by both site and season, with no consistent spatial or temporal trend (**Figure 6.8A**) among fields. However, a number of the agricultural fields showed a general rise in SR rates during the growing season, followed by a decrease during the draining period, and varied responses during the post-harvest winter. Site-specific median values ranging by a factor of 10-fold (6.9 to 69.4 nmol g^{-1} d^{-1}; **Table 6.2**). Most sites exhibited comparatively low rates throughout the year (< 100 nmol g^{-1} d^{-1}), with the exception of PW5-ow, which exceeded 300 nmol g^{-1} d^{-1} in July, and wild rice field W32, which exceeded 1200 nmol g^{-1} d^{-1}during February (**Figure 6.8A**). There were no significant differences in SR rates among agricultural fields grouped by habitat (agricultural vs non-agricultural), by block (northern vs southern) or by season (growing vs post-harvest).

In contrast to SR rates, solid-phase TRS exhibited a similar seasonal pattern among all agricultural fields, which included an increase during the growing season, a decrease during the draining period, and an increase again during the post-harvest winter period (**Figure 6.8B**), a pattern which was mirror opposite of that for sediment redox (**Figure 6.7**). Both TRS and AVS (poorly crystalline FeS) were significantly higher (approximately 10-fold) in non-agricultural sites as compared to agricultural fields (**Table 6.3** and **Figure 6.8B**), with median TRS concentrations by site ranging 77-fold (1.2 to 93.4 µmol g^{-1}) and median AVS concentrations by site ranging 128-fold (0.4 to 53.9 µmol g^{-1}) (**Table 6.2**). No significant differences in TRS or AVS concentrations were found when data was grouped by block or by season.

Pore water sulfate concentration ($pw[SO_4^{2-}]$) was significantly higher (> 5-fold) in agricultural fields than in non-agricultural wetlands (**Table 6.3; Figure 6.9A**). Similar to TRS, $pw[SO_4^{2-}]$ exhibited a similar seasonal pattern among most agricultural fields (**Figure 6.9A**). This pattern was the mirror opposite of TRS (and similar to sediment redox), including a decrease during the growing season, an increase during the draining period, and a decrease again during the post-harvest winter period. An exception to this general pattern in agricultural fields

was noted for wild rice field W65 and fallow field F66, in which pw[SO_4^{2-}] appeared to rise during the growing season (**Figure 6.9A**). However, in the case of wild rice field W65, this was largely due to an overall increase in salinity in this field during that period, as evidenced by pore water chloride concentration data (not shown). Since chloride is a conservative element in the environment, affected almost exclusively by physical processes of dilution and evaporative concentration, normalizing sulfate to chloride concentration (i.e. calculating the sulfate-to-chloride (pw[SO_4^{2-}/Cl^-]) molar ratio) allows us to separate changes in sulfate concentration due to microbiological and abiotic chemical reactions, from those based solely on physical dilution or evaporative concentration (**Marvin-DiPasquale et al., 2003b**). Time series plots of pw[SO_4^{2-}/Cl^-] ratio data (**Figure 6.9B**) more clearly show the relative changes in pw[SO_4^{2-}] concentration due to microbiological and/or abotic reaction, with field W65 also exhibiting a general decrease during the growing season. However, F66 was still shown to increase during this period, which is suggestive of the continued reoxidation of reduced-S compounds during the growing and draining periods. The significant decrease in the pw[SO_4^{2-}/Cl^-] ratio between December '08 and February '09 for all agricultural fields suggests stimulated sulfate reduction during this period. Pore water sulfide concentration (pw[H_2S]) was uniformly low for all sites, rarely exceeding 2 µmol L^{-1} (**Table 6.2**), which suggests either reoxidation or precipitation into solid-phase Fe-S minerals. There were also no significant differences in pw[H_2S] among fields grouped by habitat, by block or by season. The above results indicate comparable rates of microbial SR in the two habitat types, but a much higher degree of reduced sulfur preservation (and less reoxidation) in the non-agricultural wetland sites, most likely from the precipitation of H_2S with dissolved iron to form Fe-S minerals.

Pore water sulfate isotope data (pw[$\delta\ ^{34}SO_4^{2-}$]; June thru December 2007 data only) sheds even more light on sulfur cycling across the habitats studied, as agricultural fields were significantly lighter isotopically (lower values) compared to non-agricultural wetlands (**Table 6.3**). This is consistent with generally more microbial SR in non-agricultural fields, as the process of SR tends fractionate sulfate and sulfide such that the remaining (unused) pore water sulfate is enriched in the heavier ^{34}S isotope and the end-product reduced-sulfur (e.g. sulfide) is isotopically deplete in ^{34}S (Sharp, 2007). This trend is apparent in the positive correlation between SR rates and pw[$\delta\ ^{34}SO_4^{2-}$] (**Figure 6.10A**). Similarly, the negative correlation between the pw[SO4/Cl] ratio and pw[$\delta\ ^{34}SO_4^{2-}$] (**Figure 6.10B**) indicates that sites comparatively depleted in sulfate (also suggestive of enhanced SR) are enriched in $\delta\ ^{34}SO_4^{2-}$. So while statistically significant differences in SR rates were not found between the two field types, the data suggests that overall there was a more pw[δ 34SO42-] enrichment due to SR in non-agricultural fields, while agricultural fields spanned a much wider range of both SR rates and pw[$\delta\ ^{34}SO_4^{2-}$] enrichment factors (**Figure 6.10A**).

The pw[$\delta\ ^{34}SO_4^{2-}$] data also gives us some evidence as to the extent of reduced-sulfur reoxidation among the various habitat types. When reduced-sulfur compounds are reoxidized back to SO_4^{2-}, the isotopic signature of the resulting SO_4^{2-} is similar to the parent reduced-sulfur compound (i.e. isotopically deplete) (**Balci et al., 2007**). We note that the only instances of istoptically deplete pw[$\delta^{34}SO_4^{2-}$] (values < 0) occurred in exclusively in agricultural fields, and only at sites with high redox values (Eh > +150 mv; **Figure 6.10C**). This suggests that there is a significant amount of reduced-sulfur reoxidation that occurs on agricultural fields, compared to non-agricultural fields. Further, during the post-harvest season (December data only),

agricultural fields exhibited significantly lighter $_{pw[}\delta\ ^{34}SO_4^{2-}{}_{]\ values}$ than during the June-August growing season (**Table 6.5**), indicating that this reoxidation takes place largely during the post-harvest season.

6.3.2.3 *Sediment Iron Chemistry*

While microbial Fe(III)-reduction was not directly measured, multiple iron pools were tracked throughout the study, and provide a dynamic picture of seasonal and spatial iron cycling. As the name implies, microbial heterotrophic Fe(III)-reduction describes the process by which certain bacteria can use organic carbon as an electron donor and various forms of ferric iron (Fe(III)) as an electron acceptor, thereby reducing Fe(III) to the ferrous (Fe(II)) form. Since a) some Fe(III)-reducing bacteria have been shown to form MeHg (**Fleming et al., 2006; Kerin et al., 2006**), b) multiple forms of Fe react with both S and Hg (**Hylander et al., 2000; Slowey and Brown, 2007**), and c) there is abundant total iron (Fe_T = Fe(II)+aFe(III)+cFe(III) = 15.6 ± 0.8 mg g^{-1}, average for all sites) in the YBWA study area, understanding Fe-biogeochemistry is key to understanding Hg cycling in this system.

One measure of the general activity of Fe(III)-reducing bacteria is the build-up of the Fe(II) concentrations over time. Agricultural fields exhibited large seasonal changes in both pore water and sediment Fe(II) concentrations (**Figures 6.11A and 6.11B**), with periods of Fe(II) increase observed during the June-August growing season and the December-February post-harvest season. In contrast, while non-agricultural areas often had higher Fe(II) concentrations, temporal changes in these were much less pronounced. The large drop in Fe(II) concentrations in pore water and sediment in the agricultural fields during the September-November field draining period coincided with the increase in sediment redox conditions (**Figure 6.7**), and thus likely reflects the abiotic reoxidation of Fe(II) back to Fe(III). Median Fe(II) concentrations across all sites ranged more than 160-fold (0.03 to 4.5 mg L^{-1}) in pore water, and only 3-fold (2.4 to 7.6 mg g^{-1}) in sediment (**Table 6.2, Figure 6.11**). Agricultural sites had significantly higher sediment Fe(II), than did non-agricultural sites (**Table 6.3**). Significant differences were not found for pore water Fe(II) based on habitat, nor for sediment or pore water Fe(II) for data grouped by block or by season.

Previous studies (**Lovley and Phillips, 1987a; Roden and Zachara, 1996**) have shown that amorphous (poorly crystalline) forms of Fe(III) (herein referred to as aFe(III)) are more readily available to Fe(III)-reducing bacteria than are more crystalline forms (herein referred to as cFe(III); e.g. crystalline goethite (αFeOOH), hematite (Fe_2O_3), Ferrihydrite ($Fe(OH)_3$), lepidocrocite (γFeOOH), and magnetite (Fe_3O_4)). Average sediment aFe(III) and cFe(III) concentrations were significantly higher (> 7-fold and 2-fold, respectively) in agricultural fields, compared to non-agricultural fields, with cFe(III) concentrations being significantly larger (20X to > 180X, all sites) than aFe(III) concentrations (**Table 6.3, Figure 6.12**). There were no other significant differences for either Fe(III) species, grouped by either block or season. To the extent that aFe(III) is the preferred form of Fe(III) for microbial Fe(III)-reduction, due to increased surface area (**Roden and Zachara, 1996**), and that the aFe(III) concentration has been shown to be proportional to rates of microbial Fe(III)-reduction (**Roden and Wetzel, 2002**), the current data suggests that agricultural fields exhibit an overall higher rate of Fe(III)-reduction, than do non-agricultural fields (**Windham et al., 2009**).

6.3.2.4 *Organic Carbon*

Sediment total organic matter, as measured by %LOI, was generally constant with time and similar in magnitude among all sites, with the exception of vegetated non-agricultural sites (i.e. SW, PW5-CAT, PW5-TULE), which were somewhat more organic rich (**Figure 6.13, Table 6.2**). As a group, sediment in agricultural fields was slightly, yet significantly, less organic rich compared to non-agricultural fields (**Table 6.3**). There were no significant differences in sediment organic content for data group by block or season.

In contrast to whole sediment organic content, dissolved organic metrics (pore water DOC (pw[DOC] and pore water acetate (pw[Ac])) exhibited much more dynamic seasonal and spatial differences. While pw[Ac] is only a minor subset of the total pw[DOC] pool, it is a key indicator of substrates for heterotrophic bacteria (including sulfate and iron reducers), a low molecular weight end product of bacteria fermentation, and thus a good surrogate for the specific class of low molecular weight organic molecules that fuel microbial processes in sediment. There were there was a general rise on both pw[DOC] and pw[Ac] concentrations through the growing season, followed by a decrease during the field harvest and draining period (**Figures 6.14A and 6.14B**). There was no significant difference in the concentration of either pore water constituent when data was grouped by habitat (agricultural vs non-agricultural sites) or by block. However, pw[DOC] was statistically greater during the growing season across all agricultural fields (**Table 6.5**). Further statistical analysis indicated that among agricultural fields only, those planted with rice (white and wild) and which had decaying rice straw (post harvest), increased significantly in pw[Ac] concentration between the growing and post harvest season, while those that were held fallow during the study period, decreased in pw[Ac] between the growing and post-harvest periods (**Figure 6.15**).

6.4 Summary/Discussion

6.4.1 YBWA sediment MeHg concentrations in the larger ecosystem context

While wetlands in general are known to be important zones for MeHg production (**Zillioux et al., 1993; Rudd, 1995; St. Louis et al., 1996; Marvin-DiPasquale et al., 2003a**), there is very little known about the influence of land management and agricultural practices on the cycling of mercury in freshwater wetlands. The upper range of MeHg concentrations measured in surface sediments of the YBWA (this study; 75^{th}-100^{th} percentile range = 2.7 – 6.2 ng g^{-1} dry wt.) are high compared to other reports of surface sediment MeHg concentrations made in a number of open-water locations throughout the San Francisco Bay system, including an extensive estuarine transect from the Guadalupe R. to the SFB-Delta (0.1-1.0 ng g^{-1} dry wt., n = 52; **Conaway et al., 2003**), San Pablo Bay (< 1 ng g^{-1}; **Marvin-DiPasquale et al., 2003a**), the Frank's Tract region (SFB central delta; 75^{th}-100^{th} percentile range = 0.5-0.9 ng g^{-1}; **Marvin-DiPasquale et al., 2007**), the larger central SFB-Delta region (< 1 – 3 ng g^{-1} dry; all data; **Heim et al., 2007**) and Englebright Lake (a Sierra Nevada foothill reservoir; range = 0.7-1.5 ng g^{-1} dry; n = 12; **Alpers et al., 2006**). However, the YBWA MeHg concentrations are in the range of values measured in the Cosumnes R. region (freshwater) and it's associated floodplain (75^{th}-100^{th} percentile range = 4-22 ng g^{-1}; **Marvin-DiPasquale et al., 2007**) and in the range of salt marsh settings in the central SFB-Delta (2-8 ng g^{-1} dry; **Heim et al., 2007**), adjacent to San Pablo Bay (average = 5.4 ng g^{-1} dry wt.; **Marvin-DiPasquale et al., 2003a**), and associated with the Petaluma R. ($75^{th-1}00^{th}$ percentile range = 4.0 – 14.5 ng g^{-1} dry wt.; **Yee et al., 2008**). Thus, the

concentrations of sediment MeHg measured in this study are similar to other wetland settings (both freshwater and saline) measured throughout the larger San Francisco Bay system.

6.4.2 Controls on Methylmercury production

While the overall range of sediment MeHg concentrations in the YBWA are similar to other wetlands within the SFB watershed, large seasonal variations and differences among habitat types were observed for both MeHg concentrations (**Figure 6.5**) and MPP rates (**Figure 6.4**) in this study. To better understand what natural and land management actions controls these temporal and spatial variations, our focus is ultimately on what controls the activity of the Hg(II)-methylating community (i.e. k_{meth}) and the availability of inorganic Hg(II) to be methylated (i.e. $Hg(II)_R$), as these two terms control gross MeHg production (see **Equation 6.3**). Based on the literature and our previous research experience, we hypothesized that interactions with the biogeochemical cycles governing S, Fe and C chemistry would play a significant role in governing Hg cycling in the YBWA. The relevant interrelationships between these elemental cycles are brie discussed below.

Sulfate reducing bacteria (SRB) mediate the conversion of dissolved sulfate (SO_4^{2-}) to sulfide (H_2S), while iron reducing bacteria mediate the conversion of Fe(III) to Fe(II). Both sulfate reducing (**Gilmour et al., 1992; Jeremiason et al., 2006**) and Fe(II) reducing (**Mehrotra et al., 2003; Fleming et al., 2006; Kerin et al., 2006**) bacteria are known to carry out Hg(II)-methylation in freshwater sediments, although not all species within these two group have this capability (**King et al., 2001; Kerin et al., 2006**). Both microbial sulfate and iron reduction take place largely in sediments, typically under oxygen depleted conditions, and both are facilitated by bacteria that require suitable forms of organic C as the electron donor, as well as for cellular growth. Due to the thermodynamics of both processes, Fe(III)-reduction typically outcompetes SR for commonly used organic substrates such as acetate (**Thullner and Van Cappellen, 2007**). So it is common that when suitable forms of Fe(III) are available, microbial Fe(III)-reduction is active, and at the expense of microbial SR, at least in terms of commonly used organic substrates (**Lovley and Phillips, 1987b**). However, not all forms of Fe(III) are equally available to Fe(III)-reducing bacteria. Amorphous (poorly crystalline) forms of Fe(III) (i.e. aFe(III)) have more surface area and are more readily susceptible to microbial reduction, than are crystalline forms (i.e. cFe(III)) (**Roden and Zachara, 1996**). Thus, while Fe(III)-reducing bacteria can use both Fe(III) forms, they utilize cFe(III) much more slowly. Since electron acceptor availability is a key determinate as to which microbial groups are active at a given time or place, as aFe(III) becomes limiting, conditions for microbial SR become more favorable.

Reduced forms of both S and Fe can readily react to form a suite of solid phase reduced Fe-S minerals (e.g. FeS, FeS_2, etc…), thus diminishing the concentration of either sulfide or Fe(II) (or both) in the dissolved phase, depending on which is in limited supply. Further, both dissolved and solid phase reduced sulfur compounds can form strong bonds with inorganic Hg(II) (**Benoit et al., 1999, 2001**) and MeHg (**Qian et al., 2002**). To the extent that Hg(II) is bound to various solid phase reduced-S compounds, it may be less available for Hg(II)-methylation (**Marvin-DiPasquale and Cox, 2007; Marvin-DiPasquale et al., 2009a, 2009b**). Thus, the presence, form and concentration of both S and Fe species exert a very strong influence on each other and on the Hg cycle.

In the current study, as with our previous research (**Marvin-DiPasqule et al., 2003a, 2007; Marvin-DiPasquale and Agee, 2003; Yee et al., 2008**), the activity of the resident Hg(II)-methylating community in sediment was assessed using the radioactive ^{203}Hg(II) isotope derived k_{meth} parameter. If the community of sulfate reducing bacteria were the only microbial group involved in the Hg(II)-methylation process, we would expect to see a good correlation between k_{meth} and our independent parallel measure of microbial SR rates across all sites. While a significant positive linear relationship was found between these two parameters, microbial SR rates explained only 33% of the variability in k_{meth} values across all sites and dates of the YBWA dataset (i.e. linear regression $R^2 = 0.33$, data not shown). A much stronger relationship ($R^2 = 0.69$) was found when k_{meth} was regressed against the term [%Fe(II)/Fe_T] (**Figure 6.16**), where Fe_T (total Fe) is the sum of all solid phase Fe species (Fe(II) + aFe(III) + cFe(III)). While not a direct measure of Fe(III)-reduction rate, [%Fe(II)/Fe_T] represents a measure of the percentage of all (measured) solid phase iron species that have already been reduced to Fe(II), presumably via microbial Fe(III)-reduction. We interpret that sites with low [%Fe(II)/Fe_T] values as having a high potential for Fe(III)-reduction, as much of the Fe is still in the oxidized Fe(III) form. Conversely, high [%Fe(II)/Fe_T] values would suggest sites with a lower potential for further Fe(III)-reduction, as much of the Fe(III) pool (includes aFe(III) + cFe(III)] has already been converted to Fe(II). Since aFe(III) is more readily available and always much lower in concentration than cFe(III) (**Table 6.2**, **Figure 6.12**), we would also expect that as [%Fe(II)/Fe_T] values increase, the actual rate of Fe(III)-reduction slows, as the remaining Fe(III) is in the less available crystalline form. Further, since Fe(III)-reduction is thermodynamically more favorable than microbial SR, sites with a high potential for Fe(III)-reduction (low [%Fe(II)/Fe_T] values) would be expected to have a low potential for SR, and vice versa. Therefore, the [%Fe(II)/Fe_T] metric also provides some measure of the geochemical conditions along a continuum of sites and dates that transition from those more favorable to Fe(III)-reduction (low [%Fe(II)/Fe_T]) to those more favorable for SR (high [%Fe(II)/Fe_T]) (**Figure 6.16**).

The distribution of data along the regression line indicates that for agricultural sites (white rice, wild rice and fallow fields), [%Fe(II)/Fe_T] ranges anywhere from 5-60%, depending on the site and time (**Figure 6.16**). For non-agricultural fields [%Fe(II)/Fe_T] ranges from 30-75% for most sites. For data grouped by these two habitat types, [%Fe(II)/Fe_T] was statistically larger for non-agricultural sites compared to agricultural sites (**Table 6.3**). These results suggests that the agricultural fields are generally more poised for microbial Fe(III)-reduction, while the non-agricultural fields are generally more poised for SR. This is supported by the fact that there was significantly higher aFe(III) and cFe(III) concentrations in the agricultural sites (**Table 6.3**), since the concentration of aFe(III) has been shown to be proportional to the actual rate of Fe(III)-reduction in wetland settings (**Roden and Wetzel, 2002; Bonneville, et al., 2004**). However, there is certainly overlap in both processes in both settings, as evidenced by the fact that there was no statistical difference in SR rates between the two habitat types, even though the non-agricultural sites had significantly more solid phase AVS and TRS and lower concentrations of pw[SO_4^{2-}] (**Table 6.3**). Overall, this data indicates that the community of Hg(II)-methylating bacteria is active under conditions favoring both Fe(III)-reduction and SR, but as conditions transition from those favoring the former to those favoring the latter, the activity of the Hg(II)-methylating community increases.

Apart from the activity of the Hg(II)-methylation bacterial community, the other factor that ultimately mediates MeHg production is the availability of inorganic Hg(II) for methylation. The concentration of $Hg(II)_R$ exhibited a strong negative linear relationship with the solid phase TRS concentration ($R^2 = 0.62$; **Figure 6.17**). Agricultural sites, which had significantly lower TRS concentrations (**Table 6.3**) had much higher $Hg(II)_R$ concentrations, while the reverse was true for the non-agricultural sites. Similar relationship between $Hg(II)_R$ and TRS (or AVS) have been shown in a number of recent studies, including San Francisco Bay saltmarshes and the central Delta region (**Marvin-DiPasquale et al., 2007; Yee et al., 2008**), southern Louisiana wetlands (**Marvin-DiPasquale, *unpublished data***), and across a diversity of stream systems (**Marvin-DiPasquale et al., 2009b**). This is interpreted to reflect the strong binding of Hg(II) to the surfaces of solid phase reduced-S compounds, making less of the total $Hg(II)_R$ available with increasing TRS concentration.

6.4.3 Agricultural vs Non-agricultural Fields

Agricultural fields differed from non-agricultural fields in the YBWA in many ways that were reflected in the sediment chemistry associated with Hg, S, Fe and C. Most notably with respect to mercury, the resident microbial population responsible for Hg(II)-methylation was generally less active in the agricultural sites, while the pool size of $Hg(II)_R$ available for methylation was generally higher in agricultural sites (**Tables 6.2** and **6.3**; **Figures 6.2** and **6.3**). These opposing trends in k_{meth} and $Hg(II)_R$ resulted in no significant difference in calculated MPP rates between agricultural and non-agricultural sites (**Table 6.3; Figure 6.4**), although MeHg concentrations were significantly higher in agricultural fields, particularly during the post-harvest season (**Table 6.3, Figure 6.5**). The comparison of agricultural vs non-agricultural fields is potentially confounded by the general east-to-west increase in THg concentration in the study area (**Figure 6.6**), and the fact that all of the agricultural sites lay to the west and the non-agricultural sites to the east. However, we conclude that the differences observed between the two habitat groupings is much more related to actual land use, than to longitude. First, THg is generally a very poor predictor of MeHg concentrations, as may of the other factors (discussed herein) have a much stronger influence on where and when MeHg is produced by bacteria. Statistical analysis demonstrated that THg was poorly correlated with all other mercury metrics across all sites, indicating that THg alone had little impact on rates of MeHg production, or $Hg(II)_R$ and MeHg concentrations. Second, while a number of the other key mercury metrics also exhibited significant linear relationships as a function of latitude (**Table 6.6**), they also varied greatly with season for any given field. This indicates dynamic microbial and abiotic reactions are playing a dominant role. Third, within each of the two habitat groupings, there was no significant relationship between latitude and THg or any other mercury metric.

Redox sensitive species associated with both Fe and S were markedly different between the two habitat groupings. In general, the agricultural fields had higher concentrations of more oxidized species, including aFe(III), cFe(III), and $pw[SO_4^{2-}]$, while non-agricultural fields had higher concentrations of more reduced species including solid phase AVS, TRS, Fe(II), and pw[Fe(II)] (**Table 6.3, Figures 6.7, 6.8B, 6.11,** and **6.12**). Multiple land management factors likely drive these overarching differences in redox chemistry, including a) seasonal draining of agricultural fields, b) tilling of agricultural fields, and c) shallower water depths in agricultural fields, particularly compared to the open water permanent wetland sites (PW2 and PW5). As a result of these physical and hydrological manipulations, surface sediment associated with

agricultural fields tends to be more oxidized, and reduced species have a higher likelihood of getting reoxidized. Extensive reoxidation in the agricultural fields is strongly suggested by the pw[$\delta^{34}SO_4^{2-}$] data (**Table 6.5, Figure 6.10**). By extension, the reoxidation of Fe(II) to aFe(III) is presumably also better facilitated in this habitat grouping. This is evidenced by the strong seasonal changes in Fe-speciation associated with agricultural fields (but not for the non-agricultural fields) which are temporally synchronous with seasonal field draining and reflooding events (e.g. **Figures 6.7** and **6.11**). All of this supports the conclusion that agricultural fields are more poised for microbial Fe(III)-reduction (and less so for SR) than are non-agricultural fields. More importantly, these findings point to the primary influence of hydrology management on sediment chemistry, microbial processes and ultimately on Hg cycling. Previous research has also suggested that newly flooded areas (**Kelly et al., 1997**) or aquatic systems which undergo periods of both wetting and drying (**Gilmour et al., 2004**) are zones of enhanced MeHg production.

The significantly higher pore water alkalinities (pw[ALK], **Table 6.3**) in the agricultural fields also suggest a larger degree of organic carbon mineralization, compared to non-agricultural wetlands. The higher potential for the reoxidation of reduces S and Fe species in agricultural fields (as discussed above) would support of this conclusion. Further, laboratory degradation studies conducted with dominant plant material collected from each of the YBWA field types indicates that white and wild rice detritus degrades much faster than does cattail or tule detritus (see **Section 7.3.4**). Thus, while rates of overall sediment organic matter degradation were not measured directly, the above observations indicate that there may be more overall organic mineralization associated with the agricultural fields. If so, this may also be a factor that leads to significantly higher MeHg concentrations in agricultural fields, compared to the non-agricultural wetlands (**Table 6.3**).

6.4.4 Fertilizer Additions to Agricultural Fields

One of the key questions initially posed by this study was whether or not the addition of SO_4^{2-} containing fertilizers to agricultural fields stimulates microbial SR, and ultimately MeHg production. Based on fertilizer application rates used during the study and the on chemical composition of the various fertilizers (Jack DeWit, cooperating rice farmer, *personal communication*), we estimate that approximately 4-11 kg of SO_4^{2-} was applied per acre (as starter fertilizer) to white and wild rice fields during the June 2007 application, immediately prior to rice seed amendment (**Figure 3.6**). Subsequently, another 41-66 kg of SO_4^{2-} per acre was applied, as ammonium sulfate ($(NH_4)_2SO_4$), to rice growing fields during July 2007. White rice field R64 received an additional 66 kg SO_4^{2-} per acre (as $(NH_4)_2SO_4$) during August 2007. If instantaneously dissolved, these application rates would represent to an increase in overlying water SO_4^{2-} concentrations (above background) of approximately 5-26 mg L^{-1} (0.06-0.28 mmol L^{-1} for the July starter fertilizer application, and approximately 70-100 mg L^{-1} (0.7-1.1 mmol L^{-1}) for the June / August applications of $(NH_4)_2SO_4$, assuming optimal water depths of 4 inches for white rice and 7 inches for wild rice. However, actual SO_4^{2-} concentration increases due to fertilizer are likely lower, as the form of application is as a solid and dissolution is not instantaneous. Given that surface water SO_4^{2-} concentrations measured at the inlets of white and wild rice fields were 67 ± 22 mg L^{-1} (0.7 ± 0.2 mmol L^{-1}; avg. ± std. dev.; n = 19; **Appendix 3, Table A3.8**), and assuming that these represent background concentrations, the above additional

amendments from fertilizer potentially represent significant pulsed inputs of SO_4^{2-} to overlying water.

Even though the potential increase in overlying water SO_4^{2-} concentrations are significant, the direct effect of fertilizer amendments on benthic microbial SR rates and MeHg production is less clear. While all four rice fields exhibited overall higher June through December pw[SO_4^{2-}] concentrations compared to non-agricultural fields, so did the fallow fields, particularly F66 (**Figure 6.9A**). So while higher pw[SO_4^{2-}] concentrations associated with rice fields may well have been a direct result of fertilizer amendments from the current growing, the higher concentration also associated with fallow fields suggest the possibility that some of the pw[SO_4^{2-}] may be from legacy SO_4^{2-} applied in previous years and/or the reoxidation of reduced-S, which the agricultural fields appear more prone to (**Section 6.3.2.2**). Since non-agricultural fields also have higher SR rates, the relative difference in pw[SO_4^{2-}] concentrations between the two habitat groupings is in some part a function of the more rapid depletion of pw[SO_4^{2-}] in the non-agricultural settings. In 3 of 4 cases pw[SO_4^{2-}] increased in rice fields for at least part or all of the June thru August growing season (i.e. W32, W65 and R34), while declining throughout this period in white rice field R31 (**Figure 6.9A**). However, these observed increases in pw[SO_4^{2-}] largely reflected simple evaporative concentration, as all rice fields, with the exception of R64, showed steady decrease in pw[SO_4^{2-}/Cl^-] ratio through the same June thru August period (**Figure 6.9B**). Further, fallow field F66 also exhibited a rise in both pw[SO_4^{2-}] and the pw[SO_4^{2-}/Cl^-] ratio between June and August, and no fertilizer was applied to this field in 2007, again suggesting reoxidation reactions. Thus, simply considering pw[SO_4^{2-}] concentrations by site and time does not clearly illustrate the effect of fertilizer addition on the pw[SO_4^{2-}] pool.

The concentration at which SO_4^{2-} begins to limit the rate of microbial sulfate reduction is approximately 1 mmol L^{-1} in marine sediments (**Martens and Berner, 1974**) and may be even lower in freshwater systems (**Roden and Tuttle, 1993**). Through most of the study (except for February 2008) pw[SO_4^{2-}] concentrations in agricultural fields were very near or above this 1 mmol L^{-1} threshold (**Figure 6.9A**), suggesting that microbial SR was not limited by pw[SO_4^{2-}] concentrations. Whether the higher concentrations in agricultural fields was a direct result of current and/or past fertilizer applications is unclear, but to the extent that fertilizer additions pushed pw[SO_4^{2-}] concentrations much above 1 mmol L^{-1}, we would expect this to have no effect on SR rates.

While there was a general increase in microbial SR and solid phase TRS concentrations in all four rice fields during the growing season, there was also a rise in both parameters for fallow fields F20 and F66, neither of which received fertilizer during the study period (**Figures 6.8A** and **6.8B**). There was also a rise in SR rates in the non-agricultural PW5 open water site from June to July, followed by a decrease in August. Thus, any conclusions regarding the impact of fertilizer amendments based upon temporal changes in SR rates alone are also equivocal.

In addition to the assessment of the pw[SO_4^{2-}] concentration and the SR rate data discussed above, a number of other observations lead us to conclude that the addition of fertilizer did little to stimulate microbial SR rates in agricultural fields. First, rates of microbial SR were generally higher in non-fertilized non-agricultural fields during the June-August growing season (**Figures 6.8A**). Second, the high activity of Fe(III)-reducing bacteria in the agricultural fields during the

growing season, as evidenced by the overall increase in solid phase and dissolved Fe(II) (**Figure 6.11**) and the decreases in both forms of Fe(III) (**Figure 6.12**), coupled with the fact that Fe(III)-reduction generally outcompetes SR (**Lovley and Phillips, 1987b**). Since the agricultural fields were largely poised for Fe(III)-reduction, and because pw[SO_4^{2-}] concentration were already near or above levels no longer limiting to sulfate reducing bacteria, the additional SO_4^{2-} from fertilizer did little to additionally stimulate SR rates. On the contrary, SR rates were likely limited by organic substrate due to the competition with Fe(III)-reduction.

Finally, while calculated MPP rates did increase substantially in the rice fields during the growing season (**Figure 6.4B**), and it was largely due to the increase in the activity of the Hg(II)-methylating community (as measured by k_{meth}; **Figure 6.2B**), similar increases in k_{meth} were also seen on the non-fertilized fallow fields, and between June and July in the non-fertilized PW5 open water site. Temporal trends in sediment MeHg concentrations were not so consistent for either fertilized or non-fertilized fields during the growing season (**Figure 6.5B**), suggesting that variable degrees of MeHg degradation (not measured) affected the site specific MeHg concentrations. Since k_{meth} was found to be more strongly correlated with the [%Fe(II)/Fe_T] metric (**Figure 6.16**) than with SR rates (**Section 6.4.2**), we conclude that the increase in k_{meth} and associated MPP rates in fertilized rice fields reflects the overall increase in heterotrophic microbial activity (both Fe(III)-reduction and SR) brought on by the stimulatory effect of actively growing rice plants supplying organic exudates to the Hg(II)-methylating community (**Windham et al., 2009**).

6.4.5 Post-Harvest Impacts on MeHg Production in Rice Growing Fields

Another key question this study was designed to address is: How and to what extent and do post-harvest management practices impact MPP rates and MeHg concentrations? The original study design sought to compare the effects of field discing (plowing the remaining rice straw into the surface soil layer) verses allowing the standing rice straw to decay aboveground by simply draining and reflooding the field after harvest. Due to 2007 field conditions and other constraints, the cooperating rice farmer decided not to conduct discing on any of the rice fields studied during the growing season. Instead, post-harvest rice fields were reflooded and the standing rice straw was allowed to decay in all four cases. While we were not able to compare the two post-harvest approaches as planned, one benefit to the ultimate outcome was our ability to better replicate the study of the reflooding approach exclusively.

The biggest obvious effect of reflooding post-harvest rice fields and allowing the rice straw to decay aboveground, was the conversion of large amounts of particulate organic matter (rice straw) into dissolved organic matter that can fuel microbial processes. The degradation of organic matter does not happen in a single step, but instead through multiple steps each facilitated by a consortium of microbes (**Capone and Kiene, 1988**), including the exoenzymatic breakdown of particulate material into large macromolecules (polymers) by fungi, the breakdown of polymers into simpler low molecular weight monomers (e.g. simple sugars, amino acids, and fatty acids), the fermentation of monomers into even simpler organic molecules (e.g. acetate, volatile fatty acids, alcohols). It is this class of simple organic molecules that fuel terminal electron accepting processes such as Fe(III)-reduction and sulfate reduction. Statistical analysis of agricultural fields only (both previously in-rice and fallow) indicates that both MeHg concentration and the %MeHg were higher in surface sediments in the post-harvest

season, as compared to the growing season (**Table 6.5**; **Figure 6.5B**). None of the other key mercury metrics showed a significant difference for agricultural field data grouped into these two temporal classes. One factor that may have limited our ability to detect statistical differences among parameters grouped in this manner is that there were big differences in geochemical and microbial conditions between December 2007 and February 2008, both of which fell under the 'post-harvest' data grouping. Sediment metrics measured in December 2007 may be more reflective of the geochemical changes associated of recently reflooding previously drained sediments. In contrast, the geochemical data from February indicates comparatively reducing conditions have been re-established, and potentially exacerbated by the decaying rice straw. For example, compared to the last time point in the growing season (August), sediment was substantially more oxidized (**Figure 6.7**), TRS and Fe(II) concentrations were lower (**Figures 6.8B** and **6.11**), and pw[SO_4^{-2}], aFe(III) and cFe(III) concentrations were higher (**Figures 6.9A** and **6.12**) in December. However, all of these trends were reversed by February 2008. This suggests that both Fe(III)-reduction and SR were substantially enhanced between the December and February 'post-harvest' sampling dates.

In terms of the two dissolved organic parameters, pw[DOC] and pw[Acetate], the wild rice fields exhibited a much more pronounced increase in both, compared to the white rice fields (**Figure 6.14**). This may well be due to the fact that the wild rice fields were drained and harvested a full 1.5 months prior to the white rice fields (**Figure 3.6**). Thus, the remaining straw associated with the wild rice fields had that much longer to decay, and the concentrations of these parameters to build up in surface sediments. This longer time frame for organic matter decay may be reflecting in the significantly higher February pw[Fe(II)] concentrations in the wild rice fields compared to the white rice fields (**Figure 6.11A**), suggesting a stronger response of the Fe(III)-reducing bacterial community. Acetate concentration is a much better surrogate measure of the class of organic matter used by Fe(III)-reducers and sulfate reducers, than is DOC. It is thus noteworthy that only the agricultural fields with decaying rice straw exhibited a significant increase in pw[Ac] in the post-harvest season (compared to the growing season), while fallow fields exhibited a significant decrease in pw[Ac] (**Figure 6.15**). This finding, coupled with the fact that by February, Fe(II) and TRS build-up was significantly higher, and SR rates were generally higher, in fields with decaying rice straw than in fallow agricultural fields (**Figures 6.8 and 6.11**), supports our conclusion that the management practice of decaying rice straw via reflooding alone stimulates heterotrophic microbial activity, and subsequently Hg(II)-methylation, in surface sediment.

7 Detailed Results for Plant-Mercury Interactions

The data reported in this section relates to summary **Section 3.3: Methylmercury Production in Surface Sediment.**

7.1 Introduction

Vegetation can influence sediment biogeochemistry in both terrestrial and wetland ecosystems through plant:soil feedbacks (**Ehrenfeld et al., 2005**). A primary influence on sediment biogeochemistry is rhizosphere activity and physiology (**Marschner, 1986**). Root:soil interactions affect a number of processes and geochemical characteristics in the rhizosphere zone, including a) microbial community structure and activity (**Bagwell et al., 1998; Hines et al., 1989; Borga et al., 1994; Westover et al., 1997**), b) dissolved organic carbon quality (**Hines et al., 1994; Garland et al., 1996; Cheng et al., 2003**), c) the concentration and availability of electron acceptors to microbes (**Roden and Wetzel, 1996; Blaabjerg and Finster, 1998; Lee et al., 1999**), and d) nutrient/contaminant speciation (**Marins et al., 1997; Windham and Ehrenfeld, 2003; Jacob and Otte, 2003**). Further, the structure and quality of aboveground biomass influences physical dynamics (e.g. sediment irradiation) as well as the pulsed supply of decaying litter post-senescence. The abiotic processes and microbial activies that influence MeHg production are likely influenced spatially and temporally by this suite of physical, chemical and biological feedbacks from plants. Surface soils, with high root densities or supplies of aboveground labile carbon, are perhaps the most important ecosystem horizons for MeHg production, as MeHg production is typically the greatest in these zones (**Gilmour et al., 1998**) and because MeHg pools from this horizon are most likely to become suspended or diffuse into surface waters (**Langer et al., 2001**). Temporal inputs of organic matter have also been shown to drive MeHg in field and lab conditions (e.g**. Hall et al., 2004**).

7.2 Approach

7.2.1 Seasonal Comparison

In the Yolo Bypass Wildlife Area (YBWA), three types of flooded agricultural wetlands (white rice, wild rice and fallow fields) and three non-agricultural managed wetland areas (one seasonally flooded and two permanently flooded) were studied. Plant samples and structure were assessed in order to determine their physical and biogeochemical influences on mercury cycling, as well as carbon, nitrogen, sulfur, and iron. Of the two agricultural fallow fields, one was devoid of vegetation (barren fallow) and the other had a densely rooted mixed plant community (vegetated fallow). Field and dominant vegetation descriptions are given in **Table 7.1.** Vegetation sampling overlapped with sediment sampling schedules (**Figure 3.6**). Seeds were collected at the time of maturity - August for wild rice, August and December for white rice, and December for cattail and tule plants in the permanent wetland.

The above and belowground plant community was characterized for each field at all 5 major sampling events (June, July, August, December 2007 and February 2008) for total live biomass (g m^{-2}), rooting depth, and leaf area index (a ratio of leaf area to planar area). Samples were collected in triplicate for each sampling event, and a mean and standard deviation were calculated for seasonal and spatial comparisons.

Fresh leaf, root and seed tissues (50-100 g wet weight) were subsampled in the field, with ~50g refrigerated until further processing, and ~20-50 g flash frozen for Hg and MeHg analyses.

Within 72 hours of collection, refrigerated leaf surfaces and live root tissues (separated from sediments as described below) were rinsed with deionized water and a 1% EDTA solution to remove loosely sorbed THg particles and other particulates, and then freeze-dried. Tissue concentrations and isotopic ratios of carbon (C) and nitrogen (N) were measured using a Carlo-Erba elemental analyzer in tandem with a Micromass Optima system. Tissue THg concentrations were analyzed using a microwave-assisted nitric acid (HNO_3^-) digestion followed by Hg analysis on a Tekran 2600 automated CVAFS unit, according to **DeWild et al.** (**2004**), a modified version of EPA 1630. MeHg concentrations were measured with a KOH:methanol extraction followed by ethylation and CVAFS, as per **Bloom (1993**). Along with biomass data, these concentrations were used to calculate standing stocks of C, N, THg and MeHg, as well as ratios of carbon:nitrogen (an index of carbon lability) and MeHg:Hg (an index of MeHg production and uptake).

Root density and depth profiles were collected from plots using 30 cm deep cores, which were temporarily preserved on wet ice to slow microbial processes. The cores were cut into 2 cm depth intervals in the laboratory. Surface sediment (0-2 cm depth) was sampled concomitantly in neighboring devegetated and vegetated plots, using 2 cm deep (6 cm i.d.) pre-cut polycarbonate core rings. Between 5 and 10 surface sediment cores (0-2cm, "patties") were collected per plot using 6cm (i.d.) polycarbonate rings and composited into two glass mason jars (1 pt). These surface sediment composites were analyzed for sediment chemistry and physical characteristics as listed in **Table 6.1**. Three additional surface sediment cores (patties) were collected at each site for analysis of root biomass and root density in the 0-2 cm depth interval. Live roots were manually harvested with forceps and rinsed of soil particles, then visually identified by turgidity and color. A subsample of live roots were subjected to a vital stain (1% tetrazolium red) followed by dissection under 40x magnification, to assess errors of commission (< 5% for all samples collected). Live roots for each replicate surface sediment core were rinsed thoroughly and then assessed for volume by displacement of deionized water in a 50 or 100ml graduated cylinder. These samples were then freeze dried and weighed to assess root dry biomass. These root density data, collected from discrete 0-2 cm cores, were compared with the 0-2 cm data from the 0-30cm deep root profiles, and in all cases, the root profile biomass from this 0-2cm surface interval was found to be within ±1 standard deviation of the biomass calculated using the surface sediment cores.

7.2.2 Devegetation Experiment

For each vegetated plot, a neighboring devegetated plot with similar initial edaphic conditions was established. Prior to seeding and floodup, and at least 2.5 months prior to sample collection, 1 m^2 devegetation plots were established in triplicate in each of the agricultural fields to prevent the growth of plant material. In the already vegetated permanent wetlands, a single 2 m^2 plot was established by clipping aboveground biomass (live and dead) to the ground surface and removing this material from the plot. A spade was used to cut roots with a 30 cm deep slit along the edge of the plots to inhibit root growth and root-mediated inputs to the devegetated plots. All plots were covered with professional-grade water-permeable landscape cloth, to shade the sediment and inhibit vegetation regrowth during the study period. Plots were revisited 2-3 times during the growing season to retrench devegetated plots and to measure primary productivity in adjacent vegetated (control) plots.

At the growing season peak (June-December depending on the wetland type), plots were revisited and the landscape cloth lifted to access the underlying sediment surface, and sampled the same way as described in **Section 6.2**. In addition, surface sediment (0-1 cm depth) were collected to assess concentrations of benthic microalgal abundance using a modified version of **Parsons et al. (1984)**, with centrifugation, extraction and spectral analysis of chlorophyll a and phaeophytin pigments.

Net concentration changes in the three measured sediment iron species (Fe(II), aFe(III) and cFe(III)) (normalized per day) were calculated in the agricultural fields – using the *in situ* concentration difference between July and August for the fallow fields, and June and August for the rice fields, the dates most closely related to flood-up and peak biomass for a given field type. Although Fe(III)-reduction rates were not directly measured in short term incubations, as were rates of microbial sulfate reduction, total measured iron concentration in bulk sediment (Fe_T = Fe(II) + aFe(III) + cFe(III)) was generally consistent through time (17-19 mg g^{-1}), which allowed us to calculate an average net daily rate of change in each of the three iron pools as a surrogate for iron-cycling rates over the growing season. The aFe(III) concentration data was also used as an indicator of conditions favorable for iron reduction (**Roden, 2008**), as discussed in **Section 6.4.2**.

7.2.3 Decomposition Assay

Carbon mineralization and the release of THg during tissue decomposition were assessed experimentally with laboratory incubations of August 2008 samples from the six agricultural fields and the 2 permanent wetland communities. Leaves were first rinsed in a 1% EDTA solution, followed by deionized water and blotted dry. For each treatment, 4.8-5.2 g of freeze-dried ground leaf tissue were added to each of 40 Pyrex glass centrifuge tubes (50ml), with 5 additional centrifuge tubes acting as a control solution with no leaf material added. A 40.0 ml aliquot of deionized water (Ultrapur MQ) was added to each of the 45 vials at the start of the incubation. Samples were incubated under oxic conditions (tested weekly for sulfide presence) at 30°C while gently shaken (50 rpm) on a gyration table within a temperature-regulated incubator. Subsamples (5ml) were collected from each vial days 0, 1, 7, 14 and 28 for time-point processing. The incubation water was monitored for volume each week and used to correct for total mass of solution. Hg concentrations in this initial incubation water were less than 0.2 ng L^{-1}, and in control vial concentrations remained within 25% RSD of the initial concentration throughout the experiment

Upon retrieval, splits were made for dissolved THg analysis (filtration through acid-clean 0.45 nylon filters) and DOC analysis (GFF filtration at 0.6 μm and preservation at 0.1%v/v phosphoric acid). Particulate mass (detritus) removal was calculated from mass on these preweighed GFF filters. A subsample of filtrate was acid-preserved for dissolved organic carbon concentrations, analyzed on a Shimadzu TOC analyzer. The remaining filtrate was returned to the centrifuge tube and 200 ul of BrCl (0.5% v/v) was added to preserve and extract any Hg that may have adsorbed to the vial walls. This incubation filtrate was then heated overnight at 70°C and analyzed for total Hg concentration by CVAFS according to EPA 1630. Tissue decomposition rates were assessed with laboratory incubations on freezedried, ground leaf tissues from all fields except F20 (fallow, barren). A single dominant species - *Cyperus difformis* (sedge)- was chosen to represent decomposition within the mixed fallow field (F66).

Tissue samples of known weight (5g ± 0.2g) were added to pyrex centrifuge tubes, followed by 40ml of deionized water. Replicate (n=5) vials were filled for all 8 treatments (7 field treatments + 1 control). Vials were incubated at 30º C for 28 days and were kept aerobic and non-stratified by continuous shaking at 40rpm. On days 1, 7, 14, and 28, subsamples of 5ml of water were removed from the vials and prepared for analysis of particulate material, aqueous THg and DOC by filtration and preservation. Subsamples were also checked for dissolved oxygen concentrations and were > 10% saturation in all cases. Volume loss to evaporation was recorded to the nearest ml, and represented approximately 2-3ml per week. Final calculations of mass loss included the initial vs. final particulate material in each vial. These differences were used to calculate a logarithmic decay rate (k) based on laboratory conditions. To estimate decay rates under field conditions, laboratory measurements were scaled according to a Q_{10} of 2.44 (**Gu et al., 2004**), on monthly timesteps of average monthly temperatures as recorded by CDFG at El Macero Station (Yolo Bypass). These rates were then combined with initial biomass pools (aboveground biomass in August), and the date of litter deposition (harvest date or for fallow fields, drawdown date) to estimate the poolsize of surface detritus through time within each field type.

7.2.4 Statistics

Statistical analyses were performed using SPlus 7.0 (Insightful Corp. 2001). Data from the 10 sites were categorized by site and/or treatment (vegetated control plot versus devegetated plot). Data were assessed for significance between discrete field types and for Pearson correlation and/or linear or logarithmic regression analysis of parameters within given field types. Only significant correlations are reported ($p<0.05$), as assessed by comparison with t_{crit} for a two-tailed distribution and df=1. Regressions are reported for predictive relationships with $p<0.05$. We do not report absolute difference between vegetated and devegetated plots, unless explicitly noted. Instead, we focus on the relative effects of devegetation, as a way to interpret the major vegetation effects across multiple habitat types. For each site specific vegetated-devegetated plot pair, a relative metric for the magnitude and direction of the devegetation effect (%DevegEffect) had on a given parameter (e.g. X = k_{meth}, Hg(II)R, MeHg, etc…) was calculated as the % difference between devegetated and vegetated control plots, such that:

Equation 7.1

$$\%DevegEffect = (X_{vegetated\ plot} - X_{devegetated\ plot})/X_{vegetated\ plot}) \times 100$$

Normality of each parameter was assessed with Kolomogorav-Smirnov tests, and non-parametric data were log-transformed. Although the devegetation effect was profound enough for some measured parameters to warrant direct ANOVA comparisons of vegetation status (vegetated vs. devegetated), the calculation of the %DevegEffect metric for paired plots provides a clearer sense of the devegetation effect across a continuum of wetland conditions. Pairwise t-tests were used to test paired (vegetated / devegetated) plots for the signficant influence of devegetation within a given habitat category.

7.3 Results

7.3.1 Vegetation Productivity/Growth

Vegetative growth was rapid in the cropped fields (**Figure 7.1**). Over 76 days, between the June and August sampling events, the white rice fields generated 2.1 ± 0.2 kg m^{-2} above ground plus below ground biomass (average of R31 and R64), and the wild rice fields generated 1.5 ± 0.3 kg m^{-2} above ground plus below ground biomass (average of W32 and W65).

Leaf area index, a function of above ground growth, also rose quickly over the growing season for agricultural fields, reaching maximum cover in August at greater than 2.5 in three of the four rice fields (**Table 7.1**). In comparison, live aboveground biomass was consistently high in the vegetated permanent wetland sites, with leaf area indices greater than 2 for most of the year. Fallow fields were barren until flooded, and then gained 0.4 ± 0.1 kg m^{-2} at field F66. Belowground biomass (roots/rhizomes) represented less than 20 % of total biomass in white rice fields, less than 10% of total biomass in wild rice fields, but up to 35% of total biomass in the permanent wetland tule stand.

Density of live roots in surface sediments reached a seasonal maximum in August within agricultural fields, but remained constant in the permanent wetland sites. Live root densities were greatest for surface soils in white rice fields, reaching up to 10% of soil volume, whereas wild rice fields were fairly consistent with root densities of 5% (**Figure 7.2**). White and wild rice fields in the southern block (R64 and W65) had 3-9 fold greater variation between samples within a given sampling date than did fields in the northern block (R31 and W32), which is likely due to uneven early recruitment within these fields. Live root biomass and density increased over the growing season (**Figures 7.1, 7.3**), with the exception of white rice in field R31, where the average density of live roots decreased from 10% to 6% from July to August (**Figure 7.3**). High root mortality was observed on R31, where the highest surface water temperatures of the study were also observed (>38°C, see QA for water quality parameters in **Appendix 1**).

The most significant differences in tissue quality parameters were found between plant type, and not between blocks ($p>0.05$) or across season ($p>0.05$). Not only was leaf tissue biomass more abundant than seed or root biomass, they also showed the highest concentrations of nitrogen (**Table 7.2**). Tissue nitrogen concentrations varied strongly between species, with the highest leaf N concentrations observed in fallow field weeds (2.9%), followed by white rice (1.4±0.4%), and then by wildrice (0.5±0.1%). This led to over a 3-fold variation in carbon:nitrogen (C:N) ratios between the two crops, white rice (28±11) and wildrice (92±21), and to over a 4-fold variation in biomass N pools between white rice (18 ± 4 g m^{-2}) and wild rice (4 g ± 1g m^{-2}).The fallow field weed (sedge, *Cyperus difformis*) was similar to white rice in C:N ratios (20±3), but its low biomass led to a low pool of N in biomass (5.6 g ± 0.6g m^{-2}). Surprisingly, the leaf tissue C:N ratios of cattail (59±23) and tule (50±14) were similar, and tended to be lower than wild rice C:N ratios. Another notable difference by species was the high ash content (loss on ignitition, LOI) in white rice (up to 2% leaf tissue composition). Elemental analysis by ICP-AES suggested that the silica comprised the majority of this mineral component in all species. Although ash, silica or %C contents were not significantly different between species, LOI and %C were positively correlated ($r = 0.86$), suggesting that the mineral or ash component directly reduced carbon concentrations, and thus, plays a direct role in diluting carbon pools in standing stock biomass and later during litter decay on the sediment surface.

Tissue concentrations of THg also varied by species, but not between blocks ($p<0.05$) or across season ($p<0.05$). THg concentrations were greatest in roots, ranging from 104 ng g^{-1} in cattail fine roots to 282 ng g^{-1} in white rice fine roots. Analysis of aluminum concentrations in root tissues (and all tissues) illustrated that soil contamination represented less than 0.1% of the root sample, and thus cannot account for these high concentrations. No differences were observed between plant types for root concentrations of THg, but leaf concentrations varied by almost 1 order of magnitude between species, with leaf [THg] of 104 ± 8 ng g^{-1} in wild rice leaves and 14 ± 3 ng g^{-1} in white rice leaves. Non-crop species (sedges and cattails) all showed similar leaf tissue concentrations of 30-55 ng g^{-1}. The low THg concentration in white rice leaf tissue was notable, considering the comparably high THg concentrations in plant roots. Further, there was greater than a 6-fold difference in THg pools associated with leaf tissue biomass between white rice and wild rice fields (15 μg m^{-2} and 100 μg m^{-2}, respectively). The importance of these THg leaf tissue biomass pools, however, are small compared to the sediment THg pools in all agricultural fields (5240-6270 μg m^{-2} for the surface 0-2 cm interval), and comparable to sediment $Hg(II)_R$ pools (44-120 μg m^{-2} for the surface 0-2 cm depth interval), as calculated from the summary data given in **Table 6.2**.

Tissue concentrations of MeHg were similar among agricultural crops, but the permanent wetland species (tule and cattail) had 3-fold lower concentrations in their leaves (0.5 ng g^{-1}), 10-fold lower concentrations in their roots (1.1 ng g^{-1}), and 5-fold lower concentrations in their seeds (0.5 ng g^{-1}). MeHg concentrations were not correlated with THg concentrations and in many cases showed opposite patterns. While MeHg represented 8-9% of the THg pool in white rice seeds, MeHg constituted 37-60% of the THg pool in wild rice seeds (**Table 7.2**). No seasonal or block patterns were observed, but MeHg concentrations were significantly greater in agricultural crop tissues than permanent wetland species roots ($p=0.0032$), leaves ($p=0.0004$) and seeds ($p<0.0001$), following the same pattern observed in sediment MeHg concentrations (**Tables 6.2 and 6.3**). The highest tissue MeHg concentrations observed were in seeds (4.2 ± 1.1 ng g^{-1} in white rice, 6.2 ± 1.5 ng g^{-1} in wild rice), and seed [MeHg] was better correlated with root [MeHg] ($r = 0.90$) than leaf [MeHg] ($r = 0.61$). A separate analysis of [MeHg] on seed husks for wild rice showed the highest concentrations of all tissues (up to 9 ng g^{-1}), but this portion is usually removed in the crop storage and preparation process.

7.3.2 Vegetated vs. Devegetated Responses

Despite differences in hydrology and vegetation among the freshwater wetland types studied, the activity of Hg(II)-methylation bacteria (as k_{meth}) consistently decreased (17 to 87%) as a result of devegetation, in all sub-habitats except in the cattail dominated wetland (**Figures 7.4 and 7.5**, **Table 7.3**). Similarly, sediment MeHg concentration significantly decreased (13 to 55%) in all sub-habitats except for wild rice fields. The effect of devegetation on sediment $Hg(II)_R$ concentration was more varied, with a decrease in the vegetated fallow field, and an increase in the barren fallow field and in both the tule- and cattail-dominated wetlands, and non-significant changes in both rice field settings and in the Yolo seasonal wetland. The combined effect of k_{meth} and $Hg(II)_R$ concentrations on calculated MP rates thus resulted in the situation where MP significantly decreased due to devegetation in both rice field sub-habitats and the vegetated fallow field in Yolo. The concentration of pw[Ac] consistently decreased (63 to 99%) with devegetation across all freshwater sub-habitats (**Table 7.3**). While we found a significant

devegetation effect on benthic ChlA (an indicator of algal biomass in surface sediment), estimated algal biomass was quite low in all fields (<1.0 g m^{-2}), and was especially low in the white rice fields (<0.2 g m^{-2}) where the largest devegetation effects were observed. The devegetation effects on pw[Ac] and microbial activity are thus more likely to come from decreases in root density, as pw[Ac] concentrations were highly correlated with root density in agricultural fields through the growing season (r = 0.92).

Agricultural fields showed the strongest devegetation responses with respect to solid phase iron species (**Table 7.3**), including an increase in sediment Fe(II) and a decrease in sediment aFe(III) concentrations, whereas concentrations for the more abundant cFe(III) fraction were varied and not significantly different between treatments. Despite sulfate loading to both white and wild rice fields through fertilizer application (>50-75 kg SO_4^{2-} $acre^{-1}$), no significant effect from devegetation was observed in the white or wild rice fields for microbial SR rates or for reduced sulfur species concentrations. Devegetation-driven decreases in microbial SR rates were observed, however, in both fallow field settings and in the densely rooted tule permanent wetland (**Table 7.3**).

An examination of the change in Fe-species concentrations in agricultural fields showed significant decreases in cFe(III) and increases in Fe(II) over the growing season (from flood-up [June/July] until August), both trends indicative of net Fe(III)-reduction (**Figure 7.6A**). Devegetated plots showed the same general pattern of Fe(III)-reducing activity (a net decrease in cFe(III) and a net increase in Fe(II)) across all agricultural fields (**Figure 7.6B**). A direct comparison of vegetated versus devegeted plots, by difference [vegetated minus devegetated], indicates that the rates of Fe(II) increase were greater for devegetated plots (negative differences) for 5 of the 6 fields studied (**Figure 7.6C**), suggesting modestly higher net rates of Fe(III)-reduction in the devegetated sites associated with both white rice and wild rice fields, and a significantly higher net rate of Fe(III)-reduction in the devegetated site associated with fallow field F66. The exception to this trend was seen for the "devegetated" barren fallow field F20, where the [vegetated minus devegetated] difference in the Fe(II) net rate of change was clearly positive and the difference in the cFe(III) net rate of change was clearly negative (**Figure 7.6C**), suggesting that for field F20 the devegetated site had a significantly lower rate of net Fe(III)-reduction than its vegetated pair for the July thru August time period. For most of the other fields, the [vegetated minus devegeted] difference in the net rate of change for the cFe(III) pool was non-significant, based upon the error bars, the exception being wild rice field W65, which was strongly positive and again reinforces the conclusion that the devegetated site had a higher net rate of Fe(III)-reduction than did its vegetated pair.

In terms of elucidating the spatial trends in microbial Fe(III)-reduction among fields and for the vegetated versus devegetated plots (to explore the 'plant effect'), the above examination of the net changes in the Fe(II) and cFe(III) pools seems obvious, simply from their abundance on the three plots of **Figure 7.6**, relative to aFe(III). However, aFe(III) is a critical component of the Fe-cycle in that it is much more readily available to Fe(III)-reducing bacteria than is cFe(III) due to the very high surface area associated with its poorly crystalline (amorphous) structure (**Roden and Zachara, 1996**). Further, a Fe(III) is an active intermediary component of the iron cycle, and thus not likely to build up over longer periods of time. Thus, the small aFe(III) pool size in sediment relative to cFe(III) (e.g. 20 to 36-fold smaller across all agricultural fields, 33 to 850-

fold smaller across all non-agricultural wetland sites; based on mean values in **Table 6.2**) may be particularly important due to its relevance as an electron acceptor in these wetland habitats; as Fe(III)-reducing bacteria are effective at utilizing it when it is available. Further, aFe(III) concentrations were shown to be proportional to Fe(III)-reduction rates (**Roden and Wetzel, 2002**), as noted in **Section 6.4.2**. Thus, while the absolute concentrations (**Table 6.2**) and subsequently the calculated net rates of change of aFe(III) pools appear small (**Figure 7.6**), that pool is likely turning over very quickly at shorter time scales than were addressed in this study.

During the growing season, there was a significant net decrease in aFe(III) concentration over time in three of the four rice fields (R64, R31 and W32) for both the vegetated (**Figure 7.6A**) and devegetated (**Figure 7.6B**) plots, as well as the devegetated plot in fallow field F66 (**Figure 7.6B)**. All of these net changes in aFe(III) corroborate the conclusions reached from the above examination of the Fe(II) and cFe(III) data, and again suggest active Fe(III)-reduction in these locations. In further support for active Fe cycling, sites/treatments that exhibited a significant net increase in aFe(III) over time, indicative of the (re)oxidation of Fe(II) to aFe(III), included vegetated sites W65, F66 and F20 (**Figure 7.6A**), as well as devegetated site F20 (**Figure 7.6A**). In examining the [vegetated minus devegetated] differences in the aFe(III) rate of change (**Figure 7.6C**), a few things are evident: a) there is no statistical difference between vegetated and de-vegetated plots in two of the rice fields (R64 and W32); b) there is a modestly higher rate of aFe(III) production (Fe(II) reoxidation) in the vegetated sites associated with the other two rice fields (R31 and W65), and there is strong evidence for this in fallow field F66. In contrast, there is evident for a moderately lower rate of Fe(II) reoxidation in the vegetated site, compared to the devegetated site, for field F20.

The importance in considering the rate changes associated with this seemingly small aFe(III) pool is that it represents the portion of the Fe-cycle that cycling quickly between processes of Fe(III)-reduction and Fe(II)-reoxidation. While the absolute changes are small, compared to Fe(II) and cFe(III) when assessed over these relatively long time periods (1-2 months), the direction and magnitude of shift my shed some light onto what sites are most dynamic with respect to Fe-cycling in general. Thus, those sites exhibiting small but significant increases in aFe(III) in the [vegetated minus devegetated] comparison over time – and especially sites exhibiting increased aFe(III) concentrations at the same time that Fe(II) concentrations are increasing (especially F66, and W65) – may be reflective of the sites that are actually most active with respect to microbial Fe(II)-reduction, and Hg(II)-methylation, under typical vegetated conditions.

7.3.3 Relationship between microbial devegetation effects: implications for sulfur and iron cycling

Pearson correlation analysis was used to assess the correspondence of devegetation effects among the parameters, and to identify significant biogeochemical interactions. When compared across all wetland settings, %DevegEff for aFe(III) positively correlated with both the %DevegEffect for $Hg(II)_R$ ($r = 0.66$) and the %DevegEffect for MP ($r = 0.73$). Thus, in wetlands where sediment aFe(III) concentration were significantly decreased due to devegetation, MP showed the most substantial decreases (**Windham et al., 2009**). Because lower rates of aFe(III) production is indicative of a lack of Fe(II)-reoxidation back to aFe(III), this relationship suggests that Fe(II)-reoxidation may be important in driving higher rates of MP in the vegetated (control)

sites, by resupplying aFe(III) as an electron acceptor for a subset of the Fe(III)-reducing microbial community that may be involved in Hg(II)-methylation (e.g. geobacter; **Roden, 2008**). Because the most significant devegetation effects associated with mercury cycling (ie. k_{meth}, MP, %MeHg, $Hg(II)_R$ and MeHg concentration) were predominantly associated with significant changes in iron speciation, our data point to an important linkages between iron Fe biogeochemistry and MeHg production dynamics in these agricultural and managed wetlands.

.

7.3.4 Decomposition Assay

Laboratory assays of decomposition rates were rapid for rice, wild rice and fallow species (>4% day) and significantly slower for permanent wetland species tule and cattail (2%, **Table 7.4**). Log-based calculations of k (d^{-1}) were similar through the entire incubation except for intial leaching. With 5-14% of initial mass lost in the first day of incubation for rice, wild rice and the fallow species, these plant tissues were highly labile as compared with the more waxy and lignin-rich tissues of tule and cattail (<2% mass lost on the first day of incubation). Loss on ignition showed high ash contents in wild rice (1.3 ± 0.9%) and white rice (1.9± 1.0%). Elemental analyses suggest high silicate concentrations in both rice tissues, approaching 2% in white rice. Rates of mass loss were clearly a function of tissue quality, specifically C:N ratios (R^2=0.71, **Figure 7.7**) as per **Melillo et al. (1982**), and less so a function of lignin concentrations were (R^2=0.24). Multiple regression analyses support the importance of %N as the primary driver of decay dynamics.

When scaled to field conditions, surface litter areal mass was highest in white rice fields and lowest in fallow fields (**Table 7.4**). These patterns were found to be correlated with two key sediment characteristics expected to relate to labile carbon supply: pw[Ac] (r = 0.71) and microbial Hg(II)-methylation rate constants (k_{meth}, r = 0.68). The role of labile carbon as a driver of Hg(II)-methylating bacteria activity was particularly apparent during February 2008, the period during which the decay of rice straw was being actively facilitated with managed reflooding of the previously harvested rice fields and when the strongest relationship between pw[Ac] and k_{meth} was seen (**Figure 7.8**). Further, the terrestrial signal associated with the characterization of surface water DOC quality was correlated with estimates surface litter areal mass (Jacob Fleck, pers. obs).

7.4 Summary/Discussion

The role of vegetation was significant at different timepoints of the year based on the importance of key processes. During the growing season, remarkably high production of biomass in the white and wild rice fields led to large amounts of root material (180-300 g m^{-2}) concentrated within the upper 5cm of sediment. In cropped fields, root density was highly correlated with mercury methylation rates in the top 0-2cm of soil. Further, the experimental removal of active rhizosphere processes led to significant biogeochemical changes – specifically a reduction in MeHg production and sediment MeHg pools. These were accompanied by sharp drops in the concentration of pw[Ac], suggesting that the primary influence of vegetation in active ricefields is the production of labile carbon for microbial activity. Further, it suggests these relationships suggest that microbial methylation was carbon limited within these fields. In

addition, significant limitations of aFeIII supply were observed in devegetated plots, accompanied by decreases in Cl concentrations. These data, in conjunction with hydrologic estimates of evaporation (**Section 5**) and isotopic evidence of pore water sulfide reoxidation (**Section 6**), suggest that transpiration-driven oxidation of the surface soil may have played a key role in regenerating pools of amorphous iron for use by iron-reducing bacteria. These are among the first data to support the significance of iron reducing bacteria in MeHg production at the ecosystem scale (**Windham et al., 2008**).

During vegetative senescence in winter months, live roots were observed but were not correlated with MeHg production or concentration. Instead, abundant surficial detritus in white ricefields was observed and estimated poolsizes at the field scale were significantly correlated with rates of MeHg production. Estimates of surface detritus were correlated with both pw[Ac] concentrations (labile carbon) and the relative terrestrial signature of DOC in surface water (index of fresh carbon supply), suggesting that MeHg production is also carbon-limited in winter months, and that decaying ricestraw is a key driver in C supply (**Figure 7.8**).

Pools of THg and MeHg in plant biomass were <10-100 fold lower than surface sediment pools (0-1cm depth), suggesting that although uptake may be active, vegetation represents a relatively small sink for MeHg and Hg compared to sediment processes. In aboveground biomass, MeHg concentrations were lowest in stem tissue (<1 ng g^{-1}) and elevated in seed (up to 6 ng g^{-1} in wild rice).

8 Detailed Results for Methylmercury Bioaccumulation

The data reported in this section relates to summary **Section 3.4: Methylmercury Bioaccumulation.**

8.1 Introduction

It is widely recognized that MeHg biomagnifies through aquatic food chains and is a potent neurotoxin (**Wiener et al., 2003a**). In addition, wetlands often have higher rates of MeHg production than other aquatic habitats, in part because ambient conditions common within wetlands are generally conducive to MeHg production (**Zillioux et al., 1993; Marvin-DiPasquale et al., 2003; Hall et al., 2008**). Fluctuating water levels that are typical of intermittently and shallowly-flooded wetlands also can enhance the release of MeHg from sediments (**Morel et al., 1998**). As such, wetlands are known to contribute substantially to MeHg bioavailability within downstream environments (**Hurley et al., 1995; Krabbenhoft et al., 1995; Rudd, 1995; Krabbenhoft et al., 1999**) as well as to *in situ* bioaccumulation (**Snodgrass et al., 2000**). Unfortunately, specific wetland habitat types and management practices that might alter MeHg production and bioavailability remain unclear (but see **Snodgrass et al., 2000; Harmon et al., 2005; Rumbold and Fink, 2006**).

Our goal in the current study was to evaluate how different wetland management practices influenced MeHg bioavailability. We used invertebrates and fish as our indicators of Hg bioaccumulation. Specifically, our main objectives were to determine if invertebrate and fish Hg concentrations (1) differed among wetland habitat types, and (2) varied within fields from water inlets to outlets. Although not funded as part of this original study, data collected in addition to that supporting the above project objectives included Hg contamination in caged fish, and in a second species of invertebrate (Notonectidae). Subsequently, we have included that recently published data (**Ackerman and Eagles-Smith, 2010; Ackerman et al., 2010**) as part of this report for a more comprehensive assessment of Hg bioaccumulation within the Yolo Bypass.

8.2 Study Design and Methods

8.2.1 Study Site

We assessed MeHg bioaccumulation within wetlands at the Yolo Bypass Wildlife Area (38.33º N, 121.4º W). The Yolo Bypass Wildlife Area is approximately 6,475 ha and is located within the Yolo Bypass - a 23,877 ha floodway that provides flood protection as part of the Sacramento River Flood Control Project. It is common for the Yolo Bypass to flood each spring when Sacramento River waters are high due to spring runoff. During these flood events, MeHg is transported downstream into the Sacramento-San Joaquin River Delta. Both seasonal wetlands and agricultural fields are flooded during the fall and winter to provide habitat for wintering waterfowl and shorebirds.

8.2.2 Invertebrate Study

We studied MeHg bioaccumulation within two fields each of white rice, wild rice, permanent wetlands, and shallowly-flooded fallow fields. We sampled two taxa of aquatic macroinvertebrates at the inlets, centers, and outlets of each of the 8 wetlands during two time periods bounding the rice growing season and corresponding to flood-up and pre-harvest (96 total samples). White rice fields were initially flooded, then the water was discharged within two

weeks for weed control, and thereafter re-flooded; we conducted our first sampling time period immediately after the fields were re-flooded for rice production. Because fallow fields were managed for migrating shorebirds, they were not initially flooded until late July. Our pre-harvest invertebrate sampling time period occurred immediately before the wild rice harvest in mid September. Thus, our flood-up invertebrate sampling occurred from 25 June to 6 July and our pre-harvest sampling occurred from 28 August to 19 September for all habitats, with the exception that fallow fields were sampled at flood-up on 30 July 2007.

We sampled aquatic invertebrates in the water column and submerged vegetation using D-ring sweep nets with 0.5 mm mesh (diurnal) and floating light traps (nocturnal). Light traps were constructed as described by **Marchetti and Moyle (2000)**, and were set at night and retrieved at dawn the following morning. We also used sweep nets at each site during trap deployment and retrieval to increase the biomass of invertebrates captured. We transported invertebrates from the field in fresh source water on wet ice and stored them in the refrigerator for 24 hrs to allow the passage of inorganic Hg present in their digestive tracts. We then identified and sorted invertebrates with a dissecting microscope (10×) following **Merritt and Cummins (1996)**; genera were independently confirmed by the R. M. Bohart Museum of Entomology, University of California, Davis. We sampled invertebrates from each site until we reached a biomass of >3 g wet weight each of Corixidae (Order Hemiptera, Family Corixidae, Genus Corisella, water boatmen) and Notonectidae (Order Hemiptera, Family Notonectidae, Genus Notonecta, back swimmers). We stored invertebrates in Whirl-paks® (Nasco, Modesto, California, U.S.A.) at -20°C until Hg analysis.

8.2.3 Caged Fish Study

We built rectangular enclosures that were 454 L and measured 122 cm × 61 cm × 61 cm (L × W × H) using 6 mm polypropylene aquaculture mesh (Industrial Netting, Minneapolis, Minnesota, USA) affixed with cable ties to a polyvinyl chloride (PVC) pipe frame. We drilled holes in the PVC pipe frame to reduce buoyancy. A similar cage design was used successfully to examine diet and growth rates of caged juvenile chinook salmon (*Oncorhynchus tshawytscha*), and they showed that the 6 mm mesh netting allowed adequate movement of prey items such as zooplankton and macroinvertebrates to enter the enclosure (**Jeffres et al., 2008**). For cages in permanent wetlands, we affixed two 130 cm long × 7 cm diameter closed-cell foam floats to each side of the cage so that the top of the cages floated about 15 cm out of the water. In white rice and wild rice fields, we attached each cage with cable ties to 3/16 inch rebar stakes that were driven into the substrate on each side of the fish cages. To avoid fatalities from accidental drainage or low water events, we positioned the cages in slightly deeper locations of the field so that the top also was about 15 cm out of the water. We placed fish cages approximately 15 m from the water inlet and outlet within each wetland.

Western mosquitofish for our study originated from the same stock at the Sacramento-Yolo Mosquito and Vector Control District's aquaculture facility (D. Dokos, Elk Grove, California, USA). We transported mosquitofish from the aquaculture facility to the Yolo Bypass Wildlife Area (about 25 miles) during the early morning in water-filled, closed ice chests that were kept oxygenated with battery powered aerators. We measured standard length (mm) with a ruled fish board, fresh wet mass (g) using an electronic balance (Ohaus Adventurer™ Pro, Pine Brook, New Jersey, USA), and visually determined sex (**Moyle, 2002**) before their introduction into

cages. To determine baseline THg concentrations in fish at the time of introduction, we randomly selected 37 female mosquitofish from our stock population and recorded their fresh wet weight (g) and standard length (mm), and stored them frozen in Whirl-paks® (Nasco, Modesto, California, USA) at -20°C until Hg analysis.

We randomly selected 30 female mosquitofish for each cage and introduced them into cages placed at the inlet, center, and outlet of each of three wetland habitat types (white rice, wild rice, and permanent wetlands) on 28 June 2007, shortly after the white rice fields were re-flooded after being seeded. All fish were removed 60 days after introduction on 27 August 2007. Additionally, during deployment at each outlet, we placed 30 female mosquitofish into a second cage that was 15-20 m from the first outlet cage and these fish were removed at the mid-point of the 60 day exposure period on 27 July 2007 (29 days of exposure) to assess temporal bioaccumulation patterns. Each wetland habitat type was replicated twice; thus, we introduced a total of 24 fish cages (720 total fish) into six different wetlands. The density of mosquitofish introduced into cages was 0.07 fish L^{-1} of cage space, and the average biomass was 0.11 g of fish L^{-1}, which is a much lower density than most caging experiments assessing contaminant bioaccumulation (review by **Oikari, 2006**). Upon removal from cages, we re-measured each fish's fresh wet weight (g) and standard length (mm), and stored them frozen in Whirl-paks® (Nasco, Modesto, California, USA) at -20°C until Hg analysis.

8.2.4 Wild Fish Study

Using beach seines (3 mm mesh, 3 m or 6 m × 1.5 m) and dip nets, we also collected wild western mosquitofish and wild Mississippi silversides at each of the same wetland's inlets and outlets at the time when caged fish were removed (from 27 August to 19 September 2007). As with caged fish, we weighed (g) and measured the standard length (mm) of each fish, and stored them frozen in Whirl-paks® (Nasco, Modesto, California, USA) at -20°C until Hg analysis.

8.2.5 Mercury Determination

Prior to Hg analysis, invertebrates and fish were dried at 60°C for 24-48 h, ground, and then homogenized to a fine powder using a porcelain mortar and pestle. Initially, an aliquot of each Corixidae sample and a subset of caged fish were analyzed for MeHg at Battelle Marine Sciences Laboratory (Sequim, Washigton, U.S.A.) using cold vapor atomic fluorescence following EPA method 1630 (**U. S. EPA 2001**). We then analyzed the remaining aliquots of the same Corixidae samples and all the Notonectidae and fish samples for THg at the USGS Davis Field Station Mercury Lab, on a Milestone DMA-80 Direct Mercury Analyzer (Milestone Inc., Monroe, Connecticut, U.S.A.) following EPA method 7473 (**U. S. EPA 2000**). For 11 of the 92 invertebrate samples, we could not analyze THg because we were unable to collect enough biomass for both analyses. Because MeHg and THg were highly correlated (see Results), and the percent MeHg did not vary as a function of THg levels (see Results), we used MeHg concentrations and the average percent MeHg in Corixidae to estimate THg concentrations for 11 Corixidae samples. Quality assurance measures included analysis of two certified reference materials (either dogfish muscle tissue [DORM-2; National Research Council of Canada, Ottawa, Canada], dogfish liver [DOLT-3; National Research Council of Canada, Ottawa, Canada], or lobster hepatopancreas [TORT-2; National Research Council of Canada, Ottawa, Canada]), two system and method blanks, two duplicates, one matrix spike, and one matrix spike duplicate per batch. For invertebrate THg, recoveries (± SE) averaged 106.3±1.7% (*N*=9) and

101.1±1.7% (*N*=14) for certified reference materials and calibration checks, respectively. Matrix spike recoveries for THg averaged 98.3±1.3% (*N*=10), and absolute relative percent difference for all duplicates and matrix spike duplicates averaged 7.5±2.9%. For invertebrate MeHg, recoveries averaged 91.20±3.8% (*N*=3) for certified reference materials. Matrix spike recoveries for MeHg averaged 97.3±1.8% (*N*=12), and absolute relative percent difference for all duplicates and matrix spike duplicates averaged 7.8±1.6%. For fish THg, recoveries (± SE) averaged 99.4±1.8% (*N*=60) and 97.9±0.8% (*N*=90) for certified reference materials and calibration checks, respectively. Matrix spike recoveries for THg averaged 103.0±0.5% (*N*=30), and absolute relative percent difference for all duplicates and matrix spike duplicates averaged 3.4±0.5%. We report mean±SE THg and MeHg concentrations on a dry weight (dw) basis because Hg is associated with the solid protein lattice in fish tissue, and differences in moisture content among samples can substantially bias Hg results. However, for ease of comparison to other studies and regulation targets, moisture content (mean±SE) was 75.9±0.1% in caged mosquitofish, 73.1±0.2% in wild mosquitofish, and 72.8±0.1% in wild silversides.

8.2.6 Statistical Analysis: Invertebrates

We tested whether THg and MeHg concentrations in invertebrates differed among factors using backward elimination mixed effect analysis of variance (ANOVA), with alpha >0.10 to remove interactions using JMP® version 5.0 (SAS Institute, Cary, North Carolina, U.S.A.). The global mixed model included wetland habitat type (white rice, wild rice, permanent wetland, and fallow fields), site (inlet, center, and outlet), time period (flood-up and pre-harvest), taxa (Corixidae and Notonectidae; for THg model only) as fixed effects, wetland replicate as a random effect, and all 2-way and 3-way interactions of fixed effects. We found significant 2-way interactions for taxa × time period, taxa × wetland type, and time period × wetland type for the THg model, therefore we used conditional F-tests (slices) to test the effects of wetland type, time period, and taxa separately while accounting for all the other variables in the model. We then used pair-wise *t*-tests to make multiple comparisons. We calculated the proportion of THg in Corixidae that was in the form of MeHg by dividing the MeHg concentration by the THg concentration. We used linear regression to test whether MeHg concentrations were related to THg concentrations in Corixidae, and to test whether THg concentrations in Corixidae were related to THg concentrations in Notonectidae.

8.2.7 Statistical Analysis: Fish

We tested whether whole-body THg concentrations ($\log_e$-transformed) in caged mosquitofish exposed for 60 days differed among factors using a mixed effect analysis of covariance (ANCOVA) while accounting for any effects of fish size or body condition with JMP® version 8.0 (SAS Institute, Cary, North Carolina, USA). The global ANCOVA model for THg concentrations included wetland habitat type (white rice, wild rice, and permanent wetland), site (inlet, center, and outlet), fish standard length ($\log_e$-transformed), and relative body condition as fixed effects, wetland replicate as a random effect, and the wetland type × site interaction. We estimated the relative body condition of fish using the Relative Condition Factor to account for potential changes in shape as fish grow (**Anderson and Neumann, 1996**), such as often occurs in gravid female mosquitofish. The Relative Condition Factor was calculated as $K_n = W/W'$, where W was mass in g and W' was the predicted length-specific mean mass from a predictive model calculated for that population. To determine W' for the caged mosquitofish population,

we used $\log_{10}$-transformed standard length (mm) and $\log_{10}$-transformed fresh wet mass (g) data for the mosquitofish that were introduced into cages as well as the reference mosquitofish analyzed for Hg (caged mosquitofish linear regression: N=756, R^2=0.76, intercept=-4.3379, slope=2.8584). We also calculated W' for each species of wild fish using all the wild fish captured and analyzed for Hg (wild mosquitofish linear regression: N=140, R^2=0.95, intercept=-5.5443, slope=3.5573; wild silverside linear regression: N=135, R^2=0.95, intercept=-5.0217, slope=2.9583).

Total body burden of THg was calculated for each sample as the product of fish body mass (dw) and whole-body THg concentration. The global ANOVA model for total Hg burden ($\log_e$-transformed) in caged mosquitofish exposed for 60 days was similar to that for THg concentrations, except that this model did not include fish standard length or relative body condition as covariates since fish size was incorporated when calculating total body burden. Similarly, we tested whole-body THg concentrations ($\log_e$-transformed) and total Hg burden in wild mosquitofish and wild silversides using the same model structure as for caged fish, except that we only sampled wild fish from inlets and outlets, and not centers. There were significant interactions between wetland type and site in all models; we therefore used conditional F-tests (slices) to test the effects of habitat separately by site, and site separately by habitat, while also accounting for the other variables in the models. We then used pair-wise *t*-tests to examine which habitats and sites differed. We also used two-sample *t*-tests to compare THg concentrations and total Hg burdens of reference mosquitofish at introduction to values of mosquitofish removed from cages 60 days later, and we applied a sequential Bonferroni corrected alpha level to account for the number of tests performed (**Rice, 1989**). Unless otherwise noted, we reported model-based mean±SE THg concentrations and total Hg burdens based on back-transformed least-square means±SEs. The model-based SEs of the means were calculated by the delta method (**Williams et al., 2002**).

We also tested whether the size of mosquitofish removed from cages after 60 days of exposure differed among habitats and sites using a mixed effects analysis of variance (ANOVA). We performed separate ANOVAs for each of three size parameters ($\log_e$-transformed standard length [mm], $\log_e$-transformed fresh wet mass [g], and relative body condition). For each ANOVA, we included wetland habitat type (white rice, wild rice, and permanent wetland) and site (inlet, center, and outlet) as fixed effects, wetland replicate as a random effect, and the wetland type × site interaction. There were significant interactions between wetland type and site in all models (see Results); we therefore used conditional F-tests to test the effects of habitat separately by site, and site separately by habitat, while also accounting for the other variables in the models. We then used pair-wise *t*-tests to examine which pairs of habitats and sites differed. We also used two-sample *t*-tests to compare the size of fish at introduction to values 60 days later when fish were removed from cages, and we applied a sequential Bonferroni corrected alpha level to account for the number of tests performed for each variable.

Lastly, we assessed temporal THg bioaccumulation using only reference fish at introduction and mosquitofish caged at wetland outlets. For this analysis, we compared THg concentrations and body burdens among three time periods: 1) reference mosquitofish at introduction, 2) mosquitofish within the second outlet cage that was removed after 29 days of exposure, and 3) mosquitofish within the primary outlet cage that was removed after the full 60 days of exposure.

We used a similar mixed effects ANCOVA to our primary models, where THg concentration (log_e-transformed) was the dependent variable and wetland habitat type (white rice, wild rice, and permanent wetland), time period (reference, 29-day exposure, and 60-day exposure), fish standard length (log_e-transformed), and relative body condition were fixed effects, wetland replicate was a random effect, and wetland type × time period was included as an interaction. The global ANOVA model for THg body burden (log_e-transformed) was similar to that for THg concentrations, except that this model did not include fish standard length or relative body condition. For these temporal analyses, we randomly selected 12 of the 37 reference mosquitofish at introduction to be assigned to each of the three wetland habitat types at time zero to avoid pseudoreplication of reference fish among habitats.

8.3 Results

8.3.1 Invertebrates

Across all wetland habitat types and sampling time periods, THg concentrations were 0.89±0.06 µg g^{-1} dw in Corixidae (N=36) and 1.18±0.08 µg g^{-1} dw in Notonectidae (N=45). Notonectidae THg concentrations were not correlated with Corixidae THg concentrations (linear regression: N=31, R^2=0.01, P=0.96) or Corixidae MeHg concentrations (linear regression: N=43, R^2=0.02, P=0.42) collected at the same locations and time periods. MeHg concentrations in Corixidae were 0.74±0.05 µg g^{-1} dw (N=46). Corixidae MeHg concentrations were highly correlated with Corixidae THg concentrations (linear regression: N=34, R^2=0.80, p<0.0001; **Figure 8.1**). In addition, most of the THg in Corixidae was comprised of MeHg (88.0±3.1%) and the proportion of Hg in the form of MeHg was not correlated with THg concentrations (linear regression: N=34, R^2=0.01, P=0.99), indicating that the proportion of THg in the MeHg form did not vary with THg concentrations.

The final model from our backward elimination mixed effect ANOVA model for THg concentrations in invertebrates included wetland type, site, time period, and taxa as fixed effects, wetland replicate as a random effect, and taxa × time period, taxa × wetland type, and time period × wetland type as 2-way interactions (ANOVA: wetland type: $F_{3,3.94}$=3.16, P=0.15; site: $F_{2,71.88}$=3.84, P=0.03; time period: $F_{1,71.88}$=5.12, P=0.03; taxa: $F_{1,71.88}$=29.36, p<0.0001; time period × wetland type: $F_{3,71.88}$=4.03, P=0.01; taxa × wetland type: $F_{3,71.88}$=10.37, p<0.0001; taxa × time period: $F_{1,71.88}$=15.83, P=0.001). We therefore used conditional F-tests to further interpret the significant interactions to assess whether invertebrate THg concentrations differed among wetlands, taxa, and time periods.

8.3.1.1 *Site*

THg concentrations in invertebrates tended to increase from water inlets (least squares mean±SE: 0.92±0.08 µg g^{-1} dw) and wetland centers (1.01±0.08 µg g^{-1} dw) to water outlets (1.14±0.08 µg g^{-1} dw; **Figures 8.2 & 8.3**). In pairwise comparisons, THg concentrations in invertebrates at the outlet were significantly higher than THg concentrations at the inlets (difference: 0.21±0.08 µg g^{-1} dw; $t_{2,71.89}$=2.76, P=0.01) and THg concentrations at wetland centers did not differ from concentrations at inlets (difference: 0.09±0.08 µg g^{-1} dw; $t_{2,71.89}$=1.15, P=0.25) nor outlets (difference: 0.12±0.08 µg g^{-1} dw; $t_{2,71.86}$=1.61, P=0.11).

8.3.1.2 *Taxa × time*

THg concentrations in Notonectidae increased from the time of flood-up to pre-harvest (difference: 0.40±0.09 µg g^{-1} dw; $F_{1,71.86}$=18.14, p<0.0001), whereas THg concentrations in Corixidae did not differ between time periods (difference: 0.11±0.09 µg g^{-1} dw; $F_{1,71.90}$=1.60, *P*=0.21; **Figure 8.4**). Accordingly, THg concentrations in Corixidae did not differ from Notonectidae during the flood-up time period (difference: 0.09±0.10 µg g^{-1} dw; $F_{1,71.90}$=0.94, *P*=0.33), but Notonectidae were higher than Corixidae during the pre-harvest time period (difference: 0.61±0.09 µg g^{-1} dw; $F_{1,71.86}$=48.99, p<0.0001).

8.3.1.3 *Wetland type × time*

THg concentrations in invertebrates, overall, increased from the time of flood-up to pre-harvest in permanent wetlands (difference: 0.40±0.14 µg g^{-1} dw; $F_{1,71.86}$=7.57, *P*=0.01) and wild rice (difference: 0.29±0.13 µg g^{-1} dw; $F_{1,71.95}$=5.19, *P*=0.03), but not white rice (difference: 0.10±0.12 µg g^{-1} dw; $F_{1,71.86}$=0.62, *P*=0.43) or shallowly-flooded fallow fields (difference: 0.20±0.12 µg g^{-1} dw; $F_{1,71.86}$=2.54, *P*=0.12; **Figure 8.4**). THg concentrations in invertebrates did not significantly differ between wetland habitats within the flood-up time period ($F_{3,6.64}$=3.14, *P*=0.10; differences: permanent wetland vs white rice: 0.21±0.21 µg g^{-1} dw; permanent wetland vs wild rice: 0.48±0.21 µg g^{-1} dw; fallow vs permanent wetland: 0.09±0.21 µg g^{-1} dw; fallow vs white rice: 0.29±0.20 µg g^{-1} dw; fallow vs wild rice: 0.57±0.20 µg g^{-1} dw; white rice vs wild rice: 0.27±0.20 µg g^{-1} dw) or pre-harvest time period ($F_{3,5.78}$=3.78, *P*=0.08; differences: permanent wetland vs white rice: 0.51±0.20 µg g^{-1} dw; permanent wetland vs wild rice: 0.59±0.20 µg g^{-1} dw; permanent wetland vs fallow: 0.50±0.20 µg g^{-1} dw; fallow vs white rice: 0.01±0.20 µg g^{-1} dw; fallow vs wild rice: 0.09±0.20 µg g^{-1} dw; white rice vs wild rice: 0.08±0.20 µg g^{-1} dw).

8.3.1.4 *Wetland type × taxa*

THg concentrations differed among wetland habitats for Notonectidae ($F_{3,6.51}$=7.97, *P*=0.01). Notonectidae THg concentrations were higher in permanent wetlands than in wild rice (difference: 1.01±0.21 µg g^{-1} dw; $t_{3,6.51}$=4.81, *P*=0.002), white rice (difference: 0.72±0.21 µg g^{-1} dw; $t_{3,6.51}$=3.44, *P*=0.01), and fallow fields (difference: 0.67±0.21 µg g^{-1} dw; $t_{3,6.51}$=3.19, *P*=0.01), but there were no differences between white rice and wild rice (difference: 0.29±0.20 µg g^{-1} dw; $t_{3,6.51}$=1.47, *P*=0.19), white rice and fallow fields (difference: 0.05±0.20 µg g^{-1} dw; $t_{3,6.51}$=0.26, *P*=0.80), or wild rice and fallow fields (difference: 0.34±0.20 µg g^{-1} dw; $t_{3,6.51}$=1.73, *P*=0.14; **Figures 8.2 & 8.3**). Corixidae THg concentrations did not differ between wetland habitats ($F_{3,5.89}$=0.99, *P*=0.46; differences: white rice vs permanent wetland: 0.01±0.20 µg g^{-1} dw; permanent wetland vs wild rice: 0.06±0.20 µg g^{-1} dw; fallow vs permanent wetland: 0.25±0.20 µg g^{-1} dw; fallow vs white rice: 0.24±0.20 µg g^{-1} dw; fallow vs wild rice: 0.31±0.20 µg g^{-1} dw; white rice vs wild rice: 0.07±0.20 µg g^{-1} dw). THg concentrations in Notonectidae were higher than Corixidae in permanent wetlands (difference: 1.00±0.14 µg g^{-1} dw; $F_{1,71.86}$=48.39, p<0.0001) and white rice (difference: 0.27±0.12 µg g^{-1} dw; $F_{1,71.86}$=4.84, *P*=0.03), but THg concentrations in Notonectidae and Corixidae were similar in wild rice (difference: 0.05±0.13 µg g^{-1} dw; $F_{1,71.95}$=0.16, *P*=0.69) and fallow fields (difference: 0.08±0.12 µg g^{-1} dw; $F_{1,71.86}$=0.39, *P*=0.53).

8.3.1.5 *MeHg in Corixidae*

Because we used THg concentrations in our main model, we repeated the backward elimination ANOVA model using only the MeHg data in Corixidae and there were no significant interactions. Wetland habitat type, site, and time period were not significant factors influencing MeHg concentrations in Corixidae (ANOVA: wetland type: $F_{3,4}$=0.61, P=0.64; site: $F_{2,37}$=1.48, P=0.24; time period: $F_{1,37}$=1.17, P=0.29; **Figure 8.5**), although Corixidae MeHg concentrations in permanent wetlands and shallowly-flooded fallow fields tended to be elevated (differences: fallow vs white rice: 0.35±0.32 µg g^{-1} dw; fallow vs wild rice: 0.35±0.32 µg g^{-1} dw; permanent wetland vs white rice: 0.24±0.32 µg g^{-1} dw; permanent wetland vs wild rice: 0.24±0.32 µg g^{-1} dw; fallow vs permanent wetland: 0.12±0.32 µg g^{-1} dw; wild rice vs white rice: 0.01±0.32 µg g^{-1} dw).

8.3.2 Caged Fish

8.3.2.1 *Caged fish mercury bioaccumulation after 60-days of exposure*

Baseline THg concentrations and body burdens in reference mosquitofish at the time fish were introduced into cages within wetlands were 0.14±0.01 µg g^{-1} dw (N=37; range: 0.08-0.27 µg g^{-1} dw) and 0.05±0.01 µg $fish^{-1}$ dw (N=37; range: 0.01-0.29 µg $fish^{-1}$ dw), respectively. To confirm that most Hg in mosquitofish was in the MeHg form, we determined MeHg concentrations in a subset of individuals from both the experimental and reference samples. MeHg concentrations were highly correlated with THg concentrations (linear regression: N=9, R^2=0.98, p<0.0001; **Figure 8.6**), and MeHg accounted for 94.3±4.8% of the THg concentrations.

Across all wetland habitat types and sites, THg concentrations in mosquitofish removed from cages after 60 days of exposure were significantly higher than reference levels at introduction (**Table 8.1**). Total body burden of THg also was higher than reference levels at all sites, but some sites within permanent wetlands and at white rice inlets were not statistically significant after applying the sequential Bonferroni correction. THg concentrations and body burdens in mosquitofish caged at each site increased by a range of 135% to 1197% and 29% to 1566%, respectively (**Table 8.1**). Overall, model-based average THg concentrations in caged mosquitofish (N=304) at removal were 1.07±0.09 µg g^{-1} dw, 1.09±0.09 µg g^{-1} dw, and 0.41±0.04 µg g^{-1} dw in white rice, wild rice, and permanent wetlands, respectively, and 0.69±0.04 µg g^{-1} dw, 0.83±0.04 µg g^{-1} dw, and 0.83±0.04 µg g^{-1} dw at the inlets, centers, and outlets, respectively.

In our global models, we found that THg concentrations in mosquitofish caged for 60 days were positively related to fish length and negatively related to body condition, while accounting for wetland habitat type and cage site (**Figure 8.7A**). We found significant habitat type × site interactions for both THg concentrations (habitat: $F_{2,3.0}$=43.28, P=0.01, site: $F_{2,291.9}$=13.02, p<0.0001, habitat × site: $F_{4,290.9}$=165.66, p<0.0001, length: $F_{1,292.8}$=38.85, p<0.0001, condition: $F_{1,292.5}$=35.20, p<0.0001) and total Hg burdens (habitat: $F_{2,3.1}$=70.04, P=0.01, site: $F_{2,294.0}$=58.83, p<0.0001, habitat × site: $F_{4,293.9}$=61.89, p<0.0001). We therefore used conditional F-tests to further interpret whether THg concentrations and total Hg burdens in caged mosquitofish differed among habitats and sites.

8.3.2.1.1 THg concentrations in caged mosquitofish.

THg concentrations in caged mosquitofish differed among wetland habitats at the inlets ($F_{2,4.8}$=73.09, P=0.001), centers ($F_{2,3.5}$=56.51, P=0.01), and outlets ($F_{2,3.6}$=63.50, P=0.01; **Figure**

9.8A). At the inlets, THg concentrations were higher in wild rice than in either white rice ($t_{4.8}$=9.82, P=0.001) or permanent wetlands ($t_{4.8}$=11.00, P=0.001), but white rice and permanent wetlands did not differ ($t_{4.8}$=0.85, P=0.43). At the centers and outlets, THg concentrations were higher in white rice than in either wild rice (center: $t_{3.5}$=4.40, P=0.02; outlet: $t_{3.6}$=5.98, P=0.01) or permanent wetlands (center: $t_{3.5}$=10.61, P=0.001; outlet: $t_{3.6}$=11.26, P=0.001), and wild rice was higher than permanent wetlands (center: $t_{3.5}$=6.32, P=0.01; outlet: $t_{3.6}$=5.45, P=0.01).

THg concentrations also differed among cage sites within white rice ($F_{2,290.7}$=194.89, p<0.0001) and wild rice ($F_{2,292.0}$=70.87, p<0.0001), but not permanent wetlands ($F_{2,290.5}$=0.01, P=0.99; **Figure 8.8A**). Within white rice fields, THg concentrations were higher at field outlets than at the inlets ($t_{290.7}$=19.16, p<0.0001) or centers ($t_{290.7}$=2.25, P=0.03), and centers were higher than inlets ($t_{290.7}$=18.35, p<0.0001). Within wild rice fields, THg concentrations were higher at field inlets than at centers ($t_{292.0}$=10.27, p<0.0001) or outlets ($t_{292.0}$=11.86, p<0.0001), and centers were higher than outlets ($t_{292.0}$=2.73, P=0.01).

8.3.2.1.2 THg body burden in caged mosquitofish.

THg body burdens in caged mosquitofish differed among wetland habitats at inlets ($F_{2,8.0}$=28.34, P=0.001), centers ($F_{2,4.2}$=91.46, P=0.001), and outlets ($F_{2,4.2}$=117.33, P=0.001; **Figure 8.8B**). At the inlets, THg body burdens were higher in wild rice than in white rice ($t_{8.0}$=6.26, P=0.0001) or permanent wetlands ($t_{8.0}$=6.71, P=0.001), but body burdens in white rice and permanent wetlands did not differ ($t_{8.0}$=0.01, P=0.99). At the centers and outlets, THg body burdens were higher in white rice than in either wild rice (center: $t_{4.2}$=2.79, P=0.05; outlet: $t_{4.2}$=4.46, P=0.01) or permanent wetlands (center: $t_{4.2}$=12.96, P=0.0001; outlet: $t_{4.2}$=14.91, P=0.0001), and wild rice was higher than permanent wetlands (center: $t_{4.2}$=10.29, P=0.001; outlet: $t_{4.2}$=10.66, P=0.001).

THg body burdens also differed among cage sites within white rice ($F_{2,292.6}$=151.91, p<0.0001) and permanent wetlands ($F_{2,293.8}$=4.19, P=0.02), but not wild rice ($F_{2,293.3}$=2.31, P=0.10; **Figure 8.8B**). Within white rice fields, THg body burdens were higher at field outlets than at the inlets ($t_{292.6}$=17.04, p<0.0001) or centers ($t_{292.6}$=2.80, P=0.01), and body burdens at centers were higher than inlets ($t_{292.6}$=15.66, p<0.0001). In contrast, within permanent wetlands, THg body burdens were higher at field inlets than at centers ($t_{293.8}$=1.99, P=0.05) or outlets ($t_{293.8}$=2.88, P=0.01), but body burdens at centers and outlets did not differ ($t_{293.8}$=0.91, P=0.36).

8.3.2.2 *Caged fish growth after 60-days of exposure*

Upon introduction into cages, mosquitofish did not differ in standard length or mass among cage sites or habitat types (fish length: habitat: $F_{2,3}$=0.42, P=0.69; site: $F_{2,532}$=2.81, P=0.06; fish mass: habitat: $F_{2,3}$=0.53, P=0.64; site: $F_{2,531}$=0.60, P=0.55; **Table 8.2**). After 60 days of exposure, there were significant habitat type × site interactions for the length (habitat: $F_{2,3.0}$=4.68, P=0.12; site: $F_{2,294.4}$=34.57, p<0.0001; habitat × site: $F_{4,294.5}$=22.43, p<0.0001), mass (habitat: $F_{2,3.0}$=0.53, P=0.64; site: $F_{2,527}$=0.61, P=0.54; habitat × site: $F_{4,527}$=2.89, P=0.02), and relative condition factor (habitat: $F_{2,3.0}$=0.34, P=0.74; site: $F_{2,294.8}$=16.08, p<0.0001; habitat × site: $F_{4,294.8}$=4.65, P=0.001) of mosquitofish removed from cages. We therefore used conditional F-tests to further test whether body measurements differed among habitats or sites.

8.3.2.2.1 Fish length

The standard length of mosquitofish removed from cages differed among habitats at the centers ($F_{2,3.7}$=11.55, P=0.03) and outlets ($F_{2,3.7}$=14.51, P=0.02), but not at the inlets ($F_{2,6.1}$=1.18, P=0.37; **Figure 8.9A**). At the centers and outlets, fish length was greater in white rice (center: $t_{3.7}$=3.74, P=0.02; outlet: $t_{3.7}$=4.28, P=0.01) and wild rice (center: $t_{3.7}$=4.55, P=0.01; outlet: $t_{3.7}$=4.99, P=0.01) than in permanent wetlands, but fish length in white rice and wild rice did not differ (center: $t_{3.7}$=0.84, P=0.46; outlet: $t_{3.7}$=0.69, P=0.53).

Fish length also differed among cage sites within white rice ($F_{2,293.4}$=19.44, p<0.0001), wild rice ($F_{2,295.0}$=52.38, p<0.0001), and permanent wetlands ($F_{2,294.3}$=3.21, P=0.04; **Figure 8.9A**). Within white rice and wild rice fields, fish length was lower at field inlets than at either the centers (white rice: $t_{293.4}$=5.37, p<0.0001; wild rice: $t_{295.0}$=8.98, p<0.0001) or outlets (white rice: $t_{293.4}$=6.18, p<0.0001; wild rice: $t_{295.0}$=9.93, p<0.0001), whereas there was no difference in fish length between centers and outlets (white rice: $t_{293.4}$=1.49, P=0.14; wild rice: $t_{295.0}$=1.22, P=0.22). Within permanent wetlands, fish length was greater at field inlets than at either the centers ($t_{294.3}$=2.31, P=0.02) or outlets ($t_{294.3}$=2.23, P=0.03), whereas there was no difference in fish lengths between centers and outlets ($t_{294.3}$=0.19, P=0.85).

8.3.2.2.2 Fish mass

The fresh wet mass of mosquitofish removed from cages differed among habitats at the outlets ($F_{2,3.3}$=8.98, P=0.05), but not the inlets ($F_{2,4.4}$=1.69, P=0.28) or centers ($F_{2,3.3}$=5.78, P=0.08; **Figure 9.9B**). At the outlets, fish mass was greater in white rice ($t_{3.3}$=3.48, P=0.03) and wild rice ($t_{3.3}$=3.84, P=0.03) than in permanent wetlands, but white rice and wild rice did not differ ($t_{3.3}$=0.35, P=0.75).

Fish mass also differed among cage sites within white rice ($F_{2,293.2}$=27.07, p<0.0001), wild rice ($F_{2,294.5}$=75.40, p<0.0001), and permanent wetlands ($F_{2,293.7}$=4.23, P=0.02; **Figure 8.9B**). Within white rice and wild rice fields, fish mass was lower at field inlets than at either the center (white rice: $t_{293.2}$=6.88, p<0.0001; wild rice: $t_{294.5}$=11.14, p<0.0001) or outlet (white rice: $t_{293.2}$=7.02, p<0.0001; wild rice: $t_{294.5}$=11.68, p<0.0001), whereas there was no difference between centers and outlets (white rice: $t_{293.2}$=0.50, P=0.62; wild rice: $t_{294.5}$=0.66, P=0.51). Within permanent wetlands, fish mass was higher at the inlets than at the outlets ($t_{293.7}$=2.89, P=0.01), but did not differ between centers and inlets ($t_{293.7}$=1.48, P=0.14) or centers and outlets ($t_{293.7}$=1.49, P=0.14).

8.3.2.2.3 Fish relative body condition

The relative body condition of mosquitofish removed from cages did not differ among habitats at the inlets ($F_{2,7.4}$=1.98, P=0.20), centers ($F_{2,4.0}$=0.41, P=0.69), or outlets ($F_{2,4.0}$=1.80, P=0.28; **Figure 8.9C**). However, fish body condition varied among cage sites within white rice ($F_{2,293.5}$=6.32, P=0.01), wild rice ($F_{2,294.6}$=12.95, p<0.0001), and permanent wetlands ($F_{2,294.6}$=4.55, P=0.01; **Figure 8.9C**). Within white rice and wild rice fields, fish body condition was lower at field inlets than at either the centers (white rice: $t_{293.5}$=3.50, P=0.001; wild rice: $t_{294.6}$=5.01, p<0.0001) or outlets (white rice: $t_{293.5}$=2.35, P=0.02; wild rice: $t_{294.6}$=4.30, p<0.0001), whereas there was no difference between centers and outlets (white rice: $t_{293.5}$=1.63, P=0.10; wild rice: $t_{294.6}$=1.00, P=0.32). Within permanent wetlands, fish body condition did not differ

between inlets and centers ($t_{294.6}$=1.06, P=0.29) or inlets and outlets ($t_{294.6}$=1.61, P=0.11), but body condition at wetland centers was higher than at outlets ($t_{294.6}$=2.99, P=0.01).

8.3.2.3 *Temporal mercury bioaccumulation in caged fish*

In addition to our assessment of THg bioaccumulation in caged fish after 60 days of exposure, we also examined how quickly Hg was bioaccumulated. We did so only at wetland outlets, where we removed separate cages of fish after 29 and 60 days of exposure. We found a significant habitat type × time period interaction for both THg concentrations (habitat: $F_{2,3.4}$=18.59, P=0.01, time period: $F_{2,7.1}$=75.32, p<0.0001, habitat × time period: $F_{4,11.89}$=10.17, P=0.001, length: $F_{1,204.5}$=56.93, p<0.0001, condition: $F_{1,203.8}$=5.64, P=0.02) and THg body burdens (habitat: $F_{2,4.1}$=35.49, P=0.01, time period: $F_{2,6.9}$=35.31, P=0.001, habitat × time period: $F_{4,21.0}$=13.35, p<0.0001). We therefore used conditional F-tests to further examine whether THg concentrations and THg body burdens in caged mosquitofish differed among habitats and within habitats among time periods.

8.3.2.3.1 Temporal THg concentrations in caged mosquitofish.

THg concentrations in caged mosquitofish differed among time periods within white rice ($F_{2,8.0}$=65.09, p<0.0001), wild rice ($F_{2,7.9}$=29.26, P=0.001), and permanent wetlands ($F_{2,8.0}$=21.98, P=0.001; **Figure 8.10A**). Within white rice and wild rice fields, THg concentrations were higher after 60 days of exposure than after 29 days (white rice: $t_{8.0}$=8.01, p<0.0001; wild rice: $t_{7.9}$=4.50, p<0.0001) and both 29-day and 60-day exposed mosquitofish were higher than reference fish at introduction (29-day white rice: $t_{8.0}$=7.44, P=0.01; 29-day wild rice: $t_{7.9}$=5.76, P=0.01; 60-day white rice: $t_{8.0}$=9.54, P=0.001; 60-day wild rice: $t_{7.9}$=6.95, P=0.01). Within permanent wetlands, THg concentrations were higher after 60-days of exposure than after 29-days ($t_{8.0}$=5.97, p<0.0001) and only 60-day exposed mosquitofish were higher than reference fish at introduction (29-day: $t_{8.0}$=2.46, P=0.08; 60-day: $t_{8.0}$=4.00, P=0.02). Overall, 57%, 71%, and 50% of the THg concentrations at day 60 occurred within the first 29 days in white rice, wild rice, and permanent wetlands, respectively.

THg concentrations in caged mosquitofish did not differ among wetland habitats for reference fish at introduction ($F_{2,203.0}$=0.64, P=0.53), however THg concentrations differed among wetlands at 29 and 60 days of exposure (29-day: $F_{2,3.6}$=17.10, P=0.01; 60-day: $F_{2,3.2}$=21.79, P=0.01; **Figure 8.10A**). At 29 days of exposure, THg concentrations were higher in white rice and wild rice than in permanent wetlands (white rice: $t_{3.6}$=5.82, P=0.01; wild rice: $t_{3.6}$=3.47, P=0.03), but white rice and wild rice did not differ ($t_{3.6}$=2.36, P=0.09). At 60 days of exposure, THg concentrations were higher in white rice and wild rice than in permanent wetlands (white rice: $t_{3.2}$=6.59, P=0.01; wild rice: $t_{3.2}$=3.06, P=0.05), and white rice also was higher than wild rice ($t_{3.2}$=3.59, P=0.04).

8.3.2.3.2 Temporal THg body burden in caged mosquitofish

THg body burdens in caged mosquitofish differed among time periods within white rice ($F_{2,9.2}$=46.04, p<0.0001) and wild rice ($F_{2,9.2}$=23.45, P=0.001), but not permanent wetlands ($F_{2,9.3}$=1.93, P=0.20; **Figure 8.10B**). Within white rice and wild rice fields, THg body burdens were higher after 60 days of exposure than after 29 days (white rice: $t_{9.2}$=5.23, p<0.0001; wild rice: $t_{9.2}$=4.17, p<0.0001) and both 29-day and 60-day exposed mosquitofish were higher than

reference fish at introduction (29-day white rice: $t_{9.2}$=6.79, P=0.01; 29-day wild rice: $t_{9.2}$=4.41, P=0.01; 60-day white rice: $t_{9.2}$=9.10, P=0.001; 60-day wild rice: $t_{9.2}$=6.19, P=0.01). Overall, 49%, 53%, and 71% of the THg body burdens at day 60 were bioaccumulated within the first 29 days in white rice, wild rice, and permanent wetlands, respectively.

THg body burdens in caged mosquitofish did not differ among wetland habitats for reference fish at introduction ($F_{2,205.0}$=1.56, P=0.21), however THg body burdens differed among wetlands at 29 and 60 days of exposure (29-day: $F_{2,4.7}$=23.79, P=0.01; 60-day: $F_{2,3.4}$=46.02, P=0.01; **Figure 8.10B**). At both 29 and 60 days of exposure, fish THg body burdens were higher in white rice and wild rice than in permanent wetlands (29-day white rice: $t_{4.7}$=6.69, P=0.001; 29-day wild rice: $t_{4.7}$=4.79, P=0.01; 60-day white rice: $t_{3.4}$=9.31, P=0.001; 60-day wild rice: $t_{3.4}$=6.72, P=0.01), but white rice and wild rice did not differ (29-day: $t_{4.7}$=1.90, P=0.12; 60-day: $t_{3.4}$=2.69, P=0.07).

8.3.3 Wild Fish Mercury Bioaccumulation

THg concentrations in wild mosquitofish (N=140) were 0.67±0.13 µg g^{-1} dw, 0.75±0.15 µg g^{-1} dw, and 0.44±0.08 µg g^{-1} dw in white rice, wild rice, and permanent wetlands, respectively, and 0.47±0.06 µg g^{-1} dw and 0.79±0.09 µg g^{-1} dw at the inlets and outlets, respectively. THg concentrations in wild silversides (N=135) were 0.82±0.14 µg g^{-1} dw, 0.92±0.16 µg g^{-1} dw, and 0.28±0.05 µg g^{-1} dw in white rice, wild rice, and permanent wetlands, respectively, and 0.48±0.05 µg g^{-1} dw and 0.74±0.08 µg g^{-1} dw at the inlets and outlets, respectively.

Similar to our caged fish models, we found significant interactions between habitat type × site for wild mosquitofish (THg concentrations: habitat: $F_{2,2.7}$=2.10, P=0.28, site: $F_{1,131.8}$=51.95, p<0.0001, habitat × site: $F_{2,130.6}$=42.71, p<0.0001, length: $F_{1,126.8}$=1.57, P=0.21, condition: $F_{1,131.4}$=7.01, P=0.01; total Hg burdens: habitat: $F_{2,3.1}$=0.47, P=0.66, site: $F_{1,134.0}$=26.98, p<0.0001, habitat × site: $F_{2,133.1}$=6.07, P=0.01) and wild silversides (THg concentrations: habitat: $F_{2,2.9}$=14.70, P=0.03, site: $F_{1,126.9}$=49.94, p<0.0001, habitat × site: $F_{2,126.1}$=24.01, p<0.0001, length: $F_{1,126.6}$=53.81, p<0.0001, condition: $F_{1,126.1}$=1.77, P=0.19; total Hg burdens: habitat: $F_{2,3.2}$=10.98, P=0.04, site: $F_{1,122.7}$=7.54, P=0.01, habitat × site: $F_{2,121.6}$=8.96, P=0.001). THg concentrations were positively related to fish length for wild silversides, but not for wild mosquitofish, and negatively related to body condition for wild mosquitofish, but not wild silversides (**Figure 8.7B and 8.7C**). To interpret the effects of habitat type and site further, we used conditional F-tests.

8.3.3.1 *THg concentrations in wild fish*

THg concentrations in both wild mosquitofish and wild silversides differed among wetland habitat types at outlets (mosquitofish: $F_{2,2.9}$=8.90, P=0.05; silversides: $F_{2,3.5}$=23.92, P=0.01), but not inlets (mosquitofish: $F_{2,3.6}$=1.13, P=0.42; silversides: $F_{2,3.3}$=6.68, P=0.07; **Figure 8.11A and 8.11B**). At the outlets, THg concentrations were higher in white rice (mosquitofish: $t_{2.9}$=3.95, P=0.03; silversides: $t_{3.5}$=6.16, P=0.01) and wild rice (mosquitofish: $t_{2.9}$=3.22, P=0.05; silversides: $t_{3.5}$=5.59, P=0.01) than in permanent wetlands, but wild rice and white rice did not differ (mosquitofish: $t_{2.9}$=0.74, P=0.51; silversides: $t_{3.5}$=0.03, P=0.98).

THg concentrations in both wild mosquitofish and wild silversides also differed among sites within white rice (mosquitofish: $F_{1,130.0}$=126.60, p<0.0001; silversides: $F_{1,124.5}$=76.36, p<0.0001) and wild rice (mosquitofish: $F_{1,126.8}$=10.83, P=0.001; silversides: $F_{1,126.4}$=16.29, p<0.0001), but not permanent wetlands (mosquitofish: $F_{1,129.0}$=2.57, P=0.11; silversides: $F_{1,124.0}$=0.28, P=0.60; **Figure 8.11A and 8.11B**). Within white rice and wild rice fields, THg concentrations were higher at field outlets than at the inlets (mosquitofish in white rice: $t_{130.0}$=11.25, p<0.0001; silversides in white rice: $t_{124.5}$=8.74, p<0.0001; mosquitofish in wild rice: $t_{126.8}$=3.29, P=0.001; silversides in wild rice: $t_{126.4}$=4.04, P=0.0001).

8.3.3.2 *THg body burdens in wild fish*

Total body burden of THg in wild mosquitofish did not differ among habitats at inlets ($F_{2,4.1}$=0.95, P=0.46) or outlets ($F_{2,3.2}$=1.00, P=0.46; **Figure 8.11A**). However, total body burden differed among sites within white rice ($F_{1,131.6}$=19.54, p<0.0001) and wild rice ($F_{1,132.1}$=13.96, P=0.001), but not permanent wetlands ($F_{1,131.1}$=0.32, P=0.57; **Figure 8.11A**). Within white rice and wild rice fields, body burden was higher at field outlets than at the inlets (white rice: $t_{131.6}$=4.42, p<0.0001; wild rice: $t_{132.1}$=3.74, P=0.001).

Total body burden of THg in wild silversides differed among habitats at outlets ($F_{2,5.4}$=20.42, P=0.01), but not inlets ($F_{2,5.7}$=2.50, P=0.17; **Figure 8.11B**). At the outlets, body burden was higher in white rice ($t_{5.4}$=6.33, P=0.01) and wild rice ($t_{5.4}$=3.17, P=0.01) than in permanent wetlands, but body burdens in wild rice and white rice did not differ ($t_{5.4}$=1.57, P=0.15). Total body burden of THg in wild silversides also differed among sites within white rice ($F_{1,127.3}$=23.64, p<0.0001), but not wild rice ($F_{1,99.4}$=1.09, P=0.30) or permanent wetlands ($F_{1,126.3}$=0.91, P=0.34; **Figure 8.11B**). Within white rice fields, body burden was higher at field outlets than at the inlets ($t_{127.3}$=4.86, p<0.0001).

8.3.4 Caged vs. Wild Fish

In general, although caged mosquitofish were only introduced for 60 days, caged mosquitofish bioaccumulated THg to higher concentrations than wild mosquitofish that were exposed to Yolo Bypass Hg concentrations presumably their entire lives (**Figure 8.12**). This illustrates the value of using caged fish as site specific bioindicators of Hg contamination. Because wild fish are free to move in and out of the wetlands studied and into canals where MeHg concentrations are known to be lower, their concentrations represent exposure within each wetland for an unknown time period. Alternatively, caged fish not only allow for sampling over a known and discrete time period, but the method also allows for the calculation of bioaccumulation rates over time.

8.3.5 Biota Hg vs. Water MeHg and Sediment MeHg

We used linear regression to compare biota Hg concentrations with sediment MeHg concentrations and MeHg in unfiltered surface water using each site (inlet, center, or outlet) as an independent replicate (**Figure 8.13**). We found that caged mosquitofish THg concentrations at removal were slightly more correlated with MeHg in unfiltered surface water collected at deployment (N=13, R^2=0.44, P=0.01), than in water collected upon retrieval (N=13, R^2=0.33, P=0.04), suggesting that bioaccumulation into fish occurs rapidly upon early exposure. Interestingly, we found no correlation between THg concentrations in mosquitofish and MeHg in sediment sampled upon introduction (N=5, R^2=0.01, P=0.86) or retrieval (N=5, R^2=0.01,

P=0.85). In contrast, invertebrate (Corixidae) MeHg concentrations were more correlated with MeHg in sediment (*N*=14, R^2=0.40, p<0.01) than with MeHg in unfiltered surface water (*N*=39, R^2=0.24, p<0.01) across all time periods.

8.4 Discussion

The Yolo Bypass Wildlife Area, like many other state and federal refuges in California's Central Valley, is primarily managed as waterfowl and shorebird habitat. Therefore, wetlands are typically managed using shallow and intermittent flooding because seasonal wetlands typically have greater invertebrate abundance than permanent wetlands that have longer hydroperiods (**Neckles et al., 1990**). In particular, reverse-cycle seasonal wetlands are intermittently flooded during the spring and summer to increase invertebrate production for breeding ducks (**Neckles et al., 1990; de Szalay et al., 2003**), which switch from a diet primarily of seeds to that of invertebrates in order to attain the required protein for egg formation (reviews by **Alisauskas and Ankney, 1992; Krapu and Reinecke, 1992**), and ducklings, that require invertebrate protein for rapid growth (review by **Sedinger, 1992**). Unfortunately, cyclical wetting and drying of wetland habitats often is associated with increased MeHg production and concentrations in biota (**Hall et al., 1998; Snodgrass et al., 2000**).

We found that wetland habitat type had an important influence on Hg concentrations in invertebrates and fish, but this effect differed among taxa. Specifically, our results indicate that THg concentrations in Notonectidae, but not Corixidae, increased from wetland flood-up to draw-down, whereas invertebrate THg concentrations in temporarily flooded habitats were not higher than permanent wetlands. In fact, THg concentrations in Notonectidae were higher in permanent wetlands than in white rice, wild rice, or shallowly-flooded fallow fields, but did not differ among wetland types for Corixidae. The effect of habitat on invertebrate THg concentration was especially prevalent at the end of the rice growing season, when Notonectidae THg concentrations were higher in permanent wetlands than in any other wetland habitat. Similarly, THg concentrations in amphipods (Crangonyctidae) were highest in permanent wetlands compared to intermittently flooded sites in the Okefenokee Swamp in Georgia (**George and Batzer, 2008**).

Importantly, our results are in direct contrast to the companion studies we conducted simultaneously using caged and wild fish, highlighting the importance of evaluating multiple biosentinels simultaneously. In fish, we found strong evidence for higher THg concentrations in white rice and wild rice fields compared to permanent wetlands. However, we did find similar within-field spatial patterns between invertebrates and fish, with both taxa groups tending to have higher THg concentrations at field outlets than at field inlets. These incongruent results for THg concentrations in invertebrates and fish among wetland habitats indicate that bioaccumulation pathways in wetlands are complex and underscore the importance of using several taxa at different trophic levels to examine MeHg bioaccumulation in wetlands. The complexity of MeHg bioaccumulation in wetlands is further illustrated by the fact that we did not find a correlation between THg concentrations in Notonectidae and Corixidae, even though the paired samples were collected at the same sites and on the same days. Notonectidae (*Notonecta*) typically forage at a higher trophic level than Corixidae (*Corisella*; **Menke, 1979; Merritt and Cummins, 1996**). Thus, the lack of correlation between their THg concentrations indicates that

they are foraging on different prey items, and that the two invertebrates are not tightly linked within the foodweb.

Furthermore, we found that caged fish THg concentrations were correlated with water MeHg concentrations, but not with sediment MeHg concentrations, whereas invertebrate MeHg concentrations were more correlated with sediment MeHg concentrations than with water MeHg concentrations. Thus pelagic-feeding fish may be better indicators of MeHg availability within the water column, and demersal invertebrates better indicators for MeHg availability in sediment, however simultaneously using several bioindicators when monitoring MeHg production and bioaccumulation is important. Top predators often forage on both benthic and pelagic prey, and an important exposure source may be overlooked if bioindicators of only one habitat are examined.

Notably, Corixidae THg and MeHg concentrations were higher at the Yolo Bypass Wildlife Area wetlands than in wetlands located downstream within the same watershed in San Francisco Bay (THg: 0.63 μg g^{-1} dw, MeHg: 0.59 μg g^{-1} dw; A. K. Miles, U. S. Geological Survey, unpublished data). Overall, 75% and 48% of all Corixidae samples at the Yolo Bypass Wildlife Area exceeded reported MeHg dietary effect levels of 0.50 μg g^{-1} dw for mallard reproduction (*Anas platyrhynchos*; **Heinz, 1979**) and 0.70 μg g^{-1} dw for American kestrel reproduction (*Falco sparverius*; **Albers et al., 2007**), respectively. Considering that Corixidae are common in waterfowl diets (**Euliss et al., 1991**), higher trophic level predators may be negatively affected by current Hg concentrations in invertebrate prey within Yolo Bypass wetlands.

Furthermore, all caged fish and 99% of wild fish sampled exceeded the Central Valley Regional Water Quality Control Board's Total Maximum Daily Load (TMDL) target for Hg concentrations in small fish (0.03 μg g^{-1} ww or approximately 0.11 μg g^{-1} dw assuming 73% moisture in wild) that is meant to be protective of wildlife in the Sacramento-San Joaquin River Delta (**Wood et al., 2010a**). Although this TMDL target is likely below actual effects to many wildlife, like piscivorous waterbirds, 38% of caged mosquitofish, 19% of wild mosquitofish, and 13% of wild silversides exceeded the dietary concentration of 0.30 μg g^{-1} ww which is commonly associated with impaired bird reproduction (**Barr, 1986**; **Albers et al., 2007**; **Burgess and Meyer, 2008**). In addition to wildlife, fish health might also be affected at current concentrations. Fifty-nine percent of caged mosquitofish and 36% of wild mosquitofish and silversides sampled exceeded 0.20 μg g^{-1} ww (approximately 0.74 and 0.83 μg g^{-1} dw assuming 73% and 76% moisture in wild and caged fish, respectively), the fish health risk threshold associated with sublethal endpoints (**Beckvar et al., 2005**).

Thus, there may be substantial risk of MeHg toxicity to waterbirds and other wildlife that forage in Yolo Bypass wetlands. Of particular concern within these wetlands are wading birds such as egrets, herons, ibis, shorebirds, and ducks. Recent lab studies (**Heinz et al., 2009**) have confirmed that wading birds are among the most sensitive species to mercury-induced egg hatching failure, thus future research should evaluate potential effects to these abundant birds in the area. MeHg concentrations in these waterbirds, such as black-necked stilts, should be evaluated to determine wildlife exposure and risk. For example, within San Francisco Bay, we found that black-necked stilt chicks (*Himantopus mexicanus*) found dead near nesting sites had higher THg concentrations than those in randomly-sampled live chicks of similar age

(**Ackerman et al., 2008a**) and that failed-to-hatch Forster's tern (*Sterna forsteri*) eggs had higher THg concentrations than randomly-sampled live eggs (**Ackerman et al., 2008b**). Similar deleterious effects of Hg on waterbird reproduction may be occurring within Yolo Bypass wetlands where Hg concentrations in prey are considerably higher than in San Francisco Bay wetlands.

8.5 Summary

8.5.1 Objective

Wetlands typically have higher rates of MeHg production than other aquatic habitats, but it is unclear whether there are specific wetland habitat types that enhance MeHg bioaccumulation. We examined MeHg bioavailability in invertebrates and fish within four of the most predominant wetland habitats in California's Central Valley agricultural region during the spring and summer: white rice, wild rice, permanent wetlands, and shallowly-flooded fallow fields.

8.5.2 Mercury in Invertebrates

We sampled THg and MeHg concentrations in two aquatic macroinvertebrate taxa at the inlets, centers, and outlets of four replicated wetland habitats (8 wetlands total) during two time periods bounding the rice growing season and corresponding to flood-up and pre-harvest (96 total samples). In general, THg concentrations (mean±standard error) in Notonectidae (*Notonecta*, back swimmers; 1.18±0.08 μg g^{-1} dw) were higher than in Corixidae (*Corisella*, water boatmen; 0.89±0.06 μg g^{-1} dw, MeHg: 0.74±0.05 μg g^{-1} dw). MeHg concentrations were correlated with THg concentrations in Corixidae (R^2=0.80) and 88% of THg was in the MeHg form. Wetland habitat type had an important influence on THg concentrations in aquatic invertebrates, but this effect depended on the sampling time period and taxa. In particular, THg concentrations in Notonectidae, but not Corixidae, were higher in permanent wetlands than in white rice, wild rice, or shallowly-flooded fallow fields. THg concentrations in Notonectidae were higher at the end of the rice growing season than near the time of flood-up, whereas THg concentrations in Corixidae did not differ between time periods. The effect of wetland habitat type was more prevalent near the end of the rice growing season, when Notonectidae THg concentrations were highest in permanent wetlands. Additionally, invertebrate THg concentrations were higher at water outlets than at inlets of wetlands. Our results indicate that although invertebrate THg concentrations increased from the time of flood-up to draw-down of wetlands, temporarily flooded habitats such as white rice, wild rice, and shallowly-flooded fallow fields did not have higher THg or MeHg concentrations in invertebrates than permanent wetlands.

8.5.3 Mercury in Caged Fish

We introduced western mosquitofish (*Gambusia affinis*) into cages placed within white rice, wild rice, and permanent wetlands at hydrologic sites associated with their surface water inlets, centers, and outlets. We introduced 30 individual fish into each of the 24 cages that were used, for a total of 720 fish that were introduced into Yolo Bypass Wildlife Area wetlands. Baseline THg concentrations in reference mosquitofish at the time cages were introduced into wetlands were 0.14±0.05 μg g^{-1} dw (N=37). THg concentrations and whole body burdens of caged mosquitofish increased rapidly, exceeding reference values at introduction by 135% to

1197% and 29% to 1566% among sites, respectively, after only 60 days. Mercury bioaccumulation in caged mosquitofish was greater in rice fields than in permanent wetlands. For example, THg concentrations in mosquitofish caged at wetland outlets increased by 12.1, 5.8, and 2.9 times over reference values at introduction in white rice, wild rice, and permanent wetlands, respectively. Within wetlands, THg concentrations and body burdens of caged fish increased from water inlets to outlets in white rice fields, and tended to not vary among sites in permanent wetlands. Overall, model-based average THg concentrations in caged mosquitofish (*N*=304) at removal after 60 days of exposure were 1.07±0.09 μg g^{-1} dw, 1.09±0.09 μg g^{-1} dw, and 0.41±0.04 μg g^{-1} dw in white rice, wild rice, and permanent wetlands, respectively, and 0.69±0.04 μg g^{-1} dw, 0.83±0.04 μg g^{-1} dw, and 0.83±0.04 μg g^{-1} dw at the inlets, centers, and outlets, respectively.

8.5.4 Mercury in Wild Fish

We also collected wild western mosquitofish and wild Mississipi silversides (*Menidia beryllina*) at each wetland's inlets and outlets when caged fish were removed. Across all wetland habitat types and sites, THg concentrations in wild mosquitofish (*N*=140) were 0.67±0.13 μg g^{-1} dw, 0.75±0.15 μg g^{-1} dw, and 0.44±0.08 μg g^{-1} dw in white rice, wild rice, and permanent wetlands, respectively, and 0.47±0.06 μg g^{-1} dw and 0.79±0.09 μg g^{-1} dw at the inlets and outlets, respectively. THg concentrations in wild silversides (*N*=135) were 0.82±0.14 μg g^{-1} dw, 0.92±0.16 μg g^{-1} dw, and 0.28±0.05 μg g^{-1} dw in white rice, wild rice, and permanent wetlands, respectively, and 0.48±0.05 μg g^{-1} dw and 0.74±0.08 μg g^{-1} dw at the inlets and outlets, respectively. Similar to caged fish, THg concentrations in wild fish differed among habitats, with white rice and wild rice having higher THg concentrations than permanent wetlands. THg concentrations in wild fish were higher at outlets than inlets in white rice and wild rice, but there was no difference between sites in permanent wetlands. Our results from wild fish are similar to caged fish, except that THg concentrations in caged fish were considerably higher than wild fish that were presumably exposed to Yolo Bypass Hg concentrations their entire lives. This illustrates the importance of using caged fish as site specific bioindicators of Hg contamination since wild fish are free to move in and out of the wetlands studied and into canals where MeHg concentrations are known to be lower.

8.6 Conclusions

Our results indicate that temporarily flooded shallow wetlands, such as white rice and wild rice fields, have elevated THg concentrations in both caged and wild fish compared to permanent wetlands at the Yolo Bypass. In contrast, THg and MeHg concentrations in invertebrates were higher in permanent wetlands than in white rice or wild rice fields. These conflicting results are partially explained by the fact that fish THg concentrations were correlated with water MeHg, but not with sediment MeHg, whereas invertebrate MeHg concentrations were more correlated with sediment MeHg than with water MeHg. These results illustrate the complexity of MeHg bioaccumulation through food webs and indicate the importance of simultaneously using multiple biosentinels when monitoring MeHg production and bioaccumulation.

Hg concentrations exceeded levels that are potentially harmful to wildlife - Hg concentrations in invertebrates and fish were more than 6 and 11 times higher, respectively, in Yolo Bypass wetlands than stated TMDL target values to protect humans and wildlife (0.03 ppm ww). In fact, 99% of wild fish sampled in Yolo Bypass wetlands exceeded this TMDL target

value to protect wildlife and 75% of invertebrates sampled in Yolo Bypass wetlands exceeded MeHg dietary levels of 0.50 μg g^{-1} dw that have been previously shown to impair avian reproduction.

9 Detailed Results for Methylmercury Photodemethylation

The data reported in this section relates to summary **Section 3.2: Methylmercury Export** and **Section 3.3: Methylmercury Production in Surface Sediment.**

9.1 Introduction

MeHg photodecomposition – the destruction of MeHg to inorganic mercury (Hg(II) or Hg^0) by exposure to solar radiation – is an important process which can dramatically influence the abundance and cycling of MeHg in aquatic surface waters. In fact, photodecomposition (e.g. photodegradation) has been shown to account for 80% of the loss of MeHg from an Alaskan lake (**Hammerschmidt and Fitzgerald, 2006**). Previous work in the Bay-Delta has shown that photodecomposition is highly significant in the biogeochemical cycling of mercury, particularly during summertime low river flow conditions (**Byington et al., 2005; Byington, 2007; Stephenson et al., 2008**). It was hypothesized that agricultural rice fields are aquatic systems with high production of MeHg. If this hypothesis is supported by field measurements, then MeHg concentrations in water on agricultural rice fields will likely be elevated compared to ambient waters in the Delta region. Given their shallow water depths, photodecomposition may therefore play an important role in the biogeochemical cycling and transport of Hg in the rice fields.

This current report on the photodecomposition of MeHg in agriculturally-managed and non-agricultural wetlands in the YBWA is part of a larger effort to understand the biogeochemical cycling and transport of Hg and MeHg associated with agricultural rice field activities. The rate of MeHg destruction by photochemical processes was investigated to determine how this process varies relative to the various manipulations and Best Management Practices (BMP) of rice farmers. Special attention was focused on investigating the role of dissolved organic matter concentrations and light intensity on MeHg destruction rates.

9.2 Approach

9.2.1 Bottle Incubations

Photodemethylation experiments were conducted following the *in situ* Teflon® bottle incubation experiments described by **Byington et al. (2005)** and **Byington (2007)**. In preparation for the experiment, a large volume (~ 10 liters) of filtered surface water was collected in a polycarbonate carboy by pumping water through a 0.45 µm filter cartridge using a peristaltic pump. The peristaltic pump was equipped with C-flex pump head tubing and FEP Teflon® tubing on both the inlet and outlet. Sampling was conducted using ultra-clean protocols.

For the winter sampling event only, MeHg was added to the samples to raise the ambient MeHg concentration by ~0.4 ng L^{-1}. Spiking was deemed necessary to maintain concentrations above the method detection limits and to assure good analytical reproducibility. After rigorous mixing of the carboy, ~ 400 mL of the filtered water was aliquoted into 5 darkened (control) and 6 clear 500 mL FEP Teflon® bottles. A duplicate of one time point (usually the final time point) was collected with each experiment, which is why 6 clear bottles were used. Sample bottles were placed in a 13 mm polypropylene mesh and floated on the surface of an open water area of

the YBWA (**Figure 9.1**). One dark and one light bottle were harvested immediately before deployment, and these served as the time zero samples. A pair of samples (dark and light) was retrieved periodically over a 2-3 day exposure period providing a total of five time points of increasing total light exposure. Following retrieval, samples were immediately preserved in the field by acidification with high purity hydrochloric acid to 0.5% acid (v/v). After preservation, samples were kept dark and at ambient temperature (not exposed to heat) until analysis.

Sample bottles, carboys, and tubing were cleaned using 7.5 N reagent grade nitric acid (HNO_3) except for C-flex tubing which was cleaned using 1.2 N reagent grade hydrochloric acid (HCl). All bottles and carboys were filled with 0.5% v/v reagent grade HCl and stored until use. Ultra clean handling protocols (**EPA 1669**) were followed throughout equipment cleaning, sample collection, experimental manipulation, and analysis (**Gill and Fitzgerald, 1985**).

9.2.2 Sampling Locations and Dates

Sampling was conducted in five separate agricultural and wetland types in the YBWA: (1) two rotational white rice fields (after fallow, R31 and R64); (2) two wild rice fields (after fallow, R32 and R65); (3) two fallow fields after wild rice planting and harvesting (rotational fallow, F20 and F66); (4) a seasonal wetland (SW1); and (5) a permanent wetland (PW5). Sampling of these rice fields and wetlands were conducted in a winter (December 2007) period, and for a subset, in thesummer (July 2008) period. Whereas the summer photodecomposition sampling effort was off-cycle with most other summer measurements, the same layout of field conditions was used for comparability across years. Sampling locations and field types are given in **Table 9.1** and depicted in **Figure 4.5**. No sampling could be conducted on the seasonal wetland (SW1), field W32 and W65 during July 2008 because the seasonal wetland was dry and these two agricultural fields were in fallow and also dry.

9.2.3 Light Intensity Measurements

Measurements of ultraviolet (UV-A plus UV-B) and photosynthetically available radiation (PAR) were made continuously using a quantum sensor with nanologger from Apogee Instruments, Inc. during the experiments (December 2007 and July-August 2008) to relate light intensity to degradation rate. The light sensor was located approximately 4 km from the location used for deployment of bottle incubations. PAR measurements (mol m^{-2} s^{-1}) refer to the moles of photons in the UV or PAR wavelengths striking a square meter of (water) surface every second. PAR measurements were multiplied by the number of seconds for each PAR integration interval, giving an estimate of total light exposure (mol m^{-2}): the moles of photons per square meter. For the remainder of this report, MeHg concentrations will be presented in ng L^{-1} whereas light will be presented in units of mol m^{-2}. **Byington (2007)** determined that clear FEP Teflon® bottles have a high optically transparency for 280-800 nm light wavelengths (**Figure 9.2**). In addition to the light intensity measurements made during the degradation experiments, measurements were made of light penetration into the water column during several different periods of rice growth to assess seasonal effects of shading on light penetration into the water column.

9.2.4 Methylmercury Determinations

The MeHg concentration in the incubated waters was determined using a distillation and aqueous phase ethylation method with cold vapor atomic fluorescence spectrometry (CVAFS) detection (**Bloom, 1989; Horvat et al., 1993**). Prior to analysis, 45 to 80 mL aliquots were

distilled to minimize recovery artifacts associated with the sample matrix. The distilled sample was buffered to pH 5.0 with 2 M acetate buffer, and reacted with 35 µL of a 1% sodium tetraethylborate (NaBEt) solution to create volatile ethyl analogs of the solution mercury species. The sample was then purged with nitrogen and the ethylated complexes (e.g. monomethylmercury becomes methylethylmercury) are collected onto a Carbotrap™. The trap is then heated and the products flow into an isothermal gas chromatography (GC) column where separation occurs. At the exit of the GC the mercury species were pyrolyzed at high temperature (>500 °C) and converted to elemental mercury (Hg^o) for subsequent determination by Cold Vapor Atomic Fluorescence Spectrometry (CVAFS). The method detection limit for MeHg determinations was 0.012 ng L^{-1} based on 7 replicate measurements of a low MeHg content substrate.

9.2.5 Quality Assurance Quality Control

Because of the nature of this work, Quality Assurance and Quality Control (QA/QC) for the field sampling can be handled slightly differently than normal field sampling where replication and blank checks are used to verify quality. With each experiment, a set of exposure bottles (clear) are contrasted with a set of control (darkened bottles). Any difference between the concentration of MeHg in the clear bottles and the dark bottles can be taken to result from decomposition due to exposure to light. In addition, all 5 time points are considered together by treating them as an exposure-dependent set using linear regression analysis. In addition, one field replicate was collected with each exposure set. The replicate collected was usually the final time point in the clear bottle. The data used in calculations, and the relative percent difference (RPD) of the replicate pairs, are summarized in **Appendix 4**. QAQC associated with the analytical determinations of MeHg followed the data quality objectives outlined in EPA method 1630, *Methyl Mercury in Water by Distillation, Aqueous Ethylation, Purge and Trap, and CVAFS* (**EPA, 2001**).

9.3 Results and Discussion

9.3.1 Light Intensity (PAR) Measurements

Two types of PAR measurements were obtained during this study, continuous measurements associated with the exposure experiments, and discrete measurements in individual fields to evaluate light attenuation with depth in the water column and shading of light reaching the surface due to emergent rice. Ultra-violet (UV) exposures were assessed by established UV:PAR predictive relationships (**Byington 2007**).

9.3.2 Continuous Measurements

Continuous light intensity (PAR) measurements for the two experimental time periods are depicted in **Figures 9.3**. The integrated flux for each individual time point in an experiment is given in the appendicies. Note that the maximum intensity of light reaching the surface of the water in the winter (~ 800 µmol m^{-2} s^{-1}) is about half that observed in the summer (~ 1700 µmol m^{-2} s^{-1}). In addition, during the winter period there were periods of cloudy and stormy weather that substantially reduced light intensity reaching the water surface.

9.3.3 Discrete Water Column Profile Measurements

PAR depth profile measurements taken in the water column of the rice fields and wetlands areas are summarized in the Appendix. An example of the water column profile measurements for field R20 taken on June 26, 2008 is given in **Figure 9.4**. The attenuation of the PAR flux with depth can be determined by performing a logarithmic (natural log) regression analysis of the profiles. An attenuation coefficient is determined by taking the reciprocal (m^{-1}) of the logarithmic coefficient associated with equation of the line for a logarithmic (natural log) regression of the PAR data with depth:

$$y = m \ln(x) + b \qquad \textbf{Equation 9.1}$$

The PAR at depth (z) is then given by:

$$PAR_{(z)} = PAR_{(0)} e^{\mu(z)} \qquad \textbf{Equation 9.2}$$

Where, $PAR_{(z)}$ is the intensity of light at depth z, $PAR_{(0)}$ is the intensity of PAR at the water surface (z =0), μ is an extinction coefficient or attenuation coefficient and has units of cm^{-1}, and z is depth, in units of centimeters.

The PAR extinction coefficient was observed to be highly variably, ranging from -0.019 to -0.041 cm^{-1}, and averaging -0.029 ± 0.011 cm^{-1}. This corresponded to a light intensity at a water depth of 20 cm (the average depth of surface water on rice fields) of 38-82% of surface light intensity. Unfortunately, no UV light penetration data were obtained, so it is not possible to directly assess how UV light was attenuated with depth. Thus, PAR extinction coefficients were applied to UV-calculations to estimate UV radiation attenuation in the water column.

9.3.4 Photodecomposition Experiments

Illustrated in **Figures 9.5A, 9.5B** and **9.6** are individual photodecomposition experiment for the two time periods, December 2007 and July/August 2008. The green circles represent the bottles exposed to light, and the red circles represent samples in darkened bottles. Note that MeHg concentration data (in units of ng L^{-1}) are plotted relative to total light exposure (mol m^{-2}). Hence, this is not a typical kinetic experiment where the independent variable would time. The choice to use total light exposure rather than time stems from the fact that the photodegradation rate is linearly proportional to light exposure, and because the light exposure rate varied with time. This means that the photodegradation rate can be treated in kinetic terminology, as first-order with respect to light intensity:

$$\text{MeHg Photodegredation Rate (ng } L^{-1} \text{ mol}^{-1} \text{ m}^2) = k \text{ [light flux]} \qquad \textbf{Equation 9.3}$$

Where light flux concentration is represented by the photons of light striking a surface area (mol m^{-2}) and is independent of time. The rate constant (k) has units of ng L^{-1} mol^{-2} m^4. The slope associated with the linear regression analysis for the five exposure periods of each experiment provides the photodecomposition rate constant for the individual experiment. The results for the darkened bottles serve as the control to each experiment. A summary of the linear regression data which provides the photodecomposition rate constant for both experimental periods is given in **Tables 9.2 and 9.3** for PAR and UV as the portion of the light spectrum

driving MeHg photodecomposition. A recent paper by **Li et al. (2010)** has suggested that it is UVb radiation that is responsible for the photodegredation of MeHg. Both treatments (PAR and UV) are provided in this report.

Note that the regression slope for each individual experiment varies significantly. This preliminary information suggests that another parameter is also influencing the rate at which MeHg undergoes photodegradation. In a later section it will be demonstrated that MeHg concentration also influences the photodegradation rate and that the rate is linear with concentration. Hence, the MeHg photodegredation rate is second-order, varying with the amount of light flux and MeHg concentration:

MeHg Photodegredation Rate (ng L^{-1} mol^{-1} m^2) = k [light flux][MeHg] **Equation 9.4**

Tabulated results of the individual photodecomposition experiments for the two sampling events are given in **Appendix 4**.

9.3.5 Monomethyl Hg Concentration Dependence on Photodecomposition Rate

As noted previously, there is evidence that the photodegradation rate of mercury is dependent on another parameter besides light flux since the slopes of the individual photodegradation experiments varied significantly. Illustrated in **Figures 9.8A and 9.8B** is the dependence of MeHg concentration on the photodecomposition rate using PAR and UV, respectively, as the portion of the light spectrum responsible for MeHg photodecomposition. Rate dependence is determined by plotting the photodecomposition rate (regression slope) obtained for the individual experiments from **Table 9.2** against the initial MeHg concentration. **Figure 9.7A** represents the dependence based on PAR decomposition obtained using all the experimental data and **Figure 9.7B** represents the dependence observed when two experiments are removed (sites 20 and 31 in December). **Figures 9.8A** and **9.8B** are similarly structured to represent dependence on UV as driving photodecomposition. Removing the two experimental points from the dependence determination increases the regression coefficient significantly. In both cases, the regression is forced through zero, restricting MeHg decomposition to light driven processes only. Using the selected experimental results the concentration dependence on the photodecomposition rate is given by:

PAR Photodecomposition Rate (ng L^{-1} mol^{-1} m^2) = -0.0048 [MeHg, ng L^{-1}]$_I$ [PAR Flux, mol^{-1} m^2]
Equation 9.5

UV Photodecomposition Rate (ng L^{-1} mol^{-1} m^2) = -0.118 [MeHg, ng/L]$_I$ [UV Flux, mol^{-1} m^2]
Equation 9.6

The UV photodecomposition rate of -0.118 ng L^{-1} mol^{-1} m^2 represents the rate for all surface waters, and will be used as the starting point for all calculations involved with mass balance calculations (i.e. loss term) of MeHg from the rice fields and wetlands in the YBWA. Additional corrections on a field wide basis need to be made for light attenuation with depth and shading from emergent rice.

9.3.6 Modeling MeHg Photodecomposition in the YBWA

Mass balance modeling of the photodecomposition of MeHg in the Yolo Wildlife Area needs to account for variations due to:

1. Temporal changes in solar irradiation (both daily and seasonal)
2. MeHg concentration dependence on the photodegradation rate
3. Light attenuation with water column depth (TSS dependent)
4. Shading by emergent macrophytes

The resulting output can then be expressed as the mass of MeHg lost in a square meter of the water column per day (ng MeHg m^{-2} d^{-1}). This loss rate can also be expressed as a percent loss per day using information on the mass loading of MeHg in the YBWA. Given in **Table 9.4** is the percent loss of MeHg as a function of water column light attenuation and daily integrated PAR (Panel A) and UV (Panel B) light flux. This particular assessment was conducted for a water depth of 30 cm, approximating that of the water depths over a typical rice field in the YWA. The range in light flux spans typical winter and summer integrated light intensity conditions (**Figure 9.3**). Given in **Table 9.4** are the average water column mass losses of MeHg (ng MeHg m^{-2} d^{-1}) as function of MeHg concentration. This tabulation was conducting using an attenuation coefficient for PAR and UV of -0.029 and a total water depth of 30 cm. **Table 9.5A** shows the loss driven solely by PAR radiation and **Table 9.5B** shows the loss where UV radiation is responsible for MeHg photodecomposition. Again, the range in light flux spans typical winter and summer integrated light intensity conditions (see **Figure 9.3**).

Several important observations are apparent in these simulations of typical conditions in a rice field.

1. The loss of MeHg, when modeled as driven by UV light is significantly larger (typically greater than 2 times) than the loss that would result from a PAR driven light flux.

2. Assuming that the hydraulic residence time on a rice field is on the order of 12-25 days, then the potential for photodegrdation of MeHg, whether driven by PAR or UV becomes very significant in the mass balance of MeHg on the rice fields.

3. The photodecomposition loss of MeHg in the winter is far less than that in summer when photoperiod is longer and days are typically less cloud cover.

Shading of the water surface by emergent grasses was highly variable and difficult to incorporate into a modeling effort. While there were a paucity of measurements (~10 observations), the range in shading observed at the water surface between open water and rice fields varied between 45 and 89%. A typical shading value was around 70% of the incident light, meaning that only around 30% of the ambient light reached the water surface. The attenuation with depth in the emergent grasses appeared to be similar to that observed in the open water. To factor this into the modeling effort one would have to reduce the photodegradation predictions given in **Tables 9.3** and **9.4** by approximately 70% for that portion of the rice field where emergent grass exists, and for the time periods where emergent grass existed.

9.4 Summary

Photdecomposition of MeHg in the YWA was observed to be a direct function of both total light exposure (total photons of light, mol m^{-2}) and MeHg concentration (ng L^{-1}). No significant photodecomposition was observed with dark controls suggesting that the destruction of MeHg was abiotic and mediated by sunlight. The dependence of MeHg concentration on photodecomposition can be modeled based either on degradation by PAR or the UV portions of the light spectrum according to:

PAR Photodecomposition Rate (ng L^{-1} mol^{-1} m^2) = -0.0048 $[MeHg, ng/L]_I$ [PAR Flux, mol^{-1} m^2]

UV Photodecomposition Rate (ng L^{-1} mol^{-1} m^2) = -0.118 $[MeHg, ng/L]_I$ [UV Flux, mol^{-1} m^2]

The combination of these two controlling factors results in a much more significant MeHg photodecomposition in summer periods than in winter periods. The significant increase in summer is due primarily to two factors, more total light exposure (both intensity and period) and generally higher MeHg concentrations in the summer period compared to winter periods. A recent paper by **Li et al. (2010)** suggests that the photdegradation of MeHg is driven primarily by UV radiation, although most previous research related photodegradation to the PAR portion of the light spectrum. Both approaches are provided here, but it is clear that if driven solely by UV radiation, then the loss would be much more significant. Knowledge of environmental factors that influence photodegradation will clearly be useful in developing management strategies to mitigate MeHg problems and for controlling high MeHg inputs into the Delta. Environmental parameters that could potentially be manipulated to influence MeHg concentrations in open water areas such as YWA include: water clarity (TSS), shading by emergent aquatic vegetation, water residence time, and water depth.

10 Detailed Results for Public Outreach and Stakeholder Involvement

The data reported in this section addresses outreach support and environmental justice goals of the project.

10.1 Pre-Study Workshop

GOAL: To increase community and stakeholder understanding of MeHg exposure and share information between the research and stakeholder community.

TASK : Organize one (1) pre-study workshop in conjunction with the Yolo Bypass Working Group to discuss design and goals of project.

The Yolo Basin Foundation hosted a two-part Workshop on Mercury in the Yolo Bypass on Thursday, February 8, 2007. The meeting was facilitated by long-time Yolo Bypass Working Group facilitator, Dave Ceppos, with the Center for Collaborative Policy associated with California State University Sacramento. The morning session (10 a.m. to noon) introduced the new project. There were presentations on:

1. Mining history in northern California
2. Methylmercury and the TMDL process
3. Wetland Management in the Yolo Bypass Wildlife Area

After the presentation, project objectives, approach and expected outcome were discussed with questions and answers. There was a short break for lunch.

The second part of the meeting covered general information on mercury in the waterways of Yolo and Sacramento Counties and the status of fish-consumption advisories, TMDLs and other regulatory processes. There was an overview of ongoing education and outreach efforts including the Delta Fish Mercury Project.

10.1.1 Stakeholder Outreach for the Pre-study Workshop

TASK: Invite stakeholders representing a variety of potentially interested constituencies, including farmers, landowners, fish consumers, local and state government agencies, and other interested stakeholders.

A significant outreach effort ensured that 54 stakeholders attended the workshop. A press release announcing the workshop was sent to all of the local papers using Yolo Basin Foundation's press list. The over 200 participants on the Yolo Bypass Working Group listserve were invited by email to attend the workshop. Additionally several email invitations were sent to over 60 stakeholders in the public and private sector who are involved in water quality, environmental health, and advocacy concerns related to environmental justice issues.

The following organizations and agencies were represented at the pre-study workshop:
Government:

City of Davis Public Works
Yolo County Department of Health
Yolo County Planning Department
Irvington High School
Delta Protection Commission
Sacramento Area Flood Control Agency
State Water Resources Control Board
California State Department of Fish and Game Water Branch
California State Department of Fish and Game, Yolo Bypass Wildlife Area
California Wildlife Conservation Board
California State Department of Water Resources Division of Environmental Services
Central Valley Regional Water Quality Control Board
Office of Environmental Health Hazard Assessment, CA Environmental Protection Agency
California State Department of Water Resources
Solano County Environmental Management Department
California Department of Health Services
University of California Davis
University of California Cooperative Extension
US Geological Survey

Private Sector Business and Industry:
Techlaw Inc.
Homestake Mine
Larry Walker Associates
Shaw Environmental
Cal Test Analytical Lab
URS Corporation

Press:
Davis Enterprise

Agriculture Industry:
DeWit Farms, Rice Grower in Yolo Bypass
Schene Enterprises, Rancher in Yolo Bypass
California Rice Commission

Private Wetland Management:
Glide In Ranch (hunting club)

Conservation:
Delta Keeper
Yolo Basin Foundation
California Waterfowl Association
Ducks Unlimited
Solano Land Trust
Tuleyome

Sacramento River Watershed Program
California Indian Environmental Alliance

10.1.2 Pre-study Questionnaire

TASK: Prepare a questionnaire to be distributed at the workshops with goals of determining principal areas of stakeholder interest, level of knowledge of mercury issues with regard to fish consumption and human health, level of knowledge with regard to the THg-MeHg TMDL process.

A two-sided questionnaire was distributed to participants when they arrived for the workshop. One side had pre-workshop questions, and participants were asked to fill that out before the workshop started. The second side had the same questions but the attendees were asked to fill it out before they left.

The questionnaire listed various interests in the Bypass and the attendees were asked to check which applied to them. There were 34 respondents. Most people checked more than one area of interest. The interest tallies were as follows:

Land Use 15
Agriculture: 12
Wildlife: 15
Fishing: 13
Mercury advisories: 17
Mercury TMDL: 25
Other interests included: science behind wetland MeHg process; analytical; land management (Yolo Bypass Wildlife Area).

The first question on both the pre-workshop and post workshop questionnaires asked: “On a scale of 1 to 10 rate your knowledge of fish consumption advisories in the Yolo/Sacramento Area (1= not familiar, 10= very familiar.)” Pre-workshop responses ranged from 1 to 10 with an average of 5.79. Post-workshop responses ranged from 4 to 10 with an average of 7.10, indicating that participants felt that they had gained some more knowledge of the subject.

The second question on both the pre-workshop and post-workshop questionnaire asked: “On a scale of 1 to 10 rate your knowledge of the TMDL process with regard to mercury and methylmercury (1=not familiar, 5=moderately familiar, 10=very familiar).” The pre-workshop responses ranged from 1 to 10 with an average of 5.35. The post-workshop responses ranged from 2 to 10 with an average of 7.10, indicating that participants felt that they had also gained some additional knowledge on this subject.

Comments received included: “Helpful presentations describing recent research and upcoming studies in the Bypass;” “great gathering, looking forward to future updates;” “Good for scientific community, not so great for public health and local government attendees who deal with social issues, I enjoyed it a lot!” “Lots of information, what would be helpful next time is for all presenters to have copies of their PowerPoint presentations (maybe one big packet handed out to attendees before the meeting starts);” “Very good, thanks! Good presentations;” “would be great

to get semi-annual or annual updates on studies regarding MeHg characterization, control and BMPs;" "very good line-up of speakers;" "very informative;" "great turnout;" "good selection of speakers;" "At the beginning an objective was mentioned of including diversity and low income in this meeting – I didn't see it." "Helpful for basic overview of mercury processes and present issues."

10.1.3 Conclusion

The workshop was well attended, and many participants thanked the workshop organizers for making the opportunity available. People asked to be kept up-to-date on the issue of MeHg in the Yolo Bypass and with the research project during the year.

10.2 Post-Study Workshop

GOAL: To update the stakeholder community on research results of the project and increase community and stakeholder understanding of MeHg exposure.

TASK : Organize one (1) post-study workshop in conjunction with the Yolo Bypass Working Group to discuss design and goals of project.

The first part of the post-study workshop focused on results from the project. Dave Ceppos (with the Center for Collaborative Policy) facilitated the workshop. After Dave Feliz, Yolo Bypass Wildlife Area Manager, introduced the project, Mark Stephenson (with the Moss Landing Marine Laboratory) described the project and its hypotheses. Project scientists Mark Stephenson, Lisa Windham-Myers (with the U.S. Geological Survey, USGS), Phil Bachand (with Bachand and Associates), Charlie Alpers (USGS), Jacob Fleck (USGS), Mark Marvin-DiPasquale (USGS), and Josh Ackerman (USGS) presented the results by subject: hydrology, water quality, THg and MeHg loads, MeHg photo degradation, sediment, plants, and bioaccumulation. Part I concluded with a panel discussion by the project team on conclusions and evaluation of the hypotheses. The panel also discussed management practices that may affect MeHg bioaccumulation and export. After a lunch break, Part 2 of the workshop began with general information on mercury in Yolo and Sacramento Counties. Robert Brodberg (with the California Office of Environmental Health Hazard Assessment) discussed fish- consumption advisories related toMeHg as well as public health outreach and education. Patrick Morris (with the Regional Water Quality Control Board – Central Valley Region, RWQCB-CVR) and Dave Ceppos gave an update on the MeHg TMDL process in the Sacramento–San Joaquin Delta. Chris Foe (RWQCB-CVR) presented information based on MeHg studies conducted in the flooded Yolo Bypass in 2006. Mark Stephenson described current research on developing Best Management Practices for MeHg in the Yolo Bypass Wildlife Area. The workshop ended in a group discussion led by Dave Ceppos.

10.2.1 Stakeholder Outreach for the Post-study Workshop

TASK: Invite stakeholders representing a variety of potentially interested constituencies, including farmers, landowners, fish consumers, local and state government agencies, and other interested stakeholders.

A significant outreach effort resulted in 72 stakeholders attending the workshop. A press release announcing the workshop was sent to all of the local papers using Yolo Basin Foundation's press list. An article appeared in the *Davis Enterprise* the day before the workshop. More than 200 participants on the Yolo Bypass Working Group listserve were invited by email to attend the workshop. Additionally several email invitations were sent to over 60 stakeholders in the public and private sector that are involved in water quality, environmental health, and advocacy issues related to environmental justice issues. Members of the Lower Yolo Bypass Planning Forum were also invited.

The following organizations and agencies were represented at the post-study workshop:

Government:
City of Davis Public Works
City of Vacaville
Yolo County Department of Public Health
Delta Protection Commission
California Assembly Water, Parks and Wildlife Committee
State Water Resources Control Board
California State Department of Fish and Game Water Branch
California State Department of Fish and Game, Yolo Bypass Wildlife Area
California State Department of Fish and Game, Bay Delta Region
California State Department of Water Resources Division of Environmental Services
Central Valley Regional Water Quality Control Board
North Coast Regional Water Quality Control Board
Office of Environmental Health Hazard Assessment, CA Environmental Protection Agency
California Bay Delta Authority
North Delta Water Agency
Reclamation District 2068
Sacramento County Regional Sanitation District
Solano County Water Agency
University of California Davis
US Army Corps of Engineers
US Bureau of Land Management
US Fish and Wildlife Service
US Geological Survey

Private Sector Business and Industry:
AMEC
Burkeson Consulting
Clean Water Vision
EDAW
G. Fred Lee and Associates
A. Teichert and Son
Larry Walker Associates
Cal Test Analytical Lab
Wallace Kuhl & Associates

Agriculture Industry:
Conaway Ranch
DeWit Farms, Rice Grower in Yolo Bypass

Conservation:
Clean Water Action
Yolo Basin Foundation
California Waterfowl Association
Ducks Unlimited
Solano Land Trust
Tuleyome
The Nature Conservancy

10.2.2 Post-Study Questionnaire

TASK: Prepare a questionnaire to be distributed at the workshops with goals of determining principal areas of stakeholder interest, level of knowledge of mercury issues with regard to fish consumption and human health, level of knowledge with regard to the THg/MeHg TMDL process.

As with the pre-study workship, a two-sided questionnaire was distributed to participants when they arrived for the post-study workshop. One side had pre-workshop questions that participants were asked to fill that out before the workshop started. The second side had the same questions but the attendees were asked to fill it out before they left. There was also a space for comments.

The questionnaire listed various interests in the Bypass and the attendees were asked to check which applied to them.

There were 32 respondents. Most people checked more than one area of interest. The interest tallies were as follows:

Land Use 14
Agriculture: 12
Wildlife: 21
Fishing: 8
Mercury advisories: 12
Mercury TMDL: 24
Other interests included: research on fish, plants and microbes, mining and abandoned mine lands, impacts ofMeHg on subsistence fishing, mercury hotspots, making a documentary, wetland management, hunting, beneficial uses of the Bay-Delta, and policy issues related toMeHg and habitat restoration.

The first question on both the pre-workshop and post-workshop questionnaires asked: “On a scale of 1 to 10 rate your knowledge of fish consumption advisories in the Yolo/Sacramento Area (1= not familiar, 10= very familiar.)” Pre-workshop responses ranged from 1 to 10 with an

average of 5.75. Post-workshop responses ranged from 4 to 10 with an average of 7.83, indicating that participants felt that they had gained some more knowledge of the subject.

The second question on both the pre-workshop and post-workshop questionnaire asked: "On a scale of 1 to 10 rate your knowledge of the TMDL process with regard to mercury and methylmercury (1=not familiar, 5=moderately familiar, 10=very familiar)." The pre-workshop responses ranged from 1 to 10 with an average of 5.75. The post-workshop responses ranged from 2 to 10 with an average of 8.07, indicating that participants felt that they had gained some additional knowledge on the subject.

Comments received included: "great research project;" "very informative;" "great presentation of the study;" and "good update on status of current studies in the Yolo Bypass." The majority of comments were positive, but some indicated that the agenda was rushed and too ambitious and that the information was too technical.

10.2.3 Conclusion

The Workshop was well attended. People asked to be kept up-to-date on the issue of MeHg in the Yolo Bypass and with future research projects. Several participants expressed the opinion that MeHg research projects should be continued, as much more information is needed in order to develop effective Best Management Practices to reduce MeHg releases to the Bay Delta estuary.

10.3 PAEP Evaluation and Discussion

A Project Assessment and Evaluation Plan (PAEP) was used to evaluate the results of our field-based studies for use in developing BMP's for agricultural fields and managed wetlands within the Yolo Bypass of the S-SJ Delta. Project Goals and Desired Outcomes are as follows:

a. Project Goals for Research/Monitoring/Assessment

i. Aid in the development of an effective TMDL for MeHg in the Delta
ii. Aid in development of cost-efficient BMP's to reduce MeHg production, export and bioaccumulation

b. Desired Outcomes for Research/Monitoring/Assessment

i. Regional Water Board staff will have a better understanding of patterns and processes of MeHg production and export over an annual cycle through quantification of wetland management practices for the Yolo Bypass.

The results reported here have not yet been used directly in the TMDL for MeHg in the Delta, but are being considered by members of the SWRCB as quantitative information to modify BMP guidelines. Our goal of 50% acceptance and use of the resulting BMP guidelines for the MeHg TMDL by land managers has not yet been tested, as the BMPs have yet to be developed by the SWRCB.

c. Project Goals for Education/Outreach/Capacity-building

i. Increase community and stakeholder understanding of MeHg exposure
ii. Increase bi-directional sharing of information between the research and stakeholder community

d. Desired Outcomes for Education/Outreach/Capacity-Building

i. Wetland managers understand how to aid in reducing MeHg production and export from wetlands of the Yolo Bypass.
ii. Disadvantaged communities become more informed as to the risk and causes of Hg contamination of sport fish in the Yolo Bypass.

We exceeded targets for the following project goals in education and outreach:

GOAL 1: Greater literacy among land managers regarding Hg cycling in the Yolo Bypass and the proposed MeHg TMDL for the Delta.

RESULT: 20% greater understanding of Hg cycling in the Yolo Bypass, 20% greater understanding of fish consumption guidelines and relation to land management, and 20% greater understanding of biogeochemical conditions related to fish Hg levels

GOAL 2: Greater awareness among disadvantaged communities of the risks of consuming Hg in specific fish.

RESULT: 20% greater awareness of MeHg consumption risks among stakeholders.
We still seek to evaluate the use of MeHg risk information in an additional 20% of school and community newsletters or other documents.

GOAL 3: Direct sharing of study results with designated stakeholders.

RESULT: Formal presentation and distribution of project fact sheet with CALFED-abstracts to 100% of designated stakeholdersat post-study meeting

In summary, quantifiable goals of the PAEP research agenda have been largely met, but BMP development and implementation has a longer timeframe for evaluation. In addition to positive public evaluation of the pre- and post-study meetings, high stakeholder turnout and interaction with PI's both at the meeting and in subsequent telephone and e-mail conversations are evidence of the successful outreach effort to share the patterns and processes of MeHg production, bioaccumulation and export on managed wetlands of the YBWA.

11 REFERENCES CITED

Ackerman, J.T., and Eagles-Smith C.A., 2008, A dual life-stage approach to monitoring the effects of mercury concentrations on the reproductive success of Forster's Terns in San Francisco Bay: Final Administrative Report, U. S. Geological Survey, Western Ecological Research Center, Davis, Calif., 41 p.

Ackerman J.T., and Eagles-Smith C.A., 2010, Agricultural wetlands as potential hotspots for bioaccumulation: experimental evidence using caged fish: Environmental Science and Technology, v. 44, p. 1451–1457.

Ackerman, J.T., Miles, A.K., and Eagles-Smith, C.A., 2010, Invertebrate mercury bioaccumulation in permanent, seasonal, and flooded rice wetlands within California's Central Valley: Science of the Total Environment, v. 408, p. 666–671.

Ackerman, J.T., Takekawa, J.Y., Eagles-Smith, C.A., and Iverson, S.A., 2008, Mercury contamination and effects on survival of American avocet and black-necked stilt chicks in San Francisco Bay: Ecotoxicology, v. 17, p. 103–116.

Albers, P.H., Koterba, M.T., Rossman, R., Link, W.A., French, J.B., Bennett, R.S., and Bauer, W.C., 2007, Effects of methylmercury on reproduction in American kestrels: Environmental Toxicology and Chemistry, v. 26, p. 1856–1866.

Alisauskas, R.T., and Ankney, C.D., 1992, The cost of egg laying and its relationship to nutrient reserves in waterfowl, *in* Batt, B.D.J., Afton, A.D., and others, eds., Ecology and management of breeding waterfowl: Minneapolis, University of Minnesota Press, p. 30–61.

Allen, R.G., Pereira, L.S., Raes, D., and Smith, M., 1998, Crop evapotranspiration — guidelines for computing crop requirements: Irrigation and Drainage Paper 56, Food and Agriculture Organization of the United Nations, Rome, Italy. *http://www.fao.org/docrep/X0490E/X0490E00.htm* (accessed Sept. 30, 2010).

Alpers, C.N., Eagles-Smith, C., Foe, C., Klasing, S., Marvin-DiPasquale, M.C., Slotton, D.G., and Windham-Myers, L., 2008, Mercury conceptual model. Sacramento, Calif.: Delta Regional Ecosystem Restoration Implementation Plan, 62 p. http://www.science.calwater.ca.gov/pdf/drerip/DRERIP_mercury_conceptual_model_final_012408.pdf

Alpers, C.N., Hunerlach, M.P., Marvin-DiPasquale, M.C., Antweiler, R.C., Lasorsa, B.K., De Wild, J.F., and Synder, N.P., 2006, Geochemical data for mercury, methylmercury, and other constituents in sediments from Englebright Lake, California, 2002: U.S. Geological Survey, Data Series 151, 107 p. *http://pubs.er.usgs.gov/usgspubs/ds/ds151*

Anderson, R.O., and Neumann, R.M., 1996, Length, weight, and associated structural indices, *in* Murphy, B.R., and Willis, D.W., eds., Fisheries techniques, second edition: American Fisheries Society, Bethesda, Maryland, p. 447–482.

Bachand and Associates, Hydrofocus, Inc., University of California, Davis, U.S. Geological Survey, Ducks Unlimited, and Contra Costa Water District, 2006, Reducing non-point DOC and nitrogen exports from rice fields: A pilot study and quantitative survey to determine the effects of different hydrologic management practices: Final Report to State Water Resources Control Board, Agreement 03-165-555-0, Davis, Calif., May 19, 2006, 194 p., appendices. *http://aquacomm.fcla.edu/2072/1/FINAL_REPORT_2006.pdf* (accessed Sept. 30, 2010).

Bagwell, C.E., Piceno, Y.M., Ashburne-Lucas, A.L., and Lovell, C.R., 1998, Physiological diversity of the rhizosphere diazotroph assemblages of selected salt marsh grasses: Applied Environmental Microbiology, v. 64, no. 11, p. 4276–4282.

Balci, N., Shanks III, W.C., Mayer, B., and Mandernack, K.W., 2007, Oxygen and sulfur isotope systematics of sulfate produced by bacterial and abiotic oxidation of pyrite: Geochimica et Cosmochimica Acta, v. 71, p. 3796–3811.

Barkay, T., Gillman, M., and Turner, R.R., 1997, Effects of dissolved organic carbon and salinity on bioavailability of mercury: Applied and Environmental Microbiology, v. 63, no. 11, p. 4267–4271.

Barkay, T., and Wagner-Döbler, I., 2005, Microbial transformations of mercury — potentials, challenges, and achievements in controlling mercury toxicity in the environment: Advances in Applied Microbiology, v. 57, p. 1-52.

Barr, J.F., 1986, Population dynamics of the common loon (Gavia immer) associated with mercury-contaminated waters in northwestern Ontario: Canadian Wildlife Service Occasional Paper No. 56, Ottawa, Canada, 25 p.

Beckvar, N., Dillon, T.M., and Read, L.B., 2005, Approaches for linking whole-body fish tissue residues of mercury or DDT to biological effects thresholds: Environmental Toxicology and Chemistry, v. 24, p. 2094–2105.

Benoit J.M., Gilmour C.C., Heyes A., Mason R., and Miller, C., 2003, Geochemical and biological controls over methylmercury production and degradation in aquatic systems, *in* Chai, Y., and Braids, O.C., eds., Biochemistry of Environmentally Important Trace Elements: ACS Symposium Series 835, American Chemical Society, Washington, D.C., p. 262–297.

Benoit, J.M., Gilmour, C.C., and Mason, R.P., 2001, The influence of sulfide on solid-phase mercury bioavailability for methylation by pure cultures of *Desulfobulbus propionicus* (1pr3): Environmental Science and Technology, v. 35, no. 1, p. 127–132.

Benoit, J.M., Gilmour, C.C., Mason, R.P., and Heyes, A., 1999, Sulfide controls on mercury speciation and bioavailability to methylating bacteria in sediment porewaters: Environmental Science and Technology, v. 33, p. 951–957.

Benoit, J.M., Mason, R.P., Gilmour, C.C., and Aiken, G.R., 2001, Constants for mercury binding by dissolved organic matter isolates from the Florida Everglades: Geochimica et Cosmochimica Acta, v. 65, no. 24, p. 4445-4451.

Bird, J.A., Pettygrove, G.S., and Eadie, J.M., 2000, The impact of waterfowl foraging on the decomposition of rice straw: mutual benefits for rice growers and waterfowl: Journal of Applied Ecology, v. 37, p. 728–741.

Blaabjerg, V. and Finster, K., 1998, Sulphate reduction associated with roots and rhizomes of the marine macrophyte Zostera marina: Aquatic Microbial Ecology, v. 15, p. 311–314.

Bloom, N.S.,1993, Determination of picogram levels of methylmercury by aqueous phase ethylation, followed by cryogenic gas chromatography, with cold vapour atomic fluorescence detection: Canadian Journal of Fisheries and Aquatic Sciences, v. 46, p. 1131–1140.

Bonneville, S., Van Cappellen, P., and Behrends, T., 2004, Microbial reduction of iron (III) oxyhydroxides: effects of mineral solubility and availability: Chemical Geology, v. 212, p. 255–268.

Borga, P., Nilsson, M., and Tunlid, A., 1994, Bacterial communities in peat in relation to botanical composition as revealed by phospholipid fatty acid analysis: Soil Biology and Biochemistry, v. 26, p. 841–848.

Bouman, B.A.M., Wopereis, M.C.S., Kropff, M.J., ten Berge, H.F.M., and Tuong, T.P., 1994, Water use efficiency of flooded rice fields. II. Percolation and seepage losses: Agricultural Water Management, v. 26, p. 291–304.

Brady, N.C. and Weil, R.R., 2002, The Nature and Properties of Soils (13th ed.): Upper Saddle River, N.J., Prentice Hall, 960 p.

Branfireun, B., Heyes, A., and Roulet, N., 1996, The hydrology and methylmercury dynamics of a Precambrian Shield headwater peatland: Water Resources Research, v. 32, no. 6, p. 1785–1794.

Brumbaugh, W.G., Krabbenhoft, D.P., Helsel, D.R., Wiener, J.G., and Echols, K.R., 2001, A national pilot study of mercury contamination of aquatic ecosystems along multiple gradients — Bioaccumulation in fish: U.S. Geological Survey, Biological Science Report USGS/BRD/BSR-2001-0009, 26 p.

Burgess N.M., and Meyer, M.W., 2008, Methylmercury exposure associated with reduced productivity in common loons: Ecotoxicology, v. 17, p. 83–91.

Byington, A., 2007, Photo-degradation of methylmercury in the Sacramento–San Joaquin Delta Estuary: San Jose, Calif., San Jose State University and Moss Landing Marine Laboratory, Master's thesis, 64 p.

Byington, A., Coale, K., Gill, G., and Choe, K.-Y., 2005, Photo-degradation of methyl mercury (MeHg) in the Sacramento-San Joaquin Delta [abs.]: State of the San Francisco Estuary Conference, 7th Biennial, Oakland, Calif., October 4–6, 2005. *http://www.abag.ca.gov/abag/events/estuary/pdfs/SOE_2005_abstracts_poster.pdf* (accessed Sept. 30, 2010)

Capone, D.G., and Kiene, R.P., 1988, Comparison of microbial dynamics in marine and freshwater sediments: Contrasts in anaerobic carbon catabolism: Limnology and Oceanography, v. 33, p. 725–749.

Carmody, R.W., Plummer, L.N., Busenberg, E., and Coplen, T.P., 1998, Methods for collection of dissolved sulfate and sulfide and analysis of their sulfur isotopic composition: U.S. Geological Survey Open-File Report 97-234, 91 p.

Cheng, S., Johnson, D.W., and Fu, S., 2003, Rhizosphere effects on decomposition: controls of plant species, phenology, and fertilization: Soil Science Society of America Journal, v. 67, p. 1418–1427.

Clark, I.D., and Fritz, P., 1997, Environmental Isotopes in Hydrogeology: New York, Lewis Publishers, 328 p.

Compeau, G., and Bartha, R., 1984, Methylation and demethylation of mercury under controlled redox, pH, and salinity conditions: Applied and Environmental Microbiology, v. 50, p. 498–502.

Compeau, G.C., and Bartha, R., 1985, Sulfate-reducing bacteria — Principal methylators of mercury in anoxic estuarine sediment: Applied and Environmental Microbiology, v. 50, p. 498-502.

Conaway, C.H., Squire, S., Mason, R.P., and Flegal, A.R., 2003, Mercury speciation in the San Francisco Bay estuary: Marine Chemistry, v. 80, p. 199–225.

Dahl, T.E., 1990, Wetland losses in the United States 1780's to 1980's: U.S. Department of the Interior, Fish and Wildlife Service, Washington, D.C., 13 p. *http://www.fws.gov/wetlands/_documents/gSandT/NationalReports/WetlandsLossesUS1780sto1980s.pdf* (accessed Sept. 30, 2010)

Davis, J.A., Yee, D., Collins, J.N., Schwarzbach, S.E., and Louma, S.N., 2003, Potential for increased mercury accumulation in the estuary food web, *in* Brown, L.R., ed., Issues in San Francisco Estuary Tidal Wetlands Restoration: San Francisco Estuary and Watershed Science:

v. 1, issue 1, article 4 http://repositories.cdlib.org/jmie/sfews/vol1/iss1/art4 (accessed Sept. 30., 2010)

de Szalay, F.A., Carroll, C., Beam, J.A, and Resh, V.H., 2003, Temporal overlap of nesting duck and aquatic invertebrate abundances in the Grasslands Ecological Area, California, USA: Wetlands, v. 23, p. 739–749.

Del Vecchio, R., and Blough, N.V., 2002, Photobleaching of chromophoric dissolved organic matter in natural waters: kinetics and modeling: Marine Chemistry, v. 78, p. 231–253.

DeWild, J., Olund, S.D., Olson, M.L., Tate, M.T., 2004, Methods for the preparation and analysis of solids and suspended solids for methylmercury: U.S. Geological Survey Techniques and Methods for Water Investigations, Book 5, A-7, 21 p. http://pubs.usgs.gov/tm/2005/tm5A7/

Downing, B.D., Bergamaschi, B.A., Evans, D.G., and Boss, E., 2008, Estimating source-specific contributions of DOC into a drinking-water reservoir using optical profiling: Lake and Reservoir Management, v. 24, p. 381–391.

Drexel, R.T., Haitzer, M., Ryan, J.N., Aiken, G.R., and Nagy, K.L., 2002, Mercury (II) sorption to two Florida Everglades peats: Evidence for strong and weak binding and competition by dissolved organic matter released from the peat: Environmental Science and Technology, v. 36, p. 4058-4064.

Driscoll, C.T., Holsapple, J., Schofield, C.L., and Munson, R., 1998, The chemistry and transport of mercury in a small wetland in the Adirondack Region of New York, USA: Biogeochemistry, v. 40, no. 2/3, p. 137–146. [Mercury as a Global Pollutant, 4th International Conference.]

Ehrenfeld, J.G., Ravit, B., and Elgersma, K., 2005, Feedback in the plant-soil system: Annual Review of Environmental Resources, v. 30, p. 75–115.

Elphick, C.S., 2000. Functional equivalency between rice fields and seminatural wetland habitats: Conservation Biology, v. 14, p. 1–13.

Elphick, C.S., and Oring, L.W., 1998, Winter management of California rice fields for waterbirds: Journal of Applied Ecology, v. 35, p. 95–108.

Fleming, E.J., Mack, E.E., Green, P.G., and Nelson, D.C., 2006, Mercury methylation from unexpected sources: molybdate-inhibited freshwater sediments and an iron-reducing bacterium: Applied and Environmental Microbiology, v. 72, p. 457–464.

Foe, C., Louie, S., and Bosworth, D., 2008, Methyl mercury concentrations and loads in the Central Valley and freshwater Delta, *task 2 of* Transport, Cycling, and Fate of Mercury and Monomethyl Mercury in the San Francisco Delta and Tributaries: An Integrated Mass Balance Assessment Approach: Final report to Calif. Dept. of Fish and Game and California Bay-Delta Authority, Sept. 2008, 41 p., 37 figs., 21 tbls. http://mercury.mlml.calstate.edu/wp-content/uploads/2008/10/04_task2mmhg_final.pdf (accessed Sept. 30, 2010)

Frayer, W.E., Peters, D.D., and Pywell, H.R., 1989, Wetlands of the California Central Valley Status and Trends: 1939 to mid-1980's: U.S. Department of the Interior, Fish and Wildlife Service, Washington, D.C. 28 p.

Frimmel, F.H., 1998a, Characterization of natural organic matter as major constituents in aquatic systems: Journal of Contaminant Hydrology, v. 35, p. 201–216.

Frimmel, F.H., 1998b, Impact of light on the properties of aquatic natural organic matter: Environment International, v. 24, p. 559–571.

Gassel, M., Brodberg, R.K., Klasing, S., and Roberts, S., 2007, Draft safe eating guidelines for fish and shellfish from the San Joaquin River and South Delta (Contra Cost, San Joaquim,

Stanislaus, Merced, Madera, and Fresno Counties): Sacramento, Calif., California Office of Environmental Health Hazard Assessment, March 2007, 124 p. http://www.oehha.ca.gov/fish/so_cal/centralsouthdelta.html (accessed Sept. 30, 2010)

Gassel, M., Brodberg, R.K., Klasing, S., and Roberts, S., 2008, Draft safe eating guidelines for fish and shellfish from the Sacramento River and Northern Delta: Sacramento, Calif., California Office of Environmental Health Hazard Assessment, April 2008, 31 p., 9 tbls., 6 figs., appendices. http://www.oehha.ca.gov/fish/so_cal/srnd041108.html (accessed Sept. 30, 2010)

George, B.M., Batzer, D., 2008, Spatial and temporal variations of mercury levels in Okefenokee invertebrates, southeast Georgia: Environmental Pollution, v. 152, p. 484–490.

Giesemann, A., Jager, H.J., Norman, A.L., Krouse, H.R., Brand, W.A., 1994, On-line sulfur-isotope determination using an elemental analyzer coupled to a mass spectrometer: Analytical Chemistry, v. 66, p. 2816–2819.

Gill, G., 2008a, Monomethylmercury photo-degradation studies, *Task 5.1 in* Transport, Cycling, and Fate of Mercury and Monomethyl Mercury in the San Francisco Delta and Tributaries: An Integrated Mass Balance Assessment Approach: Final report to the California Department of Fish and Game and the California Bay Delta Authority, 21 p. *http://mercury.mlml.calstate.edu/wp-content/uploads/2008/10/09_task5_1_final.pdf* (accessed Sept. 30, 2010)

Gill, G., 2008b, Sediment biogeochemistry studies in Delta wetlands, *Task 5.3b in* Transport, Cycling, and Fate of Mercury and Monomethyl Mercury in the San Francisco Delta and Tributaries: An Integrated Mass Balance Assessment Approach: Final report to the California Department of Fish and Game and the California Bay Delta Authority, 16 p. http://mercury.mlml.calstate.edu/wp-content/uploads/2008/10/17_task5_3b_final.pdf (accessed Sept. 30, 2010)

Gill, G.A., and Fitzgerald, W.F., 1985, Mercury sampling in open ocean waters at the picomolar level: Deep-Sea Research, v. 32, p. 287–297.

Gilmer, D.S., Miller, M.R., Bauer, R.D., LeDonne, J.R., 1982, California's Central Valley wintering waterfowl: concerns and challenges: Transactions, North American Wildlife and Natural Resources Conference, v. 47, p. 441–452.

Gilmour, C.C., Henry, E.A., and Mitchell, R., 1992, Sulfate stimulation of mercury methylation in freshwater sediments: Environmental Science and Technology, v. 26, p. 2281–2287.

Gilmour, C., Krabbenhoft, D., Orem, W., and Aiken, G., 2004, Influence of drying and rewetting on mercury and sulfur cycling in Everglades and STA Soils, *Appendix 2B-1 in* 2004 Everglades Consolidated Report: South Florida Water Management District and Florida Department of Environmental Protection, 19 p. *https://my.sfwmd.gov/pls/portal/docs/PAGE/PG_GRP_SFWMD_SFER/PORTLET_PREVREPORT/FINAL/INDEX.HTML* (accessed Sept. 30, 2010)

Grenier, L., Marvin-DiPasquale, M., Drury, D., Hunt, J., Robinson, A., Bezalel, S., Melwani, A., Agee, J., Kakouros, E., Kieu, L., Windham-Myers, L., and Collins, J., 2010, South Baylands Mercury Project. Cooperator Report prepared for the California State Coastal Conservancy by San Francisco Estuary Institute, U.S. Geological Survey, and Santa Clara Valley Water District, February 10, 2010, 97 p. http://www.sfei.org/sites/default/files/SBMP_Final%20Report%2010FEB2010.pdf

Gu, L., Post, W.M., and King, A.W., 2004, Fast labile carbon turnover obscures sensitivity of heterotrophic respiration from soil to temperature: a model analysis: Global Biogeochemical Cycles, v.18, GB1022, doi:10.1029/2003GB002119

Haitzer, M., Aiken, G.R., and Ryan, J.N., 2003, Binding of mercury (II) to aquatic humic substances: influence of pH and source of humic substances: Environmental Science and Technology, v. 37, p. 2436–2441.

Hall, B.D., Aiken, G.R., Krabbenhoft, D., Marvin-DiPasquale, M., Swarzenski, C.M., 2008, Wetlands as principal zones of methylmercury production in southern Louisiana and the Gulf of Mexico region: Environmental Pollution, v. 154, p.124–134.

Hall, B.D., Rosenberg, D.M., Wiens, A.P., 1998, Methyl mercury in aquatic insects from an experimental reservoir: Canadian Journal of Fisheries and Aquatic Sciences, v. 55, p. 2036–2047.

Hall, B.D., St. Louis, V.L., and Bodaly, R.A., 2004, The stimulation of methylmercury production by decomposition of flooded birch leaves and jack pine needles: Biogeochemistry, v. 68, p.107–129.

Hammerschmidt, C.R. and Fitzgerald, W.F., 2006, Photodecomposition of methylmercury in an Arctic Alaskan Lake: Environmental Science and Technology, v. 40, p. 1212–1216.

Harmon, S.M., King, J.K., Gladden, J.B., Chandler, G.T, Newman, L.A., 2005, Mercury body burdens in *Gambusia holbrooki* and *Erimyzon sucetta* in a wetland mesocosm amended with sulfate: Chemosphere, v. 59, p. 227–233.

Heald, C.C., ed., 2002, Cameron Hydraulic Data -- A handy reference on the subject of hydraulics and steam (19th ed.): Irving, Tex., Flowserve, Inc.

Hecky, R.E., Ramsey, D.J., Bodaly, R.A., and Strange, N.E., 1991, Increased methylmercury contamination in fish in newly formed freshwater reservoirs, *in* Suzuki, T., Imura, N., and Clarkson, T.W., eds., Advances in Mercury Toxicity: Proceedings of a Conference held in Tokyo, Japan, Aug. 1–3, 1990. Springer, p. 33–52.

Heim, W., Coale, K., Stephenson, M., Choe, K.-Y., Gill, G., and Foe, C., 2007, Spatial and habitat-based variations in total and methyl mercury concentrations in surficial sediments in the San Francisco Bay-Delta: Environmental Science and Technology, v. 41, p. 3501–3507.

Heim, W.A., Deverel, S., Ingrum, T., Piekarski, W., and Stephenson, M., 2009, Assessment of Methylmercury Contributions from Sacramento-San Joaquin Delta Farmed Islands: Final report submitted to the Central Valley Regional Water Quality Control Board, contract 04-235-150-0, August 2009, 54 p. *http://www.waterboards.ca.gov/centralvalley/water_issues/tmdl/central_valley_projects/delta_hg/other_technical_reports/* (accessed Sept. 30, 2010)

Heinz, G.H., 1979, Methylmercury: reproductive and behavioral effects on three generations of mallard ducks: Journal of Wildlife Management, v. 43, p. 394–401.

Heinz, G.H., Hoffman, D.J., Klimstra, J.D., Stebbins, K.R., Konrad, S.L., and Erwin, C.A., 2009, Species differences in the sensitivity of avian embryos to methylmercury: Archives of Environmental Contamination and Toxicology, v. 56, p. 129–138.

Hines, M.E, Banta, G.T., Giblin, A.E., Hobbie, J.E., and Tugel, J.B., 1994, Acetate concentrations and oxidation in salt-marsh sediments: Limnology and Oceanography, v. 39, p.140–148.

Hines, M.E., Knollmeyer, S.L., and Tugel, J.B., 1989, Sulfate reduction and other sedimentary biogeochemistry in a northern New England salt marsh: Limnology and Oceanography, v. 34, p. 578–590.

Horvat, M., Bloom, N.S., and Liang, L., 1993, A comparison of distillation with other current isolation methods for the determination of methyl mercury compounds in low level environmental samples. Part 2, water: Analytica Chimica Acta, v. 282, p. 153–168.

Hurley, J.P., Benoit, J.M., Babiarz, C.L., Shafer, M.M., Andren, A.W., Sullivan, J.R., Hammond, R., Webb, D.A.,1995, Influences of watershed characteristics on mercury levels in Wisconsin rivers: Environmental Science and Technology, v. 29, p. 1867–1875.

Hylander, L.D., Meili, M., Oliveira, L.J., de Castro e Silva, E., Guimaraes, J.R.D., Araujo, D.M., Neves, R.P., Stachiw, R., Barros, A.J.P., and Silva, G.D., 2000, Relationship of mercury with aluminum, iron and manganese oxy-hydroxides in sediments from the Alto Pantanal, Brazil: The Science of the Total Environment, v. 260, no. 1-3, p. 97–107.

International Wild Rice Association, 2007, The Manomin News: v. 17, no. 4, November 2007, Outing, Minn.

Jacob, D.L. and Otte, M.L., 2003, Conflicting processes in the wetland plant rhizosphere: metal retention or mobilization?: Water, Air, and Soil Pollution, v. 3, p. 91–104.

Jeffres, C.A., Opperman, J.J., Moyle, P.B., 2008, Ephemeral floodplain habitats provide best growth conditions for juvenile Chinook salmon in a California river: Environmental Biology of Fishes, v. 83, p. 449–458.

Jeremiason, J.D., Engstrom, D.R., Swain, E.B., Nater, E.A., Johnson, B.M., Almendinger, J.E., Monson, B.A., and Kolka, R.K., 2006, Sulfate addition increases methylmercury production in an experimental wetland: Environmental Science and Technology, v. 40, p. 3800–3806.

Kelly, C.A., Rudd, J.W.M., Bodaly, R.A., Roulet, N.P., St.Louis, V.L., Heyes, A., Moore, T.R., Schiff, S., Aravena, R., Scott, K.J., Dyck, B., Harris, R., Warner, B., and Edwards, G., 1997, Increases in fluxes of greenhouse gases and methyl mercury following flooding of an experimental reservoir: Environmental Science and Technology, v. 31, p. 1334–1344.

Kerin, E., Gilmour, C.C., Roden, E., Suzuki, M.T., Coates, J.D., and Mason, R.P., 2006, Mercury methylation among the dissimilatory iron-reducing bacteria: Applied and Environmental Microbiology, v. 72, p. 7919–7921.

King, J.K., Kostka, J.E., Frischer, M.E., Saunders, F.M., and Jahnke, R.A., 2001, A quantitative relationship that demonstrates mercury methylation rates in marine sediments are based on the community composition and activity of sulfate-reducing bacteria: Environmental Science and Technology, v. 35, no. 12, p. 2491–2496.

Krabbenhoft, D.P., Benoit J.M., Babiarz C.L., Hurley J.P., and Andren A.W., 1995, Mercury cycling in the Allequash Creek Watershed, northern Wisconsin: Water, Air, and Soil Pollution, v. 80, p. 425–433.

Krabbenhoft, D.P., Wiener, J.G., Brumbaugh, W.G., Olson, M.L., DeWild, J.F., Sabinal, T.J., 1999, A national pilot study of mercury contamination of aquatic ecosystems along multiple gradients, *in* Morganwalp, D.W., and Buxton, H.T., eds., , U.S. Geological Survey Toxic Substances Hydrology Program — Proceedings of the Technical Meeting, Charleston, SC, March 8-12, 1999 – Volume 2 of 3 – Contamination of Hydrologic Systems and Related Ecosystems, USGS Water-Resources Investigations Report: 99-4018, p. 147-160. Available at: *http://toxics.usgs.gov/pubs/wri99-4018/Volume2/sectionB/2301_Krabbenhoft/pdf/2301_Krabbenhoft.pdf* (accessed: August, 2007)

Krapu, G.L., and Reinecke, K.J., 1992, Foraging ecology and nutrition, *in* Batt, B.D.J., Afton, A.D., Anderson, M.G., Ankney, C.D., Johnson, D.H., Kadlec, J.A., and Krapu, G.L., eds.,

Ecology and management of breeding waterfowl: Minneapolis, University of Minnesota Press, p. 1–29.
Krumme, U., Brenner, M., and Saint-Paul, U., 2008, Spring-neap cycle as a major driver of temporal variations in feeding of intertidal fishes: Evidence from the sea catfish *Sciades herzbergii* (Ariidae) of equatorial west Atlantic mangrove creeks: Journal of Experimental Marine Biology and Ecology, v. 367, no. 2, p. 91–99.
Lacerda, L.D., and Fitzgerald, W.F., 2001, Biogeochemistry of mercury in wetlands: Wetlands Ecology and Management, v. 9, p. 291-293.
Langer, C.S., Fitzgerald, W.F., Visscher, P.T., and Vandal, G.M., 2001, Biogeochemical cycling of methylmercury at Barn Island Salt Marsh, Stonington, CT, USA: Wetlands Ecology and Management, v. 9, p. 295–310.
Lee, R., Kraus, D.W., and Doeller, J.E., 1999, Oxidation of sulfide by Spartina alterniflora roots: Limnology and Oceanography, v. 44, p. 1155–1159.
Li, Yanbin, Mao, Y., Liu, G., Tachiev, G., Roelant, D., Feng. X., Cai, Y., 2010, Degradation of methylmercury and its effects on mercury distribution and cycling in the Florida Everglades: Environmental Science and Technology, v. 44, p. 6661–6666.
Lovley, D.R., and Phillips, E.J.P., 1987a, Rapid assay for microbially reducible ferric iron in aquatic sediments: Applied and Environmental Microbiology, v. 53, p. 1536–1540.
Lovley, D.R., and Phillips, E.J.P., 1987b, Competitive mechanisms for inhibition of sulfate reduction and methane production in the zone of ferric iron reduction in sediments: Applied and Environmental Microbiology, v. 53, p. 2636–2641.
Liu, C.W., Chen, K., Jou, S.W., and Kuo, S.F., 2001, Estimation of the infiltration rate of a paddy field in Yun-Lin, Taiwan: Agricultural Systems, v. 68, p. 41–54.
Marchetti, M.P., and Moyle, P.B., 2000, Spatial and temporal ecology of native and introduced fish larvae in lower Putah Creek, California: Environmental Biology of Fishes, v. 58, p. 75–87.
Marins, R.V., Lacerda, L.D., Goncalves, G.O., de Paiva, E.C., 1997, Effect of root metabolism on the post-depositional mobilization of mercury in salt marsh soils: Bulletin of Environmental Contamination and Toxicology, v. 58, p. 733–738.
Marschner, H., 1995, The mineral nutrition of higher plants (2nd ed.): London, Academic Press, 889 p.
Martens, C.S., and Berner, R.A., 1974, Methane production in the interstitial waters of sulfate depleted marine sediments: Science, v. 185, p. 1167–1169.
Marvin-DiPasquale, M., and Agee, J.L., 2003, Microbial mercury cycling in sediments of the San Francisco Bay-Delta: Estuaries, v. 26, no. 6, p. 1517–1528.
Marvin-DiPasquale, M., Agee, J., Bouse, R., and Jaffe, B., 2003a, Microbial cycling of mercury in contaminated pelagic and wetland sediments of San Pablo Bay, California: Environmental Geology: v. 43, no. 3, p. 260–267.
Marvin Di-Pasquale, M., Alpers, C.N., and Fleck, J.A., 2009a, Mercury, methylmercury, and other constituents in sediment and water from seasonal and permanent wetlands in the Cache Creek Settling Basin and Yolo Bypass, Yolo County, California, 2005−06: U.S. Geological Survey, Open File Report 2009-1182, 69 p. *http://pubs.usgs.gov/of/2009/1182/* (accessed Sept. 30, 2010)
Marvin-DiPasquale, M.C., Boynton, W.R., and Capone, D.G., 2003b, Benthic sulfate reduction along the Chesapeake Bay central channel. II. Temporal controls: Marine Ecology Progress Series, v. 260, p. 55–70.
Marvin-DiPasquale, M., and Cox, M.H., 2007, Legacy mercury in Alviso Slough, South San Francisco Bay, California: Concentration, speciation and mobility: U.S. Geological Survey

Open-File Report 2007-1240, 98 p. http://pubs.usgs.gov/of/2007/1240/ (accessed Sept. 30, 2010)

Marvin-DiPasquale, M.C., Lutz, M.A., Brigham, M.E., Krabbenhoft, D.P., Aiken, G.R., Orem, W.H., and Hall, B.D., 2009b, Mercury cycling in stream ecosystems. 2. Benthic methylmercury production and bed sediment-pore water partitioning: Environmental Science and Technology, v.43, p. 2726–2732.

Marvin-DiPasquale, M.C., Lutz, M.A., Krabbenhoft, D.P., Aiken, G.R., Orem, W.H., Hall, B.D., DeWild, J.F., and Brigham, M.E., 2008, Total mercury, methylmercury, methylmercury production potential, and ancillary streambed-sediment and pore-water data for selected streams in Oregon, Wisconsin, and Florida, 2003–04: U.S. Geological Survey Data Series 375, 24 p.

Marvin-DiPasquale, M., Stewart, A.R., Fisher, N.S., Pickhardt, P., Mason, R.P., Heyes, A., and Windham-Myers, L., 2007, Evaluation of mercury transformations and trophic transfer in the San Francisco Bay/Delta: Identifying critical processes for the Ecosystem Restoration Program: final report to California Bay Delta Authority, project ERP-02-P40, 40 p.

McKnight, D.M., Boyer, E.W., Westerhoff, P.K., Doran, P.T., Kulbe, T., and Anderson, D.T., 2001, Spectrofluorometric characterization of dissolved organic matter for indication of precursor organic material and aromaticity: Limnology and Oceanography, v. 46, no. 1, p. 38–48.

Mehrotra, A.S., Horne, A.J., and Sedlak, D.L., 2003, Reduction of net mercury methylation by iron in Desulfobulbus propionicus (1pr3) cultures: implications for engineered wetlands: Environmental Science and Technology, v. 37, p. 3018–3023.

Melillo, J.M., Aber, J.D., and Muratore, J.M., 1982, Nitrogen and lignin control of hardwood leaf litter decomposition dynamics: Ecology, v. 63, p. 621–626.

Menke, A.S.,ed., 1979, The semiaquatic and aquatic Hemiptera of California: Bulletin of the California Insect Survey, v. 21, p. 1–166.

Merritt, K.A., and Amirbahman, A., 2009, Mercury methylation dynamics in estuarine and coastal marine environments — A critical review: Earth-Science Reviews, v. 96, p. 54-66.

Merritt, R.W., Cummins, K.W., eds., 1996, An introduction to the insects of North America (3rd ed.): Dubuque, Iowa, Kendall-Hunt Publishing Co., 862 p.

Morel, F.M.M., Kraepiel, A.M.L., and Amyot, M., 1998, The chemical cycle and bioaccumulation of mercury: Annual Review of Ecology and Systematics, v. 29, p. 543–566.

Moyle, P.B., 2002, Inland Fishes of California (2nd ed.): Berkeley, Calif., Univ. of California Press, 517 p.

Neckles, H.A., Murkin, H.R., and Cooper, J.A., 1990, Influences of seasonal flooding on macroinvertebrate abundance in wetland habitats: Freshwater Biology, v. 23, p. 311–322.

Oikari, A., 2006, Caging techniques for field of fish to chemical contaminants: Aquatic Toxicology, v. 78, p. 370–381.

Olson, M.L., and Dewild, J.F., 1999, Techniques for the collection and species-specific analysis of low levels of mercury in water.: U. S. Geological Survey - Toxic Substance Hydrology Program. Water-Resources Investigation Report 99-4018B, 191-199 p.

Parsons, T. R., Y. Maita and C. M. Lalli, 1984. A manual of chemical and biological methods for seawater analysis. Pergamon Press.Oxford, UK. 173 pp.

Qian, J., Skyllberg, U., Frech, W., Bloom, P.R., and Petit, P.E., 2002, Bonding of methyl mercury to reduced sulfur groups in soil and stream organic matter as determined by X-ray

absorption spectroscopy and binding affinity studies: Geochemica et Cosmochemica Acta, v. 66, no. 22, p. 3873–3885.
Ravichandran, M., 2004, Interactions between mercury and dissolved organic matter—a review: Chemosphere, v. 55, no.3: p. 319–331.
Rice, W.R., 1989, Analyzing tables of statistical tests: Evolution, v. 43, p. 223–225.
Roden, E.E., 2008, Microbiological controls on geochemical kinetics 1: Fundamentals and case study on microbial Fe(III) oxide reduction, *in* Brantley, S.L., Kubicki, J.D., and White, A.F., eds., Kinetics of Water-Rock Interactions: New York, Springer, p. 335–415.
Roden, E.E., and Tuttle, J.H., 1993, Inorganic sulfur turnover in oligohaline estuarine sediments: Biogeochemistry, v. 22, p. 81–105.
Roden, E.E., and Wetzel, R.G., 2002, Kinetics of microbial Fe(III) oxide reduction in freshwater wetland sediments: Limnology and Oceanography, v. 47, p. 198–211.
Roden, E.E., and Zachara, J.M., 1996, Microbial reduction of crystalline iron(III) oxides: Influence of oxide surface area and potential for cell growth: Environmental Science and Technology, v. 30, p.1618–1628.
Rudd, J.W.M., 1995, Sources of methyl mercury to freshwater ecosystems: a review: Water, Air, and Soil Pollution, v. 80, p. 697–713.
Rumbold, D.G., and Fink, L.E., 2006, Extreme spatial variability and unprecedented methylmercury concentrations within a constructed wetland: Environmental Monitoring and Assessment, v. 112, p. 115–135.
Sassone, E., Bonnema, A., Stephenson, M., Heim, W.A., Newman, A., Fleck, J., and Coale, K., 2008, Methylmercury loading studies in Delta wetlands – Twitchell Island, *task 5.3a in* Transport, Cycling, and Fate of Mercury and Monomethyl Mercury in the San Francisco Delta and Tributaries: An Integrated Mass Balance Assessment Approach: Final report to the California Department of Fish and Game and the California Bay Delta Authority, 13 p. *http://mercury.mlml.calstate.edu/wp-content/uploads/2008/10/12_task5_3a_twitchell_final.pdf* (accessed Sept. 30, 2010)
Schlemel, L.E., Cox, M.H., Runkel, R.L., and Kimball, B.A., 2006, Multiple injected and natural conservative tracers quantify mixing in a stream confluence affected by acid mine drainage near Silverton, Colorado, Hydrologic Processes, v. 20, p. 2727–2743.
Seal II, R.R., Alpers, C.N., and Rye, R.O., 2000, Stable isotope systematics of sulfate minerals, *in* Alpers, C.N., Jambor, J.L, and Nordstrom, D.K., eds., Sulfate Minerals: Crystallography, Geochemistry, and Environmental Significance: Washington, D.C., Mineralogical Society of America and Geochemical Society, Reviews in Mineralogy and Geochemistry, v. 40, p. 541–602.
Sedinger, J.S., 1992, Ecology of prefledging waterfowl, *in* Batt, B.D.J., Afton, A.D., Anderson, M.G., Ankney, C.D., Johnson, D.H., Kadlec, J.A., and Krapu, G.L., eds., Ecology and management of breeding waterfowl: Minneapolis, University of Minnesota Press, p.109–127.
Sharp, Z., 2007, Principles of Stable Isotope Geochemistry: New Jersey, Pearson-Prentice Hall, 344 p.
Skyring, G.W., 1987, Sulfate reduction in coastal ecosystems: Geomicrobiology Journal, v. 5, p. 295-374.
Slowey, A.J., and Brown Jr., G.E., 2007, Transformations of mercury, iron, and sulfur during the reductive dissolution of iron oxyhydroxide by sulfide: Geochimica et Cosmochimica Acta, v. 71, p. 877–894.

Snodgrass, J.W., Jagoe, C.H., Bryan, Jr. A.L., Brant, H.A., and Burger, J., 2000, Effects of trophic status and wetland morphology, hydroperiod, and water chemistry on mercury concentrations in fish: Canadian Journal of Fisheries and Aquatic Sciences, v. 57, p. 171–180.

Sommer, T., Harrell, B., Nobriga, M., Brown, R., Moyle, P., Kimmerer, W. and Schemel, L., 2001, California's Yolo Bypass — Evidence that flood control can be compatible with fisheries, wetlands, wildlife, and agriculture: Fisheries, v. 26, p. 6-16.

Sommer, T.R., Harrell, W.C., and Swift, T.J., 2008, Extreme hydrologic banding in a large-river floodplain, California, U.S.A.: Hydrobiologia, v. 598, p. 409–415.

St. Louis, V.L., Rudd, J.W.M., Kelly, C.A., and Barrie, L.A., 1995, Wet deposition of methylmercury in northwestern Ontario compared to other geographic locations: Water, Air, and Soil Pollution, v. 80, p. 405–414.

St. Louis, V.L., Rudd, J.W.M., Kelly, C.A., Beaty, K.G., Bloom, N.S. and Flett, R.J., 1994, Importance of wetlands as sources of methylmercury to boreal forest ecosystems: Canadian Journal of Fisheries and Aquatic Sciences, v. 51, p. 1065–1076.

St. Louis, V.L., Rudd, J.W.M., Kelly, C.A., Beaty, K.G., Robert, J.F., Roulet, N.T., 1996, Production and loss of methylmercury and loss of total mercury from boreal forest catchments containing different types of wetlands: Environmental Science and Technology, v. 30, p. 2719–2729.

Stephenson, C., Foe, C., Gill, G.A., and Coale, C., 2008, Transport, Cycling, and Fate of Mercury and Monomethyl Mercury in the San Francisco Delta and Tributaries: An Integrated Mass Balance Assessment Approach: Final report to the California Department of Fish and Game and the California Bay Delta Authority, September, 2008. *http://mercury.mlml.calstate.edu/reports/reports/* (accessed Sept. 30, 2010)

Thamdrup, B., 2000, Bacterial manganese and iron reduction in aquatic sediments: in Schink, Bernhard (Ed.), Advances in Microbial Ecology, Vol 16. Springer, p. 41-84

Thullner, M., and Van Cappellen, P., 2007, Modeling microbially induced carbon degradation in redox-stratified subsurface environments: concepts and open questions: Geomicrobiology Journal, v. 24, p. 139–155.

Trust, B.A., and Fry, B., 1992, Stable sulfur isotopes in plants - a review: Plant, Cell, and Environment, v.15, p. 1105–1110.

U.S. Department of Agriculture, National Agricultural Statistics Service, 2007, *http://www.nass.usda.gov/* (accessed July 22, 2009)

U.S. Environmental Protection Agency, 2000a, Mercury in solids and solutions by thermal decomposition, amalgamation, and atomic absorption spectrophotometry: Method 7473, Test methods for evaluating solid waste, physical/chemical methods SW 846, Update IVA, Washington, D.C.

U.S. Environmental Protection Agency, 2000b, Water Quality Standards - Establishment of Numeric Criteria for Priority Toxic Pollutants for the State of California, 40 CFR Part 131. *http://www.epa.gov/fedrgstr/EPA-WATER/2000/May/Day-18/w11106.pdf* (accessed Sept. 30, 2010)

U.S. Environmental Protection Agency, 2001, Methyl mercury in water by distillation, aqueous ethylation, purge and trap, and cold-vapor atomic fluorescence spectrometry: Method 1630, EPA-821-R-01-020. Office of Water and Office of Science and Technology, Washington, D.C.

U.S. Fish and Wildlife Service, 1978, Concept plan for waterfowl wintering habitat and preservation, Central Valley, California: Portland, Oregon.

U.S. Geological Survey, 2006, Collection of water samples (ver. 2.0): U.S. Geological Survey Techniques of Water-Resources Investigations, book 9, chap. A4, revised September 2006, accessed May, 23, 2007 at http://pubs.water.usgs.gov/twri9A4/

U.S. Geological Survey, Calif. Department of Fish and Game, Yolo Basin Foundation, Moss Landing Marine Lab, and Battelle Marine Sciences, 2008, Quality Assurance Project Plan (version 3.1), Methylmercury cycling and export from agricultural and natural wetlands in the Yolo Bypass: prepared for the California State Water Resources Control Board, January 7, 2008, 419 p.

Ullrich, S.M., Tanton, T.W., and Abdrashitova, S.A., 2001, Mercury in the aquatic environment: A review of factors affecting methylation: Critical Reviews in Environmental Science and Technology, v. 31, p. 241-293.

Waples, J.S., Nagy, K.L., Aiken, G.R., and Ryan, J.N., 2005, Dissolution of cinnabar (HgS) in the presence of natural organic matter: Geochemica et Cosmochemica Acta, v. 69, p. 1575-1588.

Westover, K.M., Kennedy, A.C., and Kelley, S.E., 1997, Patterns of rhizosphere microbial community structure associated with co-occurring plant species: Journal of Ecology, v. 85, p. 863–873.

Wiener, J.G., Gilmour, C.C., Krabbenhoft, D.P., 2003b, Mercury strategy for the Bay-Delta ecosystem: a unifying framework for science, adaptive management, and ecological restoration: Final report to the California Bay Delta Authority, Sacramento, California. *http://calwater.ca.gov/science/pdf/MercuryStrategyFinalReport.pdf* (accessed Sept. 30, 2010)

Wiener, J.G., Krabbenhoft, D.P., Heinz, G.H., Scheuhammer, A.M., 2003a, Ecotoxicology of Mercury, *Chapter 16 in* Hoffman, D.J., Rattner, B.A., Burton, G.A., Jr., and Cairns J., Jr., eds., Handbook of Ecotoxicology (2nd ed.): Boca Raton, Fla., CRC Press, p. 409–463.

Williams, B.K., Nichols, J.D., Conroy, M.J., 2002, Analysis and management of animal populations: Modeling, estimation, and decision making: San Diego, Calif., Academic Press, 818 p.

Windham, L. and Ehrenfeld, J.G., 2003, Net impact of a plant invasion on nitrogen cycling processes within a brackish tidal marsh: Ecological Applications, v. 13, p. 883–897.

Windham-Myers, L., Marvin-DiPasquale, M., Krabbenhoft, D.P., Agee, J.L., Cox, M.H., Heredia-Middleton, P., Coates, C., and Kakouros, E., 2009, Experimental removal of wetland emergent vegetation leads to decreased methylmercury production in surface sediment: Journal of Geophysical Research, Biogeosciences, v. 114, G00C05, doi:10.1029/2008JG000815 *http://www.agu.org/journals/pip/jg/2008JG000815-pip.pdf* (accessed Sept. 30, 2010)

Wood, M.L., Foe, C., Cooke, J., and Louie, S.J., 2010a, Sacramento – San Joaquin Delta Estuary TMDL for Methylmercury: Staff report, Regional Water Quality Control Board – Central Valley Region, Sacramento, Calif., April 2010, 234 p. *http://www.swrcb.ca.gov/rwqcb5/water_issues/tmdl/central_valley_projects/delta_hg/april_2010_hg_tmdl_hearing/index.shtml* (accessed Sept. 30, 2010)

Wood, M.L., Morris, P., Cooke, J., and Louie, S.J., 2010b, Amendments to the Water Quality Control Plan for the Sacramento River and San Joaquin River Basins for the Control of Methylmercury and Total Mercury in the Sacramento-San Joaquin Delta Estuary: Staff Report, Regional Water Quality Control Board – Central Valley Region, April 2010, 332 p. *http://www.swrcb.ca.gov/rwqcb5/water_issues/tmdl/central_valley_projects/delta_hg/april_2010_hg_tmdl_hearing/index.shtml* (accessed Sept. 30, 2010)

Wopereis, M.C.S., Bouman, B.A.M., Kropff, M.J., ten Berge, H.F.M., and Maligaya, A.R., 1994, Water use efficiency of flooded rice fields. I. Validation of the soil-water balance model SAWAH: Agricultural Water Management, v. 26, p. 277–289.

Yee, D., Collins, J., Grenier, L., Takekawa, J., Tsao-Melcer, D., Woo, I., Schwarzbach, S., Marvin-DiPasquale, M., Windham, L., Krabbenhoft, D., Olund, S., and DeWild, J., 2008, Mercury and Methylmercury Processes in North San Francisco Bay Tidal Wetland Ecosystems – Final Report for Project # ERP02D-P62. Cooperator Report to CALFED Ecosystem Restoration Program, Prepared by the San Francisco Estuary Institute and the U.S. Geological Survey. May 2, 2008, 65 p.

YSI, Inc., 2009, YSI 6-series Multiparameter Water Quality Sondes — User's Manual (revision F): Yellow Springs, Ohio, Sept. 2009, 377 p. *http://www.ysi.com/media/pdfs/069300-YSI-6-Series-Manual-RevF.pdf* (accessed Sept. 30, 2010)

Zillioux, E.J., Porcella, D.B., and Benoit, J.M., 1993, Mercury cycling and effects in freshwater wetland ecosystems: Environmental Toxicology and Chemistry, v. 12, p. 2245–2264.

12 ACKNOWLEDGEMENTS

This report integrates a large and diverse data set that would be difficult to understand without review comments from two agencies: 1) the review panel within the RWQCB-CVR – especially Janis Cooke, and 2) Joann Holloway, USGS – Denver, Colorado, whose comments were invaluable as an independent sounding board, due to her detailed and comprehensive understanding of each part and how it should link together. We are grateful to the SWQCB for supporting this project with Proposition 40 funding. Task-specific acknowledgements follow here:

Acknowledgements for Section 5; Special thanks to California Department of Fish and Game staff (especially Chris Rocco), USGS field and laboratory staff (especially Frank Anderson, Elizabeth Beaulieu, and Will Kerlin), SWRCB/ RWQCB-CVR staff and the Yolo Basin Foundation staff. Thanks to the residents of California for funding from Proposition 40 and the USGS for contributions of matching funds from the Cooperative Hydrology Program as well as in-kind funds from the National Research Program in Water Resources and other USGS programs in support of the work conducted in this study. Particular USGS in-kind contributions include supportive laboratory analyses by Craig Stricker (USGS-Denver), Howard Taylor (USGS-Denver), and George Aiken (USGS-Boulder).

Acknowledgements for Sections 6 & 7: We thank Jack DeWit, of DeWit farms for sharing field-based management decisions and for sharing post-harvest estimates of yield for each field. We thank Mark Rollog (USGS, Menlo Park) for providing high quality analyses of plant tissue carbon and nitrogen concentrations and isotopic signatures. We thank many field and laboratory technicians for both initial experimental set up and for continued sampling and processing during the 1 year study, including Sherrie Wren, Steven Quistad, Justin Kanerva, and Kathy Akstin. This research was made possible by careful wetland management by California Fish and Game staff and Chris Rocco of the Yolo Bypass Wildlife Area.

Acknowledgements for Section 8: This research was funded by the California State Water Resources Control Board with additional support from the USGS Western Ecological Research Center. We thank Carson Jeffres for fish cage design and advice on deployment, Sarah Stoner-Duncan, Robin Keister, Danika Tsao, Mark Ricca, Erica Caceres, Jill Bluso, Sarah Spring, Cody Massing, Meg Harper, Jessica Mellinger, and Whitney Thornton for field and lab work, and Julie Yee for statistical advice. We also thank Dave Feliz and the California Department of Fish and Game staff of the Vic Fazio Yolo Bypass Wildlife Area, Jack DeWit and DeWit Farms, Jacob Fleck, Charlie Alpers, Lisamarie Windham-Myers, Mark Marvin-DiPasquale, Mark Stephenson, Phil Bachand, Gary Gill, and the Yolo Basin Foundation for logistical support. The use of trade, product, or firm names in this publication is for descriptive purposes only and does not imply endorsement by the U. S. Government.

Table 1.1. Individuals (alphabetically) and organizations involved in the project

Name	Affiliation	Area of Expertise	Contact Information
Josh Ackerman	U.S. Geological Survey	Biology / Fish and invertebrate Hg analyses	TEL (530) 752-0485 FAX (530) 752-9680 jackerman@usgs.gov
Charlie Alpers	U.S. Geological Survey	Trace metals and aquatic geochemistry	TEL (916) 278-3134 FAX (916) 278-3070 cnalpers@usgs.gov
Phil Bachand	Bachand and Associates	Hydrologic processes and modeling	TEL (530) 758-1336 phil@bachandassociates.com
Ann Brice	Yolo Basin Foundation	Public Outreach	TEL (530) 758-0530 FAX (530) 757-4824 abrice@yolobasin.org
Collin Eagles-Smith	U.S. Geological Survey	Biology / Fish and invertebrate Hg analyses	TEL (541) 750-0949 FAX (541) 750-1069 ceagles-smith@usgs.gov
Dave Feliz	California Dept. Fish and Game	YWMA management	TEL (530) 757-2461 FAX (530) 757-2518 dfeliz@dfg.ca.gov
Jacob Fleck	U.S. Geological Survey	Aquatic chemistry / DOM-Hg interactions	TEL (916) 278-3063 FAX (916) 278-3071 jafleck@usgs.gov
Gary Gill	Batelle Marine Science Laboratories	Aquatic geochemistry / photochemistry	TEL (360) 681-4593 FAX (360)681-3600 gary.gill@pnl.gov
Mark Marvin-DiPasquale	U.S. Geological Survey	Microbial ecology; Hg analysis in sediments	TEL (650) 329-4442 FAX (650)-329-4463 mmarvin@usgs.gov
Mark Stephenson	Moss Landing Marine Laboratories	Hg analyses of water samples; hydrologic measurements	TEL (831) 771-4177 FAX (831) 633-0805 mstephenson@mlml.calstate.edu
Lisamarie Windham-Myers	U.S. Geological Survey	Plant ecology; Hg analysis in plant material	TEL (650) 329-4447 FAX (650) 329-4463 lwindham@usgs.gov

Table 3.1. Study sampling locations and descriptions

[Site coordinates expressed in degrees,minutes,seconds (dd(d)° mm' ss") using World Geodetic System 1984 (WGS84). Field type: 'PW' = 'permanently flooded wetland', 'SW' = 'seasonally flooded wetland'.]

Field Type	Field #	Field Location	Site Code	Latitude (North)	Long itude (West)	Description
White Rice	31	Inlet 1	R31-i1	38 33' 40"	121 37' 11"	check levee weir box on west side of field
White Rice	31	Inlet 2	R31-i2	38 33' 40"	121 36' 45"	check levee weir box in NE corner of field
White Rice	31	Center	R31-c	38 33' 24"	121 36' 59"	center field levee intersection with wind breaks
White Rice	31	Outlet 1	R31-o1	38 33' 11"	121 37' 11"	outlet riser in SW corner of field, W boundary
White Rice	31	Outlet 2	R31-o2	38 33' 09"	121 36' 38"	outlet riser in SE corner of field, S boundary
White Rice	64	Inlet 1	R64-i1	38 33' 07"	121 37' 12"	check levee weir box in NW area of field
White Rice	64	Inlet 2	R64-i2	38 33' 07"	121 37' 04"	check levee weir box in SW area of field
White Rice	64	Center	R64-c	38 33' 01"	121 36' 55"	center field sampling point - levee wall
White Rice	64	Outlet 1	R64-o1	38 33' 06"	121 36' 40"	check levee weir box in NE area of field
White Rice	64	Outlet 2	R64-o2	38 32' 52"	121 36' 41"	check levee weir box in SE area of field
Wild Rice	32	Inlet 1	W32-i1	38 33' 40"	121 36' 38"	screwgate inlet at NW corner of field #32 YWA
Wild Rice	32	Center	W32-c	38 33' 24"	121 36' 32"	center field sampling point - levee wall
Wild Rice	32	Outlet 1	W32-o1	38 33' 10"	121 36' 23"	outlet riser in SE corner of field
Wild Rice	65	Inlet 1	W65-i1	38 33' 07"	121 36' 36"	screwgate inlet at NW corner , 70m E of corner
Wild Rice	65	Center	W65-c	38 32' 48"	121 36' 27"	center field sampling point at levee wall
Wild Rice	65	Outlet 1	W65-o1	38 32' 34"	121 36' 23"	outlet riser at SE corner of field
Fallow	20	Inlet 1	F20-i1	38 33' 10"	121 37' 45"	standpipe inlet in SW corner of YWA #20 lower
Fallow	20	Inlet 2	F20-i2	38 33' 30"	121 37' 45"	screwgate inlet at NW corner of YWAsouth,new structure just put in under new road intersection
Fallow	20	Center	F20-c	38 33' 15"	121 37' 30"	Unkonwn, still being reworked as of 6/20/07
Fallow	20	Outlet 1	F20-o1	38 33' 09"	121 37' 12"	outlet flashboard riser at SE corner of lower unit
Fallow	66	Inlet 1	F66-i1	38 33' 07"	121 36' 09"	screwgate inlet at NE corner of field
Fallow	66	Center	F66-c	38 32' 34"	121 36' 23"	outlet riser at SW corner of field
Fallow	66	Outlet 1	F66-o1	38 32' 34"	121 36' 07"	outlet riser at SE corner of field
PW	5	Inlet 1	PW5-i1	38 33' 08"	121 35' 26"	inlet screwgate culvert for permanent wetland
PW	5	Center	PW5-c	38 32' 57"	121 35' 27"	center openwater site for permanent wetland
PW	5	Outlet 1	PW5-o1	38 32' 34"	121 35' 33"	outlet flashboard riser for permanent wetland
SW	1	Inlet 1	SW1-i1	38 33' 08"	121 36' 05"	inlet screwgate culvert for seasonal wetland
SW	1	Center	SW1-c	38 33' 09"	121 35' 47"	center vegetated site for seasonal wetland
SW	1	Outlet 2	SW1-o1	38 32' 28"	121 36' 04"	outlet flashboard riser for seasonal wetland

Table 4.1. Field size and associated areas for hydrologic units

['Field area' represents the area as measured from the field inflow structure to the field outflow structure. The hydrologic unit (HU) area represents the area encompassed by where the inflow and outflow were actually measured, and is sometimes smaller than the field area due to the location of within-field 'checks' (water control berms). The number of 'checks' is also indicated for both the full field and the HU.]

	Field		HU	
Field	**Area, Hectares**	**# Checks**	**Area, Hectares**	**# Checks**
F20	47	11	42	9
F66	39	4	35	2
PW	16	3	16	---
R31	78	6	63	4
R64	31	6	25.5	5
SW	52	2	52	---
W32	33	5	30	4
W65	44	5	43	5

Table 4.2. Seasonal breakdown of operations at the Yolo Wildlife Management Area, by Field, March 2007 – May 2008

Season (period)	Dates / # of Days	F20	F66	R31	R64	W32	W65	SW	PW
Spring (dry-down)	Start Date	3/1/07	3/1/07	3/1/07	3/1/07	3/1/07	3/1/07	NA	NA
	End Date	7/1/07	7/1/07	5/26/07	6/2/07	6/2/07	6/8/07		
	# of days	122	122	87	94	94	98	0	0
Summer (irrigated)	Start Date	7/1/07	7/1/07	5/26/07	6/2/07	6/2/07	6/8/07	5/1/07	5/1/07
	End Date	9/5/07	9/5/07	10/9/07	10/1/07	10/2/07	10/15/07	9/30/07	9/30/07
	# days	67	67	136	121	122	131	153	153
Autumn (dry-down)	Start Date	9/5/07	9/5/07	10/9/07	10/1/07	10/2/07	10/15/07	NA	NA
	End Date	10/15/07	11/26/07	11/16/07	11/16/07	11/26/07	11/19/07		
	# days	40	82	38	47	56	35		
Winter (irrigated)	Start Date	10/15/07	11/26/07	11/16/07	11/16/07	11/26/07	11/19/07	10/1/07	10/1/07
	End Date	1/24/08	1/24/08	1/24/08	1/24/08	1/24/08	1/24/08	1/24/08	1/24/08
	# days	101	59	69	69	59	66	115	115
Winter (flood)	Start Date	1/24/08	1/24/08	1/24/08	1/24/08	1/24/08	1/24/08	1/24/08	1/24/08
	End Date	2/10/08	2/10/08	2/10/08	2/10/08	2/10/08	2/10/08	2/10/08	2/10/08
	# days	17	17	17	17	17	17	17	17
Winter (drainage)	Start Date	2/10/08	2/10/08	2/10/08	2/10/08	2/10/08	2/10/08	2/10/08	2/10/08
	End Date	2/28/08	2/28/08	2/28/08	2/28/08	2/28/08	2/28/08	4/30/08	4/30/08
	# days	18	18	18	18	18	18	80	80

Table 4.3. Water budget for agricultural and non-agricultural fields during the summer irrigated period
[Values are in centimeters (water volume normalized to field area). Percentages are based on the measured and calculated fluxes as a percent of total "INs" and "OUTs". The seasonal wetland (SW) remained dry during this period and the annual imbalance includes the "dry-down" period 5/1/2007 through 9/30/2007. The permanent wetland (PW) was periodically irrigated to maintain a set water level and once in July to flush the system, and includes the period 5/1/2007 through 9/30/2007. The 'days in season' are from **Table 4.2** and are operationally defined. The summer period is defined by the period between flood-up and dry down when surface storage equals zero. 'Seasonal imbalance' represents the imbalance for the season. 'Annual imbalance' represents the cumulative imbalance beginning in spring at the beginning of dry down. Precipitation, evaporation and transpiration vary somewhat between cells because of the different lengths of the seasons. Evapotranspiration is determined utilizing CIMIS data and crop coefficients. Evapotranspiration's components (evaporation, transpiration) were estimated using a Plug Flow Reactor Model.]

	Field ID	F20		F66		R31		R64		W32		W65		SW		PW	
	days in season	67		67		136		121		122		131		153		153	
INs	irrigation	50	100%	44	100%	113	100%	137	100%	127	100%	102	97%	0	0%	120	100%
INs	precipitation	0	0%	0	0%	0	0%	0	0%	0	0%	3	3%	0.5	100%	0.5	0%
OUTs	surface outflow	-6	12%	-6	12%	-31	26%	-43	35%	-39	32%	-15	15%	0	0%	-10	8%
OUTs	evaporation	-11	22%	-11	22%	-22	18%	-20	16%	-21	17%	-21	21%	-35	50%	-70	58%
OUTs	transpiration	-33	66%	-32	65%	-67	56%	-59	48%	-63	51%	-63	64%	-35	50%	-40	33%
	surface storage	0	0%	0	0%	0	0%	0	0%	0	0%	0	0%	0	0%	0	0%
	season imbalance	0	0%	-5	5%	-7	3%	15	6%	4	2%	6	3%	-70	99%	0.5	0%
	annual imbalance	-33	23%	-38	28%	-20	8%	1	0%	-10	4%	-8	4%	-70	99%	0.5	0%

Table 4.4. Water budget for agricultural and non-agricultural fields during the winter irrigated period
Values are in centimeters (water volume normalized to field area). Percentages are based on the measured and calculated fluxes as a percent of total "INs" and "OUTs". The 'days in season' are from **Table 4.2** and are operationally defined. 'Surface storage' is positive for this period for all fields because the regional flooding occurred during flooded conditions. 'Seasonal imbalance' represents the imbalance for the season. 'Annual imbalance' represents the cumulative imbalance beginning in spring at the beginning of dry down. Evapotranspiration is determined utilizing CIMIS data and crop coefficients. Transpiration is assumed to be equivalent to zero during this period because of vegetation senescence and/or harvest except in the permanent wetland where vegetation is present and active throughout the year.

	Field ID	F20		F66		R31		R64		W32		W65		SW		PW	
	days in season	101		59		69		69		59		66		115		115	
INs	irrigation	10	28%	18	43%	18	44%	41	64%	12	34%	17	42%	100	78%	17	37%
INs	precipitation	25	72%	23	57%	23	56%	23	36%	23	66%	23	58%	29	22%	29	63%
OUTs	surface outflow	-24	57%	-24	60%	-6	14%	-20	32%	-0.4	1%	-15	39%	0	0%	-13	27%
OUTs	evaporation	-18	43%	-8	20%	-10	24%	-10	16%	-8	23%	-10	25%	-22	17%	-18	40%
OUTs	transpiration	0	0%	0	0%	0	0%	0	0%	0	0%	0	0%	0	0%	-9	20%
	surface storage	25	72%	25	61%	25	61%	25	39%	25	71%	25	63%	30	23%	0	0%
	season imbalance	-33	32%	-17	17%	1	1%	9	7%	2	2%	-11	12%	77	42%	6	7%
	annual imbalance	-79	30%	-76	29%	-24	7%	2	0%	-18	5%	-28	8%	7	2%	7	2%

Table 4.5. Water budget estimates for agricultural fields during the 17-day winter flooded period, based on pressure transducer data

Values are in centimeters (water volume normalized to field area). Surface flood water on and off the fields were estimated from changes in surface water depth measured using pressure transducers and are conservative estimates of flood water on and off because surface waters not only likely raised water elevations but also passed through the system during this period. Based on published floodplain flow estimate of 0.1 m s^{-1}, flooded field depths and field geometry, actual flood inflow and outflow would range from 2 to 5 times greater than the estimates reported here for no-flow conditions. Percentages are based on the measured and calculated fluxes as a percent of total field inputs (flood inflow plus precipitation). The 'days in season' are from **Table 4.2** and are operationally defined. 'Seasonal imbalance' represents the imbalance for the season. Note using pressure transducers only accounts for water level changes and does not account for infiltration occurring during this period. Evapotranspiration is determined utilizing CIMIS data and crop coefficients. Transpiration is assumed to be equivalent to zero during this period because of vegetation senescence and the dominance of flowing flood waters over this short time period.

	Field ID	F20		F66		R31		R64		W32		W65		SW		PW	
	days in season	17		17		17		17		17		17		17		17	
INs	flood inflow	130	98%	200	99%	150	98%	150	98%	170	98%	170	98%	210	99%	210	99%
INs	precipitation	3	2%	3	1%	3	2%	3	2%	3	2%	3	2%	3	1%	3	1%
OUTs	flood outflow	-130	-98%	-200	-99%	-150	-98%	-150	-98%	-170	-98%	-170	-98%	-210	-99%	-210	-99%
OUTs	evaporation	-2	-2%	-2	-1%	-2	-1%	-2	-1%	-2	-1%	-2	-1%	-2	-1%	-2	-1%
OUTs	transpiration	0	0%	0	0%	0	0%	0	0%	0	0%	0	0%		0%		0%
	surface storage	0	0%	0	0%	0	0%	0	0%	0	0%	0	0%		0%		0%
	season imbalance	1	1%	1	0%	1	1%	1	1%	1	1%	1	1%		0%		0%

Table 4.6. Water budget for agricultural and non-agricultural fields during the winter drainage period

Values are in centimeters (water volume normalized to field area). Percentages are based on the measured and calculated fluxes as a percent of total “INs” and “OUTs”. The ‘days in season’ are from **Table 4.2** and are operationally defined. ‘Surface storage’ is set equal to zero because the end of the season is defined by the drainage of surface water and the change in storage is captured in the ‘surface outfall’ value. ‘Seasonal imbalance’ represents the imbalance for the season. ‘Annual imbalance’ represents the cumulative imbalance beginning in spring at the beginning of dry down. Evapotranspiration is determined utilizing CIMIS data and crop coefficients. Transpiration is assumed to be equivalent to zero during this period because of vegetation senescence except in the seasonal and permanent wetlands where viable vegetation is present.

	Field ID	F20		F66		R31		R64		W32		W65		SW		PW	
	days in season	18		18		18		18		18		18		80		80	
INs	irrigation	0	0%	0	0%	0	0%	0	0%	0	0%	0	0%	32	80%	32	80%
INs	precipitation	5	100%	5	100%	5	100%	5	100%	5	100%	5	100%	8	20%	8	20%
OUTs	surface outfall	-25	83%	-25	-12%	-25	-16%	-25	-16%	-25	-14%	-25	-14%	-30	-14%	-3	-1%
OUTs	evaporation	-5	17%	-5	-2%	-5	-3%	-5	-3%	-5	-3%	-5	-3%	-15	-7%	-25	-12%
OUTs	transpiration	0	0%	0	0%	0	0%	0	0%	0	0%	0	0%	-25	-12%	-12	-6%
	surface storage	0	0%	0	0%	0	0%	0	0%	0	0%	0	0%	0	0%	0	0%
	season imbalance	-25	71%	-25	71%	-25	71%	-25	71%	-25	71%	-25	71%	-30	27%	0	0%
	annual imbalance	-104	35%	-101	34%	-49	13%	-23	5%	-43	11%	-53	15%	-93	21%	7	2%

Table 4.7. Water budget for agricultural and non-agricultural fields during the combined winter irrigated and winter drainage periods, excluding the 17-day winter flood period

This budget combines the irrigated and drained periods in winter when water management was possible (**Tables 4.4 and 4.6**). The period during the regional flood was left out of the budget due to the high uncertainty inherent in the estimates for that period. The 'seasonal imbalance' represents the total imbalance for winter. The 'annual imbalance' represents the cumulative annual imbalance (March – February for agricultural wetlands and May – April for non-agricultural wetlands). The annual imbalance shows good closure of the water budget (< 10% in most fields) except in F20 and F66 where a larger imbalance suggests subsurface water sources provide additional water to the shallow-flooded fallow fields or a low bias in irrigation volume measurements in these fields.

	Field ID	F20		F66		R31		R64		W32		W65		SW		PW	
	days in season	119		77		87		87		77		84		195		195	
INs	irrigation	9.5	22%	17.7	36%	18.2	37%	41.1	57%	12	28%	16.7	35%	132	77%	49	55%
INs	precipitation	33	78%	31	64%	31	63%	31	43%	31	72%	31	65%	39.5	23%	40	45%
OUTs	surface outflow	-49	66%	-49	77%	-31	64%	-45	73%	-25	63%	-40	70%	-30	32%	-16	19%
OUTs	evaporation	-25	34%	-15	23%	-17	36%	-17	27%	-15	37%	-17	30%	-39	41%	-45	55%
OUTs	transpiration	0	0%	0	0%	0	0%	0	0%	0	0%	0	0%	-25	27%	-21	26%
	surface storage	0	0%	0	0%	0	0%	0	0%	0	0%	0	0%	0	0%	0	0%
	season imbalance	-32	27%	-16	14%	1.5	2%	9.9	7%	2.6	3%	-9.6	9%	77.5	29%	7	4%
	annual imbalance	-78	28%	-75	27%	-23	6%	2.9	1%	-17	5%	-27	8%	8	2%	7.5	2%

Table 4.8. Annual total water budget for agricultural and non-agricultural fields
The annual total water budget is the summation of the seasonal water budgets (including spring and autumn periods). Percentages are based upon the percent of surface water applied from either precipitation or irrigation. The annual imbalance shows good closure of the water budget (< 10% in most fields). The imbalance suggests the water demands for the fallow fields and the seasonal wetland are augmented by subsurface waters or that irrigation measurements are biased low for these fields' managements using the methodologies implemented in this study.

	Field ID	F20		F66		R31		R64		W32		W65		SW		PW	
INs	irrigation	60	59%	62	60%	131	76%	178	81%	139	77%	119	75%	132	77%	169	81%
INs	precipitation	41	41%	41	40%	41	24%	41	19%	41	23%	39	25%	41	23%	40	19%
OUTs	surface outflow	-55	31%	-55	31%	-62	32%	-88	41%	-64	33%	-55	30%	-30	13%	-26	13%
OUTs	evaporation	-36	20%	-26	15%	-57	29%	-56	26%	-70	35%	-66	36%	-109	47%	-115	57%
OUTs	transpiration	-87	49%	-97	54%	-77	39%	-72	33%	-63	32%	-63	34%	-95	41%	-61	30%
	surface storage	0	0%	0	0%	0	0%	0	0%	0	0%	0	0%	0	0%	0	0%
	annual imbalance	-78	28%	-75	27%	-23	6%	3	1%	-17	5%	-27	8%	-62	15%	8	2%

Table 5.1. Description of water-quality parameters, Yolo Bypass Wildlife Area mercury study

[ng L^{-1}, nanogram per liter; %, percent; mg L^{-1}, milligram per liter; µg L^{-1}, microgram per liter; nm, nanometer; cm, centimeter]

Parameter Notation	Units	Parameter Name
Water-quality mercury parameters		
u-THg	ng L^{-1}	total mercury in unfiltered water
f-THg	ng L^{-1}	total mercury in filtered water
u-MeHg	ng L^{-1}	methylmercury in unfiltered water
f-MeHg	ng L^{-1}	methylmercury in filtered water
% u-Me/T	%	percent of total mercury in unfiltered water as methylmercury
% f-Me/T	%	percent of total mercury in filtered water as methylmercury
Water-quality non-mercury parameters		
DOC	mg L^{-1}	dissolved organic carbon concentration
SUVA	absorbance/(mg L^{-1}*100)	specific ultraviolet absorbance at 254 nm
ChlA+Pheophytin	µg L^{-1}	chlorophyll-a plus pheophytin-a
SPM	mg L^{-1}	suspended particulate matter
SO_4	mg L^{-1}	sulfate in filtered water
Fe	µg L^{-1}	iron in filtered water
SC	microsiemens cm^{-1}	specific conductance in unfiltered water
Cl	mg L^{-1}	chloride in filtered water

Table 5.2. Statistical comparison of selected water-quality parameters for agricultural versus non-agricultural fields

[Analysis includes center field samples for interdisciplinary sampling dates only. The mean, standard error (SE, given in parentheses) and the number of observations (N) are shown, along with all results from all mercury water-quality parameters and selected non-mercury parameters. Significant differences ($p < 0.05$) using the Mann-Whitney test between agricultural and non-agricultural fields are indicated as '****' and non-significant differences are indicated as 'NS'. p-values <0.10 are indicated in **bold**. See **Table 5.1** for explanations of parameter notation and units]

	Agricultural Fields		Non-Agricultural Fields				
Parameter	**Mean ± SE**	**N**	**Mean ±**	**SE**	**N**	**Significance**	**p-value**
Water-quality mercury parameters							
u-MeHg	2.7	(0.4)	28	1.2	(0.6)	8	****	**0.012**
f-MeHg	1.3	(0.3)	27	0.6	(0.3)	8	NS	0.135
u-THg	26	(4)	28	7.8	(1.2)	6	****	**0.0008**
f-THg	7.1	(1.0)	28	1.9	(0.4)	8	****	**0.0001**
% u-Me/T	16	(4)	27	16	(6)	8	NS	0.666
% f-Me/T	23	(5)	27	24	(5)	8	NS	0.316
dissolved organic carbon concentration							
Water-quality non-mercury parameters							
DOC	15	(1)	28	9.7	(0.9)	8	****	**0.011**
SUVA	2.2	(0.1)	28	2.4	(0.1)	8	NS	0.171
ChlA+Pheophytin	28	(5)	8	22	(7)	3	NS	0.812
SPM	40	(8)	25	41	(15)	7	NS	0.715
SO_4	85	(12)	28	49	(8)	8	NS	0.102
Fe	51	(23)	28	92	(43)	8	NS	0.216
SC	990	(73)	28	722	(82)	8	****	**0.046**
Cl	96	(10)	28	56	(8)	8	NS	**0.060**

Table 5.3. Statistical comparison of selected water-quality parameters for northern versus southern agricultural fields

[Analysis includes center field samples for interdisciplinary sampling dates only. The mean, standard error (SE, given in parentheses) and the number of observations (N) are shown, along with all results from all mercury water-quality parameters and selected non-mercury parameters. Significant differences ($p < 0.05$) using the Mann-Whitney test between northern and southern agricultural fields are indicated as '****' and non-significant differences are indicated as 'NS'. p-values <0.10 are indicated in **bold**. See **Table 5.1** for explanations of parameter notation and units]

	Northern Block Fields		Southern Block Fields			
Parameter	**Mean ± SE**	**N**	**Mean ± SE**	**N**	**Significance**	**p-value**
Water-quality mercury parameters						
u-MeHg	3.1 (0.5)	14	2.3 (0.7)	14	NS	**0.073**
f-MeHg	1.4 (0.4)	14	1.1 (0.5)	13	NS	0.627
u-THg	30 (6)	14	23 (4)	14	NS	0.370
f-THg	7.2 (1.4)	14	7.0 (1.3)	14	NS	0.765
% u-Me/T	20 (6)	14	11 (3)	13	NS	0.409
% f-Me/T	28 (7)	14	18 (6)	13	NS	0.716
Water-quality non-mercury | dissolved organic carbon concentration						
DOC	16 (2)	14	14 (1)	14	NS	0.395
SUVA	2.2 (0.1)	14	2.2 (0.1)	14	NS	0.730
ChlA+Pheophytin	36 (9)	10	19 (3)	10	NS	0.184
SPM	49 (13)	12	32 (9)	13	NS	0.183
SO_4	100 (23)	14	70 (9)	14	NS	0.581
Fe	77 (46)	14	26 (7)	14	NS	0.346
SC	1081 (103)	14	898 (99)	14	NS	0.260
Cl	107 (16)	14	85 (12)	14	NS	0.370

Table 5.4. Statistical comparison of selected water-quality parameters from agricultural fields during growing season versus post-harvest season

[Analysis includes center field samples from agricultural fields for interdisciplinary sampling dates only. The mean, standard error (SE, given in parentheses) and the number of observations (N) are shown, along with all results from all mercury water-quality parameters and selected non-mercury parameters. Significant differences ($p < 0.05$) using the Mann-Whitney test between growing season (June through August, 2007) and post-harvest season (December 2007 through February 2008) are indicated as '****' and non-significant differences are indicated as 'NS'. p-values <0.10 are indicated in **bold**. See **Table 5.1** for explanations of parameter notation and units]

	Growing Season		Post-Harvest Season			
Parameter	**Mean ± SE**	**N**	**Mean ± SE**	**N**	**Significance**	**p-value**
Water-quality mercury parameters						
u-MeHg	2.8 (0.47)	16	2.5 (0.7)	12	NS	0.430
f-MeHg	0.9 (0.3)	15	1.7 (0.6)	12	NS	0.143
u-THg	27 (5)	16	25 (5)	12	NS	0.908
f-THg	8.1 (1.6)	16	5.7 (0.5)	12	NS	0.799
% u-Me/T	18 (6)	15	12 (3)	12	NS	0.922
% f-Me/T	21 (7)	15	25 (7)	12	NS	0.213
Water-quality non-mercur dissolved organic carbon concentration						
DOC	16 (1)	16	13 (2)	12	NS	0.109
SUVA	2.0 (0.1)	16	2.5 (0.1)	12	****	**0.0032**
ChlA+Pheo	24 (4)	14	36 (14)	6	NS	0.321
SPM	31 (10)	13	49 (12)	12	NS	**0.092**
SO_4	96 (11)	16	70 (25)	12	****	**0.027**
Fe	25 (7)	16	86 (53)	12	NS	0.120
SC	1177 (62)	16	740 (115)	12	****	**0.0032**
Cl	122 (11)	16	62 (14)	12	****	**0.0017**

Table 5.5. Statistical comparison of selected water-quality parameters for inlet, center and outlet sampling sites on agricultural fields

[The mean, standard error (SE, given in parentheses) and the number of observations (N) are shown, along with all results from all mercury water-quality parameters and selected non-mercury parameters. Significant differences ($p < 0.05$) using the Mann-Whitney test between inlet (I), center (C), and outlet (O) sampling sites on agricultural fields are indicated as '****' and non-significant differences are indicated as 'NS"; p-values <0.10 are indicated in bold. See **Table 5.1** for explanations of parameter notation and units]

	Inlet			Center			Outlet			Significance			p-value		
Parameter	**Mean**	**SE**	**N**	**Mean**	**SE**	**N**	**Mean**	**SE**	**N**	**I vs. C**	**I vs. O**	**C vs. O**	**I vs.. C**	**I vs. O**	**C vs. O**
Water-quality mercury parameters															
u-MeHg	1.0	(0.2)	23	2.7	(0.4)	28	2.8	(0.6)	29	****	****	NS	**0.0002**	**0.0022**	0.539
f-MeHg	0.49	(0.12)	23	1.3	(0.3)	27	1.2	(0.3)	29	****	****	NS	**0.0068**	**0.0096**	0.928
u-THg	14	(2)	23	26	(4)	28	31	(5)	29	****	****	NS	**0.011**	**0.0466**	0.898
f-THg	2.1	(0.2)	23	7.1	(1.0)	28	9.1	(1.5)	29	****	****	NS	**0.0000**	**0.0000**	0.930
% u-Me/T	8.7	(2.2)	23	16	(4)	27	14	(3)	29	NS	NS	NS	**0.098**	0.173	0.825
% f-Me/T	19	(3)	23	23	(5)	27	20	(4)	29	NS	NS	NS	0.527	0.549	0.670
Water-quality non-mer	dissolved organic carbon concentration											NS			
DOC	9.5	(0.4)	23	15	(1)	28	16	(1)	29	****	****	NS	**0.0001**	**0.0001**	0.429
SUVA	2.4	(0.00)	23	2.2	(0.1)	28	2.1	(0.1)	29	****	****	NS	**0.0019**	**0.0008**	0.962
ChlA+Pheo	47	(5)	18	28	(5)	20	27	(5)	21	****	****	NS	**0.0014**	**0.0053**	0.754
SPM	62	(9)	20	40	(8)	25	47	(12)	27	****	****	NS	**0.018**	**0.023**	0.927
SO_4	62	(5)	23	85	(12)	28	92	(13)	29	NS	NS	NS	0.229	0.107	0.702
Fe	32	(7)	22	51	(23)	28	29	(4)	29	NS	NS	NS	0.646	0.849	0.731
SC	831	(39)	23	990	(73)	28	1124	(89)	29	****	****	NS	**0.033**	**0.0033**	0.334
Cl	70	(5)	23	96	(10)	28	107	(11)	29	NS	****	NS	**0.074**	**0.0056**	0.350

Table 5.6. Non-evaporative (chloride-normalized) changes in concentrations of selected mercury species along flow paths in agricultural and non-agricultural fields during summer and winter sampling periods

[Values represent seasonal averages of ratio of outlet to inlet concentrations of mercury species normalized to aqueous chloride, except as noted. u-MeHg, unfiltered methylmercury; u-THg, unfiltered total mercury; Harvest period for wild rice fields (W32 and W65) not included because harvest activities greatly increased unfiltered methylmercury and total-mercury concentrations at outlet, affecting comparison of outlet to inlet. Fallow fields (F20 and F66) were not completely flooded during July 2007 so water-quality at field centers (rather than outlets) were compared with inlets. At permanent wetland, flow was typically in or out but not both simultaneously; comparisons of outlet to center were used in late July and early August 2007 and comparisons of center to inlet were used in early July and late August, 2007. The seasonal wetland was not flooded during summer 2007.]

		u-MeHg		u-THg	
field	unit	summer	winter	summer	winter
F20	N	0.7	0.5	2.9	2.4
R31	N	0.6	**2.8**	0.8	0.8
W32	N	1.4	**2.8**	1.0	1.6
F66	S	**5.0**	0.4	0.6	0.3
R64	S	**5.8**	**8.3**	1.1	1.5
W65	S	**2.0**	1.3	1.4	1.0
PW	S	1.0	1.0	1.6	1.0
SW	S	NA	**8.3**	NA	0.6

Table 5.7. **Methylmercury loads during the summer irrigation period for agricultural and non-agricultural fields**

[Values represent methylmercury loads in units of nanograms per square meter (ng m^{-2}) for the summer irrigation season, which varied in duration among fields, as indicated. Surface imbalance is a comparison of irrigation supply and outlet flows. Precipitation inputs are assumed to be negligible. The net imbalance is the sum of all components (inputs and outputs). Positive values are onto the fields, so a positive imbalance indicates a net loss of MeHg across the field. (Refer to **Table 4.3** for water balance information). 'Days in season' represents the number of days each field was inundated during the summer irrigation period.]

	field ID	F20	F66	R31	R64	W32	W65	SW	PW
	unit/block	North	South	North	South	North	South	South	South
	days in season	67	67	136	121	122	131	0	153
Inflows	irrigation	1429	122	748	377	1312	398	0	360
	precipitation	0	0	0	0	0	0	0	0
Outflows	surface outflow	-124	-331	-237	-642	-1188	-534	0	-50
	transpiration	-660	-640	-1675	-995	-950	-1071	0	-200
S	storage	0	0	0	0	159	80	0	0
	Surface imbalance	1305	-209	511	-265	124	-136	0	310
	Net imbalance	645	-849	-1164	-1259	-985	-1287	0	110

Table 5.8. Methylmercury loads for agricultural and non-agricultural fields during the winter, excluding the 17-day winter flood period

[Values reflect methylmercury loads in units of nanograms per square meter (ng m^{-2}) for the winter, excluding the 17-day winter flood period. Surface imbalance is the comparison of the irrigation supply and outlet flows. Precipitation inputs are assumed to be negligible. The total imbalance is the sum of all Inflows and Outflows. Positive values are onto the fields, and a positive imbalance indicates a net loss of MeHg across the field. See **Section 4** for detailed information on flows and dates included in the season definition. 'Days in season' represents the number of days each field was inundated during winter, excluding the 17-day flood period.]

	field ID	F20	F66	R31	R64	W32	W65	SW	PW
	unit/block	North	South	North	South	North	South	South	South
	days in season	119	77	87	87	77	84	195	195
Inflows	irrigation	207	97	243	213	348	105	529	247
	precipitation	0	0	0	0	0	0	0	0
Outflows	surface outflow	-696	-1167	-1641	-2910	-509	-680	-990	-74
	transpiration	0	0	0	0	0	0	-825	-91
S	storage	0	0	0	0	0	0	0	0
	Surface imbalance	-490	-1070	-1398	-2697	-161	-575	-461	173
	Net imbalance	-490	-1070	-1398	-2697	-161	-575	-1286	82

Table 5.9. Comparison of annual average MeHg loads from Yolo Bypass Wildlife Area loads with other systems

[µg/ha/day, microgram per hectare per day. Negative values are inputs to the system; positive values are exports from the system to the surrounding environment]

Wetland type	Location	MeHg load (µg/ha/day)	Source
Mixed managed wetlands	Yolo Bypass, California	-22 to +81	This study
Subsided island drainage	Sacramento – San Joaquin Delta, California	-4 to +6	Heim et al., 2009
Natural tidal marsh	Browns Island, California	+44 to +71	Fleck et al., 2008
Impounded marsh	Twitchell Island, California	+14 to +145	Sassone et al., 2008; Heim et al., 2009
Northern peatlands	Minnesota, Canada, Sweden	+2 to +15	Lee et al. 1995; Jeremiason et al., 2006; St Louis et al., 1994
Upland forest	Wisconsin, New York, Canada	+0.2 to +4.5	Krabbenhoft et al., 1995; St Louis et al., 1995; Driscoll et al., 1998
Duck Ponds	Grizzly Island, California	+5.2	Stephenson et al., 2008b

Table 5.10. Summary of methylmercury loads for summer irrigation season

[Values represent methylmercury loads in units of nanograms per square meter (ng m^{-2}). NC, not calculated]

	Field ID		F20	F66	R31	R64	W32	W65	SW	PW
	unit/block	Arrow	North	South	North	South	North	South	South	South
	days in season	in **Fig. 5.36**	67	67	136	121	122	131	0	153
Inflows	irrigation	Lir	1429	122	748	377	1312	398	0	360
	leaching	Llc	NC	NC	NC	NC	NC	NC	NC	NC
	soil diffusion	Ld	NC	NC	NC	NC	NC	NC	NC	NC
	Precipitation / atmospheric deposition	Lad	0	0	0	0	0	0	0	0
Outflows	surface drainage	Lout	-124	-331	-237	-642	-1188	-534	0	-50
	plant biomass	Lpb	NC	NC	NC	NC	NC	NC	NA	NA
	particle settling	Lst	NC	NC	NC	NC	NC	NC	NC	NC
	photodemethylation	Lph	-268	-161	-408	-194	-683	-419	NC	-107
	transpiration and percolation	dissolved org	-660	-640	-1675	-995	-950	-1071	0	-200
	storage		0	0	0	0	159	80	0	0
	surface imbalance		1305	-209	511	-265	124	-136	0	310
	total imbalance		377	-1010	-1572	-1453	-1668	-1706	0	3

Table 6.1. Description of sediment and pore-water parameters, Yolo Bypass Wildlife Area mercury study

[Unit definitions: dry wt., dry weight; ng g^{-1}, nanogram per gram; d^{-1}, per day; %, percentage; pg g^{-1} d^{-1}, picogram per gram per day; nmol g^{-1} d^{-1}, nanomole per gram per day; g cm^{-3}, gram per cubic centimeter; wet sed., wet sediment; mL cm^{-3}, milliliters per cubic centimeter; µmol g^{-1}, micromole per gram; mg g^{-1}, milligram per gram; mV, millivolt; °C, degrees centigrade; ‰, permil = parts per thousand; mmol L^{-1}, millimole per liter; mg L^{-1}, milligram per liter; µmol L^{-1}, micromole per liter]

Parameter Notation	Units	Parameter Name
Sediment mercury parameters		
THg	ng g^{-1} (dry wt.)	total mercury
k_{meth}	d^{-1}	MeHg production potential rate constant
$Hg(II)_R$	ng g^{-1} (dry wt.)	inorganic reactive mercury
$\%Hg(II)_R$	%	percent THg as inorganic reactive mercury
MPP	pg g^{-1} d^{-1} (dry wt.)	MeHg production potential rate (calculated)
MeHg	ng g^{-1} (dry wt.)	methylmercury
% MeHg	%	percent THg as methylmercury
Sediment non-mercury parameters		
k_{SR}	d^{-1}	microbial sulfate reduction rate constant
SR	nmol g^{-1} d^{-1} (dry wt.)	microbial sulfate reduction rate
%dry wt.	%	pecent dry weight
LOI	%	weight loss on ignition
BD	g cm^{-3} (wet sed.)	bulk density
POR	mL cm^{-3} (wet sed.)	porosity
AVS	µmol g^{-1} (dry wt.)	acid volatile sulfur
TRS	µmol g^{-1} (dry wt.)	total reduced sulfur
Fe(II)	mg g^{-1} (dry wt.)	acid extractable ferrous iron [Fe(II)]
aFe(III)	mg g^{-1} (dry wt.)	amorphous (poorly crystalline) ferric Iron [Fe(III)]
cFe(III)	mg g^{-1} (dry wt.)	crystalline ferric Iron [Fe(III)]
Fe_T	mg g^{-1} (dry wt.)	total (measured) iron = Fe(II) + aFe(III) + cFe(III)
$\%Fe(II)/Fe_T$	%	percentage of total iron as ferrous iron
GS	%	percent grain size < 63 micron)
E_h laboratory	mV	oxidation-reduction potential: laboratory measurement
E_h field	mV	oxidation-reduction potential: field measurement
pH	pH Units	pH
TEMP	°C	temperature (field)
Pore-water non-mercury parameters		
$pw[\delta\ ^{34}SO_4^{2-}]$	‰, V-CDT	ratio of ^{34}S to ^{32}S in aqueous sulfate relative to the Vienna - Canyon Diablo Troilite (V-CDT) standard
$pw[SO_4^{2-}]$	mmol L^{-1}	sulfate
$pw[Cl^-]$	mmol L^{-1}	chloride
pw[SO4/Cl]	(unitless)	sulfate:chloride concentration ratio
pw[Fe(II)]	mg L^{-1}	ferrous Iron [Fe(II)]
pw[DOC]	mg L^{-1}	dissolved organic carbon
$pw[H_2S]$	µmol L^{-1}	sulfide
pw[ALK]	mg L^{-1} as HCO_3^-	bicarbonate alkalinity
pw[Ac]	µmol L-1	acetate

Table 6.2. Summary statistics for sediment and pore water parameters for individual agricultural fields and non-agricultural wetlands

[First Row = Mean ± (standard error), second row = median and **{N}**, where N = number of observations. Parameter notation definitions and units are given in **Table 6.1**.]

Parameter	Agricultural fallow field:F20	Agricultural fallow field:F66	Agricultural white rice field:R31	Agricultural white rice field:R64	Agricultural wild rice field:W32	Agricultural wild rice field:W65	Permanent Wetland open water field:PW2	Permanent Wetland open water field:PW5-ow	Permanent Wetland cattail field:PW5-cat	Permanent Wetland tule field:PW5-tule	Seasonal wetland mixed veg. field:SW
TEMP (field)	16.8 (2.5)	17.1 (3.3)	20.3 (2.2)	16.9 (3.5)	21.2 (3.6)	19.9 (3.6)	9.8 (1.8)	18.4 (3.0)	16.9 (3.9)	17.0 (4.4)	12.8 (2.3)
TEMP (field)	17.6 {4}	17.2 {4}	21.0 {5}	13.0 {5}	19.0 {5}	22.0 {5}	9.8 {2}	22.0 {5}	17.7 {4}	16.9 {4}	12.4 {3}
THg	296 (13)	276 (19)	362 (26)	373 (17)	290 (19)	354 (19)	124 (10)	135 (7)	147 (16)	132 (10)	161 (8)
THg	290 {4}	279 {4}	382 {5}	362 {5}	301 {5}	355 {5}	124 {2}	139 {5}	147 {4}	133 {4}	163 {3}
k_{meth}	0.012 (0.007)	0.061 (0.034)	0.090 (0.048)	0.055 (0.034)	0.037 (0.026)	0.077 (0.032)	0.031 (0.020)	0.199 (0.064)	0.634 (0.253)	0.330 (0.102)	0.061 (0.013)
k_{meth}	0.007 {4}	0.057 {4}	0.046 {5}	0.003 {5}	0.012 {5}	0.070 {5}	0.031 {2}	0.141 {5}	0.518 {4}	0.300 {4}	0.073 {3}
$Hg(II)_R$	5.13 (2.18)	6.31 (2.83)	2.65 (1.39)	4.84 (1.96)	4.24 (1.55)	4.56 (2.09)	0.27 (0.13)	0.27 (0.07)	0.26 (0.04)	0.17 (0.03)	0.16 (0.02)
$Hg(II)_R$	4.23 {4}	6.36 {4}	1.08 {5}	4.43 {5}	3.93 {5}	4.13 {5}	0.27 {2}	0.24 {5}	0.21 {4}	0.16 {4}	0.14 {3}
$\%Hg(II)_R$	1.72 (0.72)	2.13 (0.89)	0.68 (0.34)	1.33 (0.53)	1.40 (0.48)	1.31 (0.62)	0.21 (0.09)	0.20 (0.04)	0.17 (0.02)	0.12 (0.02)	0.10 (0.01)
$\%Hg(II)_R$	1.43 {4}	2.12 {4}	0.28 {5}	1.35 {5}	1.30 {5}	1.17 {5}	0.21 {2}	0.18 {5}	0.17 {4}	0.13 {4}	0.09 {3}
MPP	38.5 (17.9)	101.0 (44.2)	47.3 (17.3)	125.0 (87.6)	40.1 (17.7)	142.7 (88.7)	5.4 (1.2)	42.2 (13.5)	110.0 (34.2)	38.6 (4.1)	7.3 (1.4)
MPP	30.1 {4}	89.4 {4}	47.4 {5}	6.9 {5}	41.7 {5}	88.7 {5}	5.4 {2}	29.2 {5}	119.8 {4}	39.3 {4}	7.5 {3}
MeHg	2.55 (0.38)	2.31 (0.57)	2.60 (0.79)	3.00 (0.57)	2.68 (0.90)	2.84 (0.53)	0.65 (0.12)	1.27 (0.16)	2.53 (0.50)	1.80 (0.25)	2.03 (0.34)
MeHg	2.64 {4}	2.54 {4}	1.98 {5}	2.43 {5}	2.16 {5}	2.99 {5}	0.65 {2}	1.14 {5}	2.41 {4}	1.58 {4}	1.99 {3}
%MeHg	0.87 (0.12)	0.82 (0.17)	0.82 (0.35)	0.83 (0.18)	1.05 (0.46)	0.80 (0.13)	0.53 (0.14)	0.94 (0.10)	1.77 (0.36)	1.39 (0.21)	1.26 (0.18)
%MeHg	0.97 {4}	0.96 {4}	0.53 {5}	0.65 {5}	0.69 {5}	0.89 {5}	0.53 {2}	0.89 {5}	1.80 {4}	1.28 {4}	1.36 {3}
SR	6.9 (2.8)	48.8 (41.9)	31.2 (9.7)	12.6 (7.2)	303.4 (290.9)	45.7 (18.5)	9.7 (6.1)	98.0 (51.5)	14.4 (3.9)	71.3 (26.5)	11.9 (4.7)
SR	6.9 {4}	10.2 {4}	25.5 {5}	9.4 {5}	18.6 {4}	25.8 {5}	9.7 {2}	37.8 {5}	12.5 {4}	69.4 {4}	16.5 {3}
AVS	0.71 (0.24)	1.78 (1.04)	3.62 (2.10)	1.53 (0.92)	2.16 (0.98)	5.21 (2.06)	1.58 (0.86)	10.29 (2.44)	51.16 (13.80)	30.98 (13.23)	10.11 (1.49)
AVS	0.51 {4}	1.14 {4}	0.82 {5}	0.42 {5}	1.28 {5}	5.32 {5}	1.58 {2}	9.00 {5}	53.85 {4}	29.75 {4}	9.73 {3}

Parameter	Agricultural fallow field:F20	Agricultural fallow field:F66	Agricultural white rice field:R31	Agricultural white rice field:R64	Agricultural wild rice field:W32	Agricultural wild rice field:W65	Permanent Wetland open water field:PW2	Permanent Wetland open water field:PW5-ow	Permanent Wetland cattail field:PW5-cat	Permanent Wetland tule field:PW5-tule	Seasonal wetland mixed veg. field:SW
TRS	2.18 (0.66)	3.45 (1.73)	6.74 (3.33)	2.86 (1.18)	3.34 (1.52)	5.34 (2.28)	4.59 (1.09)	16.82 (4.13)	83.59 (18.76)	36.11 (8.84)	19.58 (1.68)
TRS	1.81 {4}	2.13 {4}	5.13 {5}	1.21 {5}	2.55 {5}	4.80 {5}	4.59 {2}	14.95 {5}	93.39 {4}	39.23 {4}	19.66 {3}
Fe(II)	4.05 (0.76)	4.17 (1.36)	5.34 (1.02)	3.30 (1.12)	4.08 (0.84)	5.03 (1.40)	4.07 (1.62)	6.36 (0.49)	7.16 (0.97)	7.33 (0.57)	7.53 (0.11)
Fe(II)	3.77 {4}	4.04 {4}	6.55 {5}	2.36 {5}	3.94 {5}	5.25 {5}	4.07 {2}	6.39 {5}	6.85 {4}	7.55 {4}	7.47 {3}
aFe(III)	0.55 (0.09)	0.61 (0.16)	0.55 (0.16)	0.65 (0.11)	0.59 (0.10)	0.35 (0.11)	0.28 (0.15)	0.03 (0.01)	0.05 (0.00)	0.09 (0.04)	0.01 (0.00)
aFe(III)	0.52 {4}	0.66 {4}	0.49 {5}	0.50 {5}	0.72 {5}	0.33 {5}	0.28 {2}	0.03 {5}	0.05 {4}	0.07 {4}	0.00 {3}
cFe(III)	11.71 (1.26)	12.00 (1.97)	11.53 (0.99)	14.69 (0.94)	13.26 (1.48)	12.34 (2.24)	9.08 (2.40)	5.85 (0.84)	3.97 (0.15)	8.53 (2.73)	5.92 (1.26)
cFe(III)	12.07 {4}	11.34 {4}	10.90 {5}	15.75 {5}	14.30 {5}	13.36 {5}	9.08 {2}	4.87 {5}	4.06 {4}	5.89 {4}	6.09 {3}
%Fe(II)/Fe_T	25.39 (5.66)	25.64 (8.50)	30.76 (5.90)	17.51 (5.86)	23.52 (5.71)	30.38 (9.63)	31.31 (14.21)	52.58 (5.26)	63.24 (3.65)	49.25 (7.83)	56.94 (5.81)
%Fe(II)/Fe_T	22.88 {4}	25.22 {4}	38.65 {5}	12.29 {5}	21.11 {5}	27.26 {5}	31.31 {2}	59.40 {5}	61.84 {4}	55.88 {4}	55.08 {3}
E_h laboratory	38 (43)	49 (72)	32 (57)	69 (48)	57 (65)	36 (40)	89 (46)	-20 (25)	-68 (39)	-44 (42)	-27 (37)
E_h laboratory	50 {4}	18 {4}	5 {5}	57 {5}	102 {5}	1 {5}	89 {2}	6 {5}	-65 {4}	-50 {4}	-3 {3}
E_h field	128 (10)	142 (82)	97 (38)	209 (48)	115 (46)	127 (35)	186 (73)	40 (24)	0 (23)	20 (42)	17 (12)
E_h field	131 {4}	123 {4}	69 {5}	195 {5}	76 {5}	149 {5}	186 {2}	47 {5}	9 {4}	28 {4}	12 {3}
pH	7.03 (0.10)	6.82 (0.05)	6.92 (0.09)	6.86 (0.04)	7.10 (0.07)	6.95 (0.07)	7.31 (0.15)	7.03 (0.08)	6.91 (0.10)	6.94 (0.05)	6.77 (0.16)
pH	6.96 {4}	6.83 {4}	6.88 {5}	6.84 {5}	7.05 {5}	6.96 {5}	7.31 {2}	7.06 {5}	7.00 {4}	6.91 {4}	6.79 {3}
GS	76.9 (7.4)	81.8 (6.0)	81.7 (5.3)	76.3 (7.4)	77.3 (2.5)	79.9 (4.0)	65.2 (8.4)	62.4 (6.9)	68.6 (6.8)	51.4 (6.5)	81.7 (2.7)
GS	77.9 {4}	83.5 {4}	81.6 {5}	72.1 {5}	77.6 {5}	78.9 {5}	65.2 {2}	54.2 {5}	63.1 {4}	51.9 {4}	80.1 {3}
%dry wt.	59.3 (1.0)	63.6 (1.7)	56.8 (2.6)	57.5 (1.5)	59.4 (0.3)	56.3 (1.2)	62.4 (0.9)	49.1 (2.3)	31.9 (2.1)	48.8 (4.8)	56.4 (1.7)
%dry wt.	59.3 {4}	65.0 {4}	59.1 {5}	57.6 {5}	59.4 {5}	56.9 {5}	62.4 {2}	46.1 {5}	30.6 {4}	48.9 {4}	55.0 {3}
LOI	6.66 (0.34)	6.80 (0.45)	6.85 (0.38)	7.31 (0.29)	6.55 (0.20)	7.01 (0.29)	4.44 (0.27)	6.71 (0.24)	10.22 (0.29)	8.60 (0.74)	8.94 (0.40)
LOI	6.55 {4}	6.72 {4}	6.76 {5}	7.27 {5}	6.64 {5}	6.91 {5}	4.44 {2}	6.87 {5}	10.14 {4}	8.23 {4}	8.83 {3}

Parameter	Agricultural fallow field:F20	Agricultural fallow field:F66	Agricultural white rice field:R31	Agricultural white rice field:R64	Agricultural wild rice field:W32	Agricultural wild rice field:W65	Permanent Wetland open water field:PW2	Permanent Wetland open water field:PW5-ow	Permanent Wetland cattail field:PW5-cat	Permanent Wetland tule field:PW5-tule	Seasonal wetland mixed veg. field:SW
BD	1.51 (0.02)	1.53 (0.02)	1.47 (0.05)	1.46 (0.03)	1.52 (0.01)	1.46 (0.04)	1.61 (0.08)	1.40 (0.04)	1.19 (0.02)	1.39 (0.05)	1.42 (0.02)
BD	1.52 {4}	1.52 {4}	1.51 {5}	1.44 {5}	1.52 {5}	1.47 {5}	1.61 {2}	1.41 {5}	1.18 {4}	1.37 {4}	1.43 {3}
POR	0.61 (0.02)	0.56 (0.03)	0.63 (0.02)	0.62 (0.02)	0.62 (0.01)	0.64 (0.00)	0.60 (0.02)	0.71 (0.02)	0.81 (0.01)	0.71 (0.04)	0.62 (0.02)
POR	0.61 {4}	0.54 {4}	0.63 {5}	0.62 {5}	0.62 {5}	0.64 {5}	0.60 {2}	0.70 {5}	0.82 {4}	0.70 {4}	0.63 {3}
pw[Cl^-]	2.59 (0.68)	2.76 (0.68)	3.79 (0.82)	3.17 (0.52)	4.66 (1.44)	5.68 (1.99)	1.80 (0.46)	2.46 (0.51)	2.01 (0.38)	1.95 (0.34)	1.32 (0.18)
pw[Cl^-]	2.76 {4}	2.89 {4}	4.40 {5}	3.72 {5}	3.99 {5}	4.21 {5}	1.80 {2}	2.56 {5}	2.08 {4}	2.07 {4}	1.35 {3}
pw[SO_4^{2-}]	0.52 (0.19)	0.92 (0.40)	1.09 (0.36)	1.10 (0.46)	1.49 (0.74)	1.48 (0.56)	0.50 (0.12)	0.43 (0.10)	0.01 (0.00)	0.10 (0.04)	0.00 (0.00)
pw[SO_4^{2-}]	0.52 {4}	0.81 {4}	1.19 {5}	0.71 {5}	0.99 {5}	1.35 {5}	0.50 {2}	0.34 {5}	0.01 {4}	0.10 {4}	0.00 {3}
pw[SO_4^{2-}/Cl^-]	0.21 (0.05)	0.38 (0.15)	0.24 (0.07)	0.30 (0.11)	0.30 (0.06)	0.24 (0.06)	0.28 (0.00)	0.19 (0.04)	0.004 (0.001)	0.05 (0.02)	0.003 (0.001)
pw[SO_4^{2-}/Cl^-]	0.23 {4}	0.34 {4}	0.27 {5}	0.25 {5}	0.32 {5}	0.25 {5}	0.28 {2}	0.19 {5}	0.004 {4}	0.06 {4}	0.003 {3}
pw[H_2S]	0.49 (0.13)	0.56 (0.21)	0.76 (0.22)	2.27 (1.34)	0.43 (0.15)	0.91 (0.22)	0.22 (0.07)	0.45 (0.07)	0.93 (0.27)	0.89 (0.21)	1.54 (0.19)
pw[H_2S]	0.49 {4}	0.43 {4}	0.85 {5}	1.35 {5}	0.25 {5}	1.08 {5}	0.22 {2}	0.49 {5}	1.04 {4}	0.78 {4}	1.62 {3}
pw[Fe(II)]	0.10 (0.04)	0.20 (0.08)	0.62 (0.50)	0.85 (0.69)	0.20 (0.13)	0.55 (0.29)	0.06 (0.02)	0.24 (0.08)	0.68 (0.20)	0.55 (0.08)	8.83 (4.51)
pw[Fe(II)]	0.08 {4}	0.19 {4}	0.13 {5}	0.05 {5}	0.03 {5}	0.10 {5}	0.06 {2}	0.23 {5}	0.73 {4}	0.52 {4}	4.45 {3}
pw[ALK]	526 (71)	518 (81)	696 (92)	652 (97)	573 (40)	725 (196)	375 (78)	460 (46)	458 (60)	467 (61)	391 (57)
pw[ALK]	549 {4}	471 {4}	678 {5}	638 {4}	529 {5}	523 {5}	375 {2}	408 {5}	494 {4}	471 {4}	407 {3}
pw[DOC]	16.7 (4.6)	18.1 (4.6)	24.4 (5.8)	22.8 (4.3)	19.2 (3.8)	26.6 (7.4)	9.8 (0.2)	10.0 (0.7)	13.2 (0.5)	17.8 (6.1)	41.3 (19.2)
pw[DOC]	13.4 {4}	15.5 {4}	22.8 {5}	22.7 {5}	16.5 {5}	22.1 {5}	9.8 {2}	10.7 {5}	13.1 {4}	12.1 {4}	24.5 {3}
pw[Ac]	5.4 (4.4)	166.2 (81.9)	163.7 (123.6)	548.3 (413.4)	83.7 (73.8)	175.8 (145.2)	1.0 (0.0)	1.0 (0.0)	138.0 (46.3)	245.6 (182.2)	347.5 (155.6)
pw[Ac]	1.0 {4}	156.1 {4}	34.5 {5}	79.8 {5}	16.1 {5}	51.8 {5}	1.0 {2}	1.0 {5}	173.0 {4}	96.8 {4}	220.8 {3}

Table 6.3. ANOVA results comparing sediment and pore water data grouped as agricultural versus non-agricultural fields

[Analysis includes all sampling dates and excludes experimental devegetation plots. The mean, standard error (SE), and the number of observations (N) is shown, along with all results from all mercury metric comparisons. Only significant results for non-mercury metrics are shown. Significant differences between groupings ($p < 0.05$) are indicated as '****' and non-significant differences are indicated as 'NS'. Parameter notation definitions and units are given in **Table 6.1**.]

	Agricultural Fields			Non-Agricultural Fields			
Parameter	**Mean ± SE**		**N**	**Mean ± SE**		**N**	**Significant**
THg	328	(10)	28	140	(5)	18	****
k_{meth}	0.057	(0.013)	28	0.283	(0.077)	18	****
$Hg(II)_R$	4.54	(0.76)	28	0.22	(0.03)	18	****
$\%Hg(II)_R$	1.39	(0.23)	28	0.16	(0.02)	18	****
MPP	83.3	(23.0)	28	46.6	(11.8)	18	**NS**
MeHg	2.68	(0.25)	28	1.73	(0.19)	18	****
%MeHg	0.86	(0.11)	28	1.23	(0.13)	18	****
Fe(II)	4.34	(0.43)	28	6.69	(0.38)	18	****
aFe(III)	0.55	(0.05)	28	0.07	(0.02)	18	****
cFe(III)	12.6	(0.6)	28	6.4	(0.8)	18	****
$\%Fe(II)/Fe_T$	25.5	(2.8)	28	52.6	(3.4)	18	****
$pw[SO_4^{2-}]$	1.13	(0.20)	28	0.20	(0.06)	18	****
$pw[\delta\ ^{34}SO_4^{2-}]$	5.0	(1.7)	24	14.3	(3.4)	6	****
AVS	2.6	(0.6)	28	23.0	(5.8)	18	****
TRS	4.07	(0.82)	28	35.04	(7.92)	18	****
pw[ALK]	621	(45)	27	440	(24)	18	****
%LOI	6.87	(0.13)	28	8.03	(0.47)	18	****
$pw[Cl^-]$	3.85	(0.49)	28	1.98	(0.19)	18	****
E_h Field	136	(19)	28	39	(18)	18	****
E_h Lab	47	(21)	28	-25	(18)	18	****
GS	79	(2)	28	65	(4)	18	****

Table 6.4. ANOVA results comparing northern versus southern agricultural fields

[Analysis includes all sampling dates and excludes experimental devegetation plots. The mean, standard error (SE), and the number of observations (N) is shown, along with all results from all mercury metric comparisons. Only significant results for non-mercury metrics are shown. Significant differences between groupings ($p < 0.05$) are indicated as '****' and non-significant differences are indicated as 'NS'. Parameter notation definitions and units are given in **Table 6.1.**]

	Northern Block Fields			Southern Block Fields			
Parameter	**Mean ± SE**		**N**	**Mean ± SE**		**N**	**Significant**
THg	318	(15)	14	338	(15)	14	**NS**
k_{meth}	0.049	(0.020)	14	0.065	(0.018)	14	**NS**
$Hg(II)_R$	3.93	(0.93)	14	5.16	(1.21)	14	**NS**
$\%Hg(II)_R$	1.24	(0.29)	14	1.55	(0.37)	14	**NS**
MPP	42.2	(9.5)	14	124.4	(43.1)	14	**NS**
MeHg	2.61	(0.41)	14	2.75	(0.31)	14	**NS**
%MeHg	0.91	(0.20)	14	0.81	(0.09)	14	**NS**
pH	7.01	(0.05)	14	6.88	(0.03)	14	********

Table 6.5. ANOVA results comparing growing season versus post-harvest season sediment and pore water data from agricultural fields

[Analysis conducted for growing season (June through August, 2007) and post-harvest season (December 2007 through February 2008) excludes experimental devegetation plots. The mean, standard error (SE), and the number of observations (N) is shown, along with all results from all mercury metric comparisons. Only significant results for non-mercury metrics are shown. Significant differences between groupings ($p < 0.05$) are indicated as '****' and non-significant differences are indicated as 'NS'. Parameter notation definitions and units are given in **Table 6.1**.]

	growing season			post-harvest season			
Parameter	**Mean ± SE**		**N**	**Mean ± SE**		**N**	**Significant**
THg	332	(14)	16	323	(16)	12	**NS**
k_{meth}	0.053	(0.015)	16	0.061	(0.025)	12	**NS**
$Hg(II)_R$	3.90	(1.02)	16	5.40	(1.15)	12	**NS**
$\%Hg(II)_R$	1.18	(0.30)	16	1.68	(0.36)	12	**NS**
MPP	59.5	(15.9)	16	115.1	(49.2)	12	**NS**
MeHg	1.91	(0.17)	16	3.70	(0.38)	12	****
%MeHg	0.59	(0.05)	16	1.23	(0.19)	12	****
$pw[\delta\ ^{34}SO_4^{2-}]$	7.78	(1.76)	16	-0.62	(2.78)	8	****
pw[ALK]	706	(64)	16	497	(33)	11	****
$pw[Cl^-]$	4.73	(0.63)	16	2.67	(0.68)	12	****
E_h Lab	3	(27)	16	106	(24)	12	****
GS	73	(2)	16	88	(2)	12	****
pw[DOC]	25.8	(3.1)	16	16.0	(1.7)	12	****

Table 6.6. Linear regression results for longitude versus individual mercury metrics

[The linear regression slope ± standard error (SE) and Y-intercept (Y-int.) is shown, along with the number of observations (N), the regression R^2, and the statistical Type II Error probablility (p) that the slope is not significantly different from zero. Model regressions were deemed significant (****) or non-significant (NS) based on a criteria of p< 0.05. Y_Variable parameter notation definitions and units are given in **Table 6.1**.]

X_Variable	Y_Variable	slope ± SE		Y-int.	N	R^2	p	Significant
Longitude	THg	-7531	(751)	-915508	57	0.65	< 0.0001	****
Longitude	k_{meth}	9.87	(2.33)	1201	55	0.25	< 0.0001	****
Longitude	$Hg(II)_R$	-161	(44)	-19627	55	0.20	0.0006	****
Longitude	$\%Hg(II)_R$	-44.0	(13.3)	-5349	55	0.17	0.002	****
Longitude	MPP	-161	(1157)	-19560	55	< 0.001	**0.88**	**NS**
Longitude	MeHg	-30.3	(13.7)	-3688	55	0.08	0.031	****
Longitude	%MeHg	17.5	(6.4)	2129	55	0.12	0.009	****

Table 7.1. Field descriptions of dominant plant species, yield, and leaf area during the 2007–2008 study period

[Key characteristics of plant community structure during summer growing season for crops and extant vegetation in each field and during winter in permanent wetland. Field Type designations: Ag, agricultural (rice production); Non-Ag, non-agricultural (managed wetland for wildlife). Root depth measured by in-field live root presence during June and August 2007. Rice yield values provided by the farmer (Jack DeWit). Average and standard deviation (in parentheses) for leaf area was calculated by assessment of leaf area on replicate harvested leaf material (n=3) and stem density (n=3). cm, centimeter; kg ha^{-1}, kilogram per hectar; leaf area is unitless as m^2 of leaf tissue divided by m^2 of planar surface cancels the units; na, not applicable; ND; not determined]

							Leaf Area (m^2_{leaf} $m^{-2}_{planar\ surface}$)				
Field Code	Field Type	Status during study period	Dominant Plant (Common Name)	Dominant Plant (Genus species)	Maximum root depth (cm)	Rice Yield (kg ha^{-1})	June 2007	July 2007	August 2007	December 2007	February 2008
R31	Ag	vegetated	white rice	*Oryza sativa* S-102	24	1272	0	1.5 (0.1)	2.6 (0.1)	3.0 (0.1)	0
R64	Ag	vegetated	white rice	*Oryza sativa* Akita	20	704	0	1.2 (0.1)	2.5 (0.2)	2.5 (0.2)	0
W32	Ag	vegetated	wild rice	*Zizania palustris* -Franklin	30	253	0	2.0 (0.3)	2.6 (0.4)	2.7 (0.4)	0
W65	Ag	vegetated	wild rice	*Zizania palustris* -Franklin	30	226	0	0.6 (0.1)	1.9 (0.2)	1.6 (0.2)	0
F20	Ag	barren	plantain / algal	*Alisma spp.*	0	na	0	0	0	0	0
F66	Ag	vegetated	sedge	*Cyperus difformis*	14	na	0	0	0.8 (0.3)	0.8 (0.3)	0
PW5	Non-Ag	vegetated	cattail	*Typha dominguensis*	>50	na	1.5 (0.5)	1.6 (0.3)	1.8 (0.2)	1.8 (0.2)	0.6 (0.5)
PW5	Non-Ag	vegetated	tule	*Schoenolpectus acutus*	>50	na	2.0 (0.4)	2.5 (0.4)	2.6 (0.3)	2.6 (0.3)	1.0 (0.4)

Table 7.2. Concentrations of carbon, nitrogen, mercury, and methylmercury and biomass of plant tissue in individual fields

[Data for biomass and concentrations represent peak biomass conditions for all fields. Averages and standard deviations (reported in parentheses) represent a minimum of n=3 field samples. All pools and concentrations for individual tissues are provided on a dry weight basis. Ratios of C:N and MeHg/THg in plant tissues are calculated from average concentrations. No assessment of these parameters were made for vegetation associated with the seasonal wetland site. C, carbon; N, nitrogen; %, percent; THg, total mercury; MeHg, methylmercury; ng g^{-1}, nanogram per gram; g m^{-2}, gram per square meter; μg m^{-2}, microgram per

Field Code	Dominant plant type	Plant Biomas ($g\ m^{-2}$)	Carbon (%)	Nitrogen (%)	C:N Ratio	THg ($ng\ g^{-1}$)	MeHg ($ng\ g^{-1}$)	MeHg/THg Ratio	Carbon ($g\ m^{-2}$)	Nitrogen ($g\ m^{-2}$)	THg ($\mu g\ m^{-2}$)	MeHg ($\mu g\ m^{-2}$)
						LEAF DATA						
R31	white rice	1139 (27)	36.9 (1.2)	1.8 (0.6)	20	14 (4)	2.6 (0.2)	19%	420 (12)	20.7 (3.7)	16 (2)	3.0 (0.1)
R64	white rice	984 (12)	36.7 (0.8)	1.0 (0.2)	37	15 (9)	1.3 (0.4)	9%	361 (6)	9.8 (1.0)	15 (5)	1.3 (0.2)
W32	wild rice	1027 (10)	40.4 (1.1)	0.4 (0.1)	107	107 (11)	4.4 (0.5)	4%	415 (8)	3.9 (0.5)	110 (6)	4.5 (0.3)
W65	wild rice	942 (30)	38.6 (2.4)	0.5 (0.1)	77	101 (8)	1.7 (0.1)	2%	364 (17)	4.7 (0.5)	95 (5)	1.6 (0.1)
F20	plantain / algae	10 (9)	40.6 (0.1)	2.9 (0.4)	14	37 (4)	3.1 (0.9)	8%	4.1 (1.8)	0.3 (0.2)	0.4 (0.2)	0.03 (0.02)
F66	sedge	330 (34)	34.5 (1.1)	1.7 (0.2)	20	31 (5)	5.6 (0.4)	18%	114 (8)	5.6 (0.6)	10 (1)	1.8 (0.2)
PW5	tule	1404 (50)	41.0 (1.8)	0.7 (0.0)	59	50 (6)	0.5 (0.1)	1%	576 (23)	9.8 (0.2)	70 (5)	0.7 (0.1)
PW5	cattail	1188 (36)	40.3 (2.2)	0.8 (0.1)	50	55 (11)	0.4 (0.1)	1%	479 (18)	9.5 (11)	65 4	0.5 (0.1)
						ROOT DATA						
R31	white rice	424 (83)	12.2 (0.2)	0.7 (0.2)	17	273 (25)	3.1 (2.4)	1%	52 (5)	3.0 (0.7)	116 (17)	1.3 (0.6)
R64	white rice	395 (19)	16.7 (0.2)	0.8 (0.1)	21	295 (36)	10 (2.1)	3%	66 (2)	3.2 (0.2)	117 (10)	4.0 (0.5)
W32	wild rice	308 (101)	32.6 (0.8)	0.7 (0.0)	47	279 (22)	12 (1.9)	4%	100 (18)	2.2 (0.4)	86 (17)	3.8 (0.9)
W65	wild rice	107 (12)	28.3 (0.1)	0.5 (0.0)	57	105 (41)	11 (2.5)	10%	30 (2)	0.5 (0.0)	11 (3)	1.2 (0.2)
F20	plantain / algae	1.0 (3.0)	22.4 (0.2)	1.0 (0.0)	22	214 (77)	12 (1.1)	6%	0.2 (0.3)	0.01 (0.02)	0.2 (0.4)	0.01 (0.02)
F66	sedge	74 (27)	27.6 (0.1)	0.9 (0.0)	31	247 (12)	11 (0.4)	4%	20 (4)	0.7 (0.1)	18 (4)	0.8 (0.2)
PW5	tule	563 (88)	36.3 (0.1)	1.4 (0.0)	26	150 (26)	1.2 (0.6)	1%	204 (16)	7.9 (0.6)	84 (14)	0.7 (0.2)
PW5	cattail	143 (49)	38.3 (0.2)	1.2 (0.0)	32	104 (18)	1.9 (0.8)	2%	55 (10)	1.7 (0.3)	15 (4)	0.3 (0.1)
						SEED DATA						
R31	white rice	16 (11)	41.5 (0.2)	1.6 (0.1)	26	54 (12)	4.1 (1.1)	8%	6.6 (2.3)	0.3 (0.1)	0.9 (0.4)	0.1 (0.0)
R64	white rice	28 (13)	39.4 (0.1)	1.2 (0.3)	33	46 (6)	4.2 (0.6)	9%	11 (3)	0.3 (0.1)	1.3 (0.4)	0.1 (0.0)
W32	wild rice	12 (6)	44.1 (2.1)	1.6 (0.1)	28	11 (2)	6.6 (1.4)	60%	5.3 (1.4)	0.2 (0.1)	0.1 (0.0)	0.1 (0.0)
W65	wild rice	10 (8)	42.5 (0.1)	2.3 (0.2)	18	16 (12)	5.9 (1.6)	37%	4.3 (1.7)	0.2 (0.1)	0.2 (0.1)	0.1 (0.0)
F20	plantain / algae	0 (0)	ND	ND	ND	ND	ND	ND	ND	ND	ND	ND
F66	sedge	0 (0)	ND	ND	ND	ND	ND	ND	ND	ND	ND	ND
PW5	tule	4 (9)	41.0 (0.1)	1.1 (0.1)	37	150 (26)	1.2 (0.2)	1%	1.6 (1.8)	0.04 (0.05)	0.6 (0.7)	0.005 (0.006)
PW5	cattail	21 (15)	44.2 (0.5)	1.0 (0.1)	44	104 (18)	1 (0.4)	1%	9.3 (3.4)	0.2 (0.1)	2.2 (1.0)	0.02 (0.01)

Table 7.3. Devegetation effect on sediment and pore-water parameters during the period of peak plant biomass, by habitat type

[Values represent the percentage (%) decrease (-) or increase (+) for each parameter listed in devegetated plots compared to vegetated plots, as calculated by: %DevegEffect = ($X_{vegetated\ plot}$ - $X_{devegetated\ plot}$) / $X_{vegetated\ plot}$) x 100, during August 2007 for agricultural fields (Ag Management) and during December 2007 for non-agricultural fields (Non-Ag Management), where 'X' is the particular parameter of interest. Statistically significant differences between vegetated and devegetated sites for a given sub-habitat parameter (X), as assessed using pairwise t-tests ($p \leq 0.05$) on normalized data. Abbreviations: sed, sediment; pw, sediment porewater; k_{meth}, mercury-methylation rate constant; $Hg(II)_R$, inorganic "reactive" mercury; MP, microbial methylmercury production rate; MeHg, methylmercury; SR, microbial sulfate reduction rate; S^{2-}, sulfide; Fe(II), ferrous iron; aFe(III), amorphous ferric iron; DOC, dissolved organic carbon; TRS, total reduced sulfur; AVS, acid volatile sulfur; Cl, chloride; Root Density, volume of soil occupied by live root material; ns, not significant]

Field Type (dominant vegetation)	Management	sed k_{meth}	sed $Hg(II)_R$	sed MP	sed MeHg	sed %MeHg	sed SR	pw acetate	pw S^{2-}	pw Fe(II)	sed Fe(II)	sed aFe(III)	pw DOC	sed TRS	sed AVS	pw Cl	Root Density
White rice	Ag	-48	ns	-64	-38	-16	ns	-63	ns	ns	+17	-24	-47	ns	ns	-28	-99
Wild rice	Ag	-67	ns	-67	ns	ns	ns	-93	ns	ns	+16	-23	ns	ns	ns	-37	-99
Fallow-mixed (sedge)	Ag	-56	-82	-92	-55	-42	-81	-63	+68	+87	ns	-93	ns	+26	ns	-13	-95
Fallow-barren (plantain / algal)	Ag	-67	+81	ns	-49	-19	-49	-93	-72	-50	ns	+21	ns	-58	ns	ns	ns
Seasonal wetland (swamp timothy)	Non-Ag	-17	ns	ns	-35	-21	ns	-79	ns	+30	ns	ns	ns	ns	ns	ns	-87
Permanent wetland (tule)	Non-Ag	-87	+83	ns	-41	-23	-80	-98	ns	-38	ns	ns	ns	-71	-80	ns	-93
Permanent wetland (cattail)	Non-Ag	ns	+24	ns	-14	Ns	ns	-99	-45	-30	ns	ns	ns	-10	-26	ns	-99

Table 7.4. Plant litter decomposition rates and areal pool sizes

[Plant litter on the sediment surface during February 2008 was calculated based on growing season biomass (field measurements), date of litterfall via harvest (rice crop) or senescence (native wetland plants), and the decomposition rate constants (k) at 30 °C determined in the laboratory for each plant species. The temperature-dependent k value was then adjusted for mean monthly in-field air temperature (in °C) as reported by the Calif. Dept. of Fish and Game at El Macero Station, Calif., and was assumed to follow Q_{10} kinetics (increasing by a factor of 2.4 for every 10 °C change in temperature, as per **Gu et al. (2004)**). Averages and standard deviations (reported in parentheses) represent a minimum of n=3 field samples. %, percentage; °C, degree Celsius; g $m^{-2,}$ gram per square meter, on a dry weight basis]

Field Code	Plant Species	Decomposition rate constant (k) at 30 °C % per day	Litterfall Date (Estimated)	Initial Biomass at Litterfall (g m^{-2})	Surface Litter for February 2008 (g m^{-2})
R31	*Oryza sativa*	-4.2 (0.8)	10/1/07	1139	391 (31)
R64	*Oryza sativa*	-4.7 (1.2)	10/1/07	984	288 (16)
W32	*Zizania palustris*	-2.3 (1.6)	9/1/07	1027	253 (14)
W65	*Zizania palustris*	-2.8 (0.8)	9/1/07	942	163 (17)
F66	*Cyperus difformis*	-7.1 (1.0)	10/1/07	330	18 (2)
PW5	*Schoenolpectus acutus*	-2.2 (0.5)	12/15/07	1404	952 (72)
PW5	*Typha dominguensis*	-2.0 (0.8)	12/15/07	1188	836 (109)

Table 8.1. Western mosquitofish whole body total mercury concentration and body burden immediately prior to and after 60 days of caged exposure in agricultural and non-agricultural wetlands within the Yolo Bypass Wildlife Area, California

[Statistical analysis using the two-sample t-test to examine temporal changes in fish total mercury concentrations (whole body) and total mercury body burden, at the time the fish were first caged (Introduction) compared to after 60 days of in-situ exposure, for individual fields and within-field locations (inlets, center and outlet). Non-agricultural wetlands are represented by permanent wetland sites PW-2 and PW-5. Agricultural wetlands are represented by sites R31, R64, W32 and W65. Where: THg, total mercury; µg g^{-1} dw; microgram per gram fish (whole body) on a dry weight basis; µg $fish^{-1}$ dw, microgram per fish on a dry weight basis; N, number of observations; SE, standard error of the mean; DF, degrees of freedom; t, t-test statistic; P, probability of a Type II error; %, percentage; <, less than. Statistical significance found after a sequential Bonferroni correction was applied is indicated by an asterisk (*). No fish were present in the cages after 60 days, indicated as 'na'.]

	Introduction			After 60 days			*t* -test			Difference	
Field / Location	*N*	Mean	SE	*N*	Mean	SE	*DF*	*t*	*P*	Mean	%
Whole body THg concetration (µg g^{-1} dw)											
PW-2 (permanent wetlands)											
Inlet	37	0.14	0.01	6	0.49	0.08	41	8.41	<.0001*	0.35	246%
Center	37	0.14	0.01	14	0.40	0.02	49	10.62	<.0001*	0.25	176%
Outlet	37	0.14	0.01	20	0.44	0.02	55	13.77	<.0001*	0.29	204%
PW-5 (permanent wetlands)											
Inlet	37	0.14	0.01	16	0.34	0.02	51	9.08	<.0001*	0.19	135%
Center	37	0.14	0.01	14	0.34	0.02	49	9.16	<.0001*	0.19	136%
Outlet	37	0.14	0.01	15	0.34	0.02	50	9.26	<.0001*	0.20	140%
R31 (white rice)											
Inlet	37	0.14	0.01	6	0.48	0.06	41	8.58	<.0001*	0.34	237%
Center	37	0.14	0.01	24	1.57	0.05	59	33.33	<.0001*	1.42	995%
Outlet	37	0.14	0.01	14	1.64	0.05	49	27.10	<.0001*	1.50	1046%
R64 (white rice)											
Inlet	37	0.14	0.01	6	0.40	0.03	41	7.49	<.0001*	0.26	180%
Center	37	0.14	0.01	26	1.53	0.03	61	35.88	<.0001*	1.39	969%
Outlet	37	0.14	0.01	26	1.86	0.05	61	37.47	<.0001*	1.71	1197%
W32 (wild rice)											
Inlet	37	0.14	0.01	0	na	na	na	na	na	na	na
Center	37	0.14	0.01	26	0.97	0.02	61	28.56	<.0001*	0.83	579%
Outlet	37	0.14	0.01	21	0.75	0.05	56	19.30	<.0001*	0.60	422%
W65 (wild rice)											
Inlet	37	0.14	0.01	21	1.79	0.13	56	27.76	<.0001*	1.65	1153%
Center	37	0.14	0.01	24	0.92	0.02	59	27.32	<.0001*	0.78	546%
Outlet	37	0.14	0.01	25	1.02	0.04	60	26.97	<.0001*	0.88	615%
THg body burden (µg $fish^{-1}$ dw)											
PW-2 (permanent wetlands)											
Inlet	37	0.05	0.01	6	0.11	0.02	41	2.52	0.02	0.06	117%
Center	37	0.05	0.01	14	0.08	0.01	49	2.01	0.05	0.03	51%
Outlet	37	0.05	0.01	20	0.07	0.01	55	1.44	0.16	0.01	29%
PW-5 (permanent wetlands)											
Inlet	37	0.05	0.01	16	0.11	0.01	51	3.52	0.001*	0.05	106%
Center	37	0.05	0.01	14	0.09	0.01	49	2.81	0.01	0.04	78%
Outlet	37	0.05	0.01	15	0.09	0.02	50	2.72	0.01	0.04	80%
R31 (white rice)											
Inlet	37	0.05	0.01	6	0.11	0.01	41	2.42	0.02	0.06	110%
Center	37	0.05	0.01	24	0.63	0.03	59	16.06	<.0001*	0.58	1118%
Outlet	37	0.05	0.01	14	0.71	0.03	49	13.07	<.0001*	0.65	1265%
R64 (white rice)											
Inlet	37	0.05	0.01	6	0.10	0.01	41	2.16	0.04	0.05	93%
Center	37	0.05	0.01	26	0.65	0.03	61	17.05	<.0001*	0.60	1162%
Outlet	37	0.05	0.01	26	0.86	0.03	61	19.04	<.0001*	0.81	1566%
W32 (wild rice)											

	Introduction			After 60 days			*t* -test			Difference	
Field / Location	*N*	Mean	SE	*N*	Mean	SE	*DF*	*t*	*P*	Mean	%
Inlet	37	0.05	0.01	0	na	na	na	na	na	na	na
Center	37	0.05	0.01	26	0.39	0.03	61	12.76	<.0001*	0.34	656%
Outlet	37	0.05	0.01	21	0.32	0.03	56	10.18	<.0001*	0.27	527%
W65 (wild rice)											
Inlet	37	0.05	0.01	21	0.38	0.03	56	11.67	<.0001*	0.33	640%
Center	37	0.05	0.01	24	0.45	0.03	59	13.62	<.0001*	0.40	779%
Outlet	37	0.05	0.01	25	0.49	0.04	60	13.96	<.0001*	0.44	850%

Table 8.2. Western mosquitofish size and body condition immediately prior to and after 60 days of caged exposure in agricultural and non-agricultural wetlands within the Yolo Bypass Wildlife Area, California

[Statistical analysis using the two-sample t-test to examine temporal changes in fish standard length, wet mass and relative condition factor, at the time the fish were first caged (Introduction) compared to after 60 days of in-situ exposure, for individual fields and within-field locations (inlets, center and outlet). Non-agricultural wetlands are represented by Permanent Wetland sites 2 and 5. Agricultural wetlands are represented by sites R31, R64, W32 and W65. Where: mm, millimeters; g, gram; N, number of observations; SE, standard error of the mean; DF, degrees of freedom; t, t-test statistic; P, probability of a Type II error; %, percentage; <, less than. Statistical significance found after a sequential Bonferroni correction was applied is indicated by an asterisk (*). No fish were present in the cages after 60 days, indicated as 'na'.]

	Introduction			After 60 days			*t* -test			Difference	
Location	*N*	Mean	SE	*N*	Mean	SE	*DF*	*t*	*P*	Mean	%
Fish standard length (mm)											
PW-2 (permanent wetlands)											
Inlet	30	39.13	0.78	6	38.32	0.42	34	-0.46	0.65	-0.81	-2%
Center	30	35.91	0.40	14	37.08	0.67	42	1.54	0.13	1.17	3%
Outlet	30	38.24	0.38	20	35.80	0.64	48	-3.41	0.001*	-2.44	-6%
PW-5 (permanent wetlands)											
Inlet	30	40.37	0.93	16	41.43	1.16	44	0.69	0.49	1.06	3%
Center	30	38.02	0.46	14	38.67	0.54	42	0.83	0.41	0.65	2%
Outlet	30	40.85	0.94	16	40.57	1.30	44	-0.20	0.84	-0.28	-1%
R31 (white rice)											
Inlet	30	37.11	0.63	6	38.59	0.96	34	0.95	0.35	1.48	4%
Center	30	35.95	0.61	24	43.51	0.61	52	8.47	<.0001*	7.57	21%
Outlet	30	35.41	0.46	14	44.66	0.67	42	11.01	<.0001*	9.25	26%
R64 (white rice)											
Inlet	30	39.10	0.66	6	38.24	1.11	34	-0.55	0.59	-0.85	-2%
Center	30	39.33	0.79	26	44.26	0.62	54	4.67	<.0001*	4.93	13%
Outlet	30	39.02	0.66	26	45.29	0.54	54	6.83	<.0001*	6.27	16%
W32 (wild rice)											
Inlet	30	41.14	0.78	0	na	na	na	na	na	na	na
Center	30	40.85	0.61	26	45.06	0.68	54	4.48	<.0001*	4.21	10%
Outlet	30	37.68	0.83	21	45.15	0.81	49	6.04	<.0001*	7.48	20%
W65 (wild rice)											
Inlet	30	37.37	0.78	21	37.79	0.38	49	0.37	0.71	0.41	1%
Center	30	38.78	0.70	24	45.60	0.78	52	6.35	<.0001*	6.82	18%
Outlet	30	38.51	0.85	25	47.23	0.76	53	7.29	<.0001*	8.72	23%
Fish wet mass (g)											
PW-2 (permanent wetlands)											
Inlet	30	1.48	0.10	6	1.26	0.05	34	-0.99	0.33	-0.22	-15%
Center	30	1.40	0.06	14	1.15	0.06	42	-2.71	0.01	-0.25	-18%
Outlet	30	1.69	0.09	20	0.93	0.04	48	-7.77	<.0001*	-0.76	-45%
PW-5 (permanent wetlands)											
Inlet	30	1.80	0.14	16	1.70	0.14	44	-0.46	0.65	-0.10	-6%
Center	30	1.47	0.07	14	1.48	0.06	42	0.04	0.97	0.00	0%
Outlet	30	1.79	0.13	16	1.55	0.14	43	-1.18	0.24	-0.24	-13%
R31 (white rice)											

	Introduction			After 60 days			*t* -test			Difference	
Location	*N*	Mean	SE	*N*	Mean	SE	*DF*	*t*	*P*	Mean	%
Inlet	30	1.40	0.07	6	1.20	0.04	34	-1.31	0.20	-0.20	-14%
Center	30	1.31	0.09	24	2.02	0.08	52	5.24	<.0001*	0.71	54%
Outlet	30	1.25	0.05	14	2.13	0.09	42	7.55	<.0001*	0.87	70%
R64 (white rice)											
Inlet	30	1.64	0.08	6	1.27	0.13	34	-2.10	0.04	-0.37	-23%
Center	30	1.63	0.12	26	2.18	0.08	54	3.48	0.001*	0.55	34%
Outlet	30	1.56	0.09	26	2.19	0.11	54	4.34	<.0001*	0.63	40%
W32 (wild rice)											
Inlet	30	1.87	0.13	0	na	na	na	na	na	na	na
Center	30	1.80	0.09	26	2.02	0.11	54	1.56	0.13	0.22	12%
Outlet	30	1.54	0.10	21	2.19	0.12	49	3.86	0.0003*	0.65	43%
W65 (wild rice)											
Inlet	30	1.37	0.10	21	1.11	0.04	49	-2.15	0.04	-0.25	-19%
Center	30	1.56	0.10	24	2.43	0.14	52	5.02	<.0001*	0.86	55%
Outlet	30	1.58	0.10	25	2.38	0.12	53	4.96	<.0001*	0.81	51%
					Relative condition factor						
PW-2 (permanent wetlands)											
Inlet	30	0.91	0.02	6	0.83	0.04	34	-1.80	0.08	-0.08	-9%
Center	30	1.11	0.04	14	0.83	0.04	42	-4.74	<.0001*	-0.28	-25%
Outlet	30	1.16	0.07	20	0.74	0.02	48	-4.88	<.0001*	-0.42	-36%
PW-5 (permanent wetlands)											
Inlet	30	1.01	0.02	16	0.89	0.02	44	-3.44	0.001*	-0.13	-13%
Center	30	0.99	0.03	14	0.94	0.02	42	-1.12	0.27	-0.06	-6%
Outlet	30	0.97	0.03	16	0.86	0.02	43	-2.32	0.03	-0.11	-11%
R31 (white rice)											
Inlet	30	1.00	0.03	6	0.77	0.05	34	-3.78	0.001*	-0.23	-23%
Center	30	1.03	0.03	24	0.91	0.02	52	-2.89	0.01	-0.12	-11%
Outlet	30	1.05	0.06	14	0.90	0.04	42	-1.71	0.09	-0.15	-14%
R64 (white rice)											
Inlet	30	1.01	0.03	6	0.83	0.04	34	-2.86	0.01	-0.18	-18%
Center	30	0.99	0.02	26	0.94	0.02	54	-1.36	0.18	-0.05	-5%
Outlet	30	0.97	0.02	26	0.89	0.02	54	-2.55	0.01	-0.08	-9%
W32 (wild rice)											
Inlet	30	1.00	0.03	0	na	na	na	na	na	na	na
Center	30	0.98	0.03	26	0.83	0.02	54	-4.02	0.0002*	-0.15	-16%
Outlet	30	1.05	0.02	21	0.90	0.03	49	-4.35	<.0001*	-0.15	-15%
W65 (wild rice)											
Inlet	30	0.96	0.02	21	0.76	0.02	49	-6.37	<.0001*	-0.20	-21%
Center	30	0.99	0.02	24	0.97	0.03	52	-0.51	0.62	-0.02	-2%
Outlet	30	1.01	0.02	25	0.86	0.02	53	-5.51	<.0001*	-0.16	-15%

Table 9.1 Sampling dates and locations for photodemethylation experiments

[Coordinates for water sampling, light meter, and incubation locations are given in datum WGS84 and in degrees decimal minutes (ddd mm.mmm). See **Figure 3.5** for corresponding map. Field codes varied between years based on crop rotation.]

Sampling Period	Field Number	Field Code	Field type	Latitude [dd mm.mmm]	Longitude [ddd mm.mmm]
Dec 3-7, 2007	20	F20	Fallow	38° 33.150’ N	121° 37.200’ W
Jul 29 - Aug 1, 2008	20	R20	White rice	38° 33.150’ N	121° 37.200’ W
Dec 3-7, 2007	31	R31	White rice	38° 33.150’ N	121° 36.628 W
Jul 29 - Aug 1, 2008	31	W31	Wild rice	38° 33.150’ N	121° 36.628 W
Dec 3-7, 2007	32	W32	Wild rice	38° 33.163' N	121° 36.387’ W
Dec 3-7, 2007	64	R64	White rice	38° 32.867'N	121° 36.683'W
Jul 29 - Aug 1, 2008	64	W64	Wild rice	38° 32.867'N	121° 36.683'W
Dec 3-7, 2007	65	W65	Wild rice	38° 32.567'N	121° 36.450'W
Dec 3-7, 2007	66	F66	Fallow	38° 32.567’ N	121° 36.108’ W
Jul 29 - Aug 1, 2008	66	R66	White rice	38° 32.567’ N	121° 36.108’ W
Dec 3-7, 2007	1	SW1	Seasonal Wetland	38° 32.474’ N	121° 36.068’ W
Dec 3-7, 2007	5	PW5	Permanent Wetland	38° 32.567'N	121° 35.550'W
Jul 29 - Aug 1, 2008	5	PW5	Permanent Wetland	38° 32.567'N	121° 35.550'W
Dec 3-7, 2007	Light Meter Location			38° 33.177’ N	121° 40.312’ W
Jul 29 - Aug 1, 2008	Light Meter Location			38° 33.177’ N	121° 40.312’ W
Dec 3-7, 2007	Incubation Location			38° 33.070’ N	121° 37.665’ W
Jul 29 - Aug 1, 2008	Incubation Location			38° 33.052' N	121° 37.600'W

Table 9.2. Summary of the linear regression slopes associated with the change in methylmercury concentration as a function of cumulative solar photosynthetically available radiation and ultraviolet radiation measured during the winter and summer photodemethylation experiments

[Linear least-squares regression slopes for merthylmercury (MeHg) degradation were calculated as the change in MeHg concentration as a function of the cummulative PAR or UV solar radiation exposure over a 2-3 day incubation (5 time points) of sample bottles exposed to light or dark conditions. The difference represents the dark-corrected light-induced slope for MeHg degradation. PAR, photosynthetically available radiation; UV, ultra-violet; ng L^{-1}, nanogram per liter; ng L^{-1} mol-1 m^{-2}, nanogram per liter per mole per square meter]

Field Code	Sampling Period	Initial MeHg Concentration (ng L^{-1})	PAR Regression Slope (ng L^{-1} mol^{-1} m^{-2})			UV Regression Slope (ng L^{-1} mol^{-1} m^{-2})		
			Light	Dark	Difference	Light	Dark	Difference
F20	Dec 3-7, 2007	0.7	-0.0086	-0.0032	-0.0054	-0.216	-0.078	-0.138
R31	Dec 3-7, 2007	1.75	-0.0148	0.0002	-0.0150	-0.372	0.040	-0.412
F66	Dec 3-7, 2007	0.84	-0.0047	0.0001	-0.0048	-0.124	0.004	-0.128
SW1	Dec 3-7, 2007	1	-0.0068	-0.0043	-0.0025	-0.172	-0.114	-0.058
R64	Dec 3-7, 2007	0.83	-0.0037	-0.0004	-0.0033	-0.094	-0.009	-0.084
W65	Dec 3-7, 2007	0.93	-0.0046	-0.0005	-0.0041	-0.116	0.017	-0.130
PW5	Dec 3-7, 2007	0.37	-0.0038	-0.0003	-0.0035	-0.010	-0.006	-0.094
PW32	Dec 3-7, 2007	1.06	-0.0057	0.0024	-0.0081	-0.015	0.062	-0.210
W31	Jul 29 - Aug 1, 2008	0.65	-0.0029	-0.0018	-0.0012	-0.071	-0.047	-0.024
PW5	Jul 29 - Aug 1, 2008	0.21	-0.0008	-0.0003	-0.0005	-0.020	-0.008	-0.012
W64	Jul 29 - Aug 1, 2008	3.75	-0.0165	0.0036	-0.0201	-0.397	0.086	-0.483
W66	Jul 29 - Aug 1, 2008	0.5	-0.0025	-0.0003	-0.0022	-0.064	-0.008	-0.056
W20	Jul 29 - Aug 1, 2008	1.5	-0.0079	-0.0003	-0.0076	-0.191	-0.006	-0.185

Table 9.3. Average daily percent loss of methylmercury as a function of daily integrated photosynthetically available radiation or ultraviolet radiation intensity and light attenuation with water-column depth

[Values represent the percentage (%) of methylmercury lost per day though photodecomposition. The extinction coefficient (unitless) is a measure of light attenuation with water depth, and is given for a maximum water-column depth of 30 centimeters. PAR, photosynthetically available radiation; UV, ultra-violet radiation; mol m^{-2}, moles of photons per square meter]

Extinction	Daily Integrated PAR (mol m^{-2})							
Coefficient	3	5	10	15	20	30	40	50
-0.01	1.2	2.1	4.2	6.2	8.3	12	17	21
-0.02	1.1	1.8	3.6	5.4	7.2	11	14	18
-0.03	0.95	1.6	3.2	4.8	6.3	9.5	13	16
-0.04	0.84	1.4	2.8	4.2	5.6	8.4	11	14
-0.05	0.75	1.2	2.5	3.7	5.0	7.5	9.0	12
-0.06	0.67	1.1	2.2	3.3	4.5	6.7	8.9	11
-0.07	0.60	1.0	2.0	3.0	4.0	6.0	8.0	10
-0.08	0.55	0.91	1.8	2.7	3.6	5.5	7.3	9.1
-0.09	0.50	0.83	1.7	2.5	3.3	5.0	6.6	8.3
-0.10	0.46	0.76	1.5	2.3	3.0	4.6	6.1	7.6

	Daily Integrated UV (mol m^{-2})							
	0.3	0.5	1	1.5	2	3	4	5
-0.01	3.1	5.1	10	15	20	31	41	51
-0.02	2.7	4.4	8.9	13	18	27	35	44
-0.03	2.3	3.9	7.8	12	16	23	31	39
-0.04	2.1	3.4	6.9	10	14	21	27	34
-0.05	1.8	3.1	6.1	9.2	12	18	24	31
-0.06	1.6	2.7	5.5	8.2	11	16	22	27
-0.07	1.5	2.5	4.9	7.4	9.9	15	20	25
-0.08	1.3	2.2	4.5	6.7	8.9	13	18	22
-0.09	1.2	2.0	4.1	6.1	8.2	12	16	20
-0.10	1.1	1.9	3.7	5.6	7.5	11	15	19

Table 9.4. Average daily percent loss of methylmercury as a function of daily integrated photosynthetically available radiation or ultraviolet radiation intensity and initial methylmercury concentration.

[Values represent the mass loss of methylmercury (in units of ng m^{-2} d^{-1}, nanograms per square meter per day) via photodecomposition, assuming an extinction coefficient of -0.029 and water-column depth of 30 centimeters. MeHg, methylmercury; PAR, photosynthetically available radiation; UV, ultra-violet radiation; mol m^{-2}, moles of photons per square meter]

Initial MeHg Concentration	Daily Integrated PAR (mol m^{-2})							
ng L^{-1}	3	5	10	15	20	30	40	50
0.5	0.05	0.08	0.16	0.24	0.32	0.48	0.64	0.80
1.0	0.10	0.16	0.32	0.48	0.64	0.96	1.3	1.6
1.5	0.14	0.24	0.48	0.72	0.96	1.4	1.9	2.4
2.0	0.19	0.32	0.64	0.96	1.3	1.9	2.6	3.2
2.5	0.24	0.40	0.80	1.2	1.6	2.4	3.2	4.0
3.0	0.29	0.48	0.96	1.4	1.9	2.9	3.8	4.8
4.0	0.39	0.64	1.3	1.9	2.6	3.8	5.1	6.4
5.0	0.48	0.80	1.6	2.4	3.2	4.8	6.4	8.0
6.0	0.58	0.96	1.9	2.9	3.8	5.8	7.7	9.6
8.0	0.77	1.3	2.6	3.8	5.1	7.7	10	13
10.0	0.96	1.6	3.2	4.8	6.4	9.6	13	16
	Daily Integrated UV (mol m^{-2})							
	0.3	**0.5**	**1**	**1.5**	**2**	**3**	**4**	**5**
0.5	0.02	0.04	0.08	0.12	0.16	0.24	0.32	0.39
1.0	0.07	0.12	0.24	0.36	0.47	0.71	1.0	1.2
1.5	0.12	0.20	0.39	0.59	0.79	1.2	1.6	2.0
2.0	0.24	0.39	0.79	1.2	1.6	2.4	3.2	3.9
2.5	0.36	0.59	1.2	1.8	2.4	3.6	4.7	5.9
3.0	0.47	0.79	1.6	2.4	3.2	4.7	6.3	7.9
4.0	0.59	1.0	2.0	3.0	3.9	5.9	7.9	9.9
5.0	0.71	1.2	2.4	3.6	4.7	7.1	9.5	12
6.0	1.0	1.6	3.2	4.7	6.3	9.5	13	16
8.0	1.2	2.0	3.9	5.9	7.9	12	16	20
10.0	1.4	2.4	4.7	7.1	9.5	14	19	24

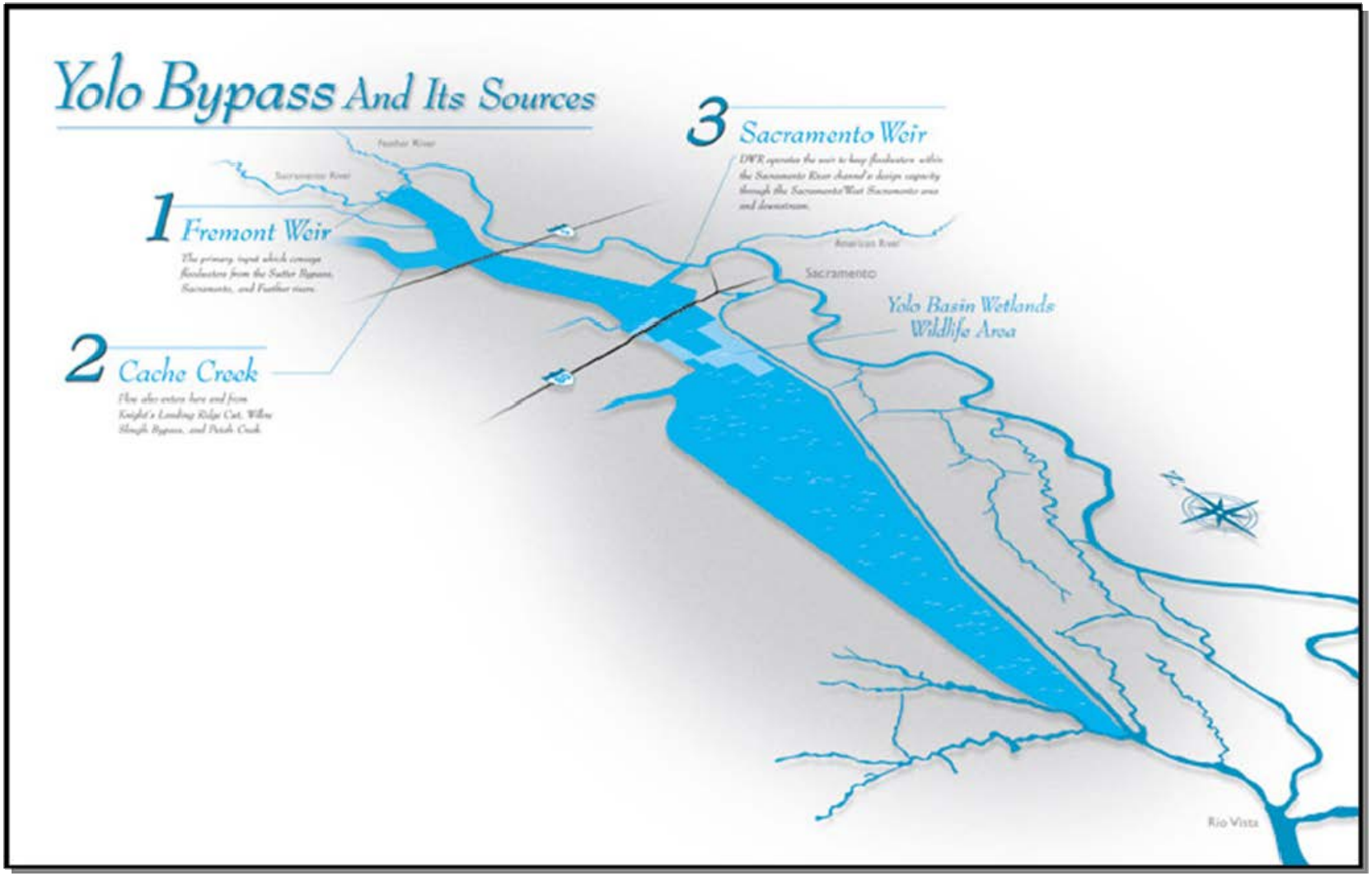

Figure 3.1. Northern-looking oblique graphic illustration of the hydrologic contribution of the Yolo Basin Wildlife Area (YBWA) to the Yolo ByPass hydrologic unit. Image taken from California Department of Water Resources news: http://geography.sierra.cc.ca.us/booth/california/9_water/Yolo_Bypass.jpg

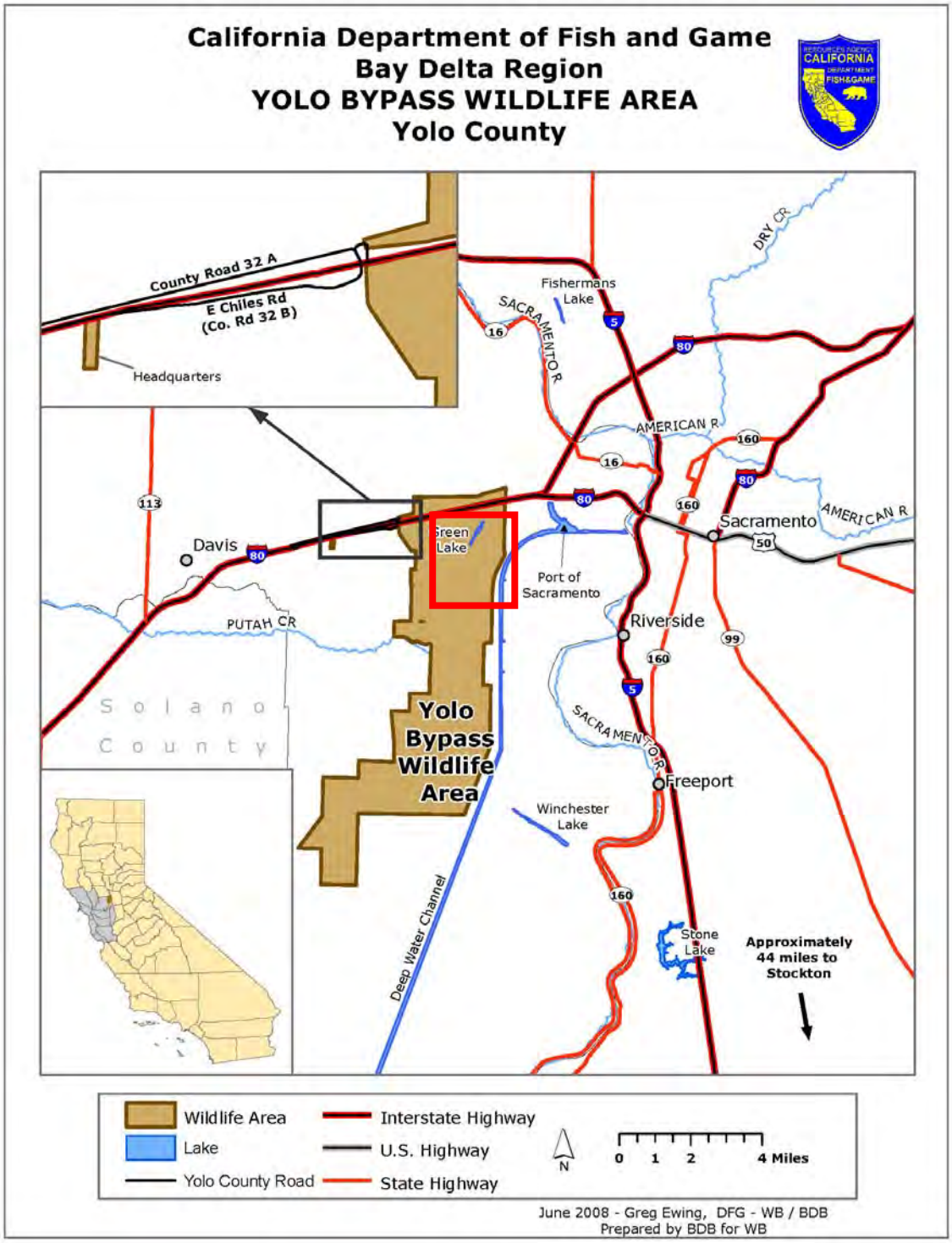

Figure 3.2. Map illustrating the location of the study area within the Yolo Bypass Wildlife Area, Yolo County, CA. The red square depicts the study area. Taken from the California Department of Fish and Game Web Site: *http://www.dfg.ca.gov/lands/wa/region3/yolo/docs/YoloBypass_WA_Web.pdf*.

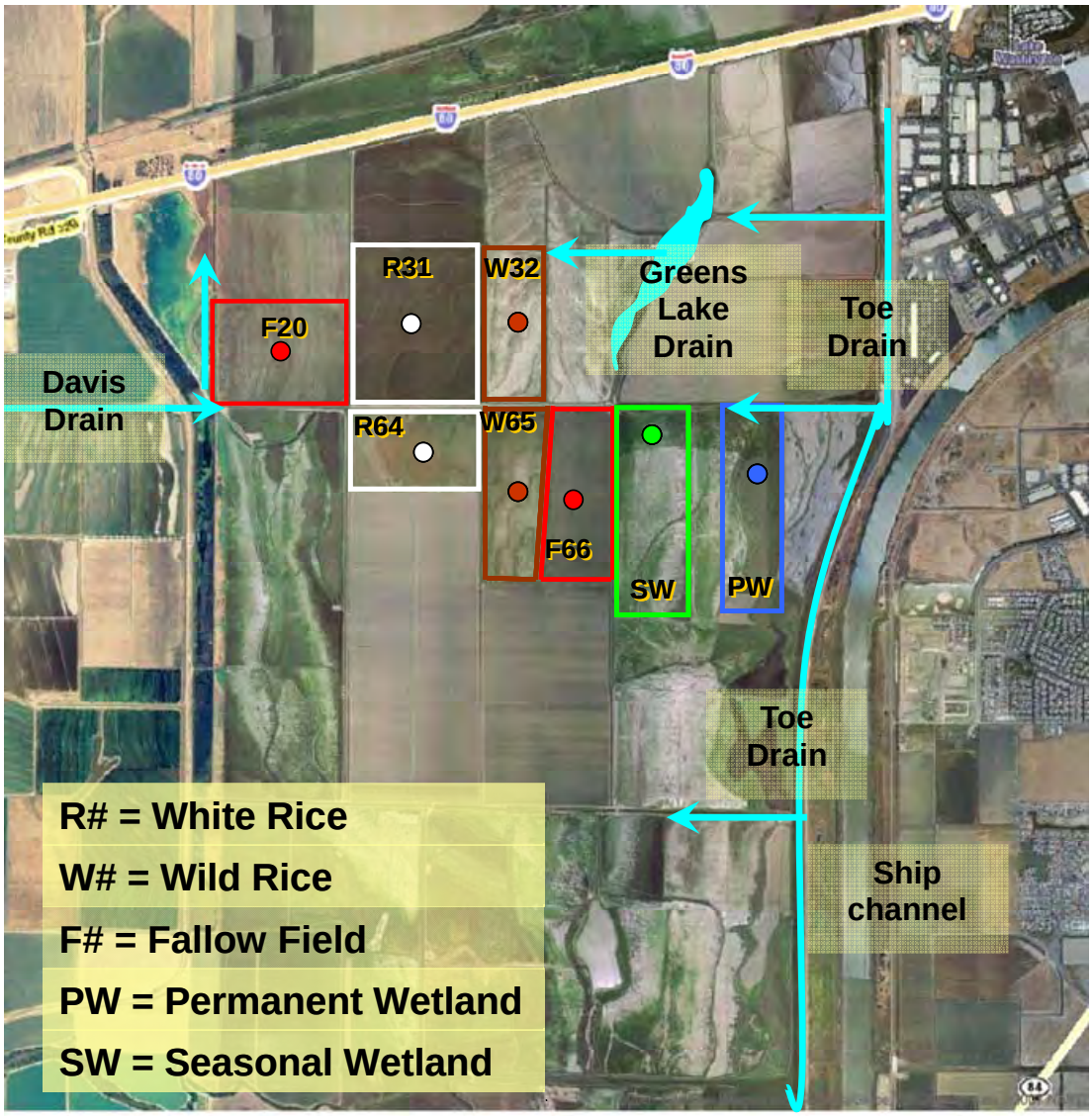

Figure 3.3 Satellite image (GoogleEarth™) of the study area depicting the five wetland types studied. Similar field types share the same color border. The circles in each field indicate the location of the primary sediment sampling sites. GPS coordinates are listed in **Table 3.1**. The turquoise lines and arrows indicate the major water flows in and around the study area.

Figure 3.4. Satellite image (GoogleEarth™) depicting sampling locations for specific matrices. Where: inlet (blue), outlet (red) and centerfield (green) sites were sampled for water (blue, red and green), sediment (green only), plant (green only) and biota (red and blue only)**.** GPS coordinates are listed in **Table 3.1**.

Figure 3.5. Satellite image (GoogleEarth™) depicting photodemethylation study sampling locations. The red dot indicates the location of the light meter. The blue dots indicate the locations where water samples were collected, and the yellow dots indicate the locations of sample deployment (photo-incubations).

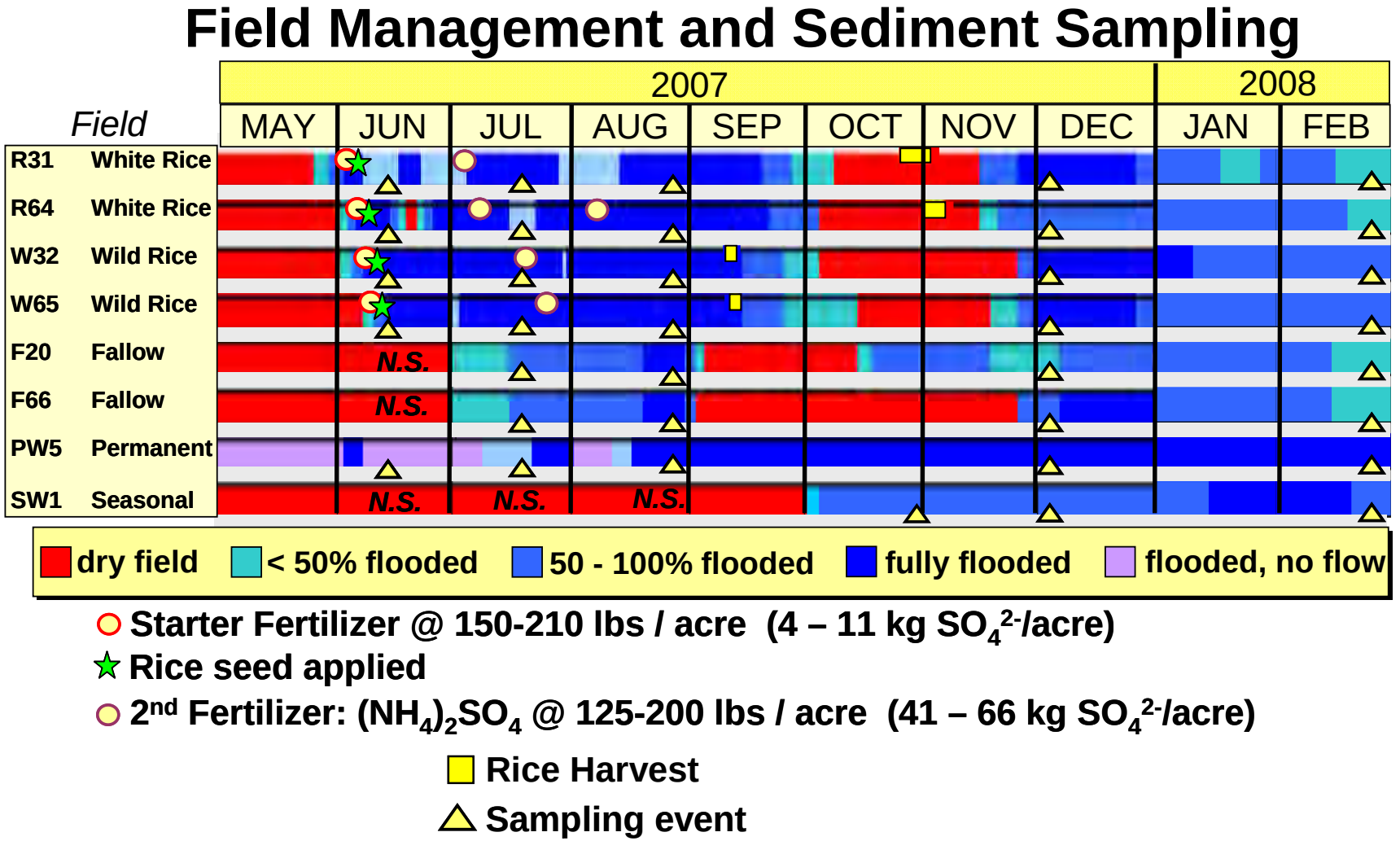

Figure 3.6. Timeline depicting field hydrology, management activities and approximate study collection dates for sediment, plants and biota samples. Water samples were also collected on these dates as well as others. See associated appendices for exact dates.

A) Continuous Flow Stirred Tank Reactor (CFSTR) **B) Plug Flow Reactor (PFR)**

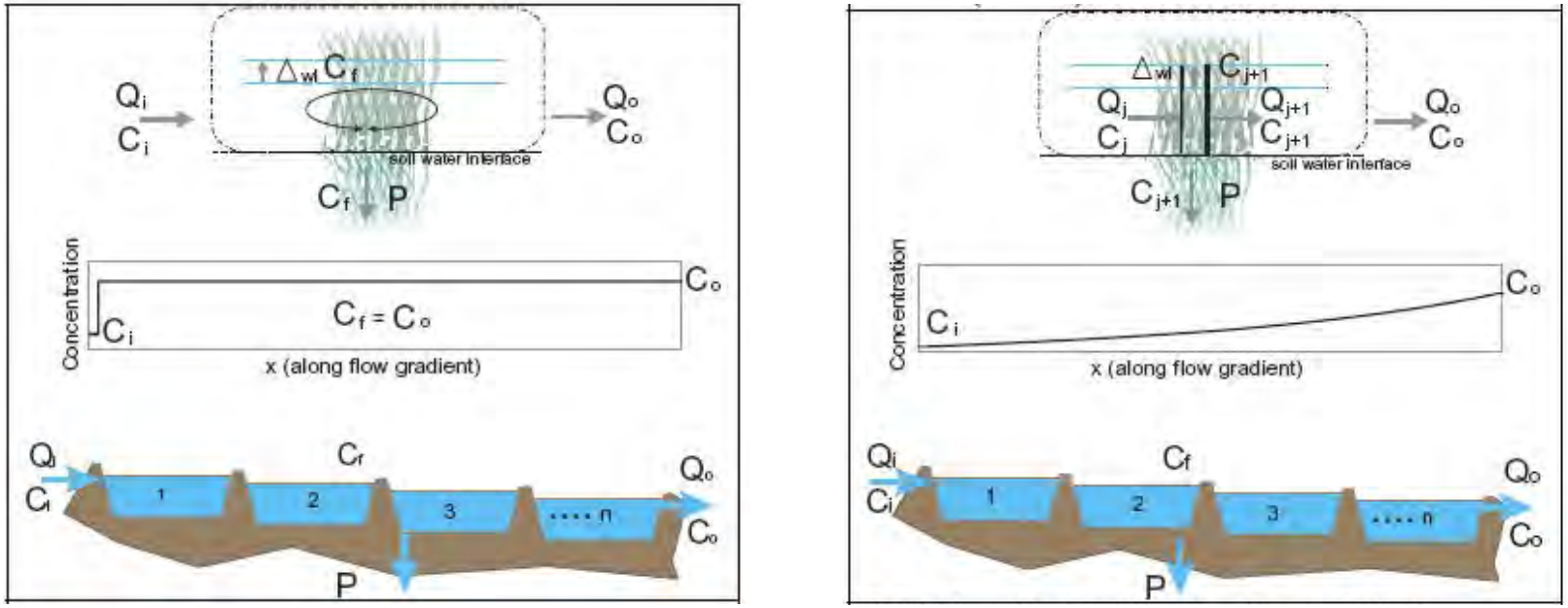

Figure 4.1. Schematics for water flow and concentration trends across the fields based on A) the Continuous Flow Stirred Tank Reactor model and B) the Plug Flow Reactor model. Where: Q_i = flow in, Q_o = flow out, C_i = concentration in, C_o = concentration out, P = percolation.

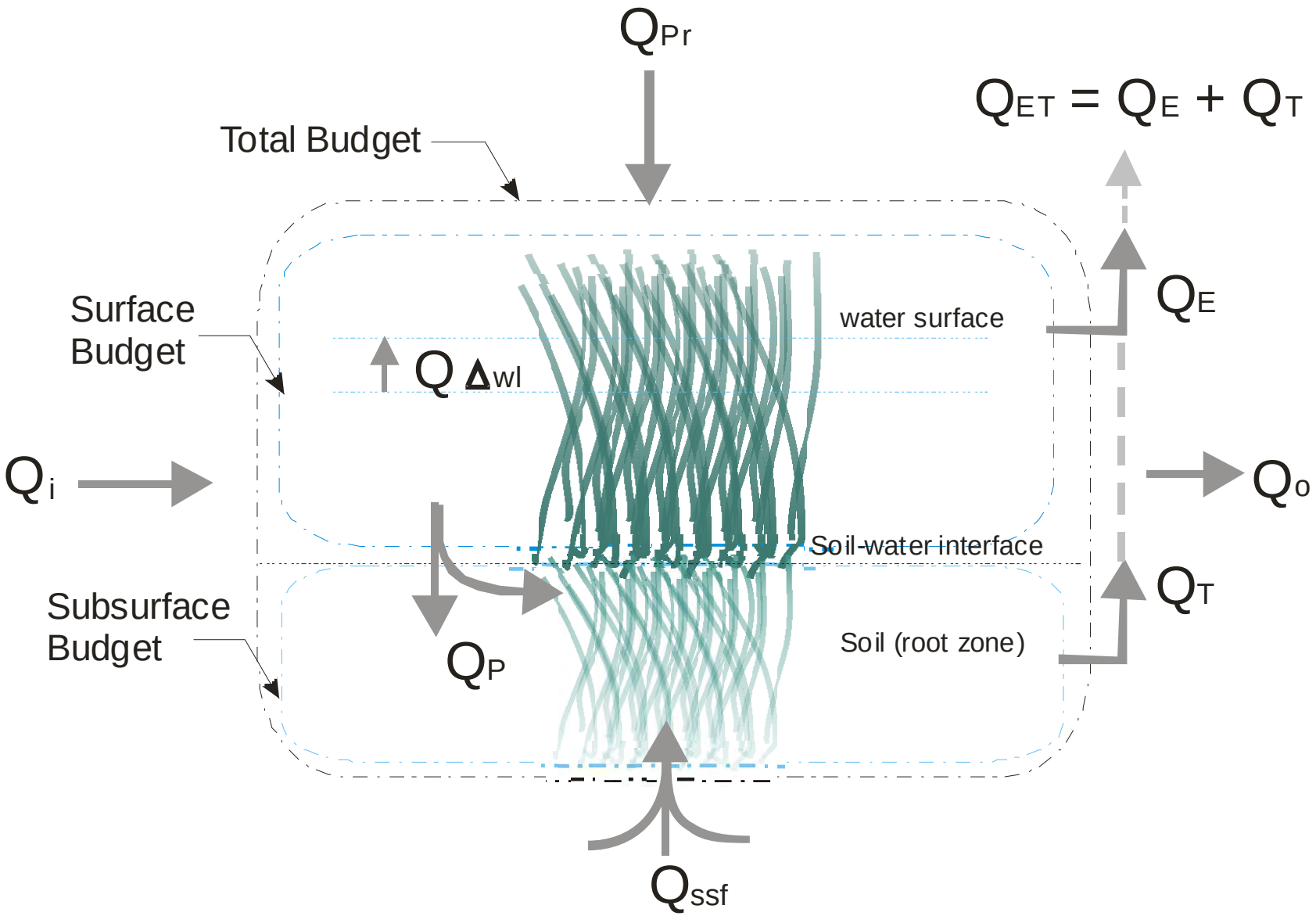

Figure 4.2. **Water budget model.** See **Section 4.2** for model parameter definitions.

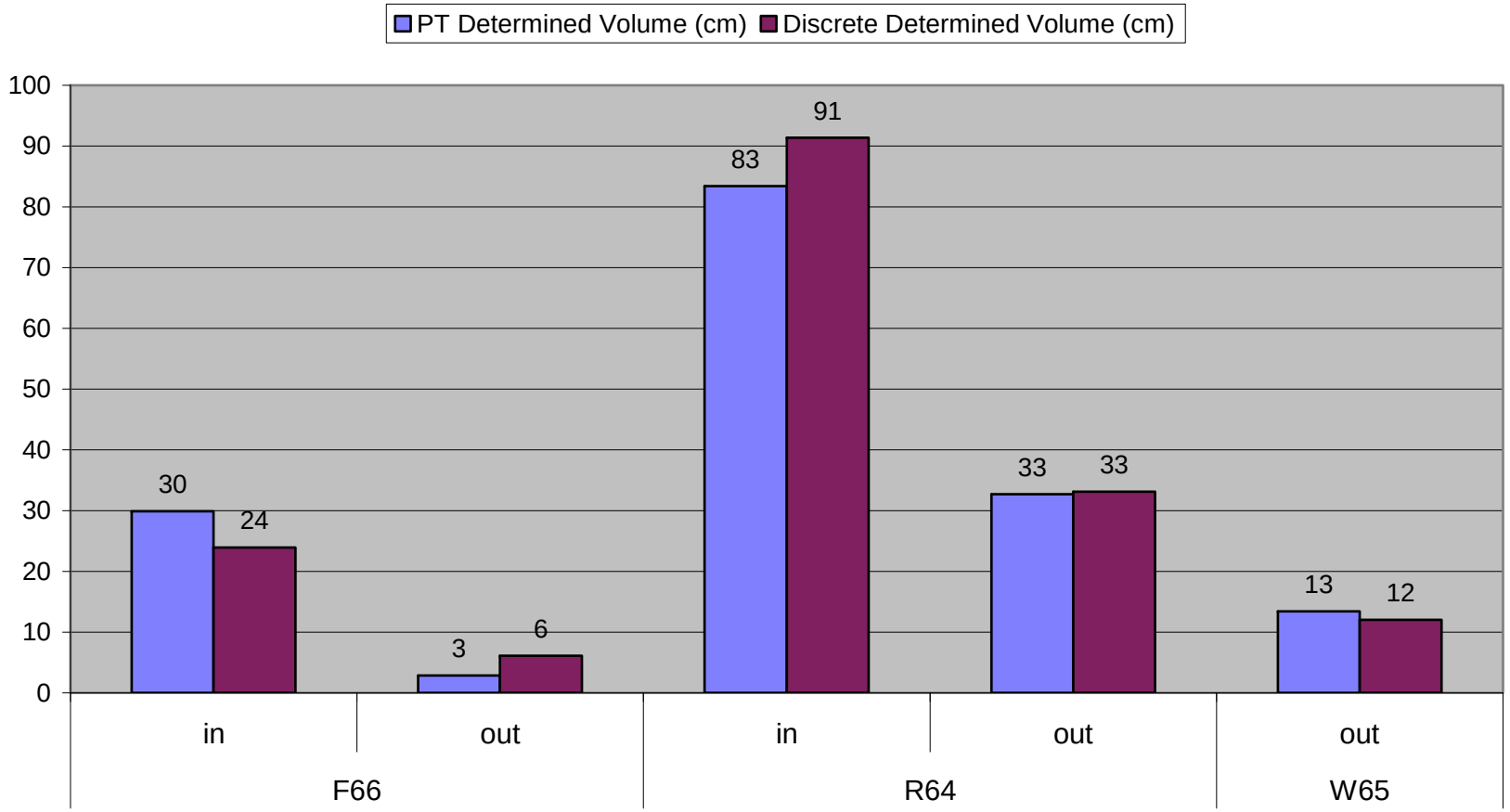

Figure 4.3. Comparison of water flux calculations using pressure transducer and manual measurements for the fields where both data were collected.

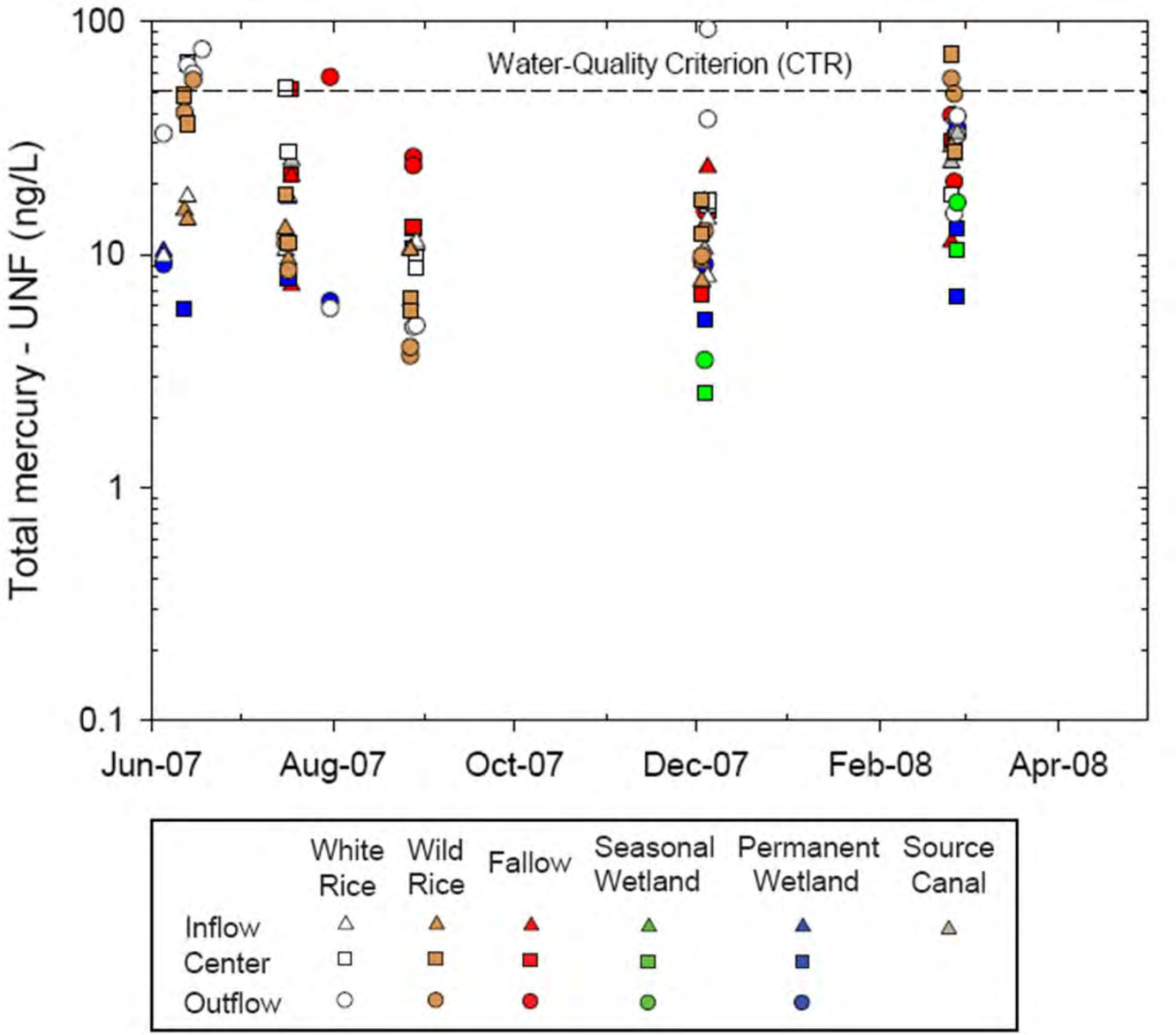

Figure 5.1. Time series plot of total mercury concentration in unfiltered surface water. The dashed line indicates the 50 ng/L water-quality criterion for unfiltered total mercury in the California Toxics Rule (CTR) (U.S. Environmental Protection Agency, 2000b).

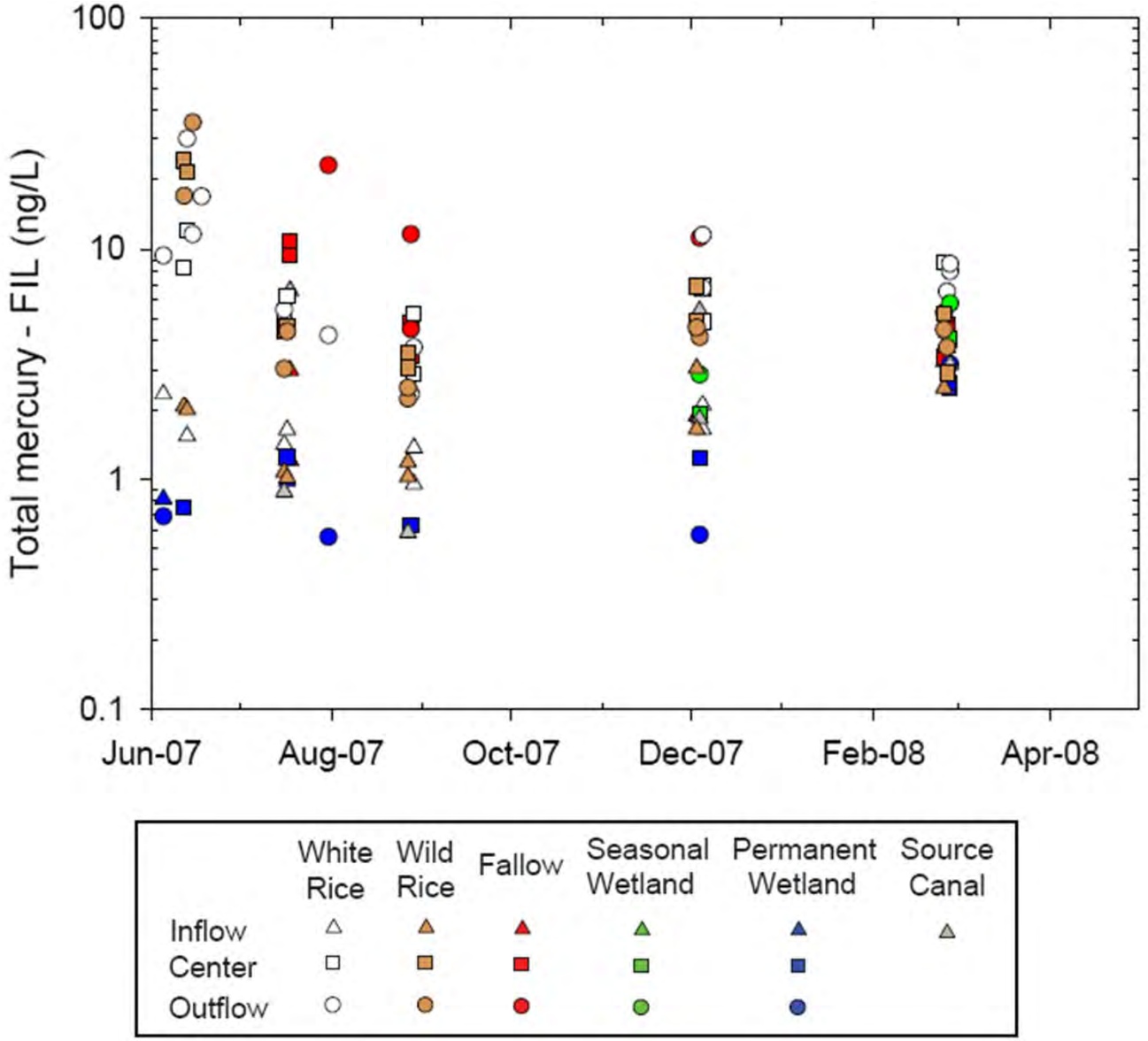

Figure 5.2. Time series plot of total mercury concentration in filtered surface water.

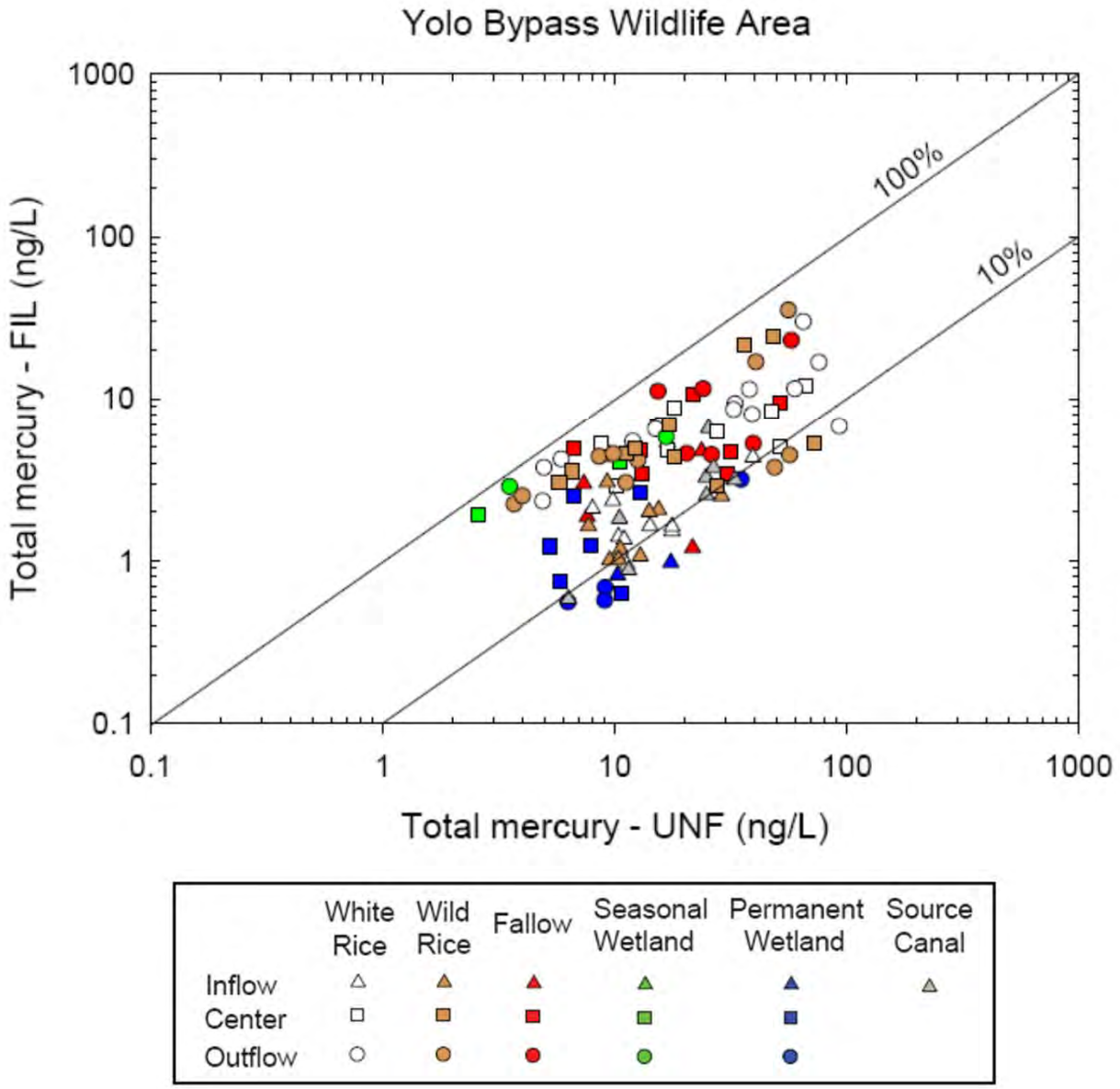

Figure 5.3. Log-log plot of total mercury concentration in unfiltered versus filtered surface water.
Diagonal lines represent lines of equal proportions of mercury passing through the filter, as indicated.

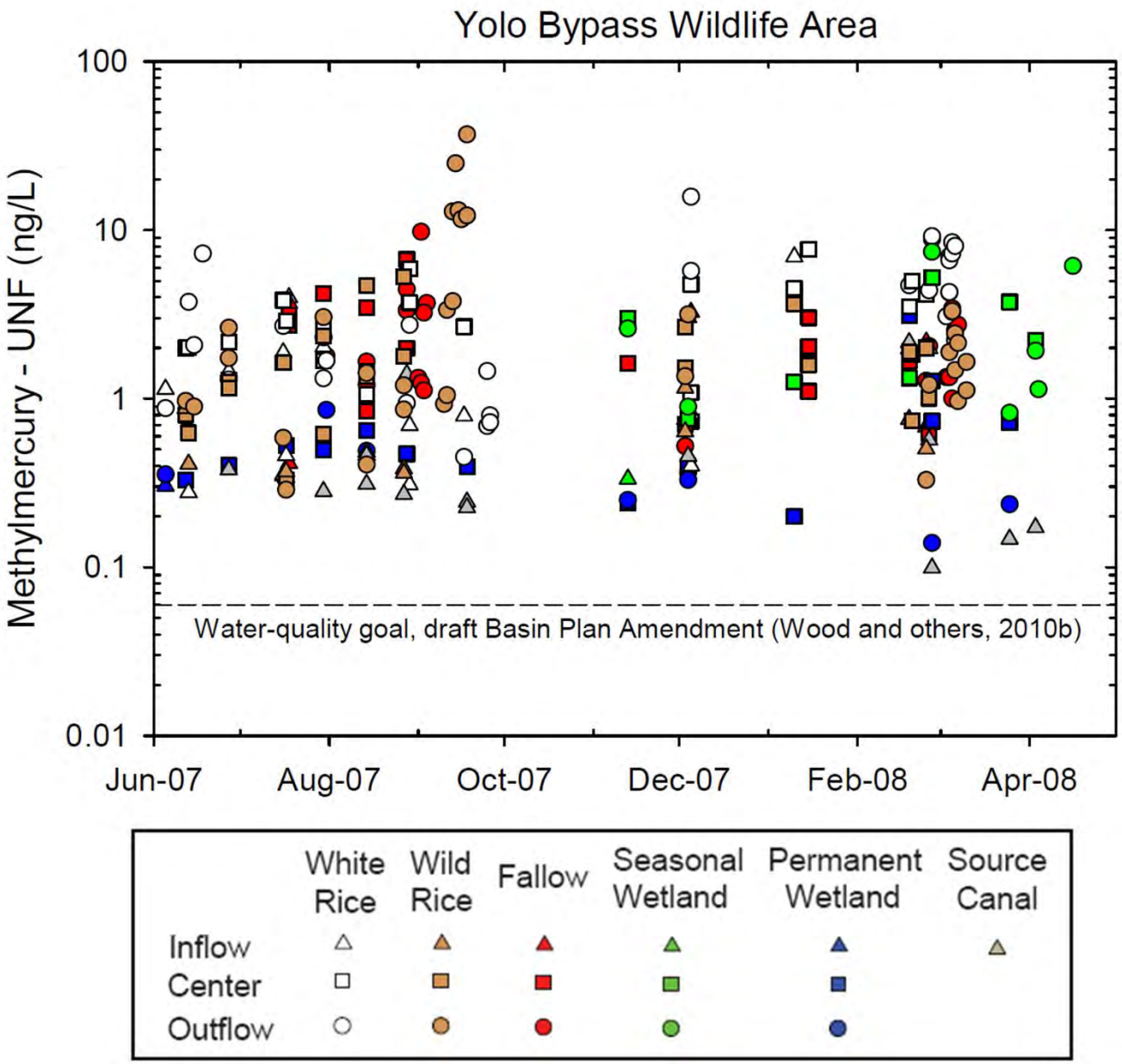

Figure 5.4. Time series plot of methylmercury concentration in unfiltered surface water. The dashed horizontal line reflects the 0.06 ng/L proposed water -quality goal for unfiltered methylmercury (Wood et al., 2010b) .

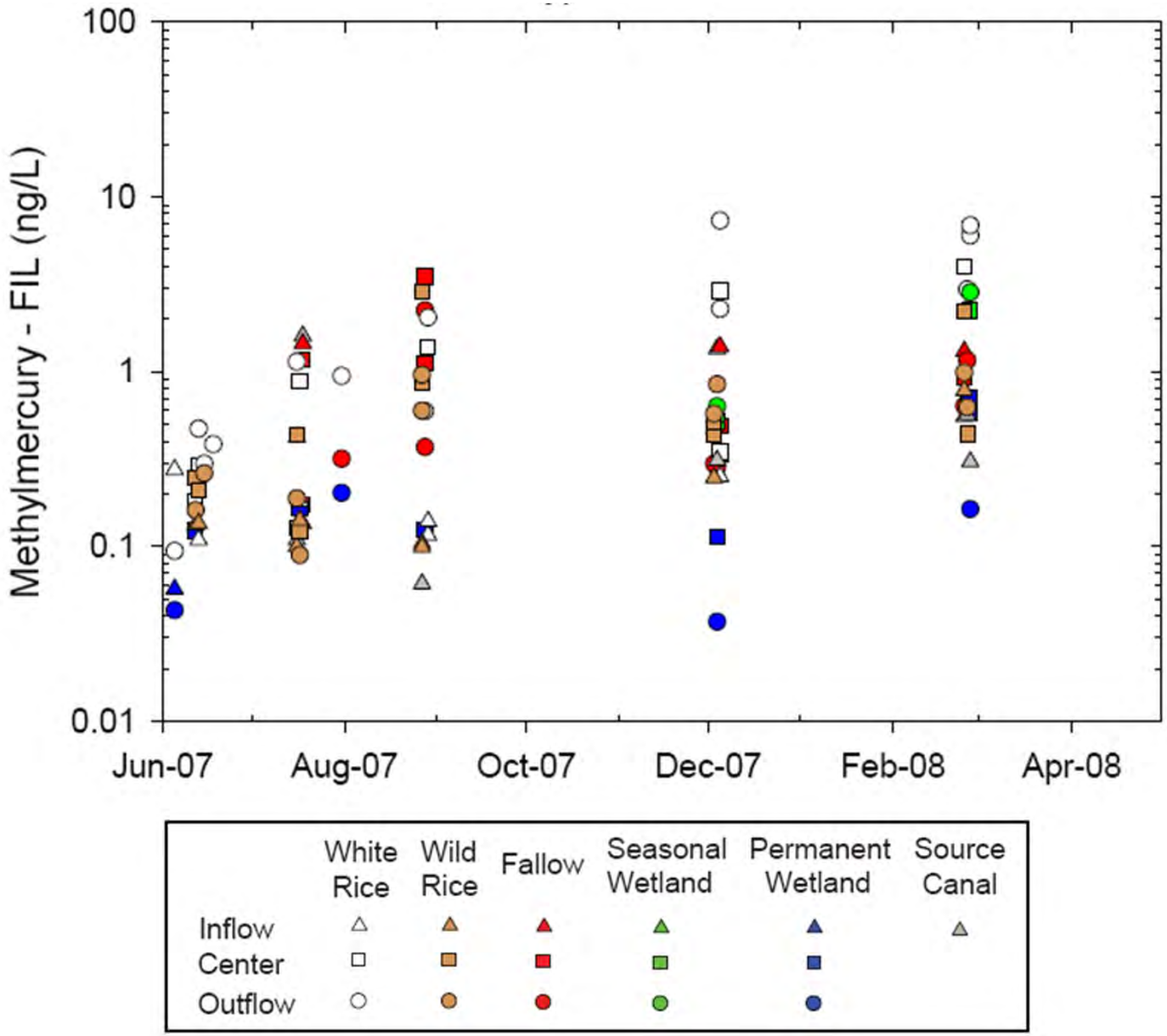

Figure 5.5. Time series plot of methylmercury concentration in filtered surface water.

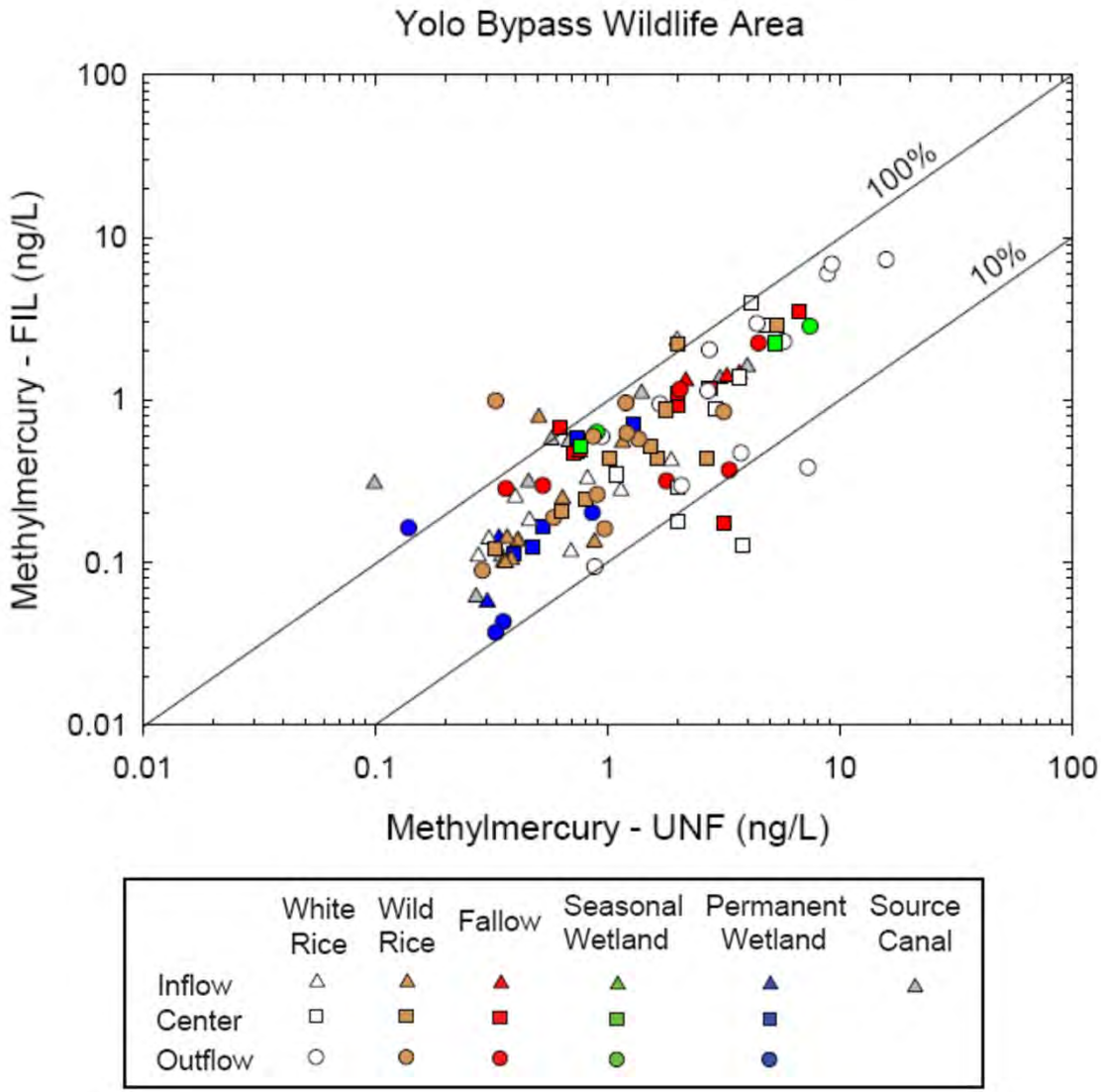

Figure 5.6. Log-log plot of methylmercury concentration in unfiltered versus filtered surface water. Diagonal lines represent lines of equal proportions of mercury passing through the filter, as indicated.

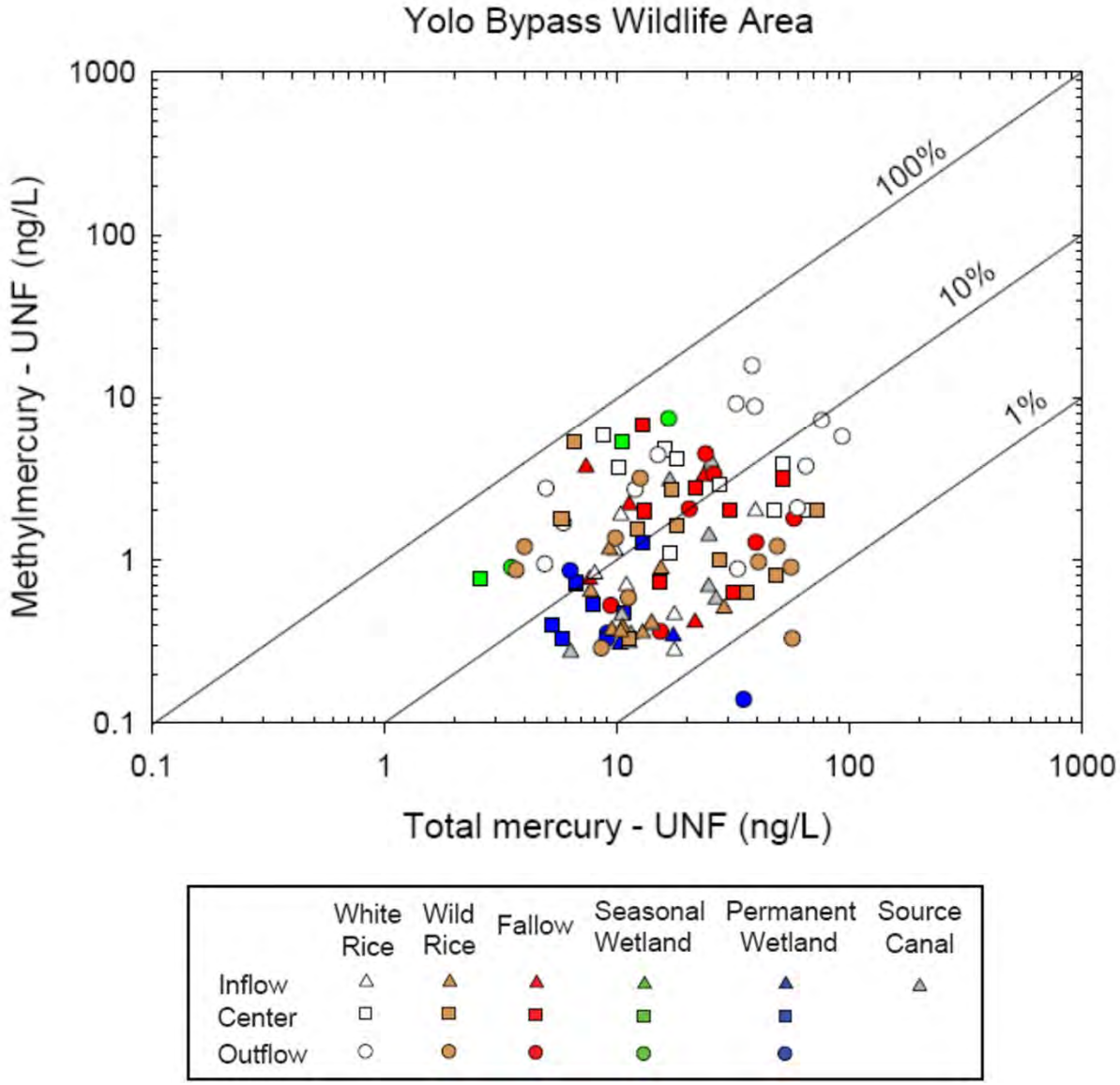

Figure 5.7. Log-log plot of total mercury concentration versus methylmercury concentration in unfiltered surface water. Diagonal lines represent lines of equal values of the ratio of methylmercury to total mercury.

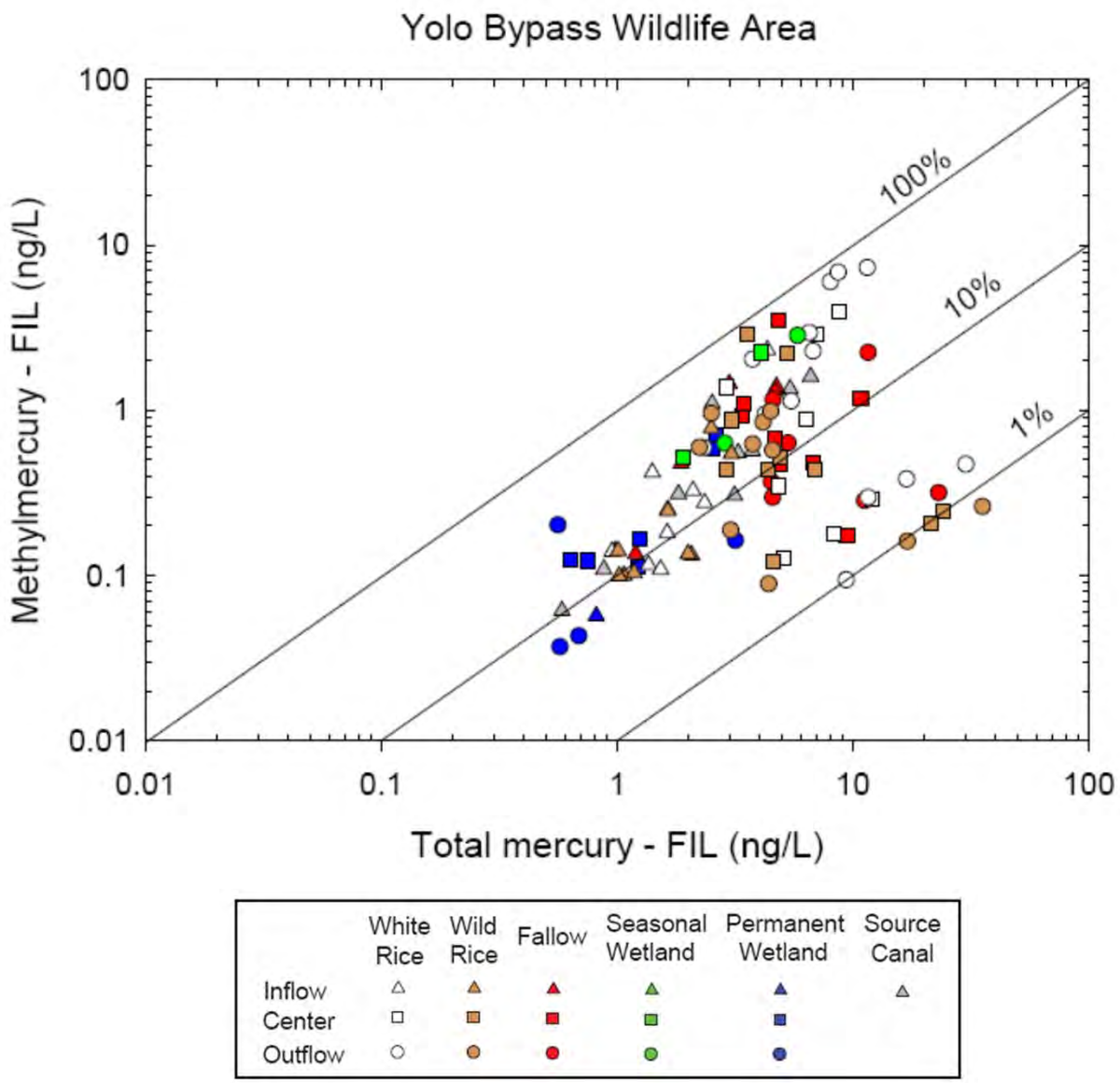

Figure 5.8. Log-log plot of total mercury concentration versus methylmercury concentration in filtered surface water. Diagonal lines represent lines of equal values of the ratio of methylmercury to total mercury.

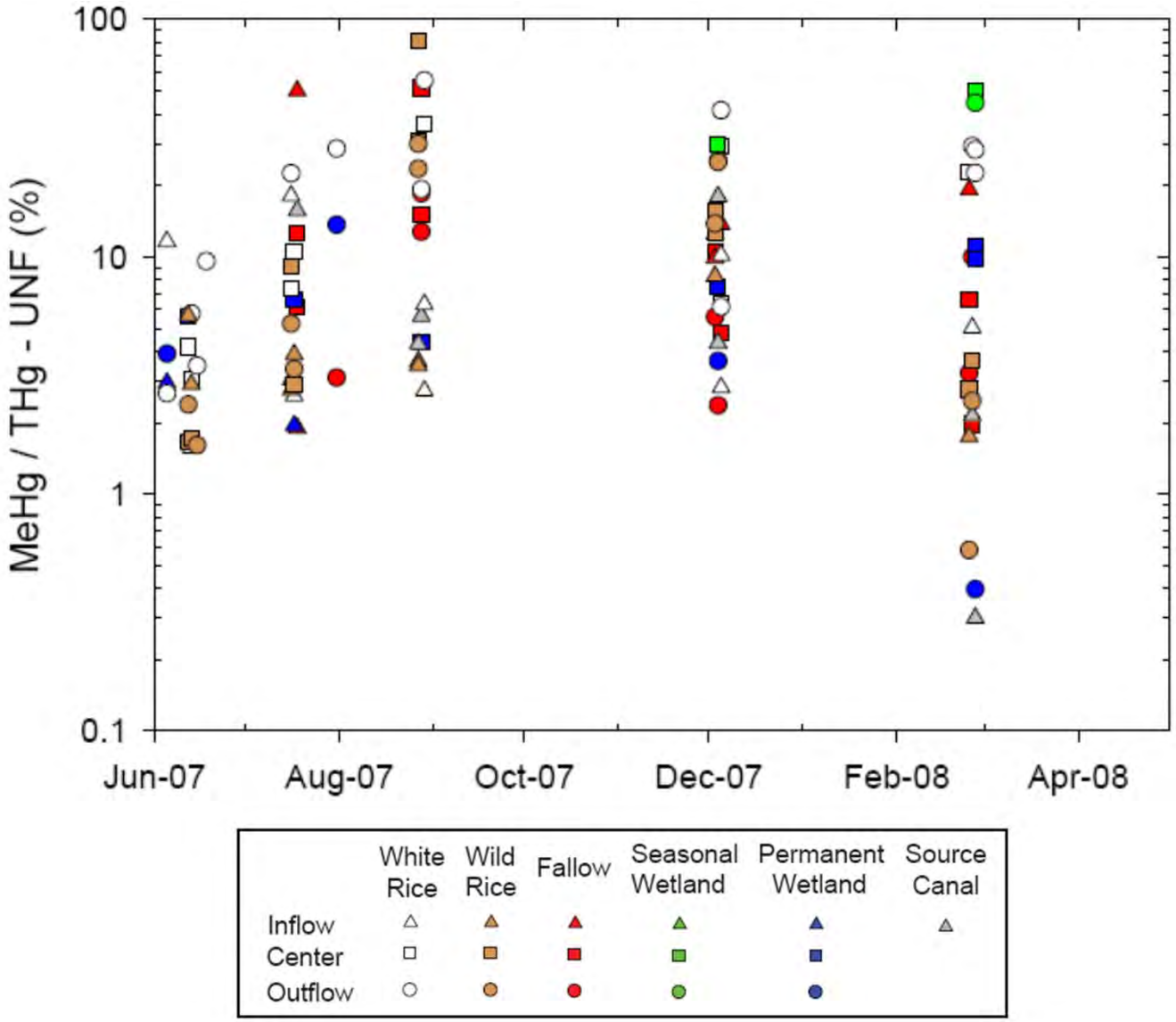

Figure 5.9. Time series plot of the methylmercury-to-total-mercury ratio (MeHg/THg) in unfiltered surface water. The ratio is expressed as a percentage (%THg as MeHg).

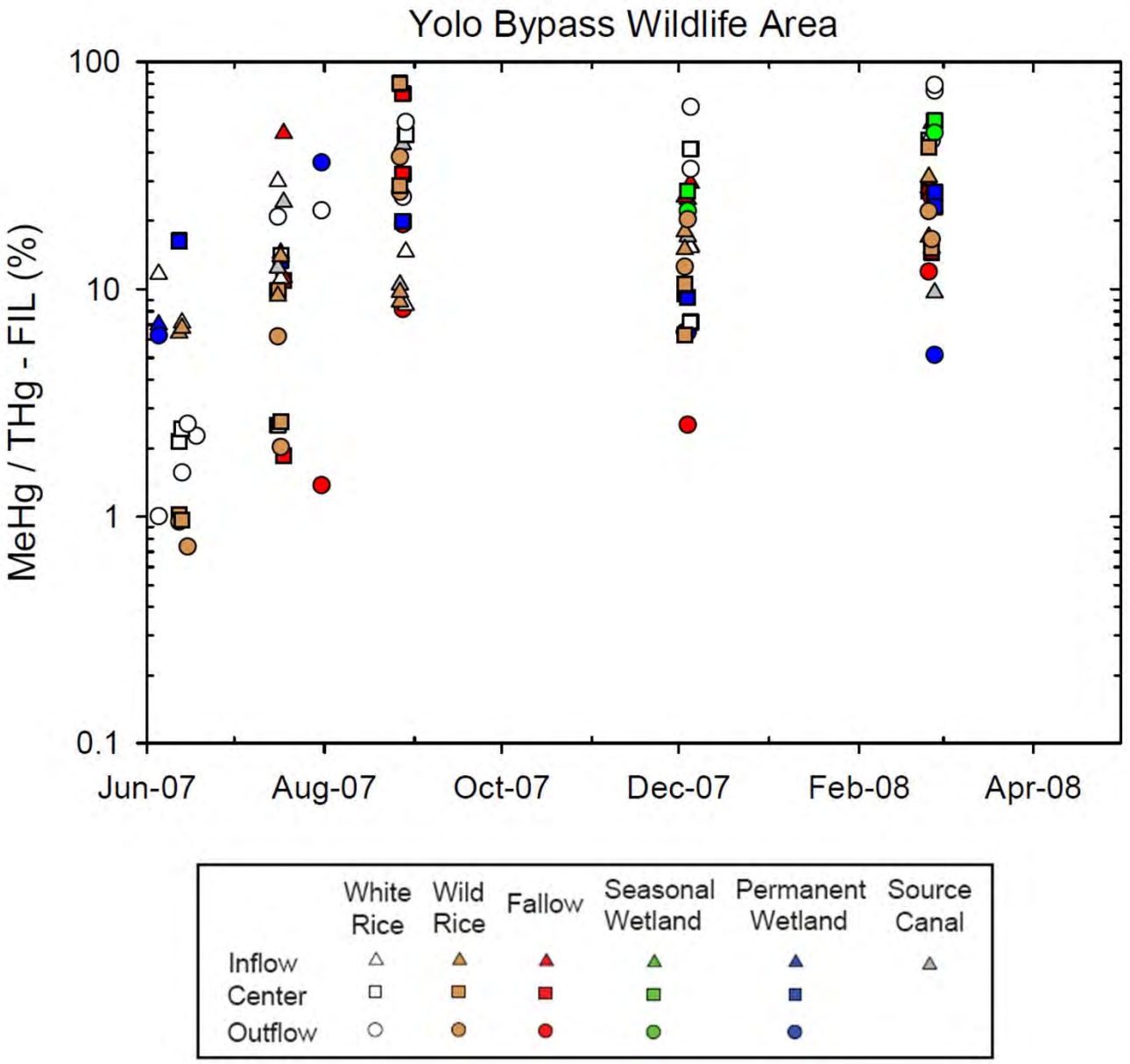

Figure 5.10. Time series plot of the methylmercury to total mercury ratio (MeHg/THg) in filtered surface water. Ratio expressed as a percentage (%THg as MeHg).

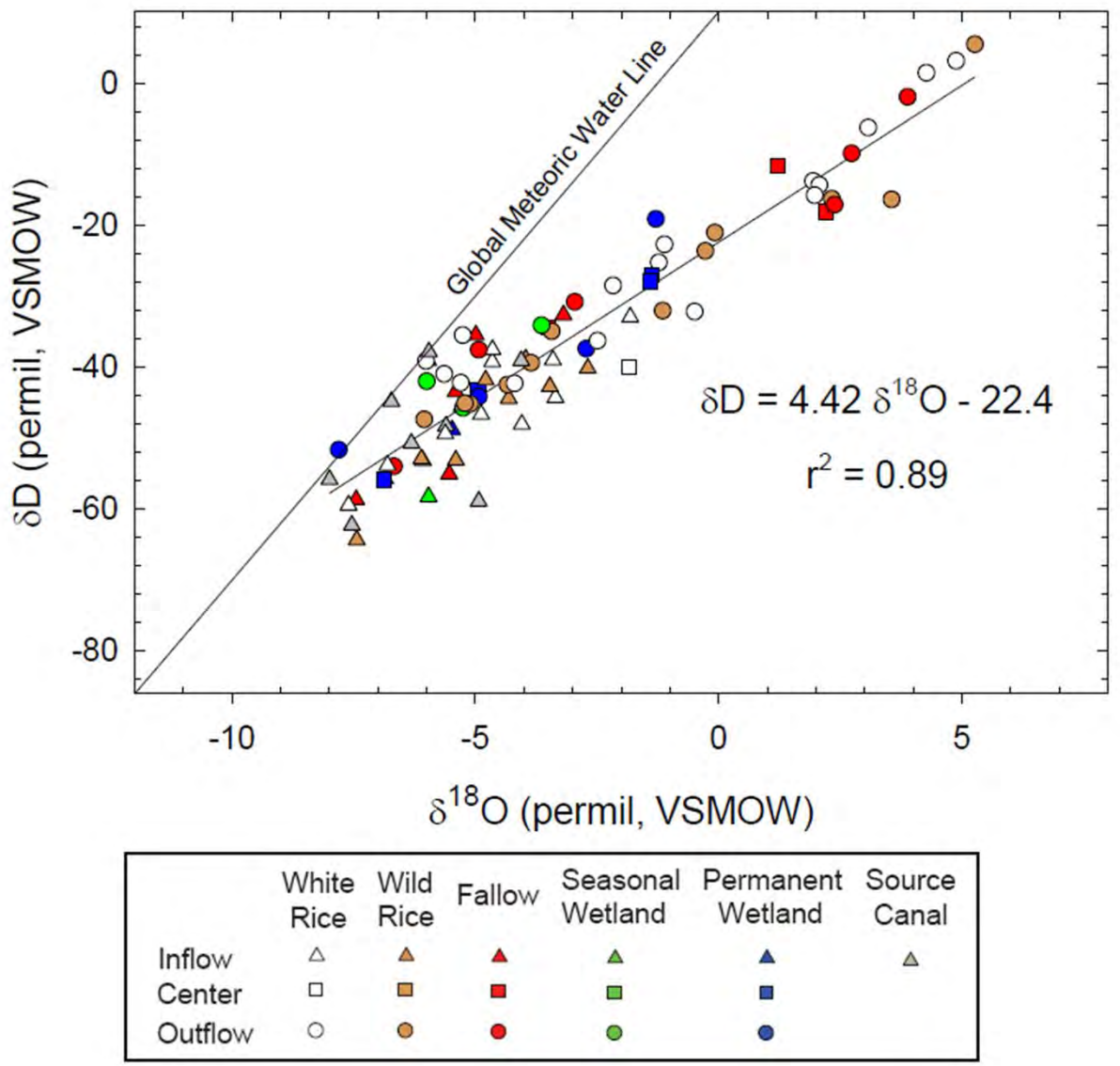

Figure 5.11. Scatter plot of oxygen isotope ratio in water versus hydrogen isotope ratio in water. Oxygen stable isotope ratio $^{18}O/^{16}O$ expressed as $\delta^{18}O$ and hydrogen isotope ratio $^{2}H/^{1}H$ expressed as δD as explained in text. Ratios are in units of permil (parts per thousand) relative to Vienna Standard Mean Ocean Water (VSMOW). Linear least-squares regression equation and correlation coefficient are indicated. Global Meteoric Water Line [$\delta D = 8\ \delta^{18}O + 10$], from Clark and Fritz (1997).

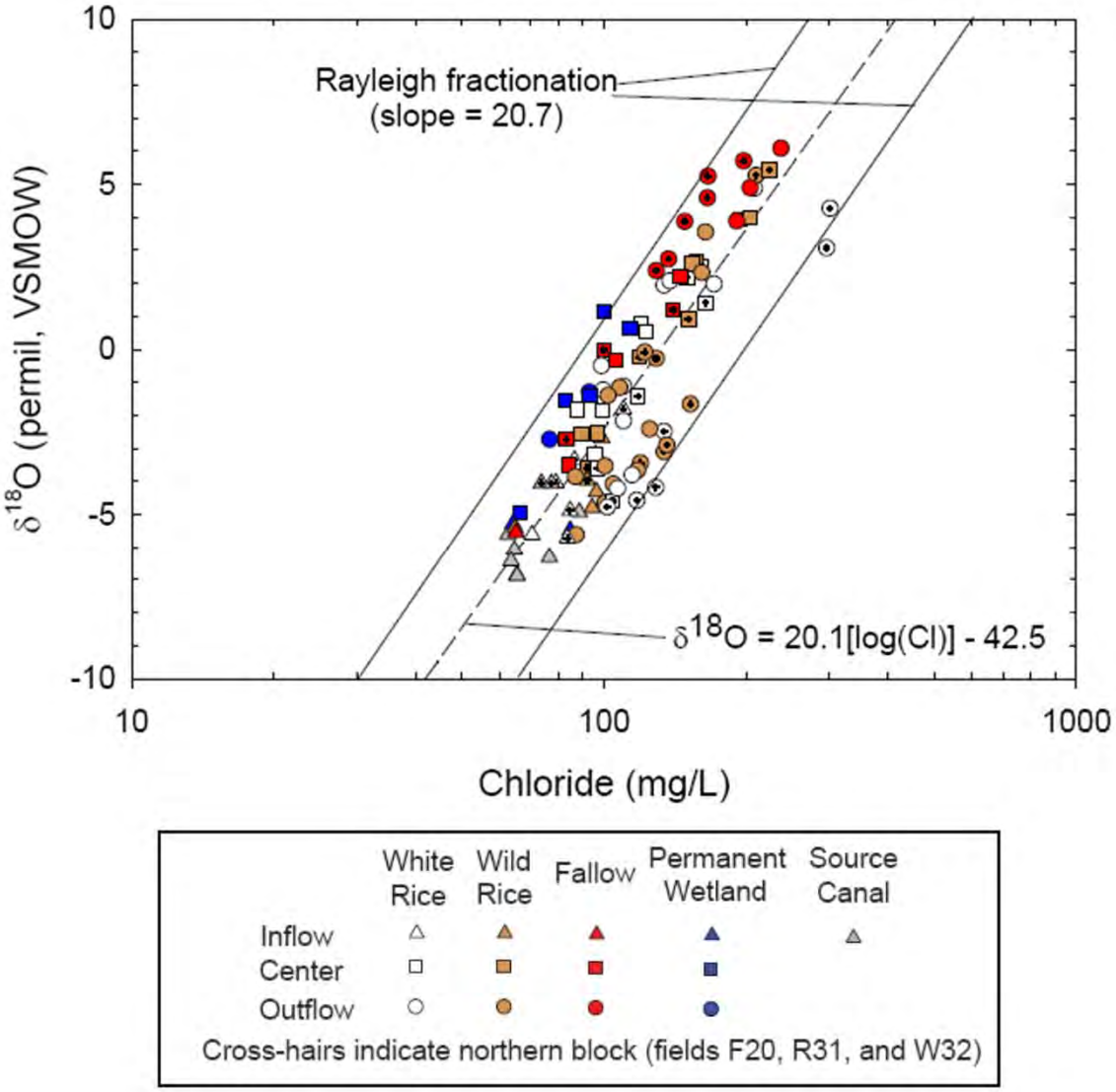

Figure 5.12. Log-linear plot showing relation between chloride concentration and $\delta^{18}O$ in water for summer irrigation season (June – September, 2007). Linear least-squares regression ($r^2 = 0.76$) compared with theoretical lines indicating Rayleigh fractionation (alpha = 1.009) (Clark and Fritz, 1997).

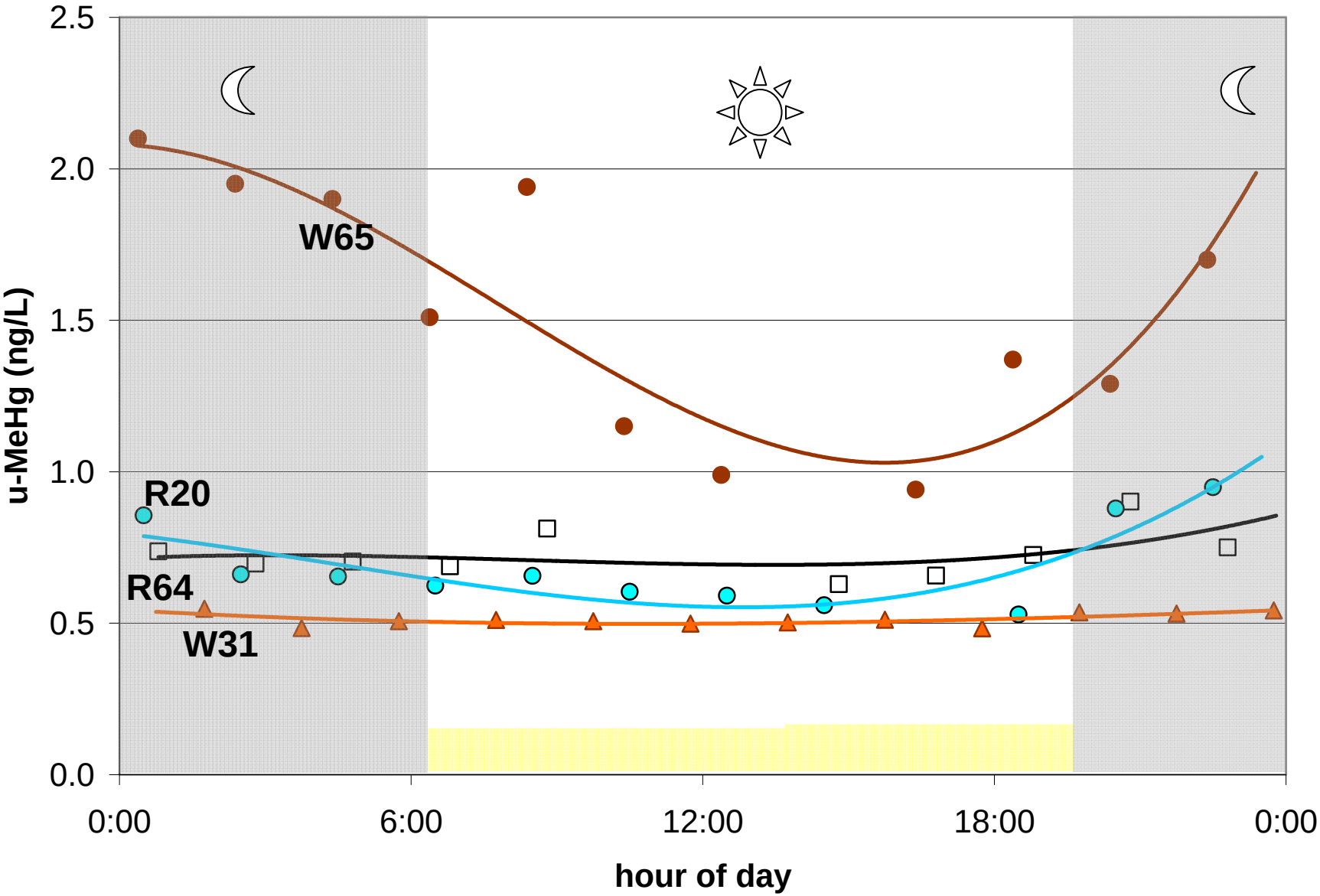

Figure 5.13. Diel time series plot of surface water unfiltered methylmercury concentration (u-MeHg) in four agricultural fields. W65 and R64 measured in summer, 2007; W31 and R20 measured in summer, 2008.

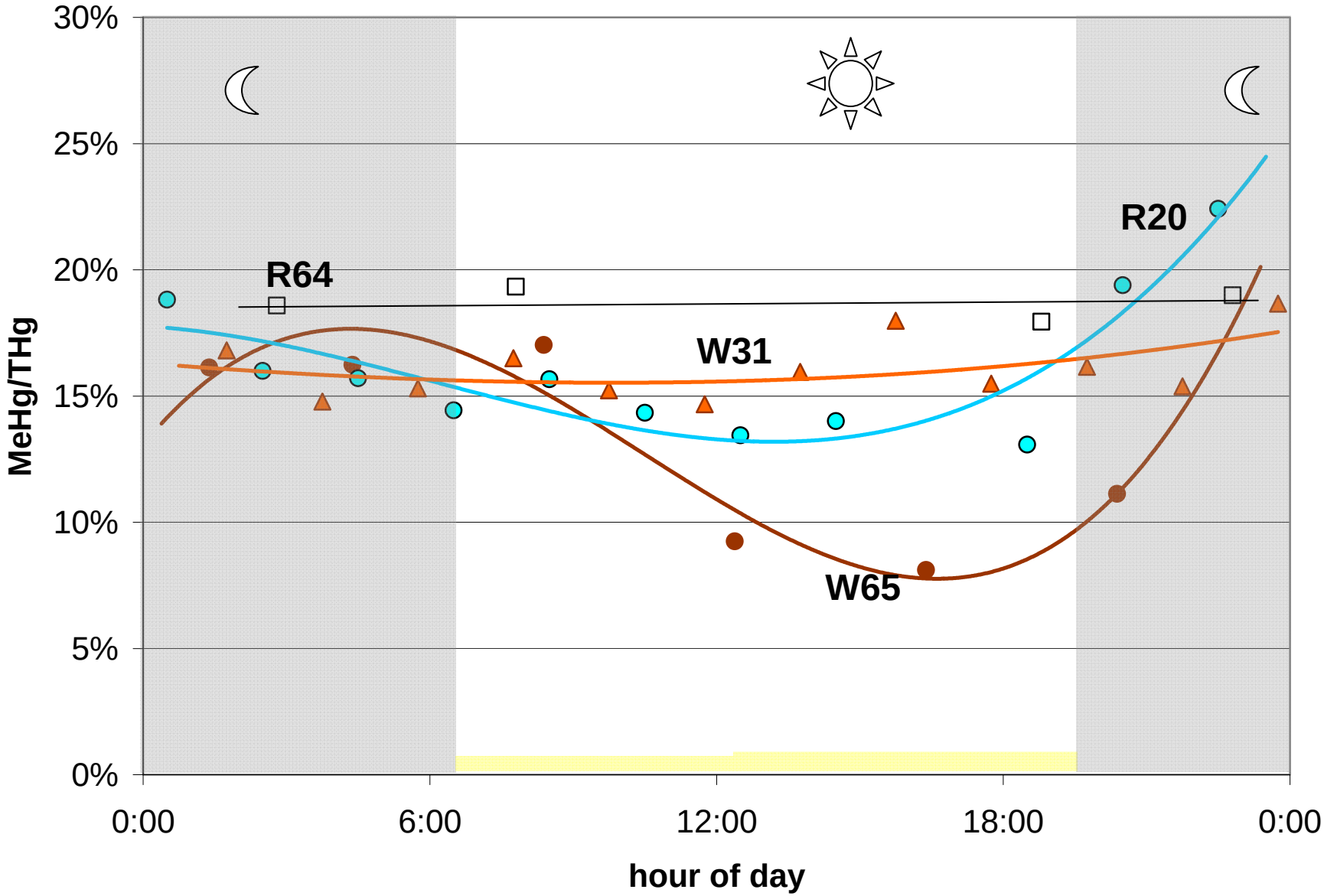

Figure 5.14. Diel time series plot of methylmecury to total mercury ratio (MeHg/THg) in unfiltered surface water from four fields of the Yolo Bypass Wildlife Area. W65 and R64 measured in summer 2007; W31 and R20 measured in summer 2008. The ratio is expressed as a percentage (%THg as MeHg).

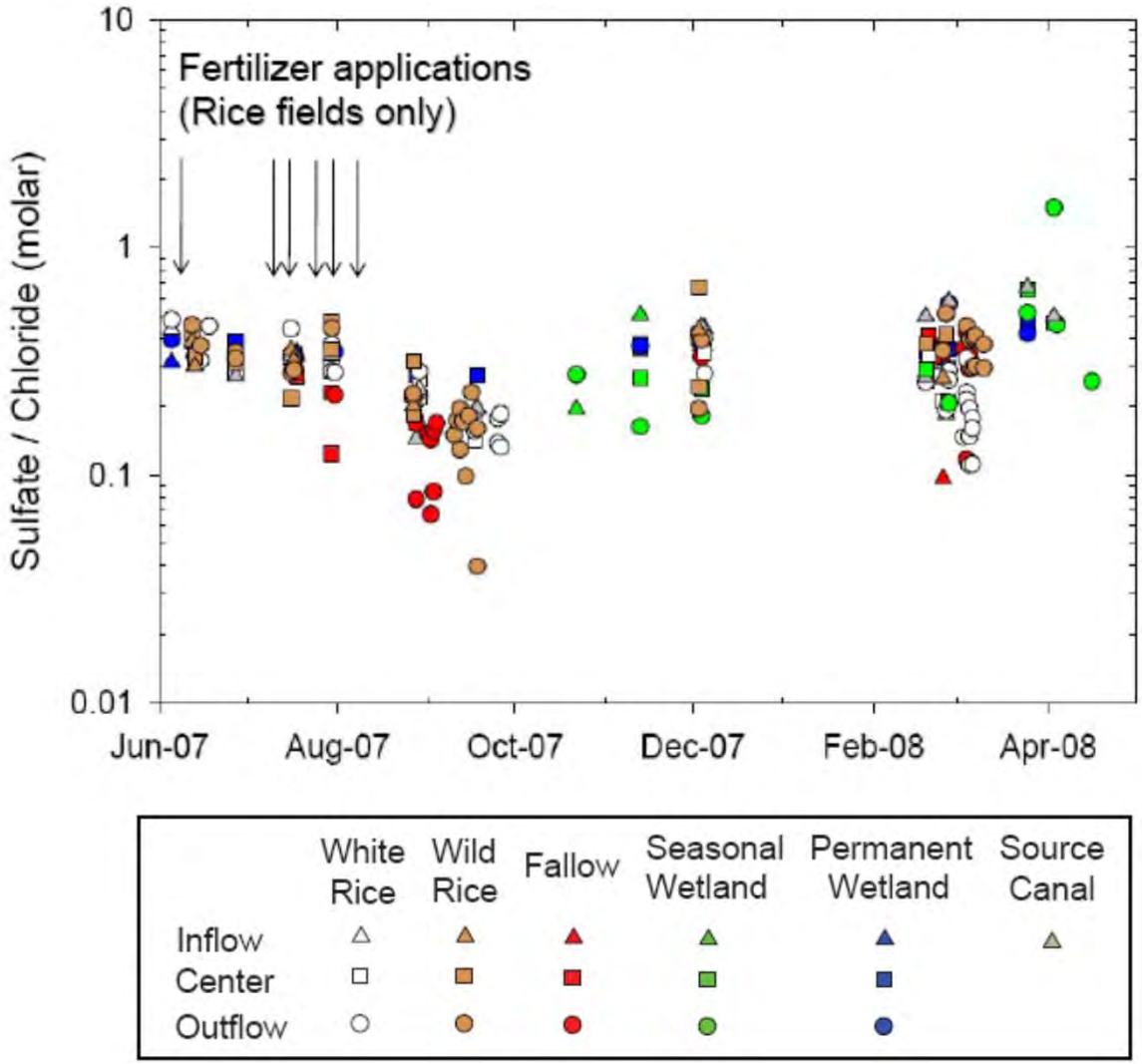

Figure 5.15. Time series plot of the sulfate-to-chloride molar ratio in filtered surface water. The timing of the application of sulfate-bearing fertilizer to white rice and wild rice fields is indicated by the arrows.

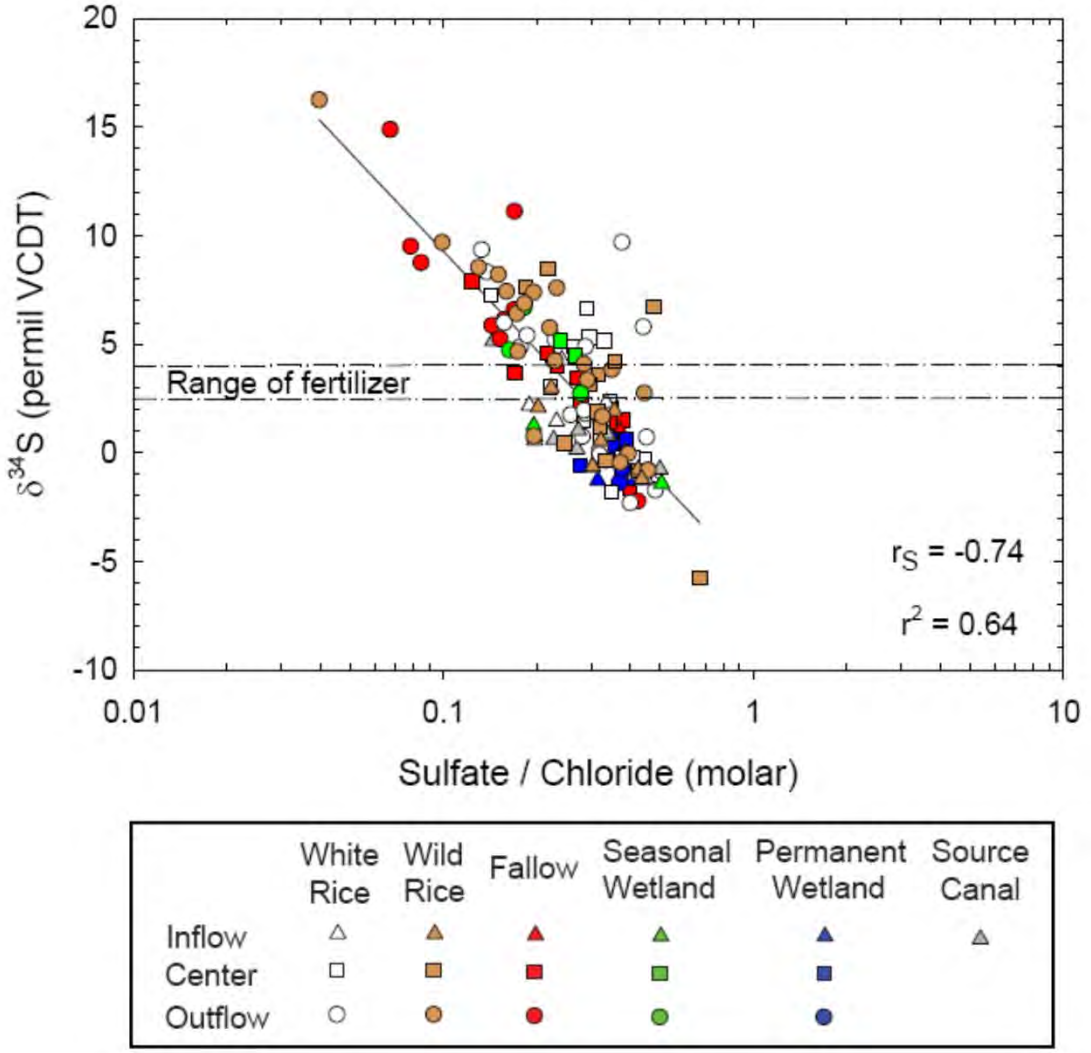

Figure 5.16. Log-log plot of sulfate-to-chloride molar ratio versus sulfur stable isotope ratio in aqueous sulfate in filtered surface water. Sulfur stable isotope ratio $^{34}S/^{32}S$ expressed as $\delta^{34}S$ as explained in text. Range of sulfur isotope values of fertilizer shown by the horizontal dashed lines. Sulfur isotope values above 4 permil indicate isotopic enrichment in pool of residual sulfate after microbial sulfate reduction has preferentially removed ^{32}S relative to ^{34}S. Linear least-squares regression coefficient (r^2) and Spearman rank order correlation coefficient (r_S) are shown.

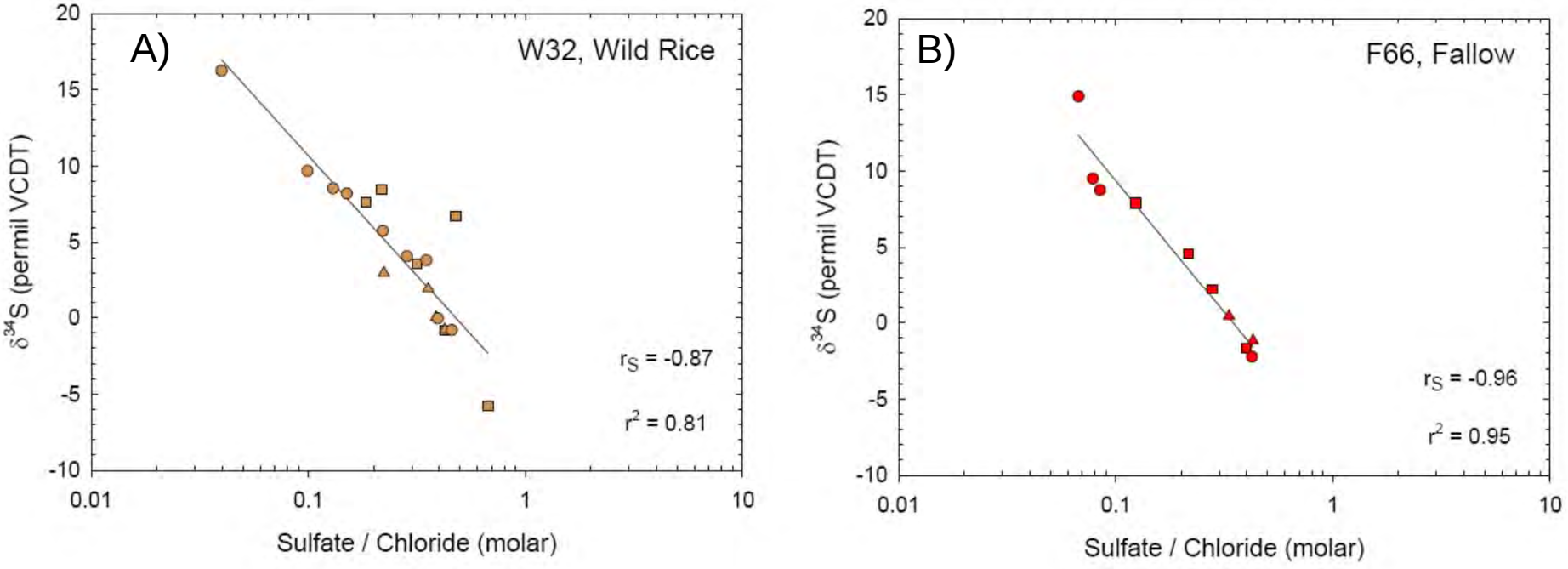

Figure 5.17. Log-linear plots of sulfate-to-chloride molar ratio versus sulfur stable isotope ratio in filtered surface water for (A) wild rice field W32, and (B) fallow field F66. Linear least-squares regression coefficients (r^2) and Spearman rank order correlation coefficients (r_S) are shown.

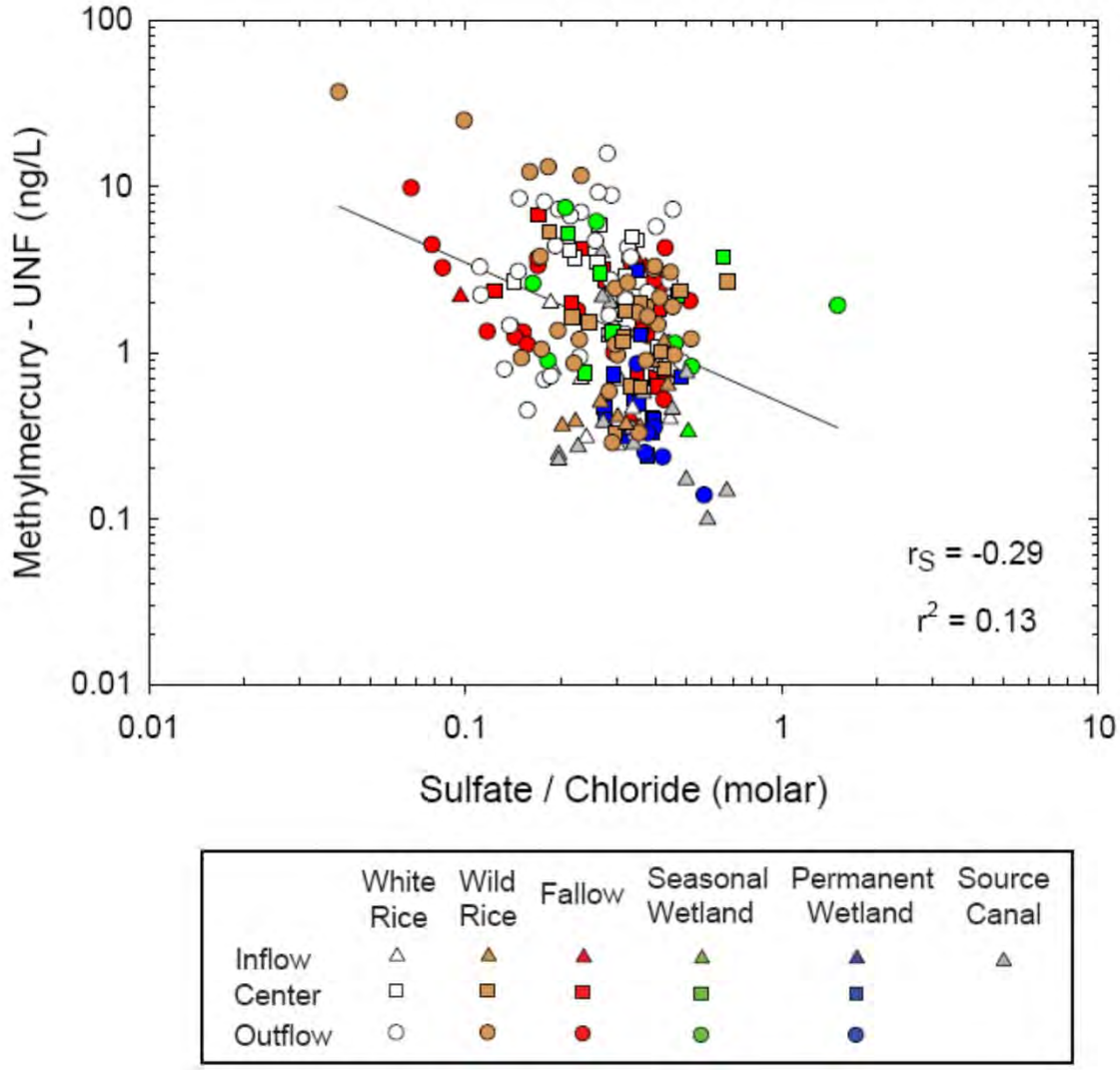

Figure 5.18. Log-log plot of sulfate-to-chloride molar ratio in filtered surface water versus methylmercury concentration in unfiltered surface water. Linear least-squares regression coefficient (r^2) and Spearman rank order correlation coefficient (r_S) are shown.

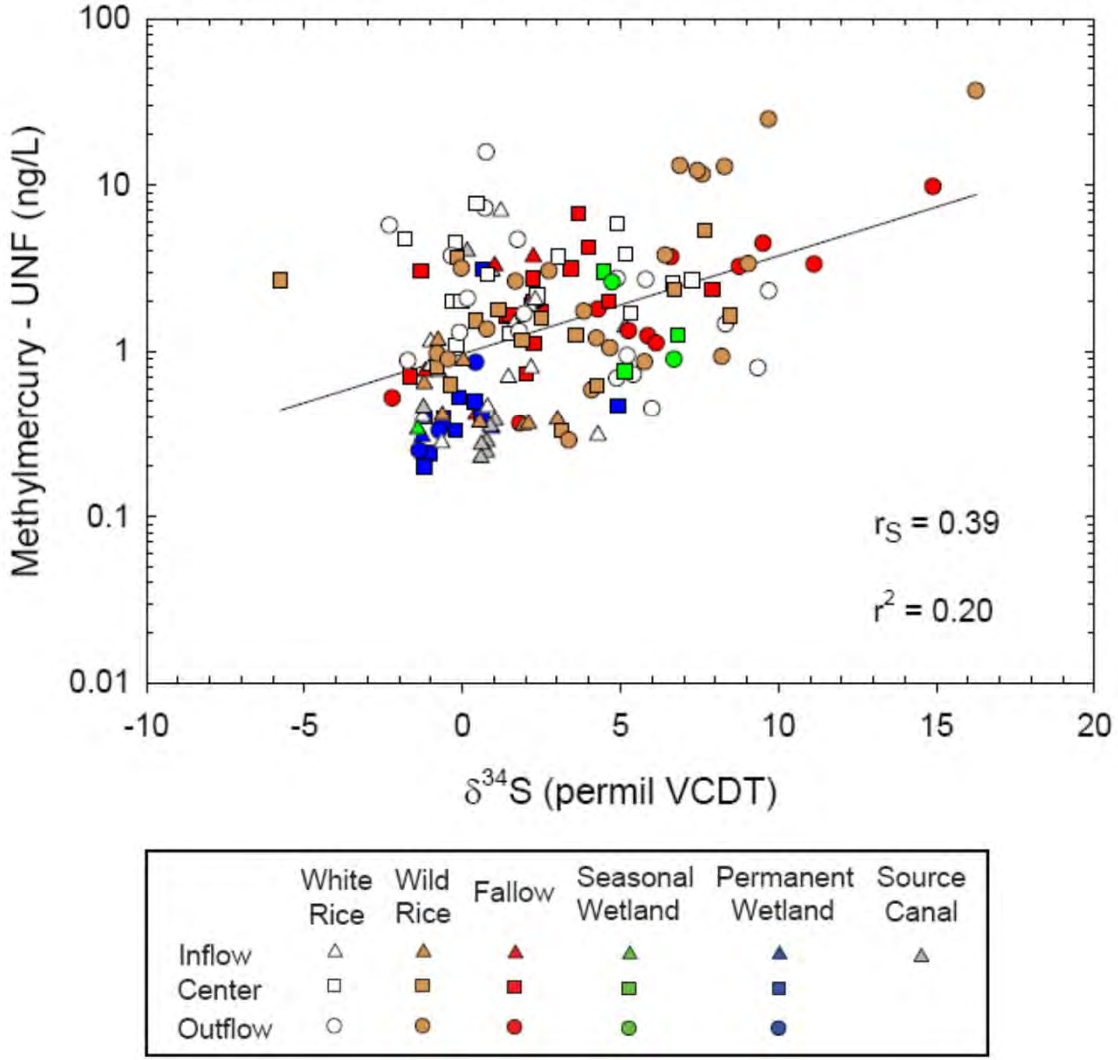

Figure 5.19. Linear-log plot of sulfur stable isotope ratio in aqueous sulfate versus unfiltered methylmercury concentration in surface water. Linear least-squares regression coefficient (r^2) and Spearman rank correlation coefficient (r_S) are shown.

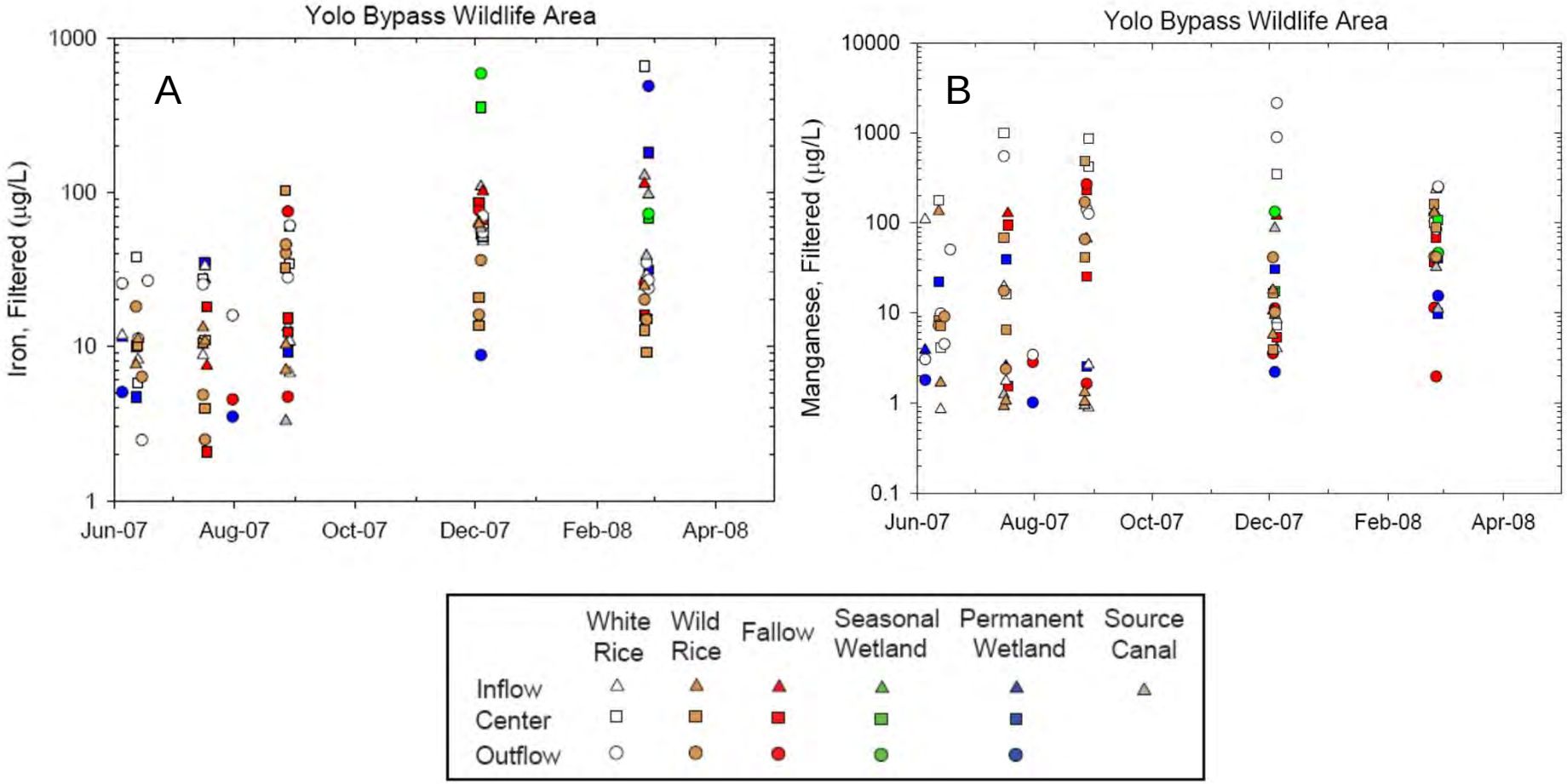

Figure 5.20. Time series plots of (A) iron concentration and (B) manganese concentration in filtered surface water. Note different logarithmic scales in A and B.

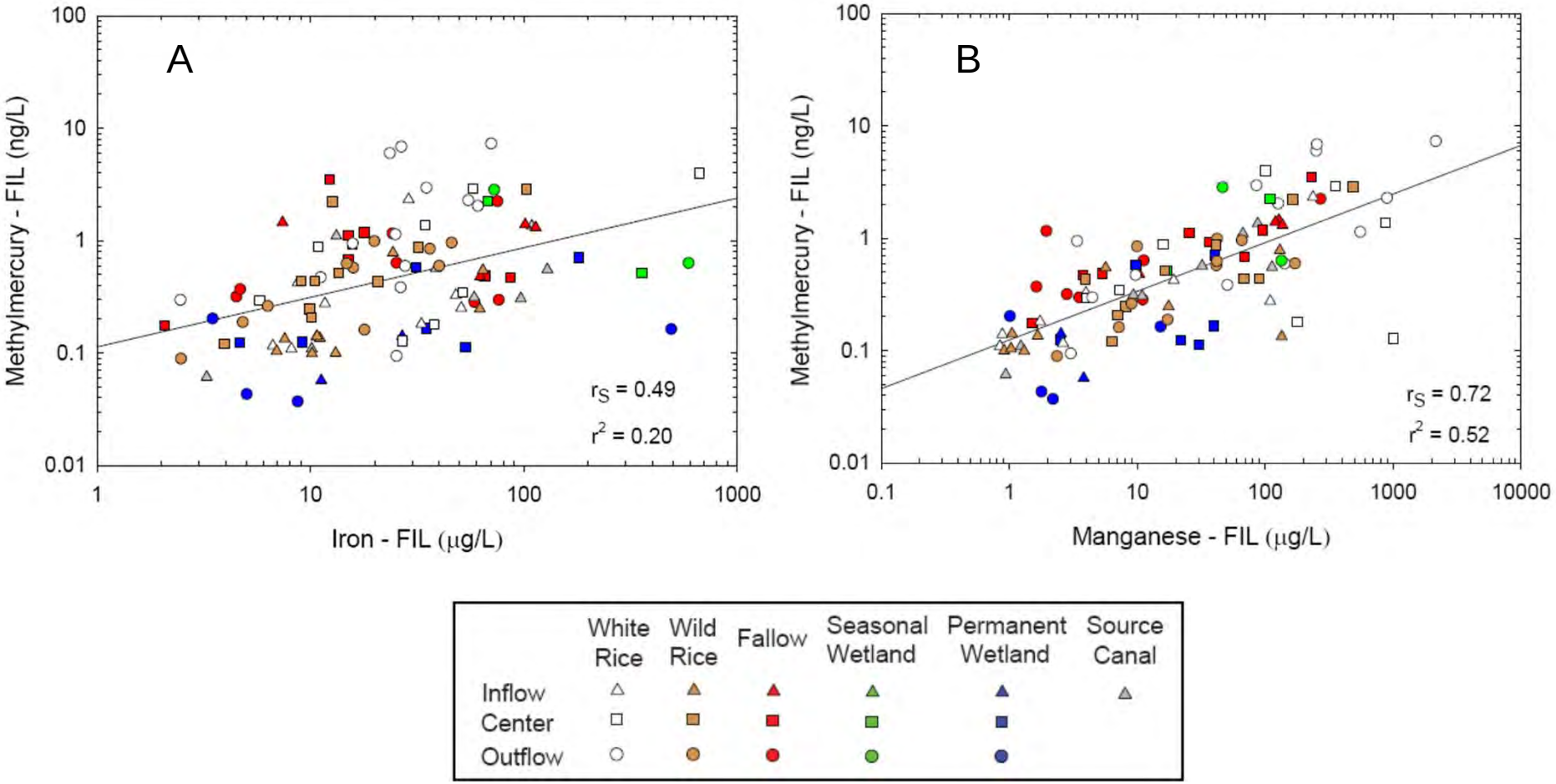

Figure 5.21. Log-log plots of (A) iron concentration and (B) manganese concentration versus methylmercury concentration in filtered surface water. Linear least-squares regression coefficients (r^2) and Spearman rank correlation coefficients (r_S) are shown.

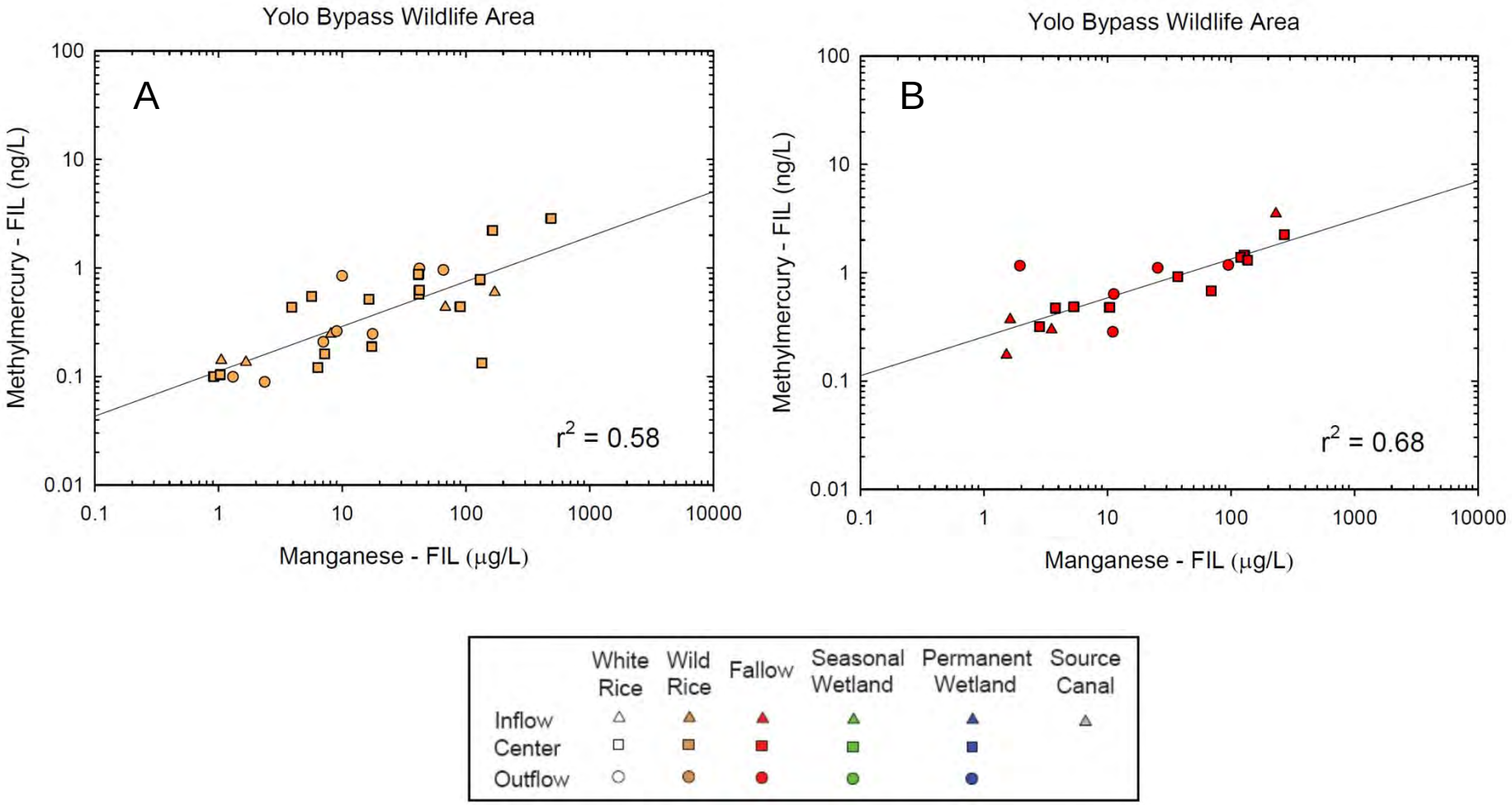

Figure 5.22. Log-log plots of manganese concentration versus methylmercury concentration in filtered surface water from (A) wild rice fields and (B) fallow fields. Linear least-squares regression coefficients are shown.

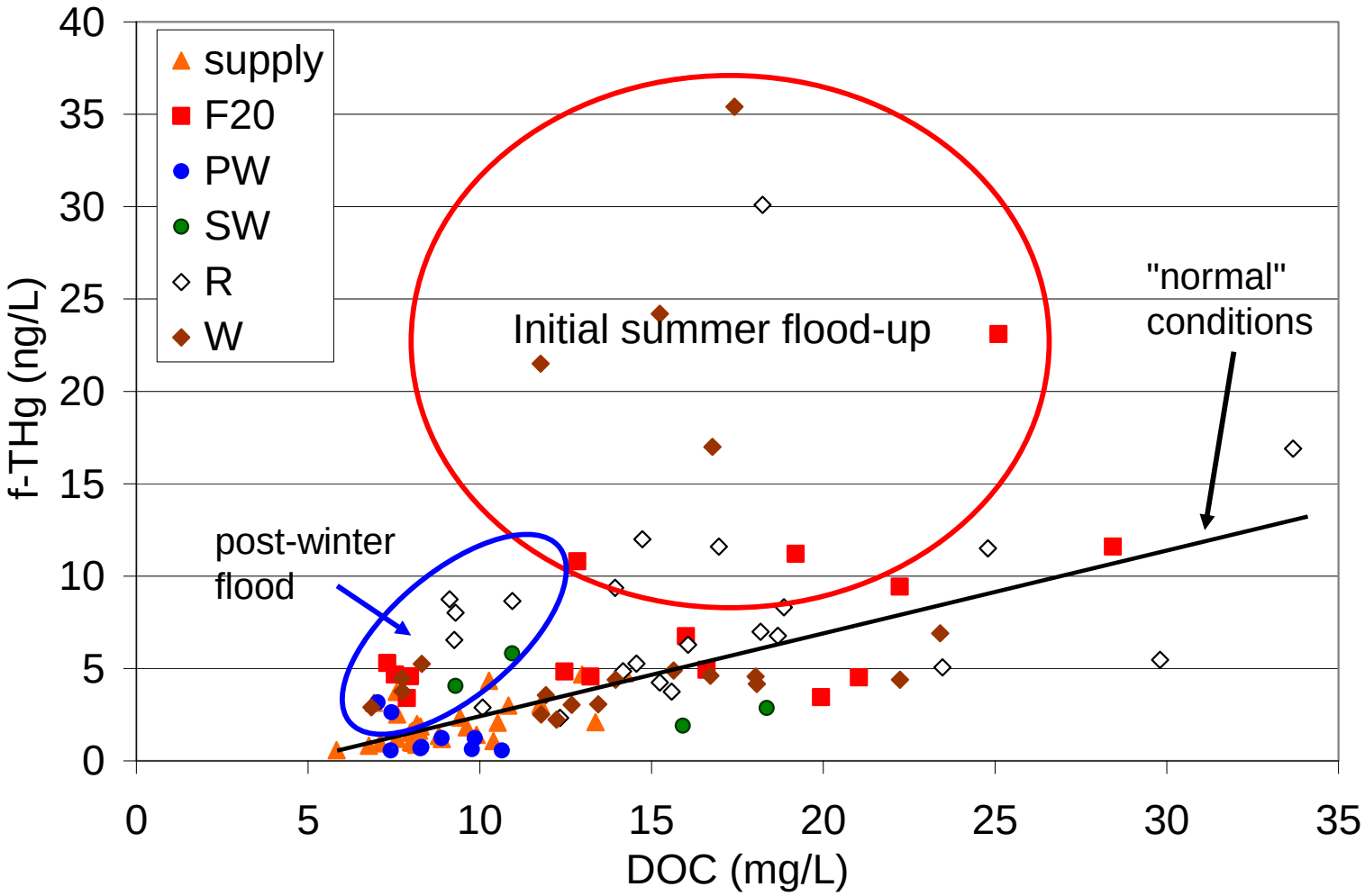

Figure 5.23. Scatter plot of surface water dissolved organic carbon (DOC) versus filtered total mercury (f-THg). This relationship varies across three conditions: initial summer irrigation, normal flow-through conditions and post-winter flood.

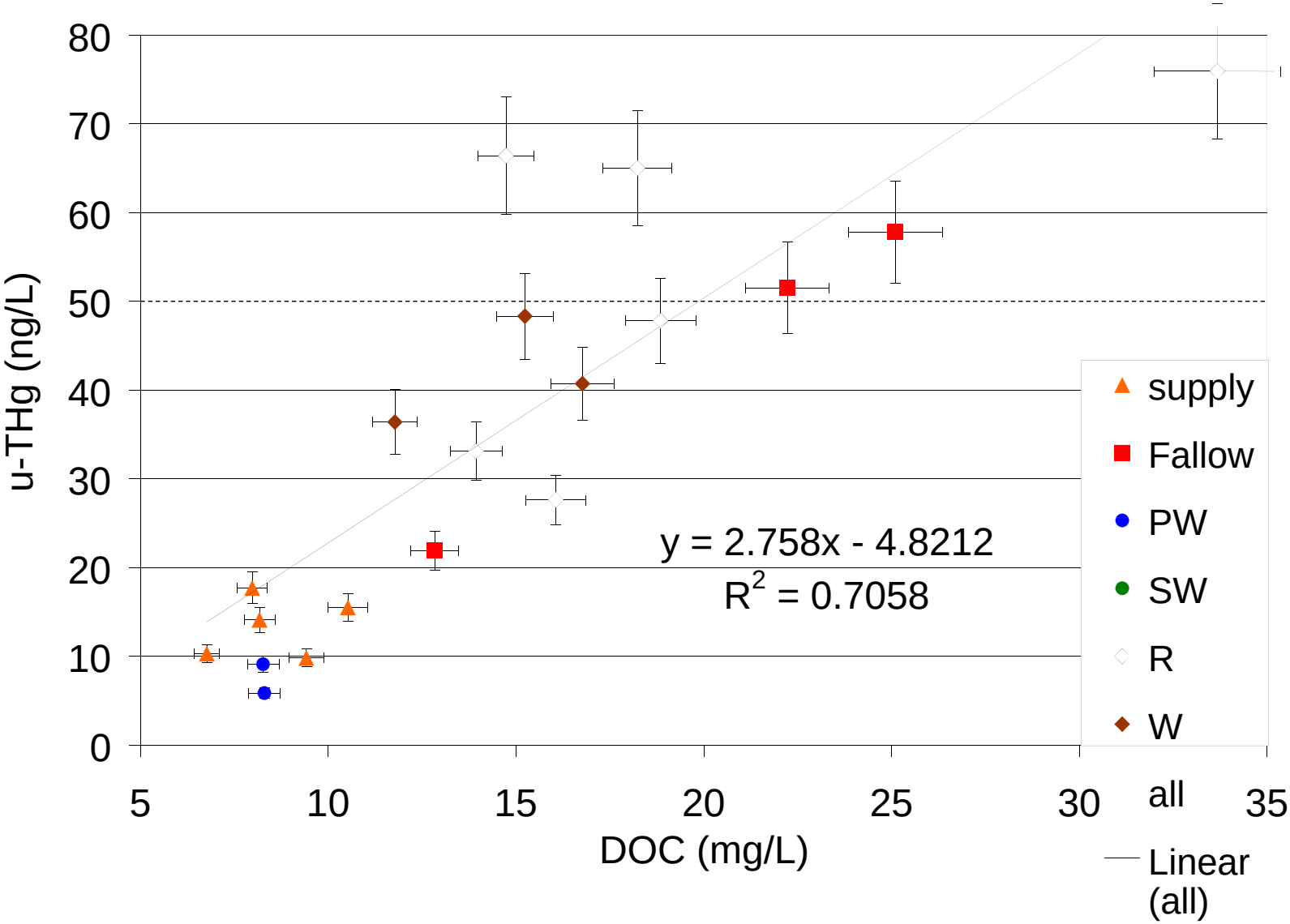

Figure 5.24. Scatter plot of surface water dissolved organic carbon (DOC) versus unfiltered total mercury (u-THg) within 30 days of the initial irrigation of the agricultural fields during early summer. During this period, DOC and filtered total mercury (f-THg) are poorly correlated (see **Figure 5.21**). Dotted line indicates concentrations of u-THg above the 50 ng/L water-quality criterion for the California Toxics Rule (CTR, U.S. Environmental Protection Agency, 2000b). Linear least-squares regression equation and coefficient are shown.

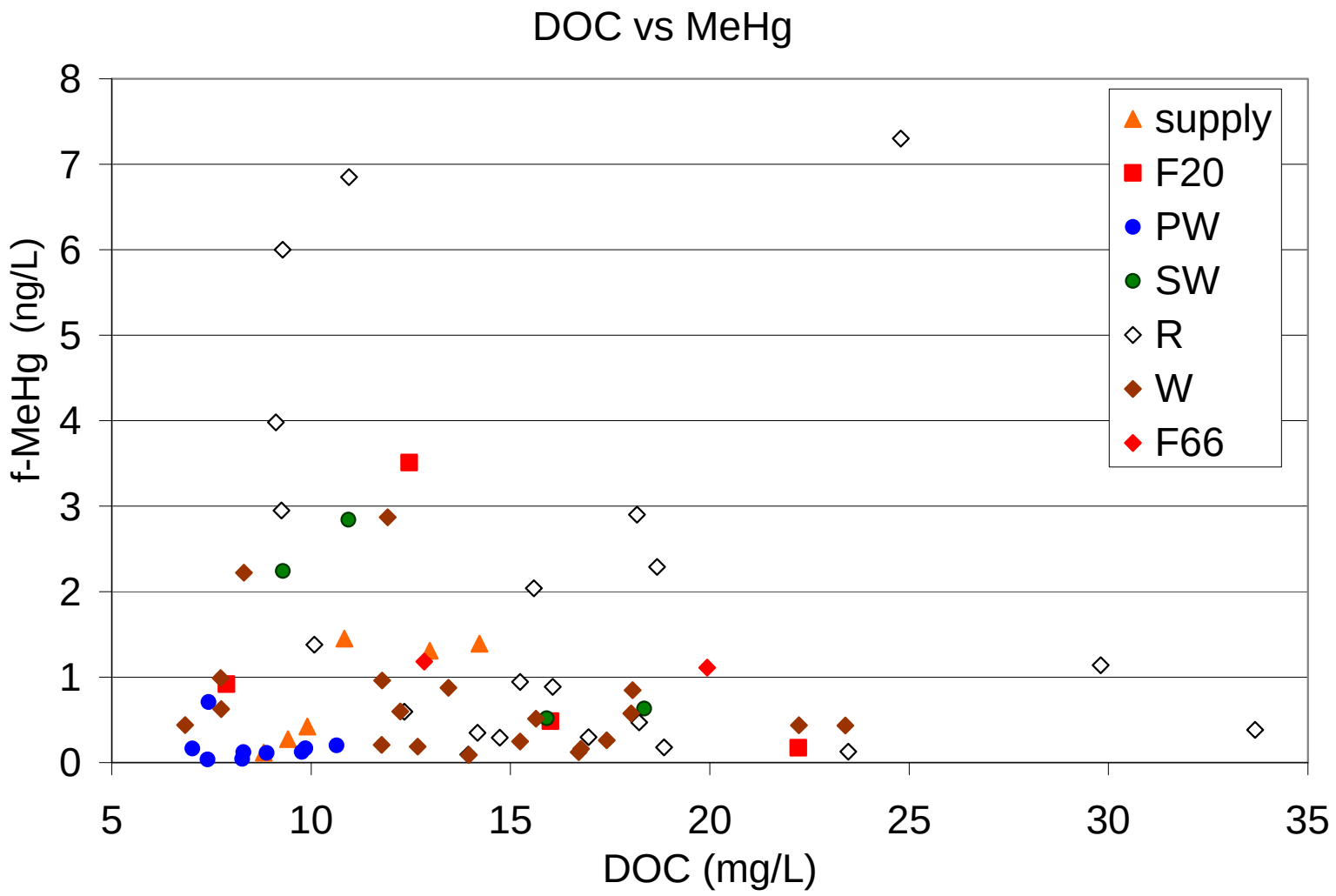

Figure 5.25. Scatter plot of surface water dissolved organic carbon (DOC) versus filtered methylmercury (f-MeHg). This relation was highly variable in agricultural fields (F20 and F66, fallow; R, white rice; W, wild rice) compared with non-agricultural wetlands (PW, permanent wetland; SW, seasonal wetland).

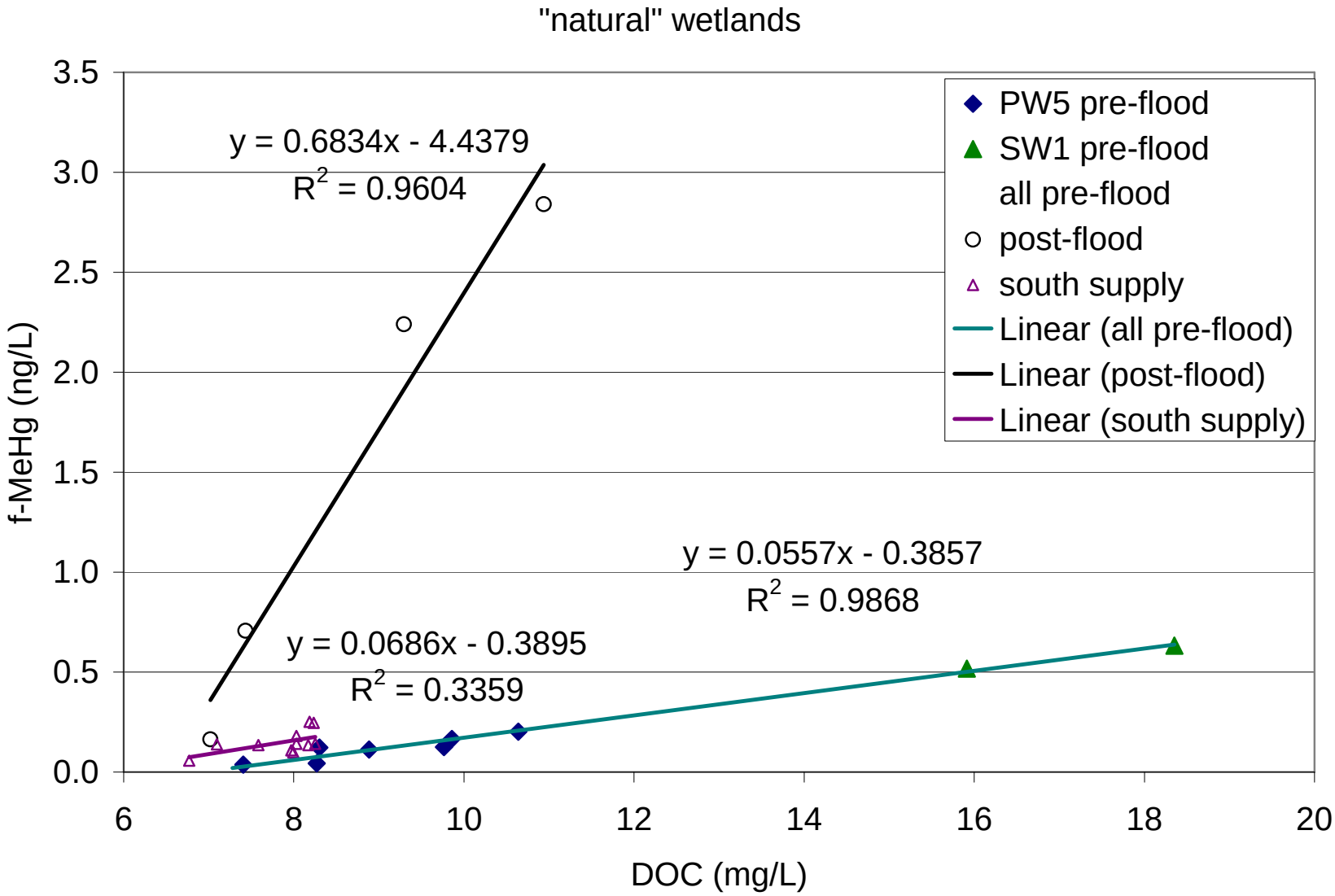

Figure 5.26. Scatter plot of surface water dissolved organic carbon (DOC) versus filtered methylmercury (f-MeHg) in the non-agricultural wetlands. The high slope of the post-flood samples shows markedly different relationship during the winter 2008 flood compared to the rest of the water year. (PW5, permanent wetland; SW1, seasonal wetland)

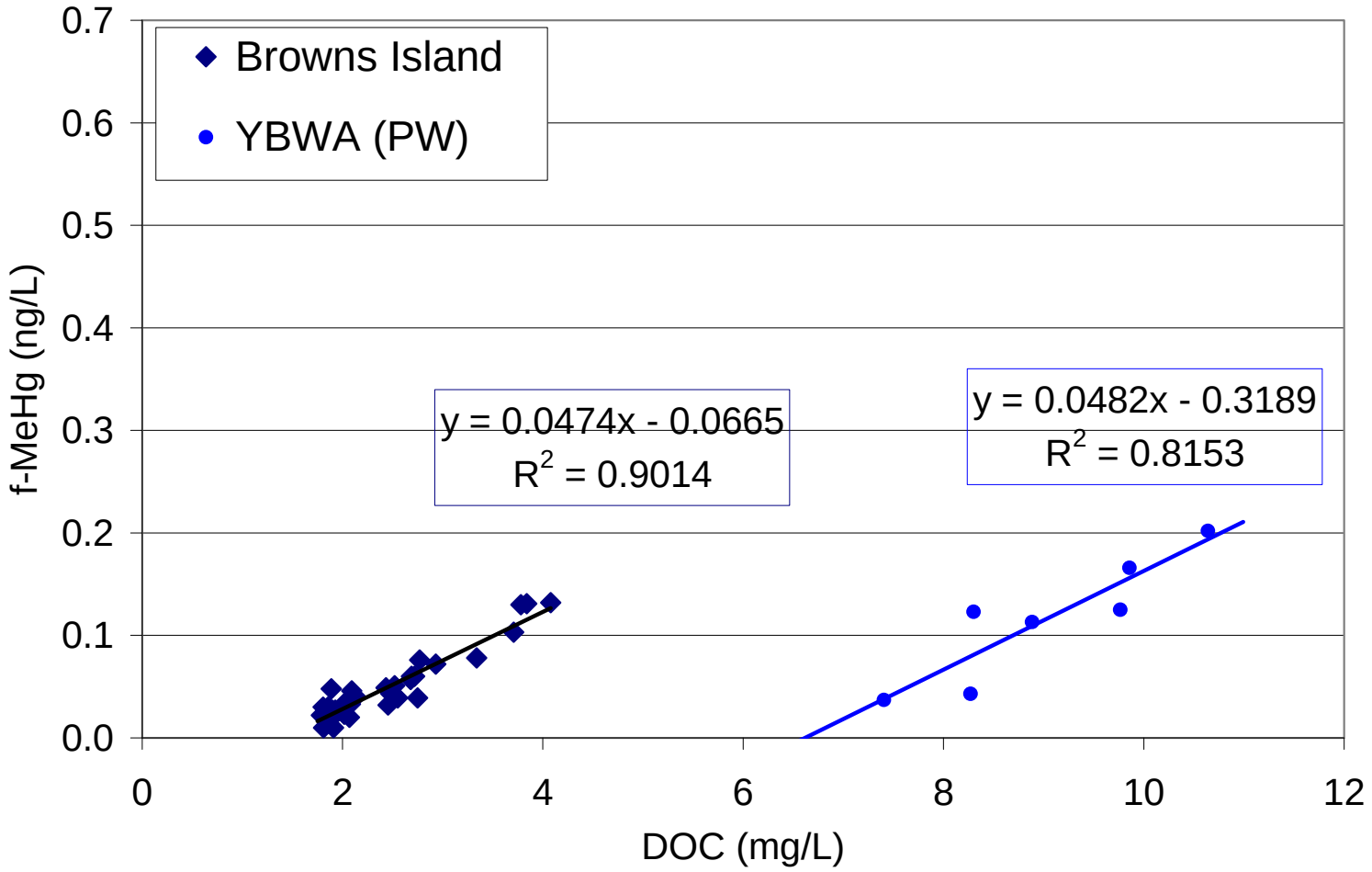

Figure 5.27. Scatter plot of surface water dissolved organic carbon (DOC) versus filtered methylmercury (f-MeHg) for the permanent wetland (PW) site in the Yolo Bypass Wildlife Area and for Browns Island, a tidal wetland in the San Francisco Bay-Delta.

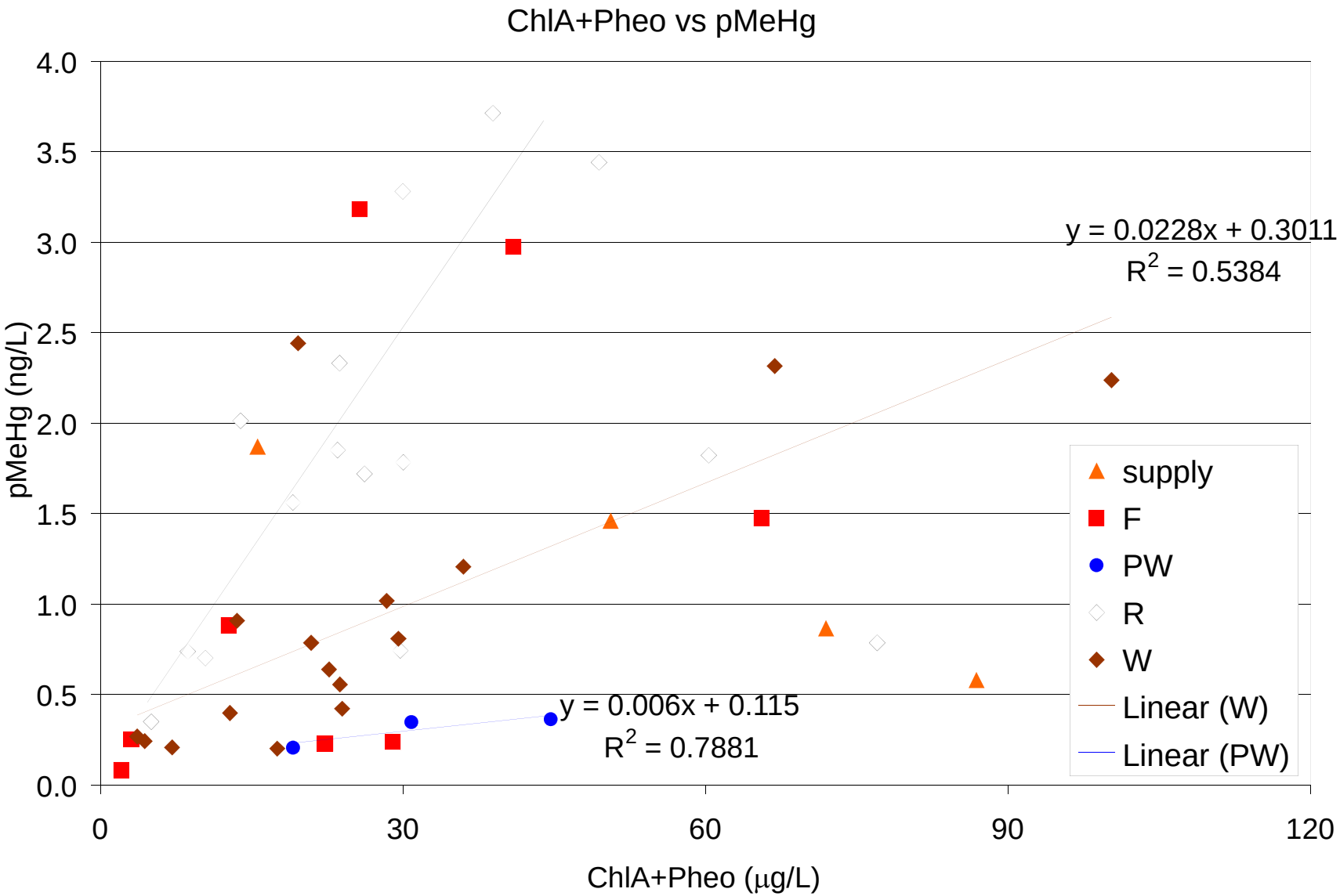

Figure 5.28. Scatter plot of surface water particulate algal concentration (as chlorophyll-a plus pheophytin; Chl-a+Pheo) versus particulate methylmercury (pMeHg) concentration. The relationship differs among field types -- fallow (F) and white rice (R) fields possess high slopes, permanent wetlands (PW) possess the lowest slope, and wild rice (W) fields fall in between. Linear least-squares regression equations and coefficients are shown for wild rice fields and the permanent wetland.

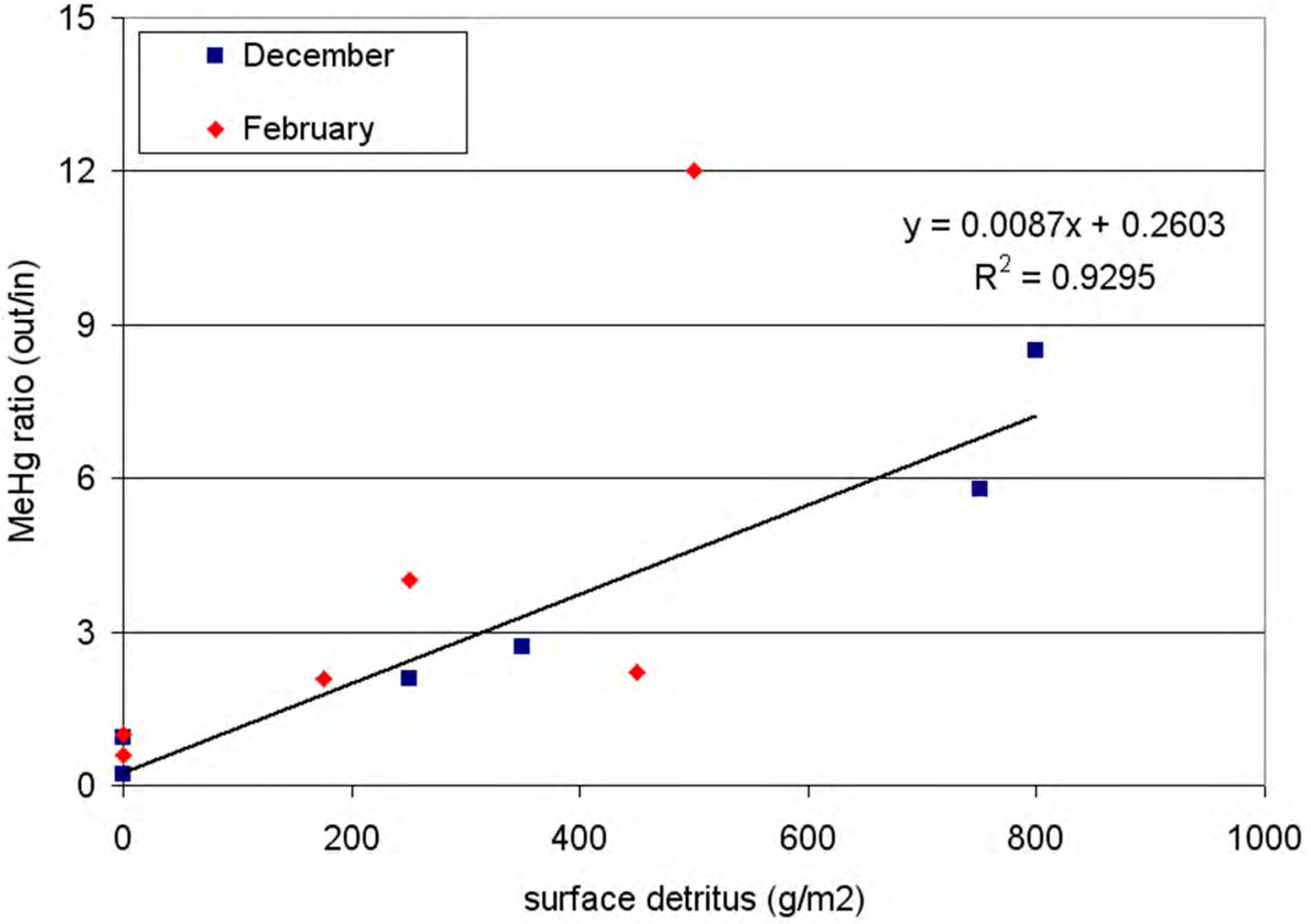

Figure 5.29. Scatter plot of surface water particulate detritus (plant residue) concentration versus the [Out/In] ratio of unfiltered methylmercury concentration along a flow path across agricultural and non-agricultural wetlands during winter (December 2007 and February 2008). Linear least-squares regression equation and coefficient are shown.

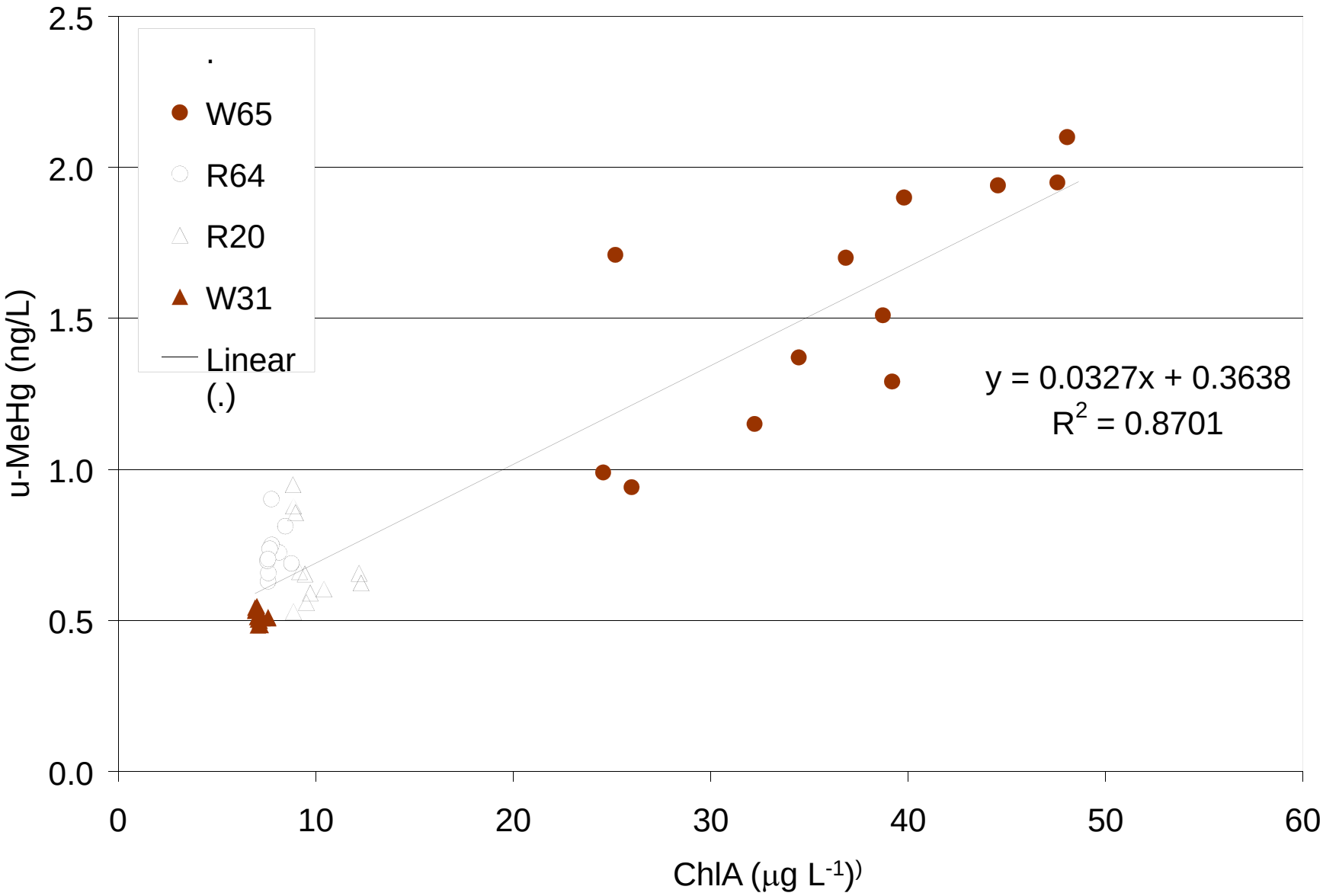

Figure 5.30. Scatter plot of surface water chlorophyll-a (ChlA) fluorescence versus unfiltered methylmercury (u-MeHg) concentration across white rice (R) and wild rice (W) fields during the diel measurements of summer 2007 (fields W65 and R64) and summer 2008 (fields R20 and W31). Linear least-squares regression equation and coefficient are shown.

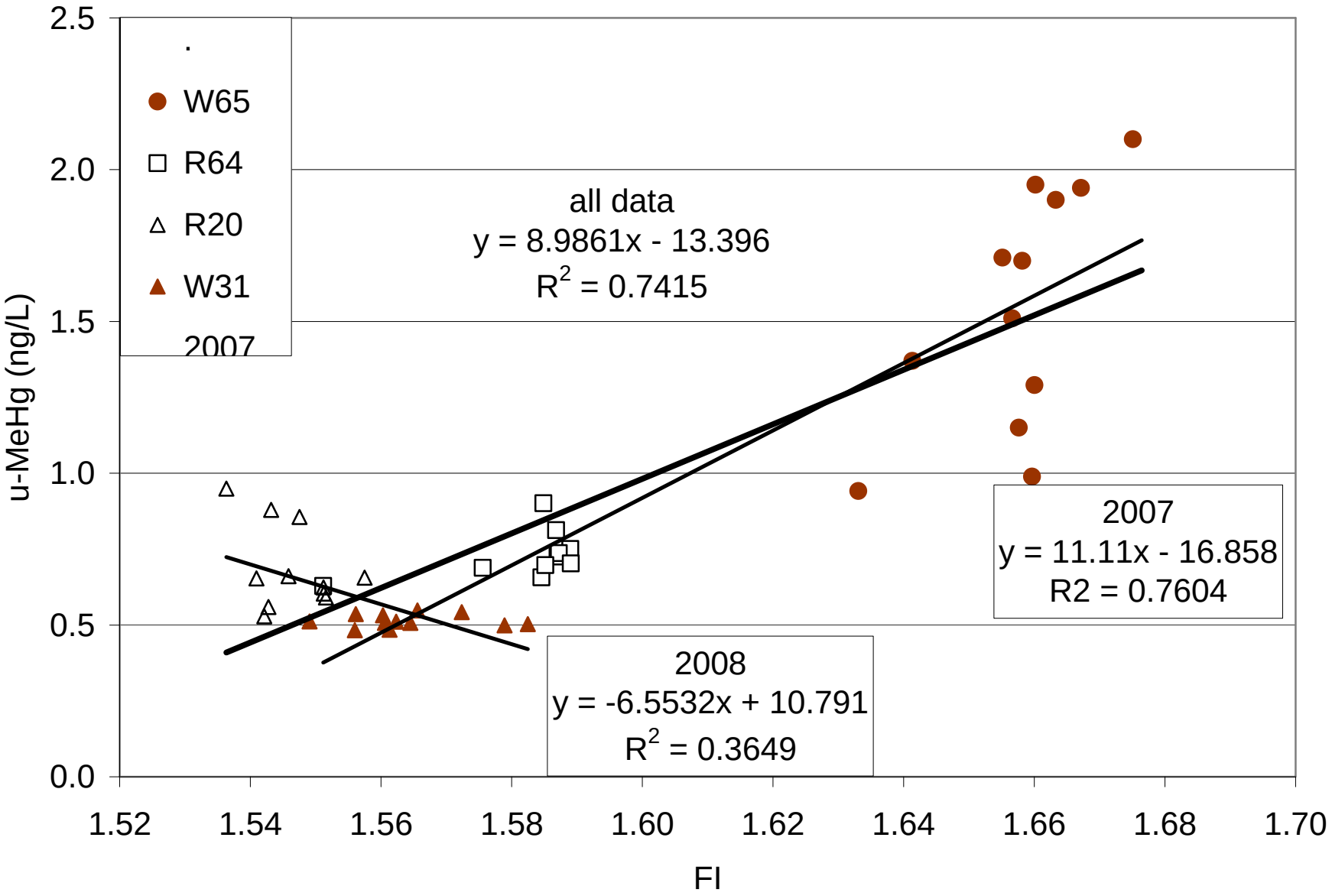

Figure 5.31. Scatter plot of fluorescence index (FI) versus unfiltered methylmercury (u-MeHg) concentration in surface water across white rice (R) and wild rice (W) fields during the diel measurements of summer 2007 (fields W65 and R64) and summer 2008 (fields R20 and W31). Linear least-squares regression equations and coefficients are shown for the 2007 data, the 2008, and all data combined.

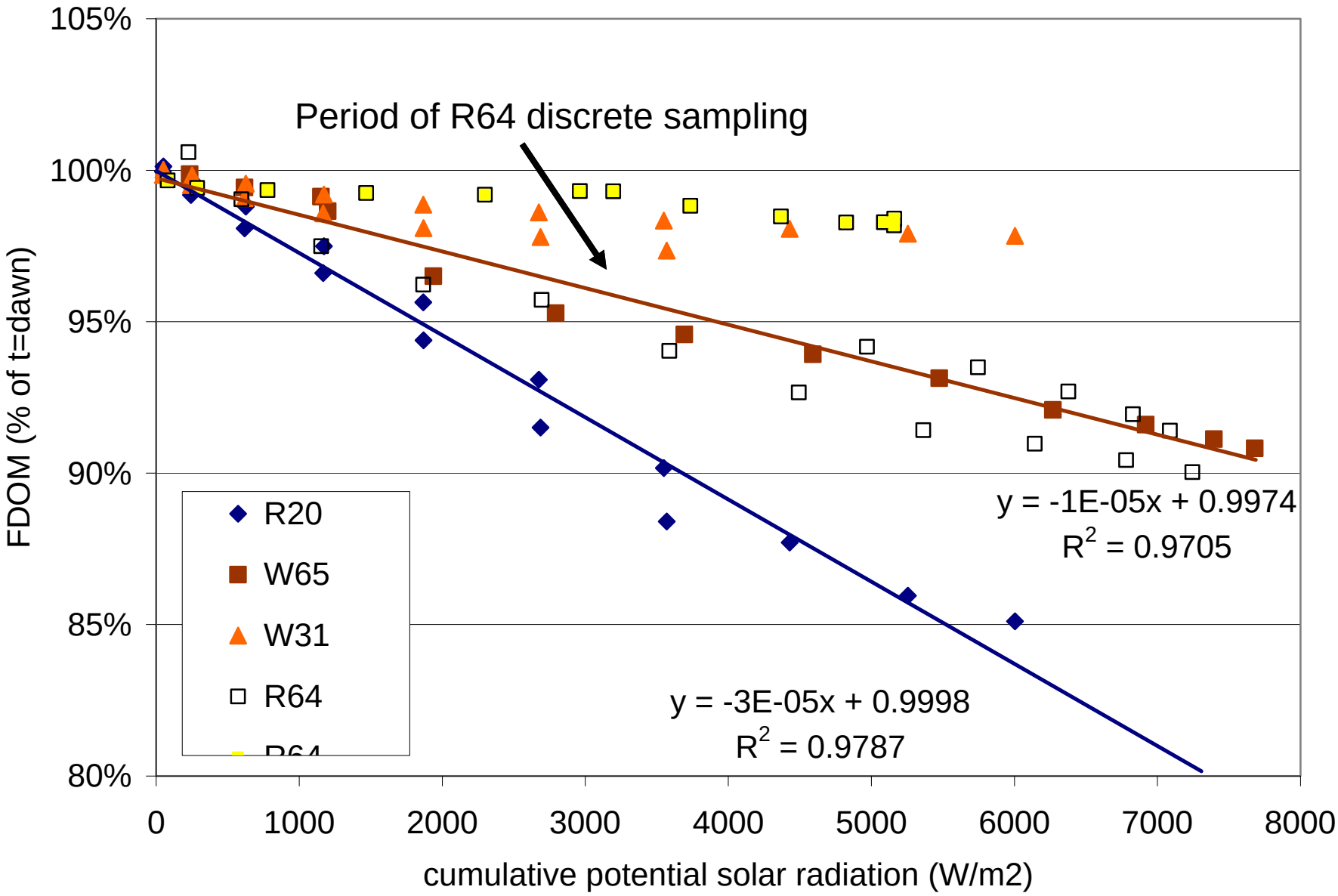

Figure 5.32. Scatter plot of cumulative potential solar radiation versus fluorescent dissolved organic matter (FDOM) in surface water during the *in situ* deployments of summer 2007 (fields W65 and R64) and summer 2008 (fields R20 and W31). Linear least-squares regression equations and coefficients are shown for fields W65 and R64..

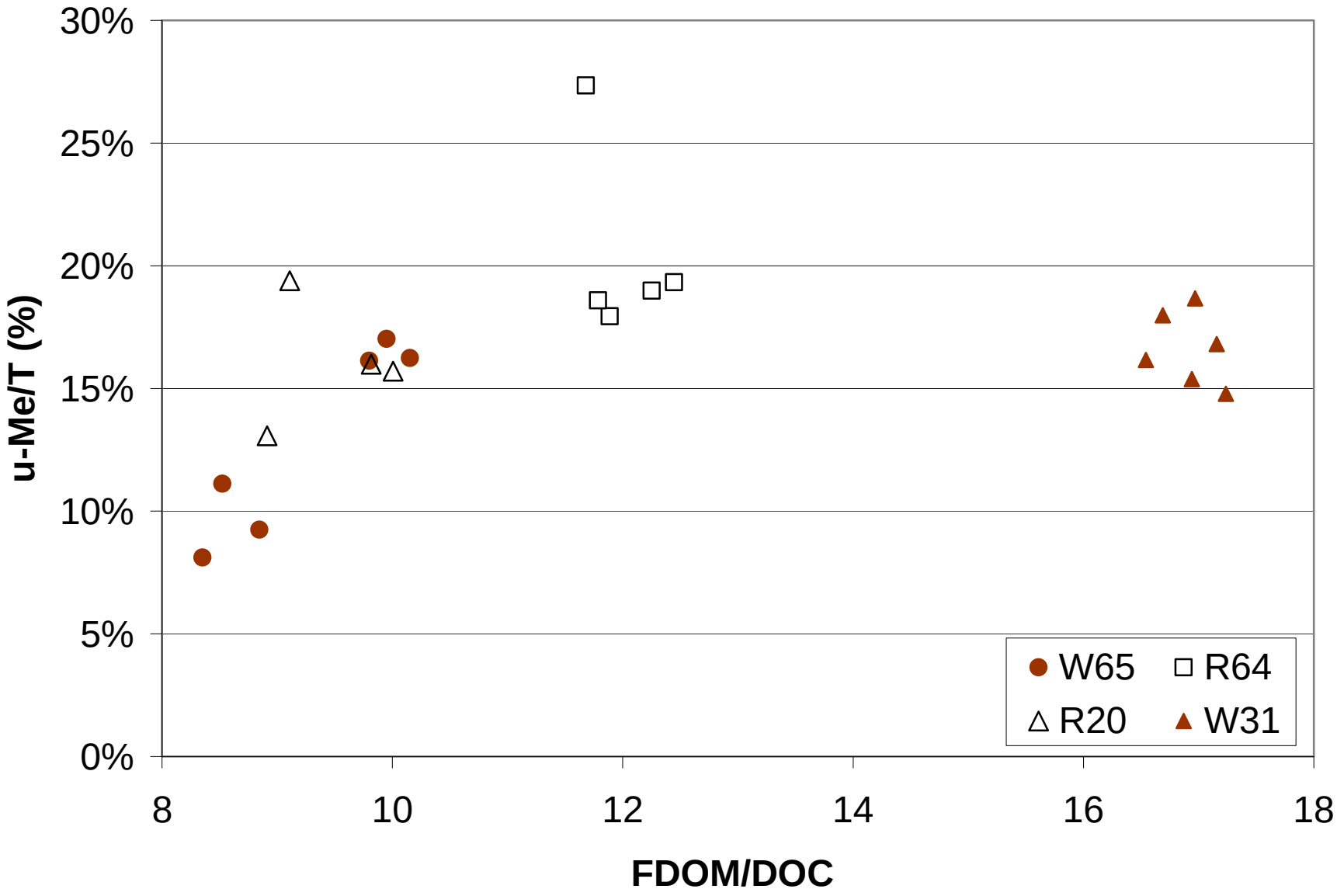

Figure 5.33. Scatter plot of the ratio of fluorescent dissolved organic matter (FDOM) to dissolved organic carbon (DOC) (FDOM/DOC) versus the ratio of unfiltered methylmercury to total mercury u-MeHg/THg) in surface water during the 2007 and 2008 diel studies. The u-MeHg/THg ratio is expressed as a percentage (% THg as MeHg).

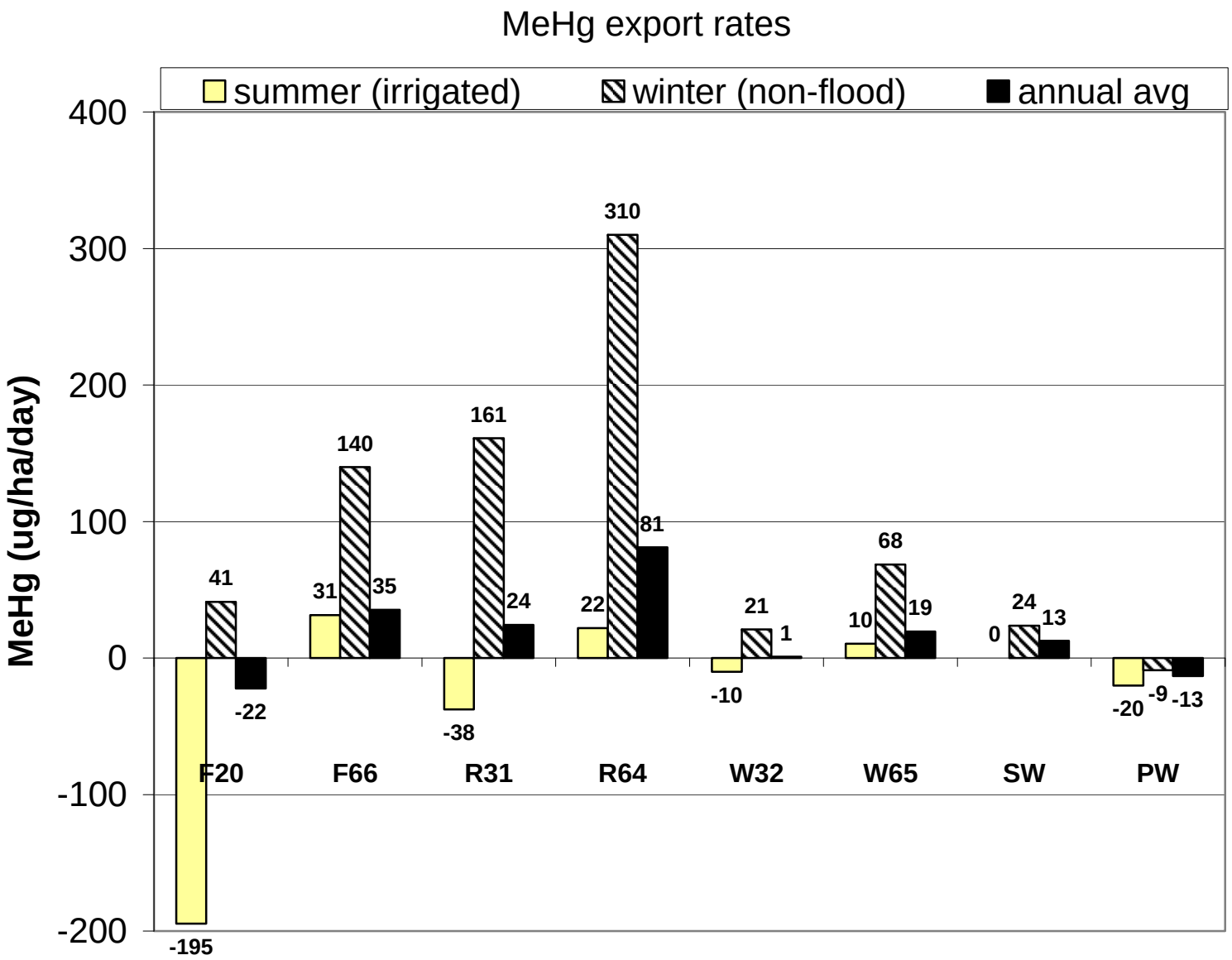

Figure 5.34. Bar graph showing methylmercury (MeHg) loads from individual fields during the summer irrigation period, the winter period (excluding the 17-day flood), and the annual average. Loads in micrograms per hectare per day (µg/ha/day). Positive values represent net export, whereas negative values represent net import.

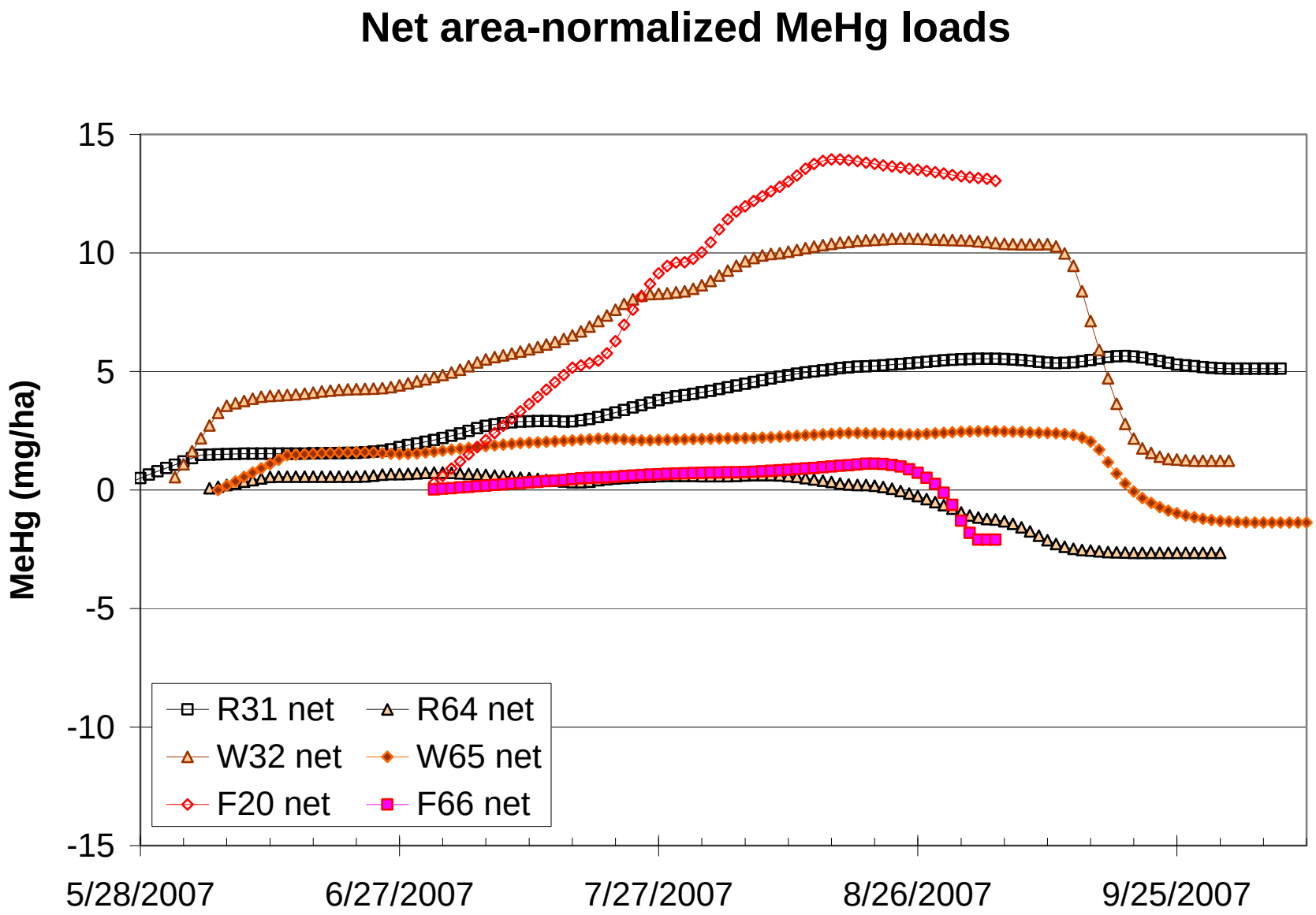

Figure 5.35. Time series plot of area-normalized, cumulative methylmercury (MeHg) mass net loading for individual fields in the Yolo Bypass Wildlife Area. Positive values represent net import, whereas negative values represent net export.

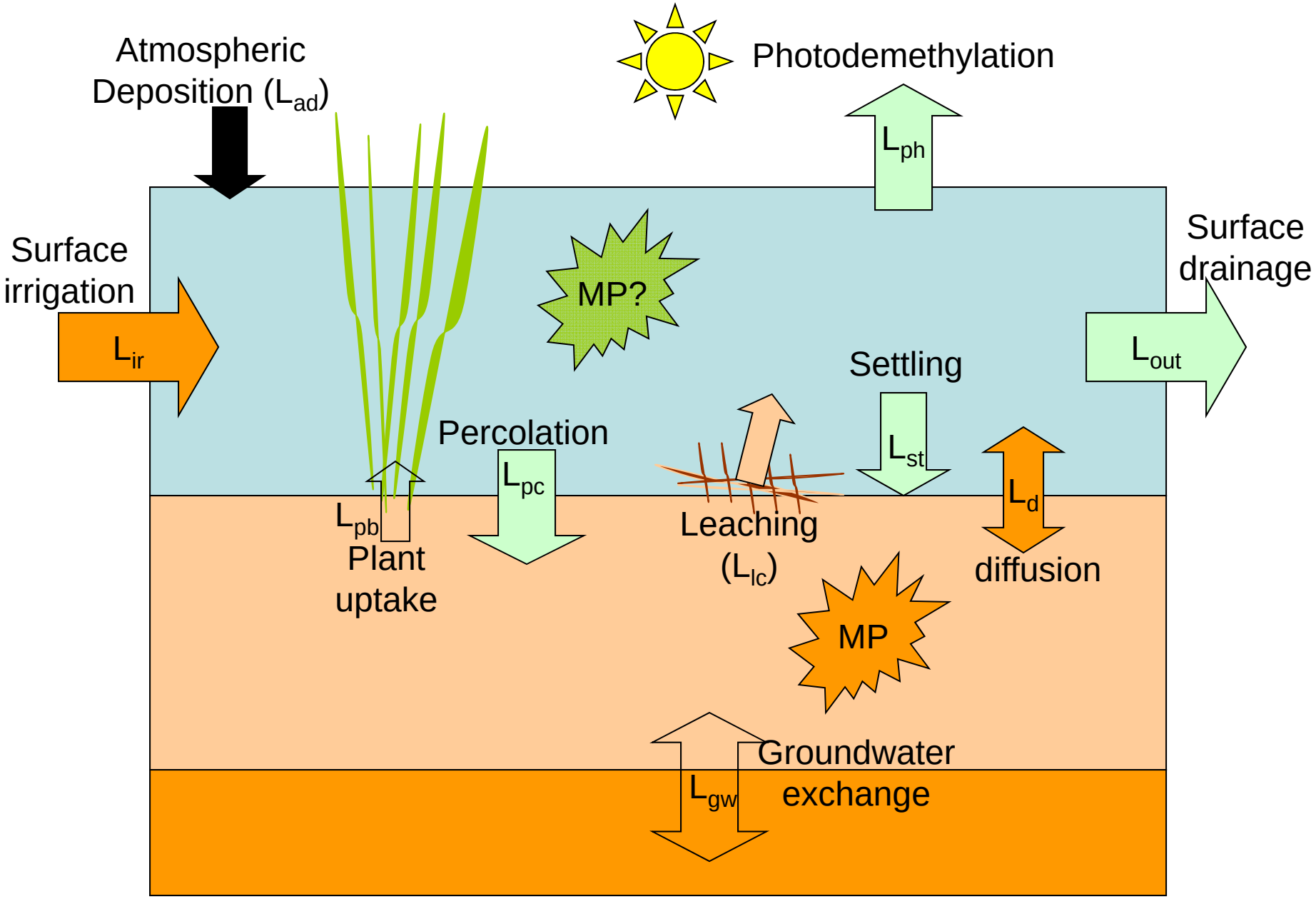

Figure 5.36. Schematic diagram showing methylmercury inputs and outputs from a generic managed wetland. See Table 5.10 for explanation of diagram notation. (MP, methylmercury production)

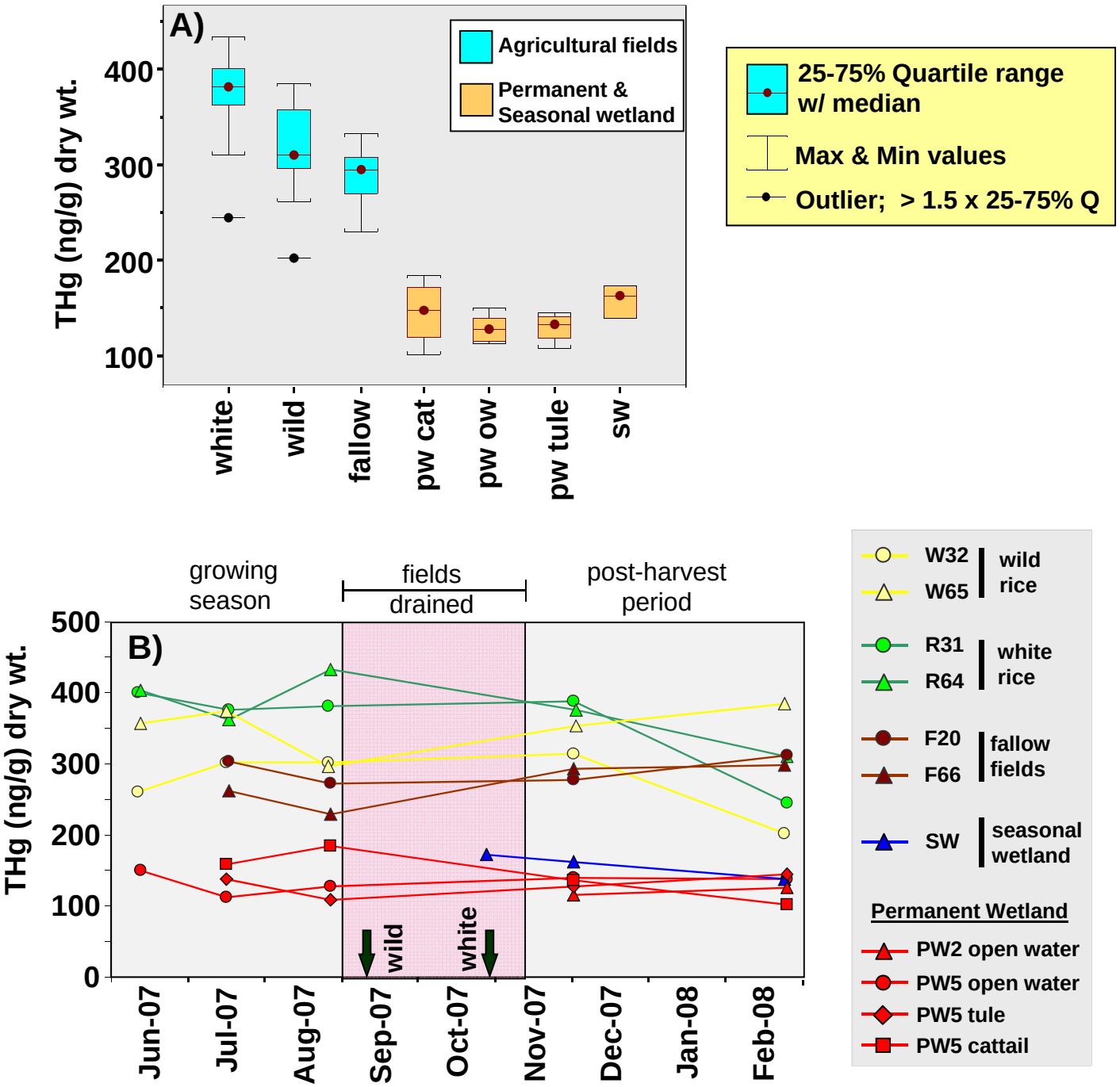

Figure 6.1. Sediment total mercury (THg) concentration data depicted as (A) a box and whisker plot by habitat type and (B) in time series for each field. (A) includes all sampling events and include replicate white rice (white), wild rice (wild) and fallow agricultural fields. Permanent wetland (pw) open water (ow) shown in (A) included data from PW5 and PW2, while cattail and tule dominated sites (pw cat and pw tule, respectively) are from PW5 only. Arrows on (B) indicate when white and wild rice fields were harvested. Temporal data groupings (growing season and post-harvest period) for agricultural field statistical comparisons (**Table 6.4**) are indicated in the grey shaded areas, and are separated by the period during which agricultural fields were drained (pink background).

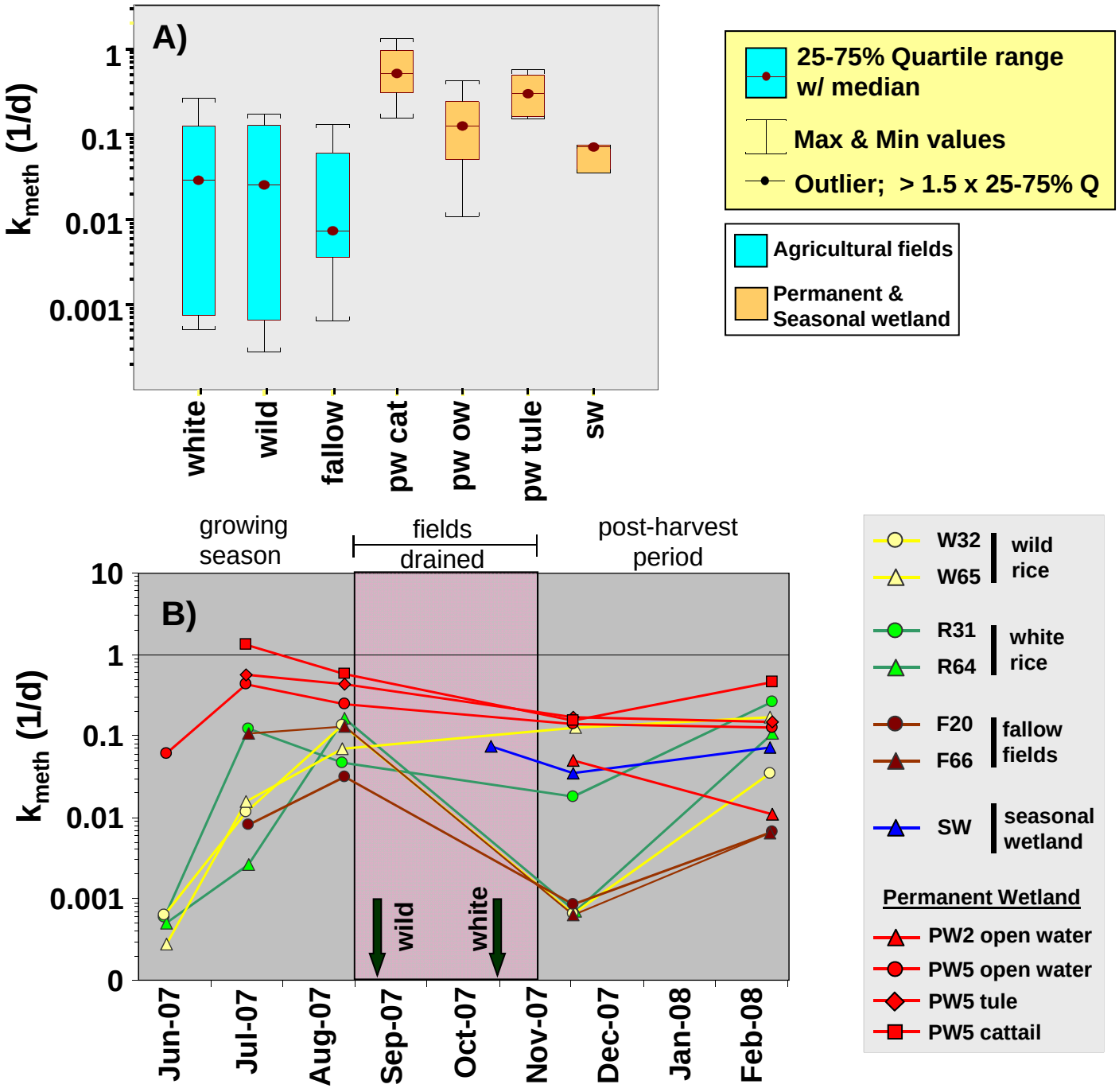

Figure 6.2. Sediment ^{203}Hg(II)-methylation rate constant (k_{meth}) data depicted as (A) a box-and-whisker plot by habitat type and (B) in time series for each field. (A) includes all sampling events and include replicate white rice (white), wild rice (wild) and fallow agricultural fields. Permanent wetland (pw) open water (ow) shown in (A) included data from PW5 and PW2, while cattail and tule dominated sites (pw cat and pw tule, respectively) are from PW5 only. Arrows and seasonal groupings on (B) are described in **Figure 6.1**.

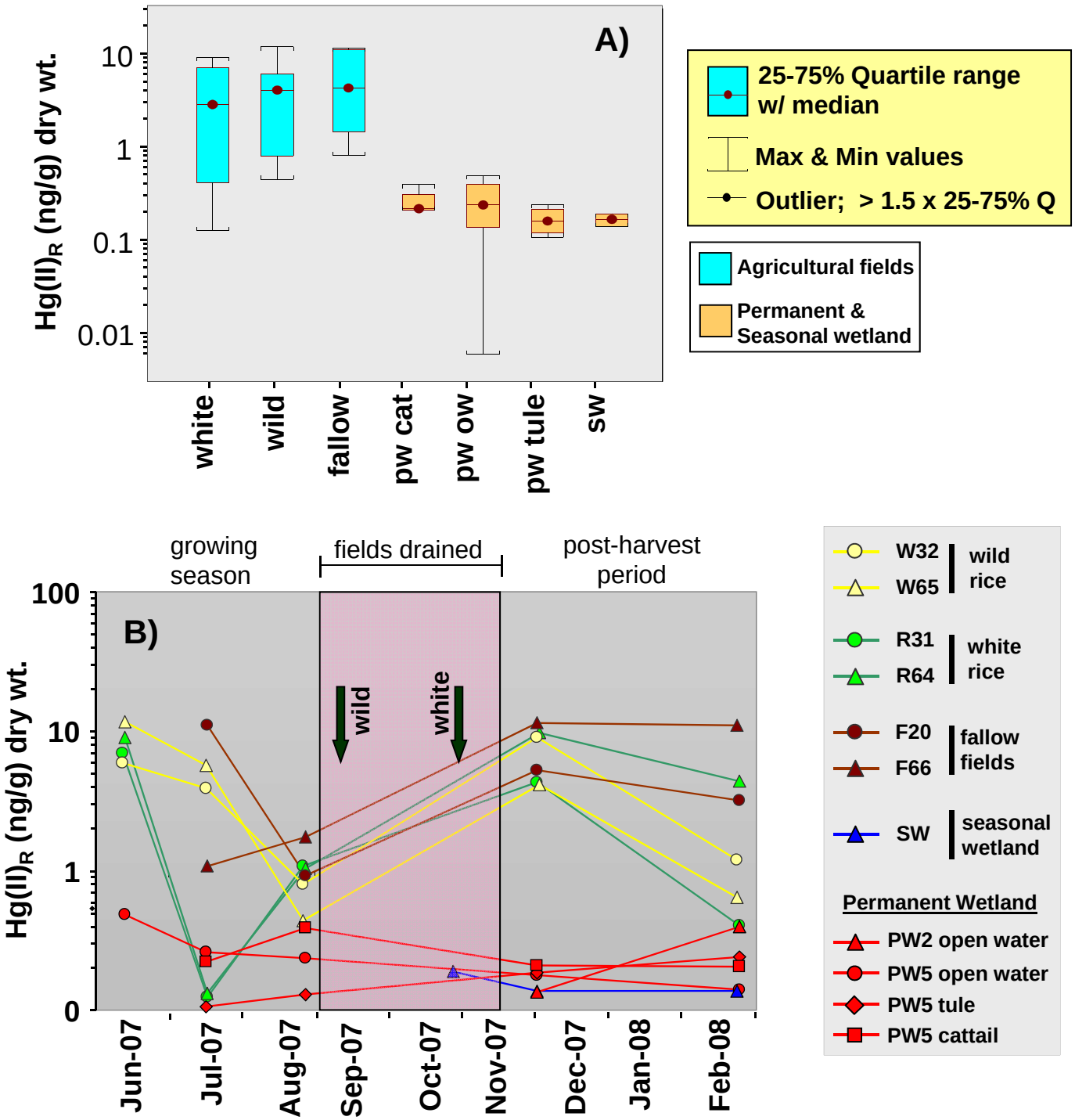

Figure 6.3. Sediment inorganic reactive mercury ($Hg(II)_R$) concentration data depicted as (A) a box-and-whisker plot by habitat type and (B) in time series for each field. (A) includes all sampling events and include replicate white rice (white), wild rice (wild) and fallow agricultural fields. Permanent wetland (pw) open water (ow) shown in (A) included data from PW5 and PW2, while cattail and tule dominated sites (pw cat and pw tule, respectively) are from PW5 only. Arrows and seasonal groupings on (B) are described in **Figure 6.1**.

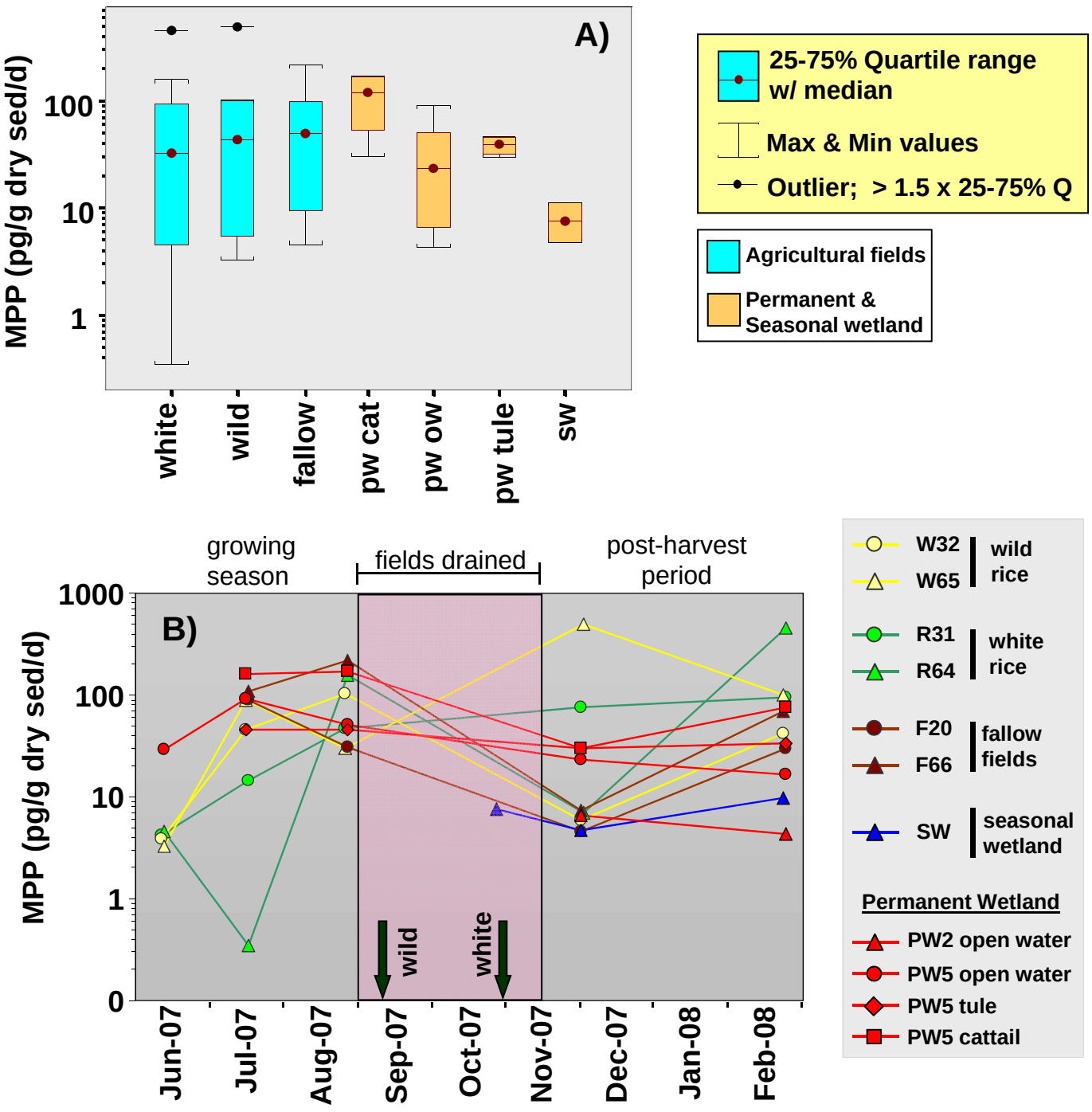

Figure 6.4. Sediment methylmercury production potential (MPP) rate data depicted as (A) a box-and-whisker plot by habitat type and (B) in time series for each field. (A) includes all sampling events and include replicate white rice (white), wild rice (wild) and fallow agricultural fields. Permanent wetland (pw) open water (ow) shown in (A) included data from PW5 and PW2, while cattail and tule dominated sites (pw cat and pw tule, respectively) are from PW5 only. Arrows and seasonal groupings on (B) are described in **Figure 6.1**.

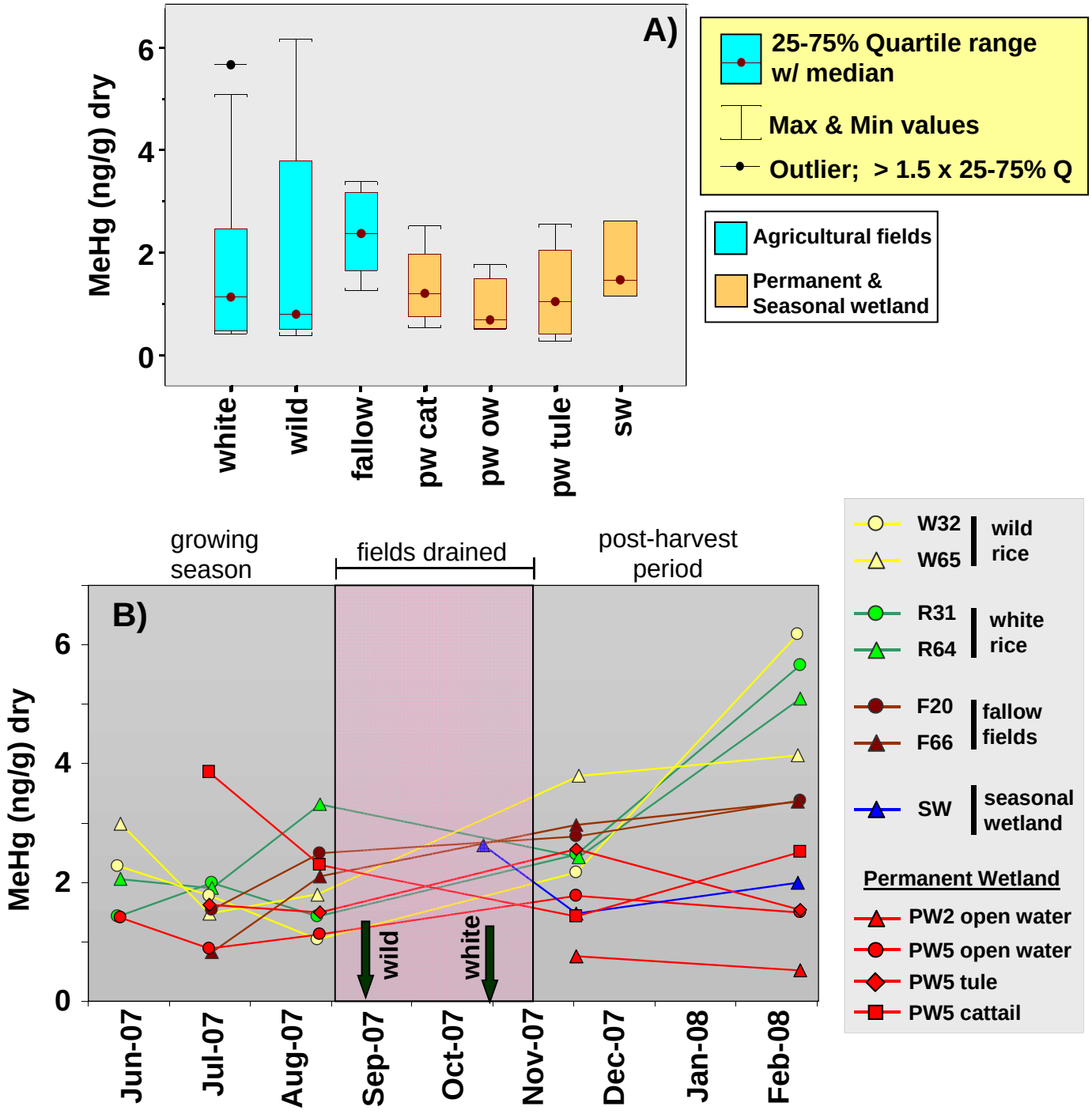

Figure 6.5. Sediment methylmercury (MeHg) concentration data depicted as (A) a box-and-whisker plot by habitat type and (B) in time series for each field. (A) includes all sampling events and include replicate white rice (white), wild rice (wild) and fallow agricultural fields. Permanent wetland (pw) open water (ow) shown in (A) included data from PW5 and PW2, while cattail and tule dominated sites (pw cat and pw tule, respectively) are from PW5 only. Arrows and seasonal groupings on (B) are described in **Figure 6.1**.

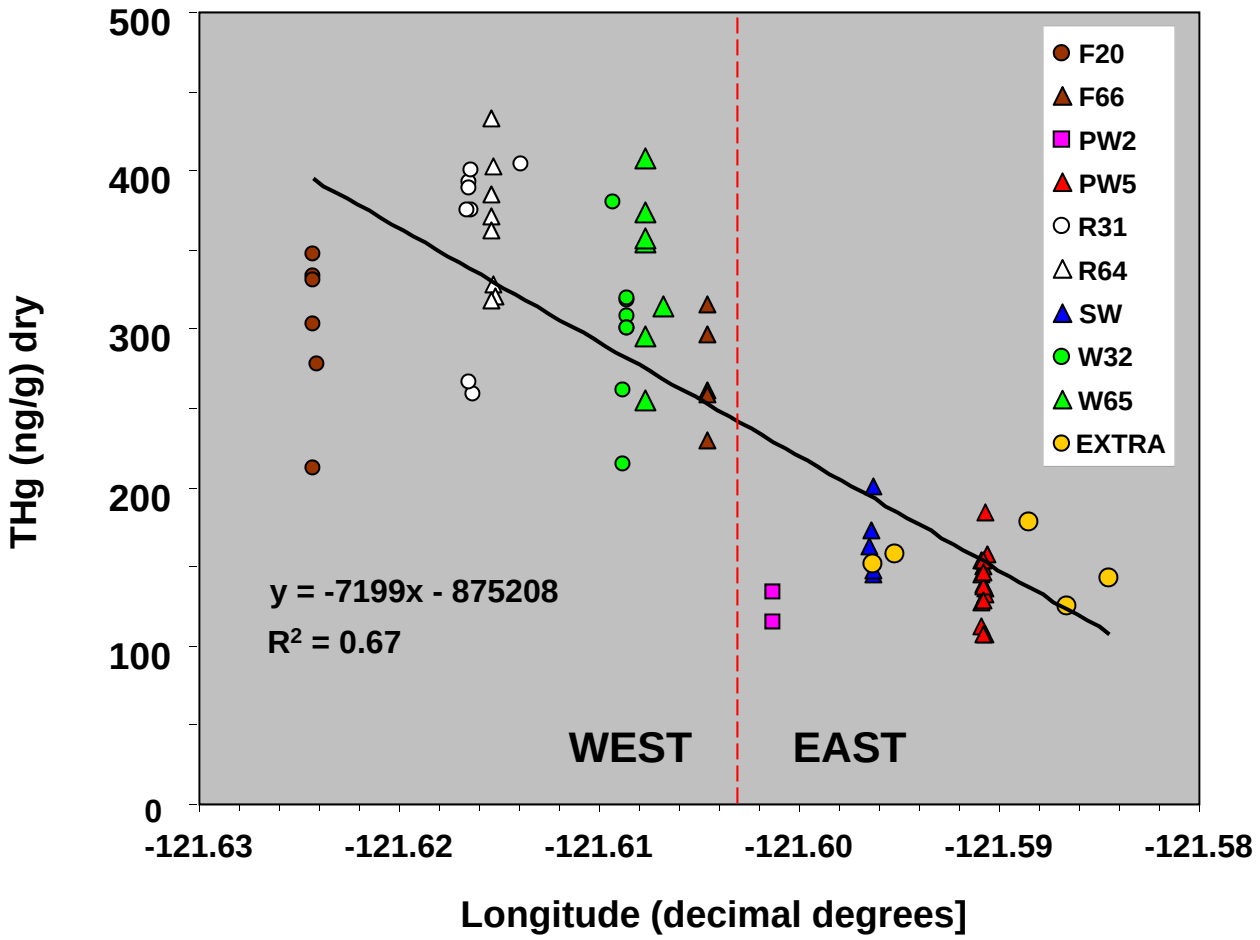

Figure 6.6. Scatter plot of sediment total mercury (THg) concentration versus longitude showing least-squares linear regression. The solid line represents the least-squares linear fit to the data, with the linear equation and R^2 value inset. The dashed red vertical line represents -121.603º longitude, and represents a visual demarkation where THg concentrations appear to abruptly shift concentration from east to west. Of the primary sampling sites in the current study, all agricultural fields were located west of this longitude, while all non-agricultural fields sampled were located to the east. Additional samples 'EXTRA' were collected during May 2008 and submitted by J. Holloway (USGS, Denver, CO) as part of the California Geochemical Landscapes project (Marty Goldhaber, USGS, Denver, CO; Project Chief).

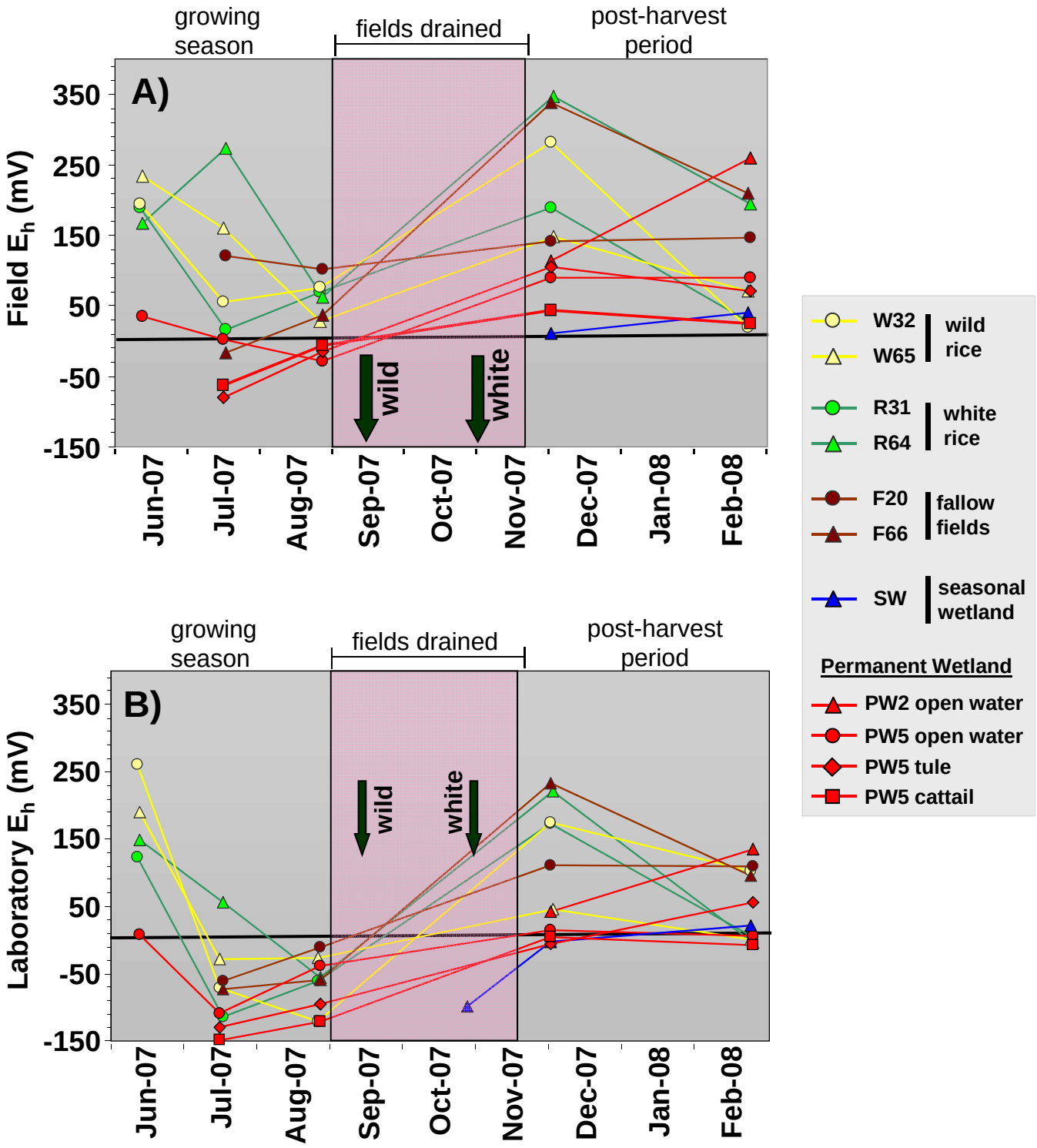

Figure 6.7. Time series plots of sediment oxidation-reduction potential (E_h) as measured in the (A) field and (B) laboratory at the time of sediment sub-sampling, by field. Sub-sampling occurred 1-4 days after field collection. Arrows and seasonal groupings on are described in **Figure 6.1**.

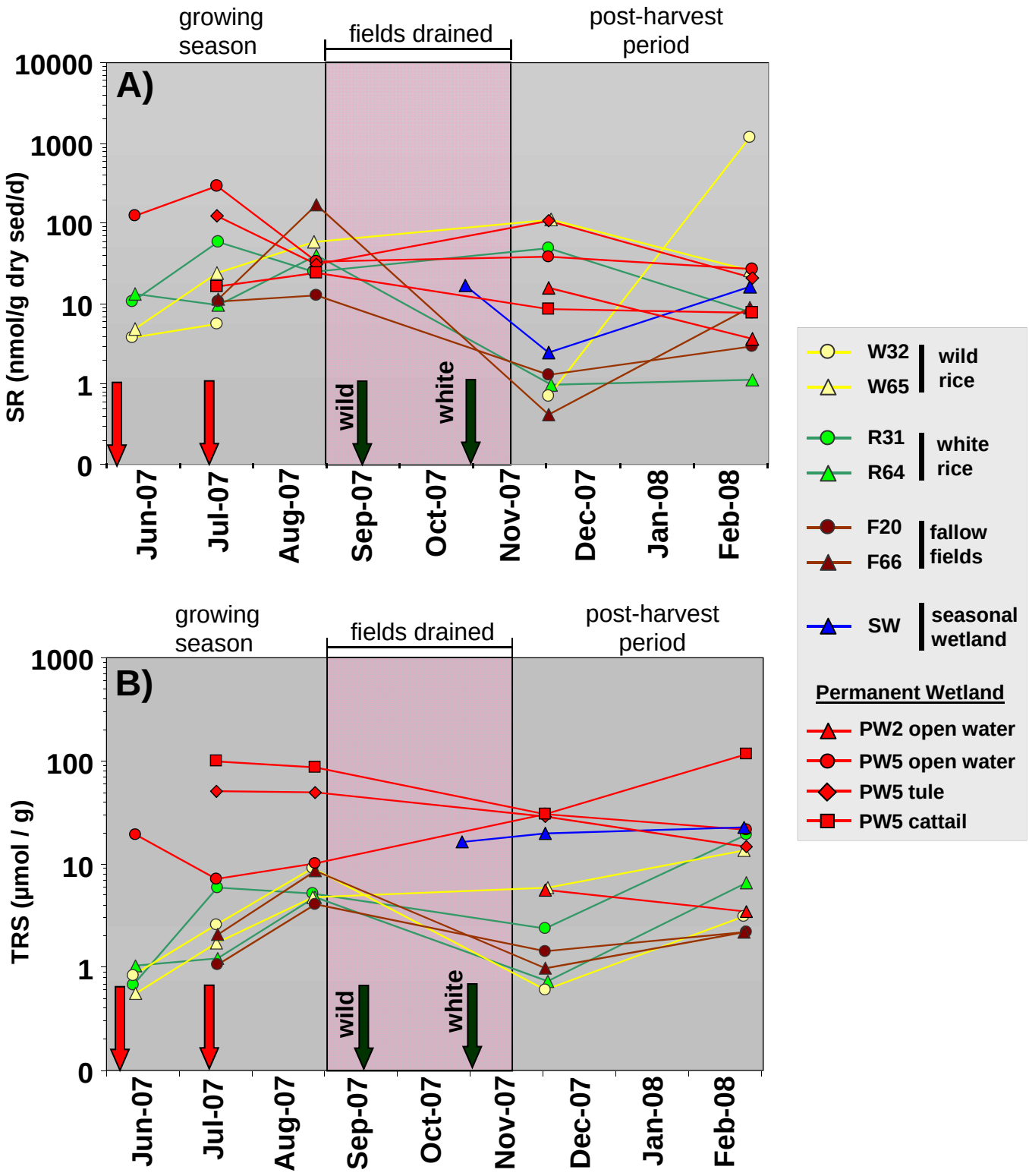

Figure 6.8. Time series plots of sediment A) microbial sulfate reduction (SR) rate and B) total reduced sulfur (TRS), by field. Red arrows and green arrows indicate when fertilizer was applied to rice fields and when rice fields were harvested, respectively. Seasonal groupings are described in **Figure 6.1**. Note: the August SR rate data for field W32 was lost during analysis.

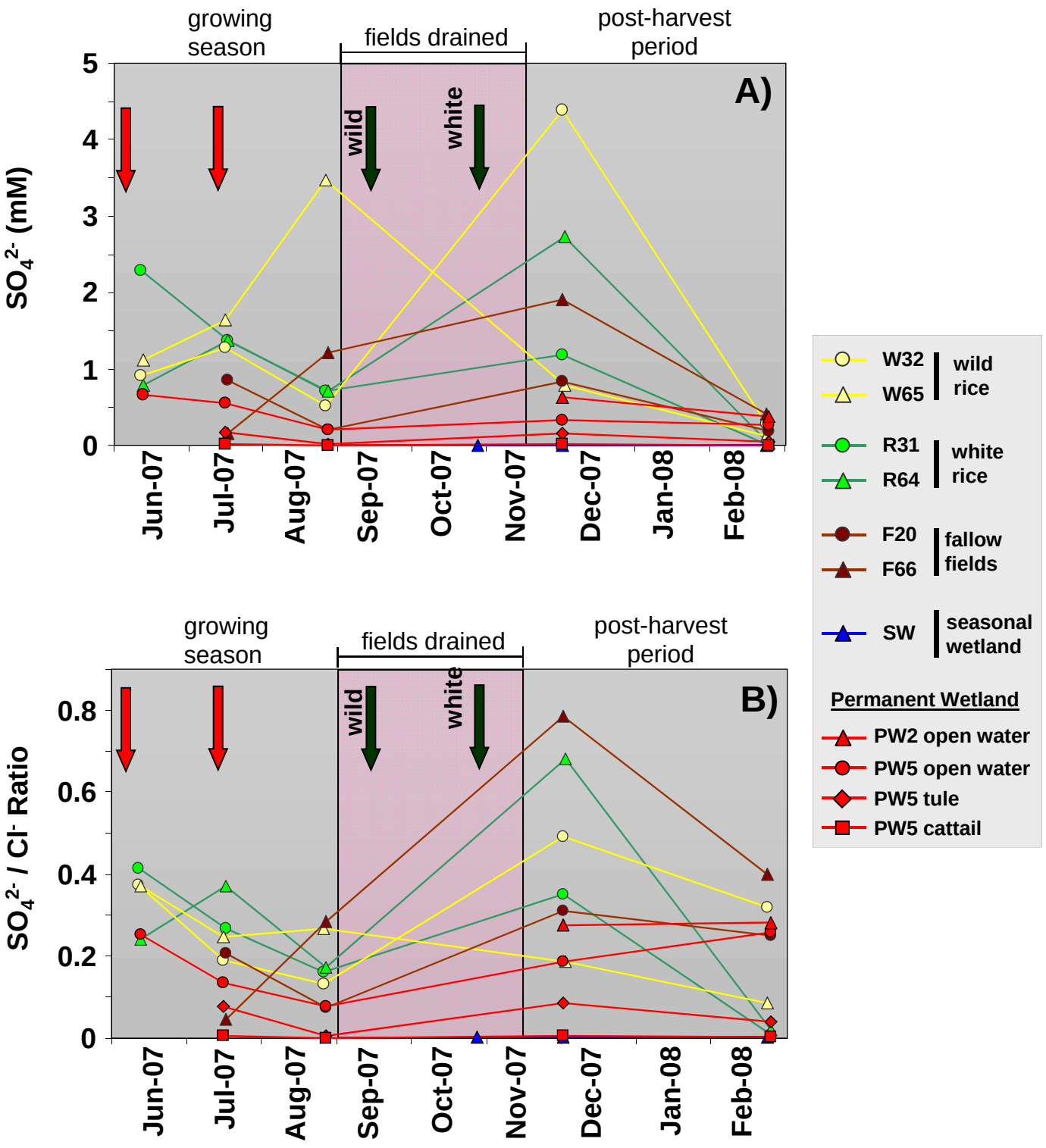

Figure 6.9. Time series plots of pore water A) sulfate (SO_4^{2-}) concentration and B) the sulfate to chloride (SO_4^{2-} / Cl^-) molar ratio, by field. Red arrows and green arrows indicate when fertilizer was applied to rice fields and when rice fields were harvested, respectively. Seasonal groupings are described in **Figure 6.1**.

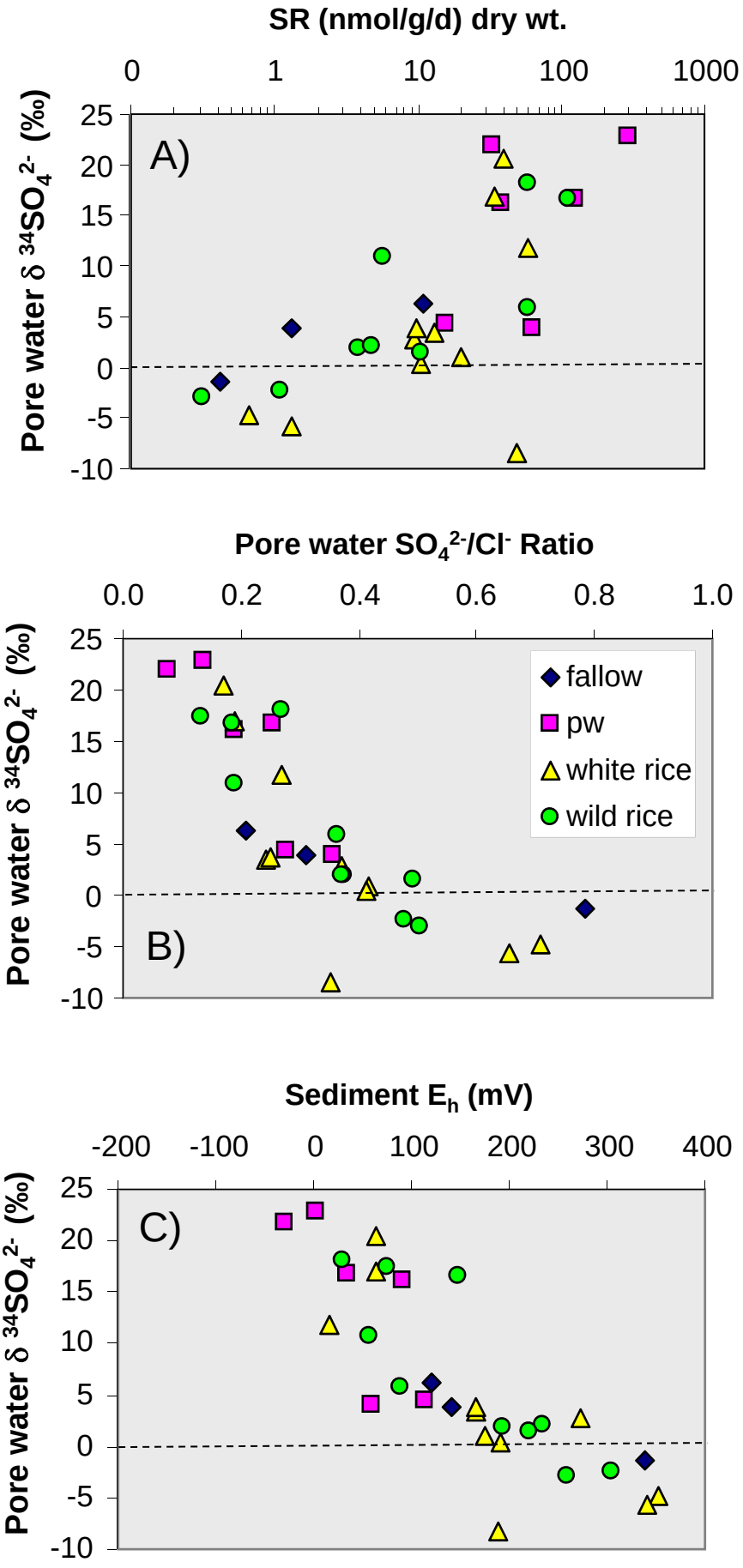

Figure 6.10. Scatter plots of pore water sulfate-sulfur stable isotope data ($\delta\ ^{34}SO_4^{2-}$) as a function of (A) sediment microbial sulfate reduction (SR) rate, (B) pore water sulfate-to-chloride concentration ratio, and (C) sediment redox (E_h). Date from the June through December (2007) sampling period. Data organized by habitat type (legend inset). Dashed line indicates the $\delta\ ^{34}SO_4^{2-}$ zero value.

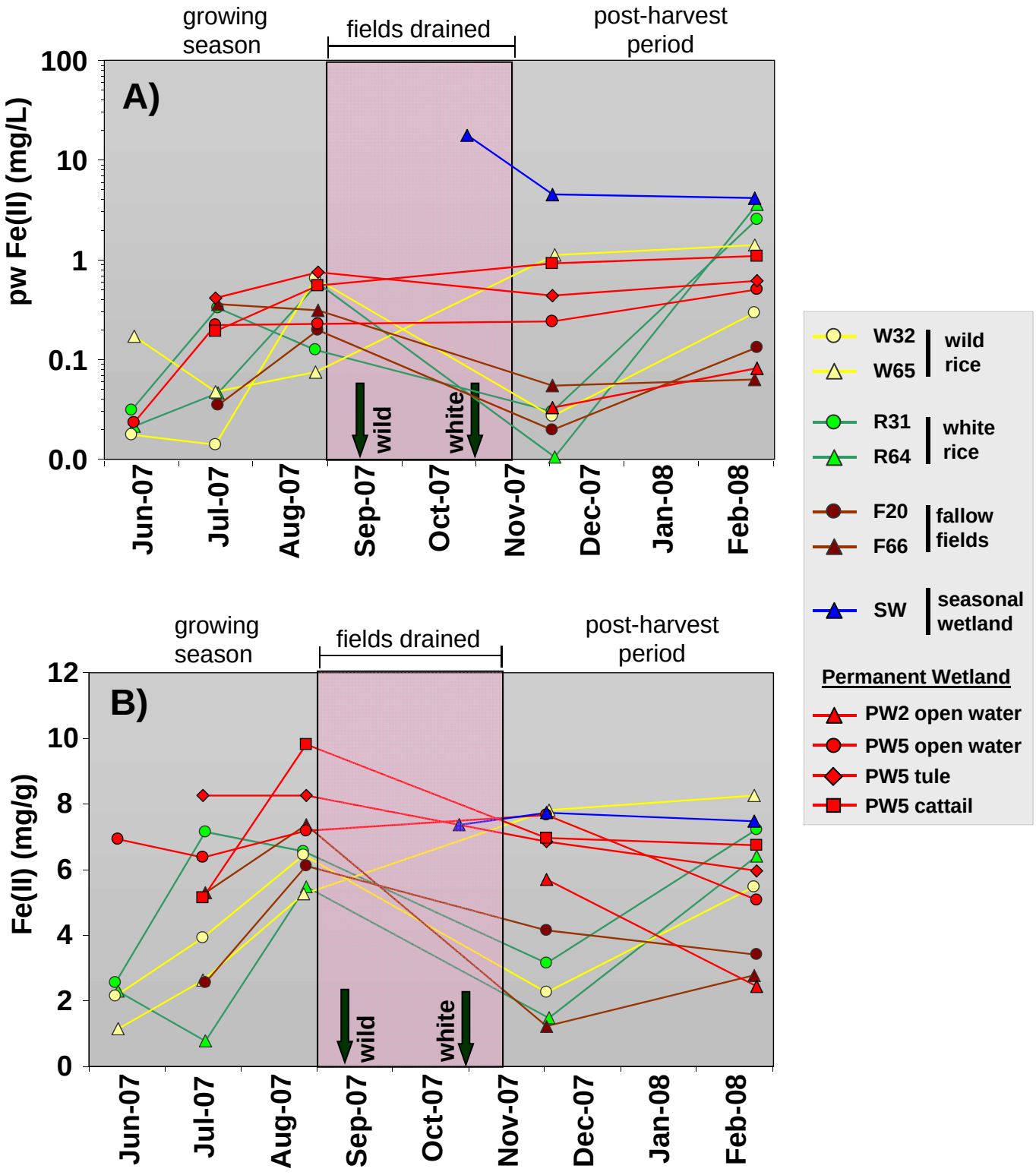

Figure 6.11. Time series plots of ferrous iron (Fe(II)) concentration in (A) pore water and (B) sediment, by field. Arrows and seasonal groupings are described in **Figure 6.1**.

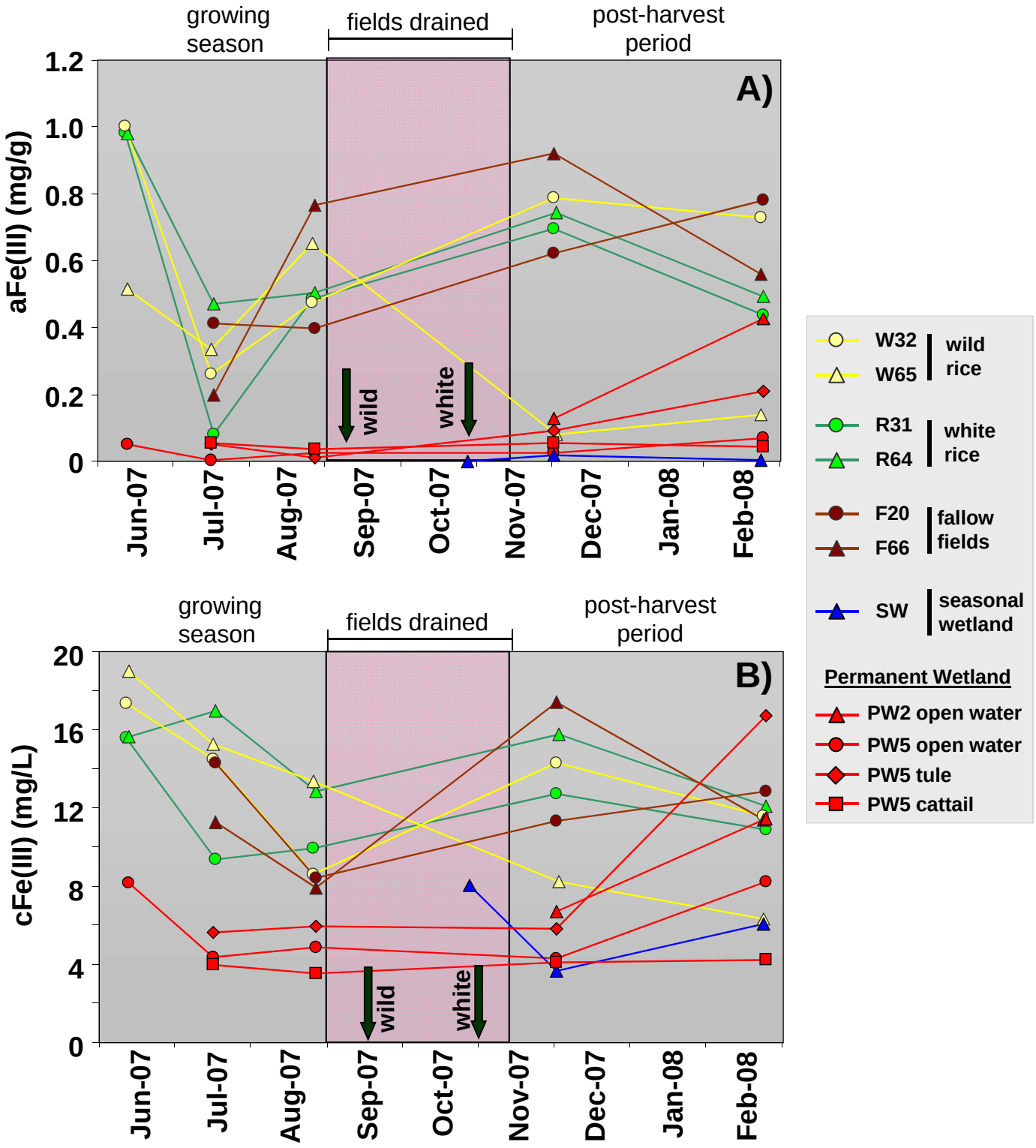

Figure 6.12. Time series plots of sediment (A) amorphous / poorly-crystalline ferric iron (aFe(III)) and (B) crystalline ferric iron (cFe(III)), by field. Arrows and seasonal groupings are described in **Figure 6.1**.

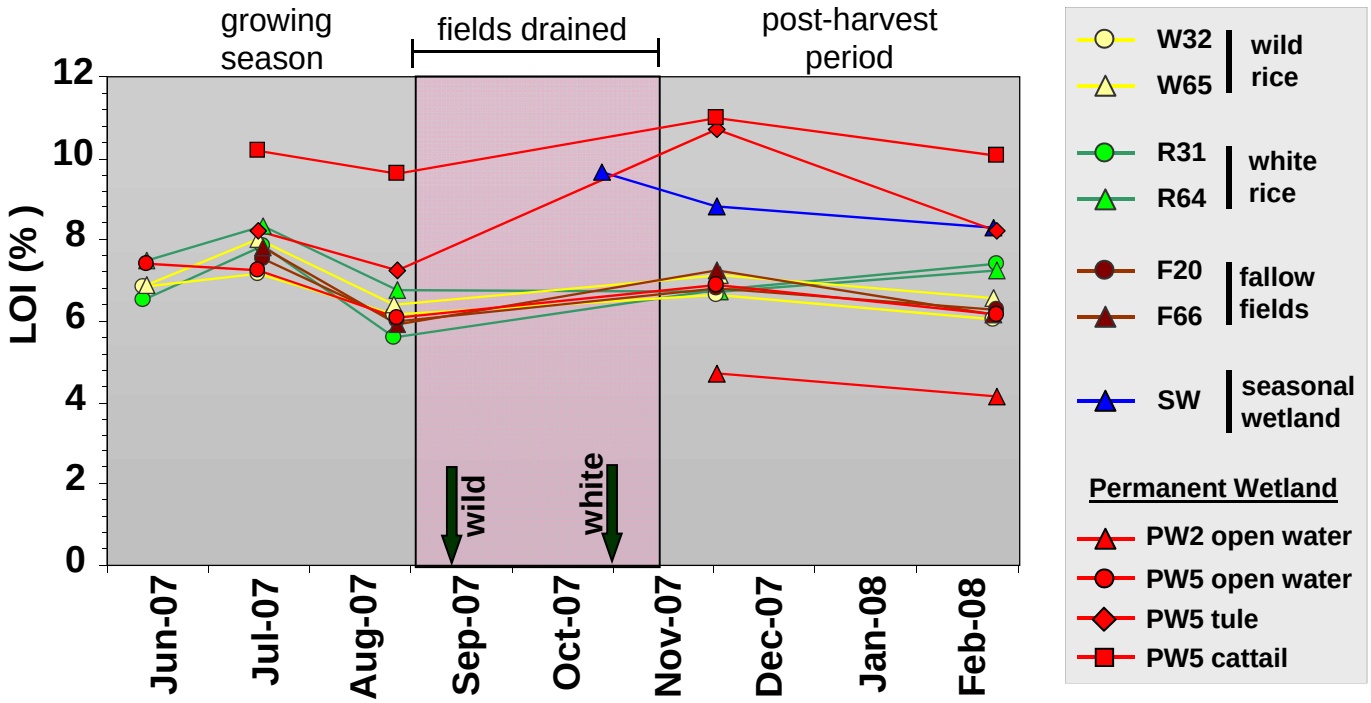

Figure 6.13. Time series plot of sediment organic content, as percent loss on ignition (%LOI), by field. Arrows and seasonal groupings are described in **Figure 6.1**.

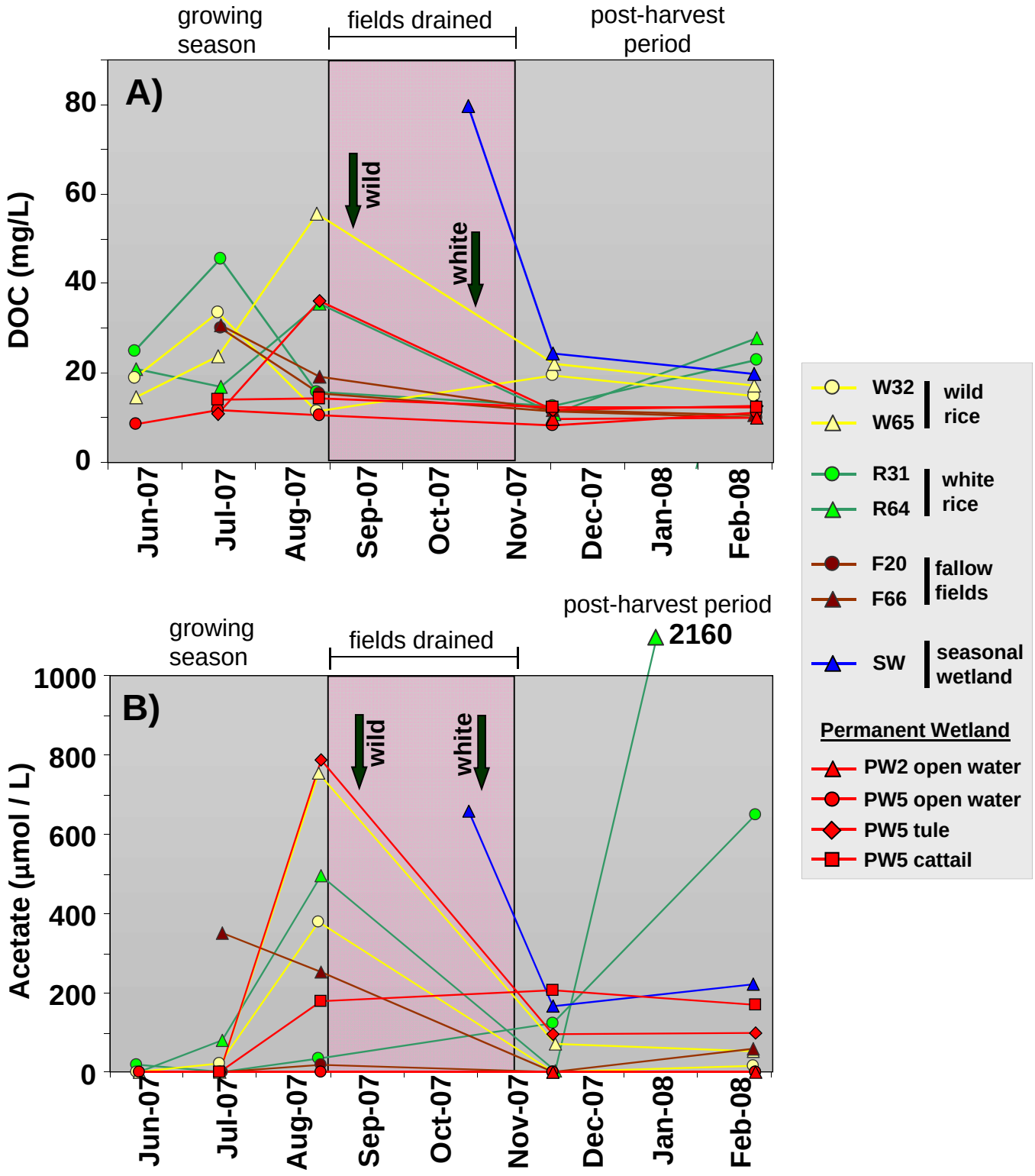

Figure 6.14. Time series plots of pore water (A) dissolved organic carbon (DOC) and (B) acetate, by field. Arrows and seasonal groupings are described in **Figure 6.1**.

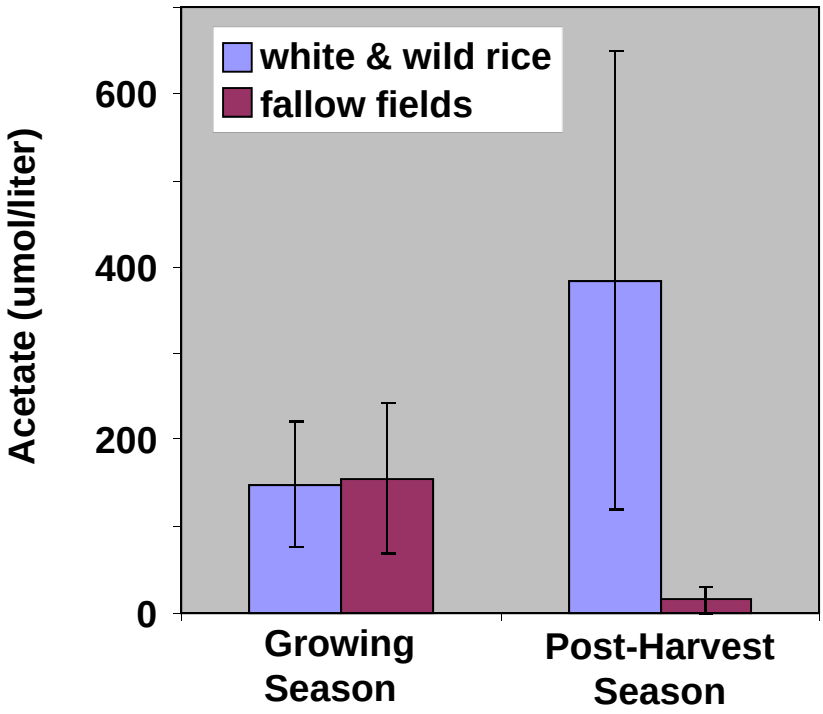

Figure 6.15. Bar graph of pore water acetate concentration by season (growing vs post-harvest) for rice (white and wild) fields and fallow fields. Error bars represent ± 1 standard error.

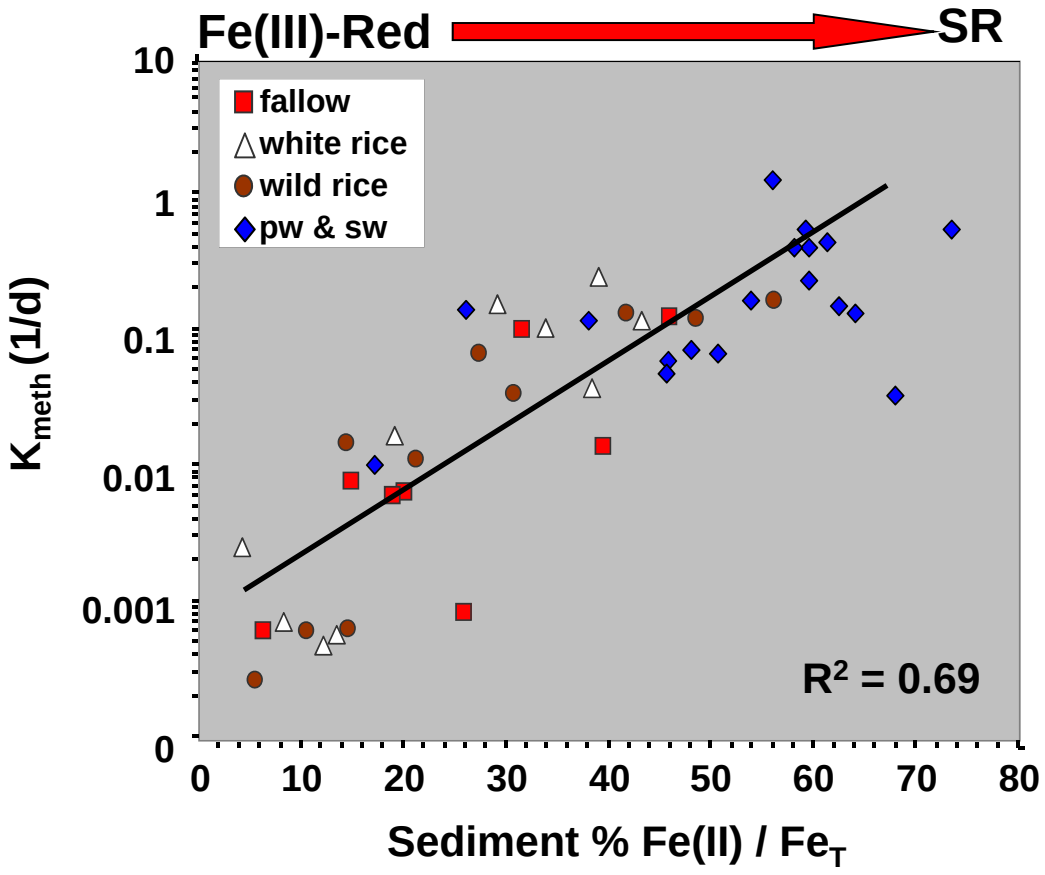

Figure 6.16. Linear-Log plot of sediment ferrous iron to total iron ratio (Fe(II)/FeT) versus ^{203}Hg(II)-methylation rate constant (k_{meth}). Where: FeT = aFe(III) + cFe(III) + Fe(II). The solid line represents the linear least squares fit. The increase in the %Fe(II)/FeT metric can be thought of as a surrogate for geochemical conditions transitioning from a state poised for microbial Fe(III)-reduction, to one poised for microbial sulfate reduction (SR), as available Fe(III) becomes exhausted. This is indicated with the red arrow above the graphic.

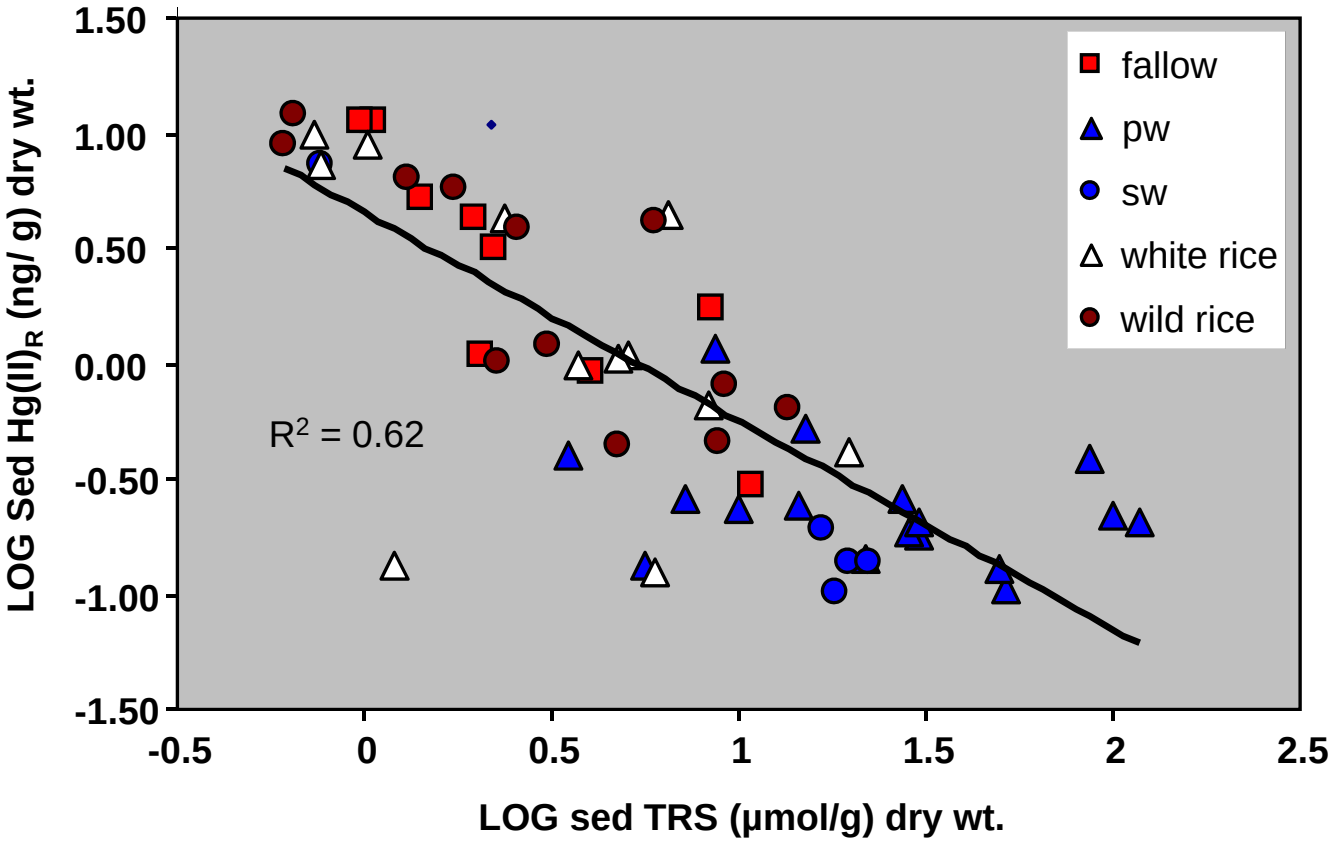

Figure 6.17. Log-Log plot of sediment total reduced sulfur (TRS) versus reactive inorganic mercury ($Hg(II)_R$). The solid line represents the linear least squares fit.

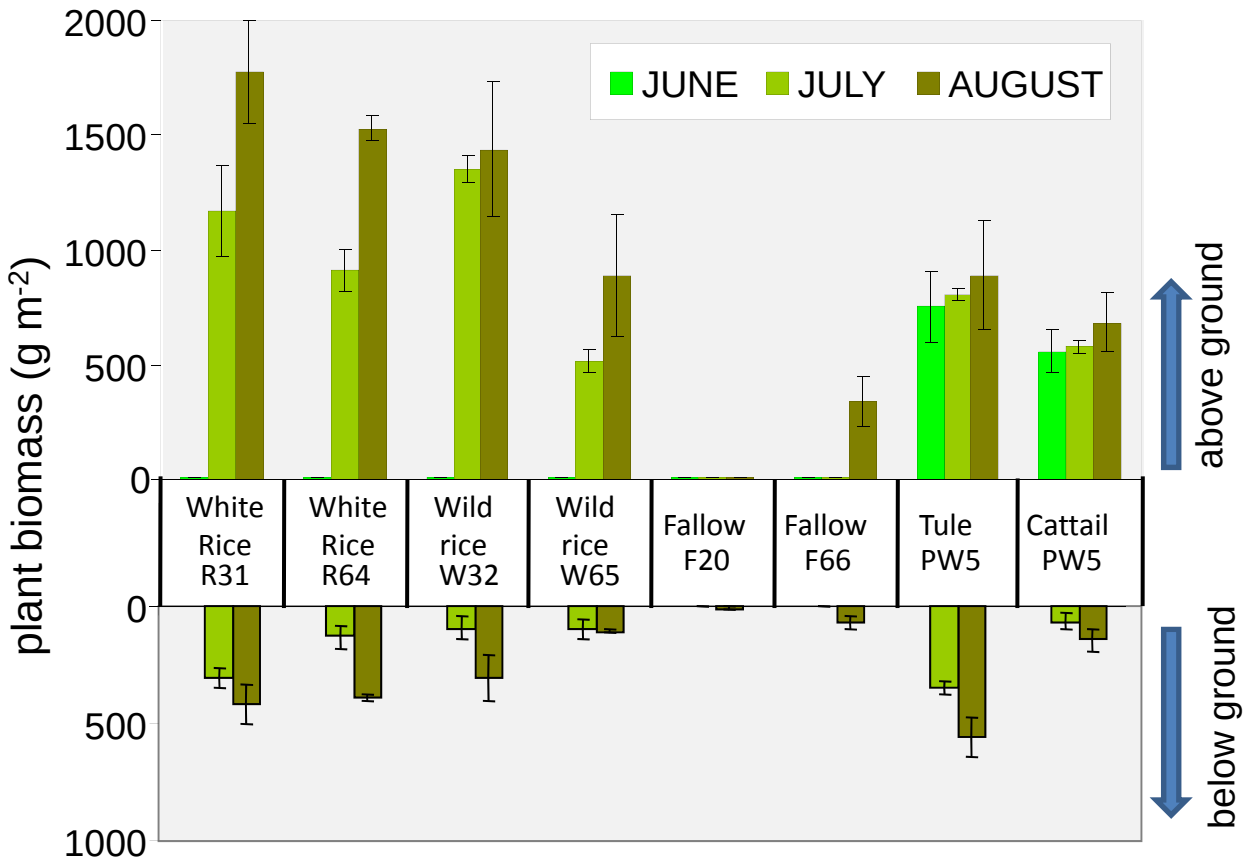

Figure 7.1 Bar graph of above and below-ground plant biomass in each field during the summer growing season, June–August 2007. Plant biomass is given on a dry weight basis. Error bars denote ± 1 standard deviation (n=3).

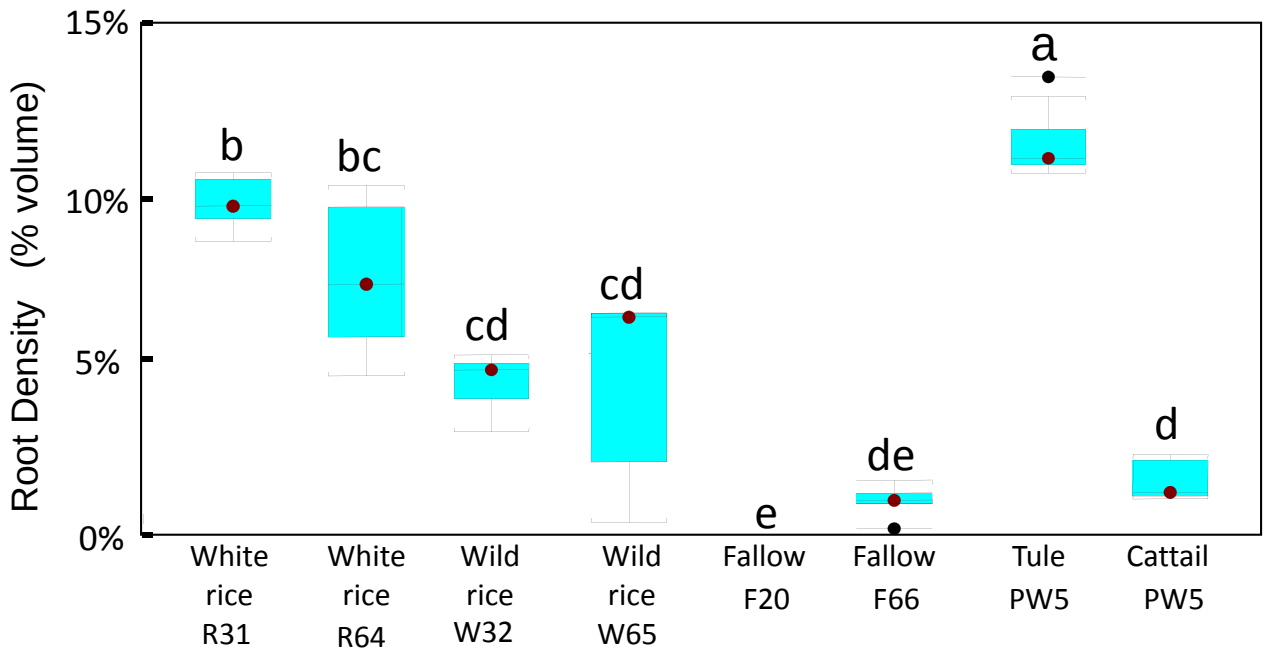

Figure 7.2. Box-and-whisker plot of live root density, expressed as the percentage of soil volume occupied by live roots in the top two centimeters of soil. Data from July (n=3) and August 2007 (n=3) are represented. Letters denote statistically significant ($p<0.05$) differences as assessed by ANOVA with Bonferonni post-hoc test. Boxes that share a common letter are not significantly different.

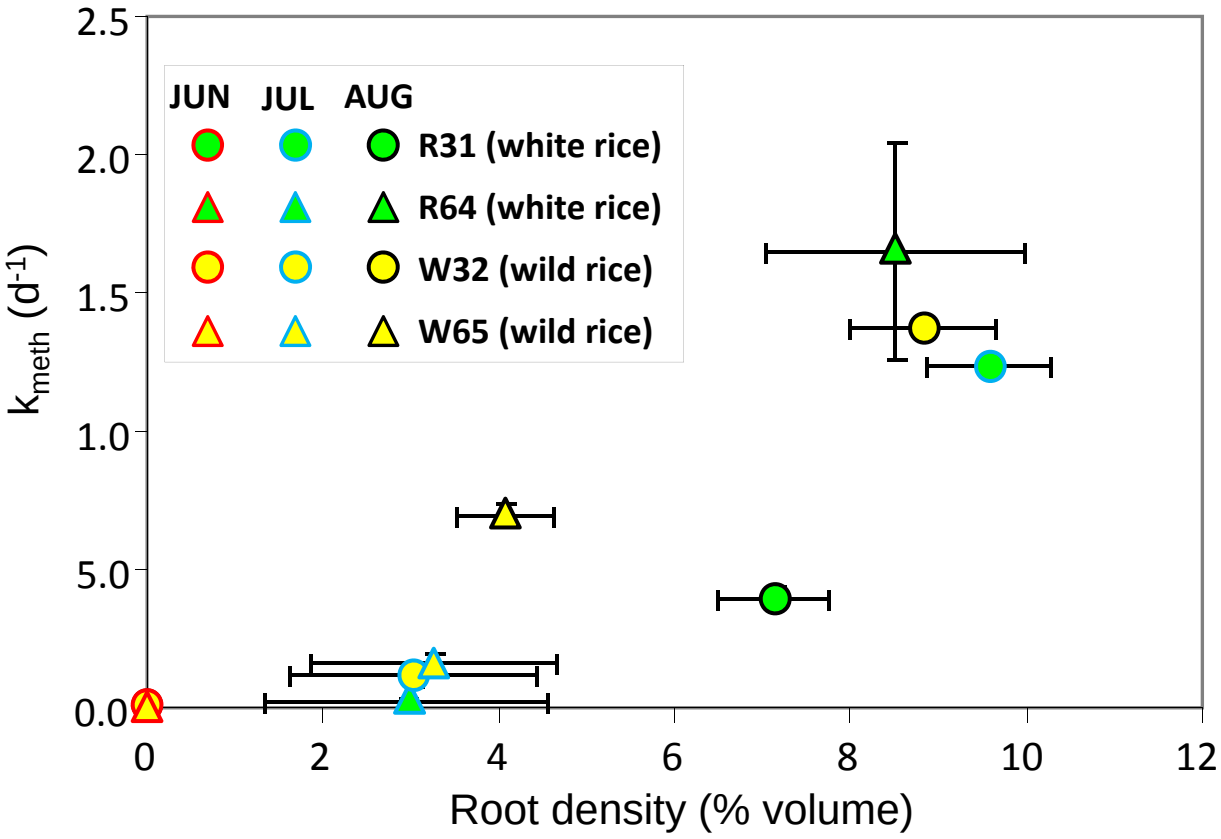

Figure 7.3. Scatterplot of live root density versus mercury methylation rate constant in actively growing rice fields during June, July and August 2007. X-axis error bars denote ± 1 standard deviation based upon n=3 observations. Y-axis error bars denote ± [absolute difference]/2 based upon n=2 observations. Months coded by symbol outline: red = June, blue = July, black = August.

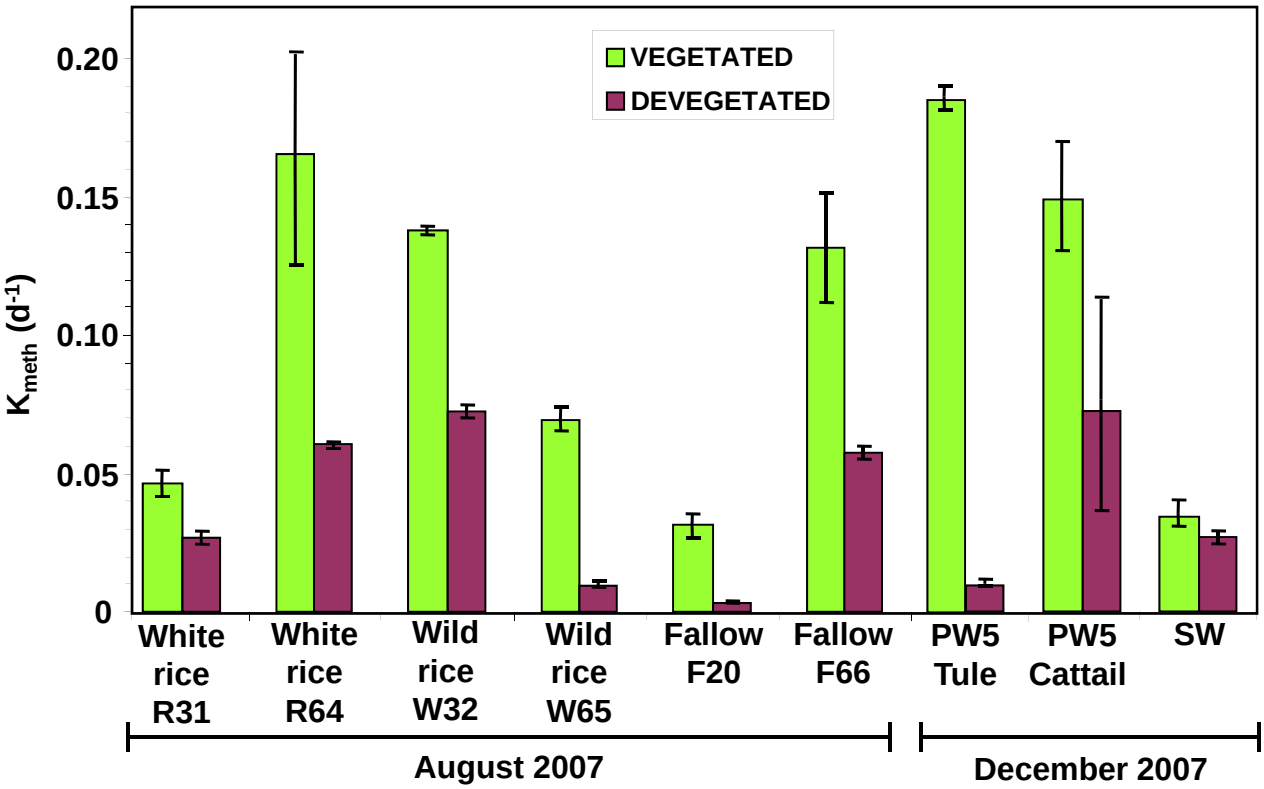

Figure 7.4. Bar graph depicting the 'devegetation effect' on the microbial mercury methylation rate constant in agricultural fields (August 2007) and non-agricultural fields (December 2007). N=2 observations for each treatment. Error bars denote ± [absolute difference]/2.

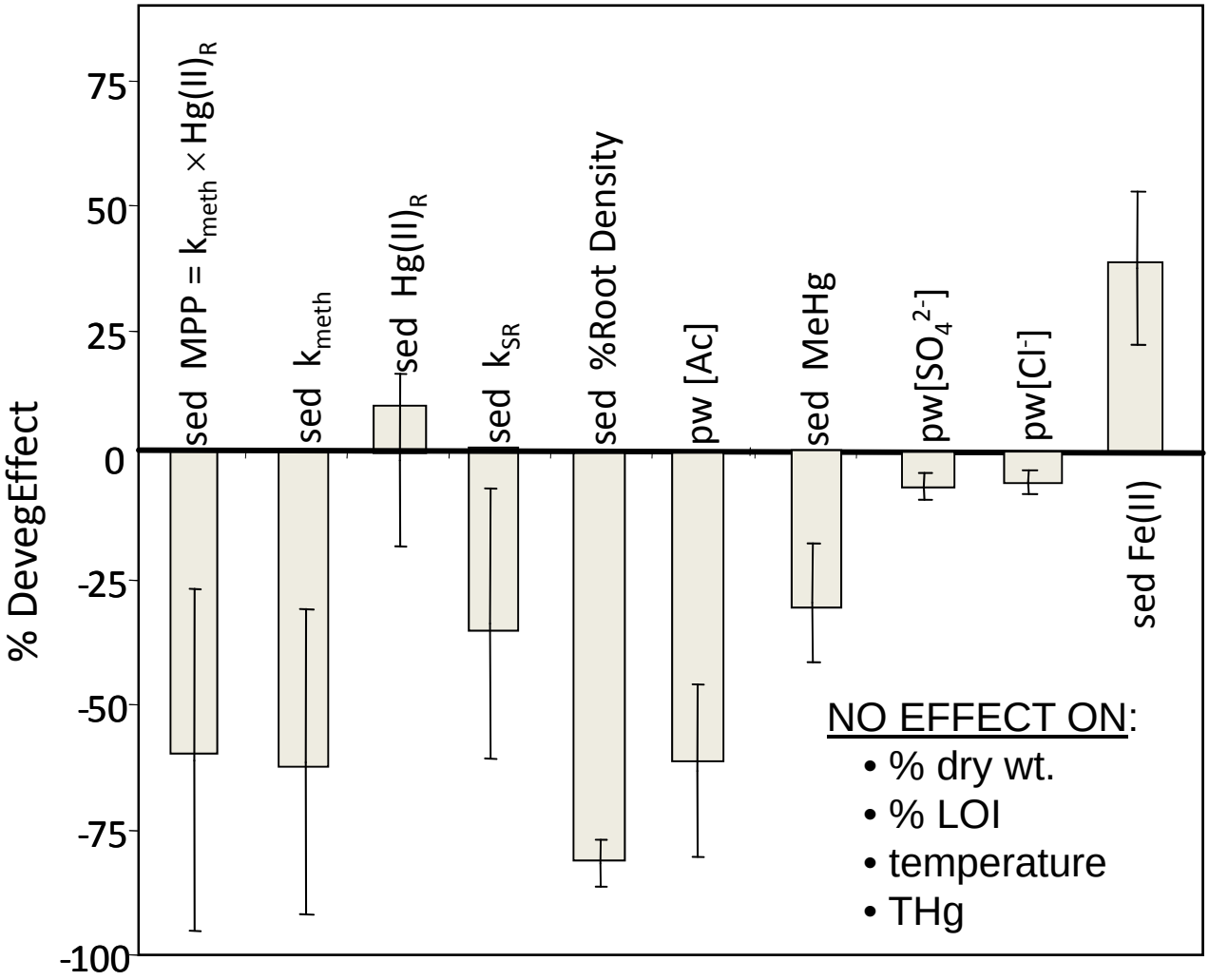

Figure 7.5. Bar graph of the percent devegetation effect on sediment and pore-water parameters in agricultural fields during the period of peak biomass (August 2007). Parameter notation as per **Table 6.1.** Percent devegetation effect (%DevegEffect) was calculated as per **Equation 7.1**. Significance assessed at $p<0.05$ with pairwise t-tests. Error bars denote ± 1 standard deviation for n=5 agricultural fields. Non-significant comparisons (e.g. percent moisture, percent loss on ignition, temperature, total mercury) are not shown.

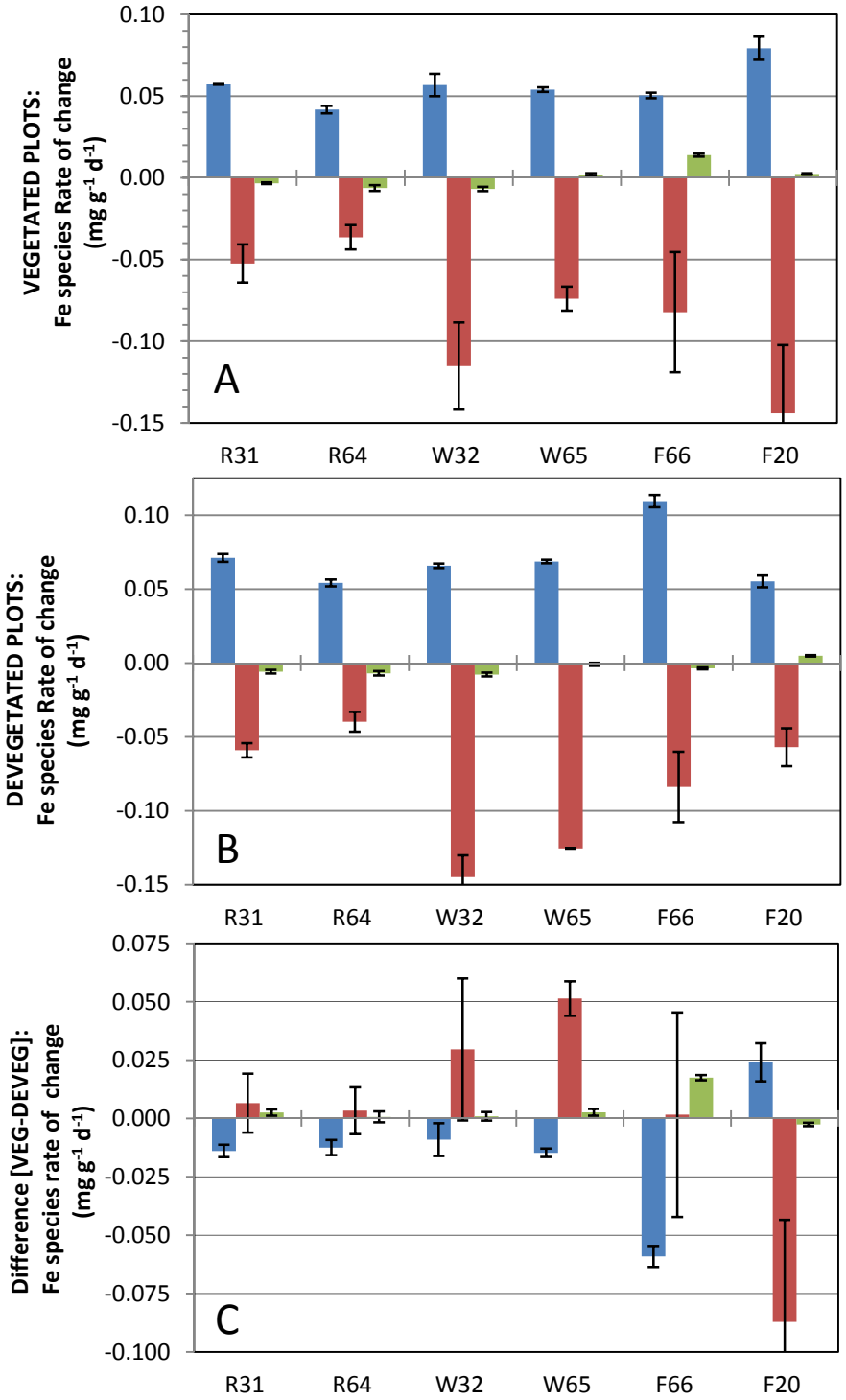

Figure 7.6. Bar graph of time-integrated daily rates of change in iron species in the surface (0-2 cm) sediment interval of individual agricultural fields for A) vegetated plots and B) devegetated plots, and C) the difference of vegetated plots minus devegetated plots. Error bars represent compounded errors. Rates were calculated based on an initial time-point of flood-up (June for white rice and wild rice, July for fallow) and a mid-season time point of peak temperatures and biomass (August for all sites). All rates are reported on a sediment dry weight basis. Iron species: Fe(II), acid-extractable ferrous iron; cFeIII, crystalline ferric iron; aFeIII, amorphous ferric iron.

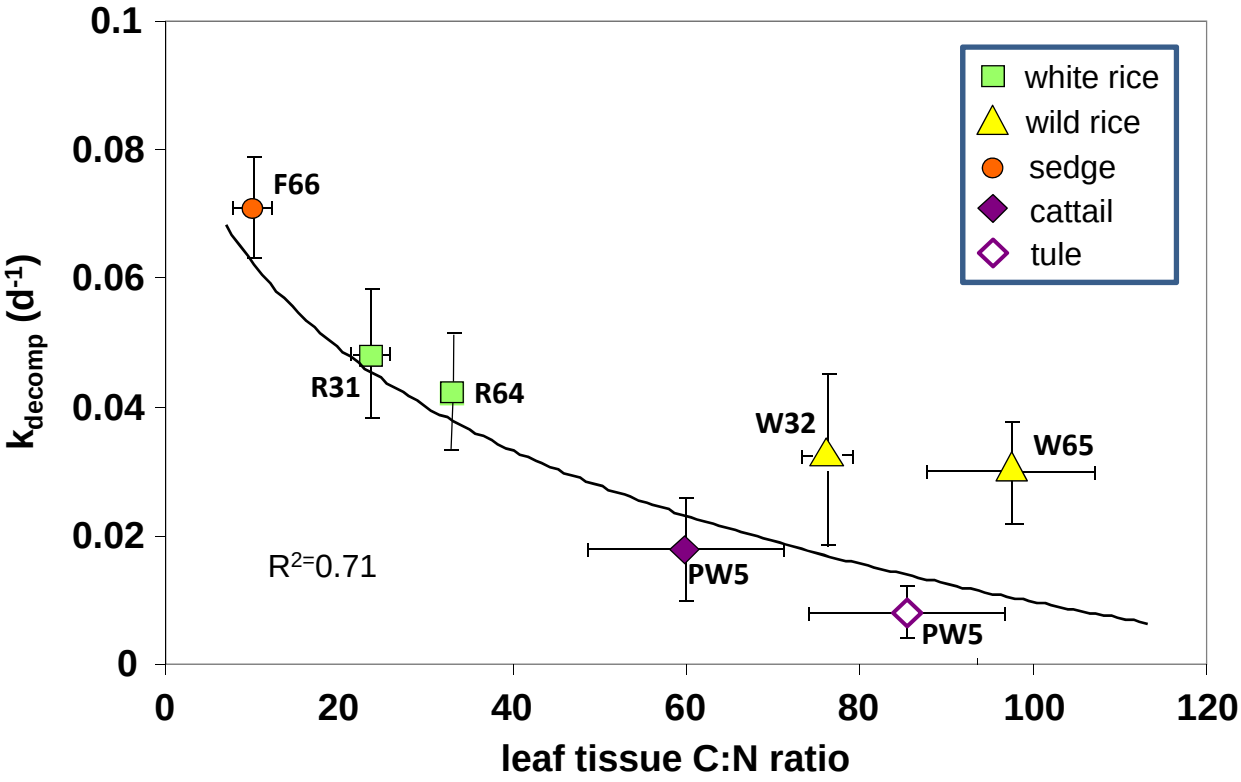

Figure 7.7. Scatterplot of leaf tissue carbon-to-nitrogen ratios versus litter decomposition rate constants for the dominant plant species in each field type. Plant tissue decomposition rate constants (k_{decomp}) were assessed experimentally in the laboratory during 28 days of incubations at 30°C. Error bars denote ± 1 standard deviation. An exponential regression was fit to the data (y= -0.12 ln(x)) and was significant at $p<0.05$.

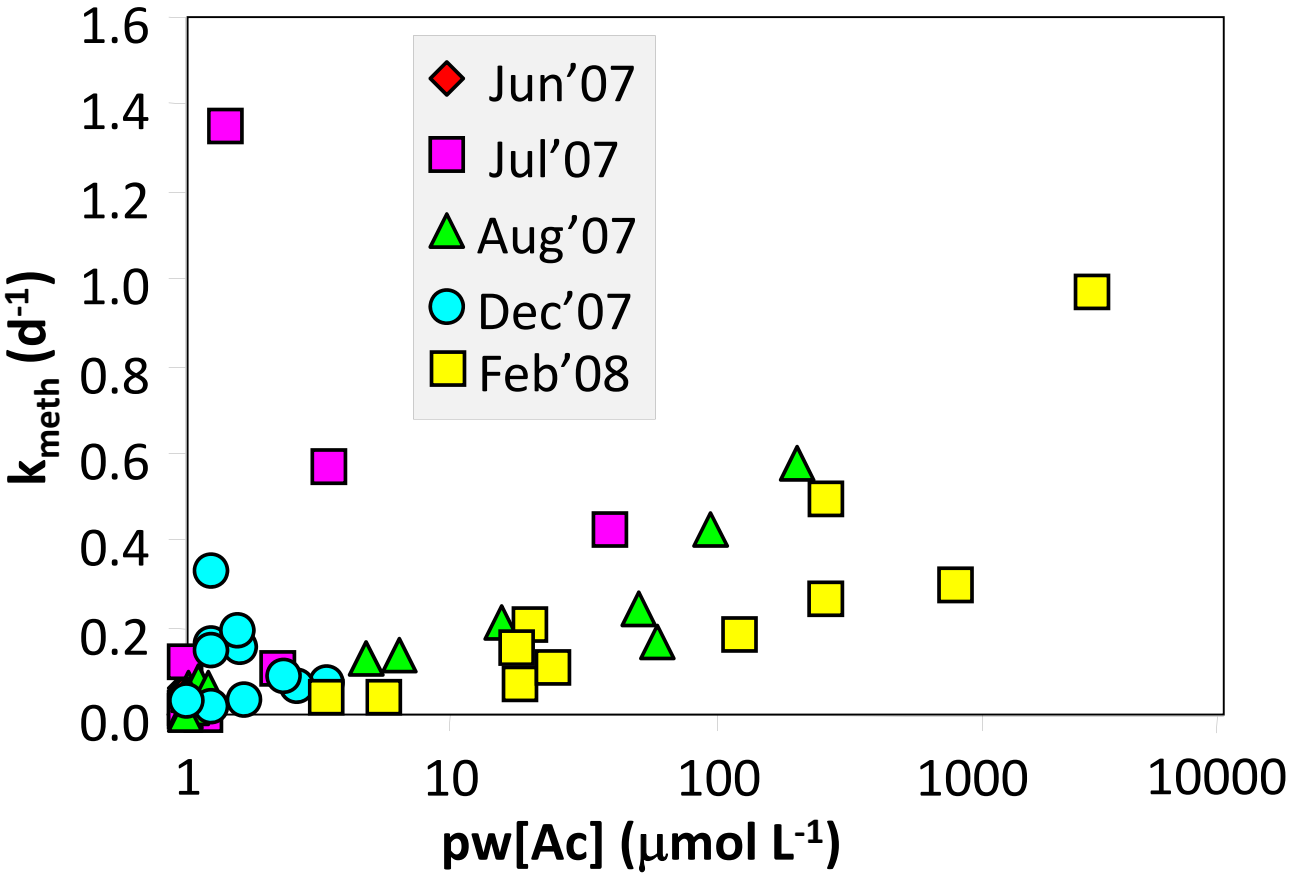

Figure 7.8. Log-linear plot of sediment pore water acetate concentration versus the mercury methylation rate constant, by sampling period. Significant ($p<0.05$) non-linear relationships were observed for the peak of the growing season (August 2007; $y=0.02 \ln(x)$, $r^2=0.42$) and for the mid-winter period during rice-straw decay (February 2008; $y=0.02 \ln(x)$, $r^2=0.39$).

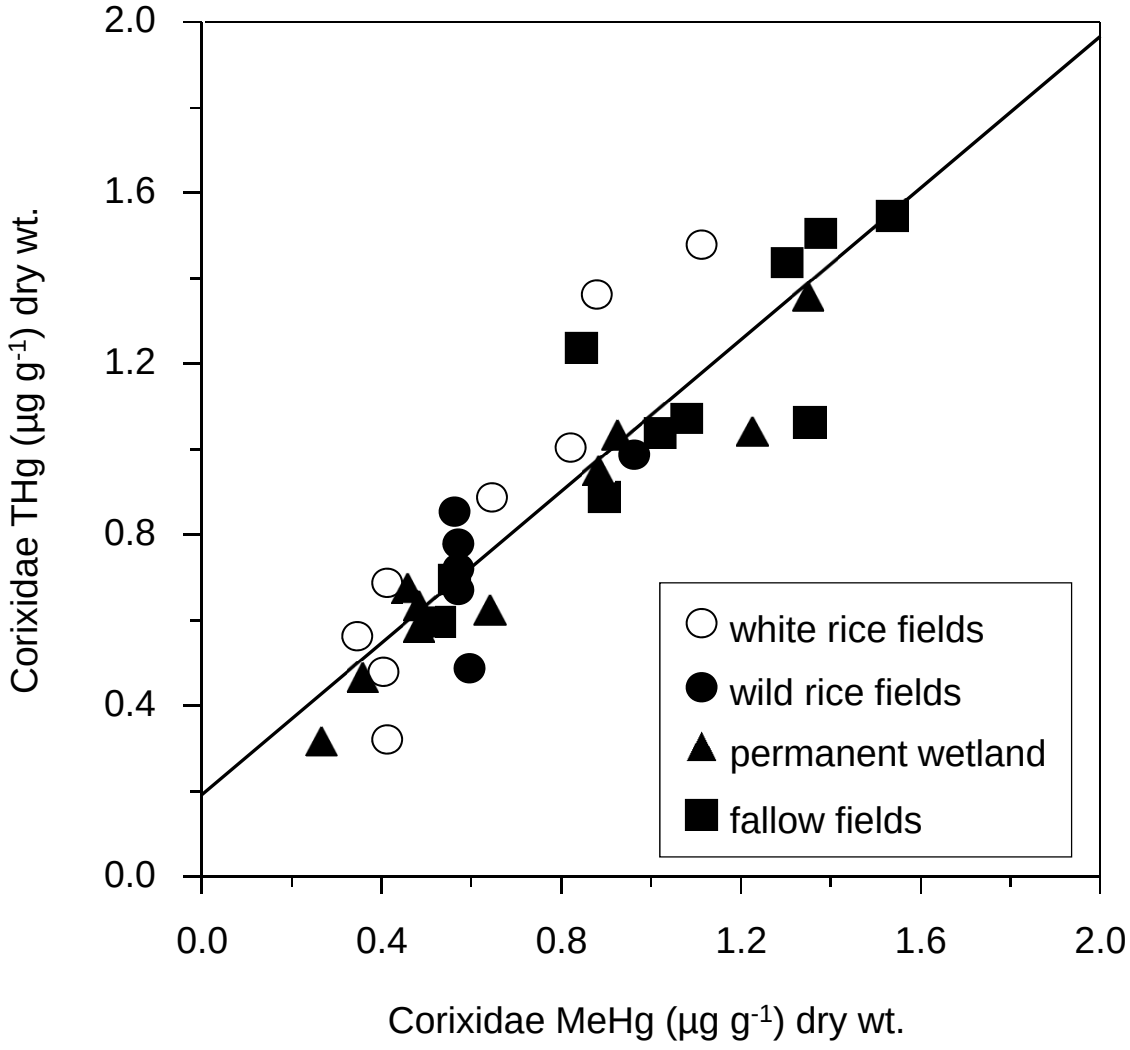

Figure 8.1. Scatter plot of Corixidae (water boatmen) methylmercury concentration versus total mercury concentration, by habitat type, in the Yolo Bypass Wildlife Area. Linear regression N=34, R^2=0.80, P<0.0001.

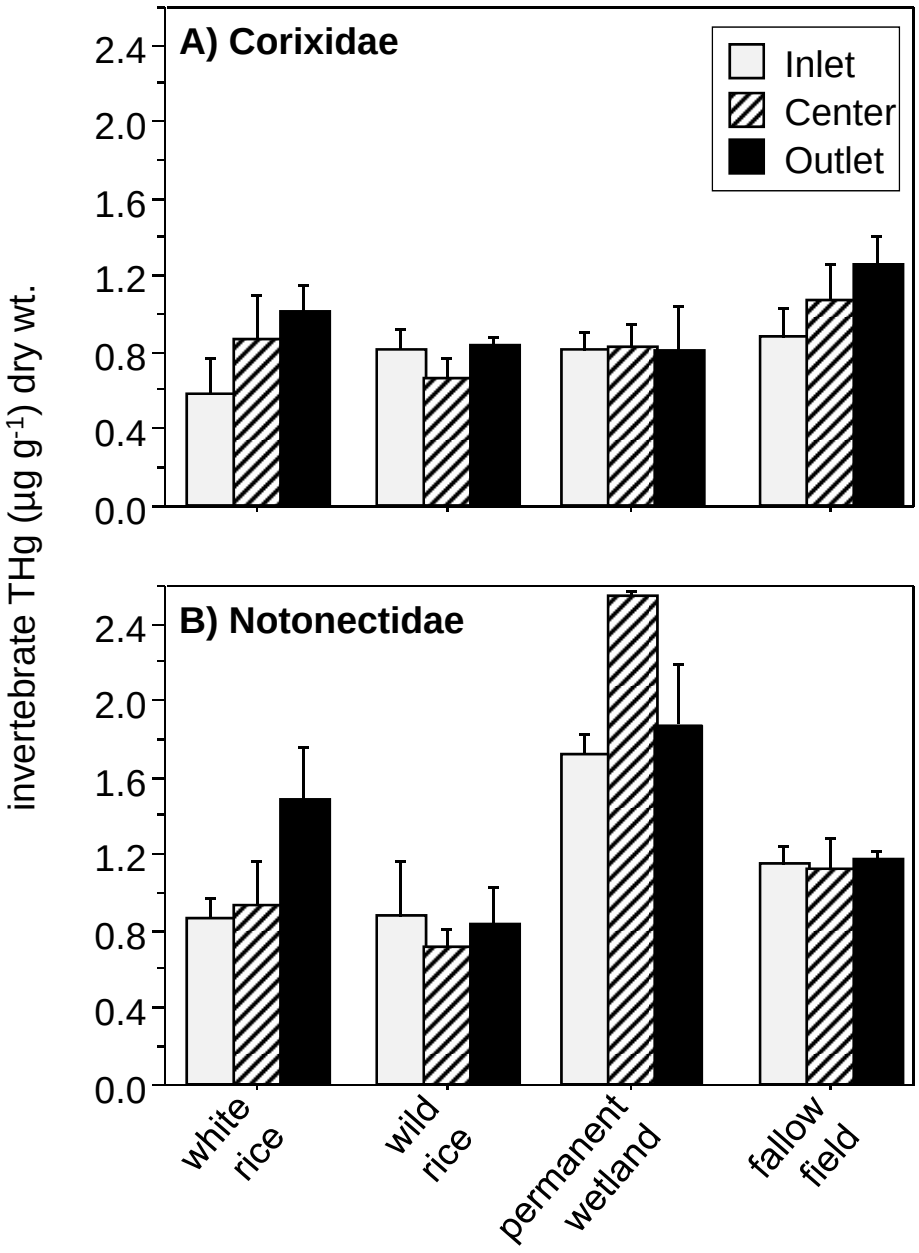

Figure 8.2. Bar graph of total mercury concentration in (A) Corixidae (water boatmen) and (B) Notonectidae (back swimmers) in agricultural fields of the Yolo Bypass Wildlife Area. Error bars reflect the standard error of the mean.

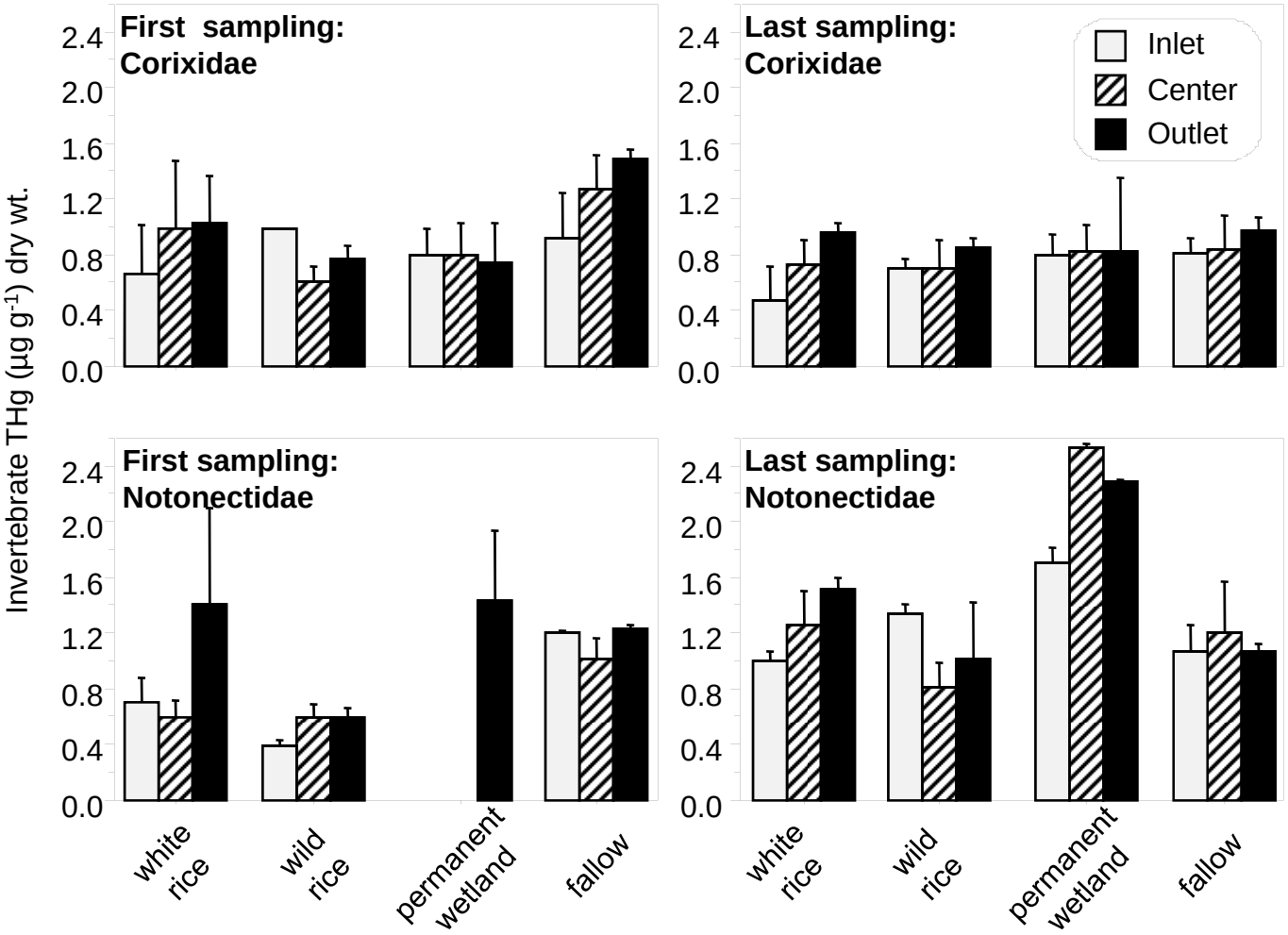

Figure 8.3. Bar graphs of total mercury concentration in Corixidae (water boatmen) and Notonectidae (back swimmers) at the inlets, centers , and outlets of shallowly-flooded fallow fields , by field type, in the Yolo Bypass Wildlife Area, during the first (25 June to 6 July 2007) and last (28 August to 19 September 2007) sampling event. Error bars reflect the standard error of the mean. The total number of observations were N=36 for Corixidae and N=45 for Notonectidae.

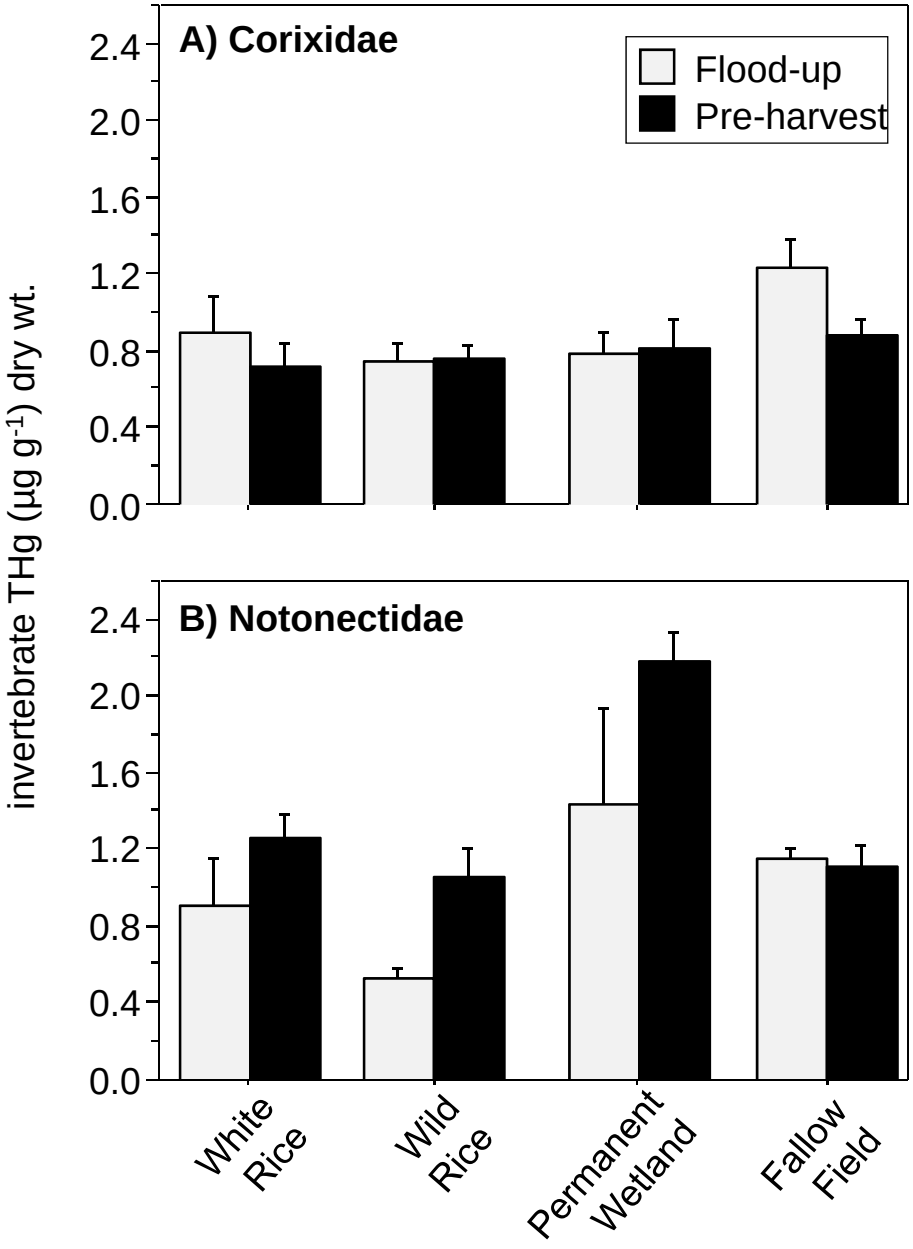

Figure 8.4. Bar graphs of total mercury concentration in (A) Corixidae (water boatmen) and (B) Notonectidae (back swimmers), by habitat type, during the field management periods of flood-up and rice pre-harvest in the Yolo Bypass Wildlife Area. Error bars reflect the standard error of the mean. The total number of observations were N=36 for Corixidae and N=45 for Notonectidae.

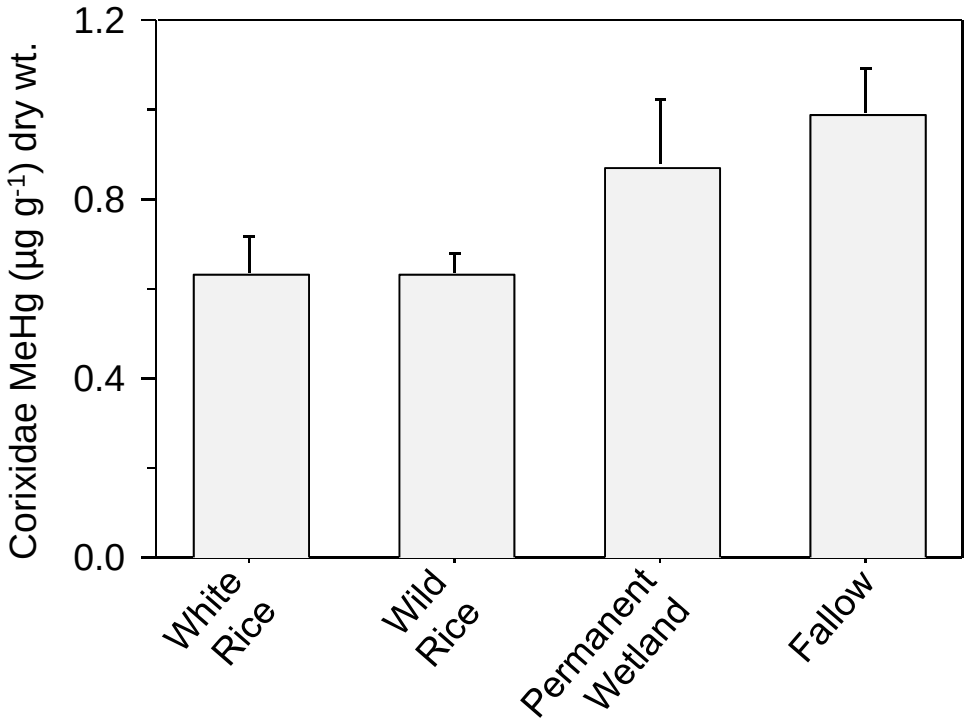

Figure 8.5. Bar graph of methylmercury concentration in Corixidae (water boatmen), by habitat type, in Yolo Bypass Wildlife Area. Error bars reflect the standard error of the mean. The total number of observations were N=36 for Corixidae and N=45 for Notonectidae.

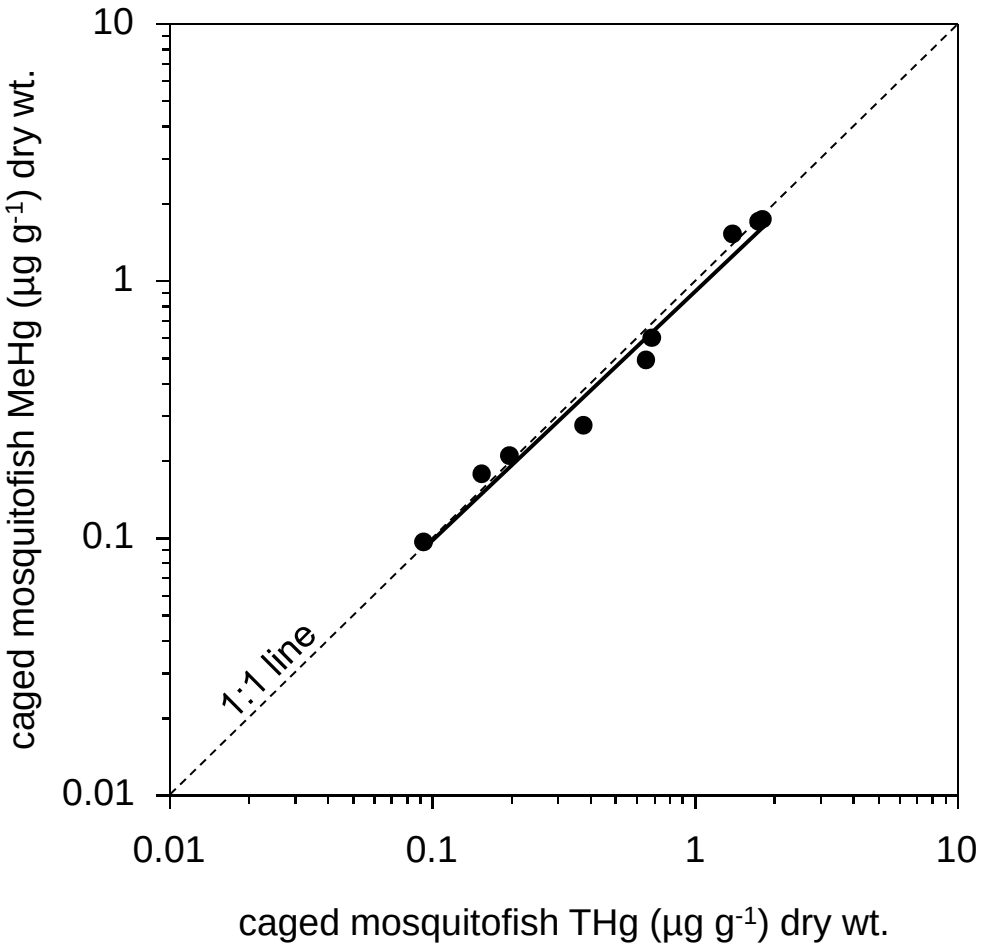

Figure 8.6. Log-Log plot of total mercury concentration versus methylmercury concentration in western mosquitofish introduced into cages within flooded agricultural fields in the Yolo Bypass Wildlife Area, California. The dashed line indicates the 1:1 relationship.

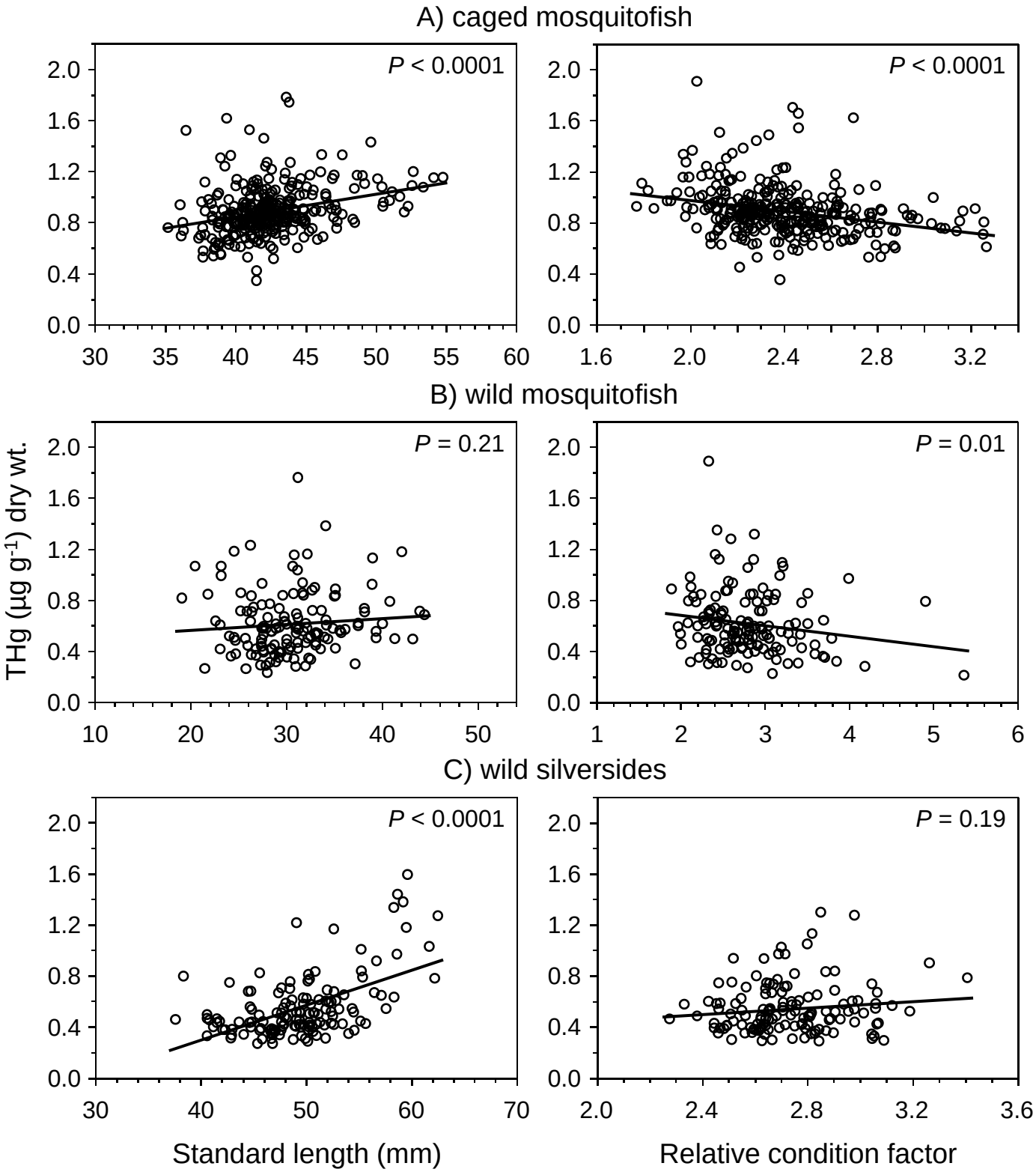

Figure 8.7. Partial leverage plots depicting the relationship between total mercury concentration and standard length or relative condition factor of (A) caged western mosquitofish, (B) wild western mosquitofish, and (C) wild Mississippi silversides in wetlands at the Yolo Bypass Wildlife Area. Partial leverage plots account for the potential effects of wetland habitat type, site within the wetland, habitat × site interaction, standard length, and the relative condition factor as fixed effects, and wetland replicate as a random effect.

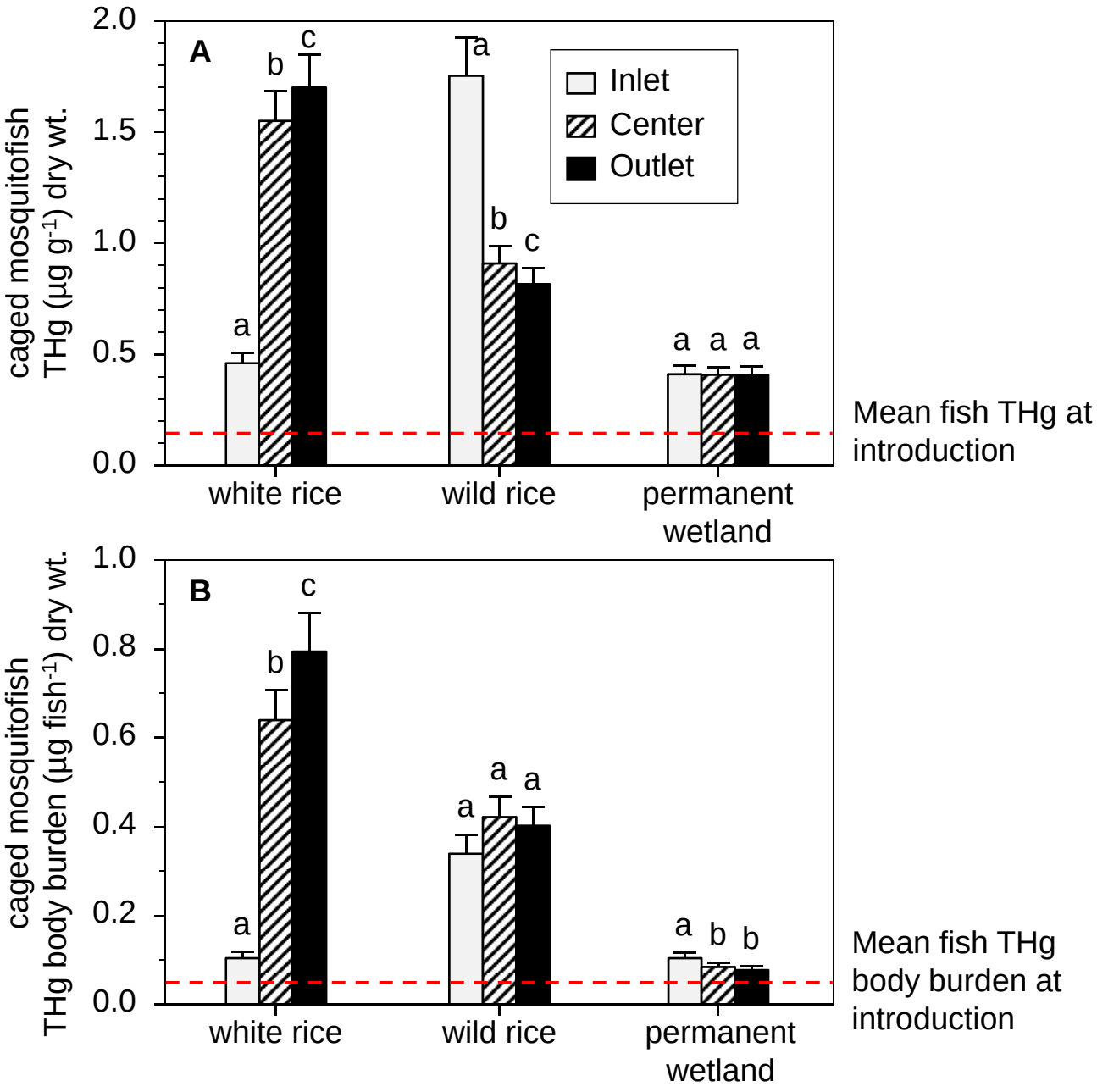

Figure 8.8. Bar graphs of (A) total mercury concentration and (B) total mercury body burden in western mosquitofish removed from cages after a 60-day of exposure period at the inlets, centers , and outlets of white rice, wild rice, and permanent wetland fields during the 2007 rice growing season at the Yolo Bypass Wildlife Area, California. The dashed lines indicate mean THg concentrations and body burdens of reference mosquitofish (*N* = 37) at the time of introduction into the cages. Different lowercase letters above bars indicate that values within a wetland habitat are statistically different ($p < 0.05$). Error bars reflect the standard error of the mean. The total number of observations was N=304 caged mosquitofish at removal.

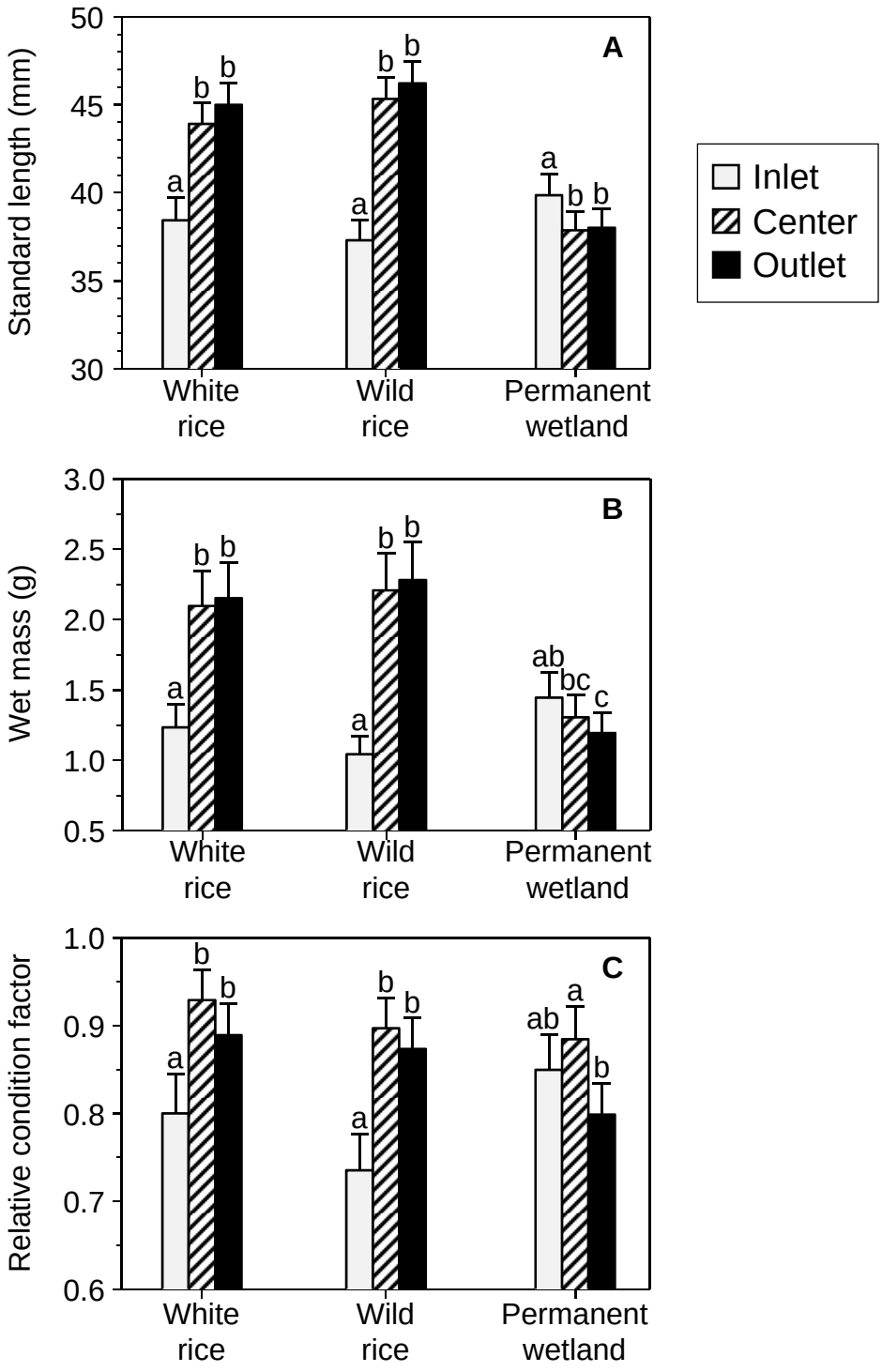

Figure 8.9. Bar graphs of (A) Standard length, (B) fresh wet mass, and (C) relative condition factor for western mosquitofish removed from cages after a 60-day exposure period at inlets, centers , and outlets of white rice fields, wild rice fields, and permanent wetlands during the 2007 rice-growing season, in the Yolo Bypass Wildlife Area, California. Different lowercase letters above bars indicate that values within a wetland habitat are statistically different ($P < 0.05$). Error bars reflect the standard error of the mean.

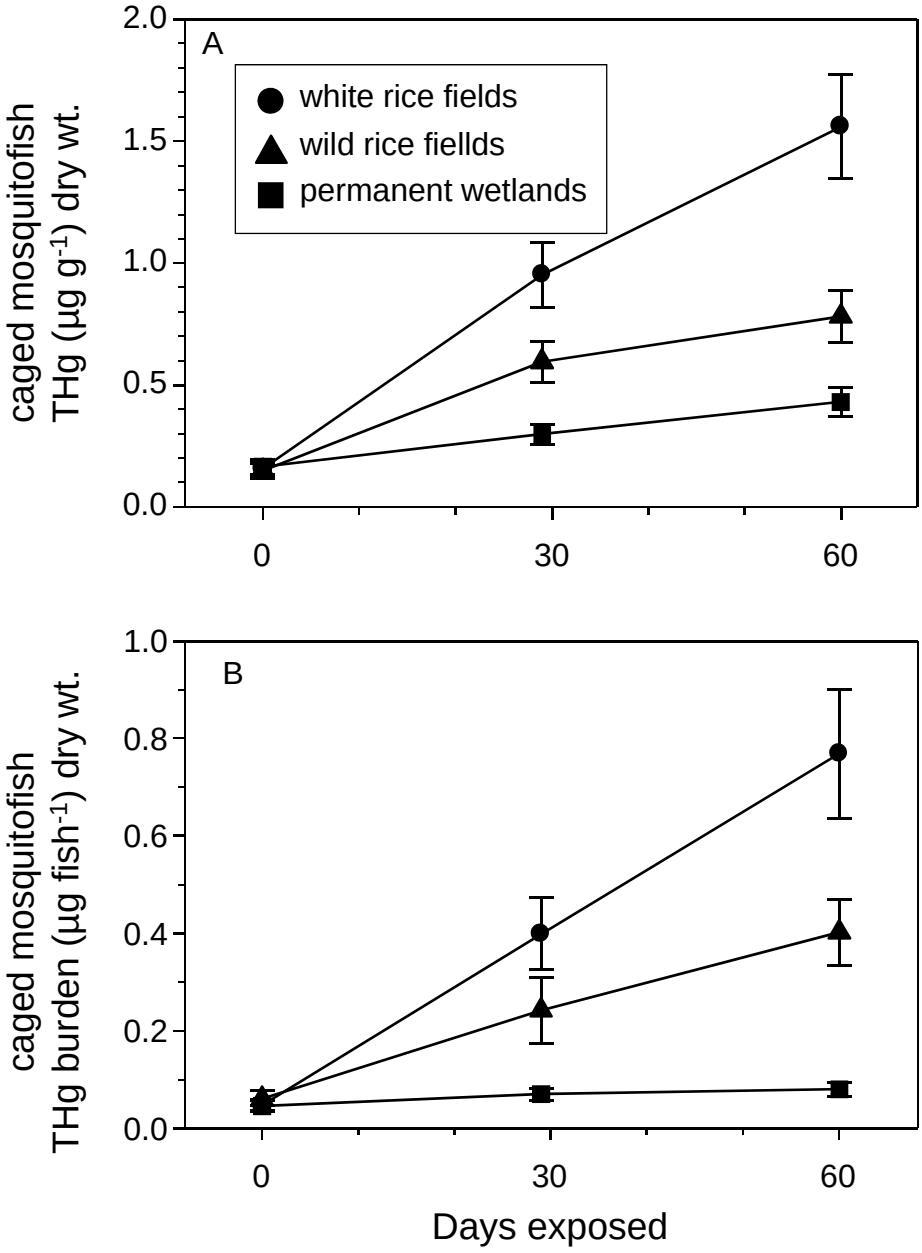

Figure 8.10. Time series plots of (A) total mercury concentration and (B) total mercury body burden of caged western mosquitofish over 60 days of exposure at the outlets of white rice, wild rice, and permanent wetland fields, during the 2007 rice growing season at the Yolo Bypass Wildlife Area, California. Error bars reflect the standard error of the mean.

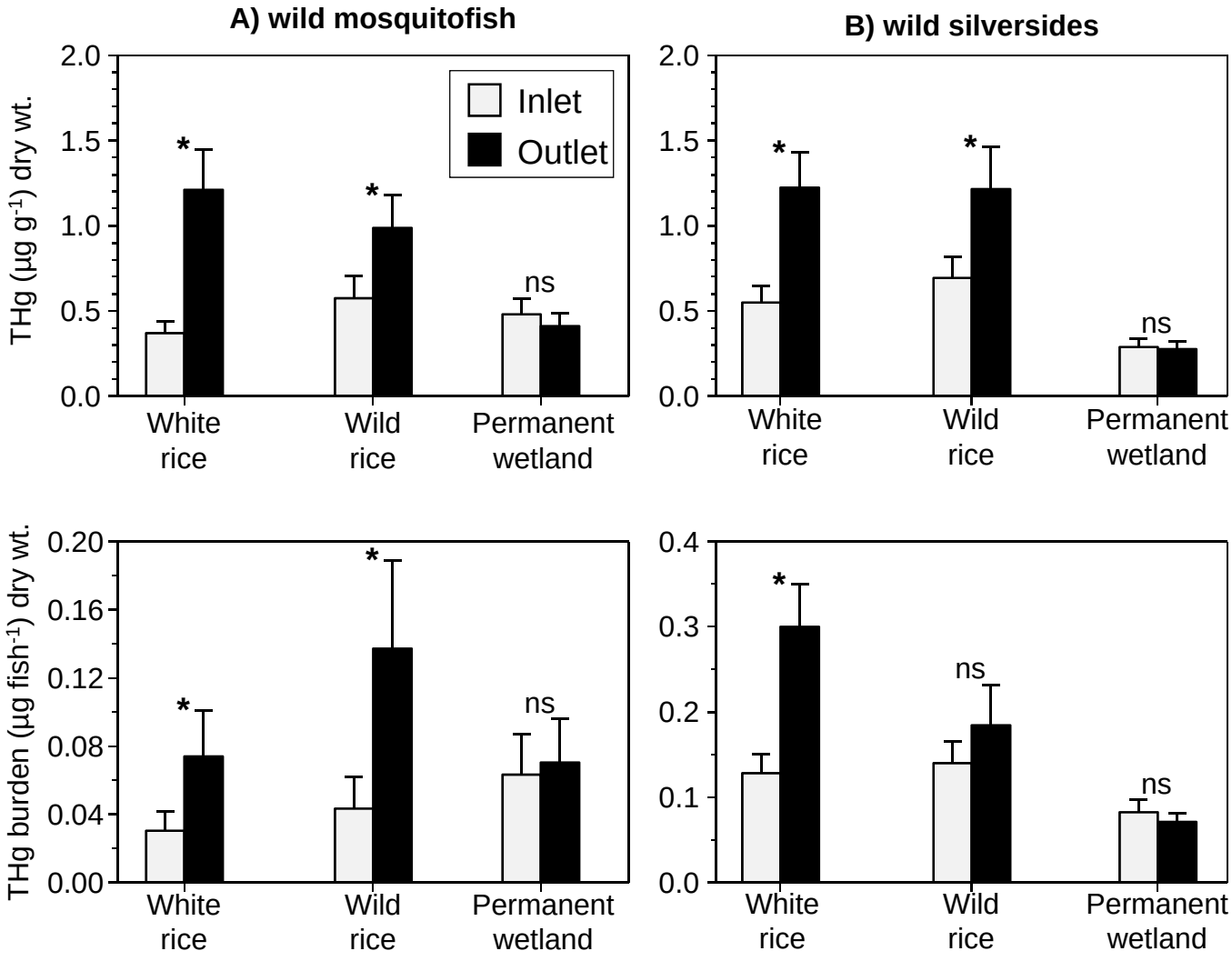

Figure 8.11. Bar graphs of total mercury concentrations and total mercury body burden in (A) wild western mosquitofish and (B) wild Mississippi silversides caught at the inlets and outlets of white rice, wild rice, and permanent wetland fields during the 2007 rice growing season at the Yolo Bypass Wildlife Area. Asterisk symbols above bars indicate that inlets and outlets within a wetland habitat are statistically different ($P < 0.05$) and "ns" indicates that values are not statistically different. Error bars reflect the standard error of the mean.

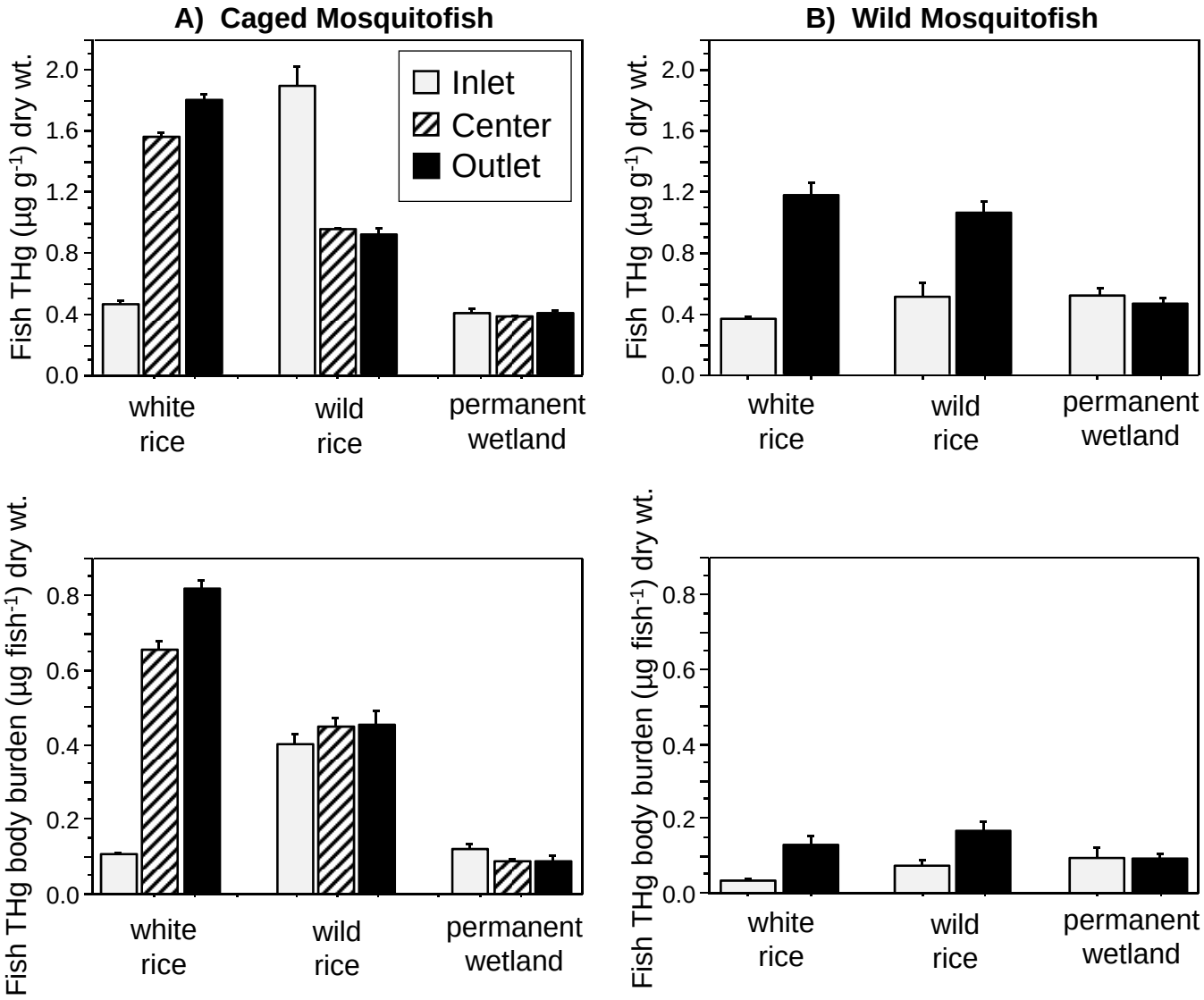

Figure 8.12. Bar graphs of (A) caged mosquitofish and (B) wild caught mosquitofish total mercury concentrations and total mercury body burden at the inlets, centers (caged only), and outlets of white rice, wild rice, and permanent wetlands during the 2007 rice growing season at the Yolo Bypass Wildlife Area. Error bars reflect the standard error of the mean.

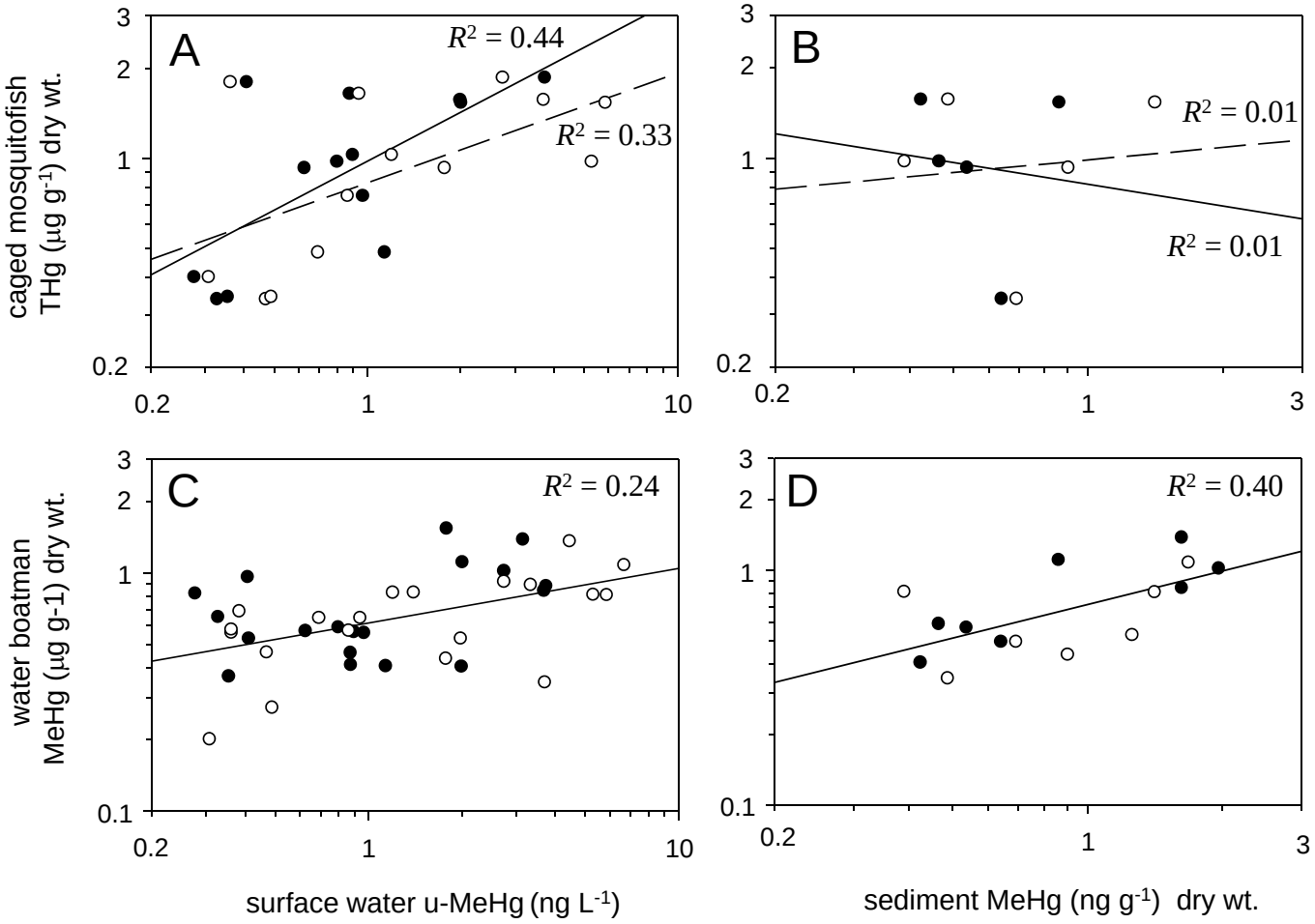

Figure 8.13. Log-Log plots of caged mosquitofish total mercury concentration versus (A) surface water unfiltered methylmercury concentration and (B) sediment methylmercury concentration, and Corixidae (water boatman) methylmercury concentration versus (C) surface water unfiltered methylmercury concentration and (D) sediment methylmercury concentration in agricultural and non-agricultural wetlands of the Yolo Bypass Wildlife Area during 2007. Closed symbols and solid lines indicate samples collected following flood-up of rice fields (early June) and open symbols and dashed lines indicate samples collected just before rice harvest (early September). Sediment only collected at centers of fields.

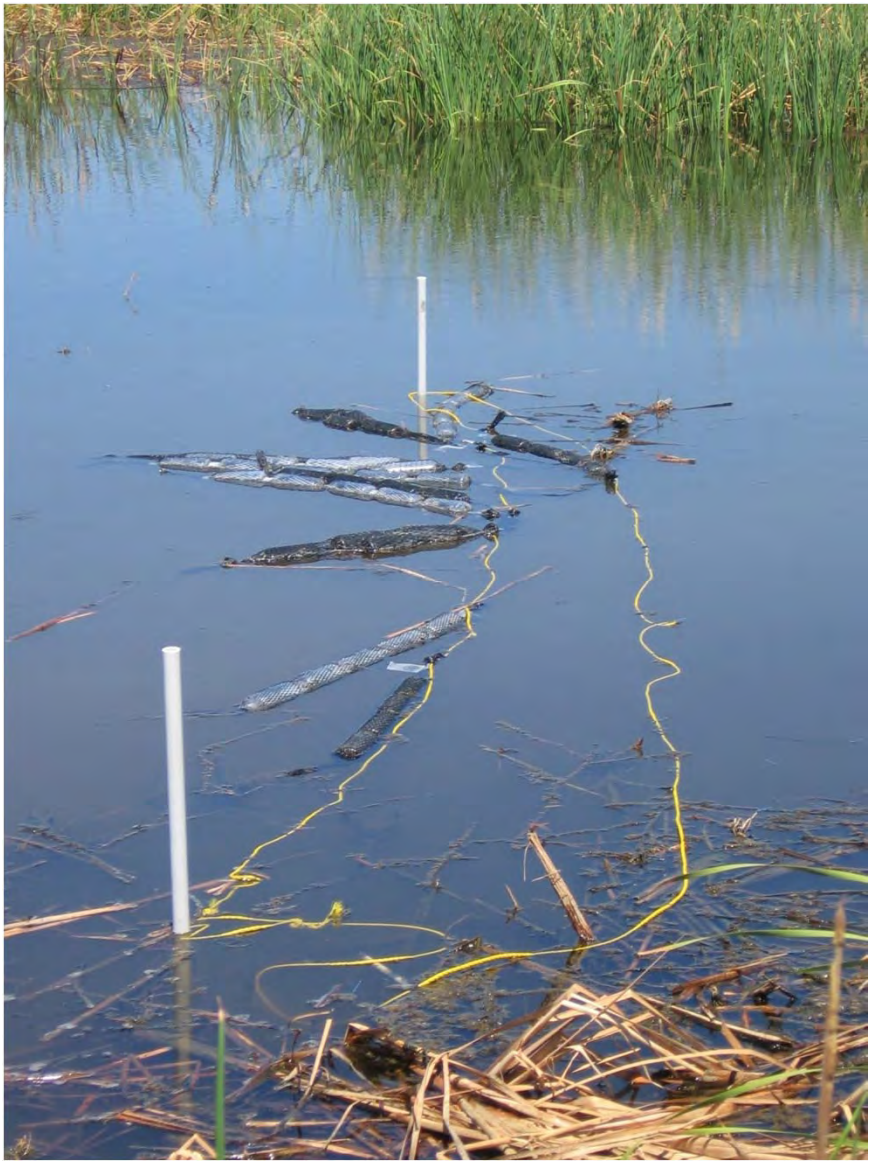

Figure 9.1. Photograph of photodemethylation experiment in the Yolo Bypass Wildlife Area, Calif.. Opaque Teflon® bottles were used as dark controls and clear Teflon® bottles were used for photo-sensitive treatments, reflecting conditions in surface waters.

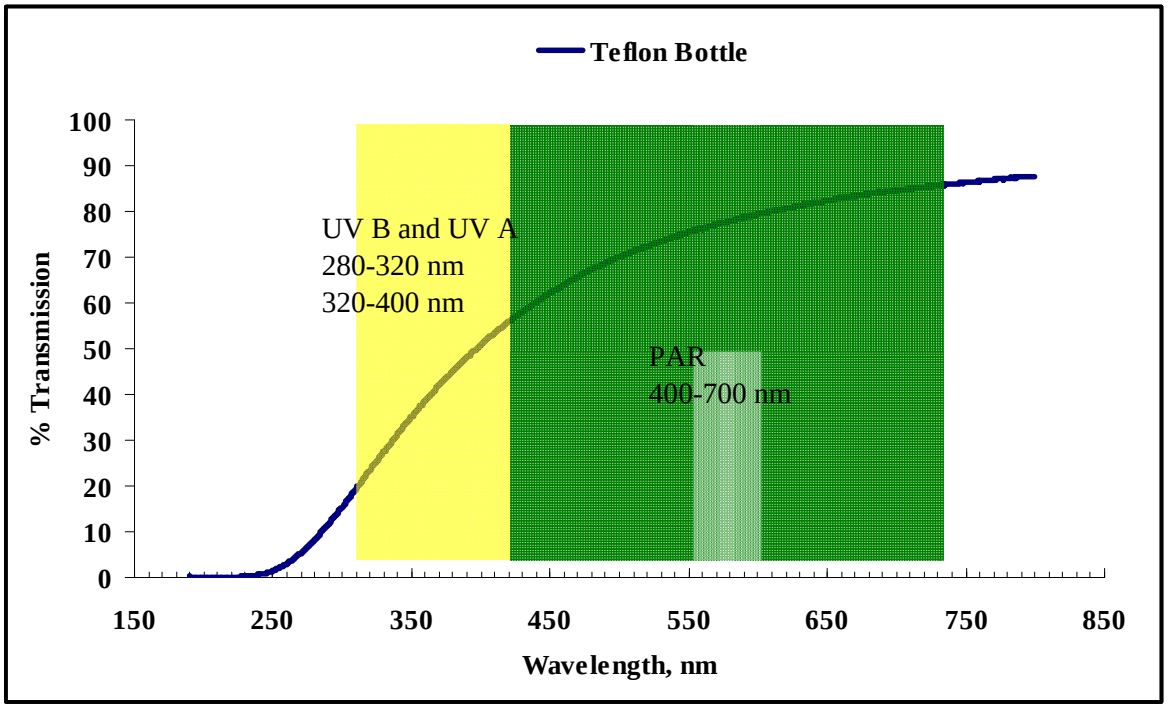

Figure 9.2. Graph showing light wavelength versus the percentage of light transmission through the incubation bottles used in the photodemethylation experiments. The percentage (%) transmission of UV-visible wavelengths through a clear FEP Teflon® bottle was determined in the laboratory with a spectrophotometer. The average light transmission in the photosynthetically available radiation (PAR) and ultra violet (UV) regions were estimated to be 69% and 35%, respectively. Figure from **Byington (2007)**.

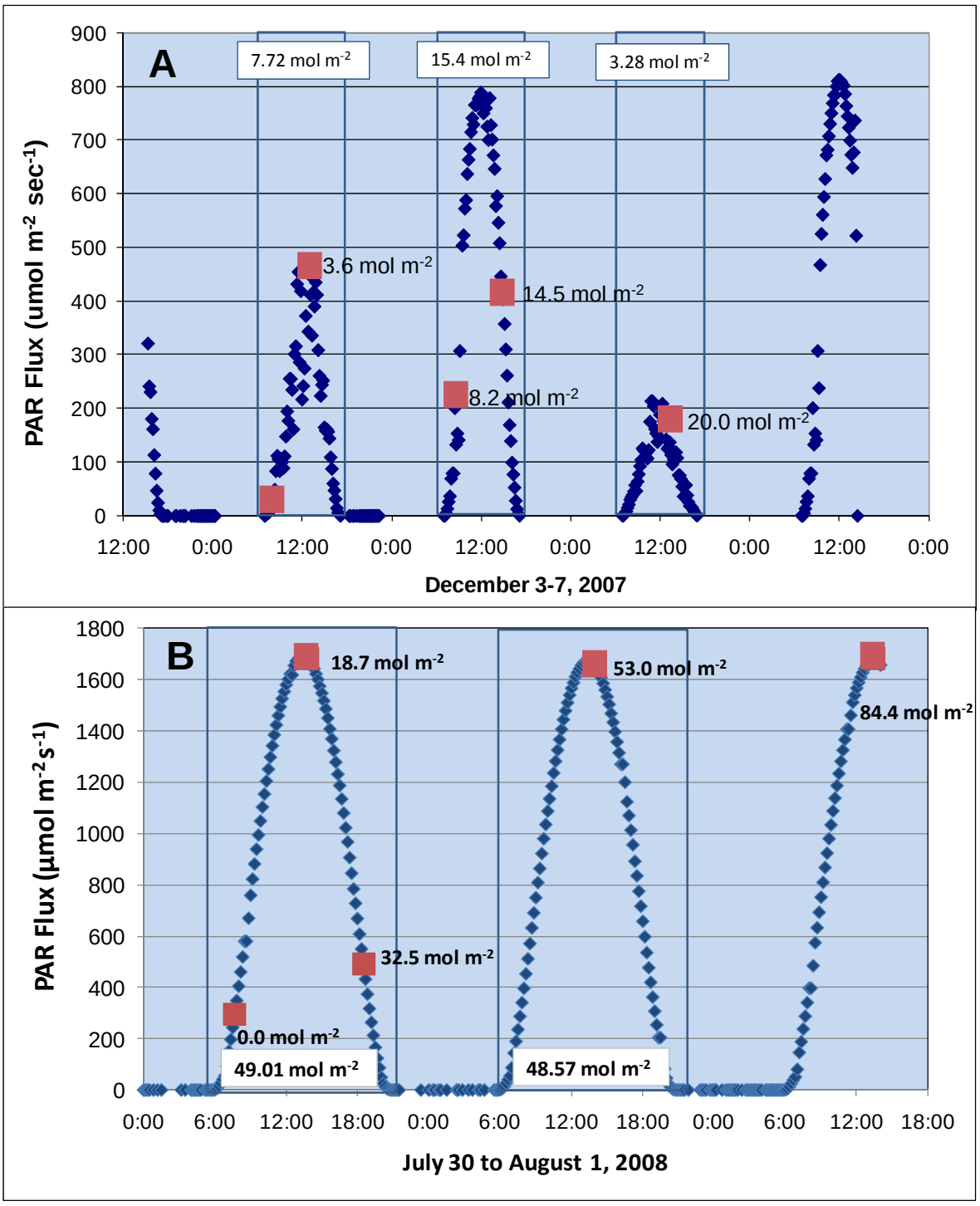

Figure 9.3. Time series plots of instantaneous flux of photosynthetically available radiation for A) December 3–7, 2007 and B) July 30 – August 1, 2008. Shaded areas for both time series are annotated with the total ultraviolet (UV, Uva + UVb) radiation flux (mol m^{-2}) for a given day, illustrating the daily variability in winter UV flux and more consistent summer UV flux. Shown in both figures are the time points (red square) and average, cumulative total in-bottle PAR flux (mol m^{-2}) at the time of sample collection.

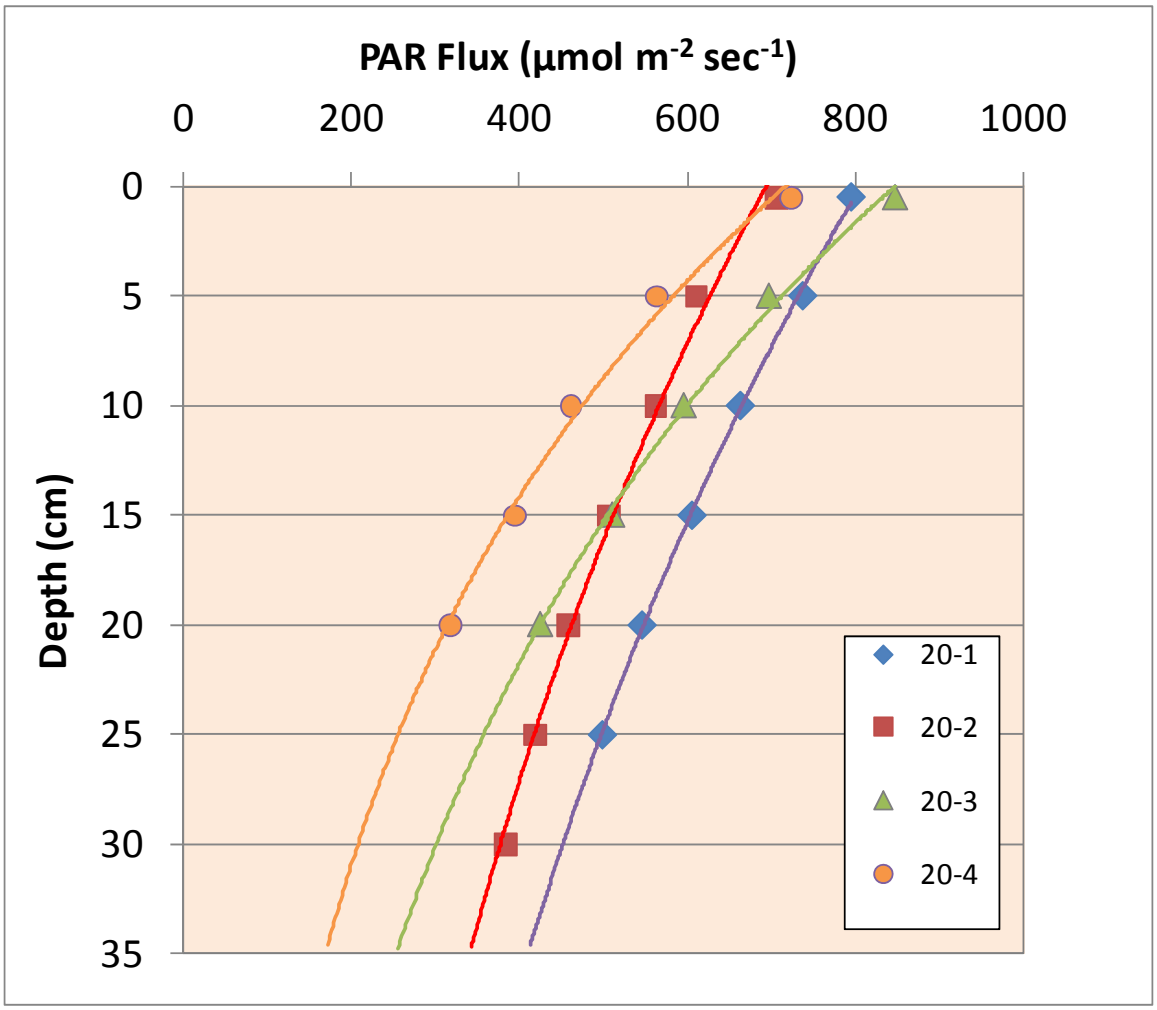

Figure 9.4 Graph showing instantaneous flux of photosynthetically available radiation versus water column depth, as a measure of light attenuation. Data collected at four replicate sites of open-water areas of field R20 on June 26, 2008. Extinction coefficients varied from 0.019 (site 20-1) to 0.041 cm^{-1} (site 20-3).

A) PAR wavelengths (400–700 nm)

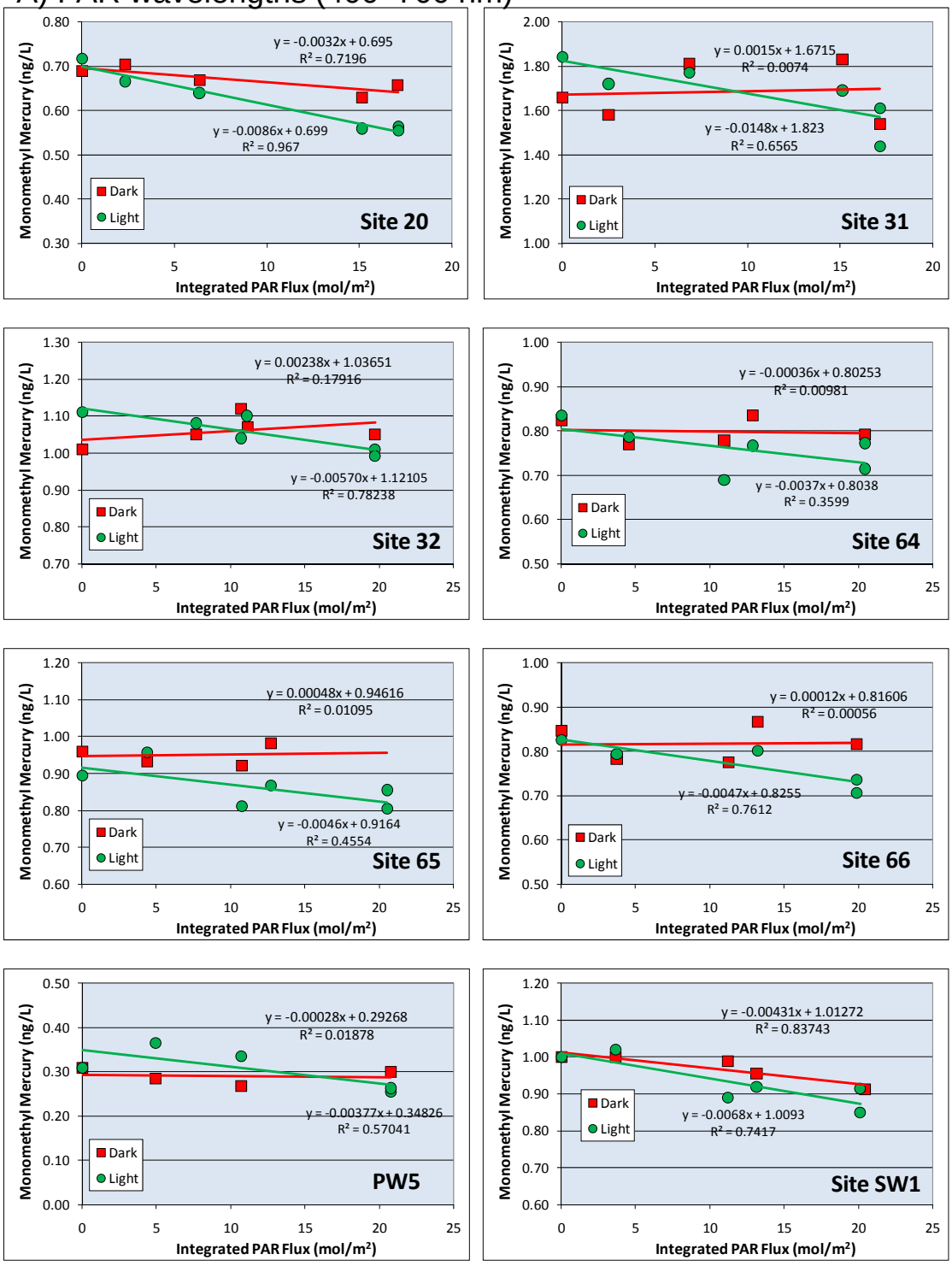

Figure 9.5. Scatter plots showing least-squares linear regressions of integrated (cumulative) solar radiation versus aqueous methylmercury concentration for December 3–7, 2007 based on A) PAR wavelengths (400–700 nm) and B) total UV wavelengths (UVa + UVb). Samples exposed to light shown in green, samples from dark control bottles shown in red.

B) UV wavelengths (UVa + Uvb; 280–400 nm).

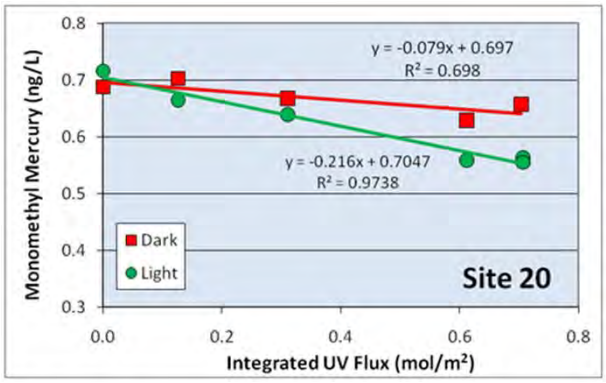

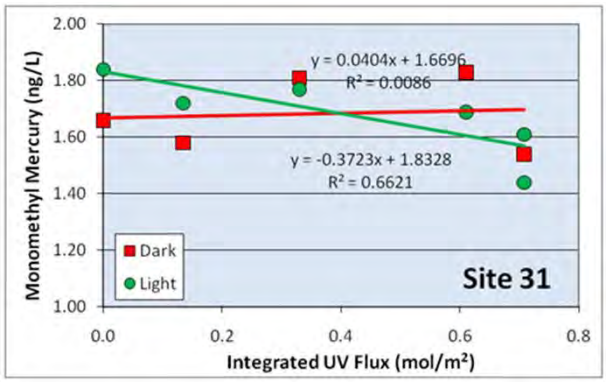

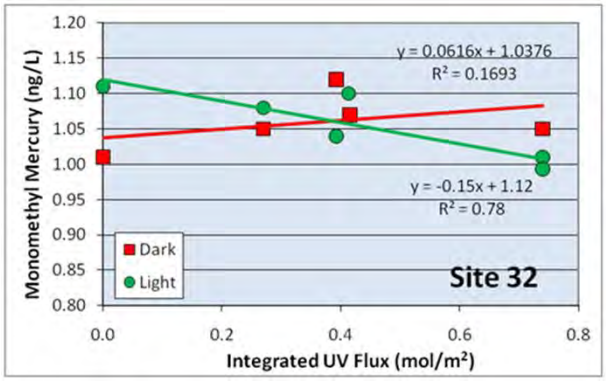

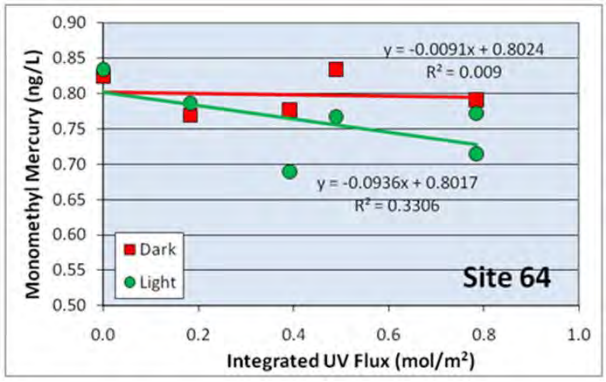

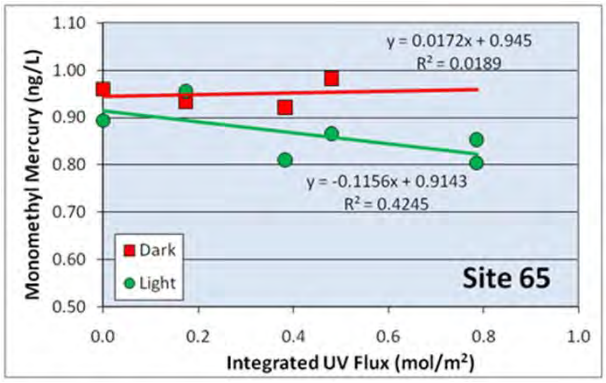

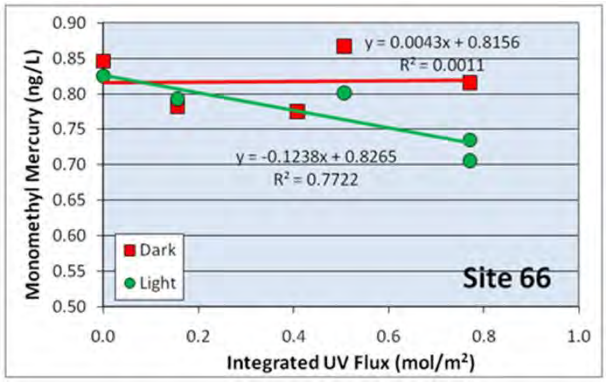

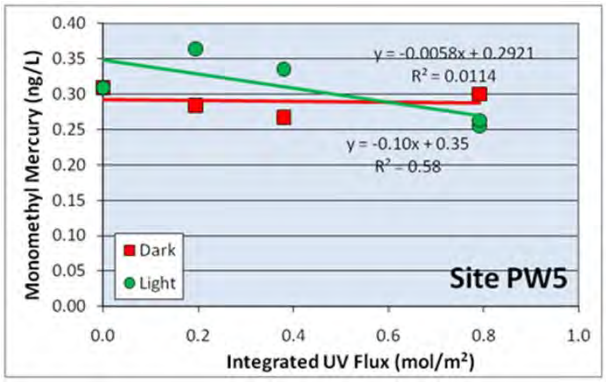

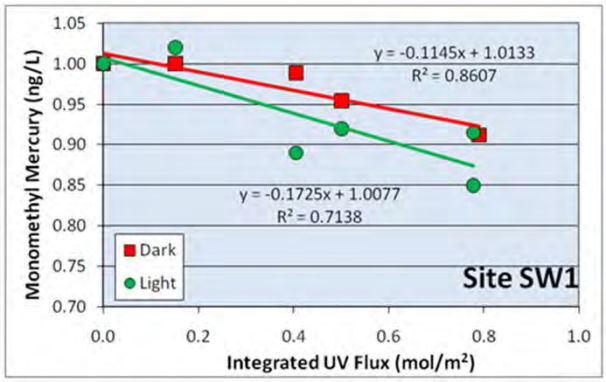

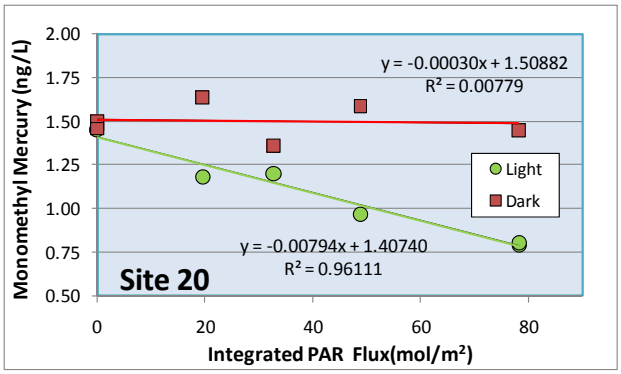

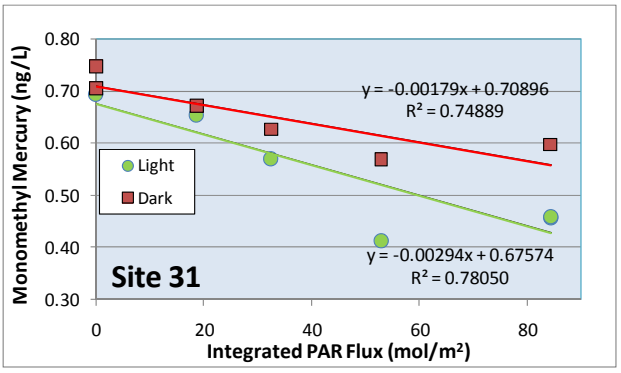

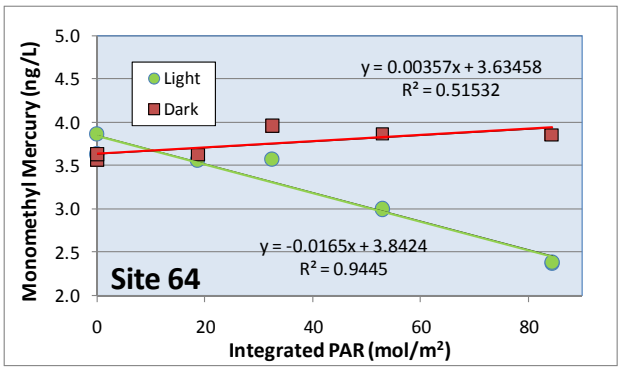

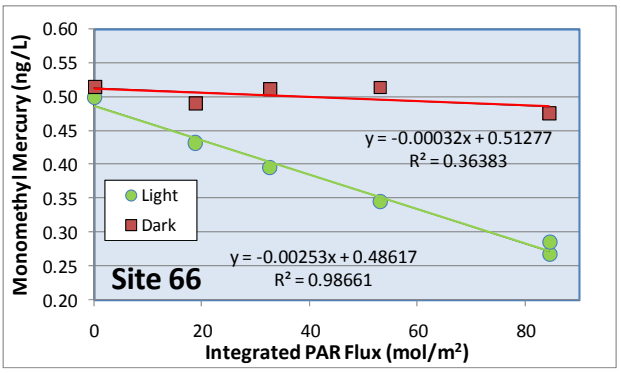

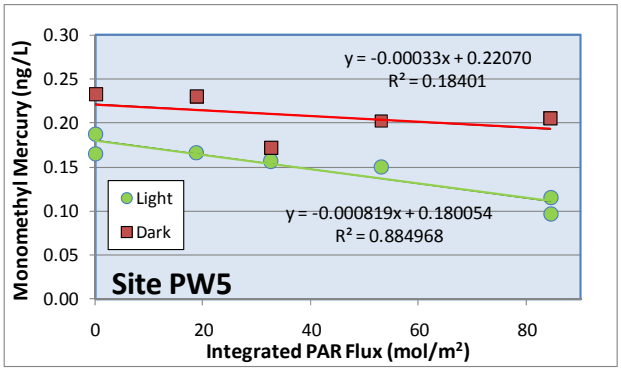

Figure 9.6. Scatter plots showing least-squares linear regressions of integrated photosynthetically available radiation versus aqueous methylmercury concentration for July–August 2008 incubations. Samples exposed to light shown in green, samples from dark control bottles shown in red.

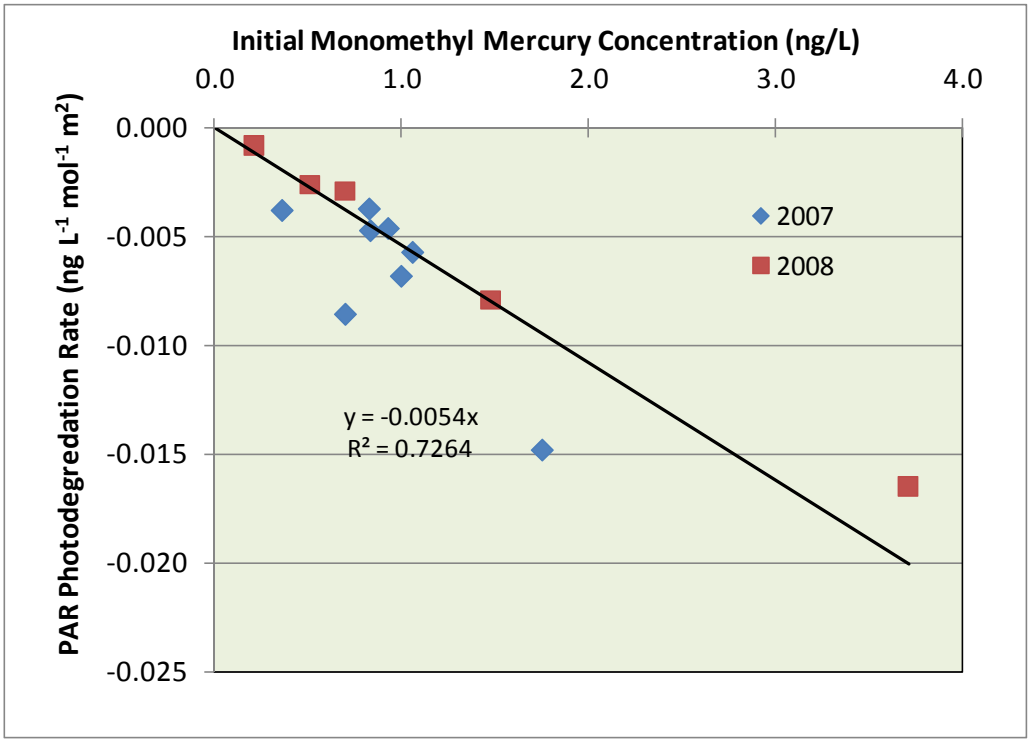

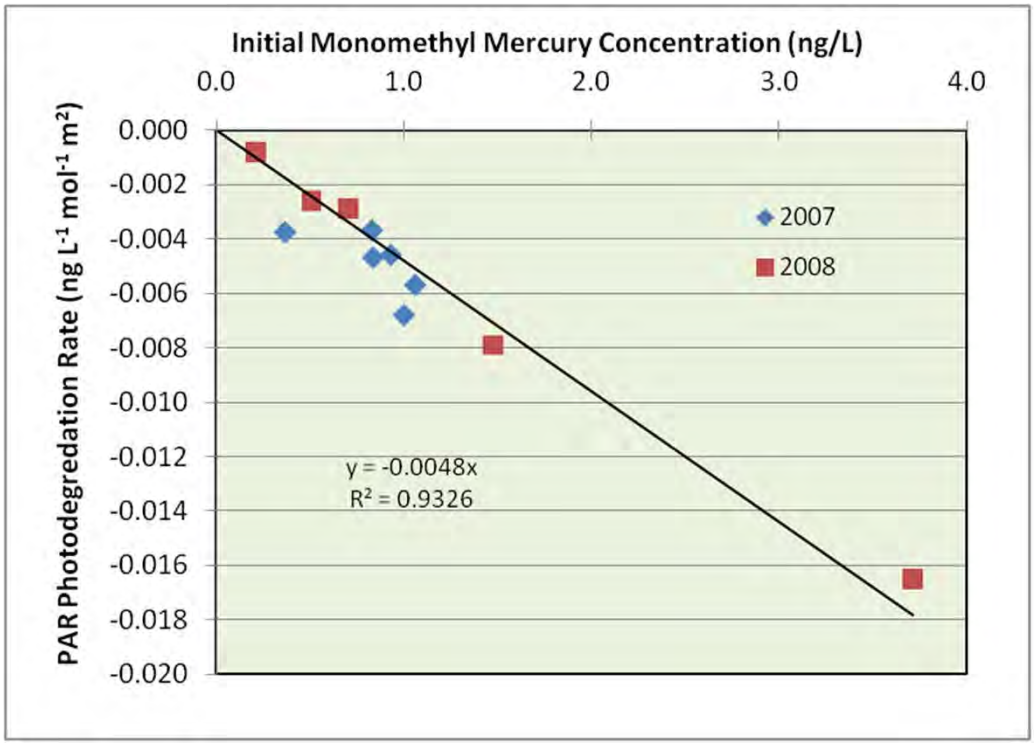

Figure 9.7. Scatter plots showing least-squares linear regressions of initial aqueous methylmercury concentration versus PAR-dependent photodecomposition rate A) data from all 13 experiments and B) data from 11 experiments (2007 data from 2 northern fields, F20 and R31, not included).

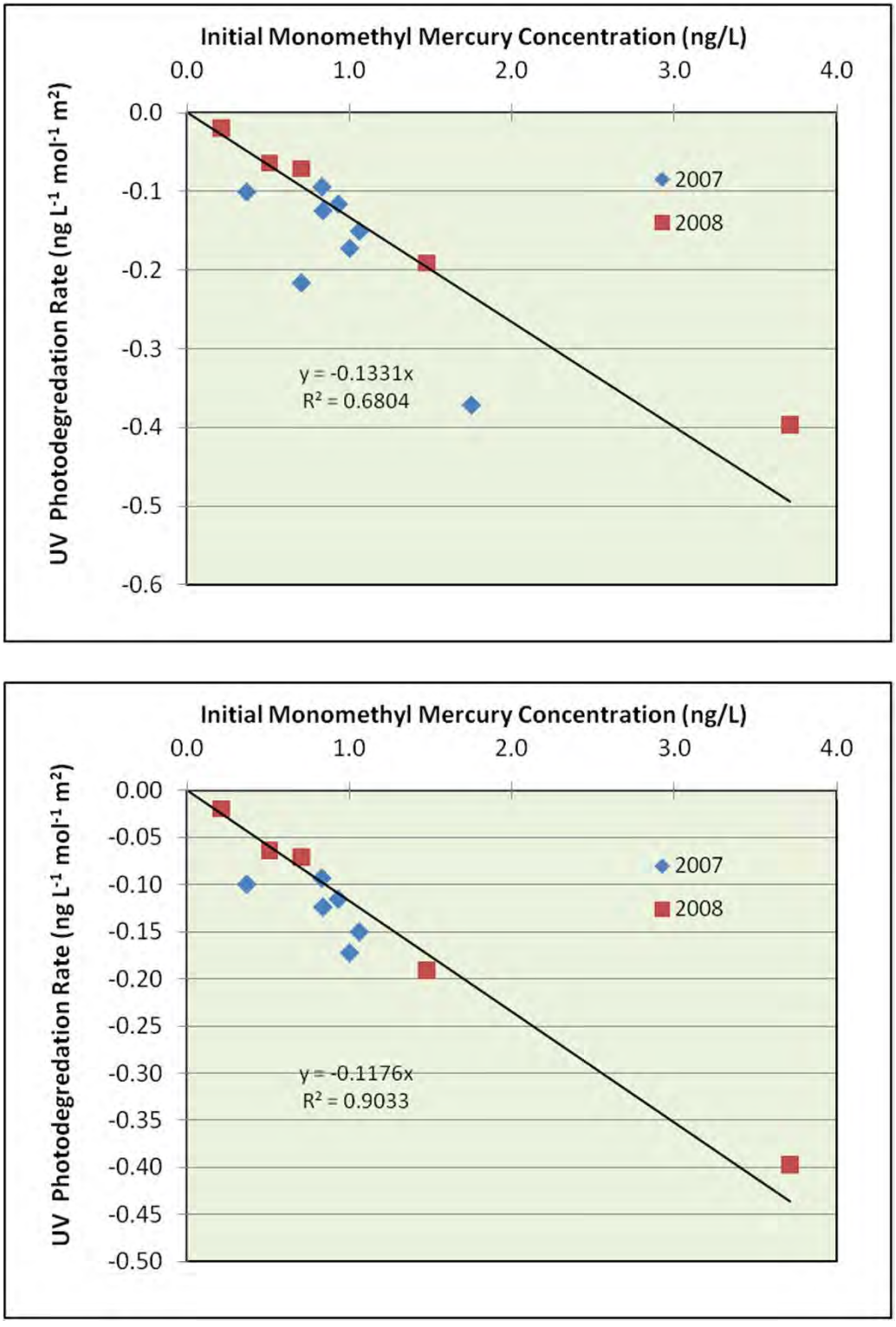

Figure 9.8. Scatter plots showing linear least-squares regressions of initial aqueous methylmercury concentration versus UV-dependent photodecomposition rate A) data from all 13 experiments and B) data from 11 experiments (2007 data from 2 northern fields, F20 and R31, not included).